

111-10
2-2-84

STS85-0118
VOLUME 1

OPERATIONAL AERODYNAMIC DATA BOOK VOLUME 1

AERODYNAMIC DESCRIPTION AND DATA USAGE

SEPTEMBER 1985

CONTRACT No. NAS9-14000
IRD SE-640D & E
WBS Nos. 10 & 14

LIBRARY
JAN 1 1986
UNCLAS
20 3
TEMPORARY HOLD

Space Transportation
Systems Division



Rockwell
International

Restriction/Classification Cancelled

| | | |
|------------------|-------------------------|---------------|
| (NASA-CR-172019) | AERODYNAMIC DESCRIPTION | X88-72411 |
| | well | |
| | NOT AVAIL: | |
| | | Unclas |
| | | 00/16 0136014 |

SPACE SHUTTLE

Transportation System



OPERATIONAL AERODYNAMIC DATA BOOK

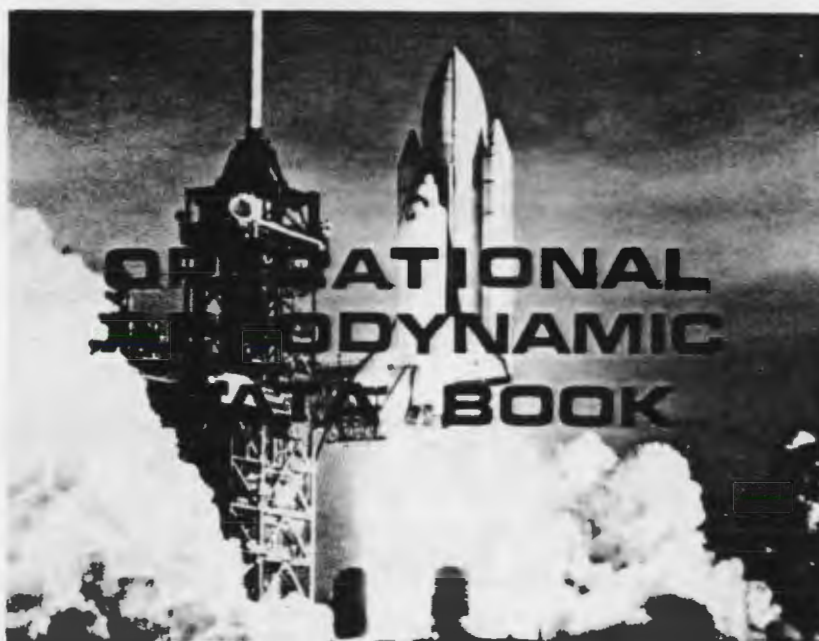


Rockwell International

Space Transportation Systems Division

Downey, California

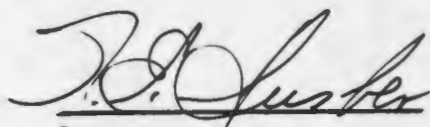
SPACE SHUTTLE TRANSPORTATION SYSTEM



AERODYNAMIC DESCRIPTION AND DATA USAGE VOLUME 1

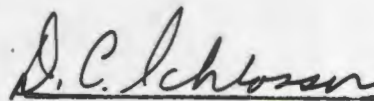
CONTRACT No. NAS9-14000
IRD SE-640D&E
WBS Nos. 10 & 14

Prepared by
AERODYNAMIC DATA
SHUTTLE AERO SCIENCES

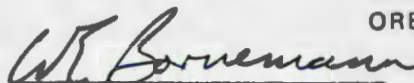


Supervisor:
LAUNCH VEHICLE

APPROVAL



Supervisor:
ORBITER VEHICLE



Manager:
AERODYNAMICS



Rockwell International

Space Transportation Systems Division

Downey California

**ORIGINAL PAGE IS
OF POOR QUALITY**

Space Systems Group



LAUNCH VEHICLE



ORBITER VEHICLE

FRONTISPIECE

STS85-0118

PREFACE

The purpose of this book is to present, in a form suitable for easy use, the operational aerodynamic data for the Rockwell Space Shuttle Vehicle. The Space Shuttle Vehicle is a combination aircraft/spacecraft designed for the express purpose of launching a variety of payloads into Earth orbit [and/or retrieving payloads from orbit], return to Earth, and land in the manner of conventional aircraft. The Space Shuttle Vehicle is comprised of three major elements: the Orbiter, External Tank, and two Solid Rocket Boosters. The external features have been designed to provide the protection and versatility required for both atmospheric and space flight regimes.

This book provides the primary reference work for all Space Shuttle Vehicle aerodynamic data appropriate to full-scale, operational, flight performance and stability and control analyses. An effort has been made to treat the data in successive steps from the launch through entry and landing. The book has been divided into five volumes, the first dealing with generalities and usage of the data which are contained in the remaining four volumes.

The book has been written to meet the needs of the practicing engineer in the areas of systems design and analyses, loads and structures, performance analyses, and manned simulations. The text is based largely on standard aerodynamic relationships and the material and data gathered during extensive wind tunnel testing of models as well as full-scale flight testing over the past few years. All the material have been used previously in this book's forerunner; the AERODYNAMIC DESIGN DATA BOOK. Since that time, the data have been revised, based largely on flight test results of the Space Transportation System Flight Test Program and NASA reviews.

The first volume presents the Space Shuttle Vehicle mission description and capability, evolution of the spacecraft configuration, systems descriptions, and the use of the aerodynamic data. The latter section presents all pertinent aerodynamic relationships necessary to the calculation of total aerodynamic forces and moments, airloads computations, and the associated uncertainties. The second volume presents the aerodynamic data for the launch configuration, including separation of the three elements and abort situations. The third volume contains the aerodynamic data for the entry configuration and includes pertinent on-orbit data. The fourth volume consists of the external airloads data for the launch configuration and the fifth volume contains external airloads data for the entry configuration. All references for a particular section are given as the last page in the single digit part of the section. For example, all references for Section 1 are on page 1.0-3. All references for Section 3 are on page 3.0-4, etc.

Many references to publications of the NASA have been used in the preparation of these volumes, for which appreciation is gratefully extended. Acknowledgement is also extended to Messers R. Wallace, P. Romere, and J. Underwood of the NASA/JSC for their help and review during the preparation of this manuscript and to those Rockwell engineers under the direction of T. E. Surber and D. C. Schlosser (supervisors) who prepared and analyzed the aerodynamic data.

JSC and Rockwell coordinated the flight test results for incorporation into the final data base. The Aero Technical Panel, whose members (JSC, LaRC, ARC, ARD/ AEDC, AFPTC, and OPRC) all contributed to this book, was of particular significance.

W. R. Russell: Editor

Rockwell International
Space Transportation Systems Division
Downey, California
September 1985

OPERATIONAL AERODYNAMIC DATA BOOK

CONTENTS

VOLUME 1 AERODYNAMIC DESCRIPTION AND DATA USAGE

| | <u>PAGE</u> |
|--|-------------|
| REVISION RECORD | a |
| PREFACE | i |
| CONTENTS | iii |
| INTRODUCTION | viii |
| NOMENCLATURE | ix |
| | |
| 1.0 SPACE SHUTTLE VEHICLE | 1.0-1 |
| 1.1 Mission Description | 1.1-1 |
| 1.2 Mission Capability | 1.2-1 |
| 2.0 SPACE SHUTTLE VEHICLE EVOLUTION | 2.0-1 |
| 2.1 Authority to Proceed (ATP) | 2.0-3 |
| 2.2 Preliminary Requirements Review (PRR) | 2.0-5 |
| 2.3 Preliminary Design Requirements (PDR) | 2.0-6 |
| 2.4 Critical Design Review (CDR) | 2.0-8 |
| 2.5 Operational Vehicles | 2.0-10 |
| 3.0 CONFIGURATION AND SYSTEMS DESCRIPTIONS | 3.0-1 |
| 3.1 Configuration and Dimensions | 3.1-1 |
| 3.1.1 Launch Vehicle | 3.1-1 |
| 3.1.2 Solid Rocket Boosters | 3.1-7 |
| 3.1.3 External Tank | 3.1-13 |
| 3.1.4 Attach Structure | 3.1-20 |
| 3.1.5 Orbiter Vehicle | 3.1-25 |
| 3.1.5.1 Wing | 3.1-35 |
| 3.1.5.2 Fuselage | 3.1-38 |
| 3.1.5.3 Vertical Tail | 3.1-39 |
| 3.1.5.4 Total Vehicle | 3.1-39 |
| 3.2 Surface Design Requirements | 3.2-1 |
| 3.2.1 Solid Rocket Boosters | 3.2-1 |
| 3.2.2 External Tank | 3.2-2 |
| 3.2.3 Orbiter Vehicle | 3.2-5 |
| 3.3 Thermal Protection System | 3.3-1 |
| 3.3.1 Solid Rocket Boosters | 3.3-1 |
| 3.3.2 External Tank | 3.3-1 |
| 3.3.3 Orbiter Vehicle | 3.3-4 |
| 3.4 Air Data System | 3.4-1 |
| 3.5 Control Systems | 3.5-1 |
| 3.5.1 Reaction Controls | 3.5-2 |
| 3.5.1.1 SRB Thrust Vector Control | 3.5-2 |
| 3.5.1.2 SSME Thrust Vector Control | 3.5-3 |
| 3.5.1.3 OMS Thrust Vector Control | 3.5-4 |
| 3.5.1.4 Reaction Control System | 3.5-5 |
| 3.5.2 Aerodynamic Controls | 3.5-8 |
| 3.5.2.1 Elevons | 3.5-10 |
| 3.5.2.2 Rudder/Speedbrake | 3.5-10 |
| 3.5.2.3 Body Flap | 3.5-11 |
| 3.6 Landing Gear | 3.6-1 |
| 3.7 Shuttle Infrared Leaside Temperature Sensing | 3.7-1 |

| | |
|---|-------------|
| 4.0 AERODYNAMIC DATA USAGE | 4.0-1 |
| 4.1 Launch Vehicle Aerodynamic Equations | 4.1-1 |
| 4.1.1 First Stage (Including Abort) | 4.1.1-1 |
| 4.1.1.1 Longitudinal Aerodynamics | 4.1.1-1 |
| 4.1.1.2 Lateral-Directional Aerodynamics | 4.1.1-10 |
| 4.1.2 Solid Rocket Booster Separation | 4.1.2-1 |
| 4.1.2.1 Longitudinal Aerodynamics | 4.1.2-12 |
| 4.1.2.2 Lateral-Directional Aerodynamics | 4.1.2-18 |
| 4.1.3 Contingency Separation | 4.1.3-1 |
| 4.1.3.1 Longitudinal Aerodynamics | 4.1.3-1 |
| 4.1.3.2 Lateral-Directional Aerodynamics | 4.1.3-2 |
| 4.1.4 Second-Stage (Including Abort) | 4.1.4-1 |
| 4.1.4.1 Longitudinal Aerodynamics | 4.1.4-1 |
| 4.1.4.2 Lateral-Directional Aerodynamics | 4.1.4-5 |
| 4.1.5 External Tank Separation | 4.1.5-1 |
| 4.1.5.1 Return-To-Launch-Site (RTLS) Abort | 4.1.5-3 |
| 4.1.5.1.1 Longitudinal Aerodynamics | 4.1.5-3 |
| 4.1.5.1.2 Lateral-Directional Aerodynamics | 4.1.5-18 |
| 4.1.5.2 Transatlantic Abort Landing | 4.1.5-28 |
| 4.1.5.2.1 Longitudinal Aerodynamics | 4.1.5-28 |
| 4.1.5.2.2 Lateral-Directional Aerodynamics | 4.1.5-32 |
| 4.1.6 Hinge Moments | 4.1.6-1 |
| 4.1.7 Uncertainties | 4.1.7-1 |
| 4.1.7.1 Launch Vehicle, Elements, and Components | 4.1.7-1 |
| 4.1.7.1.1 Trajectory Analysis / GN&C | 4.1.7-2 |
| 4.1.7.1.2 Structures | 4.1.7-7 |
| 4.1.7.1.2.1 Mated Elements | 4.1.7-7 |
| 4.1.7.1.2.2 Wing Uncertainties | 4.1.7-13 |
| 4.1.7.1.2.3 Elevon Uncertainties | 4.1.7-14 |
| 4.1.7.1.2.4 Vertical Uncertainties | 4.1.7-15 |
| 4.1.7.2 Separation | 4.1.7.2-1 |
| 4.1.7.2.1 Solid Rocket Boosters (SRB) | 4.1.7.2.1-1 |
| 4.1.7.2.2 Return-To-Launch-Site (RTLS) Intact Abort | 4.1.7.2.2-1 |
| 4.1.7.2.3 Transatlantic Abort Landing (TAL) Intact Abort | 4.1.7.2.3-1 |
| 4.1.8 Structural Analysis Data | 4.1.8-1 |
| 4.1.8.1 Longitudinal Aerodynamics | 4.1.8.1-1 |
| 4.1.8.2 Lateral Directional Aerodynamics | 4.1.8.2-1 |
| 4.1.8.3 Elevon and Wing Panel Loads | 4.1.8.3-1 |
| 4.1.8.4 Vertical Tail Loads | 4.1.8.4-1 |
| 4.2 Orbiter Vehicle Aerodynamic Equations | 4.2-1 |
| 4.2.1 Orbital and Entry Aerodynamics | 4.2.1-1 |
| 4.2.1.1 Longitudinal Aerodynamics | 4.2.1.1-1 |
| 4.2.1.2 Lateral-Directional Aerodynamics | 4.2.1.2-1 |
| 4.2.2 Hinge Moments | 4.2.2-1 |
| 4.2.2.1 Elevon Control | 4.2.2-1 |
| 4.2.2.2 Body Flap Control | 4.2.2-3 |
| 4.2.2.3 Rudder/Speedbrake Control | 4.2.2-5 |
| 4.2.3 Aerodynamic Uncertainties | 4.2.3-1 |
| 4.2.3.1 Longitudinal Aerodynamics | 4.2.3.1-1 |
| 4.2.3.2 Lateral-Directional Aerodynamics | 4.2.3.2-1 |
| 4.2.3.3 Hinge Moments | 4.2.3.3-1 |
| 4.2.3.3.1 Elevon Control | 4.2.3.3.1-1 |
| 4.2.3.3.2 Body Flap Control | 4.2.3.3.2-1 |
| 4.2.3.3.3 Rudder/Speedbrake Control | 4.2.3.3.3-1 |
| 4.2.3.4 Aerodynamic Data Uncertainty Correlation Coefficients | 4.2.3.4-1 |
| 4.3 Launch Vehicle Airloads Equations | 4.3-1 |
| 4.3.1 External Pressure Distribution and Airloads Analysis | 4.3.1-1 |
| 4.3.2 Plume Effects | 4.3.2-1 |
| 4.3.3 Skin Friction | 4.3.3-1 |
| 4.3.4 Engine Nozzle Airloads | 4.3.4-1 |
| 4.3.5 Attach Structure Airloads | 4.3.5-1 |
| 4.3.6 ET and SRB Protuberance Airloads | 4.3.6-1 |
| 4.3.6.1 Global Protuberance Aerodynamic Loads | 4.3.6-1 |
| 4.3.6.2 Protuberance Aerodynamic Loads | 4.3.6-3 |
| 4.3.7 Distributed Airloads | 4.3.7-1 |
| 4.4 Orbiter Vehicle Airloads Equations | 4.4-1 |

VOLUME 2 LAUNCH VEHICLE AERODYNAMIC DATA

| | <u>PAGE</u> |
|--|---------------|
| REVISION RECORD | a |
| PREFACE TO VOLUME 2 | i |
| CONTENTS TO VOLUME 2 | ii |
| INTRODUCTION TO VOLUME 2 | iv |
| | |
| 5.0 AERODYNAMIC DATA | 5.0-1 |
| 5.1 Launch Vehicle Aerodynamic Data | 5.1-1 |
| 5.1.1 First-Stage (Including Abort) | 5.1.1-1 |
| 5.1.1.1 Longitudinal Aerodynamics | 5.1.1.1-1 |
| 5.1.1.1.1 NORMAL FORCE | 5.1.1.1.1-1 |
| 5.1.1.1.2 AXIAL FORCE | 5.1.1.1.2-1 |
| 5.1.1.1.3 PITCHING MOMENT | 5.1.1.1.3-1 |
| 5.1.1.2 Lateral-Directional Aerodynamics | 5.1.1.2-1 |
| 5.1.1.2.1 SIDE FORCE | 5.1.1.2.1-1 |
| 5.1.1.2.2 YAWING MOMENT | 5.1.1.2.2-1 |
| 5.1.1.2.3 ROLLING MOMENT | 5.1.1.2.3-1 |
| 5.1.2 Solid Rocket Booster Separation | 5.1.2-1 |
| 5.1.2.1 Longitudinal Aerodynamics | 5.1.2.1-1 |
| 5.1.2.1.1 NORMAL FORCE | 5.1.2.1.1-1 |
| 5.1.2.1.2 AXIAL FORCE | 5.1.2.1.2-1 |
| 5.1.2.1.3 PITCHING MOMENT | 5.1.2.1.3-1 |
| 5.1.2.2 Lateral-Directional | 5.1.2.2-1 |
| 5.1.2.2.1 SIDE FORCE | 5.1.2.2.1-1 |
| 5.1.2.2.2 YAWING MOMENT | 5.1.2.2.2-1 |
| 5.1.2.2.3 ROLLING MOMENT | 5.1.2.2.3-1 |
| 5.1.3 Contingency Separation | 5.1.3-1 |
| 5.1.3.1 Longitudinal Aerodynamics | 5.1.3.1-1 |
| 5.1.3.2 Lateral-Directional Aerodynamics | 5.1.3.2-1 |
| 5.1.4 Second-Stage (Including Abort) | 5.1.4-1 |
| 5.1.4.1 Longitudinal Aerodynamics | 5.1.4.1-1 |
| 5.1.4.1.1 NORMAL FORCE | 5.1.4.1.1-1 |
| 5.1.4.1.2 AXIAL FORCE | 5.1.4.1.2-1 |
| 5.1.4.1.3 PITCHING MOMENT | 5.1.4.1.3-1 |
| 5.1.4.2 Lateral-Directional Aerodynamics | 5.1.4.2-1 |
| 5.1.4.2.1 SIDE FORCE | 5.1.4.2.1-1 |
| 5.1.4.2.2 YAWING MOMENT | 5.1.4.2.2-1 |
| 5.1.4.2.3 ROLLING MOMENT | 5.1.4.2.3-1 |
| 5.1.5 External Tank Separation | 5.1.5-1 |
| 5.1.5.1 Return-To-Launch-Site (RTLS) Abort | 5.1.5.1-1 |
| 5.1.5.1.1 Longitudinal Data | 5.1.5.1.1-1 |
| 5.1.5.1.1.1 NORMAL FORCE | 5.1.5.1.1.1-1 |
| 5.1.5.1.1.2 AXIAL FORCE | 5.1.5.1.1.2-1 |
| 5.1.5.1.1.3 PITCHING MOMENT | 5.1.5.1.1.3-1 |
| 5.1.5.1.2 Lateral-Directional Data | 5.1.5.1.2-1 |
| 5.1.5.1.2.1 SIDE FORCE | 5.1.5.1.2.1-1 |
| 5.1.5.1.2.2 YAWING MOMENT | 5.1.5.1.2.2-1 |
| 5.1.5.1.2.3 ROLLING MOMENT | 5.1.5.1.2.3-1 |
| 5.1.5.2 Transatlantic Abort Landing (TAL) | 5.1.5.2-1 |
| 5.1.5.2.1 Longitudinal Data | 5.1.5.2.1-1 |
| 5.1.5.2.1.1 NORMAL FORCE | 5.1.5.2.1.1-1 |
| 5.1.5.2.1.2 AXIAL FORCE | 5.1.5.2.1.2-1 |
| 5.1.5.2.1.3 PITCHING MOMENT | 5.1.5.2.1.3-1 |
| 5.1.5.2.2 Lateral-Directional Data | 5.1.5.2.2-1 |
| 5.1.5.2.2.1 SIDE FORCE | 5.1.5.2.2.1-1 |
| 5.1.5.2.2.2 YAWING MOMENT | 5.1.5.2.2.2-1 |
| 5.1.5.2.2.3 ROLLING MOMENT | 5.1.5.2.2.3-1 |
| 5.1.6 Hinge Moments | 5.1.6-1 |

| | | |
|-------------|--|---------------|
| 5.1.7 | Uncertainties | 5.1.7-1 |
| 5.1.7.1 | Launch Vehicle Elements and Components | 5.1.7.1-1 |
| 5.1.7.1.1 | Trajectory Analysis / GN&C | 5.1.7.1.1-1 |
| 5.1.7.1.2 | Structures | 5.1.7.1.2-1 |
| 5.1.7.1.2.1 | Mated Elements | 5.1.7.1.2.1-1 |
| 5.1.7.1.2.2 | Wing Uncertainties | 5.1.7.1.2.2-1 |
| 5.1.7.1.2.3 | Elevon Uncertainties | 5.1.7.1.2.3-1 |
| 5.1.7.2 | Separation | 5.1.7.2-1 |
| 5.1.7.2.1 | Solid Rocket Boosters (SRB) | 5.1.7.2.1-1 |
| 5.1.7.2.2 | Return-To-Launch-Site (RTL) Intact Abort | 5.1.7.2.2-1 |
| 5.1.7.2.3 | Transatlantic Abort Landing (TAL) Intact Abort | 5.1.7.2.3-1 |
| 5.1.8 | Structural Analysis Data | 5.1.8-1 |
| 5.1.8.1 | Longitudinal Aerodynamics | 5.1.8.1-1 |
| 5.1.8.1.1 | NORMAL FORCE | 5.1.8.1.1-1 |
| 5.1.8.1.2 | AXIAL FORCE | 5.1.8.1.2-1 |
| 5.1.8.1.3 | PITCHING MOMENT | 5.1.8.1.3-1 |
| 5.1.8.2 | Lateral-Directional Aerodynamics | 5.1.8.2-1 |
| 5.1.8.2.1 | SIDE FORCE | 5.1.8.2.1-1 |
| 5.1.8.2.2 | YAWING MOMENT | 5.1.8.2.2-1 |
| 5.1.8.2.3 | ROLLING MOMENT | 5.1.8.2.3-1 |
| 5.1.8.3 | Elevon and Wing Panel Loads | 5.1.8.3-1 |
| 5.1.8.4 | Vertical Tail Loads | 5.1.8.4-1 |

VOLUME 3 ORBITER VEHICLE AERODYNAMIC DATA

| | <u>PAGE</u> |
|--|-------------|
| REVISION RECORD | a |
| PREFACE TO VOLUME 3 | i |
| CONTENTS TO VOLUME 3 | ii |
| INTRODUCTION TO VOLUME 3 | iii |
| | |
| 5.0 AERODYNAMIC DATA | 5.0-1 |
| 5.1 Launch Vehicle Aerodynamic Data | VOLUME 2 |
| 5.2 Orbiter Vehicle Aerodynamic Data | 5.2-1 |
| 5.2.1 Orbital and Entry Aerodynamic Data | 5.2.1-1 |
| 5.2.1.1 Longitudinal Aerodynamics | 5.2.1.1-1 |
| 5.2.1.1.1 LIFT and NORMAL FORCE | 5.2.1.1.1-1 |
| 5.2.1.1.2 DRAG and AXIAL FORCE | 5.2.1.1.2-1 |
| 5.2.1.1.3 PITCHING MOMENT | 5.2.1.1.3-1 |
| 5.2.1.1.4 LIFT-to-DRAG RATIO | 5.2.1.1.4-1 |
| 5.2.1.2 Lateral-Directional Aerodynamics | 5.2.1.2-1 |
| 5.2.1.2.1 SIDE FORCE | 5.2.1.2.1-1 |
| 5.2.1.2.2 YAWING MOMENT | 5.2.1.2.2-1 |
| 5.2.1.2.3 ROLLING MOMENT | 5.2.1.2.3-1 |
| 5.2.2 Hinge Moments | 5.2.2-1 |
| 5.2.2.1 Elevon | 5.2.2.1-1 |
| 5.2.2.2 Body Flap | 5.2.2.2-1 |
| 5.2.2.3 Rudder/Speedbrake | 5.2.2.3-1 |
| 5.2.3 Aerodynamic Uncertainties | 5.2.3-1 |
| 5.2.3.1 Longitudinal Aerodynamics | 5.2.3.1-1 |
| 5.2.3.1.1 LIFT and NORMAL FORCE | 5.2.3.1.1-1 |
| 5.2.3.1.2 DRAG and AXIAL FORCE | 5.2.3.1.2-1 |
| 5.2.3.1.3 PITCHING MOMENT | 5.2.3.1.3-1 |
| 5.2.3.1.4 LIFT-to-DRAG RATIO | 5.2.3.1.4-1 |
| 5.2.3.2 Lateral-Directional Aerodynamics | 5.2.3.2-1 |
| 5.2.3.2.1 SIDE FORCE | 5.2.3.2.1-1 |
| 5.2.3.2.2 YAWING MOMENT | 5.2.3.2.2-1 |
| 5.2.3.2.3 ROLLING MOMENT | 5.2.3.2.3-1 |
| 5.2.3.3 Hinge Moments | 5.2.3.3-1 |
| 5.2.3.3.1 Elevon | 5.2.3.3.1-1 |
| 5.2.3.3.2 Body Flap | 5.2.3.3.2-1 |

| | |
|---|-------------|
| 5.2.3.3.3 Rudder/Speedbrake | 5.2.3.3.3-1 |
| 5.2.3.4 Uncertainty Correlation Coefficient | 5.2.3.4-1 |

VOLUME 4 LAUNCH VEHICLE AIRLOADS DATA

| | <u>PAGE</u> |
|--|--------------|
| REVISION RECORD | a |
| PREFACE TO VOLUME 4 | i |
| CONTENTS TO VOLUME 4 | ii |
| INTRODUCTION TO VOLUME 4 | iii |
| 8.0 AIRLOADS DATA | 8.0-1 |
| 8.1 Launch Vehicle Airloads Data | 8.1-1 |
| 8.1.1 External Pressure Distributions and Loads Analysis | 8.1.1-1 |
| 8.1.2 Plume Effects | 8.1.2-1 |
| 8.1.3 Skin Friction | 8.1.3-1 |
| 8.1.4 Engine Nozzle Airloads | 8.1.4-1 |
| 8.1.5 Attach Structure Airloads | 8.1.5-1 |
| 8.1.6 ET and SRB Protuberance Airloads | 8.1.6-1 |
| 8.1.6.1 Global Protuberance Aerodynamic Loads | 8.1.6.1-1 |
| 8.1.6.1 Protuberance Aerodynamic Loads | 8.1.6.2-1 |
| 8.1.7 Distributed Airloads | 8.1.7-1 |

VOLUME 5 ORBITER VEHICLE AIRLOADS DATA

| | <u>PAGE</u> |
|---|--------------|
| REVISION RECORD | a |
| PREFACE TO VOLUME 5 | i |
| CONTENTS TO VOLUME 5 | ii |
| INTRODUCTION TO VOLUME 5 | iii |
| 8.0 AIRLOADS DATA | 8.0-1 |
| 8.2 Orbiter Vehicle Airloads Data | 8.2-1 |

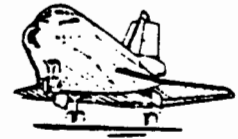
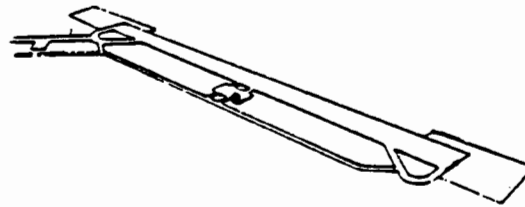
APPENDICES

| | |
|--|------------|
| A. DETAILED SEPARATION AERODYNAMIC DATA | A-1 |
| A.1 Solid Rocket Booster | A.1-1 |
| A.2 Return-To-Launch-Site (RTLS) | A.2-1 |
| B. DETAILED LAUNCH VEHICLE AIRLOADS DATA | B-1 |
| 8.1 Forebody Pressure Distributions | 8.1-1 |
| 8.1.1 Orbiter | 8.1.1-1 |
| 8.1.2 External Tank | 8.1.2-1 |
| 8.1.3 Solid Rocket Booster | 8.1.3-1 |
| C. DETAILED ORBITER VEHICLE AIRLOADS DATA | C-1 |
| (To be completed at a later date) | |

INTRODUCTION

This document, Volume 1 of the OPERATIONAL AERODYNAMIC DATA BOOK, contains information pertinent to the use of Volumes 2 through 5. Volume 1 describes the Space Shuttle Vehicle, its mission, evolution, geometry, systems, and the use of the data given in the remaining volumes. For example, the equations presented in Section 4.1 of Volume 1 direct the user to the data of Section 5.1 in Volume 2 (Launch Vehicle Aerodynamic Data) and the equations presented in Section 4.2 of Volume 1 direct the user to the data of Section 5.2 of Volume 3 (Orbiter Vehicle Aerodynamic Data). The equations given in this first volume consist of several elements or components, each of which has been defined separately and noted by reference to a particular Table or Figure number where the applicable data may be found for that particular element in the remaining four volumes. These data have been presented in a format considered useful to trajectory and flight simulation analyses and to structural engineering analyses.

The Data Book has been prepared under the terms of contract number NAS9-14000. It is specified in the Information Requirements Document, SE-640 (Schedules D and E).



NOMENCLATURE

A. ACRONYMS

| | |
|--------|--|
| AA | Accelerometer Assembly |
| AADS | Ascent Air Data System |
| AAP | Angular Accelerometer Package |
| ACIP | Aerodynamic Coefficient Identification Package |
| AADS | Ascent Air Data System |
| ADS | Air Data System |
| ADTA | Air Data Transducer Assembly |
| AFCS | Automatic Flight Control System |
| AFSCF | Air Force Satellite Control Facility |
| ALT | Approach and Landing Test |
| AMI | Alpha-Mach Indicator |
| APU | Auxiliary Power Unit |
| BET | Best Estimate Trajectory |
| BFCFS | Back-up Flight Control System |
| BITE | Built-In Test Equipment |
| CATSGT | Communications and Tracking System Ground Test |
| CCB | Configuration Control Board |
| CCT | Computer Compatible Tape |
| CCTV | Closed Circuit Television |
| CDR | Critical Design Review |
| CEI | Contract End Item |
| CG | Center of Gravity |
| COMSEC | Communications Security |
| CSS | Control Stick Steering |
| C&T | Communications and Tracking |
| C&W | Caution and Warning |
| D&C | Display(s) and Control(s) |
| DCR | Design Certification Review |
| DFI | Development Flight Instrumentation |
| DOD | Department of Defense |
| DOF | Degree(s) of Freedom |
| DTO | Detailed Test Objective |
| EAFB | Edwards Air Force Base |
| EMI | Electromagnetic Interference |
| EMS | Engineering Master Schedule |
| ESTL | Electronic Systems Test Laboratory |
| ET | External Tank |
| ETR | Eastern Test Range |
| EVA | Extravehicular Activity |
| F | Ferry |
| FAA | Federal Aviation Agency |
| FCF | Functional Checkout Flight |
| FCS | Flight Control System |
| FEWG | Flight Evaluation Working Group |
| FF | Free Flight |
| FMOF | First Manned Orbital Flight |

A. ACRONYMS (Continued)

| | |
|-------|---|
| FOF | First Operational Flight |
| FRC | Flight Research Center |
| FRD | Flight Requirements Document |
| FRF | Flight Readiness Firing |
| FRR | Flight Readiness Review |
| FSSR | Functional Subsystem Software Requirement |
| FTR | Flight Test Requirement |
| FTRD | Flight Test Requirements Document |
| | |
| GFE | Government Furnished Equipment |
| GMT | Greenwich Mean Time |
| GN&C | Guidance Navigation and Control |
| GSE | Ground Support Equipment |
| GSFC | Goddard Space Flight Center |
| | |
| HAC | Heading Alignment Circle |
| HOSC | Huntsville Operations Support Center |
| HQ | Handling Qualities |
| HSI | Horizontal Situation Indicator |
| HW | Head Wind |
| | |
| I | Inert |
| ICD | Interface Control Document |
| IDSD | Institutional Data Systems Division |
| ILS | Instrument Landing System |
| IMU | Inertial Measurement Unit |
| | |
| JSC | Johnson Space Center |
| | |
| KBPS | Kilobits per second |
| KEAS | Knots-Equivalent Airspeed |
| KSC | Kennedy Space Center |
| | |
| L&L | Launch and Landing |
| LPS | Launch Pad Station |
| LV | Launch Vehicle |
| | |
| M | Manned or Mandatory |
| MDM | Modulate - Demodulate |
| MECO | Main Engine Cut-Off |
| MER | Mission Evaluation Room |
| MET | Mission Elapsed Time |
| MEWG | Mission Evaluation Working Group |
| MFTAD | Master Flight Test Assignments Document |
| MILA | Merrit Island Launch Area |
| MMDB | Master Measurement Data Book |
| MML | Master Measurement List |
| MMLE | Modified Maximum Likelihood Estimate |
| MOF | Manned Orbital Flight |
| MPAD | Mission Planning and Analysis Division |
| MPS | Main Propulsion System |
| MRC | Moment Reference Center |
| MSFC | Marshall Space Flight Center |
| MSR | Mission Support Room |

A. ACRONYMS (Continued)

| | |
|-------|--|
| MVP | Master Verification Plan |
| N/A | Not Applicable |
| NAV | Navigation (System) |
| NRZ | Non-Return Zero |
| OAA | Orbiter Access Arm |
| OFI | Operational Flight Instrumentation |
| OFT | Orbital Flight Test |
| OI | Operational Instrumentation |
| OMI | Operations and Maintenance Instruction |
| OMRSD | Operations and Maintenance Requirements Specification Document |
| OMS | Orbital Maneuvering System |
| OPF | Orbiter Processing Facility |
| OV | Orbiter Vehicle |
| PCM | Pulse Code Modulation |
| PDR | Preliminary Design Review |
| P/L | Payload |
| PSRD | Program Support Requirements Document |
| PTI | Programmed Test Input |
| RCS | Reaction Control System |
| RF | Radio Frequency |
| RGA | Rate Gyro Assembly |
| RID | Review Item Disposition |
| RMS | Remote Manipulator Subsystem or Root-Mean-Square |
| RSS | Range Safety System or Root-Sum-Square |
| SAIL | Shuttle Avionics Integration Laboratory |
| SESL | Shuttle Engineering Simulation Laboratory |
| SILTS | Shuttle Infrared Leeside Temperature Sensor |
| SMVP | Shuttle Master Verification Plan |
| SODB | Shuttle Operational Data Book |
| SPAN | Spacecraft Analysis |
| SPI | Surface Position Indicator |
| SPS | Samples per Second |
| SRB | Solid Rocket Booster |
| S/C | Spacecraft or Stability and Control |
| SSME | Space Shuttle Main Engine |
| SSPM | Space Shuttle Program Manager |
| SSV | Space Shuttle Vehicle |
| STAR | Shuttle Turnaround Analysis Report |
| STC | Supplemental Type Certificate |
| STS | Space Transportation System |
| TAEM | Terminal Area Energy Management |
| TBD | To Be Determined |
| TDRS | Tracking and Data Relay Satellite |
| TM | Telemetry |
| TO | Take-Off |
| TOGW | Take-Off Gross Weight |
| TPS | Thermal Protection System |
| TRS | Test Requirements Specification Document |

A. ACRONYMS (Continued)

| | |
|---------|---------------------------------|
| TV | Television |
| T/W | Thrust-to-Weight Ratio |
| UHF | Ultra-High Frequency |
| VCN | Verification Completion Notice |
| VFT | Vertical Flight Test |
| VHF | Very-High Frequency |
| VIS | Verification Information System |
| VOR/LOC | Visual OMNI-Range/Localizer |
| WTR | Western Test Range |

B. GENERAL

| | | |
|---------------------|---|--------------------------------|
| A | Acceleration | ft/sec ² (also g's) |
| | Subscripts: X axial Y lateral Z normal | |
| BL | Buttock Line | |
| BP | Buttock Plane | |
| CL | Centerline | |
| F | Force | lb |
| | Subscripts: (see Acceleration, above) | |
| FRL | Fuselage Reference Line | |
| FRP | Fuselage Reference Plane | |
| FS | Fuselage Station | |
| H _L or H | Hingeline | |
| M | Mach Number | |
| | Subscripts: 0 dive MO maximum operating | |
| P | Pressure | lbs/ft ² (psf) |
| | Subscripts: a ambient (or freestream) s static T Total o } SL } sea level | |
| R | Universal Gas Constant | |
| ReN | Reynolds Number | |
| T | Temperature | °F, °R, or °K |

B. GENERAL (Continued)

| | | |
|------------------|--|---------------------------|
| T | Thrust | lbs. |
| L | Thrustline | |
| V | Velocity | fps or knots |
| u | linear perturbed velocity along x-axis (positive forward) | |
| v | linear perturbed velocity along y-axis (positive out right wing) | |
| w | linear perturbed velocity along z-axis (positive downward) | |
| Subscripts: | | |
| | c | calibrated |
| | e | equivalent |
| | i | indicated |
| | D | dive |
| | MCA | minimum control in air |
| | MCG | minimum control on ground |
| | MO | maximum operating |
| | ∞ | freestream |
| \bar{V}_∞ | Viscous Parameter | |
| W | Weight | lbs |
| WL | Waterline | |
| WP | Water Plane | |
| WDP | Wing Datum Plane | |
| a | Speed of Sound in Air | ft/sec or knots |
| a.c. | Aerodynamic Center | |
| b | Span | ft |
| c | Chord | inches |
| \bar{c} | or MAC - mean aerodynamic chord | |
| Subscripts: | | |
| | bf | body flap |
| | e | elevon |
| | r | rudder |
| | sb | speed brake |
| | w | wing |
| cg | Center of gravity | |
| cp | Center of pressure | |
| g | Acceleration due to gravity | ft/sec ² |
| h | Altitude (or height) | ft or nautical miles |
| m | Mass | slugs |
| n | Load Factor | g's |
| \bar{q} | dynamic pressure = $1/2 \rho V^2$ | lb/ft ² (psf) |

B. GENERAL (Continued)

| | | |
|----------------|---|-----------------------------|
| t | time | secs, mins, hrs |
| Δ | increment | |
| ζ | Nondimensional change in MRC with regard to WP; $(Z_{MRC} - Z_{MRC, REF})/\bar{c}$ | |
| η | (1) Semi-Span Parameter - $y/b/2$ (2) Flexible-to-Rigid Ratio | |
| i, i | Incidence | degrees |
| Λ | Sweep Angle | degrees |
| λ | Taper Ratio | |
| λ _m | Mean Free Path | inches |
| ξ | Non dimensional change to MRC with regard to Fuselage Station $= (X_{MRC} - X_{MRC, REF})/\bar{c}$ | |
| ρ | (1) Mass density of air (2) Correlation Coefficient | slug/ft ³ --- |
| σ | (1) Ratio of freestream density at a given altitude to standard sea level air density (2) Standard Deviation | |
| ω | Frequency | Hz (cycles/sec) |
| ★ | Angle | |
| > | Greater than | |
| < | Less than | |

C. CONFIGURATION

| | | |
|----|----------------|--------|
| L | Body Length | inches |
| LE | Leading Edge | |
| S | Reference Area | |

C. CONFIGURATION (Continued)

Subscripts: a aileron
bf body flap
e elevon (elevator)
r rudder
sb speedbrake
w wing
v vertical tail

TE Trailing Edge

X Longitudinal axis

Y Lateral axis

Z Vertical axis

δ (1) Control Surface Deflection degrees

Subscripts: a aileron (positive for positive rolling moment)
bf body flap (positive for nosedown pitching moment)
e elevon (positive for nosedown pitching moment)
r rudder (positive for nose-left yawing moment)
sb speed brake

(2) Dihedral Angle degrees

D. MOMENT & PRODUCTS OF INERTIA

1. Moment of Inertia slug-ft²

I_x rolling

I_y pitching

I_z yawing

2. Product of Inertia slug-ft²

I_{xy}, I_{xz}, I_{yz}

E. FORCES

A Axial; aerodynamic force along the X-body axis (positive aft) pounds

C_A Axial force coefficient = $A/\bar{q}S$

E. FORCES (Continued)

| | | |
|-------|---|--------|
| D | Drag; aerodynamic force along the total velocity vector in plane of symmetry (positive aft) | pounds |
| C_D | Drag coefficient = $D/\bar{q}S$ | |
| L | Lift; aerodynamic force perpendicular to total velocity vector in plane of symmetry (positive upward) | pounds |
| C_L | Lift coefficient = $L/\bar{q}S$ | |
| N | Normal; aerodynamic force along the Z-body axis (positive upward) | pounds |
| C_N | Normal force coefficient = $N/\bar{q}S$ | |
| Y | Side; aerodynamic force along the Y-body axis (positive out right wing) | pounds |
| C_Y | Side force coefficient = $Y/\bar{q}S$ | |

F. MOMENTS

| | | |
|--------------------|--|-----------|
| HM | Hinge; moment about hinge line | ft-pounds |
| C_h | Hinge moment coefficient = $HM/\bar{q}S\bar{c}$ | |
| | Subscripts: bf body flap e elevon r rudder sb speed brake | |
| \mathcal{L} | Rolling; moment about the X-axis due to aerodynamic torques (positive right-wing down) | ft-pounds |
| C_l | Rolling moment coefficient = $\mathcal{L}/\bar{q}SL$ | |
| M or \mathcal{M} | Pitching; moment about the Y-axis due to aerodynamic torques (positive nose-up) | ft-pounds |
| C_m | Pitching moment coefficient = $M/\bar{q}SL$ | |
| \mathcal{N} | Yawing; moment about the Z-axis due to aerodynamic torques (positive nose-right) | ft-pounds |
| C_n | Yawing moment coefficient = $\mathcal{N}/\bar{q}SL$ | |

G. ANGLES

| | | |
|------------|---|---------|
| α | Angle of attack; angle between the projection of the resultant velocity vector on the X-Z plane and the X-body (reference) axis | degrees |
| β | Sideslip; angle between the resultant velocity vector and the plane of symmetry (positive nose-left) = $-\psi$ | degrees |
| γ | Flight path; inclination of flight path to the horizontal | degrees |
| ϵ | Downwash | degrees |
| σ | Sidewash | degrees |
| θ | Pitch; displacement of reference axis from the horizontal (positive nose-up) | degrees |
| ϕ | Roll or Bank (positive right-wing down) | degrees |
| ψ | Yaw; angle between the resultant velocity vector and the plane of symmetry (positive nose-right) = $-\beta$ | degrees |

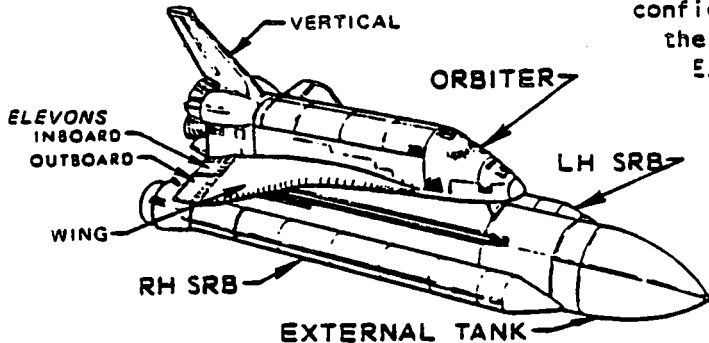
H. TIME-RELATED PARAMETERS

| | | |
|----------------|---|---------------------|
| a | Acceleration = $\dot{v} = \frac{\partial v}{\partial t}$ | ft/sec ² |
| g | Acceleration due to gravity | ft/sec ² |
| \dot{h} | Altitude rate | ft/sec |
| p | Roll rate; angular velocity about the X-axis (positive right-wing down) | radians/sec |
| q | Pitch rate; angular velocity about the Y-axis (positive nose-up) | radians/sec |
| r | Yaw rate; angular velocity about the Z-axis (positive nose-right) | radians/sec |
| $\dot{\alpha}$ | Rate of change of angle of attack | radians/sec |
| $\dot{\beta}$ | Sideslip rate | radians/sec |

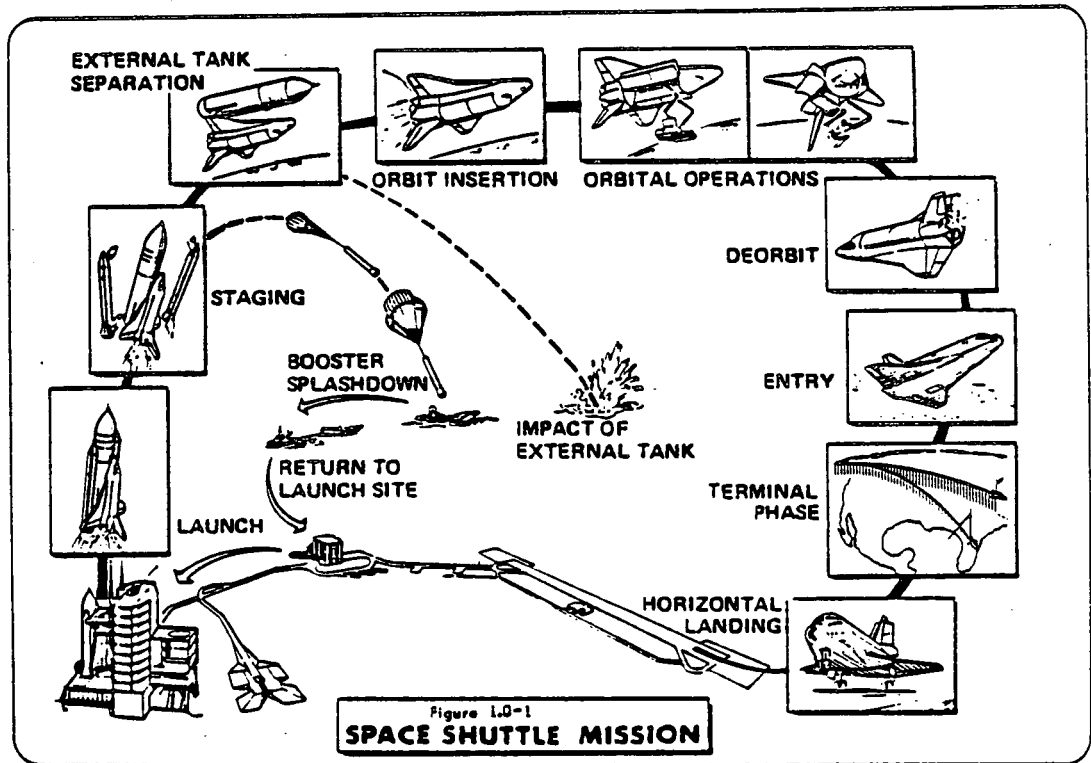
1.0 SPACE SHUTTLE VEHICLE

1.0 SPACE SHUTTLE VEHICLE

The Rockwell Space Shuttle has been designed to launch a variety of payloads into [and/or retrieve from] Earth orbit. The launch configuration consists of the Orbiter Vehicle, the External Tank, and two Solid Rocket Boosters.



The Orbiter Vehicle is launched in a vertical attitude by means of the Space Shuttle Main Engines and the two Solid Rocket Boosters. Landing of the Orbiter Vehicle is accomplished in a horizontal manner, similar to conventional aircraft. Figure 1.0-1 summarizes a typical Space Shuttle Mission.



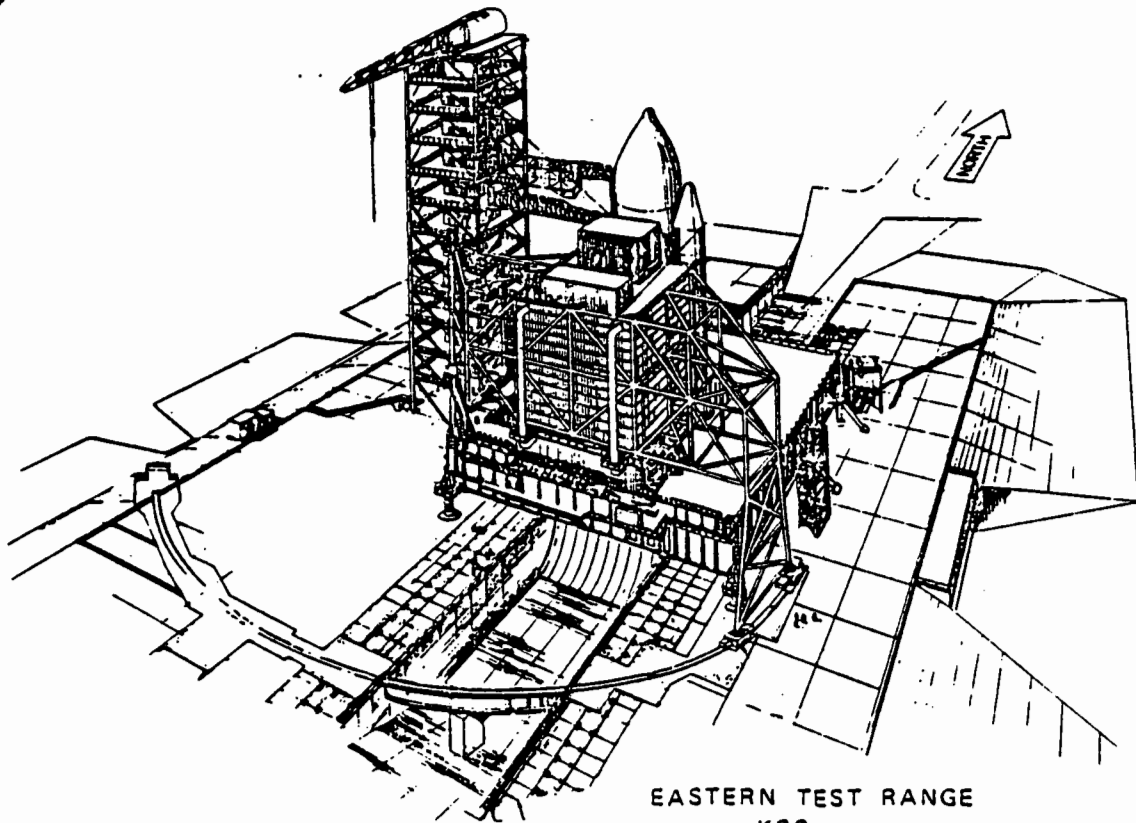
Maximum payload capability is 65,000 pounds for an easterly launch from the Eastern Test Range (ETR) at Kennedy Space Center (KSC) and 32,000 pounds for a polar orbit launch from the Western Test Range (WTR) at Vandenberg Air Force Base (VAFB). Figure 1.0-2 presents sketches of the two launch facilities.

ORIGINAL PAGE IS
OF POOR QUALITY

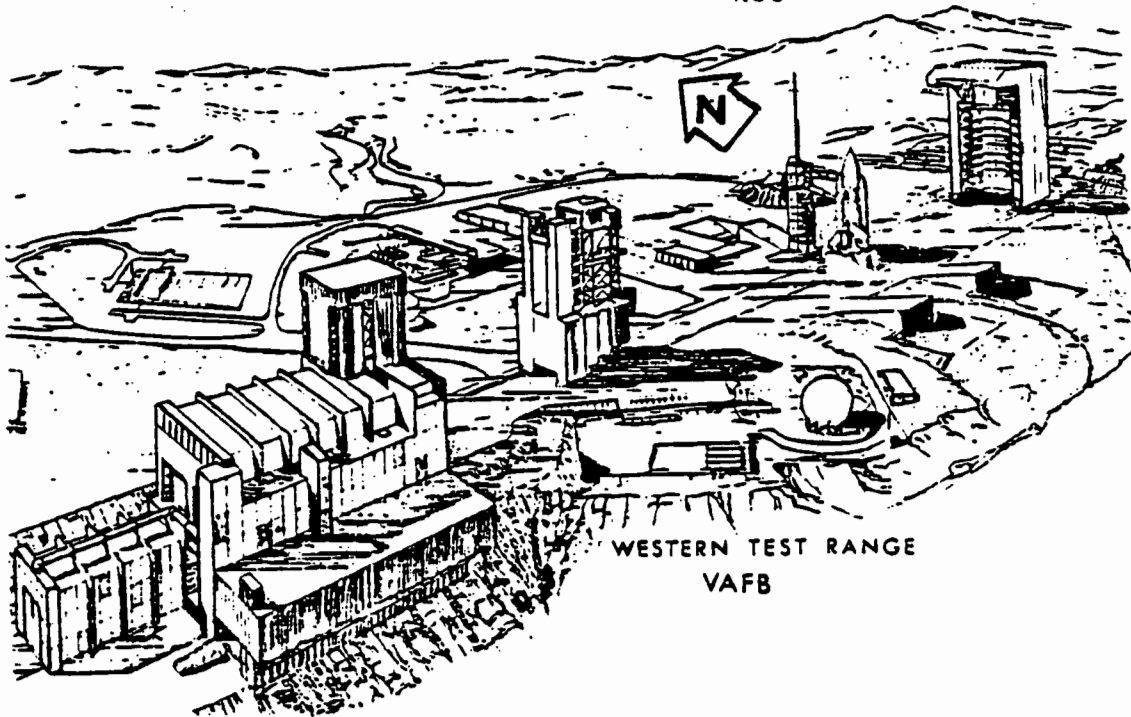
Space Transportation
Systems Division



Rockwell
International



EASTERN TEST RANGE
KSC



WESTERN TEST RANGE
VAFB

Figure 1.0-2

SPACE SHUTTLE LAUNCH FACILITIES

REFERENCES

- 1-1 SD73-SH-0178-1, "Flight Systems Performance Data Book, Volume 1, Ascent," Rockwell International, Space Division, Downey, California (December 1975)
- 1-2 JSC-IN-73-FM-47, "Space Shuttle System Baseline Reference Missions (Vols. I, II, III, and IV)," Johnson Space Center Internal Note, Houston, Texas (August 1975)
- 1-3 SD73-SH-0180F, "Space Shuttle Separation Data Book," Rockwell International, Space Division, Downey, California (July 1976)
- 1-4 SD76-SH-0133, "Space Shuttle Abort Baseline and Criteria Document," Rockwell International, Space Division, Downey, California (July 1976)

- 1.1 MISSION DESCRIPTION: The launch vehicle is transported from the vertical assembly building to the launch pad, standing in the vertical position, on a large tracked platform or "crawler" as shown in Figure 1.1-1.

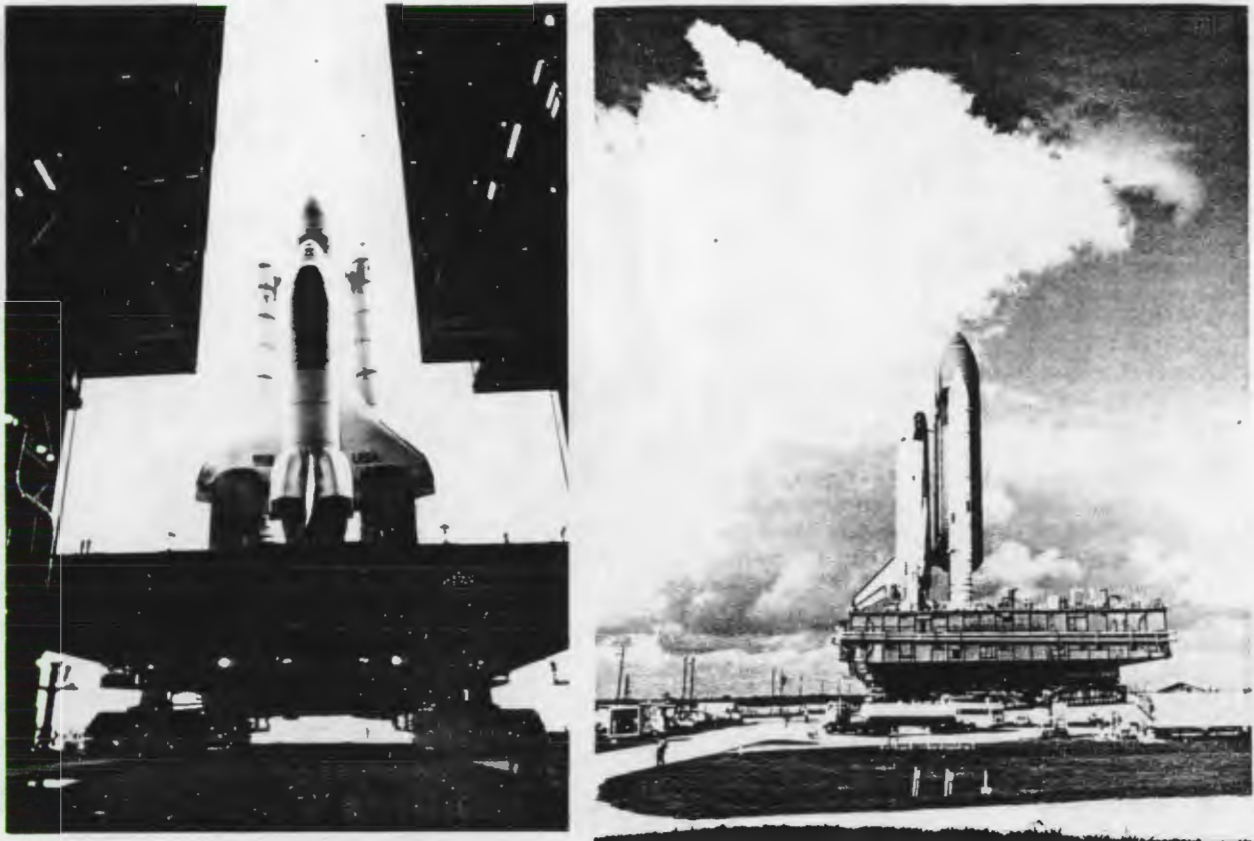


Figure 1.1-1
LAUNCH VEHICLE ON CRAWLER

Following flight readiness and checkout, the Space Shuttle Orbiter, attached to the External Tank (ET), is launched by means of two Solid Rocket Boosters (SRB) and the Space Shuttle Main Engines (SSME). Figure 1.1-2 shows the Space Shuttle Vehicle (SSV) being prepared for launch.

ORIGINAL PAGE IS
OF POOR QUALITY



Figure 1.1-2
EASTERN TEST RANGE LAUNCH PREPARATION

NASA Photo

The initial Launch of the Space Shuttle Vehicle, STS-1, is shown in the photograph at right. Launch of the STS-1 Vehicle, COLUMBIA, occurred on 12 April 1981 and was the first of several flights designed to verify the aerodynamic data base presented in this report.



ORIGINAL PAGE IS
OF POOR QUALITY

12 APRIL 1981

The launch is accomplished in two stages: the first stage terminating with SRB separation and the second stage terminating with Orbiter separation from the ET. The separation profile is illustrated in Figure 1.1-3. Mission abort capability is provided all along the launch trajectory with two options as indicated on the figure: Abort-Once-Around (AOA) and Return-To-Launch-Site (RTL).

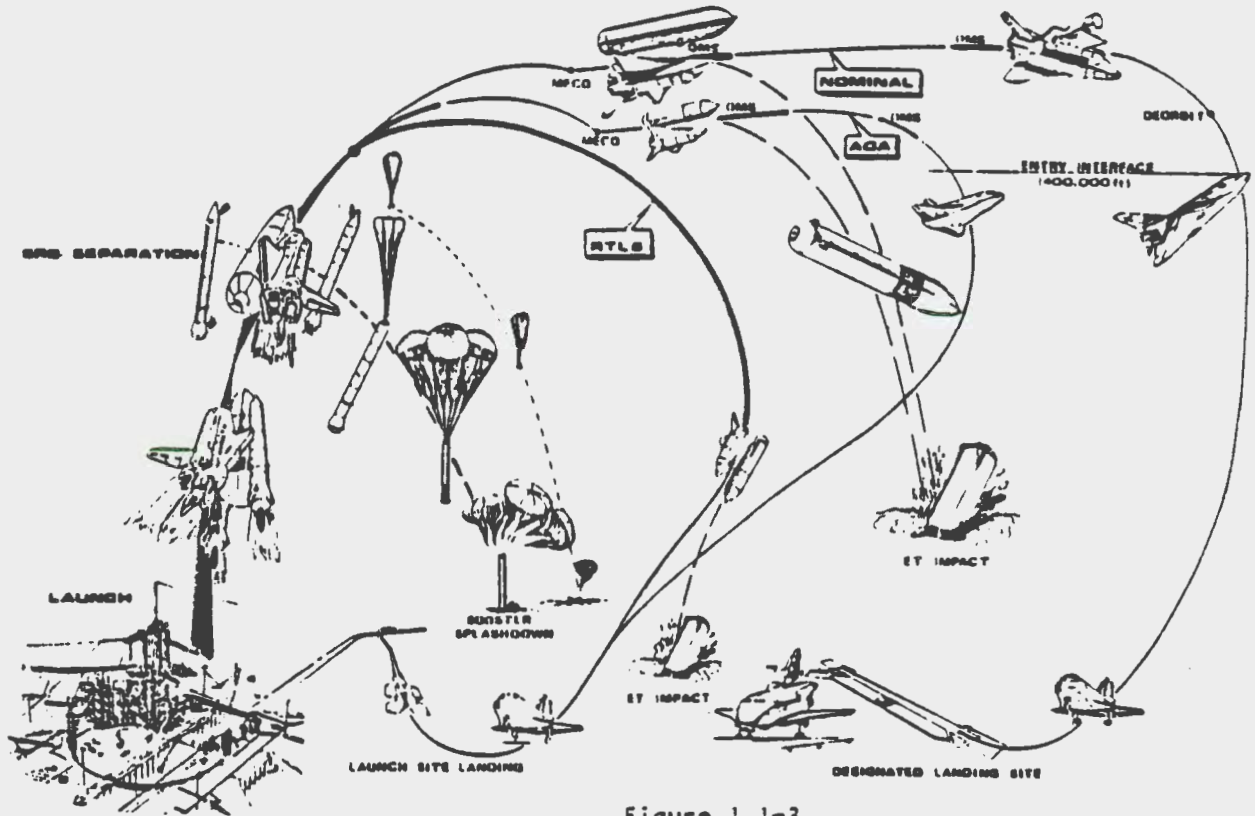


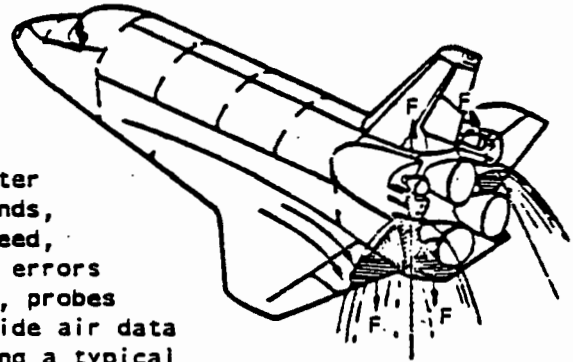
Figure 1.1-3
SEPARATION PROFILE

Subsequent to nominal separation from the ET, the Orbiter Vehicle will be inserted into Earth orbit where a payload may be deployed and/or retrieved. The Orbiter Vehicle can also function as a Space Laboratory for a moderate duration and will provide accommodations for up to five mission specialists in addition to the normal crew of commander and co-pilot. An on-orbit stay period of seven days is required and could be extended for up to thirty days during the operational phase of the program.

After completion of the orbital operations phase, deorbit is accomplished by retro-fire of the Orbital Maneuvering System (OMS) and the Orbiter Vehicle descends to the atmospheric entry interface (nominally, an altitude of 400,000 feet). The initial entry phase extends to a dynamic pressure level of 20 psf (approximately 250,000 feet) during which RCS attitude control from two aft OMS pods is blended with aerodynamic surface controls, the latter gaining in effectiveness with increasing dynamic pressure.



The entry flight phase from a dynamic pressure level of 20 psf to a Mach number of less than five, is accomplished at a high angle of attack during which the blanketing effect of the wing essentially precludes any rudder control. Coordinated lateral-directional control is provided by combined yaw RCS and aileron control. The terminal phase occurs as angle of attack is reduced below 18-degrees. As the Orbiter descends to altitudes where winds, in conjunction with vehicle speed, can result in relatively large errors in inertially derived air data, probes are extended ($M \approx 3.5$) to provide air data relative to the vehicle. During a typical normal entry, range control is achieved by bank angle while angle of attack follows a predetermined schedule to achieve (at approximately $M = 1.5$) an angle somewhat smaller than that corresponding to a maximum lift-to-drag ratio. A down-range capability of up to 4300 nautical miles with a cross-range capability of 980 nautical miles may be realized.



Equilibrium, subsonic, gliding flight is attained at an altitude of approximately 40,000 feet. Range control during the gliding descent is obtained by angle of attack modulation with velocity control maintained by the speedbrake. The approach and landing interface occurs at 10,000 feet above ground level and a pre-flare is initiated at an appropriate altitude, followed by a deceleration float and touchdown. The initial approach target and flare altitude are scheduled to provide a minimum of 25 seconds between flare initiation and touchdown.

Representative time histories of six entry trajectory parameters are given in Figure 1.1-4. This trajectory is the TPS Design Entry Trajectory (14414.1) and represents a high cross-range return from a 100 nautical mile orbit with a 25,000 pound payload and an aft center of gravity.

1.1-5

STS85-0118-1

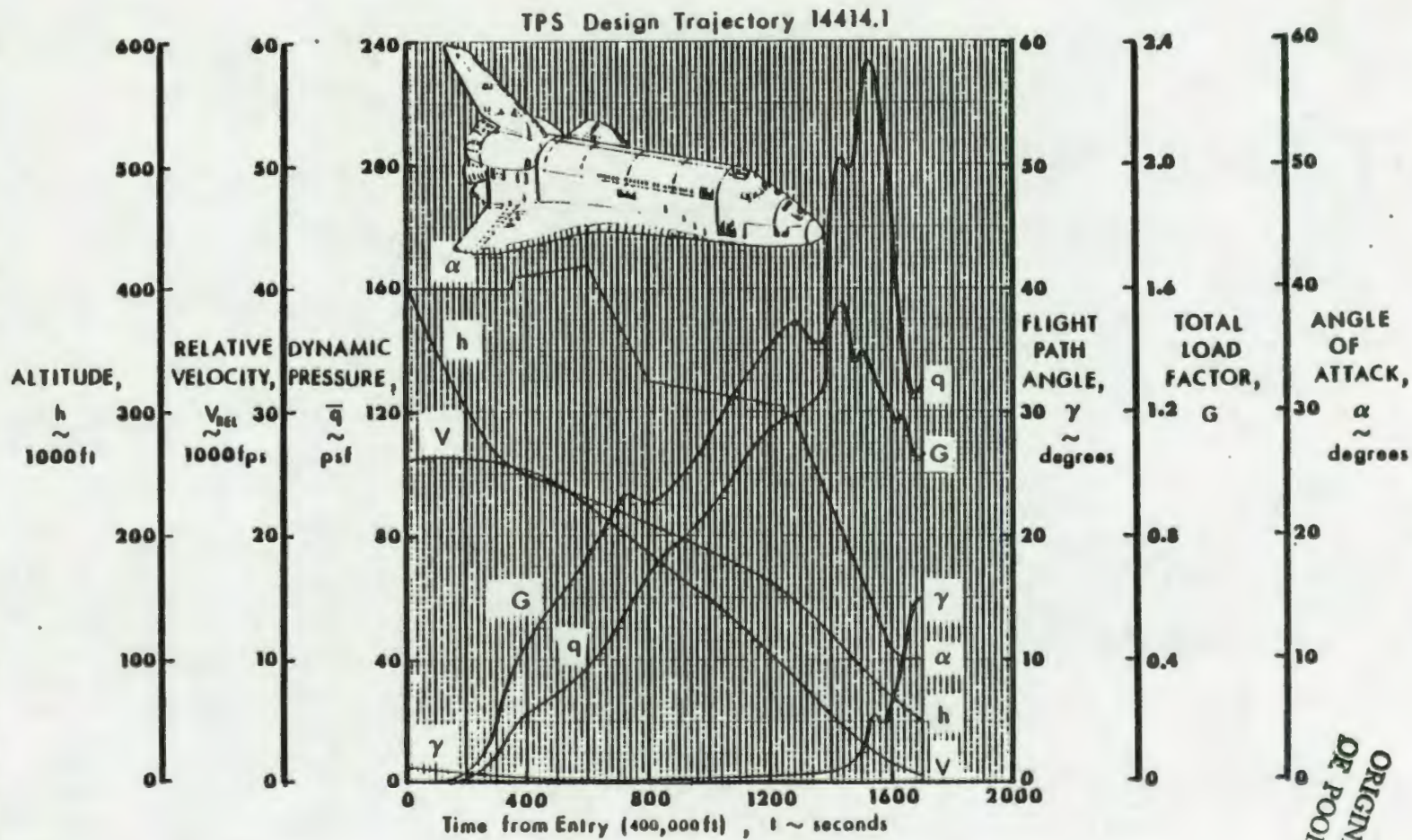
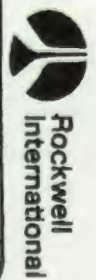


Figure 1.1-4
ORBITER ENTRY TRAJECTORY

ORIGINAL PAGE IS
OF POOR QUALITY

Space Transportation
Systems Division



1.2 MISSION CAPABILITY. The Space Shuttle "Mission Capability Envelope" is defined by four baseline reference missions. Table 1.2-1 summarizes these baseline missions. From the standpoint of launch, the Mission 3A ascent trajectory has been provided for information only. Descriptions of the other reference missions for the Space Shuttle should be obtained from the Flight Performance Data Book, Volume 1, Ascent (Reference 1-1).



Table 1.2-1
BASELINE REFERENCE MISSIONS

| BRM | OBJECTIVE | ORBIT | | DURATION | PAYLOAD | |
|-----|---|-------------|----------|----------|------------------------|---------|
| | | INCLINATION | ALTITUDE | | ASCENT | DESCENT |
| | | degrees | NAM | | 10 ³ pounds | |
| ① | PAYLOAD DELIVERY | 28.5 | 150 | 7 Days | 65.0 | 32.0 |
| ② | COMBINED REVISIT TO ORBITING ELEMENT & SPACELAB | 55.0 | 270 | 7 Days | — | — |
| ③ | A: PAYLOAD DELIVERY | 104.0 | 100 | 1 Rev | 32.0 | 2.5 |
| | B: PAYLOAD RETRIEVAL | | | | 2.5 | 25.0 |
| ④ | DELIVERY AND RETRIEVAL | 98.0 | 150 | 7 Days | 32.0 | 22.5 |

Mission 3A, which sizes the Solid Rocket Booster and External Tank

propellant capacities, is comprised of a southerly launch from the Western Test Range with a 32,000-pound payload to a 50 by 100 nautical mile orbit at an inclination of 104 degrees. Time histories of dynamic pressure, altitude, Mach number, and freestream pressure are presented in Table 1.2-2 and on Figure 1.2-1 from lift-off to Main Engine Cut-Off (MECO). These time histories are based on a reference December launch. Trajectory data include the separate AOA and RTLS data (denoted by dashed lines on the figure).

From the standpoint of entry, these baseline reference missions become essentially two types - a ramped angle of attack, characterized by long down-range and high cross-range and a high angle of attack, characterized by short down-range and low cross-range. Typical entry trajectories representing these two mission types are presented in Figure 1.2-2 (typical of Mission 1) and Figure 1.2-3 for the latter (typical of Mission 3B).

More complete and detailed mission data are available in the Mission Data Book, Reference 1-2. References 1-3 and 1-4 contain detailed information relative to separation and abort.

ORIGINAL PAGE IS
OF POOR QUALITY

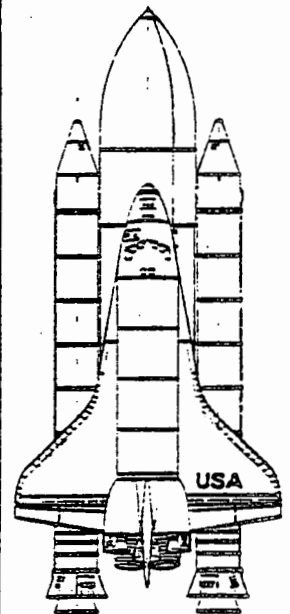
Table 1.2-2
MISSION 3A ASCENT TRAJECTORY
-DECEMBER LAUNCH-

| EVENT | TIME | MACH | \bar{q}_{∞} | P_{∞} | ALTITUDE |
|-------|-------|------|--------------------|--------------|----------|
| | sec | No | psf | psf | feet |
| (1) | 0.0 | 0.00 | 0.0 | 2088.87 | 519.1 |
| (2) | 0.3 | 0.00 | 0.0 | 2088.87 | 519.1 |
| | 2.0 | 0.02 | 1.0 | 2087.41 | 535.8 |
| | 3.5 | 0.04 | 2.0 | 2083.80 | 583.8 |
| | 4.0 | 0.05 | 3.0 | 2022.04 | 607.1 |
| | 4.4 | 0.05 | 4.0 | 2080.41 | 628.7 |
| (3) | 6.0 | 0.08 | 9.0 | 2071.93 | 741.8 |
| | 8.0 | 0.11 | 17.0 | 2055.58 | 947.4 |
| | 10.0 | 0.14 | 30.0 | 2035.78 | 1228.6 |
| | 12.0 | 0.18 | 48.0 | 2009.34 | 1589.3 |
| | 14.0 | 0.22 | 87.0 | 1977.29 | 2033.0 |
| (4) | 18.0 | 0.28 | 92.0 | 1939.83 | 2583.0 |
| | 18.0 | 0.30 | 121.0 | 1880.48 | 3182.0 |
| | 20.0 | 0.35 | 156.0 | 1848.00 | 3893.2 |
| | 22.0 | 0.39 | 195.0 | 1794.41 | 4899.3 |
| | 24.0 | 0.44 | 230.0 | 1738.19 | 5800.1 |
| | 26.0 | 0.48 | 275.0 | 1674.28 | 6588.3 |
| | 28.0 | 0.53 | 314.0 | 1609.44 | 7658.4 |
| | 30.0 | 0.57 | 353.0 | 1542.29 | 8807.1 |
| | 32.0 | 0.62 | 391.0 | 1473.30 | 10031.7 |
| | 34.0 | 0.68 | 427.0 | 1403.15 | 11330.3 |
| | 36.0 | 0.70 | 462.0 | 1332.10 | 12700.9 |
| | 38.0 | 0.75 | 495.0 | 1280.61 | 14142.0 |
| | 40.0 | 0.80 | 526.0 | 1188.08 | 15652.1 |
| | 42.0 | 0.84 | 554.0 | 1117.84 | 17229.9 |
| | 44.0 | 0.89 | 579.0 | 1047.27 | 18873.7 |
| | 46.0 | 0.94 | 600.0 | 977.69 | 20581.7 |
| | 48.0 | 0.98 | 618.0 | 909.44 | 22351.8 |
| | 50.0 | 1.04 | 633.0 | 843.08 | 24175.4 |
| | 52.0 | 1.09 | 642.0 | 778.13 | 26070.5 |
| | 54.0 | 1.13 | 645.0 | 715.88 | 28007.7 |
| | 56.0 | 1.19 | 648.0 | 650.27 | 29981.4 |
| | 58.0 | 1.24 | 649.0 | 599.42 | 32022.6 |
| | 60.0 | 1.30 | 650.0 | 545.14 | 34103.6 |
| (5) | 62.0 | 1.37 | 649.0 | 483.54 | 36238.7 |
| | 63.4 | 1.42 | 650.0 | 458.57 | 37799.2 |
| | 64.0 | 1.44 | 650.0 | 444.86 | 38440.5 |
| | 66.0 | 1.52 | 649.0 | 398.98 | 40721.4 |
| | 68.0 | 1.61 | 644.0 | 355.97 | 43007.1 |
| | 70.0 | 1.70 | 635.0 | 315.89 | 45541.8 |
| | 72.0 | 1.79 | 624.0 | 278.8 | 48089.0 |
| | 74.0 | 1.89 | 609.0 | 244.75 | 50731.0 |
| | 76.0 | 1.99 | 591.0 | 213.73 | 53469.3 |
| | 78.0 | 2.09 | 587.0 | 185.72 | 56304.9 |
| | 80.0 | 2.19 | 537.0 | 160.47 | 59239.2 |
| | 82.0 | 2.29 | 509.0 | 138.59 | 62273.0 |
| | 84.0 | 2.39 | 478.0 | 119.01 | 65406.0 |
| | 86.0 | 2.50 | 443.0 | 101.72 | 68635.3 |
| | 88.0 | 2.60 | 410.0 | 86.64 | 71957.7 |
| | 90.0 | 2.71 | 378.0 | 73.62 | 75370.3 |
| | 92.0 | 2.82 | 347.0 | 62.43 | 78871.1 |
| | 94.0 | 2.93 | 319.0 | 52.68 | 82458.0 |
| | 96.0 | 3.05 | 291.0 | 44.65 | 86128.4 |
| | 98.0 | 3.17 | 265.0 | 37.57 | 89879.6 |
| | 100.0 | 3.29 | 239.0 | 31.51 | 93709.6 |

| EVENT | TIME | MACH | \bar{q}_{∞} | P_{∞} | ALTITUDE |
|-------------|-------|--------|--------------------|--------------|----------|
| | sec | No | psf | psf | feet |
| | 102.0 | 3.40 | 214.0 | 28.43 | 97815.9 |
| | 104.0 | 3.52 | 192.0 | 22.14 | 101995.9 |
| | 106.0 | 3.63 | 171.0 | 18.51 | 105846.9 |
| | 108.0 | 3.75 | 152.0 | 15.48 | 109788.4 |
| | 110.0 | 3.87 | 135.0 | 12.91 | 113951.7 |
| | 112.0 | 3.98 | 119.0 | 10.77 | 118199.6 |
| | 114.0 | 4.09 | 105.0 | 8.98 | 122506.6 |
| | 116.0 | 4.19 | 92.0 | 7.51 | 126865.7 |
| | 118.0 | 4.26 | 80.0 | 6.28 | 131258.7 |
| | 120.0 | 4.30 | 68.0 | 5.26 | 135858.5 |
| | 122.0 | 4.33 | 58.0 | 4.42 | 140042.7 |
| | 124.0 | 4.35 | 48.0 | 3.73 | 144393.7 |
| | 126.0 | 4.35 | 42.0 | 3.16 | 148899.4 |
| (6) | 127.2 | 4.354 | 38.0 | 2.86 | 151301.7 |
| | 128.0 | 4.352 | 36.0 | | 152954.9 |
| | 144.0 | 4.749 | 12.0 | | 185570.5 |
| | 160.0 | 5.390 | 5.0 | | 215704.2 |
| | 178.0 | 6.147 | 1.6 | | 243413.7 |
| | 192.0 | 7.130 | 0.6 | | 268759.6 |
| | 208.0 | 7.717 | 0.0 | | 291804.9 |
| | 224.0 | 8.012 | | | 312615.6 |
| | 240.0 | 8.286 | | | 331260.8 |
| | 256.0 | 8.489 | | | 347814.5 |
| (7) | 258.7 | 8.535 | | | 350449.4 |
| | 272.0 | 8.745 | | | 361761.6 |
| | 288.0 | 8.958 | | | 372141.6 |
| | 304.0 | 9.376 | | | 379153.5 |
| | 318.0 | 9.889 | | | 382730.1 |
| | 320.0 | 9.974 | | | 383061.2 |
| | 336.0 | 10.750 | | | 384179.8 |
| | 352.0 | 11.718 | | | 382882.0 |
| | 368.0 | 12.894 | | | 379814.4 |
| | 377.2 | 13.679 | | | 377040.2 |
| | 384.0 | 14.308 | | | 374917.9 |
| | 392.0 | 15.110 | | | 372235.5 |
| | 400.0 | 15.977 | | | 369455.2 |
| (8) | 404.0 | 16.438 | | | 368053.5 |
| | 408.0 | 16.904 | | | 366682.9 |
| | 416.0 | 17.859 | | | 364007.9 |
| | 424.0 | 18.829 | | | 361498.2 |
| | 432.0 | 19.707 | | | 359225.9 |
| | 440.0 | 20.545 | | | 357268.6 |
| | 448.0 | 21.388 | | | 355708.8 |
| | 456.0 | 22.186 | | | 354634.6 |
| | 464.0 | 22.930 | | | 354138.3 |
| | 472.0 | 23.647 | | | 354316.7 |
| | 478.3 | 24.187 | | | 354992.2 |
| | 479.9 | 24.282 | | | 355258.2 |
| | 480.0 | 24.286 | | | 355289.7 |
| (9) | 485.9 | 24.607 | | | 356436.2 |
| END NOMINAL | | | | | |

Table 1.2-2 (cont)
MISSION 3A ASCENT TRAJECTORY
-DECEMBER LAUNCH-

| BEGIN RTLS | | | | BEGIN AOA | | | | | |
|------------|-------|----------|----------|-----------|----------|----------|----------|----------|----------|
| EVENT | TIME | MACH | ALTITUDE | EVENT | TIME | MACH | ALTITUDE | | |
| | sec | No | feet | | sec | No | feet | | |
| (10) | 258.7 | 8.535 | 350449.4 | (17) | 258.7 | 8.535 | 350449.4 | | |
| | 260.0 | 8.484 | 351832.3 | (18) | 266.8 | 8.501 | 357728.7 | | |
| | 262.0 | 8.475 | 353499.4 | | 272.0 | 8.487 | 362142.2 | | |
| | 264.0 | 8.475 | 355371.8 | | 288.0 | 8.378 | 373949.8 | | |
| | (11) | 266.0 | 8.388 | 357266.8 | (19) | 297.0 | 8.364 | 379523.0 | |
| | | 268.8 | 8.357 | 357988.9 | | 304.0 | 8.418 | 383349.3 | |
| | | 270.3 | 8.177 | 361312.2 | (20) | 305.0 | 8.425 | 383683.4 | |
| | | 272.0 | 8.048 | 362905.1 | | 320.0 | 8.581 | 390452.7 | |
| | | 288.0 | 7.048 | 375108.3 | | 338.0 | 8.788 | 395381.4 | |
| | | 304.0 | 6.308 | 383009.8 | (21) | 350.8 | 9.018 | 398169.0 | |
| 320.0 | | 5.719 | 386799.6 | | | 352.0 | 9.039 | 398320.5 | |
| 336.0 | | 5.233 | 388898.3 | | | 380.0 | 9.221 | 399072.7 | |
| 352.0 | | 4.818 | 382981.2 | | | 388.0 | 9.442 | 399388.1 | |
| 368.0 | | 4.646 | 375883.4 | | | 378.0 | 9.701 | 399227.2 | |
| 384.0 | 4.108 | 365805.4 | | 384.0 | | 10.002 | 398672.3 | | |
| 400.0 | 3.888 | 353119.9 | | 392.0 | | 10.344 | 397728.6 | | |
| 418.0 | 3.208 | 338280.4 | | 400.0 | | 10.733 | 395414.8 | | |
| 432.0 | 2.853 | 321811.2 | | 408.0 | | 11.172 | 384782.8 | | |
| 448.0 | 2.039 | 304319.6 | | 418.0 | | 11.621 | 392798.1 | | |
| (12) | 464.0 | 1.445 | 288510.9 | | 424.0 | 12.053 | 390550.8 | | |
| | 480.0 | 1.220 | 269207.1 | | 432.0 | 12.519 | 389051.6 | | |
| | 481.6 | 1.235 | 267522.1 | | 440.0 | 13.021 | 385334.6 | | |
| | (13) | 489.6 | 1.397 | 259422.1 | | 448.0 | 13.582 | 382435.4 | |
| | | 498.0 | 1.632 | 253330.5 | | 456.0 | 14.143 | 379392.4 | |
| | | 512.0 | 2.430 | 239990.6 | | 464.0 | 14.768 | 376248.9 | |
| | | 528.0 | 3.384 | 230284.3 | | 472.0 | 15.433 | 373043.3 | |
| | | (14) | 533.8 | 3.779 | 228068.7 | | 480.0 | 16.143 | 369829.2 |
| | | | 536.0 | 3.932 | 227414.9 | | 488.0 | 16.895 | 360658.2 |
| | | | 544.0 | 4.507 | 228090.1 | | 496.0 | 17.691 | 363580.0 |
| (15) | | | 547.1 | 4.748 | 226035.7 | | 504.0 | 18.512 | 360681.1 |
| | | | 552.0 | 5.133 | 226905.3 | | 512.0 | 19.219 | 357984.7 |
| | | | (16) | 560.0 | 5.795 | 228758.7 | | 520.0 | 19.946 |
| | 562.5 | | | 6.013 | 229845.7 | | 528.0 | 20.888 | 353532.5 |
| | | | | | | | 538.0 | 21.441 | 351958.4 |
| | | | | | | | 544.0 | 22.198 | 350932.7 |
| | | | | | | (22) | 550.6 | 22.821 | 350563.1 |
| | | | | | | 552.0 | 22.947 | 350548.2 | |
| | | | | | | 560.0 | 23.658 | 350908.9 | |
| | | | | | | 564.2 | 24.008 | 351418.2 | |
| | | | | | 568.0 | 24.245 | 352068.0 | | |
| | | | | (23) | 569.2 | 24.290 | 352294.4 | | |
| | | | (23) | 575.0 | 24.472 | 353555.5 | | | |



| No | EVENT | No | EVENT |
|------|--|------|-------------------------------|
| (1) | SRB IGNITION COMMAND | (13) | BEGIN RCS BURN |
| (2) | LIFT-OFF (T/W = 1.0) | (14) | OMS AND RCS CUTOFF |
| (3) | END VERTICAL RISE, BEGIN PITCH PROGRAM | (15) | 3-G LIMIT |
| (4) | END PITCH PROGRAM | (16) | RTLS MECO - 15 sec OMS CUTOFF |
| (5) | MAXIMUM DYNAMIC PRESSURE | (17) | RTLS/AQA POINT |
| (6) | SRB JETTISON | (18) | BEGIN OMS DUMP |
| (7) | RTLS/AQA POINT | (19) | END OMS DUMP |
| (8) | NOMINAL MISSION 3-G LIMIT | (20) | BEGIN RCS BURN |
| (9) | NOMINAL MECO | (21) | OMS AND RCS CUTOFF |
| (10) | RTLS/AQA POINT, BEGIN OMS BURN | (22) | 3-G LIMIT |
| (11) | BEGIN OMS DUMP | (23) | AQA MECO |
| (12) | END OMS DUMP | | |

FOR INFORMATION ONLY

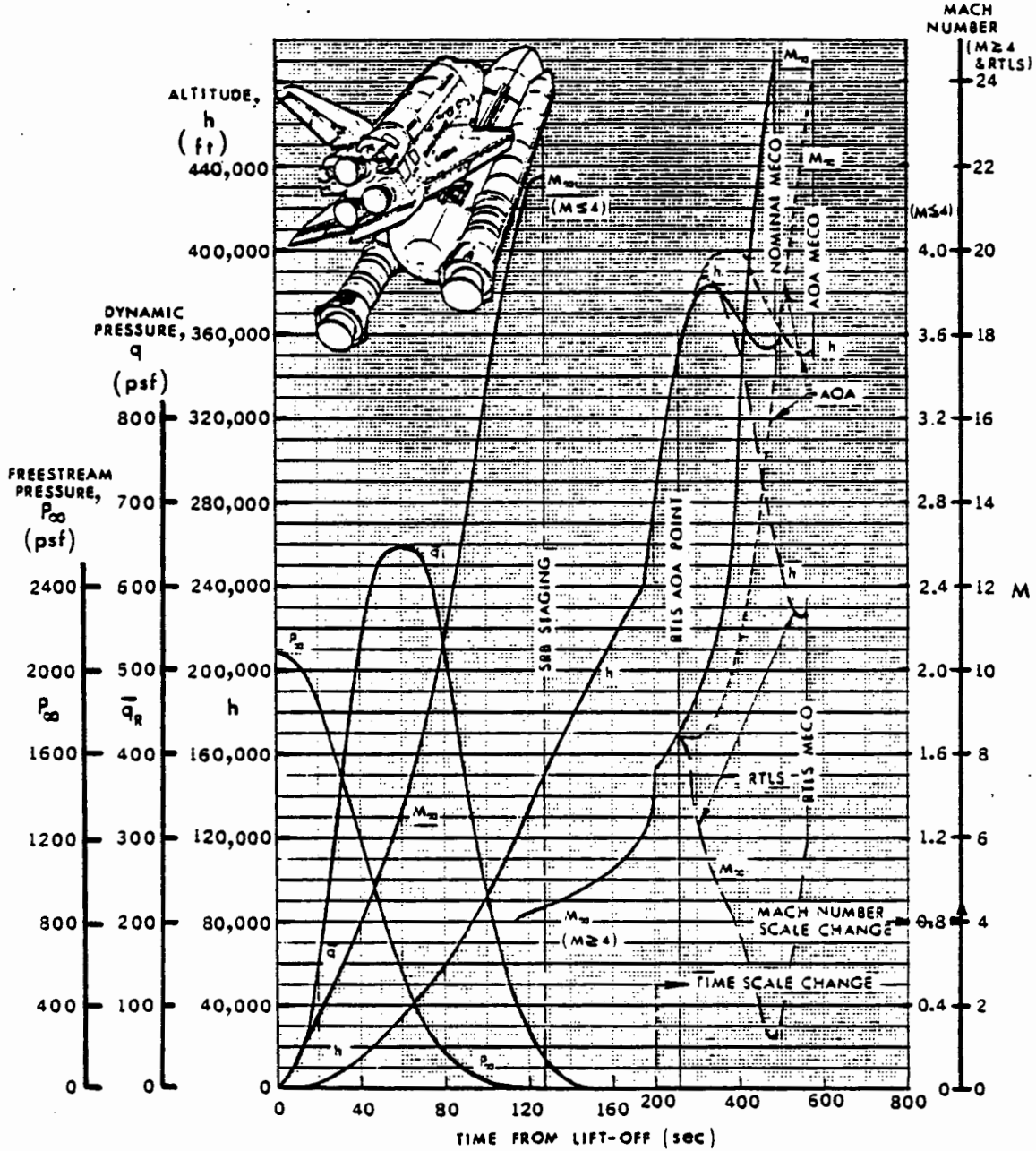
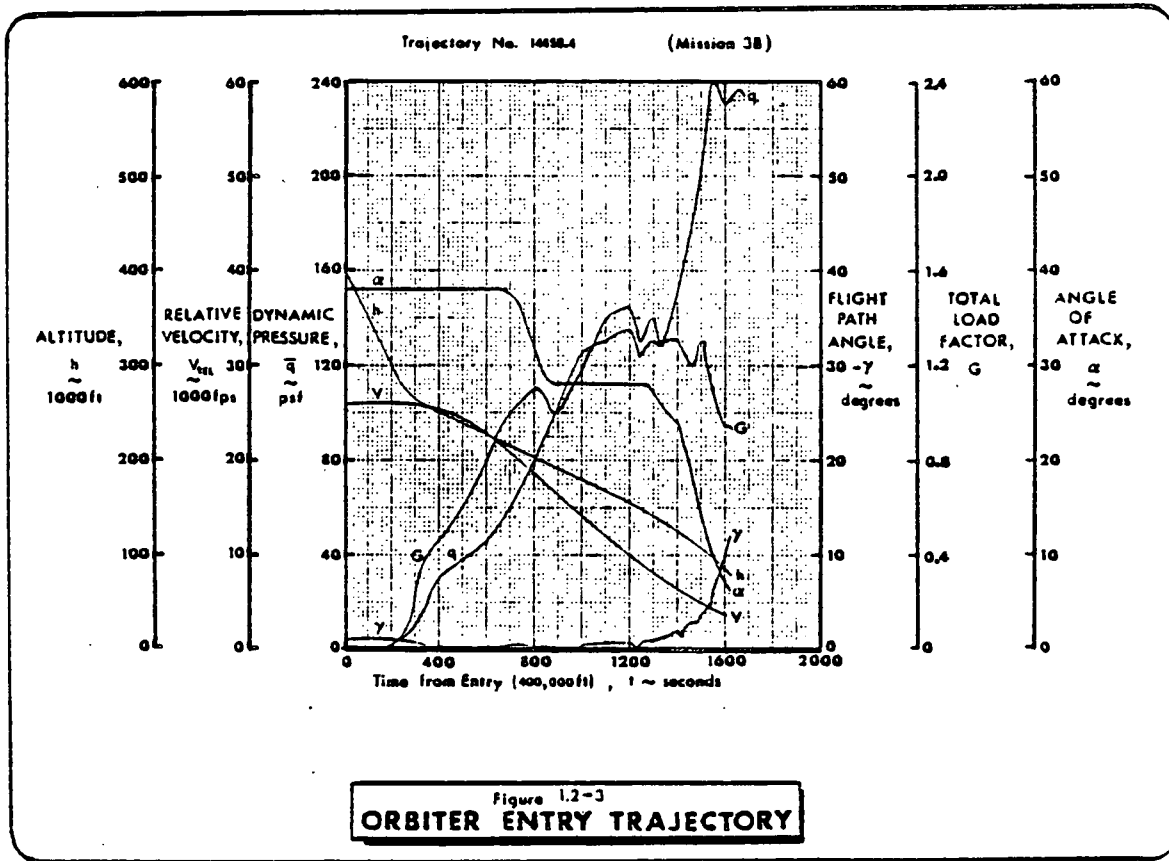
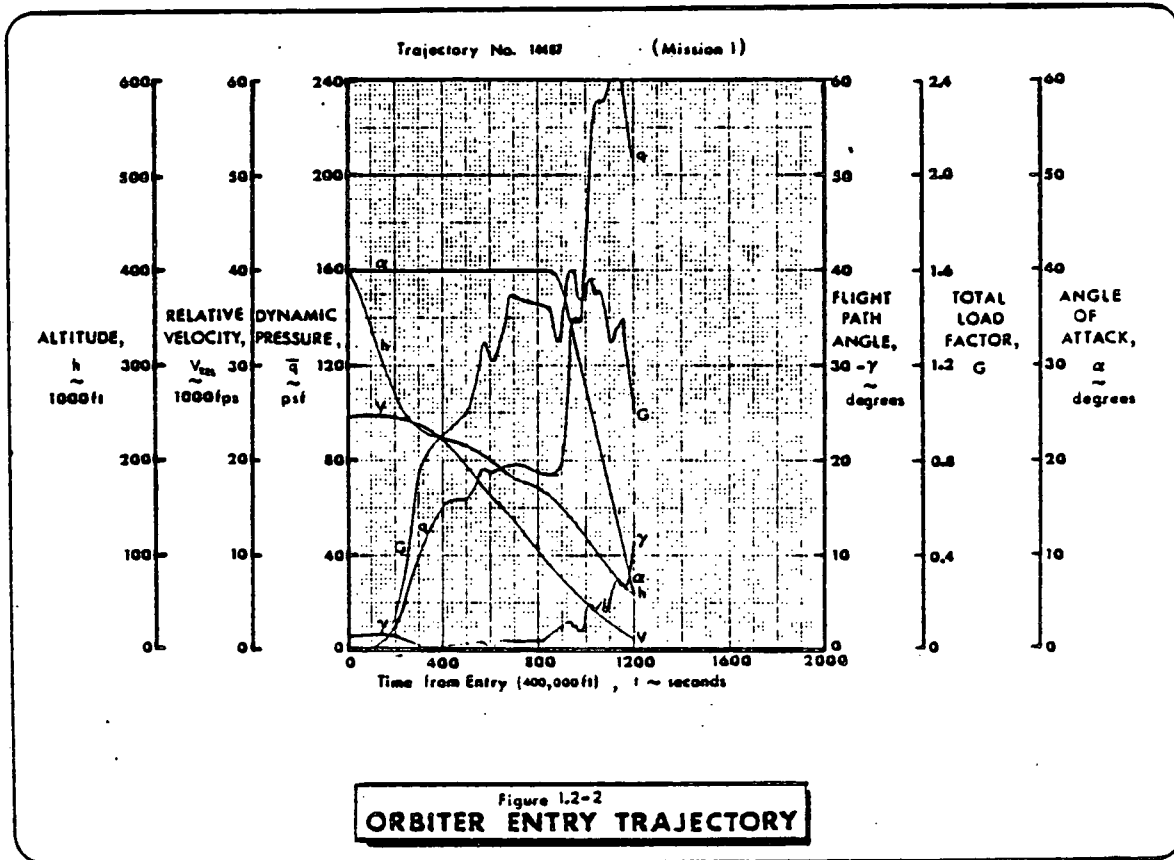


Figure 1.2-1
MISSION 3A TRAJECTORY PARAMETERS
-DECEMBER LAUNCH-

ORIGINAL PAGE IS
OF POOR QUALITY

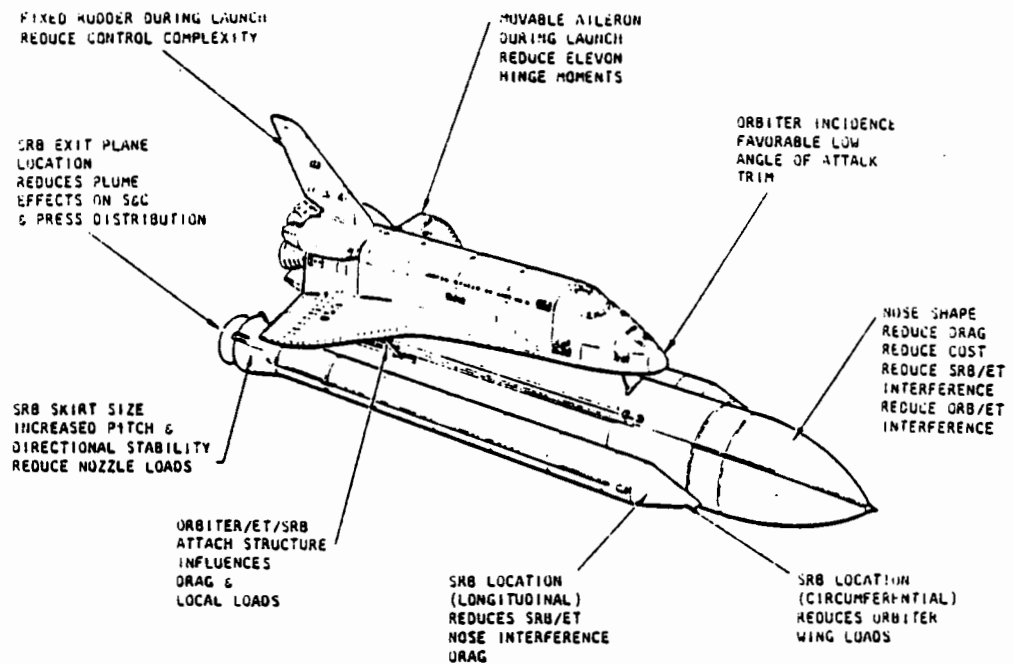


2.0 SPACE SHUTTLE VEHICLE EVOLUTION

2.0 SPACE SHUTTLE VEHICLE EVOLUTION

Evolution of the Space Shuttle Vehicle from Authority-To-Proceed (ATP) to the current operational configuration is provided in this section. The major program requirements influencing the aerodynamic design were delineated in the Space Shuttle Program Request For Proposal and subsequent directives from the NASA. The Space Shuttle Vehicle was designed to satisfy specific funding constraints and minimize technical risk. During the relatively brief launch phase of flight, the aerodynamic design is primarily related to performance and structural loads. During the entry flight phase, the aerodynamic design is primarily related to performance, stability, and control.

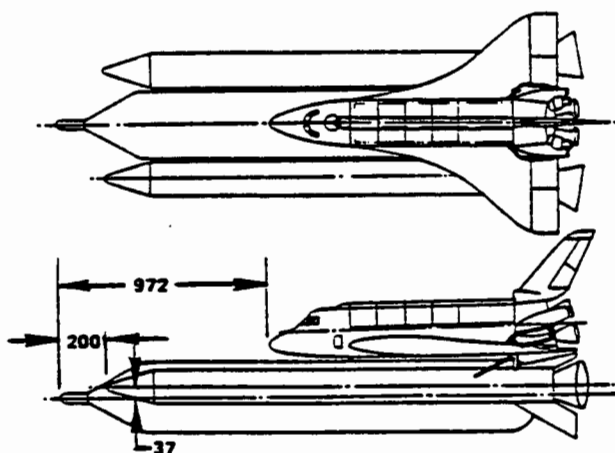
Aerodynamic design considerations for the ascent phase involved shaping to reduce drag and optimization of the element (Orbiter Vehicle, External Tank, and Solid Rocket Boosters) locations to reduce structural loading and weight. The External Tank nose shape evolved from trades of cost, drag, and reduced SRB/ET and ET/Orbiter interference. The Solid Rocket Boosters were located on the periphery of the External Tank to reduce Orbiter wing loads and, longitudinally, to decrease SRB/ET nose interference drag. The Solid Rocket Booster skirt was sized to reduce nozzle loads and increase pitch and directional stability. The rudder was fixed in the neutral position for launch to simplify control system design and the elevons incorporate a load relief system to reduce hinge moments at high dynamic pressures during launch. The SRB nozzle exit plane is located well aft to minimize the effect of plumes on stability, control, and airloads.



The Orbiter Vehicle evolved from detailed aerodynamic trade studies. The moderate fineness ratio-soft chine nose evolved from trade studies of hypersonic lift-to-drag ratio and wing-body matching to provide desirable stability characteristics. The wing evolved from trade studies of wing weight with aspect ratio, leading and trailing edge sweep, and taper ratio. Wing airfoil section and twist were optimized to provide high lift efficiency. The vertical tail was designed to provide directional stability and control at low angles of attack. The speedbrake (split rudder type) was designed to increase directional stability at hypersonic speeds and to modulate drag. The body flap was designed to shield the main engine nozzle from the high thermal environment during entry and to augment pitch trim. Full-span elevons provide good effectiveness in both pitch and roll control for minimum weight.

Aerodynamic design trade studies performed early in the Shuttle Vehicle development established the primary configuration details. Vertical tail trades included a centerline vertical, centerline vertical with ventrals, wing tip fins, and butterfly fins. The centerline vertical resulted in minimum weight for specified stability and handling qualities. Vertical tail airfoil trades indicated that a ten-degree wedge airfoil provided the required stability level at minimum weight. Location of the speedbrake on the vertical provided multiple use with flared rudder and represented the minimum weight approach. The tail scrape attitude was based on a compromise between reduced wing size/weight and increased landing gear length/weight. Nose camber, cross-section, and upward sloping forebody sides were selected to improve hypersonic pitch trim and directional stability and, in conjunction with wing/body blending, to reduce entry heating on the fuselage sides. Early baseline wing selection provided good maximum lift, good low to high speed aerodynamic balance, good low speed lift characteristics, reduced wing size, and minimized landing trim losses. The wing/body integration baseline selection provided a good allowable payload envelope without major configuration impact, met the cross-range requirement, and allowed high angle of attack.

- 2.1 AUTHORITY TO PROCEED (ATP). The Space Shuttle Vehicle concept at ATP in August of 1972 was based on pre-contract studies and configured to meet initial Shuttle Program requirements. This configuration was specified in MCR 001. The ATP configuration is shown in the sketch based on control drawing VL 72-000001 (Launch Vehicle). The overall length of the ATP vehicle was 208.7 feet.

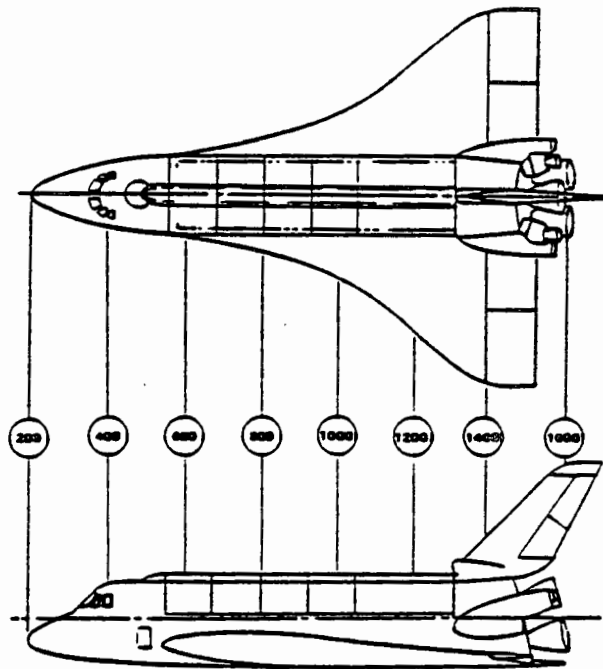


The ATP Solid Rocket Boosters (control drawing VL 77-000001) had an overall length of 184.75 feet and a diameter of 13 feet. The

SRB nose radius was 13 inches and the cone semi-vertex angle was 18 degrees. The SRB nose was located 200 inches aft of the ET nose and 37 inches above the ET centerline. The SRB's were mounted parallel to the ET. The nozzles had a large cant (11 degrees outboard in the yaw plane) such that the thrust vector would be through the approximate vehicle center of gravity during launch. There were no provisions for Thrust Vector Control (TVC).

The ATP External Tank (control drawing VL 78-000001) was essentially a cone-cylinder arrangement fitted with a retro Solid Rocket Motor (SRM) at the tank nose to facilitate External Tank de-orbit. The conical nose portion of the ET had a semi-vertex angle of 30 degrees and blended smoothly into the cylindrical section. The shoulder blending radius at the cone-cylinder juncture was identical to the cylinder radius of 13.25 feet (26.5 ft. dia.). Overall length of the ET was 182 feet. The external shape of the retro SRM was a small hemisphere-cylinder with a nose radius of 20.5 inches and a length of 124 inches.

The ATP Orbiter Vehicle (Control drawing VL 70-000001) was located piggy-back on the ET with the Orbiter nose 972 inches aft of the ET

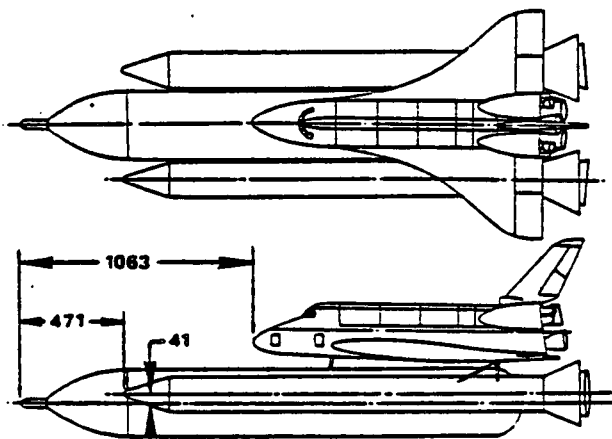


nose mounted at an incidence angle of -1.2 degrees. The Orbiter had a 50-degree blended delta wing planform. Dry weight was 170,000 pounds and the landing weight was 215,115 pounds with a payload weight of 40,000 pounds. The center of gravity range was 65% to 68% of body length. The wing span was 84 feet and wing area was 3220 ft². Minimum design touchdown speed was 150 knots at an angle of attack of 18-degrees. The performance of this configuration was intensively evaluated in studies conducted between ATP and the Preliminary Requirements Review.

VL 70-000001
ATP

2.2

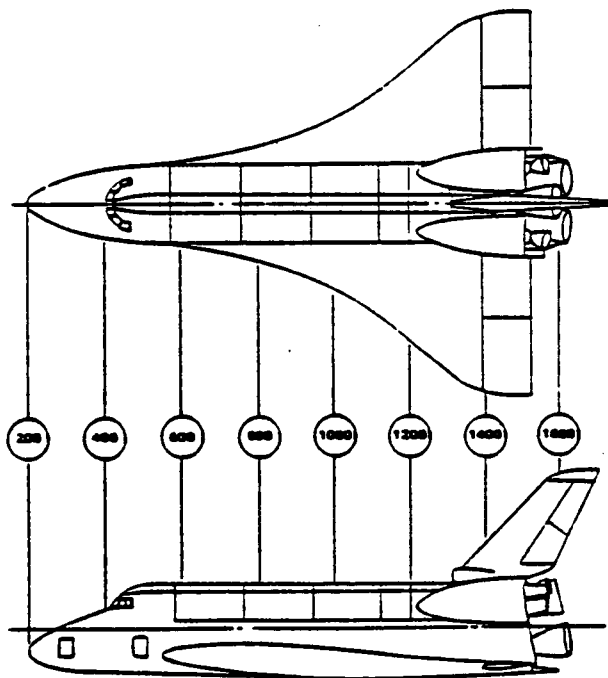
PRELIMINARY REQUIREMENTS REVIEW (PRR). The Space Shuttle baseline configuration at the PRR in November of 1972 had evolved into that shown in the sketch. This configuration was specified in MCR 0026. The PRR sketch is based on control drawings VL 72-000030 (Launch Vehicle) and VL 70-000040 (Orbiter Vehicle). The overall length of the PRR vehicle was 214.33 feet.



The PRR Solid Rocket Boosters (control drawing VL 77-000006) had an overall length of 175.083 feet and a diameter of 13.5 feet. The nose radius was 13 inches and the cone

semi-vertex angle was 18 degrees. The SRB nose was located 471 inches aft of the ET nose and 41 inches above the ET centerline. The SRB's were mounted parallel to the ET. The nozzles were canted outboard 3.5 degrees in the yaw plane with a gimbal range of 15 degrees for Thrust Vector Control.

The PRR External Tank (Control drawing VL 78-000011) was an ogive-cylinder arrangement fitted with a retro SRM at the nose of the same dimensions as the ATP retro package. The ogive nose portion of the tank had a radius of 567.8 inches and blended smoothly into the cylindrical section which had a diameter of 304 inches. Overall length of the ET was 2278 inches (189.33 feet).



VL70-000040

The PRR Orbiter Vehicle (control drawing VL 70-000040) was attached piggy-back to the External Tank with the Orbiter nose 1063 inches aft of the ET nose mounted at an incidence angle of +0.5 degree. The abort Solid Rocket Motors (ASRM) were removed and the Orbital Maneuvering System (OMS) pods were relocated to the fuselage shoulder.

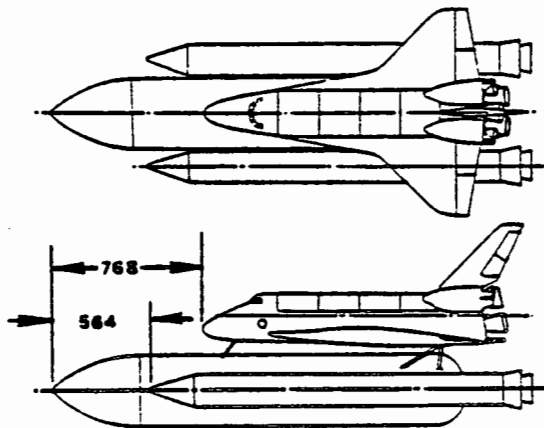
The Orbiter had a 50 degree blended delta wing planform. Dry weight was 170,000 pounds and the landing weight was 215,115 pounds with a payload weight of 40,000 pounds. The center of gravity range was 65 to 68 percent of the body length. The wing span was 84 feet and the wing area was 3220 ft². The landing weight and payload, minimum design touchdown speed and angle of attack were identical to the ATP configuration.

Continued trade studies of the PRR configuration indicated a need to re-size the Space Shuttle to a lighter weight configuration. These studies led to a reduction in Orbiter Vehicle weight from 180,000 pounds to 150,000 pounds and a reduction in the weight of the Launch Vehicle. Orbiter wing size was reduced from 3220 ft² to 2690 ft². Static stability limits changed from positive to negative and center of gravity travel was reduced from 3-percent to 2.5-percent of body length. The manipulator arm housing was removed and the landing speed and angle of attack were changed. All of these changes contributed to a lighter weight system between the PRR and Preliminary Design Requirements review.

2.3

PRELIMINARY DESIGN REQUIREMENTS (PDR). The Space Shuttle baseline configuration at the time of the PDR review in March of 1975 had

evolved into the light-weight configuration shown in the sketch. This configuration was specified in MCR 0074. The sketch is based on control drawings VL 72-000061 (Launch Vehicle) and VL 70-000089B (Orbiter Vehicle). The overall length of the PDR vehicle was 192.083 feet.



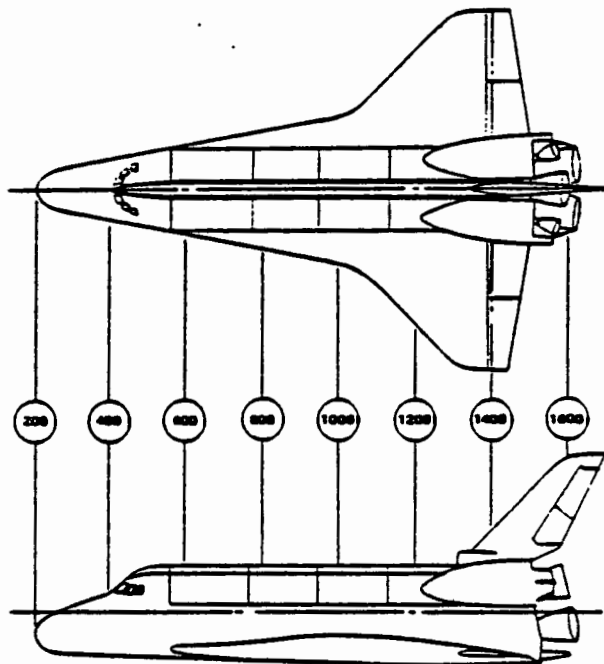
The PDR Solid Rocket Boosters (control drawing VL 77-000012A) had an overall length of 145.083 feet and a diameter of 142 inches.

The nose radius was 13 inches and the cone semi-vertex angle was 18 degrees. The SRB nose was located 564 inches aft of the ET nose and on the ET centerline. The SRB's were mounted parallel to the ET. The nozzles had a zero degree null position (pitch and yaw) with ± 5 degrees gimbal limits (pitch and yaw) for Thrust Vector Control.

The PDR External Tank (control drawing VL 78-000018) was basically an ogive-cylinder arrangement fitted with a retro SRM at the tank nose. The SRM had a nose radius of 20.5 inches and a length of 139 inches. The ogive nose portion of the tank had a planform radius of 605 inches and blended smoothly into the 324 inches diameter cylindrical section. Overall length of the ET was 1989 inches (165.75 feet).

The PDR Orbiter Vehicle (control drawing VL 74-000089B) was attached piggy-back to the External Tank with the Orbiter nose 768 inches aft

of the ET nose mounted at an incidence angle of ± 0.5 degree. Refinements in the aerodynamic configuration led to an increased



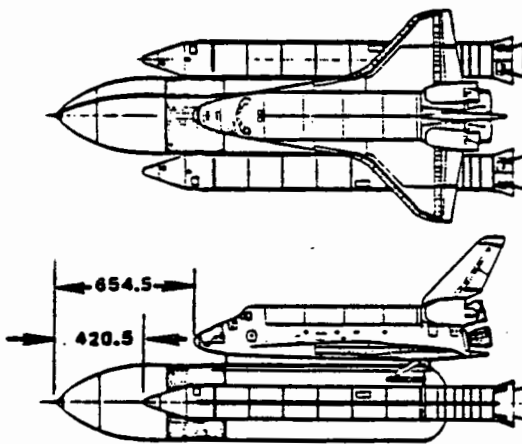
VL70-000089
PDR

nose radius and to a $45^\circ/79^\circ$ double delta wing planform incorporating a more efficient lifting surface than the 50 degree blended delta. Orbiter dry weight was reduced to 150,000 pounds. The landing weight was 179,800 pounds with a payload of 25,000 pounds. The center of gravity range was 65 to 67.5 percent of body length. The wing span was 78.1 feet and the wing area was 2690 ft². The vehicle had an overall length of 125 feet. The minimum design touchdown speed for this configuration was 165 knots at an angle of attack of 15 degrees.

Further trade studies refined the PDR base point design to the configuration for Critical Design Review conducted in October 1977.

2.4

CRITICAL DESIGN REVIEW (CDR). The Space Shuttle baseline configuration at the time of CDR in October 1977 had evolved into that shown in the sketch. This configuration was specified in MCR 3570. The sketch is based on control drawings VC 72-000002G (Launch Vehicle) and VC 70-000002B (Orbiter Vehicle). The overall length of the CDR vehicle was 184.17 feet.



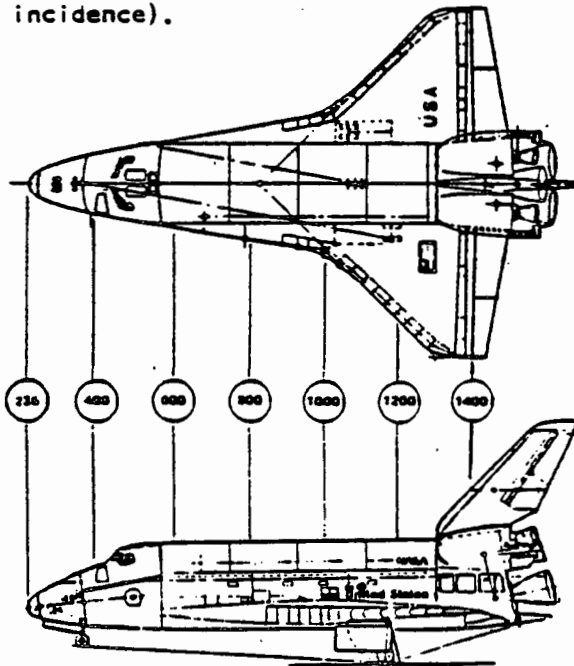
The CDR Solid Rocket Boosters (control drawing VC 77-000002J) had an overall length of 149.13 feet and a diameter of 146 inches. The nose radius was 13.28 inches and the cone semi-vertex angle was 18 degrees.

The SRB nose was located 420.5 inches aft of the ET nose along the ET centerline.

The SRB's were mounted parallel to the ET. The nozzles had a zero degree null position (pitch and yaw) with ± 5 degrees gimbals limits (pitch and yaw) for Thrust Vector Control.

The CDR External Tank (control drawing VC 78-000002G) was basically an ogive-cylinder arrangement. The ogive nose portion of the tank had a planform radius of 612 inches and blended smoothly into the 331 inch diameter cylindrical section. The retro SRM at the tank nose was replaced by the Ascent Air Data System (AADS) spike probe. The overall length of the ET was 1850.525 inches.

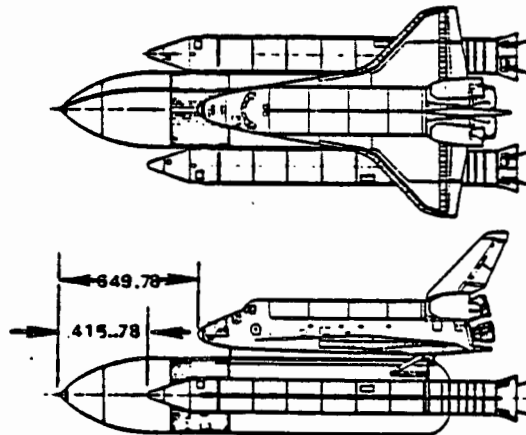
The CDR Orbiter Vehicle (control drawing VC 70-000002B) was attached piggy-back to the External Tank with the Orbiter nose 654.5 inches aft of the ET nose mounted parallel to the ET (zero degree incidence).



Aerodynamic refinements included decreased nose radius and a $45^\circ/81^\circ$ double-delta wing planform. The OMS pods had a blunt nose in place of the faired nose formerly used. The dry weight was 150,000 pounds. The landing weight was 187,900 pounds with a 32,000 pound payload. The center of gravity range was 65 to 67.5 percent of body length. The wing span was 78 feet and wing area was 2690 ft². The vehicle had an overall length of 122.3 feet. The minimum design touchdown speed for this configuration was 171 knots at 15 degrees angle of attack.

2.5

OPERATIONAL VEHICLES (OPS). The Operational Vehicles are characterized by the Interface Control Document (ICD) ICD-2-00001 Revision F dated January 31, 1980. The overall length of the OPS Vehicles is 183.77 feet.

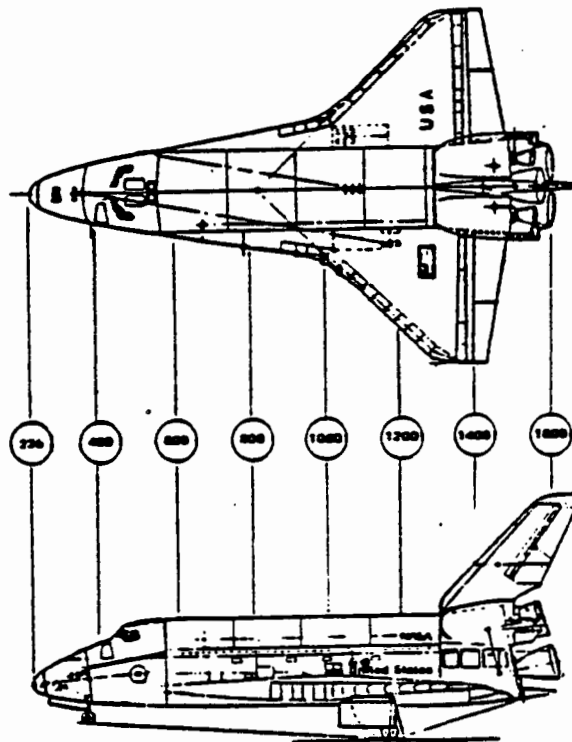


The OPS Solid Rocket Boosters (steelcase SRB's) have an overall length of 149.13 feet and a diameter of 146 inches. The nose radius is 13.27 inches and the nose, as well as the aft frustum semi-vertex angles, are both 18 degrees. The SRB nose is located 415.78 inches aft of the ET nose parallel to the ET centerline. The distance between ET and SRB

centerlines is 250.5 inches in the ET waterplane 400. The nozzles have a zero degree null position (pitch and yaw) with 5 degree gimbal limits (pitch and yaw) for Thrust Vector Control.

The OPS External Tank (lightweight ET) is basically an ogive-cylinder-ellipsoidal base configuration. The ogive nose has a planform radius of 612 inches which blends smoothly into the 331 inch diameter cylindrical section. The Ascent Air Data System (AADS) spike probe has been replaced by a non-functional probe having the same OML. Simplification of the protuberances by redesign, relocation, and/or elimination distinguishes the lightweight ET from the CDR ET. The overall length of the ET is 1845.805 inches.

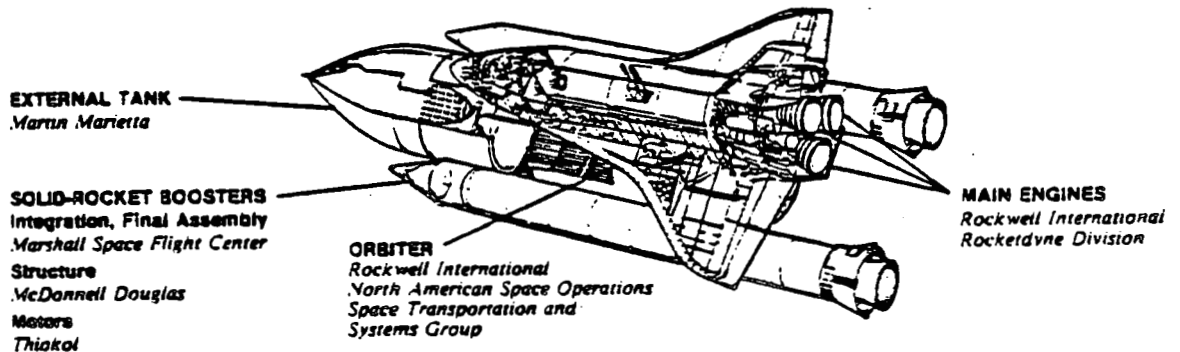
The OPS Orbiter Vehicle is attached piggy-back to the External Tank with the Orbiter nose 649.78 inches aft of the ET nose mounted parallel to the ET (zero degree incidence). The Orbiter Vehicle remains essentially unchanged from the CDR configuration.



3.0 CONFIGURATION AND SYSTEMS DESCRIPTIONS

3.0 CONFIGURATION AND SYSTEMS DESCRIPTIONS.

The Space Shuttle Vehicle configuration is comprised of essentially three elements; (1) the Orbiter Vehicle (OV) mounted on top of, (2) a non-recoverable LOX-Hydrogen External fuel Tank (ET) to which are also attached, (3) two Solid Rocket Boosters (SRB) which are recoverable for refurbishing and reuse on subsequent missions. Rockwell International is the NASA prime contractor for the development and building of the Space Shuttle Orbiter and Main Engines (SSME) and for the integration of the entire system.



Design of the integrated Launch Vehicle is such that it meets all requirements established in the Contract End Item Specification, Volume 10 [Reference 3-1]. The design is based on satisfying the prescribed boost criteria consisting of; (1) nominal SRB staging, (2) ET separation, and (3) Abort-Once-Around (AOA) capability at the time Return-To-Launch-Site (RTLS) capability is lost. The design angle of attack and sideslip envelopes are shown in Figure 3.0-1.

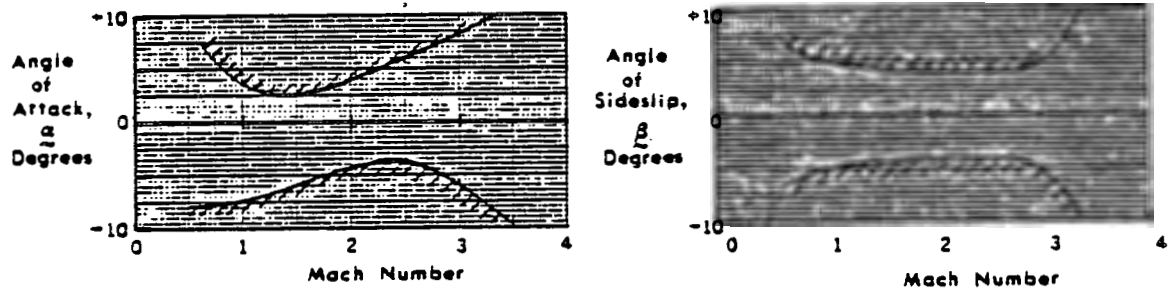


Figure 3.0-1
LAUNCH VEHICLE ENVELOPES

The Rockwell Space Shuttle Orbiter Vehicle has been designed to function as both spacecraft and aircraft and must, therefore, provide the protection and versatility necessary for both space and atmospheric flight operations. The Orbiter Vehicle meets all requirements set forth in the Orbiter Vehicle End Item Specification [Reference 3-2]. Atmospheric (or aerodynamic) requirements are predicated, for the most part, on the entry flight phase of the Orbiter mission(s) [cf. Section 1.0]. The aerodynamic lines ensure acceptable performance over hypersonic, supersonic, transonic, and

subsonic speed regimes while providing the specified down-range and cross-range capabilities and meeting the specified landing requirements shown in Figure 3.0-2.

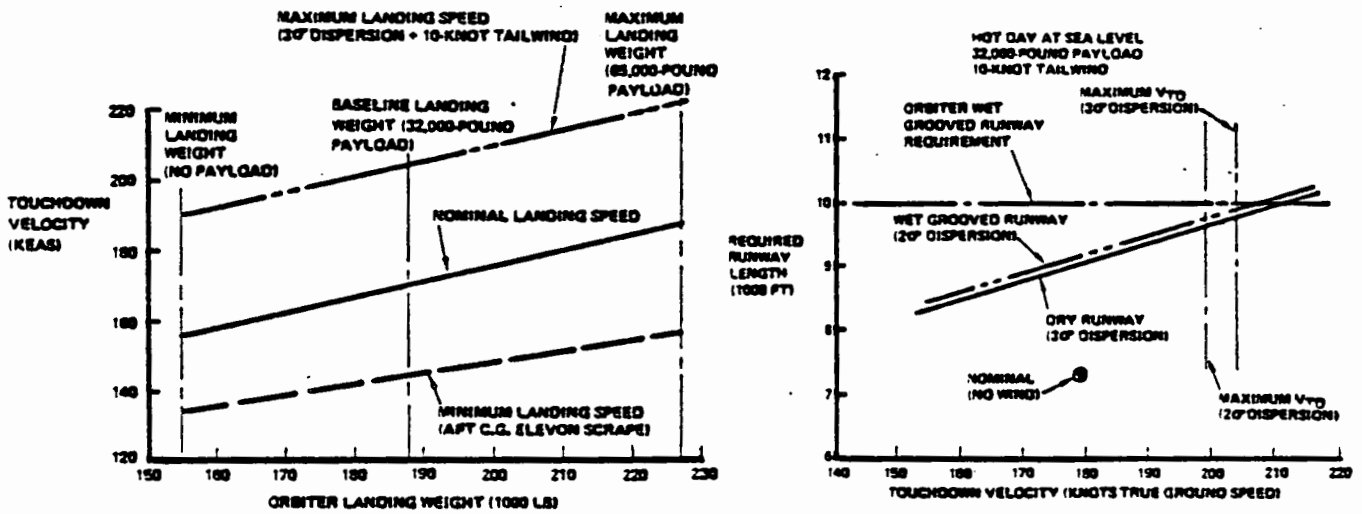


Figure 3.0-2
LANDING REQUIREMENTS

The design data angle of attack and sideslip envelopes are shown in Figure 3.0-3.

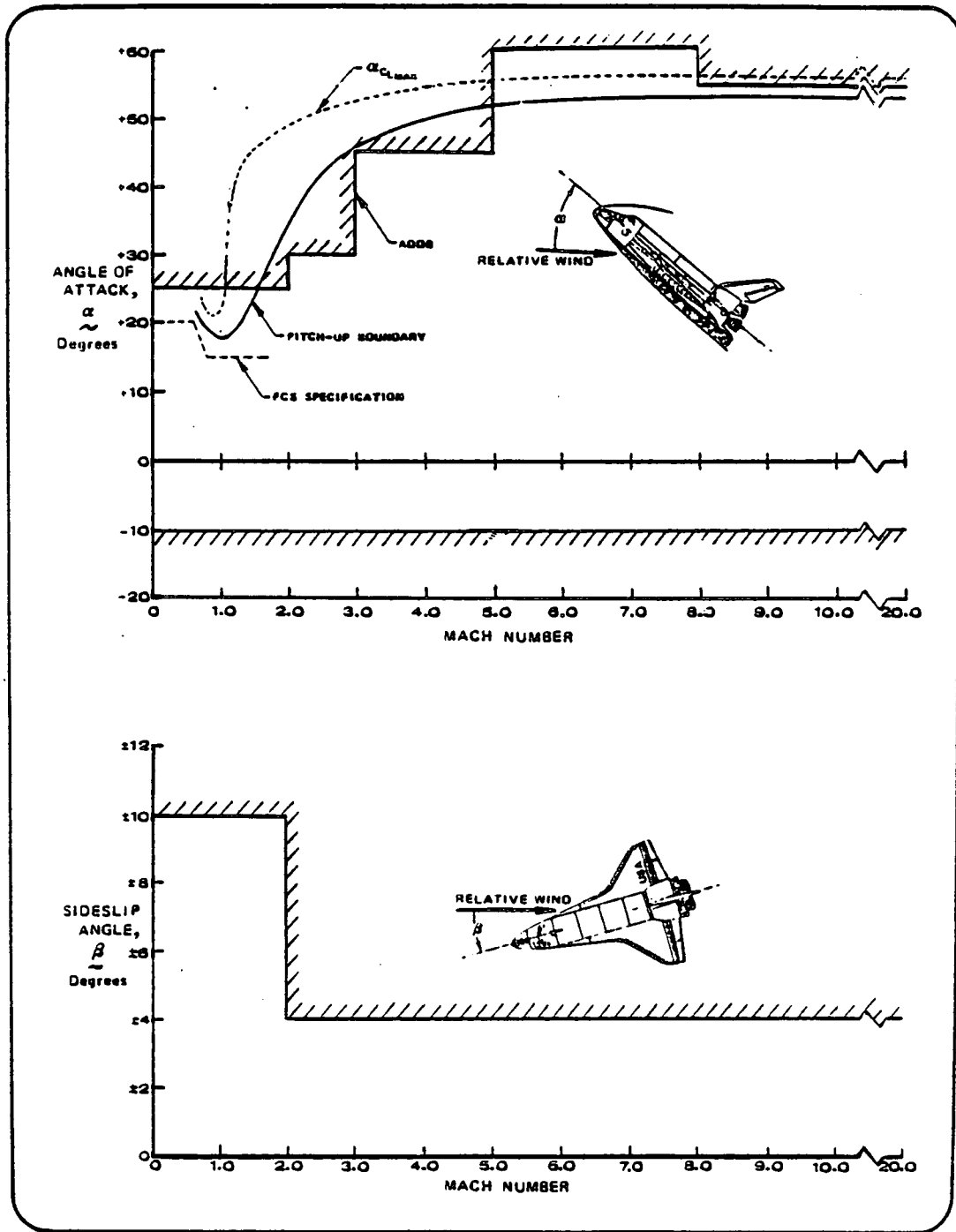


Figure 3.0-3
DESIGN DATA ANGLE OF ATTACK AND SIDESLIP ENVELOPES

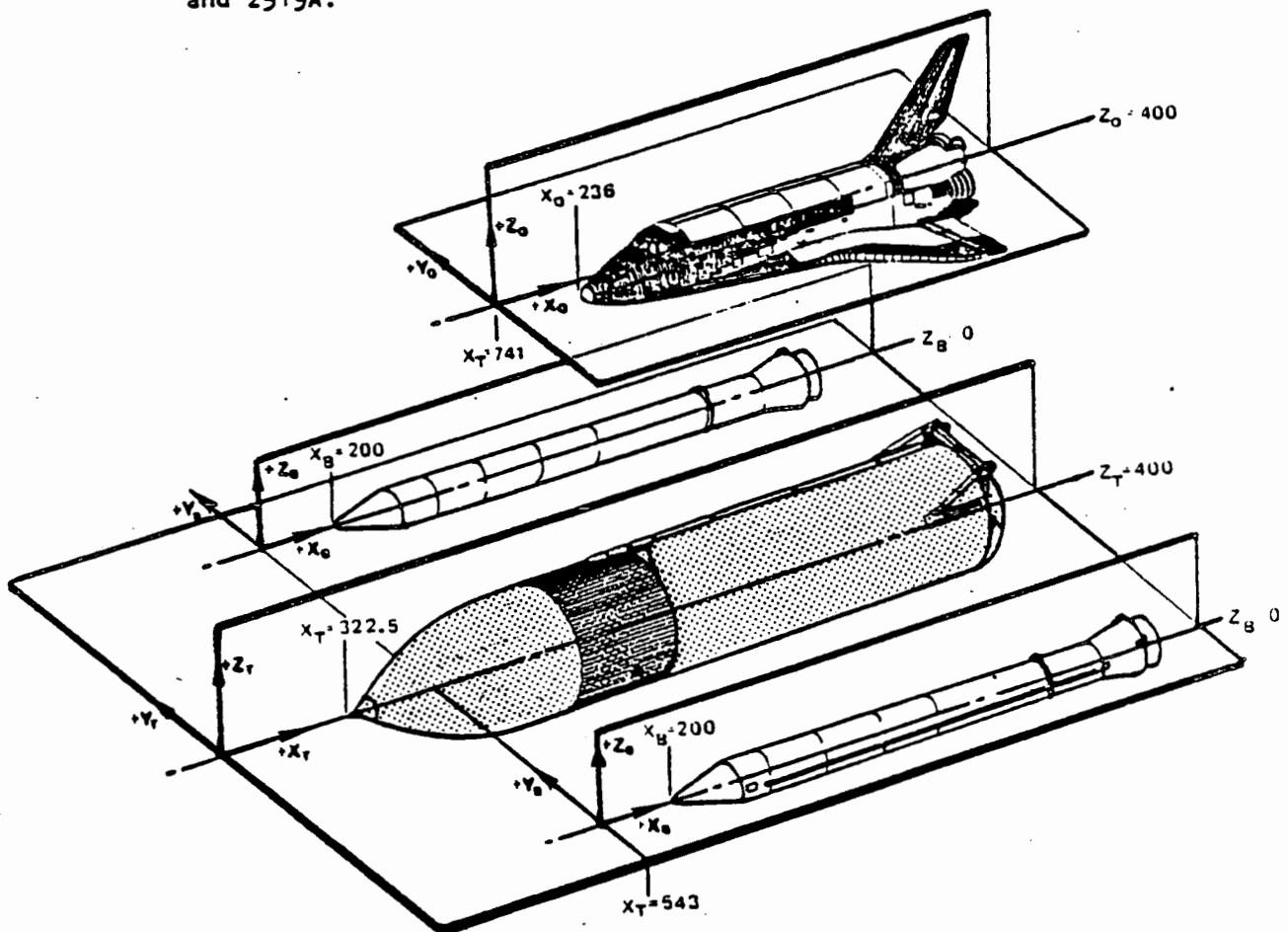
REFERENCES

- 3-1 JSC-07700-10, "Flight and Ground System Specification, Volume 10," NASA-JSC, Houston, Texas.
- 3-2 MJ070-0001-1B, "Orbiter Vehicle End Item Specification", Rockwell International, Space Division, Downey, California (January 1976).
- 3-3 SD MASTER CHANGE RECORD, MCR 3570, "Shuttle Baseline Control Drawings", Rockwell International, Space Division, Downey, California (August 30, 1976).
- 3-4 SE-019-983-2H, "SRB Systems Data Book," George C. Marshall Space Flight Center, NASA, Huntsville, Alabama (August 1977).
- 3-5 MMC-ET-SE25-0, "Space Shuttle External Tank, System Definition Handbook," Martin Marietta Corporation, Michoud Operations, New Orleans, Louisiana (August 1980)
- 3-6 NASA-JSC-17379, "Flight Definition and Requirements Directive," NASA-JSC- (Rev. 0), Houston, Texas, June 22, 1982.
- 3-7 MD-V70, "Master Dimensions Specification", Rockwell International, Space Division, Downey, California (June 1976)
- 3-8 ICD-2-00001/IRN 0078, "Shuttle Vehicle Mold Lines and Protuberances", NASA, Johnson Space Center, Houston, Texas (5 June 1982)
- 3-9 S073-SH-0226-2, "Thermal Protection Subsystem", Rockwell International Space Division, Downey, California (November 1975)
- 3-10 JSC-08934 (Vol. 1), "Shuttle Operational Data Book, Vol. 1, Shuttle Systems Performance and Constraint Data,"(includes Amendment 83), NASA/JSC, Houston, Texas (October 1976)
- 3-11 STS-85-0239, "Venting Operational Design Data Book-Entry," Rockwell International, Space Division, Downey, California (September 1985)

3.1 CONFIGURATION AND DIMENSIONS

- 3.1 CONFIGURATION AND DIMENSIONS. The Space Shuttle configuration was selected on the basis of performing certain representative missions [cf. Section 1.2] from both the ETR (Missions 1 and 2) and the WTR (Missions 3 and 4) with variable payloads. Detail drawings and dimensional parameters defining the vehicle configuration as established by MCR 3570 [Reference 3-3] are presented in this section.

Reference axes and sign convention are consistent with those for conventional aircraft. The axis systems for vehicle design and mass properties statements are defined in the sketch below for the Orbiter Vehicle, External Tank, and Solid Rocket Boosters. The axis systems are also defined in the Space Shuttle Master Dimensions Specification, Reference 3-7. All vehicle design drawing axis systems are in accordance with the NASA Phase B Technical Directives 2519 and 2519A.



- 3.1.1 LAUNCH VEHICLE. The aerodynamic design of the launch configuration is the result of drag reduction shaping and optimized element locations for the purpose of reduced structural loading and weight. A general arrangement drawing of the Launch vehicle with pertinent dimensions and relative locations of each element is given in Figure 3.1.1-1.

The operational Space Shuttle Vehicle consists of three basic elements: the Orbiter Vehicle, the External Tank, and two solid Rocket Boosters. The overall length of the Launch Vehicle is 184.17 feet. The Orbiter Vehicle is mounted on top of, and parallel to, the External Tank with the Orbiter nose located 654.5 inches aft of the ET nose. The Solid Rocket Boosters are attached to the left and right hand sides of the External Tank and are parallel to the ET with the SRB nose located 420.5 inches aft of the ET nose.

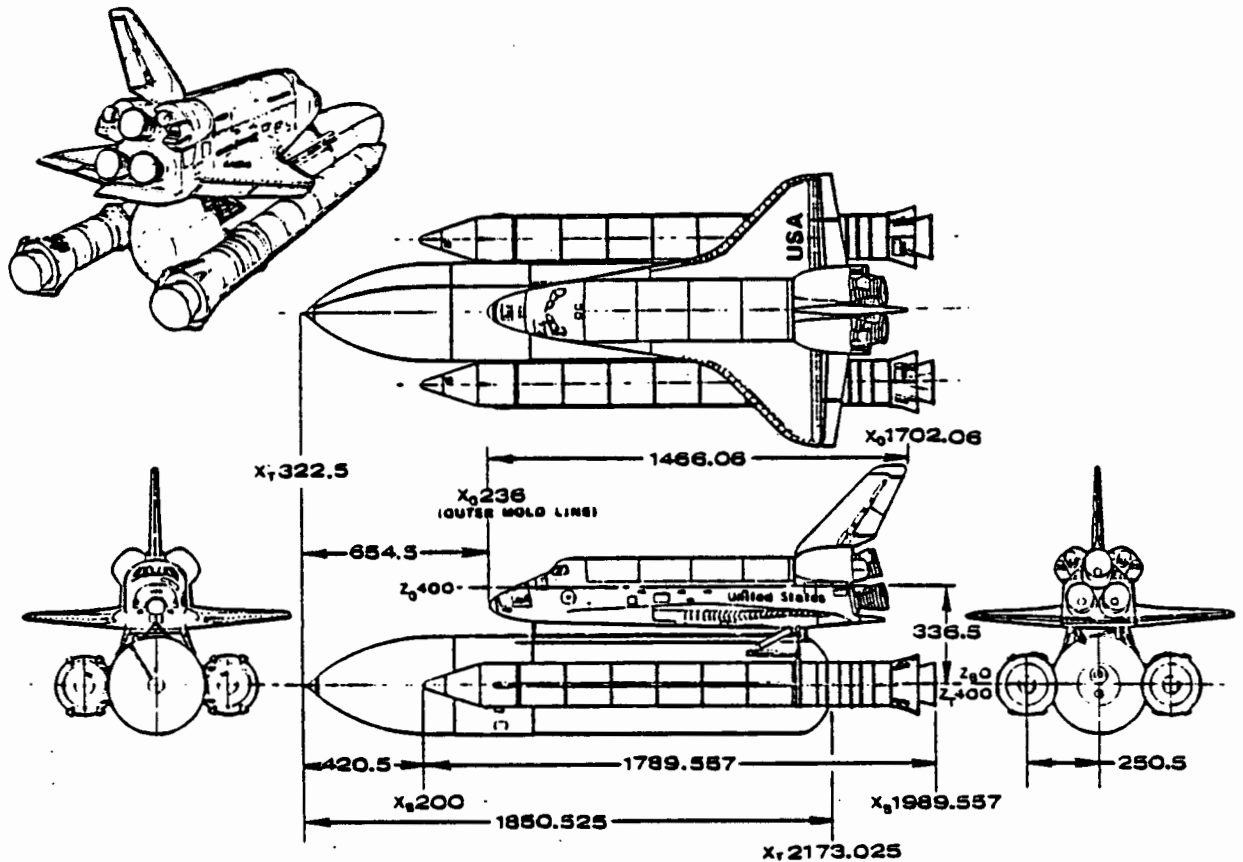
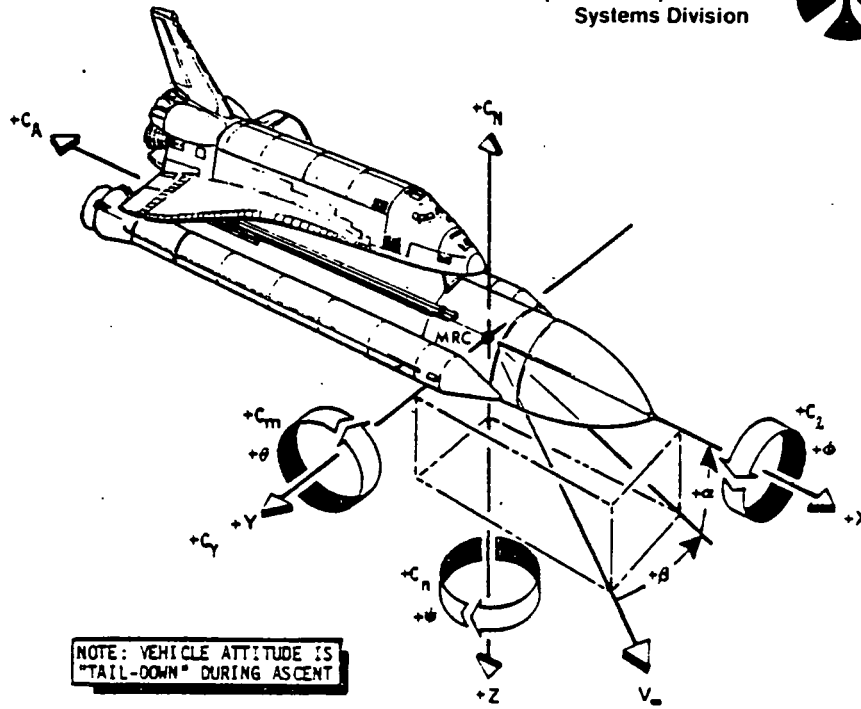


Figure 3.1.1-1
LAUNCH VEHICLE GEOMETRY

Aerodynamic forces and moments are measured with respect to a given Moment Reference Center (MRC) which is specified in each of the aerodynamic data sections. The Launch Vehicle aerodynamic data are given in the body axis systems which is illustrated in Figure 3.1.1-2. The body axis system is a conventional, right hand, orthogonal axis system with the X- and Z-axes in the plane of symmetry and with the positive X-axis along the External Tank centerline and directed out the tank nose.



NOTE: VEHICLE ATTITUDE IS
"TAIL-DOWN" DURING ASCENT

MOMENT REFERENCE CENTER (MRC) $\begin{cases} X_T=976 & \text{ORBITER NOSE} \\ Y_T=0 & \text{ET CENTERLINE} \\ Z_T=+00 \end{cases}$

X_T, Y_T, Z_T REFERENCE SYSTEM DEFINED ON PAGE 3.1-1

Figure 3.1.1-2
AERODYNAMIC BODY-AXIS REFERENCE SYSTEM

The aerodynamic force and moment sign convention is illustrated in Figure 3.1.1-3. All directions on the figure are positive as shown.

BODY AXES

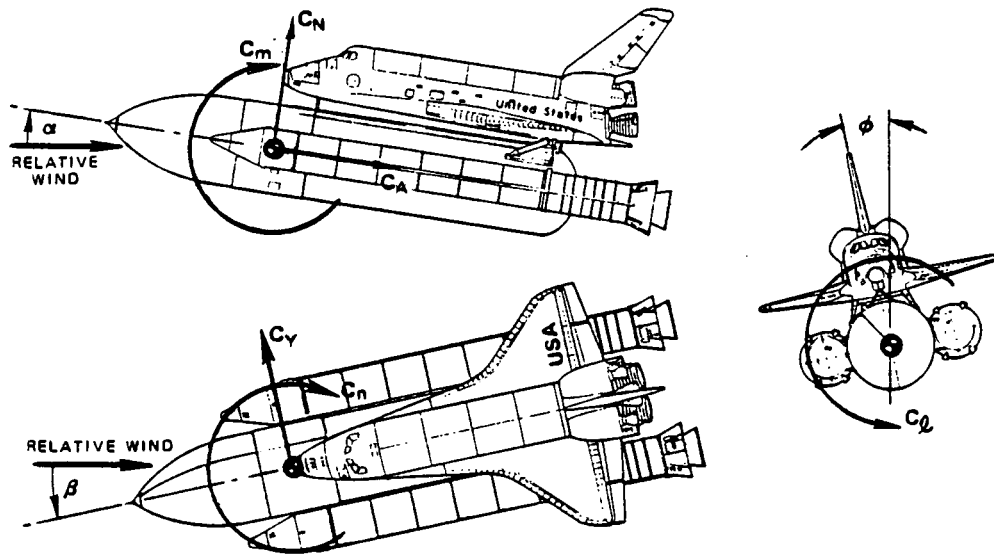
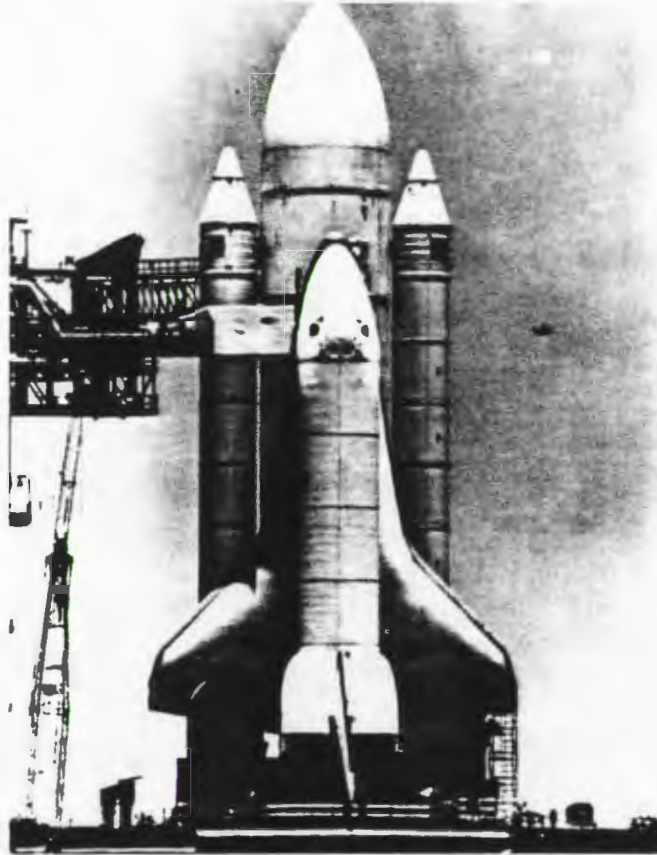


Figure 3.1.1-3
LAUNCH VEHICLE SIGN CONVENTION

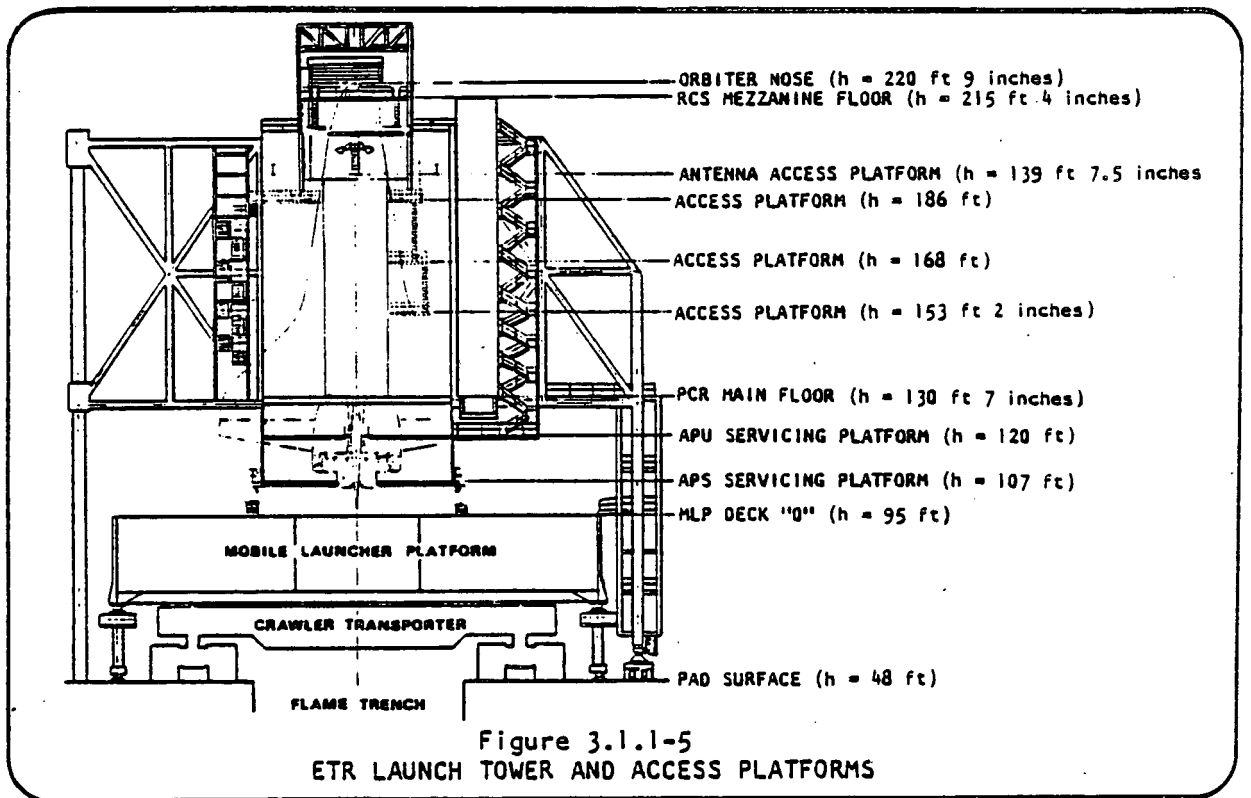
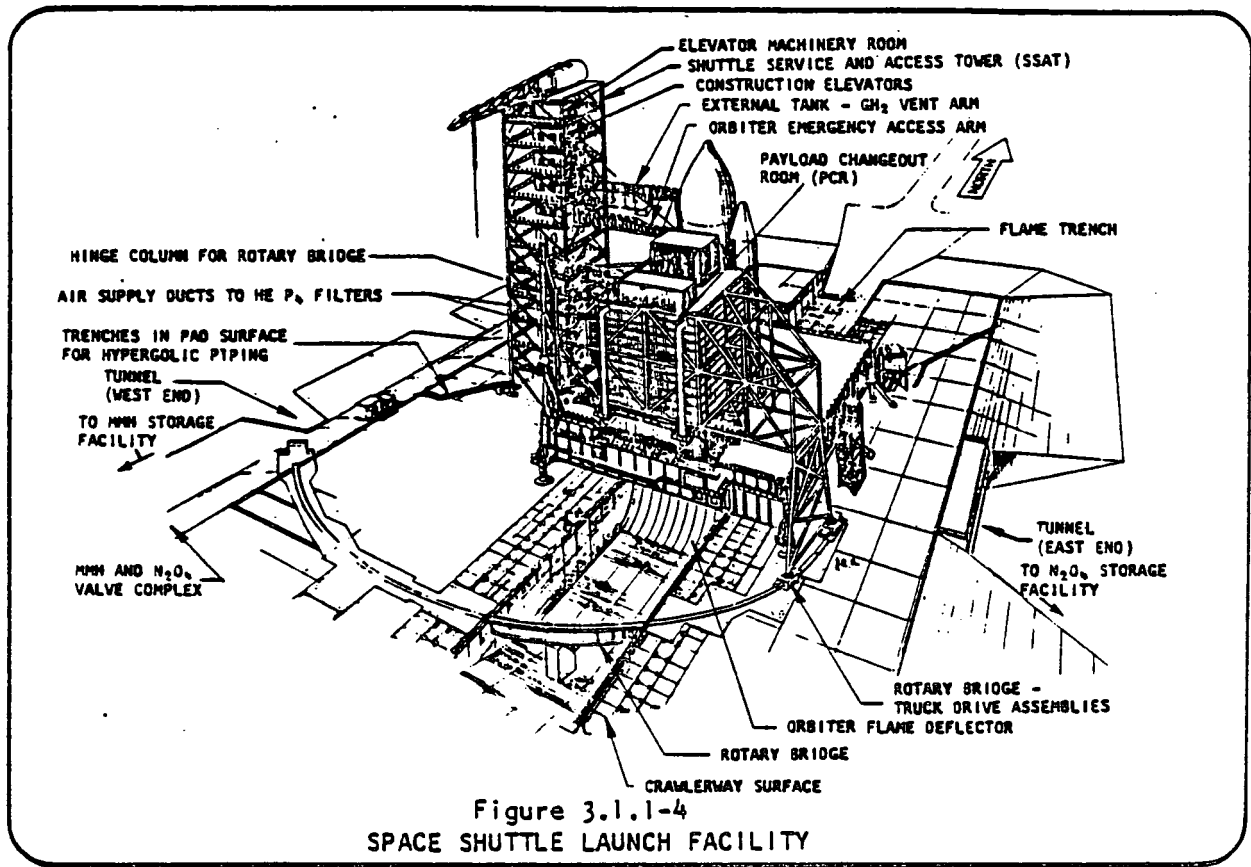


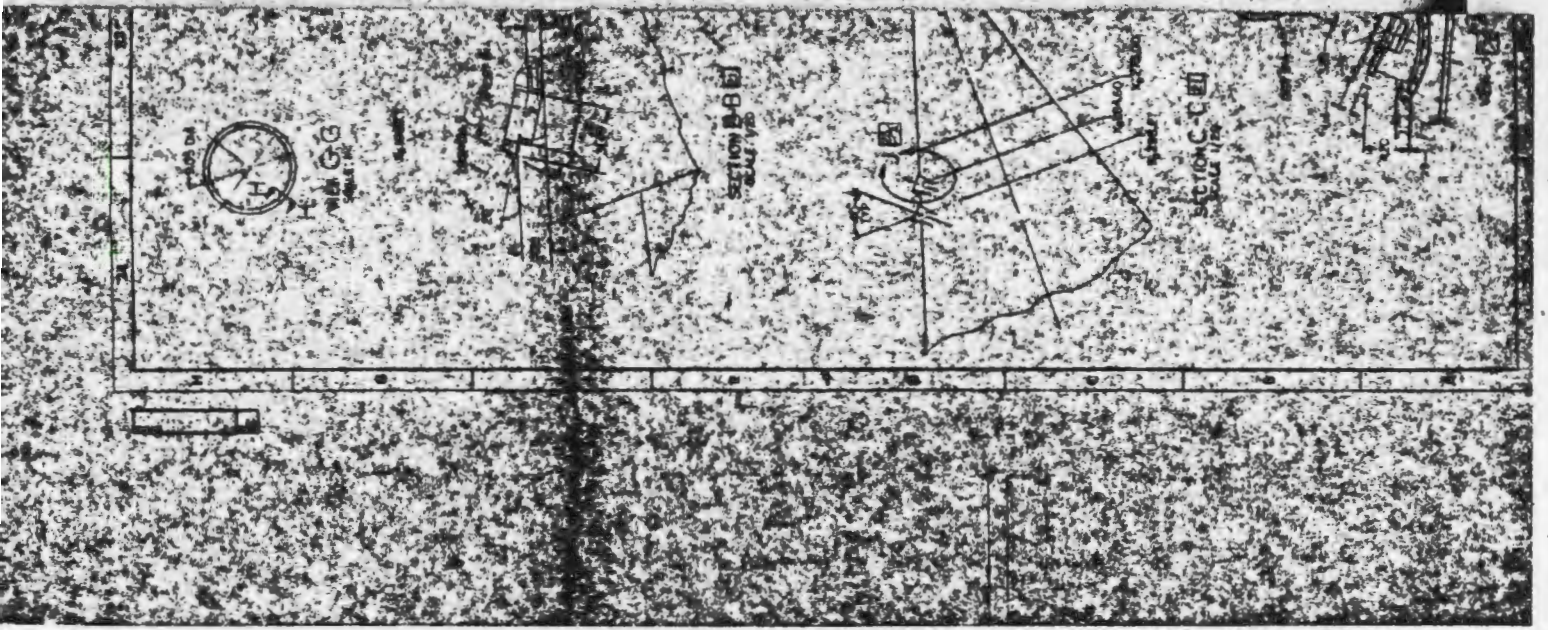
Launch complex 39A at the Eastern Test Range, Kennedy Space Center, has been used throughout the flight test program and for the first operational flights. The Space Shuttle Vehicle is shown in the photograph being readied for launch at KSC.



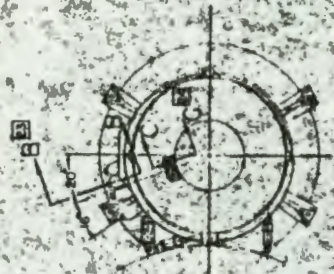
Pertinent information regarding the ETR launch facilities is given in Figures 3.1.1-4 and 3.1.1-5. These figures are considered useful in describing camera coverage during launch, debris damage assessment analyses, and for ice suppression studies. The Launch Vehicle Design drawing is given in Figure 3.1.1-6.

ORIGINAL PAGE IS
OF POOR QUALITY



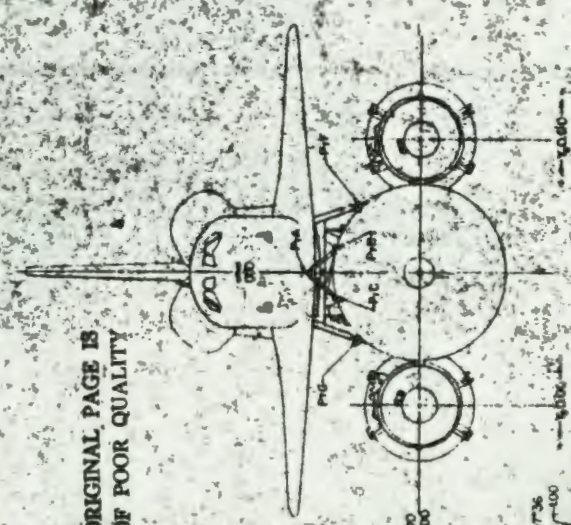


ORIGINAL PAGE IS
OF POOR QUALITY



VIEW A-A @ SCALE 1/50

ORIGINAL PAGE IS
OF POOR QUALITY



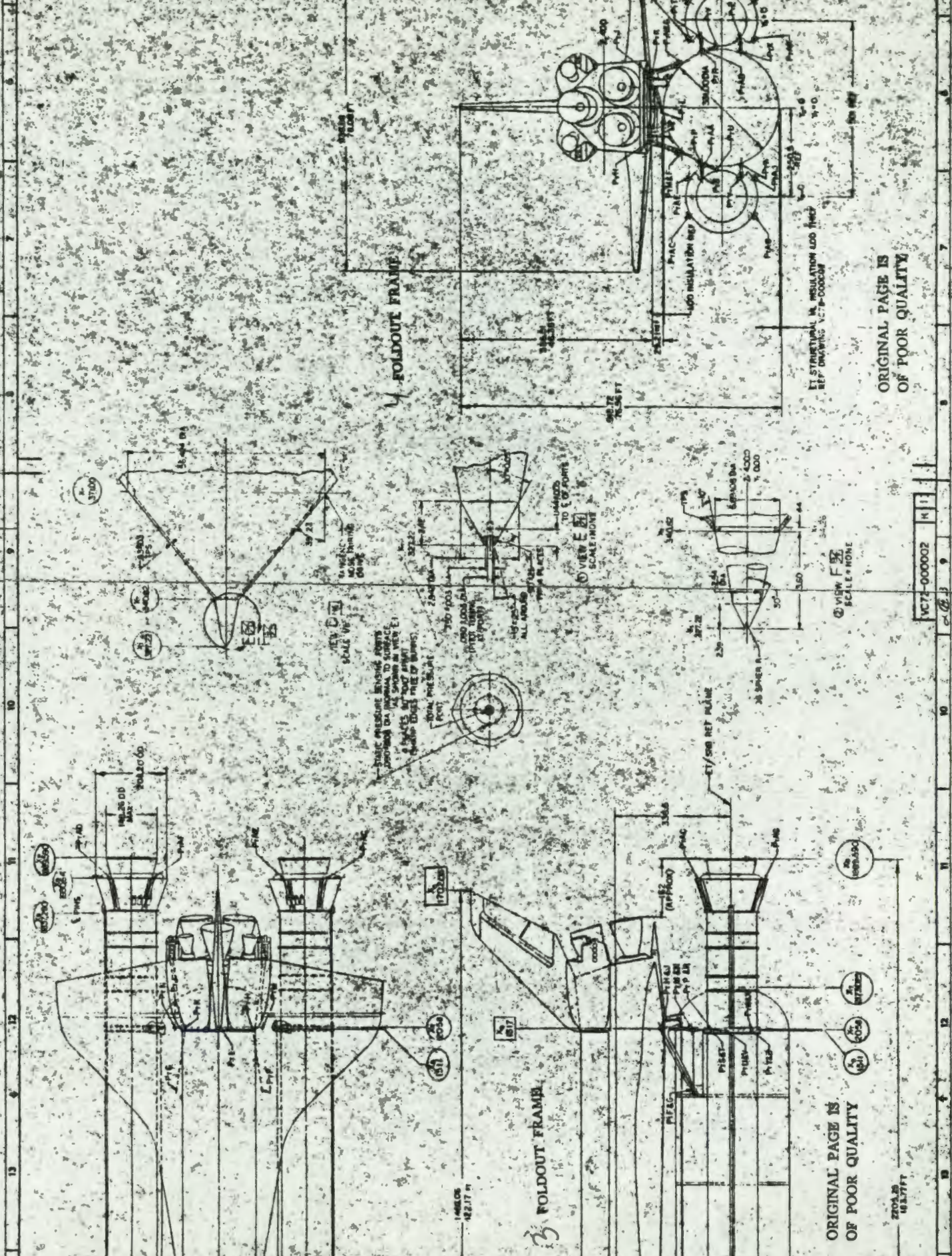
FOLDOUT FRAME

FOLDOUT FRAME

SHUTTLE ELEMENTS ATTACH COORDINATES

| h | Orbiter | E1 | X1 | Y1 | Z1 | X2 | Y2 | Z2 | SSV |
|----|---------|-------|-------|-------|-------|----|----|----|-------------------|
| A | 20500 | 0 | 20504 | | | | | | 20500 0 |
| B | | | 18290 | -4765 | 89000 | | | | 18290 -4765 89000 |
| C | | | 18290 | -4765 | 89000 | | | | 18290 -4765 89000 |
| D | | | | | | | | | |
| E | | | | | | | | | |
| F | | | | | | | | | |
| G | | | | | | | | | |
| H | 1817 | 14650 | 80000 | | | | | | 2056 14650 80000 |
| I | 1817 | 14650 | 80000 | | | | | | 2056 14650 80000 |
| J | | | | | | | | | |
| K | | | | | | | | | |
| L | | | | | | | | | |
| M | | | | | | | | | |
| N | | | | | | | | | |
| O | | | | | | | | | |
| P | | | | | | | | | |
| Q | | | | | | | | | |
| R | | | | | | | | | |
| S | | | | | | | | | |
| T | | | | | | | | | |
| U | | | | | | | | | |
| V | | | | | | | | | |
| W | | | | | | | | | |
| X | | | | | | | | | |
| Y | | | | | | | | | |
| Z | | | | | | | | | |
| AA | | | | | | | | | |
| AB | | | | | | | | | |
| AC | | | | | | | | | |
| AD | | | | | | | | | |
| AE | | | | | | | | | |
| AF | | | | | | | | | |
| AG | | | | | | | | | |
| AH | | | | | | | | | |
| AI | | | | | | | | | |
| AJ | | | | | | | | | |
| AK | | | | | | | | | |

VC72-000002 K11



FOLDOUT FRAME

ET STRUCTURAL W. INSULATION LOD (REF)
REF DRAWING VC72-000004

ORIGINAL PAGE IS
OF POOR QUALITY

VIEW D-D
SCALE 1/4"

Basic Pressure Exposed Joints
Approved by INMMA TO SURFACE
ALL SPACES IN VIEW E1
SHALL BE FILLED WITH
INSULATION (SEE E1)

VIEW E-E
SCALE 1/4"

VIEW F-F
SCALE 1/4"

VC72-000002 H 11

FOLDOUT FRAME

ORIGINAL PAGE IS
OF POOR QUALITY

2204.25
113.77 FT

| | |
|----|---|
| 1 | REVISION TO WORK AND CLARIFY AT FIG. 15 DIMS/RELEASE, SHUTTLE LOCATIONS ACCORDS SIB ESTIMATION TOLERANCES FOR REF LOCATION Simplified drawing depicts depicting error in the drawing, see page revision, see, 80 DA |
| 2 | SEE BY 2 DIRECT DIMENSIONS CHANGES INCORPORATED AND RELEASED AT REVISION SEE 69 1-91 DIRECT DIMENSIONS CHANGES INCORPORATED AND RELEASED AT REVISION |
| 3 | SEE BY 3 DIRECT DIMENSIONS CHANGES INCORPORATED AND RELEASED AT REVISION |
| 4 | SEE BY 4 DIRECT DIMENSIONS CHANGES INCORPORATED AND RELEASED AT REVISION |
| 5 | SEE BY 5 DIRECT DIMENSIONS CHANGES INCORPORATED AND RELEASED AT REVISION |
| 6 | SEE BY 6 DIRECT DIMENSIONS CHANGES INCORPORATED AND RELEASED AT REVISION |
| 7 | SEE BY 7 DIRECT DIMENSIONS CHANGES INCORPORATED AND RELEASED AT REVISION |
| 8 | SEE BY 8 DIRECT DIMENSIONS CHANGES INCORPORATED AND RELEASED AT REVISION |
| 9 | SEE BY 9 DIRECT DIMENSIONS CHANGES INCORPORATED AND RELEASED AT REVISION |
| 10 | SEE BY 10 DIRECT DIMENSIONS CHANGES INCORPORATED AND RELEASED AT REVISION |

| PROBLEMS | MINIMAL ALTERATION |
|---|---|
| 1. PROBLEM 2. PROBLEM 3. PROBLEM 4. PROBLEM 5. PROBLEM 6. PROBLEM 7. PROBLEM 8. PROBLEM 9. PROBLEM 10. PROBLEM | 1. MINIMAL ALTERATION 2. MINIMAL ALTERATION 3. MINIMAL ALTERATION 4. MINIMAL ALTERATION 5. MINIMAL ALTERATION 6. MINIMAL ALTERATION 7. MINIMAL ALTERATION 8. MINIMAL ALTERATION 9. MINIMAL ALTERATION 10. MINIMAL ALTERATION |



FOLDOUT FRAME

PRECEDING PAGE BLANK NOT FILMED

ORIGINAL PAGE IS
OF POOR QUALITY

1. FOR ET-5 ON
2. FOR ET-1, ET-4, ET-5 ONLY
3. REFERENCE DIMS 2-0000, 2-0001 & 2-1001
4. IN STACKED CONFIGURATION ALL RELATED SHUTTLE ELEMENT AXIS ARE PARALLEL
5. FOR SIB CONFIGURATION SEE V671-000002
6. FOR ET CONFIGURATION SEE V678-000002
7. FOR ORBITER CONFIGURATION SEE V670-000002
8. THIS DRAWING SUPERSEDES V670-000002 & V672-000043

NOTES: UNLESS OTHERWISE SPECIFIED

| | |
|--------|---------|
| DESIGN | REVISED |
| DATE | BY |
| 1 | 1 |
| 2 | 2 |
| 3 | 3 |
| 4 | 4 |
| 5 | 5 |
| 6 | 6 |
| 7 | 7 |
| 8 | 8 |
| 9 | 9 |
| 10 | 10 |

3.1.2 SOLID ROCKET BOOSTERS. Two Solid Rocket Boosters (SRB's) are used for each flight which, together with the Space Shuttle Main Engines (SSME's), provide the initial launch thrust. Design of the SRB's was predicated on minimizing the Launch Vehicle drag during boost. Aerodynamic considerations were sacrificed to some extent by protuberances formed by the forward (see photo) and aft Booster Separation Motors, launch pad tie down struts, stiffener rings and other miscellaneous surface protrusions.

The two Solid Rocket Boosters are separated from the External Tank at burnout by pyrotechnic devices and use of the eight Booster Separation Motors (BSM's). The SRB is illustrated in Figure 3.1.2-1.

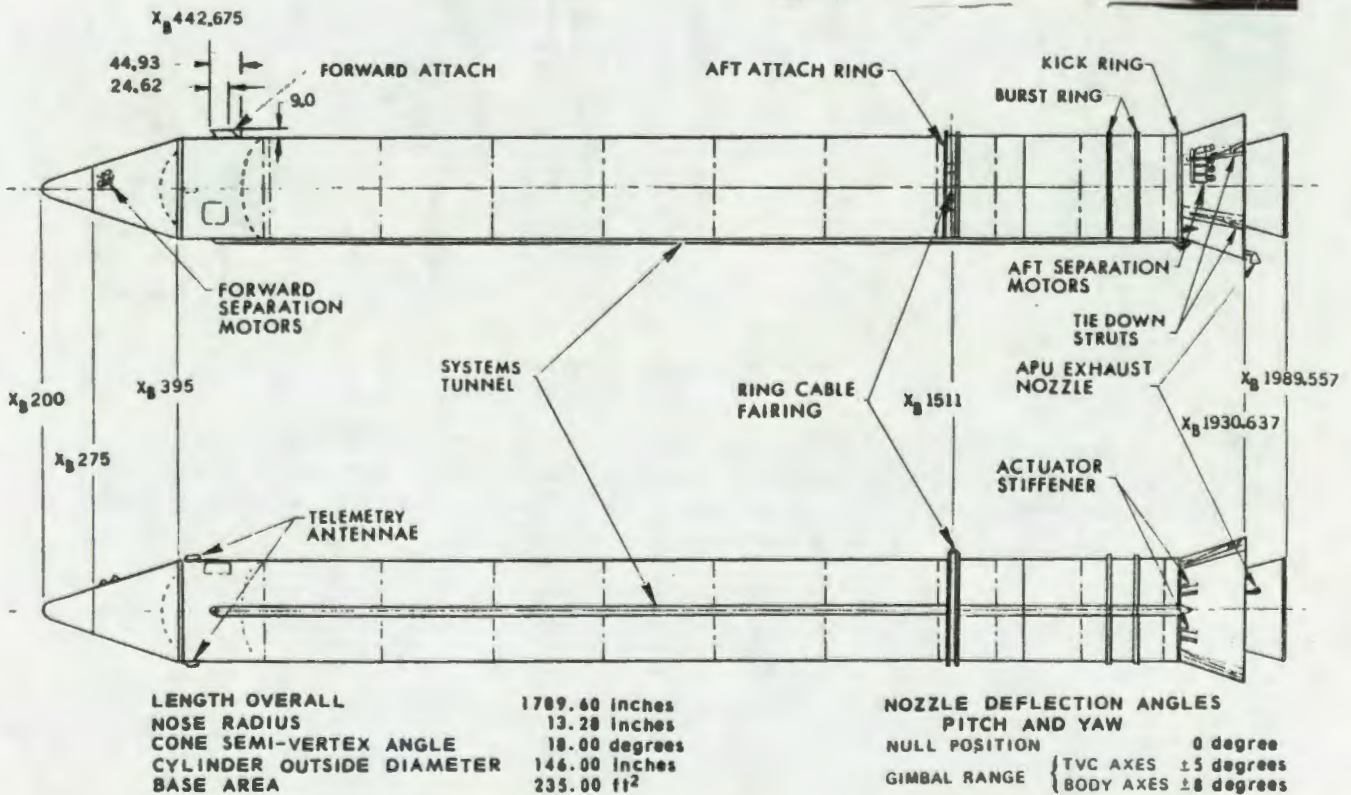
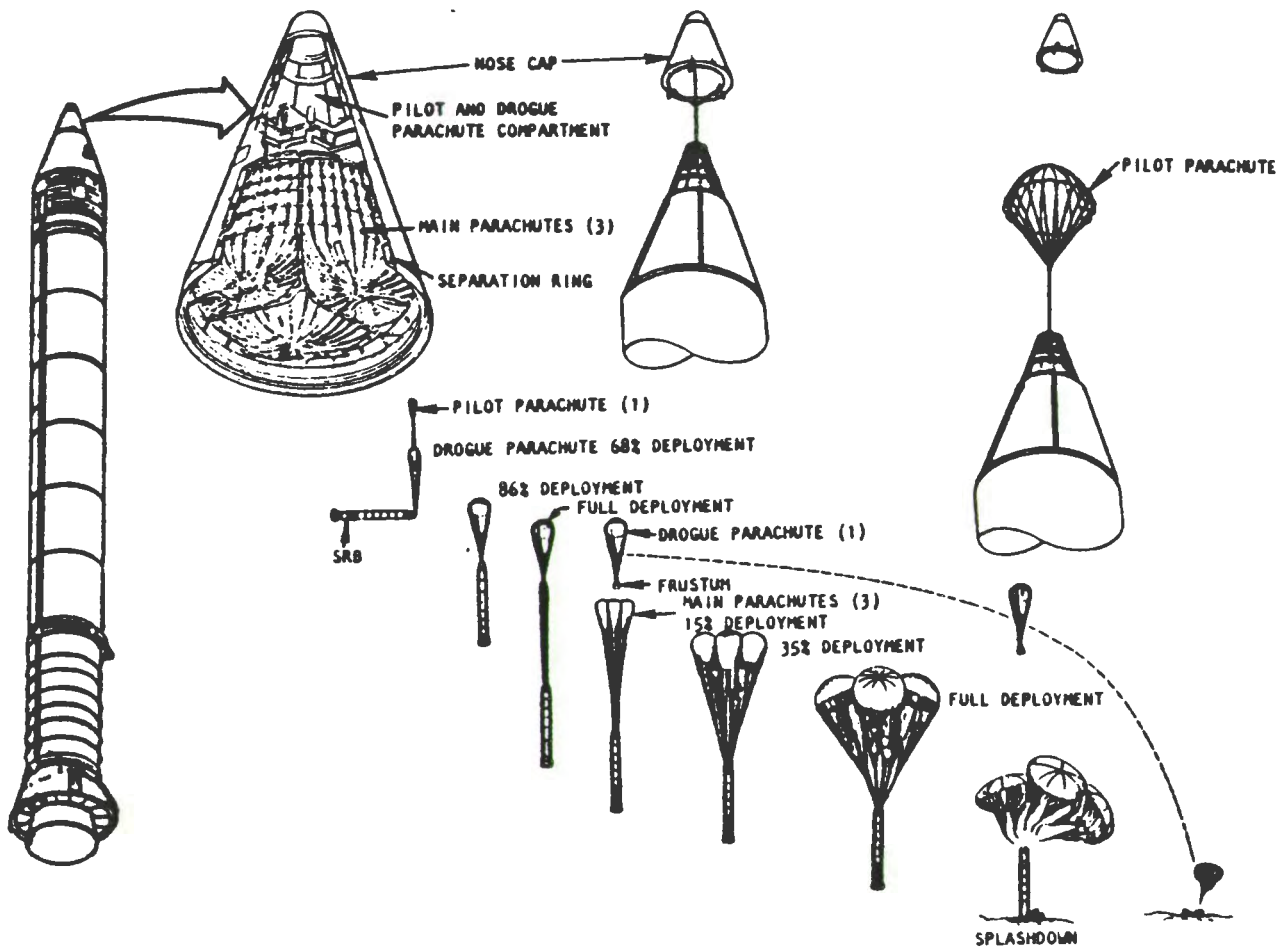


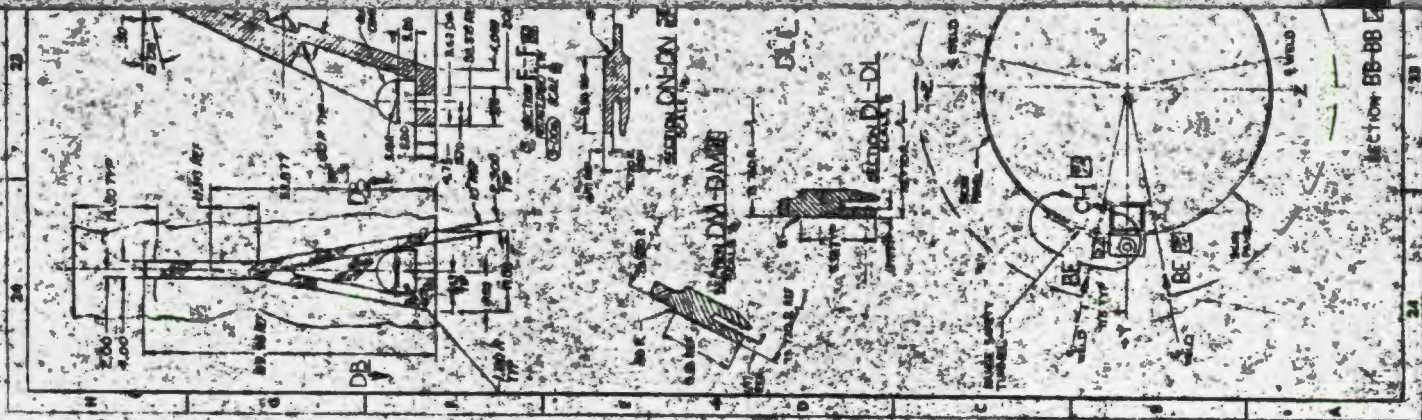
Figure 3.1.2-1
SOLID ROCKET BOOSTER

The Solid Rocket Boosters are reusable and contain parachute recovery systems and location aids in the forward section of each booster as shown in the sketch below.



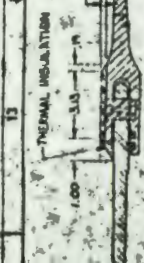
SRB RECOVERY SYSTEM

Two basic types of SRB's are maintained in the inventory; the steel case and filament wound case motors. Both types use the high performance nozzle. Design geometry for these configurations is given in Figure(s) 3.1.2-2 (a through d).

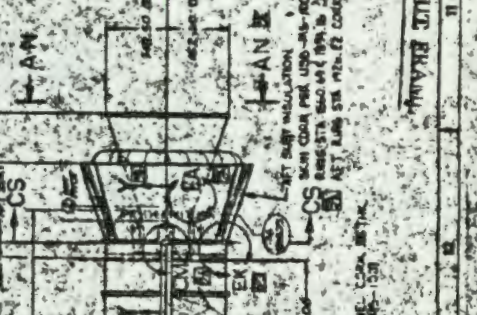
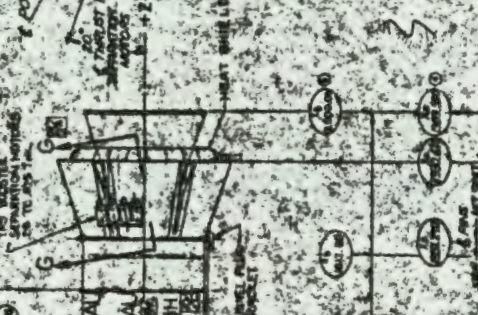
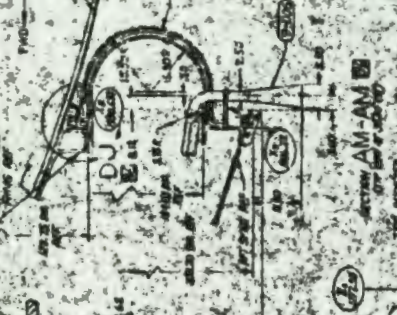


AC 10000000 13

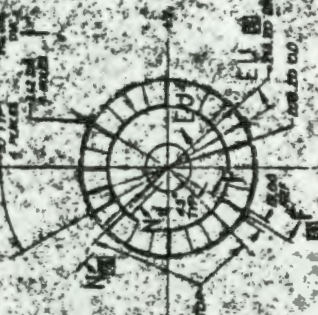
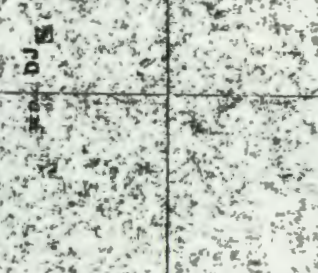
SECTION BE-BE



FORM DDE
 FROM PLANT AND TO BE INSTALLED
 AS SHOWN IN DRAWING TO BE USED
 AS PER DRAWING AND TO BE USED
 AS PER DRAWING AND TO BE USED



ORIGINAL PAGE IS
 OF POOR QUALITY



ORIGINAL PAGE IS
 OF POOR QUALITY

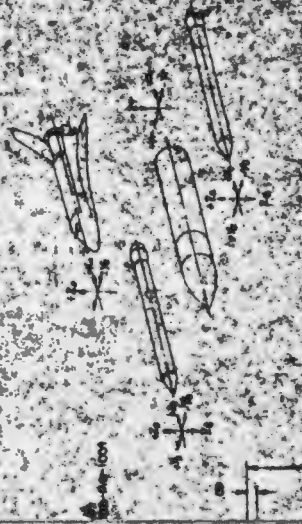
VC71-000002

FOLDOUT FRAME

ORIGINAL PAGE IS
 OF POOR QUALITY

FOLDOUT FRAME

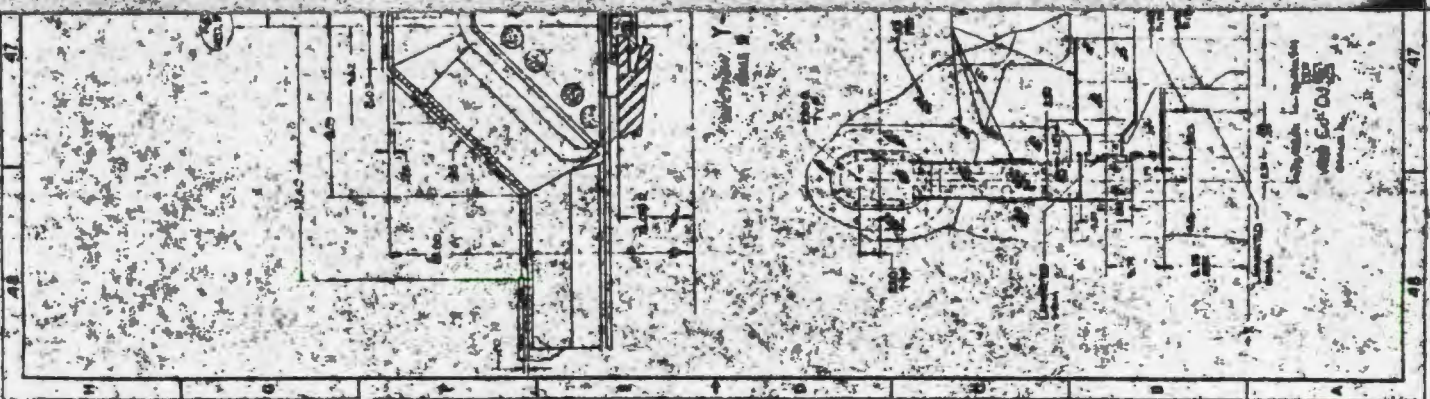
ORIGINAL PAGE IS
 OF POOR QUALITY



FOLDOUT FRAME

ORIGINAL PAGE IS
OF POOR QUALITY

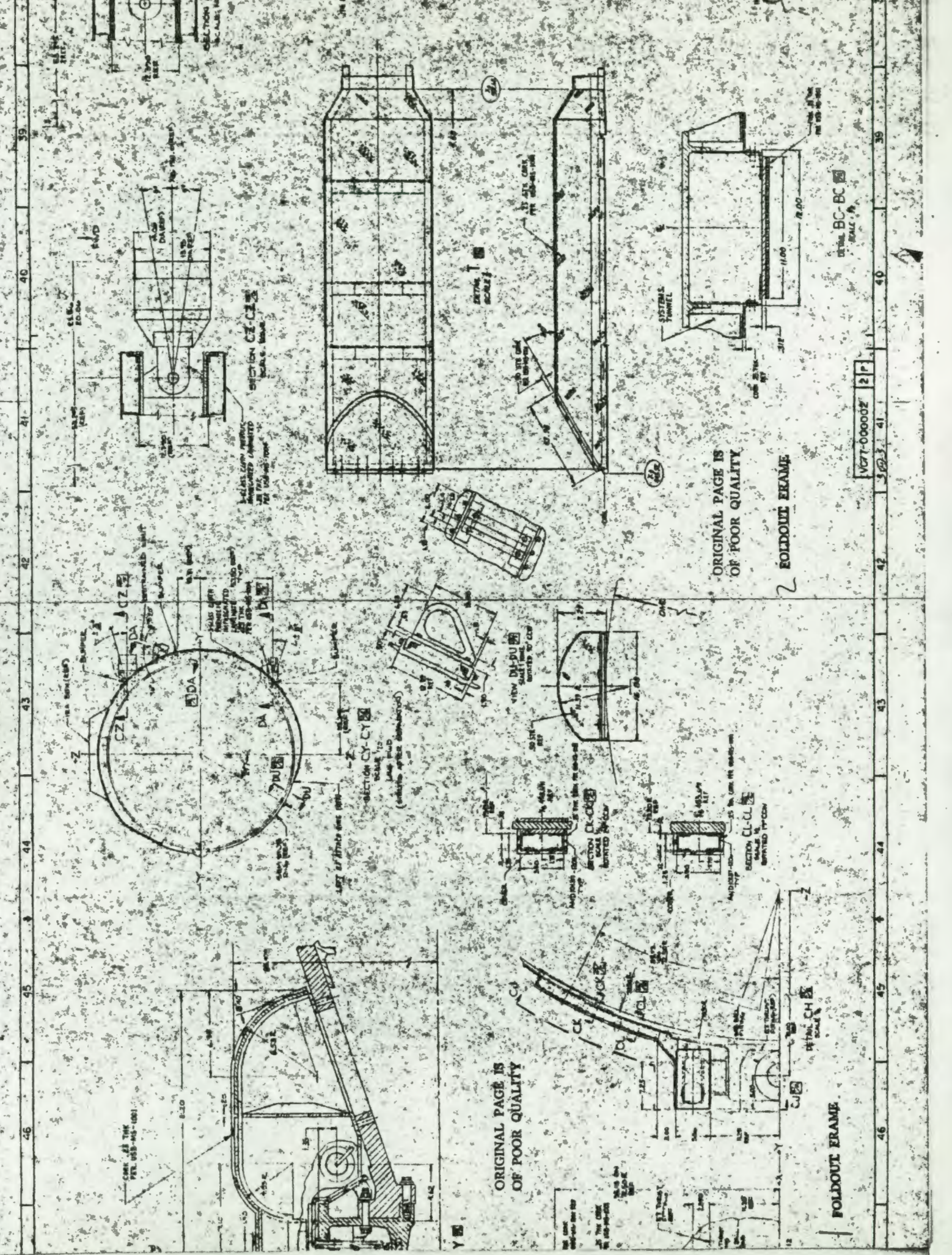
1. 13 100-100
2. 14 100-100
3. 15 100-100
4. 16 100-100
5. 17 100-100
6. 18 100-100
7. 19 100-100
8. 20 100-100
9. 21 100-100
10. 22 100-100
11. 23 100-100
12. 24 100-100
13. 25 100-100
14. 26 100-100
15. 27 100-100
16. 28 100-100
17. 29 100-100
18. 30 100-100
19. 31 100-100
20. 32 100-100
21. 33 100-100
22. 34 100-100
23. 35 100-100
24. 36 100-100
25. 37 100-100
26. 38 100-100
27. 39 100-100
28. 40 100-100
29. 41 100-100
30. 42 100-100
31. 43 100-100
32. 44 100-100
33. 45 100-100
34. 46 100-100
35. 47 100-100
36. 48 100-100
37. 49 100-100
38. 50 100-100
39. 51 100-100
40. 52 100-100
41. 53 100-100
42. 54 100-100
43. 55 100-100
44. 56 100-100
45. 57 100-100
46. 58 100-100
47. 59 100-100
48. 60 100-100
49. 61 100-100
50. 62 100-100
51. 63 100-100
52. 64 100-100
53. 65 100-100
54. 66 100-100
55. 67 100-100
56. 68 100-100
57. 69 100-100
58. 70 100-100
59. 71 100-100
60. 72 100-100
61. 73 100-100
62. 74 100-100
63. 75 100-100
64. 76 100-100
65. 77 100-100
66. 78 100-100
67. 79 100-100
68. 80 100-100
69. 81 100-100
70. 82 100-100
71. 83 100-100
72. 84 100-100
73. 85 100-100
74. 86 100-100
75. 87 100-100
76. 88 100-100
77. 89 100-100
78. 90 100-100
79. 91 100-100
80. 92 100-100
81. 93 100-100
82. 94 100-100
83. 95 100-100
84. 96 100-100
85. 97 100-100
86. 98 100-100
87. 99 100-100
88. 100 100-100



1:25000000

Section Y

Section Z



ORIGINAL PAGE IS
OF POOR QUALITY

FOLDOUT FRAME

FOLDOUT FRAME

VC77-000002 2 P

DETAIL BC-BC
SCALE 1/2"

ORIGINAL PAGE IS
OF POOR QUALITY

Y B

CASE 43 THK
PRT. 053-445-1001

SEE DETAIL BC-BC FOR
DIMENSIONS

SEE DETAIL BC-BC FOR
DIMENSIONS

SECTION CL-CL
SCALE 1/2"
SHOWN IN OPEN POSITION

SECTION DK-DK
SCALE 1/2"
SHOWN IN OPEN POSITION

SECTION CY-CY
SCALE 1/2"
LEFT OF FRAME AND RIGHT
(INTERNAL SPRING OMITTED)

VIEW DI-DI
SCALE 1/2"
SHOWN IN OPEN POSITION

DETAIL CH-CH
SCALE 1/2"

SECTION CL-CL
SCALE 1/2"
SHOWN IN OPEN POSITION

SECTION DK-DK
SCALE 1/2"
SHOWN IN OPEN POSITION

SECTION CY-CY
SCALE 1/2"
LEFT OF FRAME AND RIGHT
(INTERNAL SPRING OMITTED)

VIEW DI-DI
SCALE 1/2"
SHOWN IN OPEN POSITION

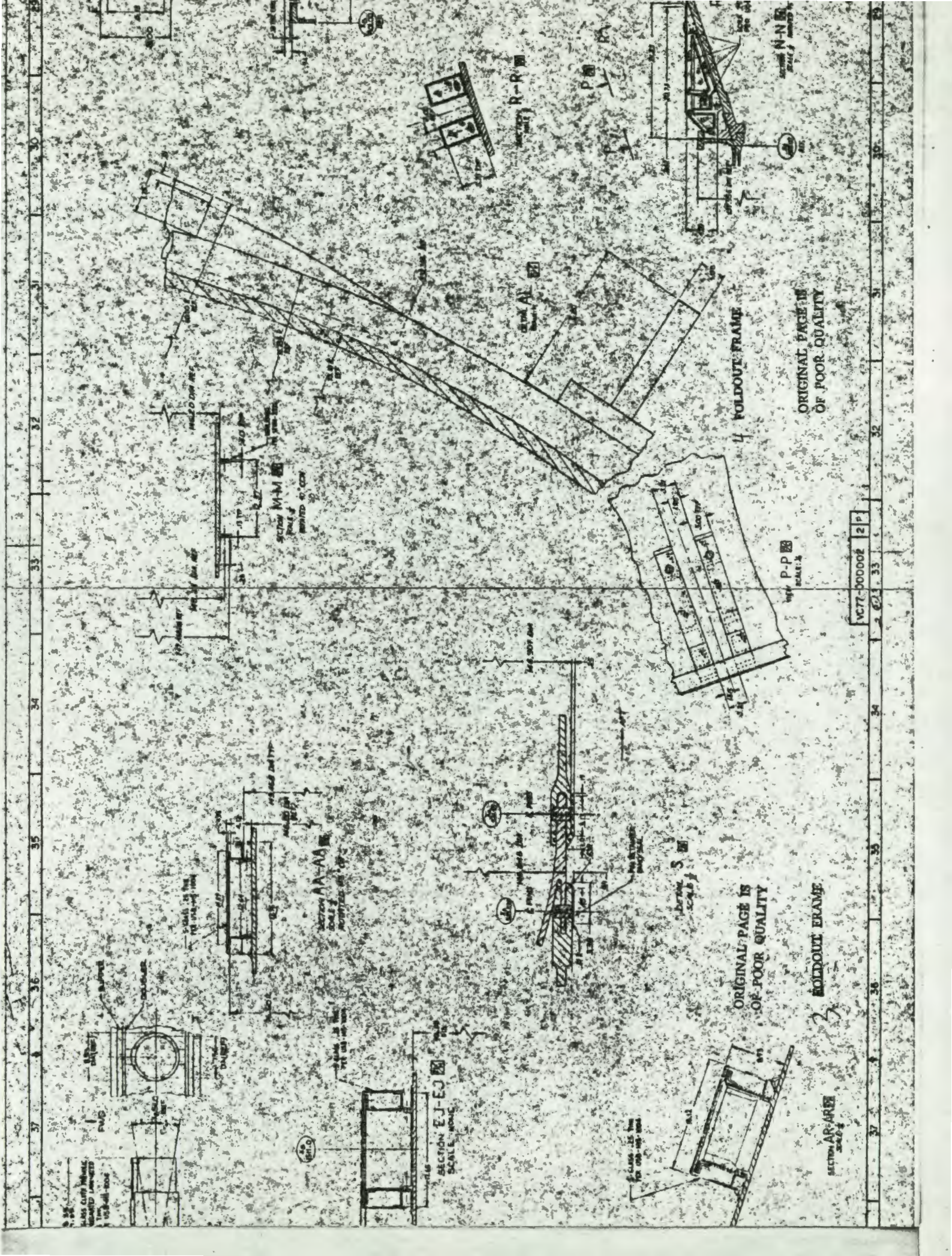
DETAIL CH-CH
SCALE 1/2"

SECTION CL-CL
SCALE 1/2"
SHOWN IN OPEN POSITION

SECTION DK-DK
SCALE 1/2"
SHOWN IN OPEN POSITION

SECTION CY-CY
SCALE 1/2"
LEFT OF FRAME AND RIGHT
(INTERNAL SPRING OMITTED)

VIEW DI-DI
SCALE 1/2"
SHOWN IN OPEN POSITION



ORIGINAL PAGE IS OF POOR QUALITY

FOLDOUT FRAME

SECTION P-P
SCALE: 1/4"

VC77-000002 2 P

ORIGINAL PAGE IS OF POOR QUALITY

FOLDOUT FRAME

SECTION A-A
SCALE: 1/4"

SECTION E-E
SCALE: 1/4"

SECTION U-U
SCALE: 1/4"

SECTION S-S
SCALE: 1/4"

SECTION M-M
SCALE: 1/4"

SECTION R-R
SCALE: 1/4"

SECTION N-N
SCALE: 1/4"

SECTION V-V
SCALE: 1/4"

SECTION W-W
SCALE: 1/4"

SECTION X-X
SCALE: 1/4"

SECTION Y-Y
SCALE: 1/4"

SECTION Z-Z
SCALE: 1/4"

SECTION T-T
SCALE: 1/4"

SECTION U-U
SCALE: 1/4"

SECTION V-V
SCALE: 1/4"

SECTION W-W
SCALE: 1/4"

SECTION X-X
SCALE: 1/4"

SECTION Y-Y
SCALE: 1/4"

SECTION Z-Z
SCALE: 1/4"

SECTION A-A
SCALE: 1/4"

SECTION B-B
SCALE: 1/4"

SECTION C-C
SCALE: 1/4"

SECTION D-D
SCALE: 1/4"

SECTION E-E
SCALE: 1/4"

SECTION F-F
SCALE: 1/4"

SECTION G-G
SCALE: 1/4"

SECTION H-H
SCALE: 1/4"

SECTION I-I
SCALE: 1/4"

SECTION J-J
SCALE: 1/4"

SECTION K-K
SCALE: 1/4"

SECTION L-L
SCALE: 1/4"

SECTION M-M
SCALE: 1/4"

SECTION N-N
SCALE: 1/4"

SECTION O-O
SCALE: 1/4"

SECTION P-P
SCALE: 1/4"

SECTION Q-Q
SCALE: 1/4"

SECTION R-R
SCALE: 1/4"

SECTION S-S
SCALE: 1/4"

SECTION T-T
SCALE: 1/4"

SECTION U-U
SCALE: 1/4"

SECTION V-V
SCALE: 1/4"

SECTION W-W
SCALE: 1/4"

SECTION X-X
SCALE: 1/4"

SECTION Y-Y
SCALE: 1/4"

SECTION Z-Z
SCALE: 1/4"

SECTION A-A
SCALE: 1/4"

SECTION B-B
SCALE: 1/4"

SECTION C-C
SCALE: 1/4"

SECTION D-D
SCALE: 1/4"

SECTION E-E
SCALE: 1/4"

SECTION F-F
SCALE: 1/4"

SECTION G-G
SCALE: 1/4"

SECTION H-H
SCALE: 1/4"

SECTION I-I
SCALE: 1/4"

SECTION J-J
SCALE: 1/4"

SECTION K-K
SCALE: 1/4"

SECTION L-L
SCALE: 1/4"

SECTION M-M
SCALE: 1/4"

SECTION N-N
SCALE: 1/4"

SECTION O-O
SCALE: 1/4"

SECTION P-P
SCALE: 1/4"

SECTION Q-Q
SCALE: 1/4"

SECTION R-R
SCALE: 1/4"

SECTION S-S
SCALE: 1/4"

SECTION T-T
SCALE: 1/4"

| | | | | | | | | | |
|---|----|----|----|----|----|----|----|----|----|
| 1 | 20 | 21 | 22 | 23 | 24 | 25 | 26 | 27 | 28 |
| | | | | | | | | | |
| | | | | | | | | | |
| | | | | | | | | | |
| | | | | | | | | | |
| | | | | | | | | | |
| | | | | | | | | | |
| | | | | | | | | | |
| | | | | | | | | | |
| | | | | | | | | | |
| | | | | | | | | | |
| | | | | | | | | | |
| | | | | | | | | | |
| | | | | | | | | | |
| | | | | | | | | | |
| | | | | | | | | | |
| | | | | | | | | | |
| | | | | | | | | | |
| | | | | | | | | | |
| | | | | | | | | | |
| | | | | | | | | | |
| | | | | | | | | | |

ORIGINAL PAGE IS
OF POOR QUALITY



view DE-FR END
(each showing section
TYP. 1 PLACE)
SCALE 1/2"



FOLDOUT FRAME

DETAIL AT 28



SECTION DC-FR END
SCALE 1/2"

18958 VC77-00000

CS-000001



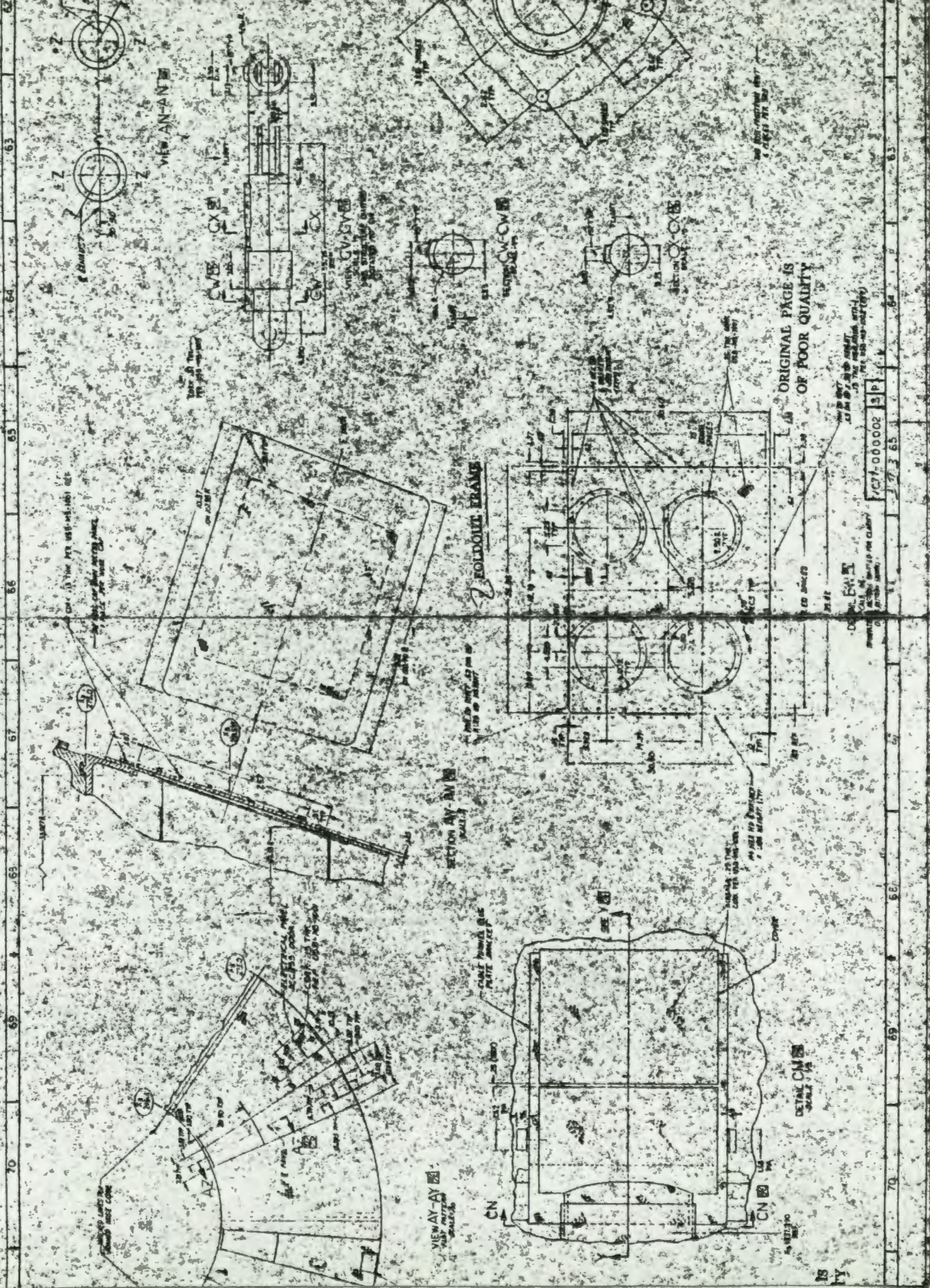
THIRTY FEET AND UP
(SEE SECTION A-2)



SECTION A-2
SCALE 1/4" = 1'-0"

FLOOR PLAN

ORIGINAL PAGE
OF FOUR QUALITY



ORIGINAL PAGE IS
OF POOR QUALITY

00000000

00000000

00000000

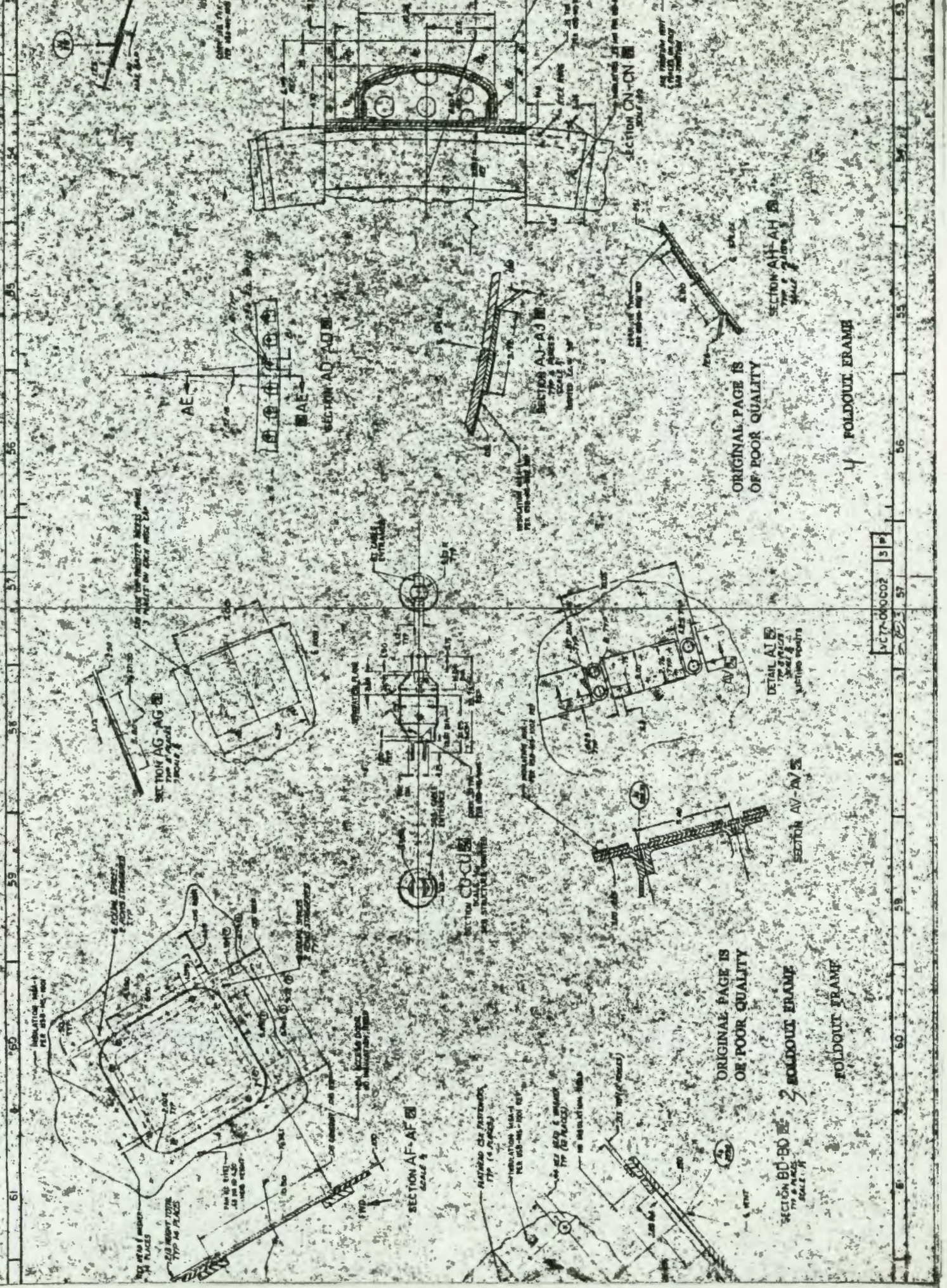
00000000

00000000

00000000

00000000

00000000



ORIGINAL PAGE IS
OF POOR QUALITY

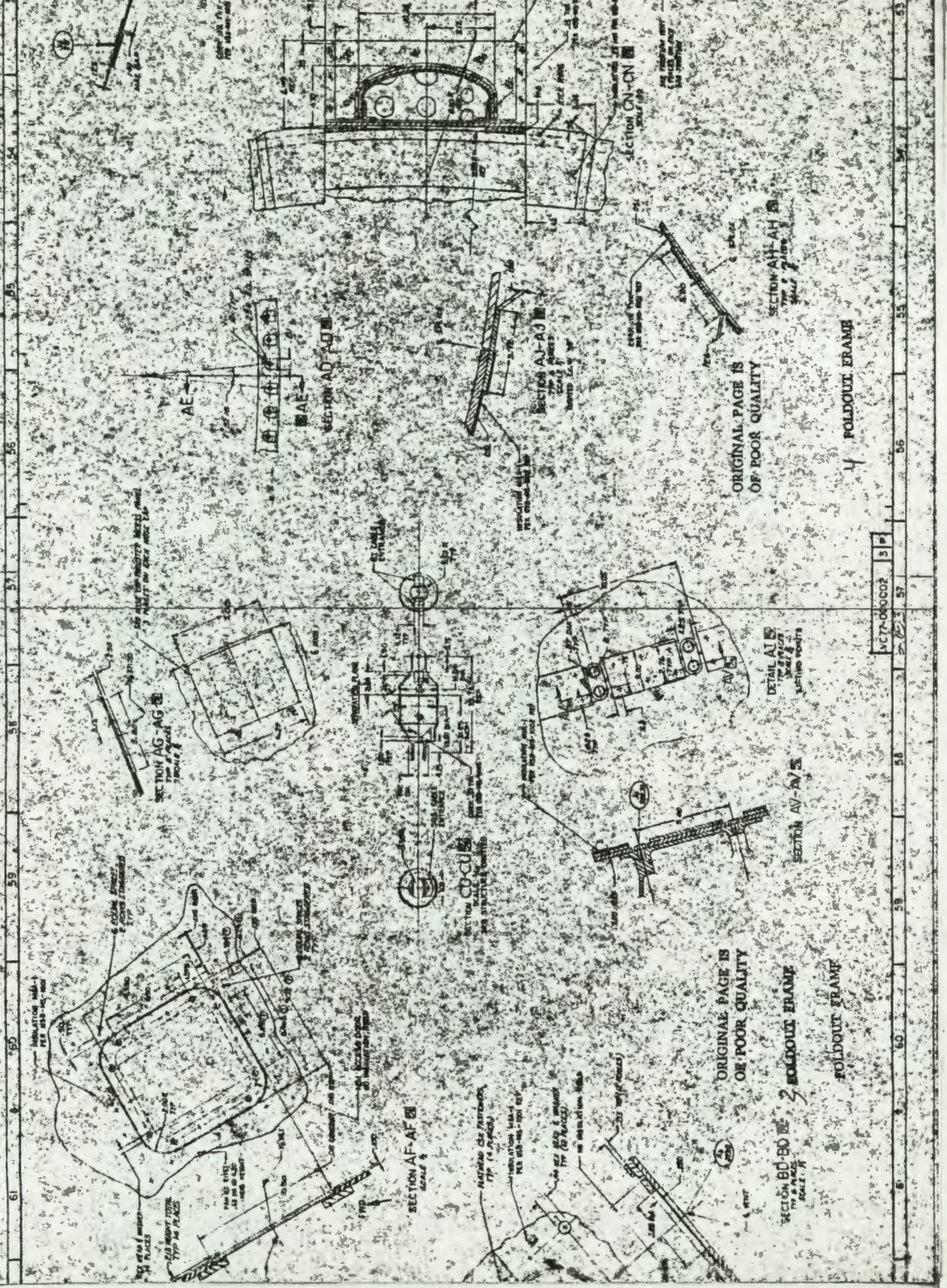
ORIGINAL PAGE IS
OF POOR QUALITY

FOLDOUT FRAME

FOLDOUT FRAME

FOLDOUT FRAME

VC7-00002 3 P

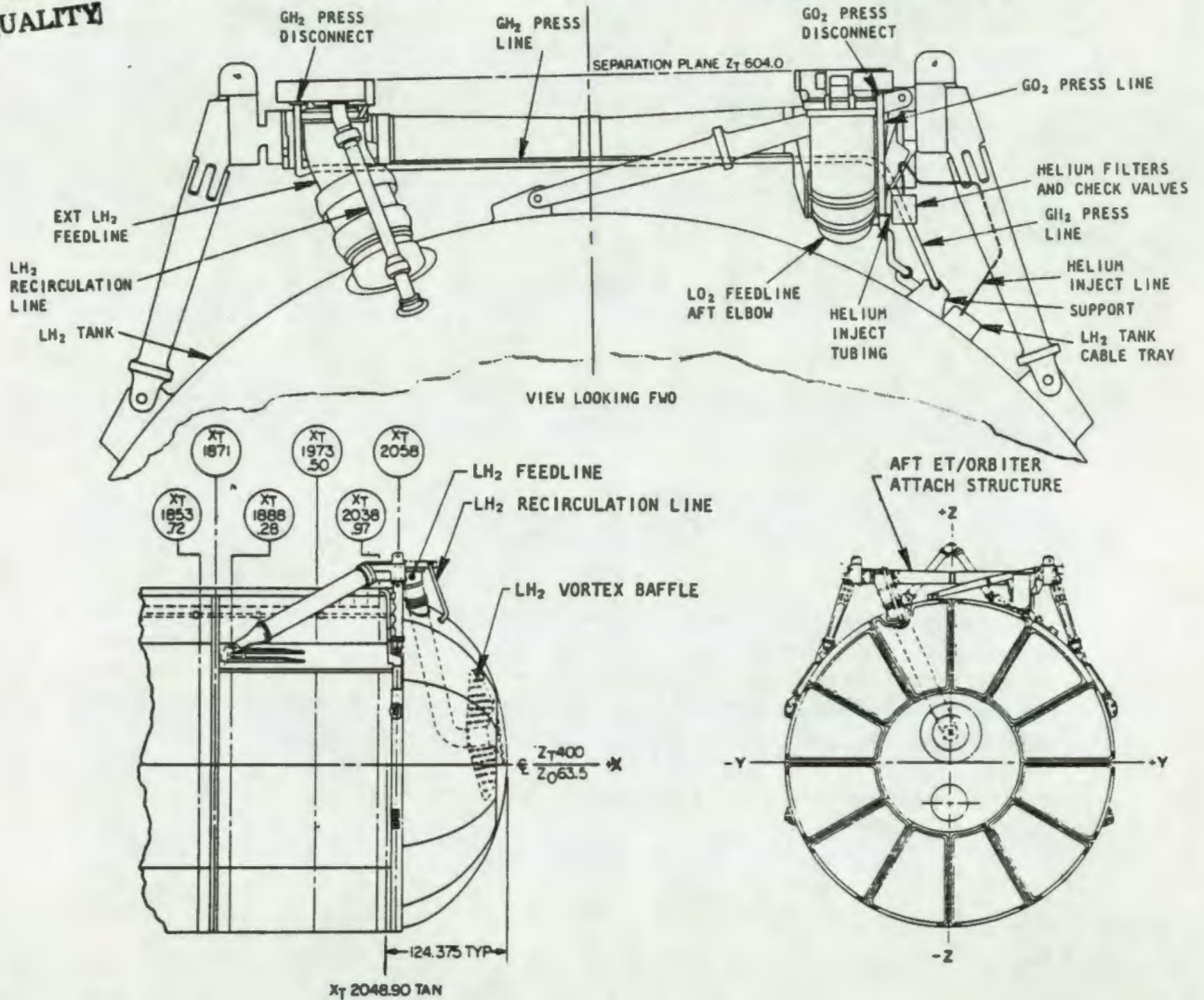


3.1.3 EXTERNAL TANK. The External Tank (ET), which supplies propellant and oxidizer to the Orbiter Vehicle's three main engines during both first and second-stage boost, has been configured to minimize drag of the Launch Vehicle during ascent. As a separate entity, subsequent to second-stage separation or RTLS abort separation, the ET includes all attach structure between the Orbiter and Tank, as well as a portion of the ET/SRB attach structure. The aft Orbiter/ET attach structure is shown in the photograph. The design of the ET is complicated by the feeder lines between the Tank and Orbiter which are mounted behind the aft attach structure as shown below. These lines include the LH₂ feedline, LH₂ recirculation line, the GO₂ pressure line, and LH₂ tank cable tray, as well as the Helium injection line, filters, check valves and support brackets.

States



ORIGINAL PAGE IS
OF POOR QUALITY



The External Tank is the only expendable element of the Space Shuttle Vehicle. Operational Launch Vehicles will employ two versions (either heavy or light weight) of the ET. Reference 3-6 delineates the particular tank to be used for any given operational flight. The External Tank is shown in Figure 3.1.3-1.

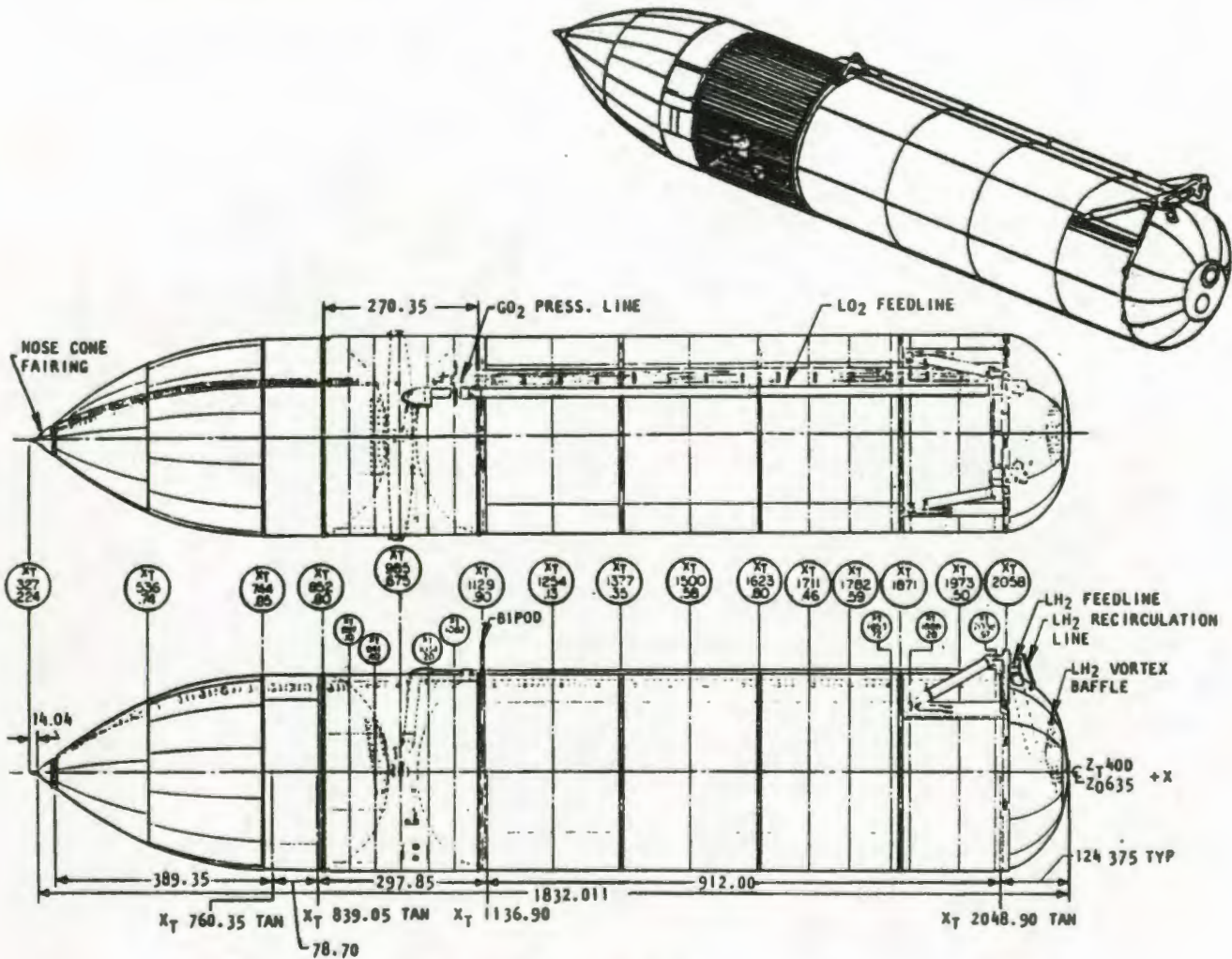
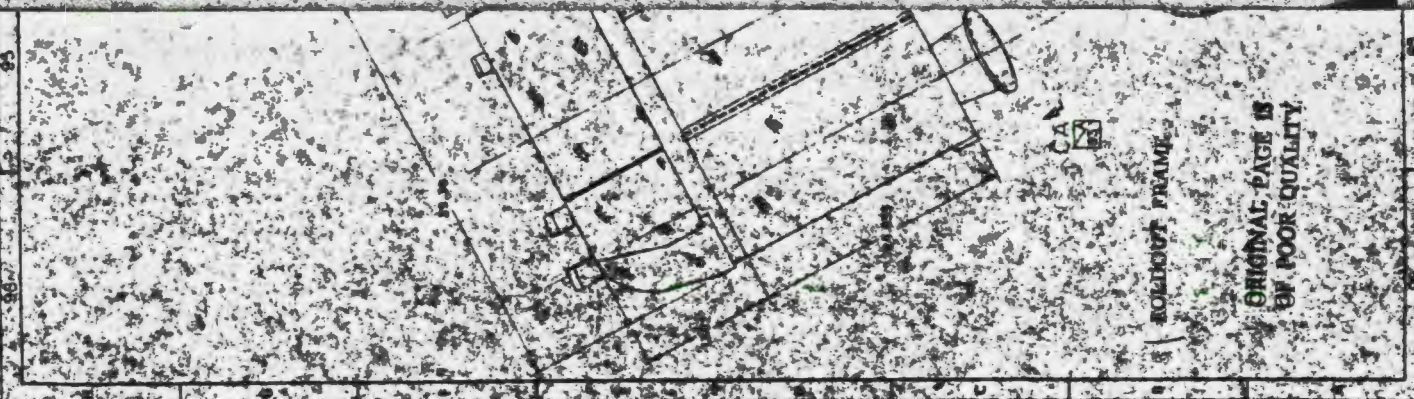


Figure 3.1.3-1
EXTERNAL TANK

The LO_2 anti-geyser line has been removed from the operational tanks as part of a weight reduction program, to remove a potential source of ice debris, and to cut costs. The elimination of this line saves approximately 600 pounds. The LH_2 pressure line has also been relocated from the left-hand side of the tank to the right-hand side.

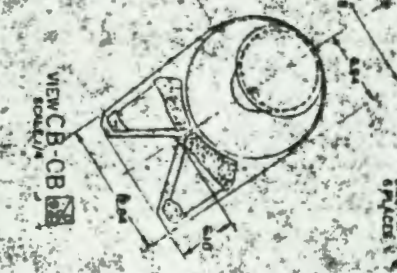
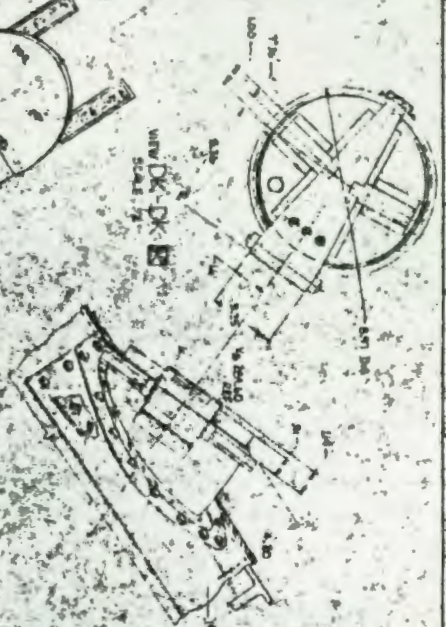
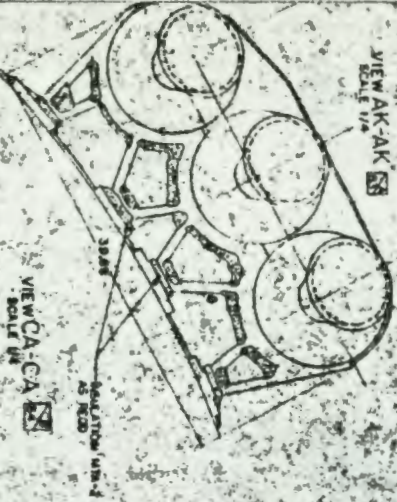
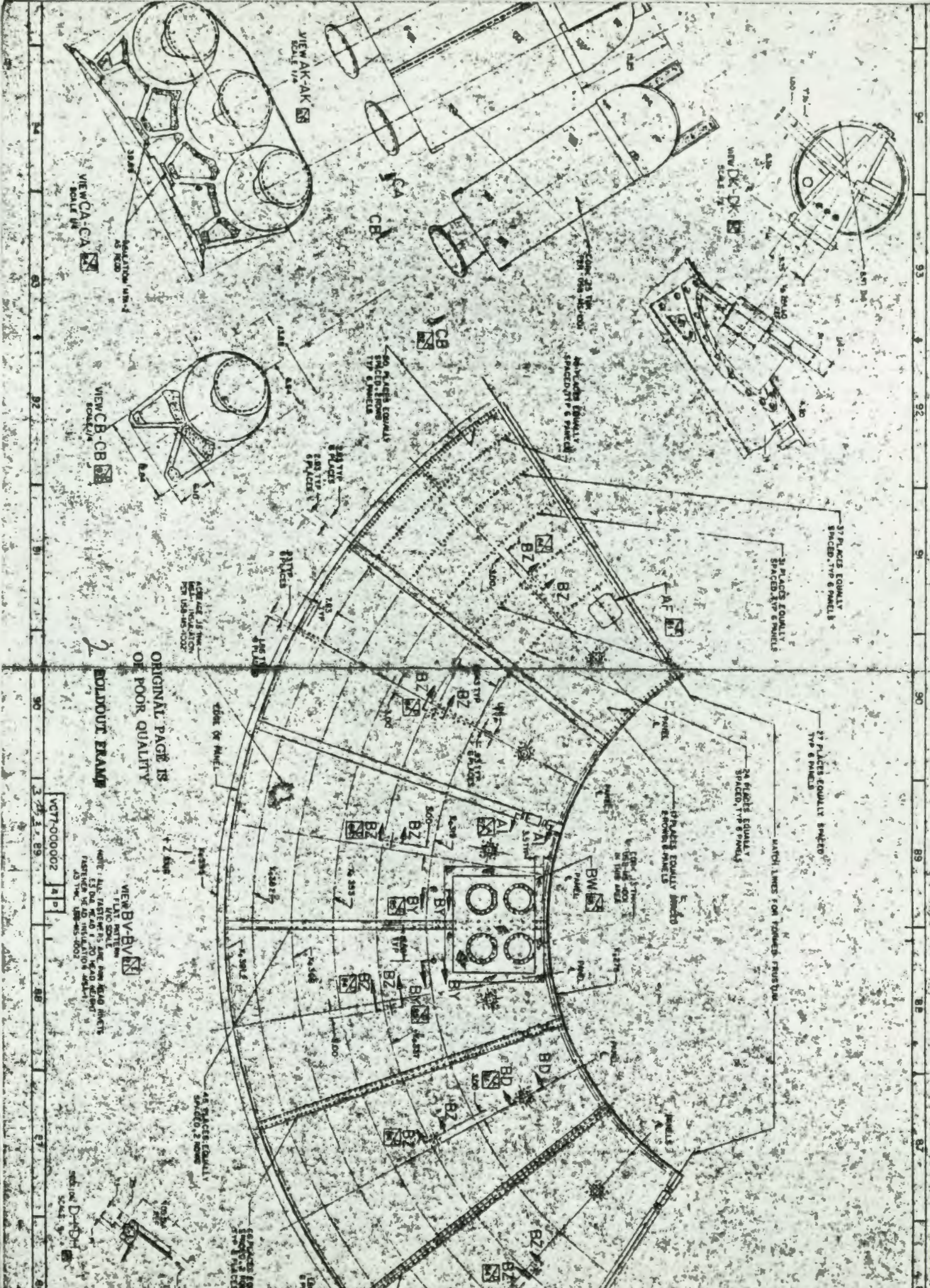
Design drawings for the External Tank are given in Figure(s) 3.1.3-2 (a through e).



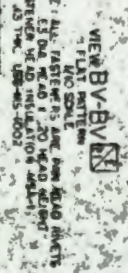
SOLIDITY FRAME

ORIGINAL PAGE IS
OF POOR QUALITY

ADAL-000000 0



2
ORIGINAL PAGE IS
OF POOR QUALITY
BOLDOUT FRAME

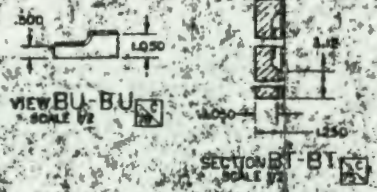
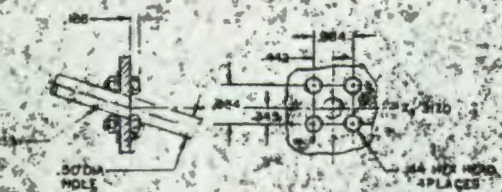


VCT7-000002 2 P

86 87 88 89 90 91 92 93 94

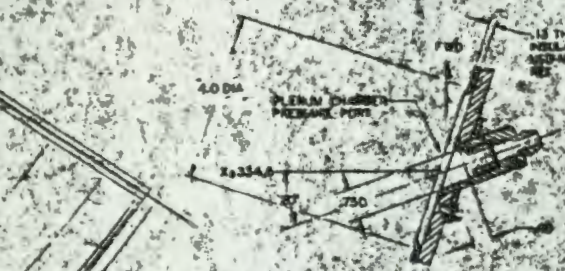
FOLDOUT FRAME

ORIGINAL PAGE IS OF POOR QUALITY



SECTION BY-BY SCALE 1/2

SECTION BT-BT SCALE 1/2



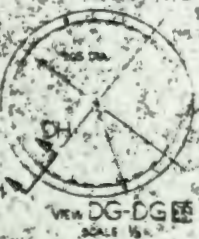
SECTION BZ-BZ SCALE 1/2



ORIGINAL PAGE IS OF POOR QUALITY

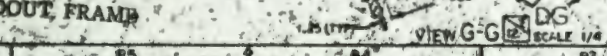


SECTION AK-AK SCALE 1/2

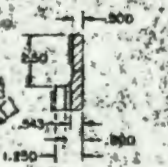


VIEW DG-DG SCALE 1/2

FOLDOUT FRAME



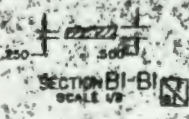
VIEW G-G SCALE 1/4



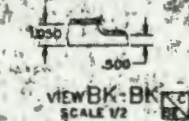
SECTION BF-BF SCALE 1/2



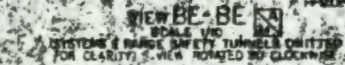
SECTION BL-BL SCALE 1/2



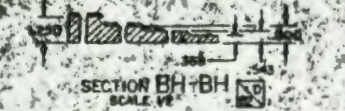
SECTION BI-BI SCALE 1/2



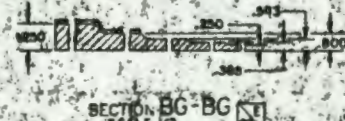
VIEW BK-BK SCALE 1/2



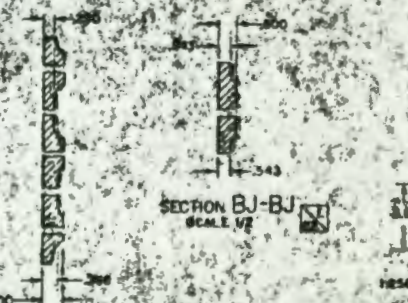
VIEW BE-BE SCALE 1/2



SECTION BH-BH SCALE 1/2



SECTION BG-BG SCALE 1/2



SECTION BJ-BJ SCALE 1/2

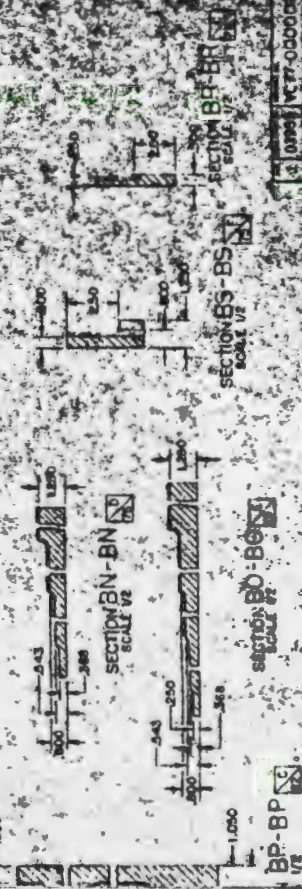
SECTION BM-BM SCALE 1/2

VC77-000002 4 P.

| | |
|-----|-----------------------|
| 1 | SEE PLAN FOR LOCATION |
| 2 | SEE PLAN FOR LOCATION |
| 3 | SEE PLAN FOR LOCATION |
| 4 | SEE PLAN FOR LOCATION |
| 5 | SEE PLAN FOR LOCATION |
| 6 | SEE PLAN FOR LOCATION |
| 7 | SEE PLAN FOR LOCATION |
| 8 | SEE PLAN FOR LOCATION |
| 9 | SEE PLAN FOR LOCATION |
| 10 | SEE PLAN FOR LOCATION |
| 11 | SEE PLAN FOR LOCATION |
| 12 | SEE PLAN FOR LOCATION |
| 13 | SEE PLAN FOR LOCATION |
| 14 | SEE PLAN FOR LOCATION |
| 15 | SEE PLAN FOR LOCATION |
| 16 | SEE PLAN FOR LOCATION |
| 17 | SEE PLAN FOR LOCATION |
| 18 | SEE PLAN FOR LOCATION |
| 19 | SEE PLAN FOR LOCATION |
| 20 | SEE PLAN FOR LOCATION |
| 21 | SEE PLAN FOR LOCATION |
| 22 | SEE PLAN FOR LOCATION |
| 23 | SEE PLAN FOR LOCATION |
| 24 | SEE PLAN FOR LOCATION |
| 25 | SEE PLAN FOR LOCATION |
| 26 | SEE PLAN FOR LOCATION |
| 27 | SEE PLAN FOR LOCATION |
| 28 | SEE PLAN FOR LOCATION |
| 29 | SEE PLAN FOR LOCATION |
| 30 | SEE PLAN FOR LOCATION |
| 31 | SEE PLAN FOR LOCATION |
| 32 | SEE PLAN FOR LOCATION |
| 33 | SEE PLAN FOR LOCATION |
| 34 | SEE PLAN FOR LOCATION |
| 35 | SEE PLAN FOR LOCATION |
| 36 | SEE PLAN FOR LOCATION |
| 37 | SEE PLAN FOR LOCATION |
| 38 | SEE PLAN FOR LOCATION |
| 39 | SEE PLAN FOR LOCATION |
| 40 | SEE PLAN FOR LOCATION |
| 41 | SEE PLAN FOR LOCATION |
| 42 | SEE PLAN FOR LOCATION |
| 43 | SEE PLAN FOR LOCATION |
| 44 | SEE PLAN FOR LOCATION |
| 45 | SEE PLAN FOR LOCATION |
| 46 | SEE PLAN FOR LOCATION |
| 47 | SEE PLAN FOR LOCATION |
| 48 | SEE PLAN FOR LOCATION |
| 49 | SEE PLAN FOR LOCATION |
| 50 | SEE PLAN FOR LOCATION |
| 51 | SEE PLAN FOR LOCATION |
| 52 | SEE PLAN FOR LOCATION |
| 53 | SEE PLAN FOR LOCATION |
| 54 | SEE PLAN FOR LOCATION |
| 55 | SEE PLAN FOR LOCATION |
| 56 | SEE PLAN FOR LOCATION |
| 57 | SEE PLAN FOR LOCATION |
| 58 | SEE PLAN FOR LOCATION |
| 59 | SEE PLAN FOR LOCATION |
| 60 | SEE PLAN FOR LOCATION |
| 61 | SEE PLAN FOR LOCATION |
| 62 | SEE PLAN FOR LOCATION |
| 63 | SEE PLAN FOR LOCATION |
| 64 | SEE PLAN FOR LOCATION |
| 65 | SEE PLAN FOR LOCATION |
| 66 | SEE PLAN FOR LOCATION |
| 67 | SEE PLAN FOR LOCATION |
| 68 | SEE PLAN FOR LOCATION |
| 69 | SEE PLAN FOR LOCATION |
| 70 | SEE PLAN FOR LOCATION |
| 71 | SEE PLAN FOR LOCATION |
| 72 | SEE PLAN FOR LOCATION |
| 73 | SEE PLAN FOR LOCATION |
| 74 | SEE PLAN FOR LOCATION |
| 75 | SEE PLAN FOR LOCATION |
| 76 | SEE PLAN FOR LOCATION |
| 77 | SEE PLAN FOR LOCATION |
| 78 | SEE PLAN FOR LOCATION |
| 79 | SEE PLAN FOR LOCATION |
| 80 | SEE PLAN FOR LOCATION |
| 81 | SEE PLAN FOR LOCATION |
| 82 | SEE PLAN FOR LOCATION |
| 83 | SEE PLAN FOR LOCATION |
| 84 | SEE PLAN FOR LOCATION |
| 85 | SEE PLAN FOR LOCATION |
| 86 | SEE PLAN FOR LOCATION |
| 87 | SEE PLAN FOR LOCATION |
| 88 | SEE PLAN FOR LOCATION |
| 89 | SEE PLAN FOR LOCATION |
| 90 | SEE PLAN FOR LOCATION |
| 91 | SEE PLAN FOR LOCATION |
| 92 | SEE PLAN FOR LOCATION |
| 93 | SEE PLAN FOR LOCATION |
| 94 | SEE PLAN FOR LOCATION |
| 95 | SEE PLAN FOR LOCATION |
| 96 | SEE PLAN FOR LOCATION |
| 97 | SEE PLAN FOR LOCATION |
| 98 | SEE PLAN FOR LOCATION |
| 99 | SEE PLAN FOR LOCATION |
| 100 | SEE PLAN FOR LOCATION |

REVISIONS

ORIGINAL PAGE
OF POOR QUALITY



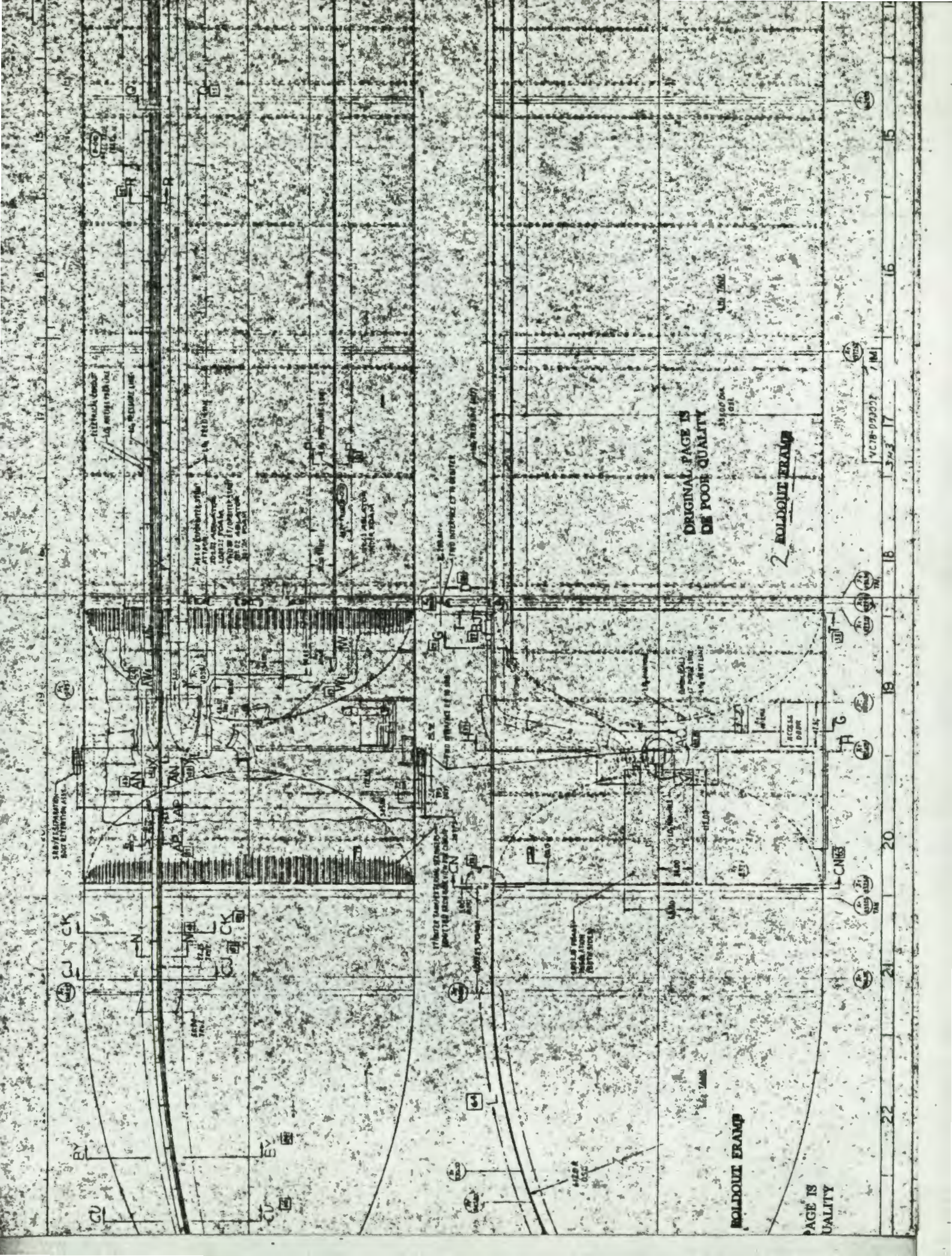
10000 VCT-00000



ORIGINAL
OF POOR Q

24
25

AC 1000000



ORIGINAL PAGE IS OF POOR QUALITY

RAILROAD YARD

RAILROAD YARD

PAGE IS OF POOR QUALITY

1 MILE

VC78-033002

343

18

19

20

21

22

23

24

25

26

27

28

29

30

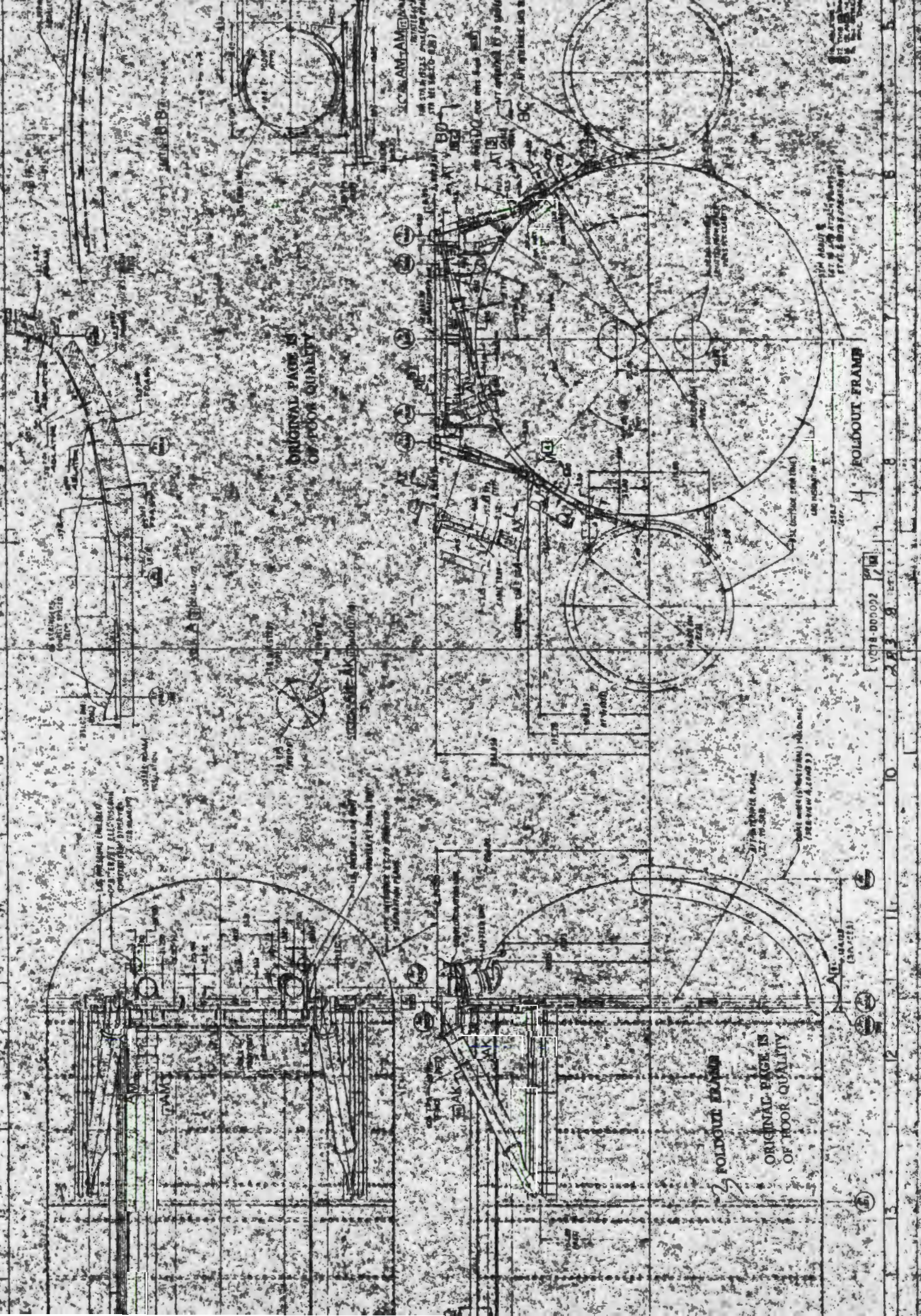
ORIGINAL PAGE IS
OF POOR QUALITY

FOLDOUT FRAME

VQ78-00002

FOLDOUT FRAME

ORIGINAL PAGE IS
OF POOR QUALITY



ORIGINAL PAGE IS
OF POOR QUALITY

UPPER
PARTS

FIG. 1 (CONT'D)
SUPPORT BRACKET
BY THE SPEC.



UPPER PARTS

UPPER PARTS TO BE ATTACHED TO THE LOWER PARTS



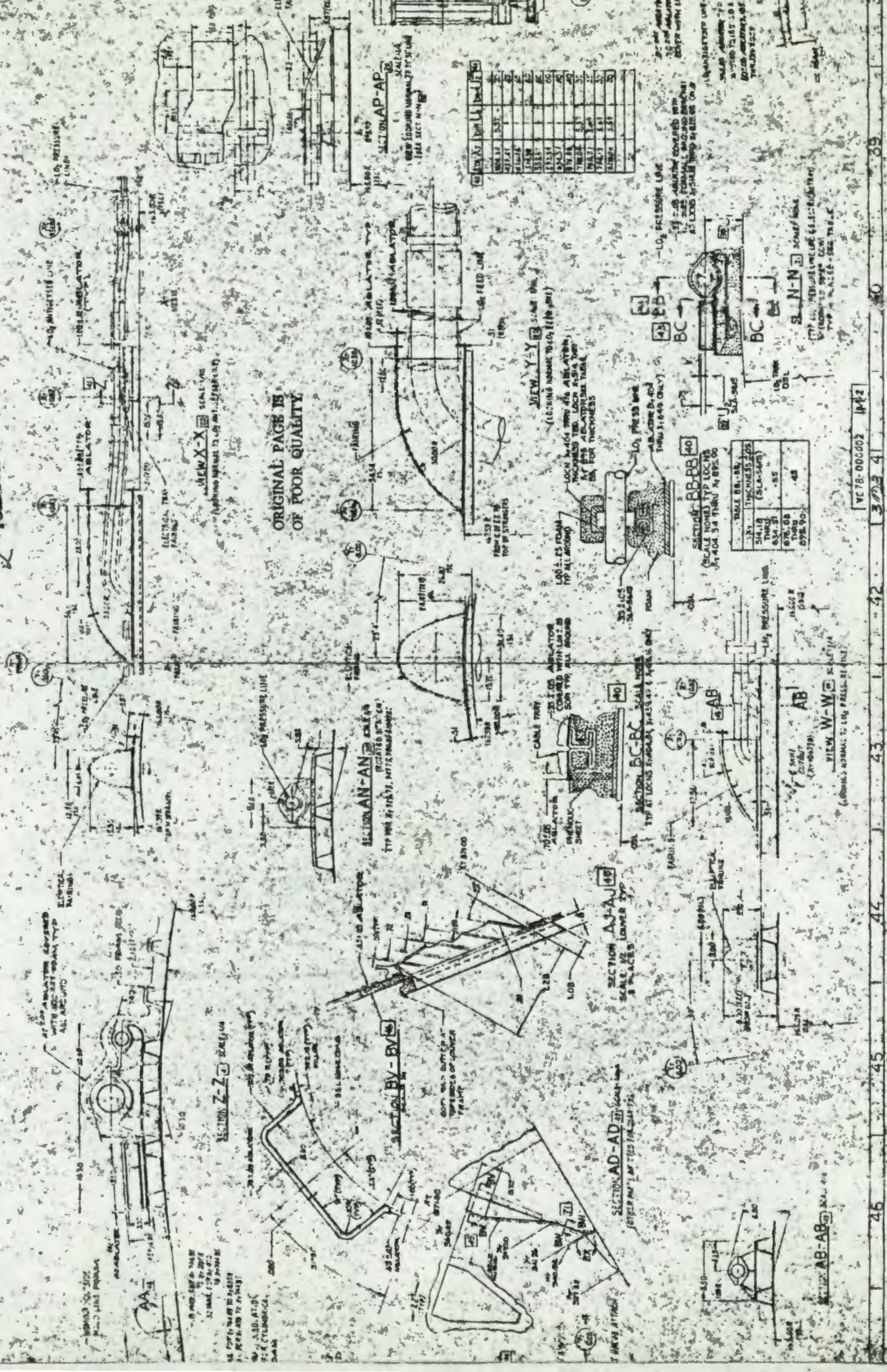
UPPER PARTS

FOLDOUT FRAME

AC 19-00000B 5

2 FOLDOUT ERAMP

ORIGINAL PAGE IS
OF POOR QUALITY



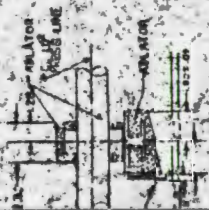
| ITEM NO. | DESCRIPTION | QTY | UNIT |
|----------|-------------|-----|------|
| 1001 | ... | ... | ... |
| 1002 | ... | ... | ... |
| 1003 | ... | ... | ... |
| 1004 | ... | ... | ... |
| 1005 | ... | ... | ... |
| 1006 | ... | ... | ... |
| 1007 | ... | ... | ... |
| 1008 | ... | ... | ... |
| 1009 | ... | ... | ... |
| 1010 | ... | ... | ... |

| ITEM NO. | DESCRIPTION | QTY | UNIT |
|----------|-------------|-----|------|
| 1011 | ... | ... | ... |
| 1012 | ... | ... | ... |
| 1013 | ... | ... | ... |
| 1014 | ... | ... | ... |
| 1015 | ... | ... | ... |
| 1016 | ... | ... | ... |
| 1017 | ... | ... | ... |
| 1018 | ... | ... | ... |
| 1019 | ... | ... | ... |
| 1020 | ... | ... | ... |

VC 78-000002 142

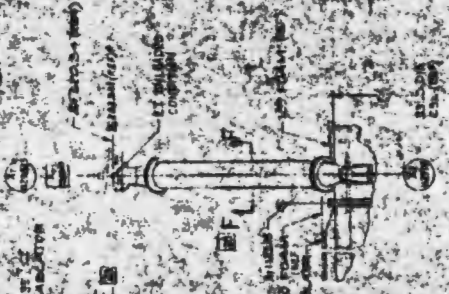
46 45 44 43 42 41 40 39

| | | |
|-----|---------------|--------------|
| 1 | SECTION C1-C1 | 1/4" = 1'-0" |
| 2 | SECTION F-F | 1/4" = 1'-0" |
| 3 | SECTION D-D | 1/4" = 1'-0" |
| 4 | SECTION A1-A1 | 1/4" = 1'-0" |
| 5 | SECTION B1-B1 | 1/4" = 1'-0" |
| 6 | SECTION C1-C1 | 1/4" = 1'-0" |
| 7 | SECTION D-D | 1/4" = 1'-0" |
| 8 | SECTION E-E | 1/4" = 1'-0" |
| 9 | SECTION F-F | 1/4" = 1'-0" |
| 10 | SECTION G-G | 1/4" = 1'-0" |
| 11 | SECTION H-H | 1/4" = 1'-0" |
| 12 | SECTION I-I | 1/4" = 1'-0" |
| 13 | SECTION J-J | 1/4" = 1'-0" |
| 14 | SECTION K-K | 1/4" = 1'-0" |
| 15 | SECTION L-L | 1/4" = 1'-0" |
| 16 | SECTION M-M | 1/4" = 1'-0" |
| 17 | SECTION N-N | 1/4" = 1'-0" |
| 18 | SECTION O-O | 1/4" = 1'-0" |
| 19 | SECTION P-P | 1/4" = 1'-0" |
| 20 | SECTION Q-Q | 1/4" = 1'-0" |
| 21 | SECTION R-R | 1/4" = 1'-0" |
| 22 | SECTION S-S | 1/4" = 1'-0" |
| 23 | SECTION T-T | 1/4" = 1'-0" |
| 24 | SECTION U-U | 1/4" = 1'-0" |
| 25 | SECTION V-V | 1/4" = 1'-0" |
| 26 | SECTION W-W | 1/4" = 1'-0" |
| 27 | SECTION X-X | 1/4" = 1'-0" |
| 28 | SECTION Y-Y | 1/4" = 1'-0" |
| 29 | SECTION Z-Z | 1/4" = 1'-0" |
| 30 | SECTION AA-AA | 1/4" = 1'-0" |
| 31 | SECTION BB-BB | 1/4" = 1'-0" |
| 32 | SECTION CC-CC | 1/4" = 1'-0" |
| 33 | SECTION DD-DD | 1/4" = 1'-0" |
| 34 | SECTION EE-EE | 1/4" = 1'-0" |
| 35 | SECTION FF-FF | 1/4" = 1'-0" |
| 36 | SECTION GG-GG | 1/4" = 1'-0" |
| 37 | SECTION HH-HH | 1/4" = 1'-0" |
| 38 | SECTION II-II | 1/4" = 1'-0" |
| 39 | SECTION JJ-JJ | 1/4" = 1'-0" |
| 40 | SECTION KK-KK | 1/4" = 1'-0" |
| 41 | SECTION LL-LL | 1/4" = 1'-0" |
| 42 | SECTION MM-MM | 1/4" = 1'-0" |
| 43 | SECTION NN-NN | 1/4" = 1'-0" |
| 44 | SECTION OO-OO | 1/4" = 1'-0" |
| 45 | SECTION PP-PP | 1/4" = 1'-0" |
| 46 | SECTION QQ-QQ | 1/4" = 1'-0" |
| 47 | SECTION RR-RR | 1/4" = 1'-0" |
| 48 | SECTION SS-SS | 1/4" = 1'-0" |
| 49 | SECTION TT-TT | 1/4" = 1'-0" |
| 50 | SECTION UU-UU | 1/4" = 1'-0" |
| 51 | SECTION VV-VV | 1/4" = 1'-0" |
| 52 | SECTION WW-WW | 1/4" = 1'-0" |
| 53 | SECTION XX-XX | 1/4" = 1'-0" |
| 54 | SECTION YY-YY | 1/4" = 1'-0" |
| 55 | SECTION ZZ-ZZ | 1/4" = 1'-0" |
| 56 | SECTION AA-AA | 1/4" = 1'-0" |
| 57 | SECTION BB-BB | 1/4" = 1'-0" |
| 58 | SECTION CC-CC | 1/4" = 1'-0" |
| 59 | SECTION DD-DD | 1/4" = 1'-0" |
| 60 | SECTION EE-EE | 1/4" = 1'-0" |
| 61 | SECTION FF-FF | 1/4" = 1'-0" |
| 62 | SECTION GG-GG | 1/4" = 1'-0" |
| 63 | SECTION HH-HH | 1/4" = 1'-0" |
| 64 | SECTION II-II | 1/4" = 1'-0" |
| 65 | SECTION JJ-JJ | 1/4" = 1'-0" |
| 66 | SECTION KK-KK | 1/4" = 1'-0" |
| 67 | SECTION LL-LL | 1/4" = 1'-0" |
| 68 | SECTION MM-MM | 1/4" = 1'-0" |
| 69 | SECTION NN-NN | 1/4" = 1'-0" |
| 70 | SECTION OO-OO | 1/4" = 1'-0" |
| 71 | SECTION PP-PP | 1/4" = 1'-0" |
| 72 | SECTION QQ-QQ | 1/4" = 1'-0" |
| 73 | SECTION RR-RR | 1/4" = 1'-0" |
| 74 | SECTION SS-SS | 1/4" = 1'-0" |
| 75 | SECTION TT-TT | 1/4" = 1'-0" |
| 76 | SECTION UU-UU | 1/4" = 1'-0" |
| 77 | SECTION VV-VV | 1/4" = 1'-0" |
| 78 | SECTION WW-WW | 1/4" = 1'-0" |
| 79 | SECTION XX-XX | 1/4" = 1'-0" |
| 80 | SECTION YY-YY | 1/4" = 1'-0" |
| 81 | SECTION ZZ-ZZ | 1/4" = 1'-0" |
| 82 | SECTION AA-AA | 1/4" = 1'-0" |
| 83 | SECTION BB-BB | 1/4" = 1'-0" |
| 84 | SECTION CC-CC | 1/4" = 1'-0" |
| 85 | SECTION DD-DD | 1/4" = 1'-0" |
| 86 | SECTION EE-EE | 1/4" = 1'-0" |
| 87 | SECTION FF-FF | 1/4" = 1'-0" |
| 88 | SECTION GG-GG | 1/4" = 1'-0" |
| 89 | SECTION HH-HH | 1/4" = 1'-0" |
| 90 | SECTION II-II | 1/4" = 1'-0" |
| 91 | SECTION JJ-JJ | 1/4" = 1'-0" |
| 92 | SECTION KK-KK | 1/4" = 1'-0" |
| 93 | SECTION LL-LL | 1/4" = 1'-0" |
| 94 | SECTION MM-MM | 1/4" = 1'-0" |
| 95 | SECTION NN-NN | 1/4" = 1'-0" |
| 96 | SECTION OO-OO | 1/4" = 1'-0" |
| 97 | SECTION PP-PP | 1/4" = 1'-0" |
| 98 | SECTION QQ-QQ | 1/4" = 1'-0" |
| 99 | SECTION RR-RR | 1/4" = 1'-0" |
| 100 | SECTION SS-SS | 1/4" = 1'-0" |

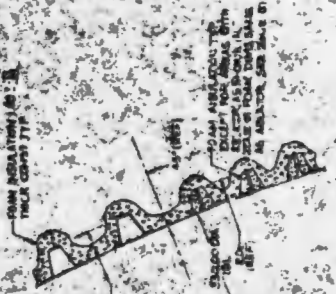


SECTION C1-C1

SECTION F-F



SECTION D-D



SECTION A1-A1

FOLDOUT FRAME

ORIGINAL PAGE IS OF POOR QUALITY

JACOBS VCM-3060

26 27 28



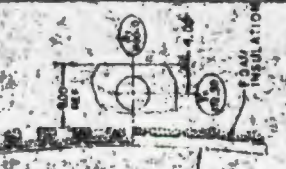
SECTION BW-BY



VIEW BX-BX

FOURTH FLOOR

ORIG
OF I



SECTION BA-BA
SCALE NONE

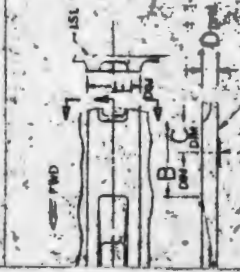
| | | | | |
|-----|------|----|------|-------------|
| REV | DATE | BY | CHKD | DESCRIPTION |
| 1 | | | | |
| 2 | | | | |
| 3 | | | | |
| 4 | | | | |
| 5 | | | | |

| | |
|---------|----------|
| SECTION | POSITION |
| NO. 1 | NO. 1 |
| NO. 2 | NO. 2 |
| NO. 3 | NO. 3 |
| NO. 4 | NO. 4 |
| NO. 5 | NO. 5 |

| ITEM NO. | DESCRIPTION | QTY | UNIT | REMARKS |
|----------|-------------|-----|------|---------|
| 1 | ... | ... | ... | ... |
| 2 | ... | ... | ... | ... |
| 3 | ... | ... | ... | ... |
| 4 | ... | ... | ... | ... |
| 5 | ... | ... | ... | ... |
| 6 | ... | ... | ... | ... |
| 7 | ... | ... | ... | ... |
| 8 | ... | ... | ... | ... |
| 9 | ... | ... | ... | ... |
| 10 | ... | ... | ... | ... |
| 11 | ... | ... | ... | ... |
| 12 | ... | ... | ... | ... |
| 13 | ... | ... | ... | ... |
| 14 | ... | ... | ... | ... |
| 15 | ... | ... | ... | ... |
| 16 | ... | ... | ... | ... |
| 17 | ... | ... | ... | ... |
| 18 | ... | ... | ... | ... |
| 19 | ... | ... | ... | ... |
| 20 | ... | ... | ... | ... |
| 21 | ... | ... | ... | ... |
| 22 | ... | ... | ... | ... |
| 23 | ... | ... | ... | ... |
| 24 | ... | ... | ... | ... |
| 25 | ... | ... | ... | ... |
| 26 | ... | ... | ... | ... |
| 27 | ... | ... | ... | ... |
| 28 | ... | ... | ... | ... |
| 29 | ... | ... | ... | ... |
| 30 | ... | ... | ... | ... |
| 31 | ... | ... | ... | ... |
| 32 | ... | ... | ... | ... |
| 33 | ... | ... | ... | ... |
| 34 | ... | ... | ... | ... |
| 35 | ... | ... | ... | ... |
| 36 | ... | ... | ... | ... |
| 37 | ... | ... | ... | ... |
| 38 | ... | ... | ... | ... |
| 39 | ... | ... | ... | ... |
| 40 | ... | ... | ... | ... |
| 41 | ... | ... | ... | ... |
| 42 | ... | ... | ... | ... |
| 43 | ... | ... | ... | ... |
| 44 | ... | ... | ... | ... |
| 45 | ... | ... | ... | ... |
| 46 | ... | ... | ... | ... |
| 47 | ... | ... | ... | ... |
| 48 | ... | ... | ... | ... |
| 49 | ... | ... | ... | ... |
| 50 | ... | ... | ... | ... |

ORIGINAL PAGE IS
OF POOR QUALITY

FOLDOUT PLATE

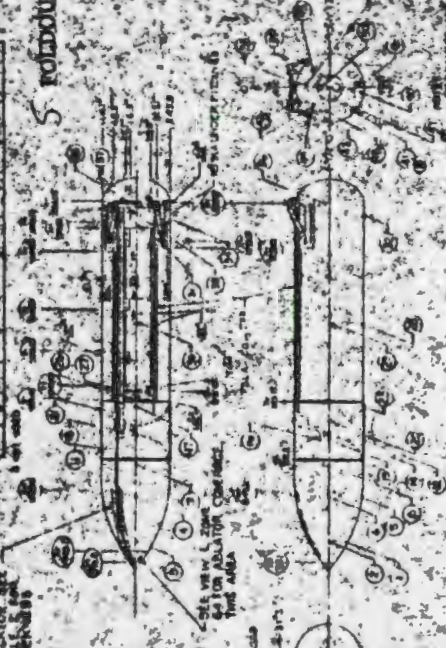


LAND NO 18 IS 80 ZI
QUANTITY ON INTERMEDIATE
AND STEEL THRUST BAND.



ISLAND 27
ON 11g DRAW

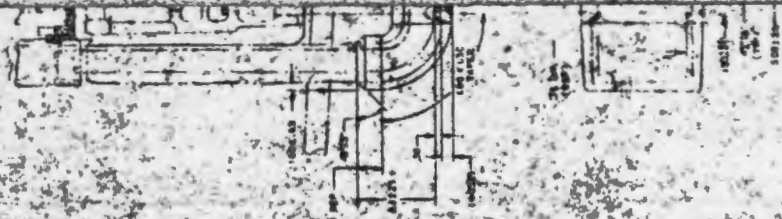
CALLOUT SEE
THICKNESS



| TABLE 3 | THICKNESS |
|---------|-----------|
| 1 | 415.1 |
| 2 | 428.2 |
| 3 | 441.3 |
| 4 | 454.4 |
| 5 | 467.5 |
| 6 | 480.6 |
| 7 | 493.7 |
| 8 | 506.8 |
| 9 | 519.9 |
| 10 | 533.0 |
| 11 | 546.1 |
| 12 | 559.2 |
| 13 | 572.3 |
| 14 | 585.4 |
| 15 | 598.5 |
| 16 | 611.6 |
| 17 | 624.7 |
| 18 | 637.8 |
| 19 | 650.9 |
| 20 | 664.0 |
| 21 | 677.1 |
| 22 | 690.2 |
| 23 | 703.3 |
| 24 | 716.4 |
| 25 | 729.5 |
| 26 | 742.6 |
| 27 | 755.7 |
| 28 | 768.8 |
| 29 | 781.9 |
| 30 | 795.0 |
| 31 | 808.1 |
| 32 | 821.2 |
| 33 | 834.3 |
| 34 | 847.4 |
| 35 | 860.5 |
| 36 | 873.6 |
| 37 | 886.7 |
| 38 | 899.8 |
| 39 | 912.9 |
| 40 | 926.0 |
| 41 | 939.1 |
| 42 | 952.2 |
| 43 | 965.3 |
| 44 | 978.4 |
| 45 | 991.5 |
| 46 | 1004.6 |
| 47 | 1017.7 |
| 48 | 1030.8 |
| 49 | 1043.9 |
| 50 | 1057.0 |

THIS PART FABRICATED TO SPECIFICATION
STANDARD FOR 752 SEE PART 75203 (SUBS 1, 2)
SMALL HOLES

9-2



10

SECTION EG-C6E
(REVISED 5-27-60)
FOR USE IN THE
SECTION OF
STATION AND ORION
PLANS A, B, C, D, E, F, G, H, I, J, K, L, M, N, O, P, Q, R, S, T, U, V, W, X, Y, Z

ORIGINAL PAGE IS
OF POOR QUALITY

SECTION GZ
BOLDDOUT FRAME

ORIGINAL PAGE IS
OF POOR QUALITY

FOLDOUT FRAME

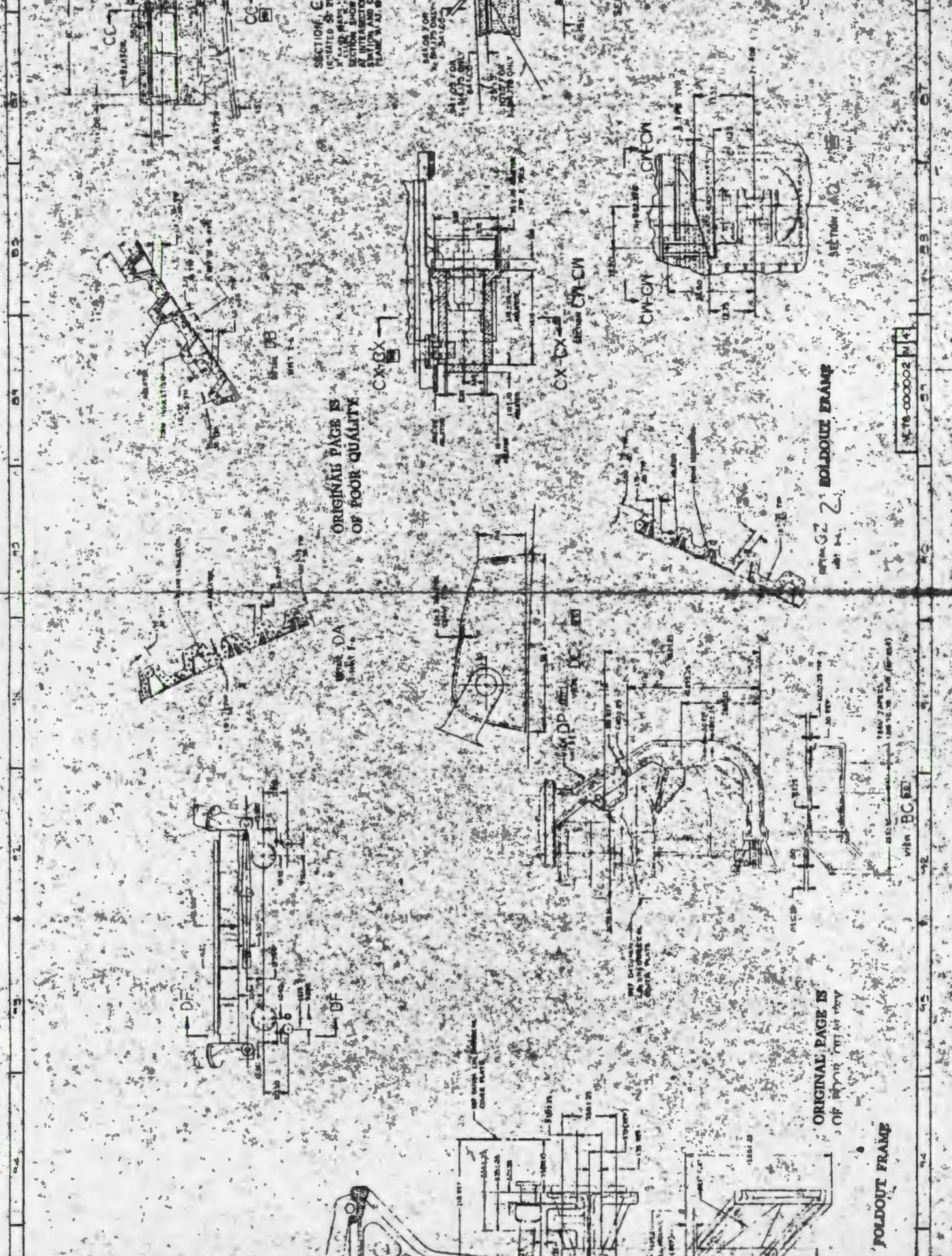
SECTION BC

SECTION DA

SECTION CX

SECTION CW

SECTION AG



44 43 42 41 40 39 38 37 36 35 34 33 32 31 30 29 28 27 26 25 24 23 22 21 20 19 18 17 16 15 14 13 12 11 10 9 8 7 6 5 4 3 2 1

44 43 42 41 40 39 38 37 36 35 34 33 32 31 30 29 28 27 26 25 24 23 22 21 20 19 18 17 16 15 14 13 12 11 10 9 8 7 6 5 4 3 2 1

SECTION EG-C6E

SECTION DA

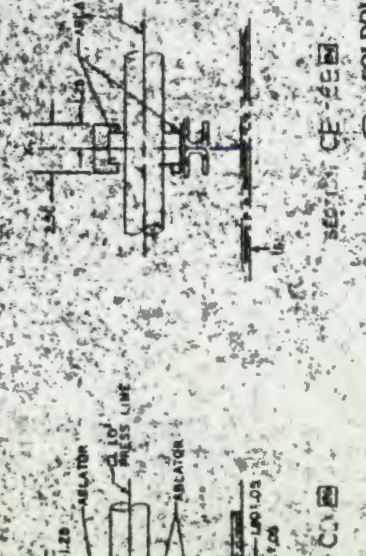
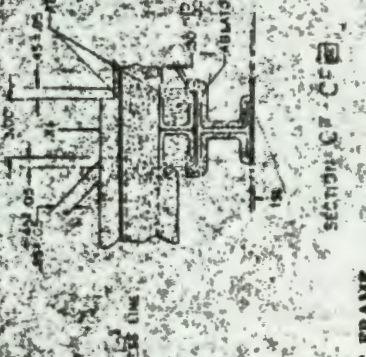
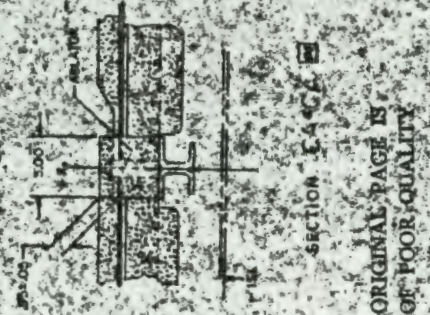
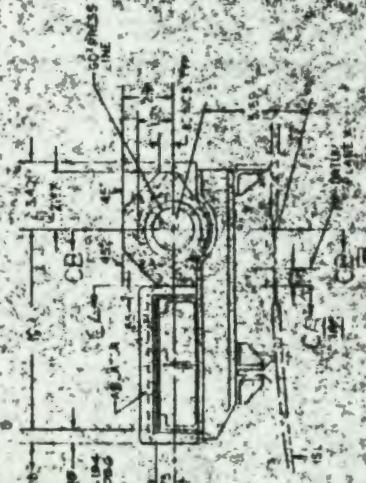
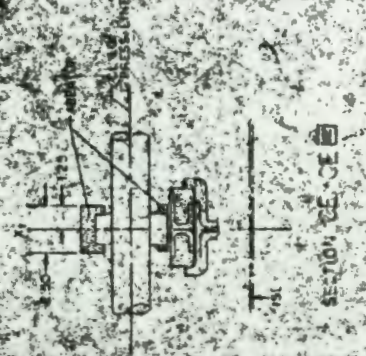
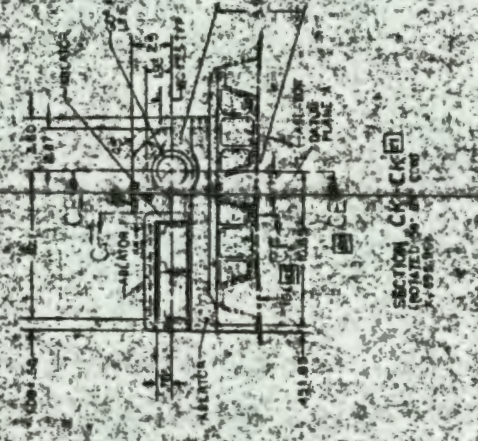
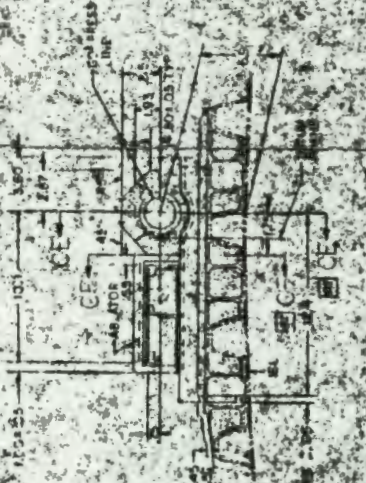
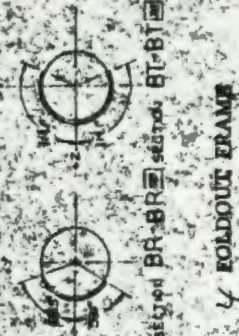
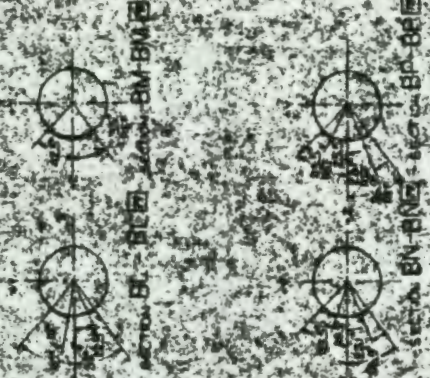
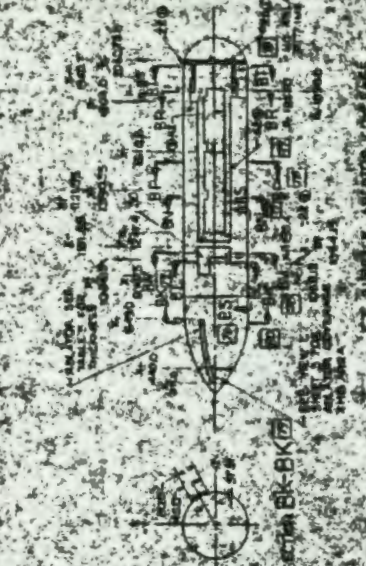
SECTION CX

SECTION CW

SECTION AG

SECTION BC

| NO. | REV. | DATE | BY | CHKD. | APP. |
|-----|------|------|----|-------|------|
| 1 | | | | | |
| 2 | | | | | |
| 3 | | | | | |
| 4 | | | | | |
| 5 | | | | | |
| 6 | | | | | |
| 7 | | | | | |
| 8 | | | | | |
| 9 | | | | | |
| 10 | | | | | |



FOLDOUT FRAME

FOLDOUT FRAME

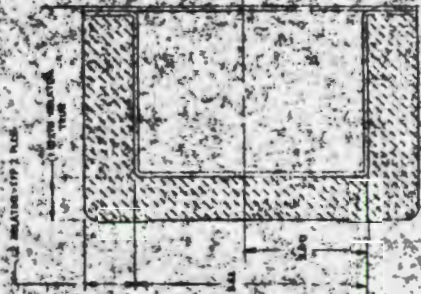
100-000002

100-000002

100-000002

ORIGINAL PAGE IS
OF POOR QUALITY

COLLAPSE FRAME



3F-BF 65

SECTION CX-CX 65

76

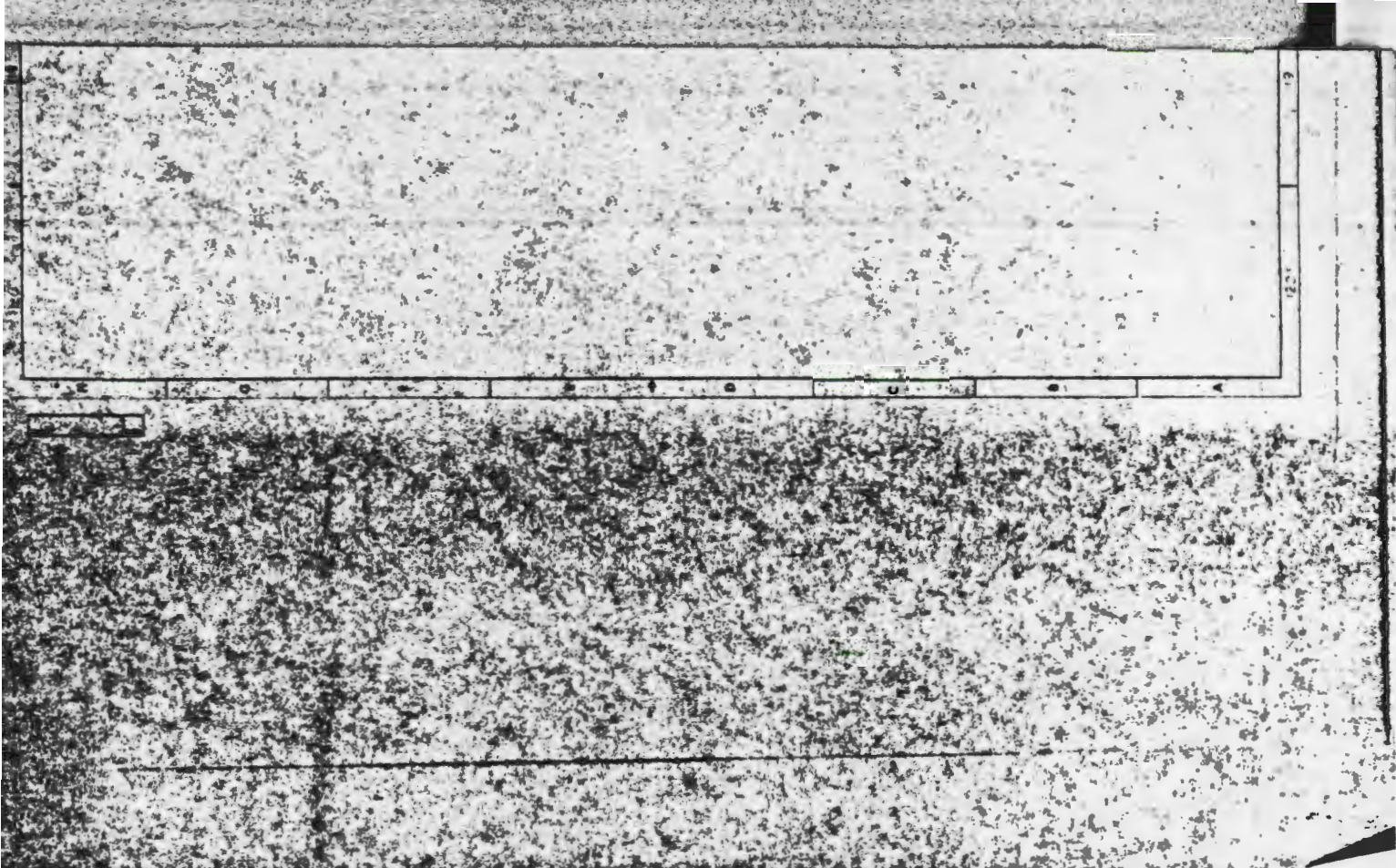
75

74

73

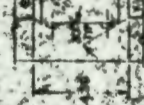
72

1





DETAIL D1



DETAIL D2



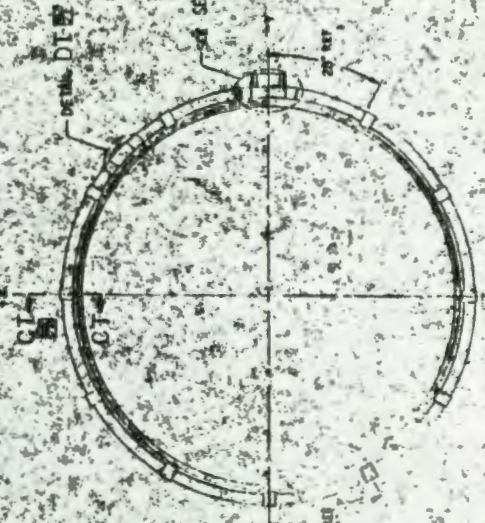
SECTION ON-CRIB



SECTION ED-ED



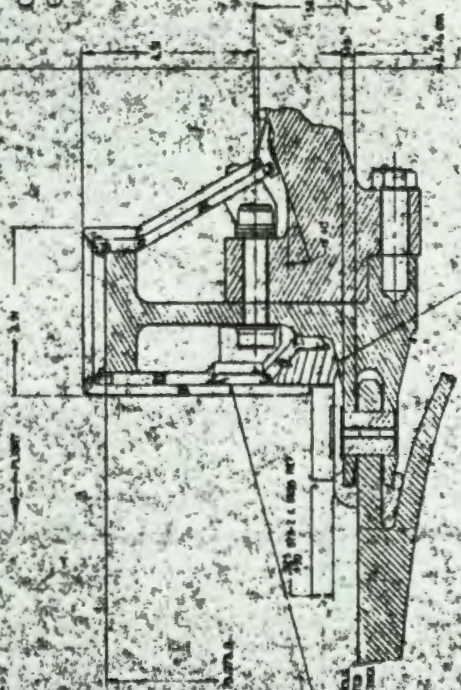
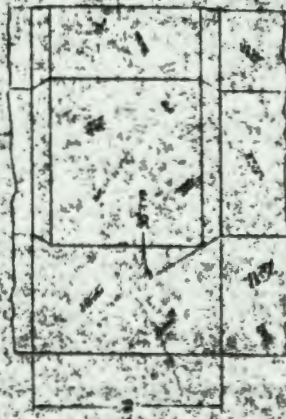
VIEW EB-EB



SECTION CS-CS

ORIGINAL PAGE IS
OF POOR QUALITY

FOLDOUT FRAME



VIEW EK

FOLDOUT FRAME

ORIGINAL PAGE IS
OF POOR QUALITY

VC 77-000002 5 P



| | | |
|-----|------|-------------|
| NO. | DATE | DESCRIPTION |
| | | |
| | | |
| | | |

200000-14A

03953 K 17-00002

97 98 99 100



SECTION DS-DS
SCALE 1/2"



NOT TO SCALE

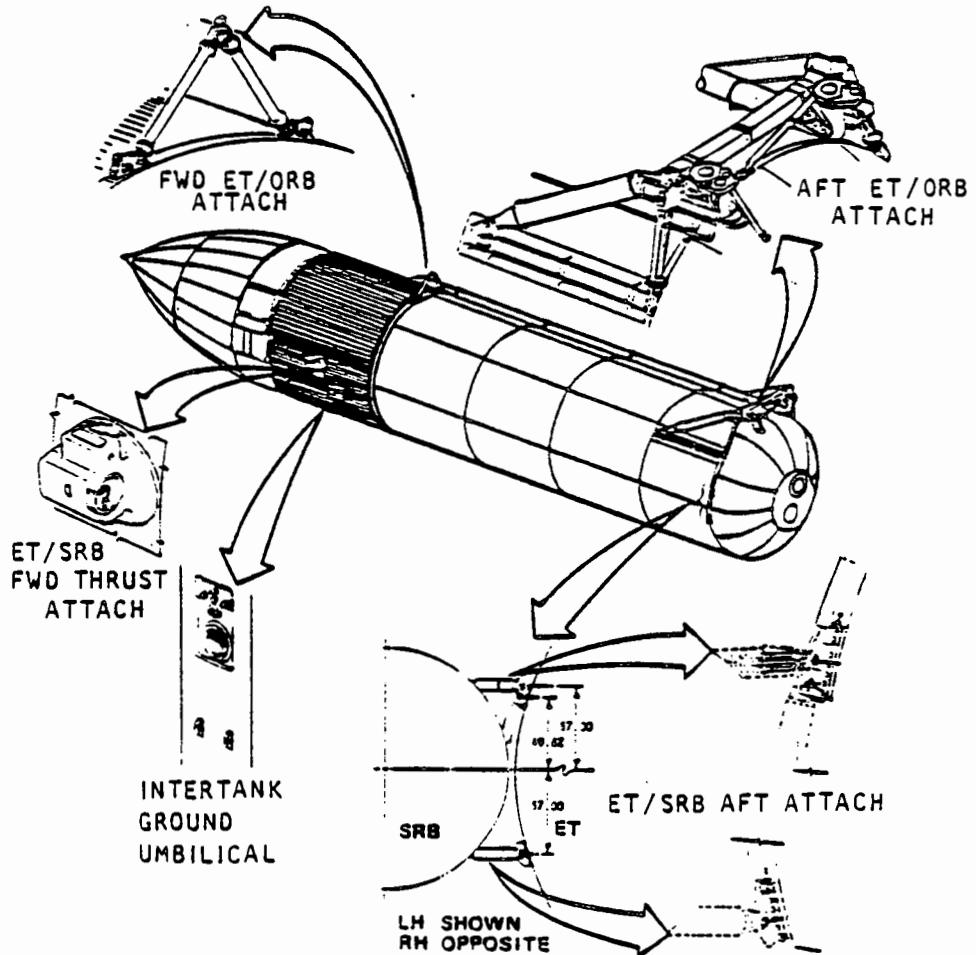
SECTION DS-DS
SCALE 1/2"

FOLIOUT FRAME

ORIGINAL PAGE IS
OF POOR QUALITY

CPOTS

- 3.1.4 **ATTACH STRUCTURE.** The External Tank includes the structural interconnections with the two Solid Rocket Boosters and the Orbiter as illustrated below. These interconnections consist of the forward and aft attach points for the SRB's and for the Orbiter, the propellant and electrical interfaces with the Orbiter, and the Orbiter to SRB interface cables.

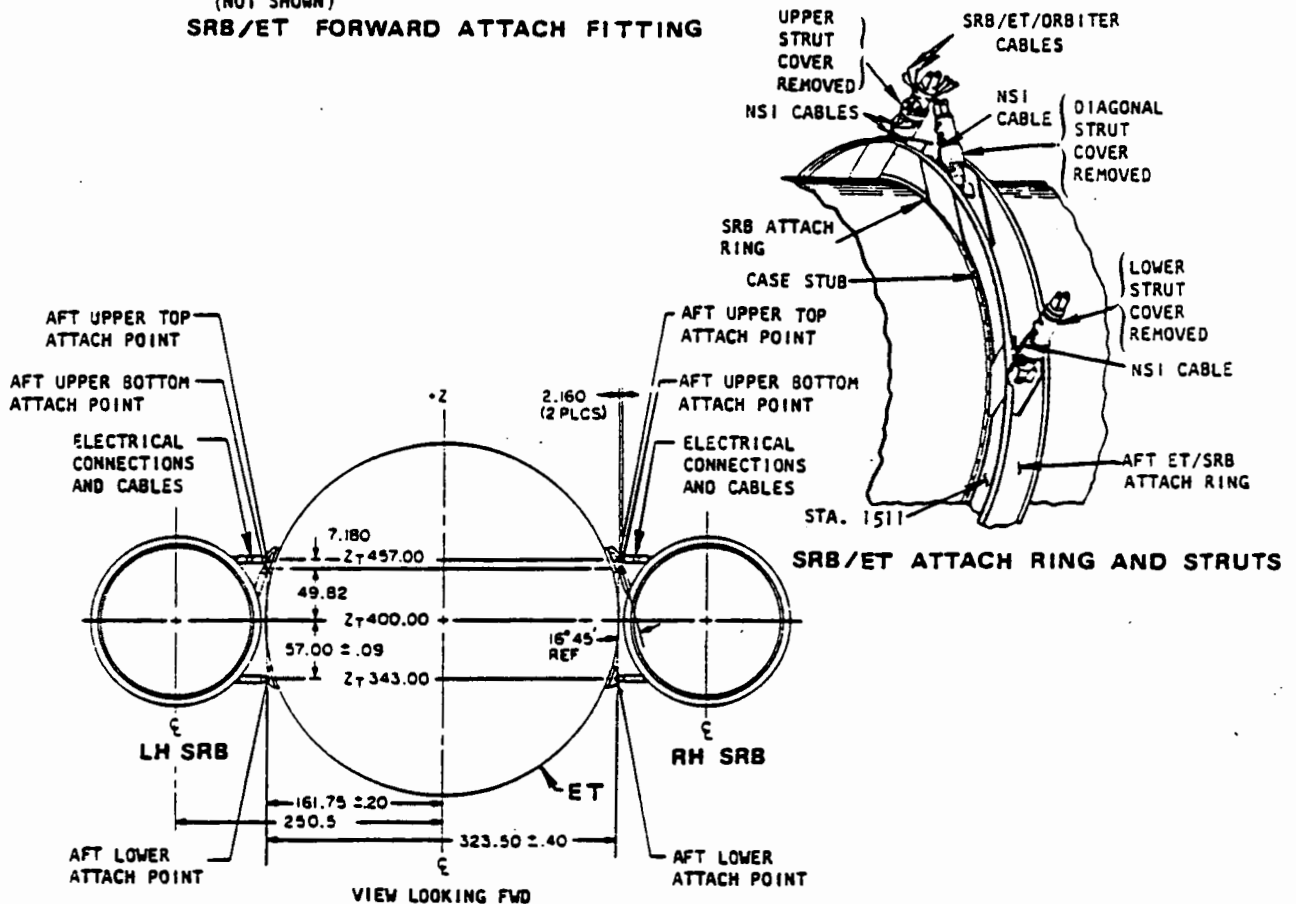
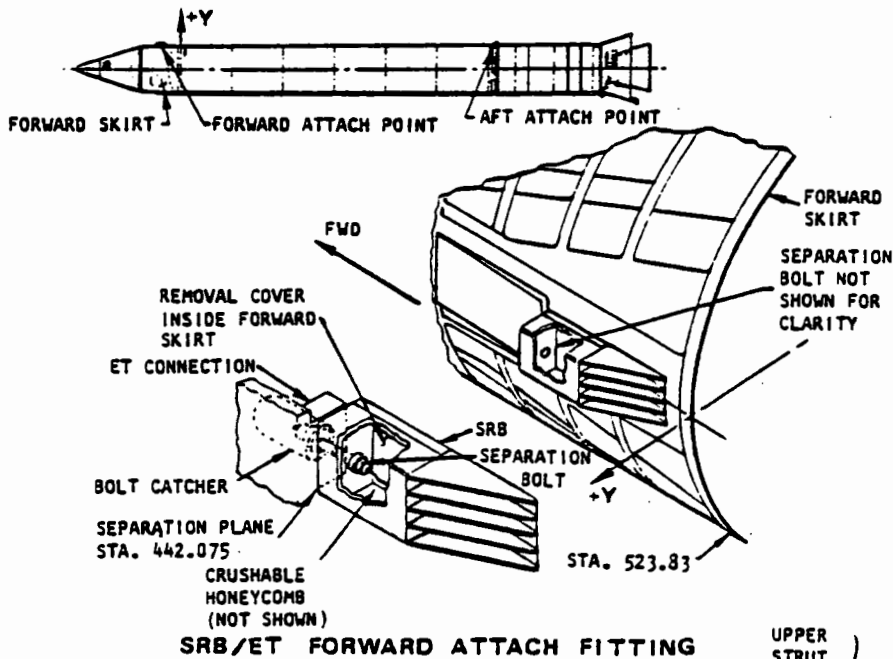


One forward thrust fitting for each SRB attachment and thrust transmission is located on each side of the ET at Tank station 985.675. The aft stabilization points, consisting of upper and lower fittings, for SRB attachment are located on each side of the ET aft major ring frame at Tank station 2058. Provisions for adjustment and alignment of the SRB and ET centerlines are located on the SRB sides of each interface. Detailed discussion of the SRB forward and aft attachments is contained in References 3-4 and 3-5.

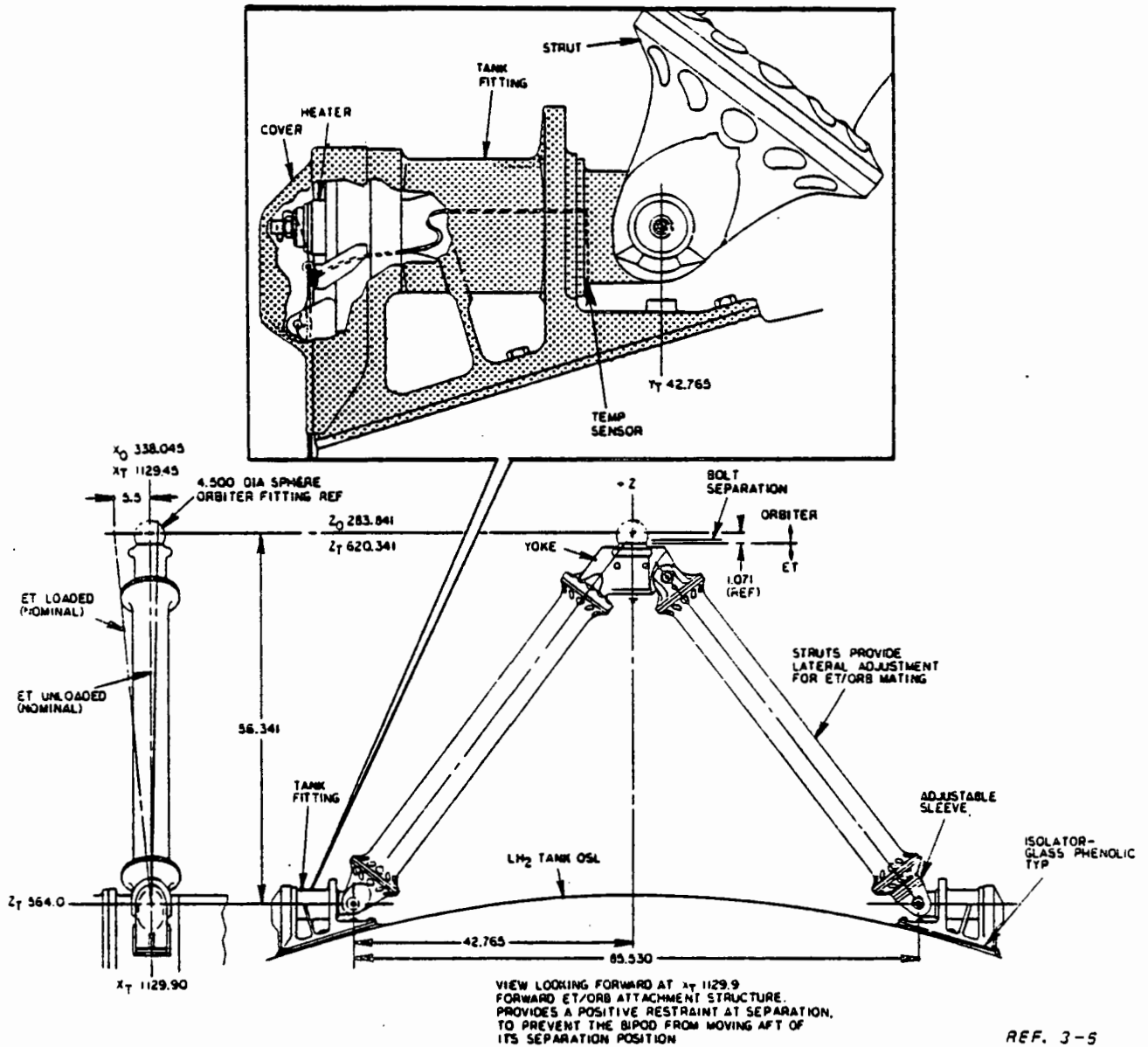
PRECEDING PAGE BLANK NOT FILMED

3.1-15 - to - 3.1-19

The SRB's are attached to the External Tank as shown below. The forward attach fitting is located on the SRB forward skirt and the aft attach fittings are on the SRB attach ring at station 1511 as illustrated.

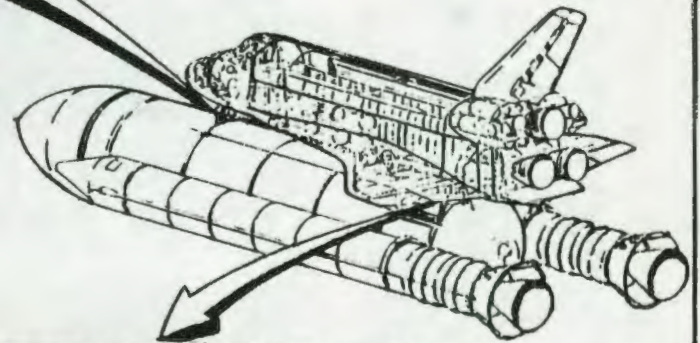
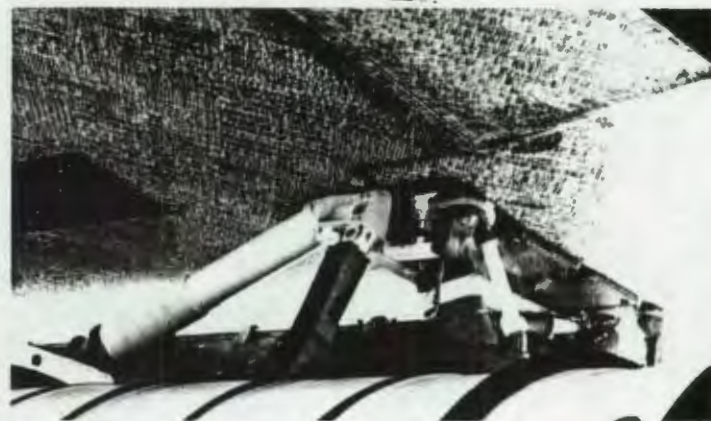
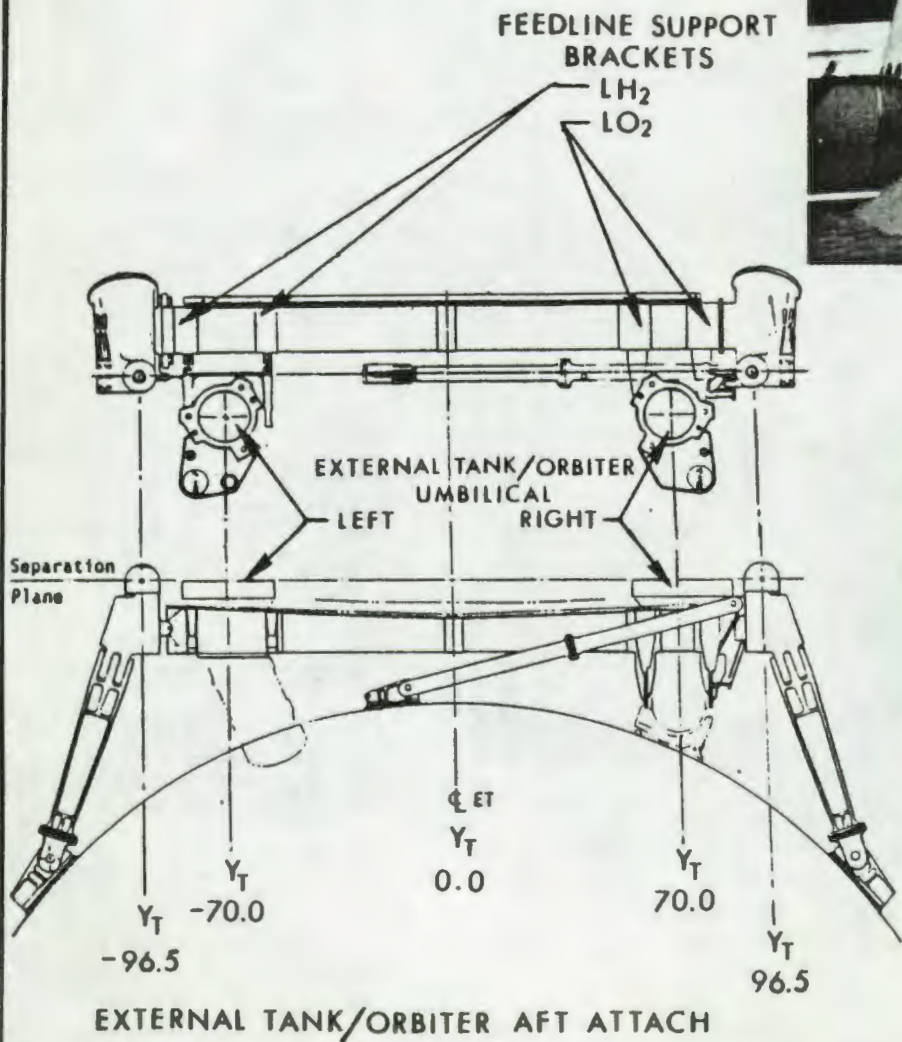


Structural attach points between the Orbiter and the ET consist of one forward fitting supported by the LH₂ tank forward ring frame and two aft fittings and support structure at the aft major ring frame. The forward attach structure is a bipod possessing rotational freedom at the attach points on the ET and rotates about a Y-axis reference line so that thermally induced changes in the Tank length will not induce load changes in the Orbiter. The bipod is canted 0.5 degree forward when mated to the Orbiter and cryogenic shrinkage of the ET results in an additional 5.5 degrees forward cant. The structure is constrained to carry loads in the Y-Z plane and is designed to be partially retracted forward at Orbiter separation. This retraction, or pivot action, is accomplished with leaf springs on the spindles which attach the struts to the tank.



ORBITER/ET FORWARD ATTACH STRUCTURE

3.1-24



ORIGINAL PAGE IS
OF POOR QUALITY

Figure 3.1.4-1

3.1.5 ORBITER VEHICLE. The aerodynamic design of the Orbiter Vehicle configuration is the result of a selection which would achieve high cross-range aerodynamically and which would be capable of trimmed flight over a wide range of angles of attack. The double-delta wing planform, combined with a moderately low fineness ratio (approximately 5) body, minimizes interference heating effects, provides the required L/D ratio to meet cross-range requirements, and possesses an acceptable trim range over the flight Mach regime. Figure 3.1.5-1 presents a general arrangement drawing of the Orbiter Vehicle.

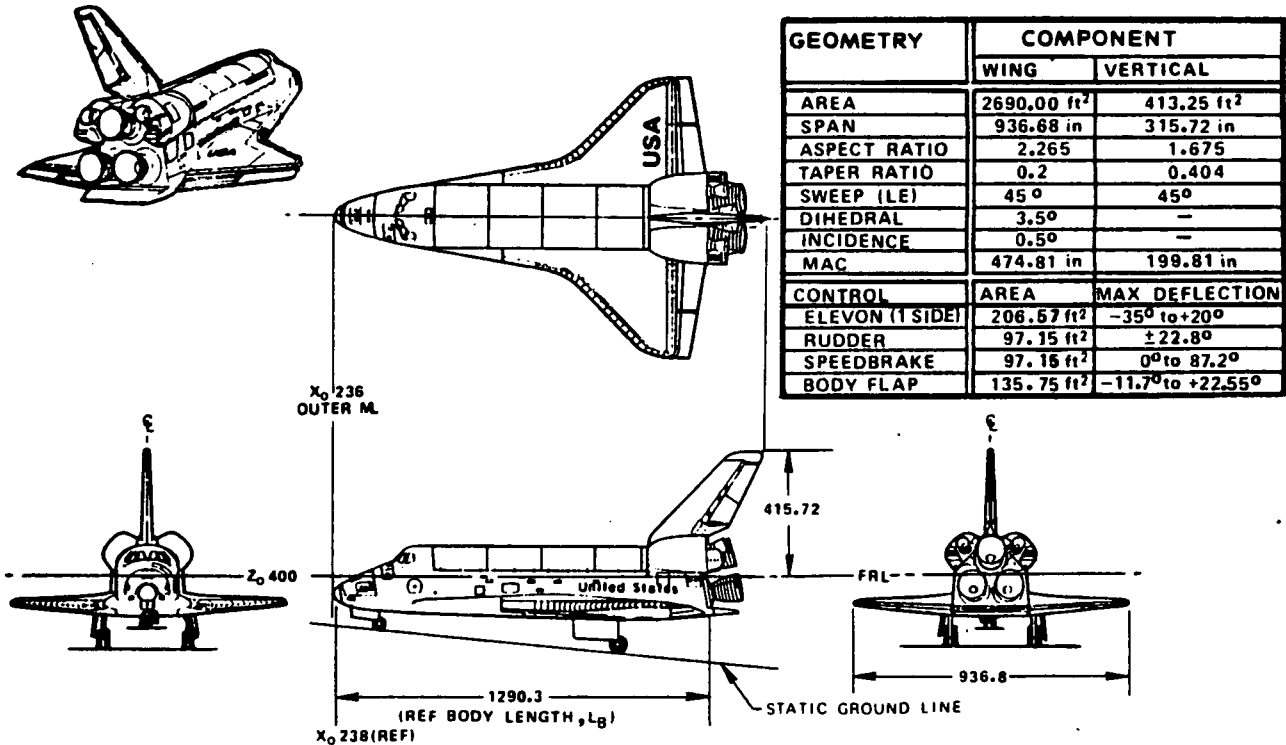
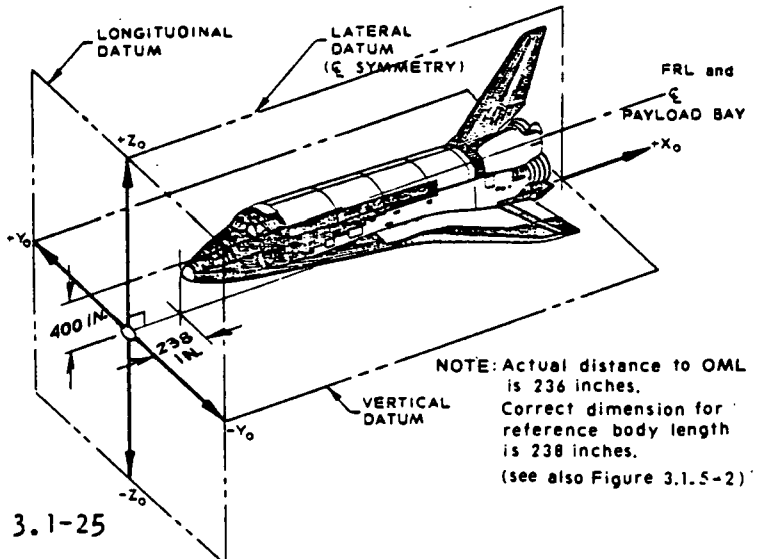


Figure 3.1.5-1
ORBITER GEOMETRY

Orbiter Vehicle design geometry is presented in Figure(s) 3.1.5-2 (a through f). The Orbiter Vehicle axis system for design drawing and mass properties statements is illustrated in the sketch. This axis system is defined in the Space Shuttle Master Dimensions Specification (Reference 3-7) and on Figure 3.1.5-2. All vehicle and design drawing axes systems are in accordance with NASA Phase B Technical Directives 2519 and 2519A.



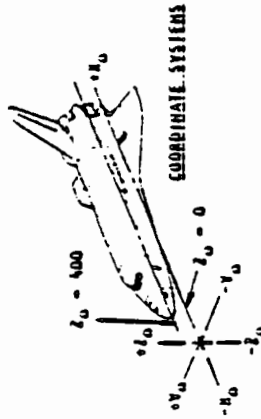


| ZONE | LET | DESCRIPTION | DATE | APPROVED |
|------|-----|--|---------|------------------------|
| 8C | A | 1. CARGO DOOR AFT TRIM X_0 1306.9 2. WAS 1107 3. REVISED GEO. NOTES 4. MPS VERT. ENG. SPACING 108 5. CONNECTED TO BEAD 103 6. 2 446 HOLE WAS 2 448 $\frac{1}{4}$ MANIP 7. C/A DIM 1136.83 WAS 1016.84 8. ET ATTACH LOC. AIT 95.5 CORR'D. 9. TO BEAD 96.5 10. ADDED X_0 238 AS END LOC OF 11. REF BODY LENGTH 1290.3 12. REMOVED 162° 45' DIM FROM SEC 13. X_0 610.5 14. ADDED 17° 50' FOR RAD DEPLOY 15. ANGLE AT SEC X_0 610.5 16. REMOVED NOT TO EXCEED - FROM 17. SEC VIEW X_0 610.5 AND X_0 1072 | 9-12-74 | |
| 8D | B | 1. SEE E.O. 801 FOR DIRECT DRAWING 2. CHANGES INCORPORATED AND RELEASED | 1-16-76 | |
| 8E | C | 1. SEE E.O. 801 FOR DIRECT DRAWING 2. CHANGES INCORPORATED AND RELEASED | 3-10-77 | J.D. GREEN |
| 8F | D | 1. SEE E.O. 801 FOR DIRECT DRAWING 2. CHANGES INCORPORATED AND RELEASED | 9-16-77 | J.F. GREEN |
| 8G | E | 1. SEE E.O. 801 FOR DIRECT DRAWING 2. CHANGES INCORPORATED AND RELEASED | 3-30-78 | J.M. COA J.F. GREEN |

ORIGINAL PAGE IS
OF POOR QUALITY

△ MPS ANGULAR ANGLES SHOWN INCLUDE 0° 30'
HYDRAULIC OVERTHROW AND 0° 30' THINUST
MISALIGNMENT

2 TRACEABILITY NOT REQD
NOTES: UNLESS OTHERWISE SPECIFIED



| DIMENSION DATA | |
|--|-----------------------------|
| INERT CONTROL WEIGHT | REFER TO CONTRACT END ITEM |
| DESIGN LANDING WEIGHT | SPECIFICATION M1070-0001-1A |
| PAYLOAD DOWN WEIGHT | |
| DESIGN LANDING SPEED | |
| PROPULSION | |
| THRUST - VACUUM - LBS | 470K |
| PROPPELLANT TYPE | H_2/O_2 |
| NUMBER | 3 |
| MAIN | OMS |
| THRUST | 6K |
| M_2/O_2 | $M_2/O_2/MHH$ |
| NUMBER | 2 |
| RELS | 0.5K |
| $M_2/O_2/MHH$ | $M_2/O_2/MHH$ |
| NUMBER | 40 |
| 66 VERNIERS | |
| 25 LBF | |
| LINES AND CONTIGUES | |
| THIS DRAWING DEPICTS OUTER HOLD LINE (OHL) ONLY. | |
| REFER TO MASTER DIMENSION SPECIFICATION | |
| M1070 FOR DETAIL DATA | |

| GEOMETRY | | VERTICAL | FLAP |
|---------------------------------------|--------------------|----------------|--------|
| S_w FT ² | 3.690 | 411.25 | 135.75 |
| AR or ASPECT RATIO | 2.285 | 1.875 | |
| λ | 0.20 | 0.404 | |
| DIRECTIONAL | 45° | 45° | |
| (CHORD PLANE & TRAILING EDGE) | 1° 30' | | |
| α BASIC WING | 40° 30' | | |
| $1/2 C V_0 = 0$ (C BODY) | 0.1137 | | |
| $1/2 C V_0 = 199$ | 0.113 | | |
| $1/2 C V_0 = 468.34$ | 0.42 | | |
| b IN. | 316.68 | 315.72 | |
| Cd IN. | 689.24 | 268.50 | |
| Cf IN. | 137.85 | 108.47 | |
| C IN. | 474.81 | 199.81 | |
| MAC | $Y_0 = 182.13$ | $Z_0 = 635.52$ | |
| AIRFOIL | TRP. 0012-64 | 10° SW | |
| | MOD | | |
| | $Y_0 = 199.0010$ | 60-40 WEDGE | |
| | MOD | | |
| V_w (TAIL VOLUME) | 2012.4 (INC. GL J) | .0537 | |
| S_w EXPOSED FT ² (TOTAL) | 290.8 | 365.1 | |
| S_w ONE EXPOSED FT ² | 4001.2 | | |
| S_w TOTAL WETTED FT ² | 206.57 | 738.82 | |
| SELEVOM FT ² (ONE SIDE) | | | |
| SRUD FT ² | | 97.148 | |

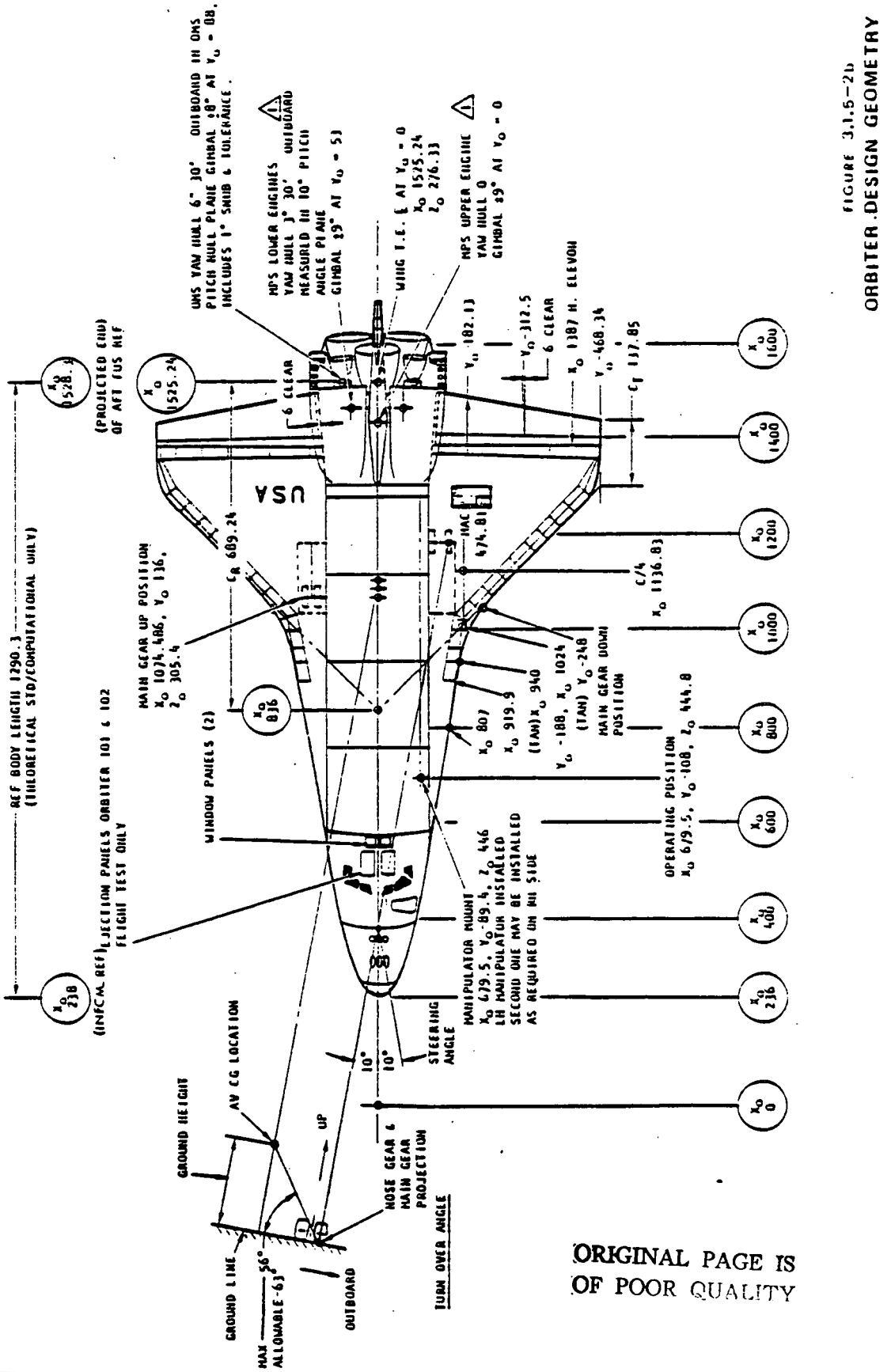
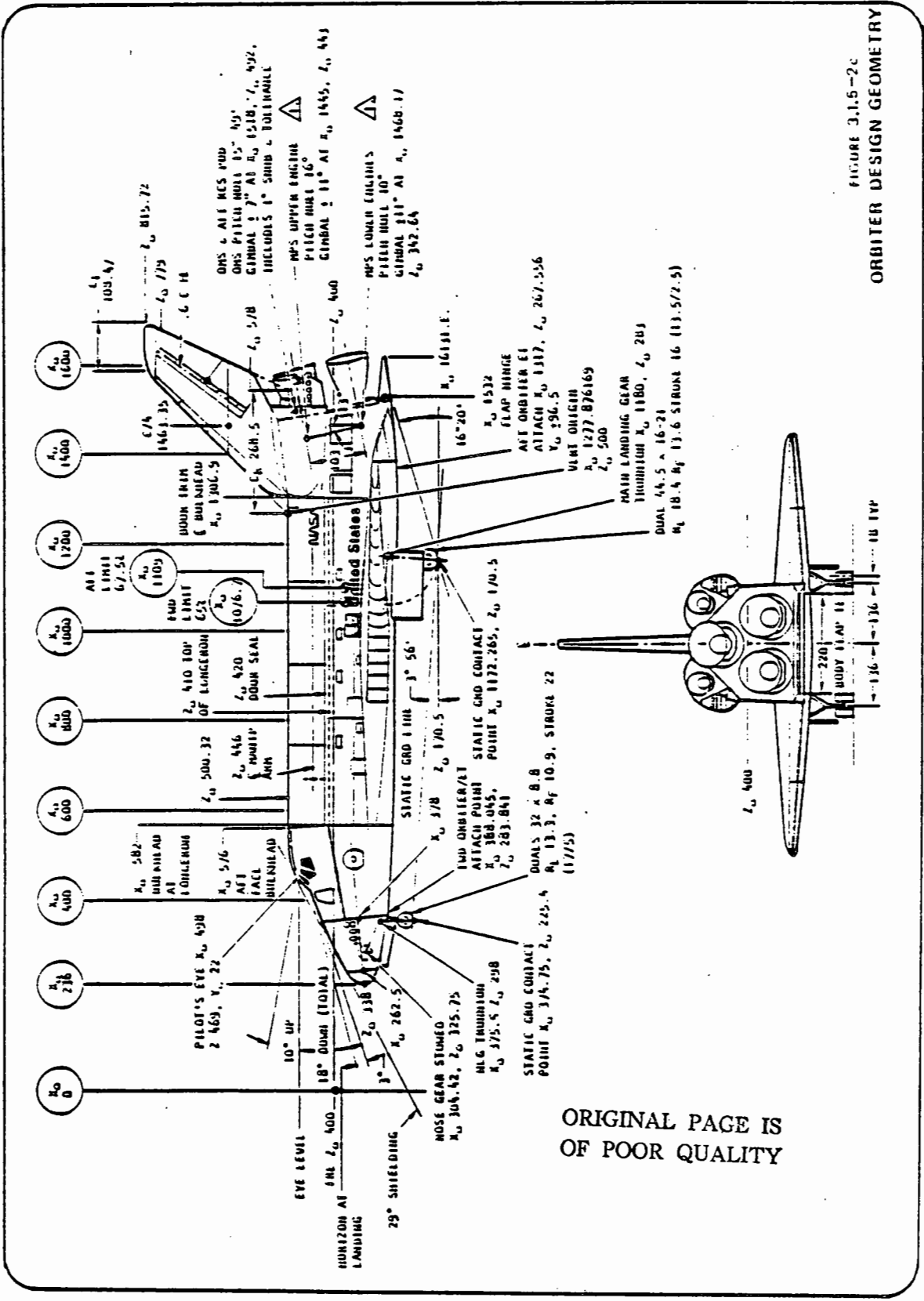


FIGURE 3.1.5-2b
ORBITER DESIGN GEOMETRY

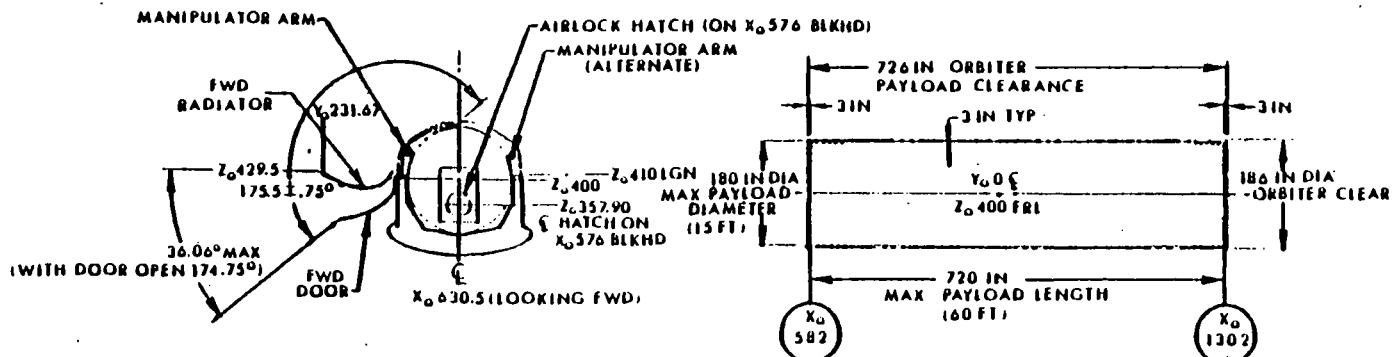
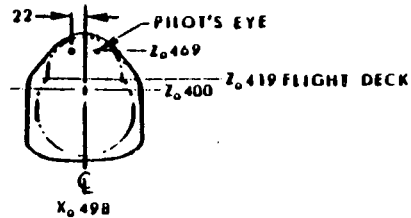
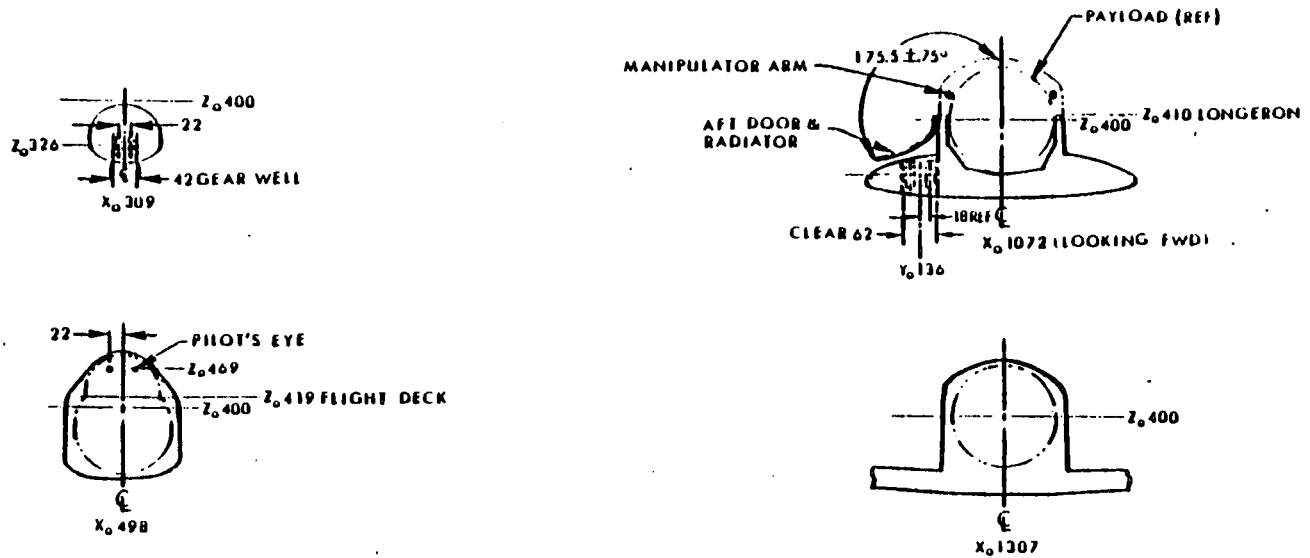
ORIGINAL PAGE IS
OF POOR QUALITY



ORIGINAL PAGE IS
OF POOR QUALITY

FIGURE 3.1.5-2c
ORBITER DESIGN GEOMETRY

3.1-29



PAYLOAD ENVELOPE/ORBITER CLEARANCE

FIGURE 3.1.5-2d
ORBITER DESIGN GEOMETRY

STS85-0118-1



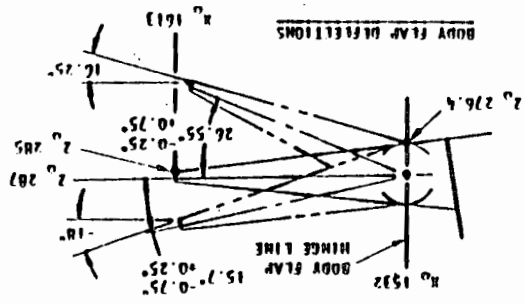
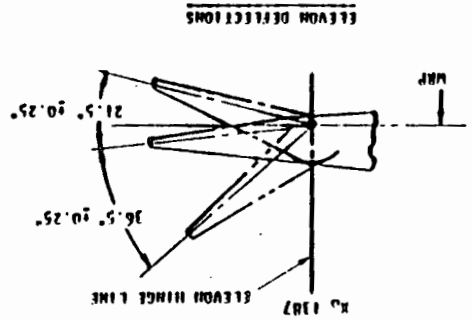
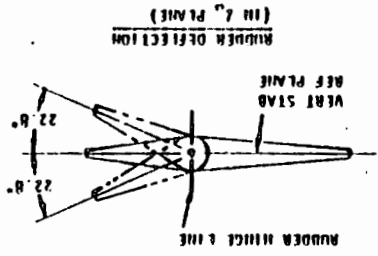
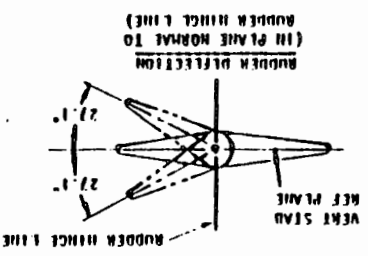
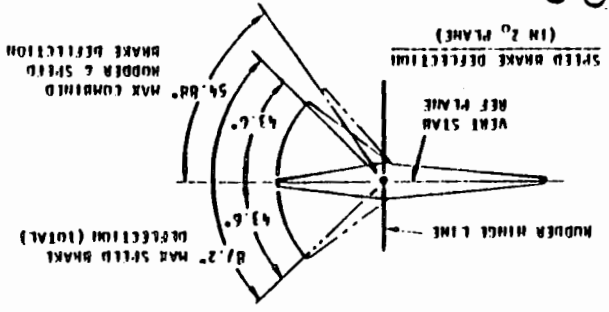
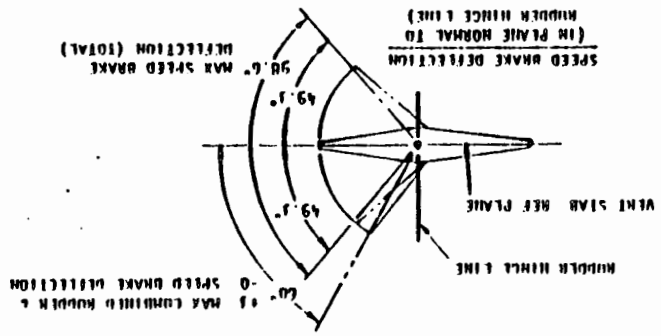


FIGURE 3.1-5-2e
ORBITER DESIGN GEOMETRY

ORIGINAL PAGE IS
OF POOR QUALITY

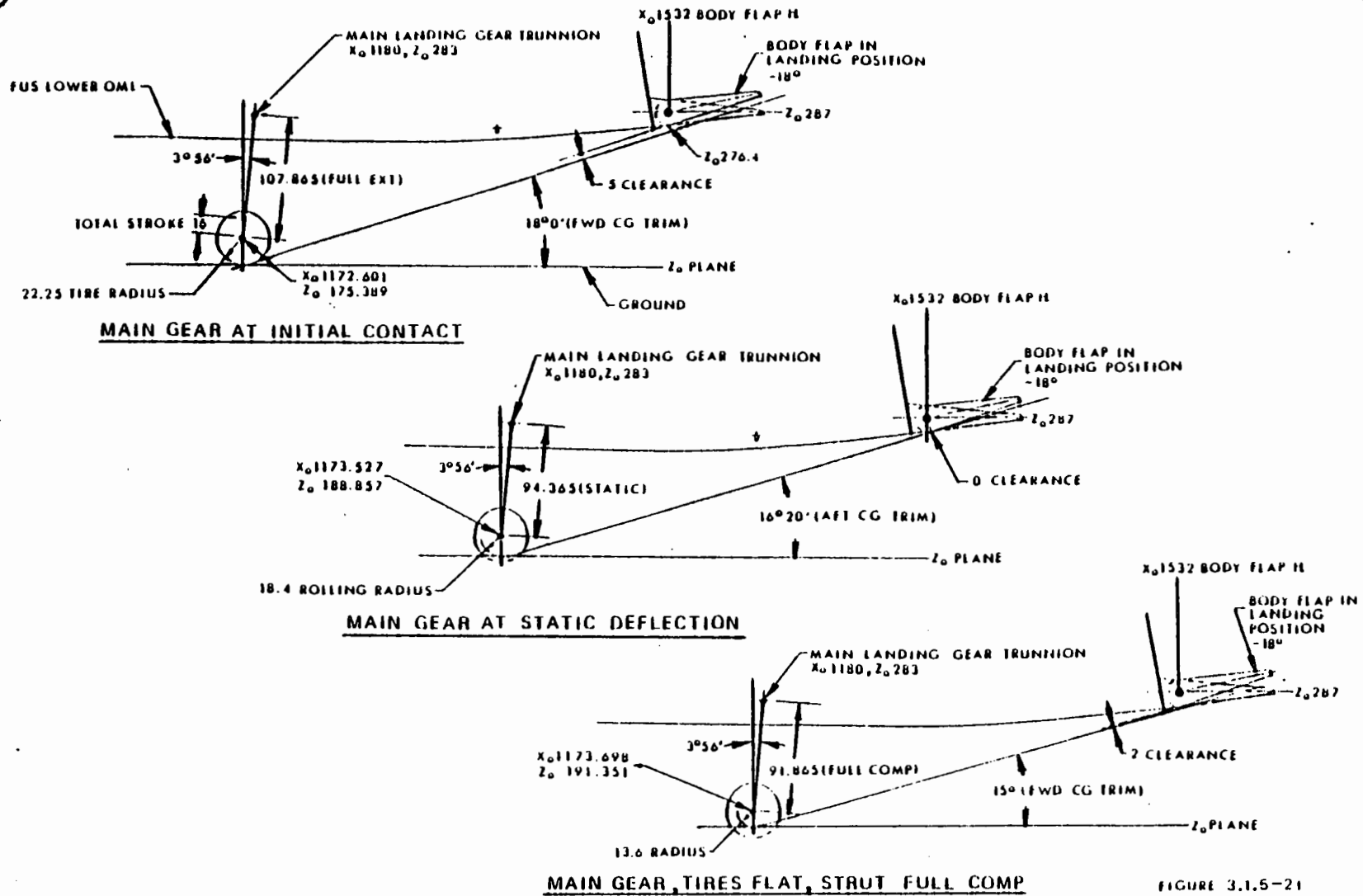
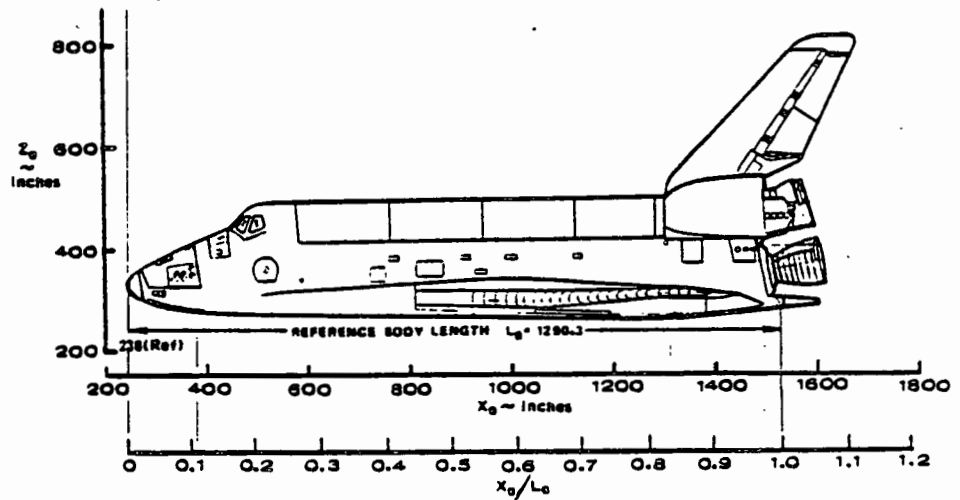


FIGURE 3.1.5-21
ORBITER DESIGN GEOMETRY

3.1-31

STS85-0118-1

The sketch below shows the relationship between the design drawing coordinates and the fuselage station expressed in percent of body length.



Aerodynamic forces and moments are measured with respect to a given Moment Reference Center (MRC) which is specified in each of the aerodynamic data sections. The Orbiter Vehicle longitudinal data are given in both stability and body axes systems and the lateral-directional data are given in the body axis system only. These aerodynamic reference axis systems are sets of conventional, right-hand, orthogonal axes with the X- and Z-axes in the plane of symmetry and with the positive X-axis directed out the nose (in the body axis system) or pointing into the component of the wind (in the stability axis system) which lies in the plane of symmetry as illustrated in Figure 3.1.5-3. All directions on the figure are positive as shown.

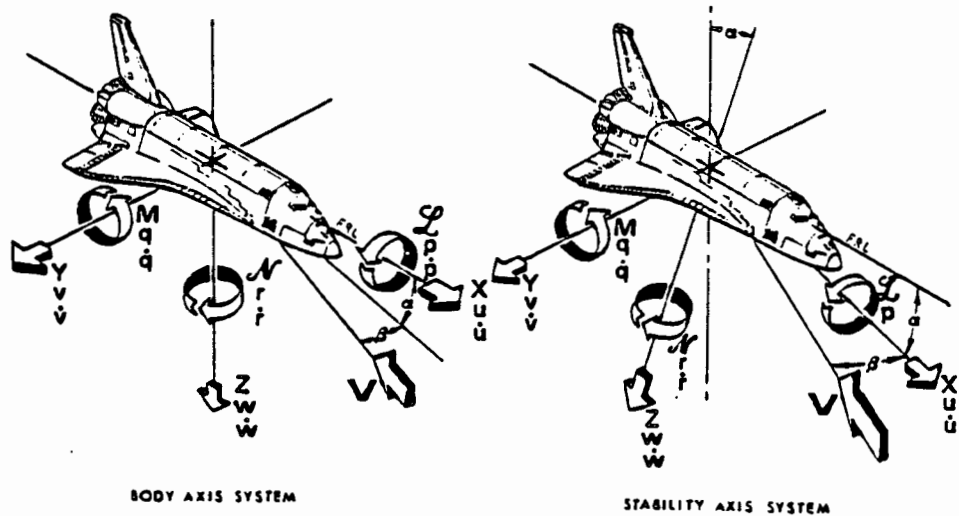


Figure 3.1.5-3
ORBITER REFERENCE AXIS SYSTEMS

The aerodynamic force and moment sign convention is illustrated in Figure 3.1.5-4 which also includes the longitudinal equations for conversion from stability to body axis system.

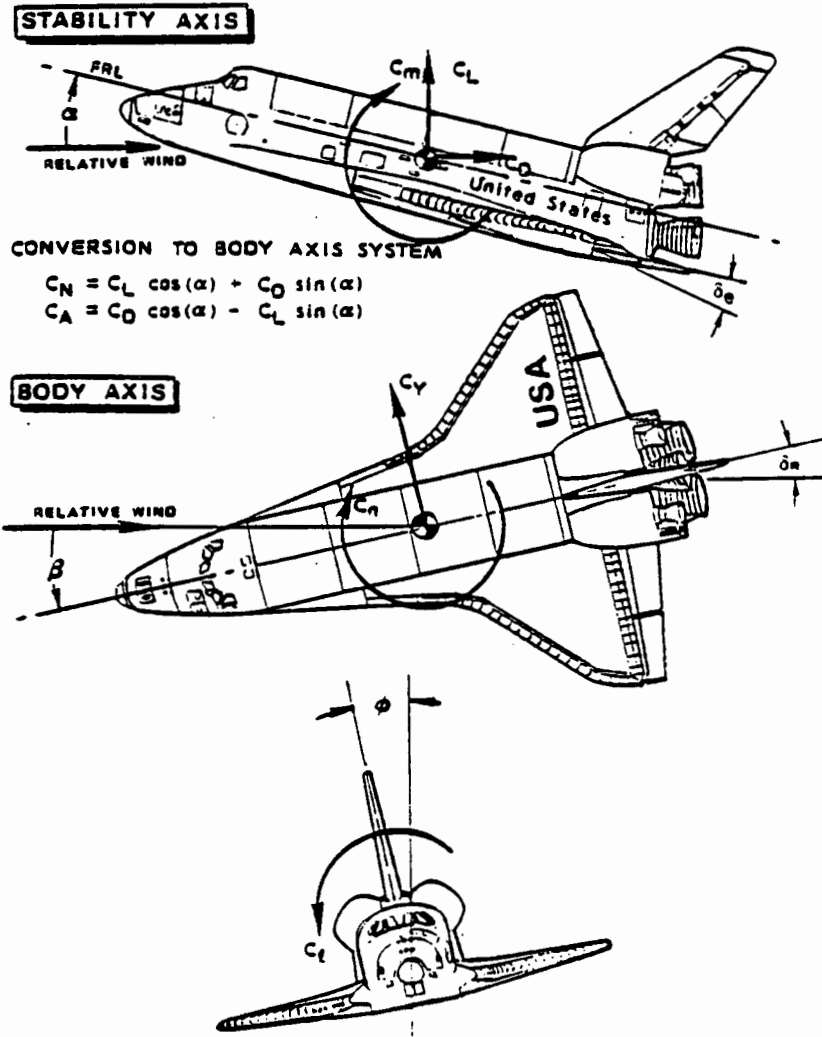


Figure 3.1.5-4
ORBITER SIGN CONVENTION

NOTE: Normal and Axial Force coefficients may be computed from Lift and Drag coefficients with wind axes system and Side Force coefficient in the body axis system as follows:

$$C_N = C_D \frac{\sin \alpha}{\cos \beta} + C_Y \frac{\sin \alpha \cos \beta}{\cos \beta} + C_L \cos \alpha$$

$$C_A = C_D \frac{\cos \alpha}{\cos \beta} + C_Y \frac{\cos \alpha \sin \beta}{\cos \beta} - C_L \sin \alpha$$

CAUTION. Reference areas and lengths used to normalize aerodynamic forces and moments are presented in the table below. In some cases (notably control surface hinge moments) the reference dimensions differ from the existing geometry. REFERENCE VALUES ARE BASED ON THEORETICAL AND NOT TRUE DIMENSIONS.

AERODYNAMIC FORCE AND MOMENT REFERENCE DIMENSIONS

| PARAMETER | REFERENCE VALUE |
|--|--------------------------------|
| LONGITUDINAL AND LATERAL/DIRECTIONAL COEFFICIENTS | |
| Wing Area, S | 2690.000 ft ² |
| Wing Span b | 78.057 ft |
| Mean Aerodynamic chord (M.A.C), \bar{c} | 39.568 ft |
| HINGE MOMENT COEFFICIENTS | |
| ELEVON | |
| Area, S | 210.000 ft ² |
| Chord c | 90.700 in |
| Area Moment | 19,047.000 ft ² -in |
| BODY FLAP | |
| Area, S | 135.000 ft ² |
| Chord, c | 81.000 in |
| Area Moment | 10,935.000 ft ² -in |
| RUDDER/SPEEDBRAKE | |
| Area, S | 100.150 ft ² |
| Chord, c | 73.200 in |
| Area Moment | 7331.000 ft ² -in |

3.1.5.1 WING. The Orbiter wing was sized to provide a 171-knot touchdown speed (V_D) at a 15-degree angle of attack (tail scrape attitude for main gear strut compressed, tire flat) with body flap retracted and the center of gravity at the forward limit (see also Figure 3.6-2). The leading edge sweep (45 degrees) and aspect ratio (2.265) were selected on the basis of aerothermodynamic trade studies to provide the design touchdown speed for a center of gravity at the forward limit with minimum wing size and to optimize the wing leading edge thermal protection system (TPS) for a re-use cycle of 100 flights prior to major rework. Spanwise twist distribution and chordwise camber are illustrated in Figure 3.1.5.1-1.

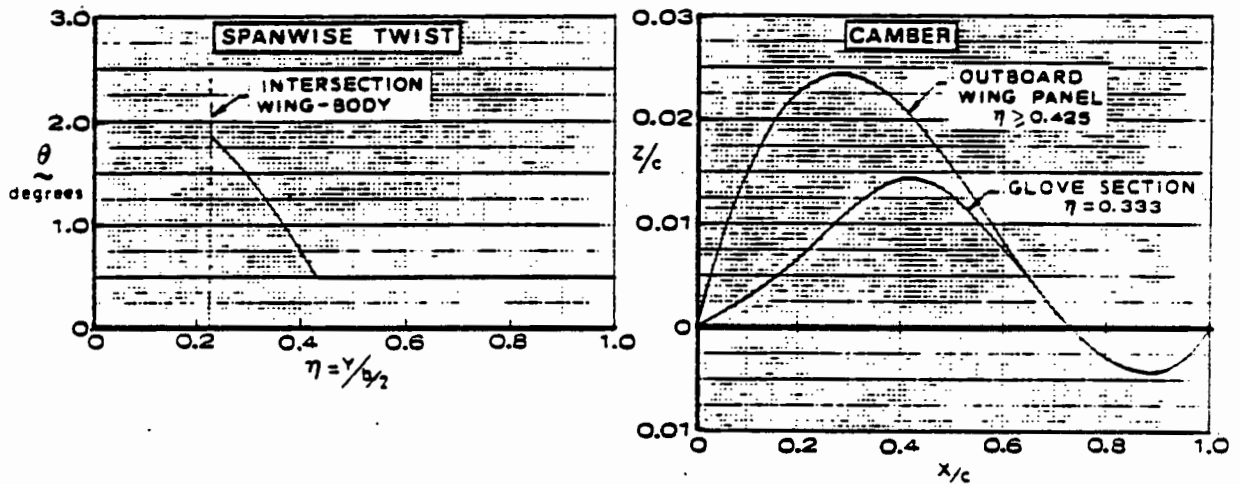
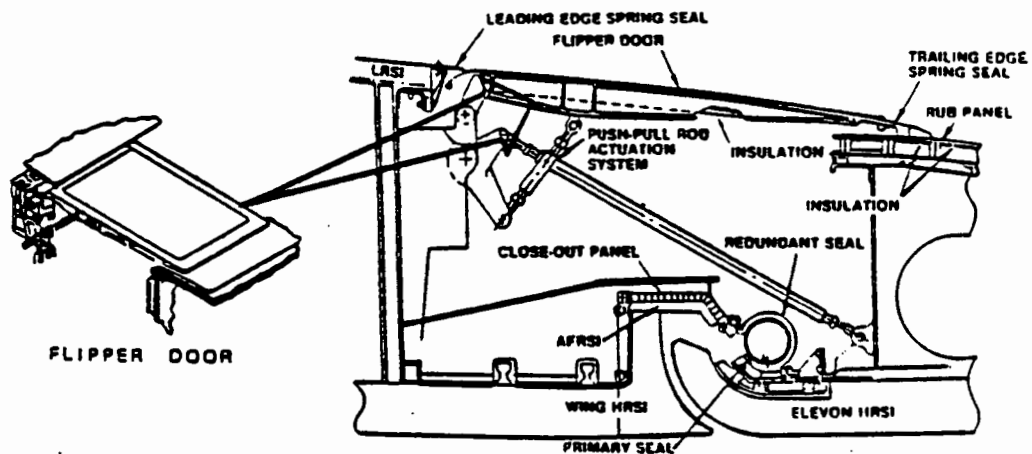


Figure 3.1.5.1-1
WING TWIST AND CAMBER

Control surfaces located in the wing consist of the elevons (elevator-aileron) with elevon seal (or "flipper") doors which effectively seal the resultant gaps when the elevons are deflected by following the control surface leading edge.



The wing planform reference area (2690 ft²) includes that portion of the basic planform covered by the fuselage. It does NOT include the areas formed by wing-body fairings or areas clipped from the equivalent "delta" by the faired wing tips. Pertinent dimensional parameters are summarized in Table 3.1.5.1-1 (see also, Figures 3.1.5.4-1 through 3.1.5.4-4 for areas and perimeters).

Table-3.1.5.1-1
WING DIMENSIONAL PARAMETERS

| PARAMETER | SYMBOL | VALUE | UNITS |
|--|---|---|---|
| AIRFOIL SECTION (Y_0 199.045) (Y_0 468.340) | --- | 0.0010 (mod) 0012 - 64 (mod) | --- |
| DIHEDRAL (at trailing edge) | δ_{TE} | 3.5 | degrees |
| AREA Planform (total) Planform (exposed) Wetted Surface (exposed) | S_{TOT} S_{EXP} S_{WET} | 2690 2012.4 4001.2 | ft ² ft ² ft ² |
| SPAN | b_w | 78.056 (936.68) | ft (Inch) |
| ASPECT RATIO | M_w | 2.265 | --- |
| TAPER RATIO | $\lambda = c_t/c_r$ | 0.20 | --- |
| SWEEP Leading Edge Trailing Edge | Λ_{LE} Λ_{TE} | 45 -10 | degrees degrees |
| CHORD Root (theoretical) Fuselage Station (0.25c) (F.S.) Buttock Line (B.L.) Length Root (exposed) Fuselage Station (0.25c) (F.S.) Buttock Line (B.L.) Length Tip Fuselage Station (0.25c) (F.S.) Buttock Line (B.L.) Length Mean Aerodynamic Fuselage Station (0.25c) (F.S.) Buttock Line (B.L.) Length | X_0 Y_0 $c_{r_{THEO}}$ X_0 Y_0 c_r X_0 Y_0 c_t MAC X_0 Y_0 \bar{z}_w | 1008.31 0 57.44 (689.24) 778.5 108.0 80.83 (970) 1338.80 468.34 11.48 (137.95) 1136.83 182.13 39.56 (474.81) | inches inches ft (Inch) inches inches ft (Inch) inches inches ft (Inch) inches inches ft (Inch) |
| GLOVE Sweep Theoretical Intersection Fuselage Station (F.S.) Buttock Line (B.L.) | Λ_{GLOVE} X_0 Y_0 | 81 1024.0 188.0 | degrees inches inches |
| ELEVON INBOARD Area (equivalent) Span (equivalent) Aspect Ratio Distance (centroid to hingeline) OUTBOARD Area (equivalent) Span (equivalent) Aspect Ratio Distance (centroid to hingeline) TOTAL (one side) Inboard/Outboard Split (BL) Area (equivalent) Span (equivalent) Aspect Ratio Chord Fuselage Station (0.25c) (F.S.) Distance (centroid to hingeline) | S_{ei} b_{ei} M_{ei} -- S_{eo} b_{eo} M_{eo} -- Y_0 S_e b_e M_e MAC, \bar{c}_e X_0 -- | 131.12 15.77 1.90 50.35 75.45 13.10 2.27 35.03 311.00 206.57 28.87 4.03 7.46 (89.5) 1409.375 44.75 | ft ² ft --- inches ft ² ft --- inches inches ft ² ft --- ft (Inches) inches inches |

3.1.5.2 FUSELAGE (OR BODY). The Orbiter fuselage was designed to accommodate a variety of payloads and house the crew and maneuvering control systems. Nose camber, cross section, and upward sloping forebody sides were selected to improve hypersonic pitch trim and directional stability and, in conjunction with wing-body blending, to reduce entry heating on the body sides. Attitude Control Propulsion Systems (ACPS) pods have been incorporated with the OMS and are located in the aft body fairings. Hinged surfaces attached to the fuselage include the cargo bay doors and the body flap. The cargo bay doors have 13 hinges on each side of the fuselage. The six forward hinges on each side are covered with TPS and faired fore and aft. The aft seven hinges have no TPS and no fairings. The body flap is used to protect the Shuttle main engines (SME) during entry and to provide trim capability to relieve elevon loads. Pertinent dimensional parameters are summarized in Table 3.1.5.2-1.

Table 3.1.5.2-1
FUSELAGE DIMENSIONAL PARAMETERS

| PARAMETER | SYMBOL | VALUE | UNITS |
|-------------------------------|------------|-------------|-----------------|
| LENGTH | | | |
| Reference | L_0 | 1290.3 | inches |
| Nose Fuselage Station (F.S.) | X_0 | 238 | inches |
| DEPTH | | | |
| Maximum at F.S. | h_0 | 19.92 (239) | ft (Inch) |
| WIDTH | | | |
| Maximum at F.S. | w_0 | 22.0 (264) | ft (Inch) |
| AREA | | | |
| Planform | S_0 | 1914.4 | ft ² |
| Wetted Surface | S_{WET} | 5634 | ft ² |
| Base | S_{BASE} | 365.7 | ft ² |
| OMS Pods | S_{PODS} | 71.0 | ft ² |
| CARGO BAY | | | |
| Diameter | d_{CB} | 15 | ft |
| Length | l_{CB} | 60 | ft |
| GLOVE | | | |
| Fuselage Intersection (F.S.) | X_0 | 500 | inches |
| (B.L.) | Y_0 | 102 | inches |
| (Based on OML - TPS included) | | | |
| BODY FLAP | | | |
| Area (planform) | S_{BF} | 135.75 | ft ² |
| Span (equivalent) | b_{BF} | 241.33 | inches |
| Chord | c_{BF} | 81 | inches |
| Hinge Line (F.S.) | X_0 | 1532 | inches |

3.1.5.3 VERTICAL TAIL. The vertical tail has been sized to provide a low-speed $C_{n\beta}$ of 0.0013 at an angle of attack of 13 degrees about a center of gravity located at the aft limit and has a reference area of 413.25 ft², including the rudder/speed brake. The rudder is split along the Orbiter buttock plane to provide directional stability augmentation in the hypersonic/supersonic flight regimes and to apply drag modulation for the subsonic flight phases, approach and landing. The section profile is a five-degree half-angle, 60 to 40 percent double wedge airfoil. Dimensional parameters are summarized in Table 3.1.5.3-1.

Table 3.1.5.3-1
VERTICAL TAIL DIMENSIONAL PARAMETERS

| PARAMETER | SYMBOL | VALUE | UNITS |
|-------------------------------|-----------------------|--|-----------------|
| AIRFOIL SECTION (root-tip) | --- | 10° Symmetrical 60% - 40% double wedge | --- |
| AREA | S_v | 413.25 | ft ² |
| SPAN | b_v | 26.31 (315.72) | ft (inch) |
| ASPECT RATIO | A | 1.675 | --- |
| TAPER RATIO | $\lambda_v = c_t/c_r$ | 0.404 | --- |
| SWEEP | | | |
| Leading Edge | $\Delta_{v_{LE}}$ | 45 | degrees |
| Trailing Edge | $\Delta_{v_{TE}}$ | 26.2 | degrees |
| CHORD | | | |
| Root | c_r | 22.37 (268.5) | ft (inch) |
| Tip | c_t | 9.04 (108.47) | ft (inch) |
| Mean Aerodynamic | \bar{c}_v | 16.65 (199.81) | ft (inch) |
| Fuselage Station (0.25C) F.S. | x_o | 1463.35 | inch |
| Waterline W.L. | z_o | 635.5 | inch |
| RUDDER/SPEED BRAKE | | | |
| AREA | S | 97.84 | ft ² |
| SPAN | b | 16.55 (198.61) | ft (inch) |
| CHORD | | | |
| Mean Aerodynamic | \bar{c} | 6.07 (72.84) | ft (inch) |
| Fuselage Station (0.25c) F.S. | x_o | 1575.77 | inch |
| Waterline W.L. | z_o | 670.41 | inch |

3.1.5.4 TOTAL VEHICLE. Cross Sectional data defining the total Orbiter Vehicle geometry are presented in Figures 3.1.5.4-1 through 3.1.5.4-4. These figures provide the cross sectional area variation for components and total vehicle and the perimeter distribution for components and total vehicle. Total vehicle dimensional parameters are summarized in Table 3.1.5.4-1.

Table 3.1.5.4-1
TOTAL VEHICLE DIMENSIONAL PARAMETERS
(fuselage plus exposed wing)

| PARAMETER | SYMBOL | VALUE | UNITS |
|-----------------------------|-----------------|-----------------|-----------------|
| AREA | | | |
| Planform | S_{TOTAL} | 3952 | ft ² |
| Wetted Surface | $S_{WET,TOTAL}$ | 11,136 | ft ² |
| LENGTH | | | |
| Overall | L | 122.0 (1464) | ft (inch) |
| Reference | L_0 | 107.5 (1290.3) | ft (inch) |
| SPAN | | | |
| | b_w | 78.056 (936.68) | ft (inch) |
| HEIGHT | | | |
| Gear-Up | $h_{GEAR UP}$ | 46.14 (553.68) | ft (inch) |
| Gear-Down (static position) | $h_{GEAR DOWN}$ | 53.76 (645.12) | ft (inch) |

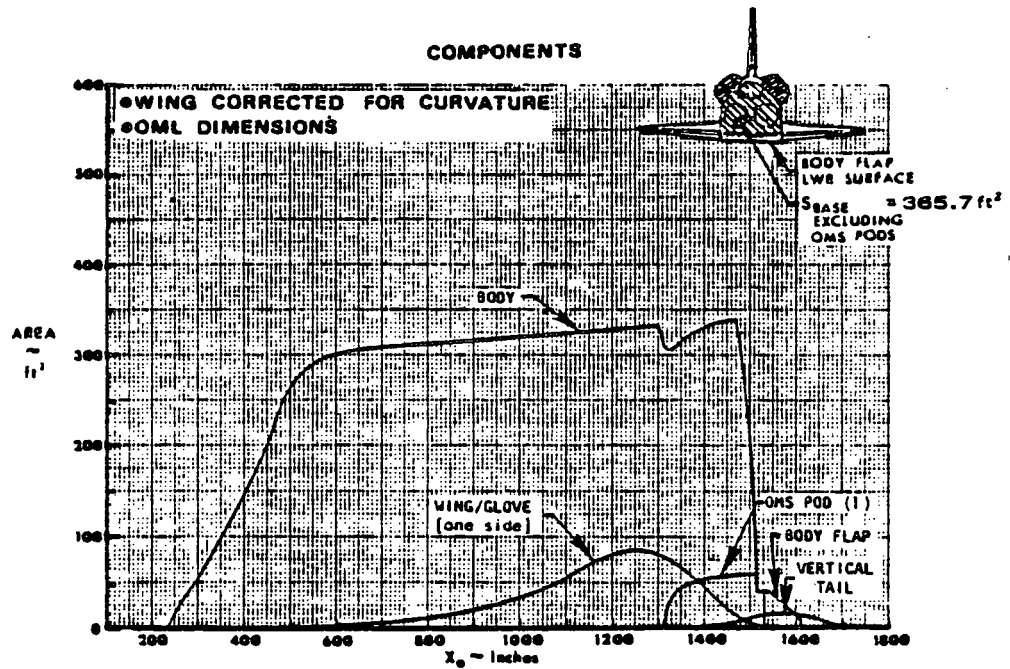


Figure 3.1.5.4-1
CROSS-SECTIONAL AREA VARIATION

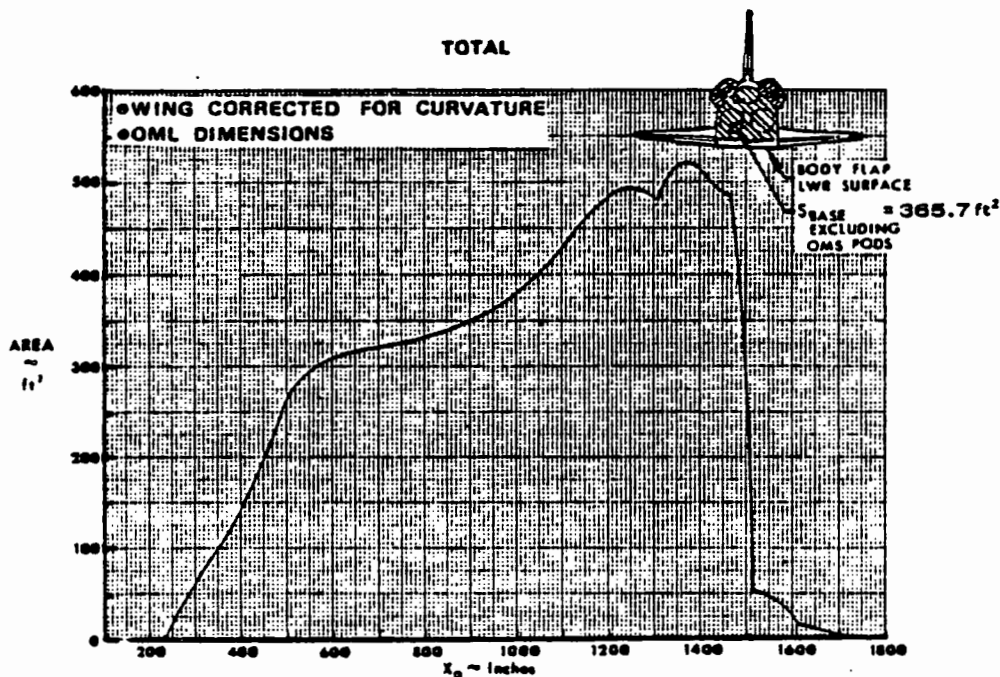


Figure 3.1.5.4-2
CROSS-SECTIONAL AREA VARIATION

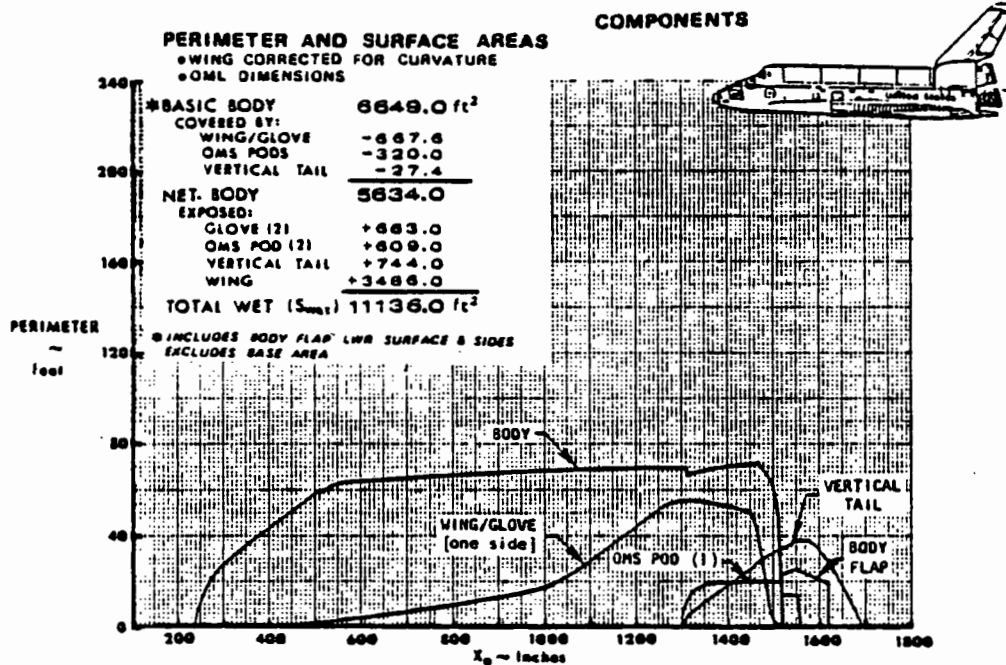


Figure 3.1.5.4-3
PERIMETER DISTRIBUTION

ORIGINAL PAGE IS
OF POOR QUALITY

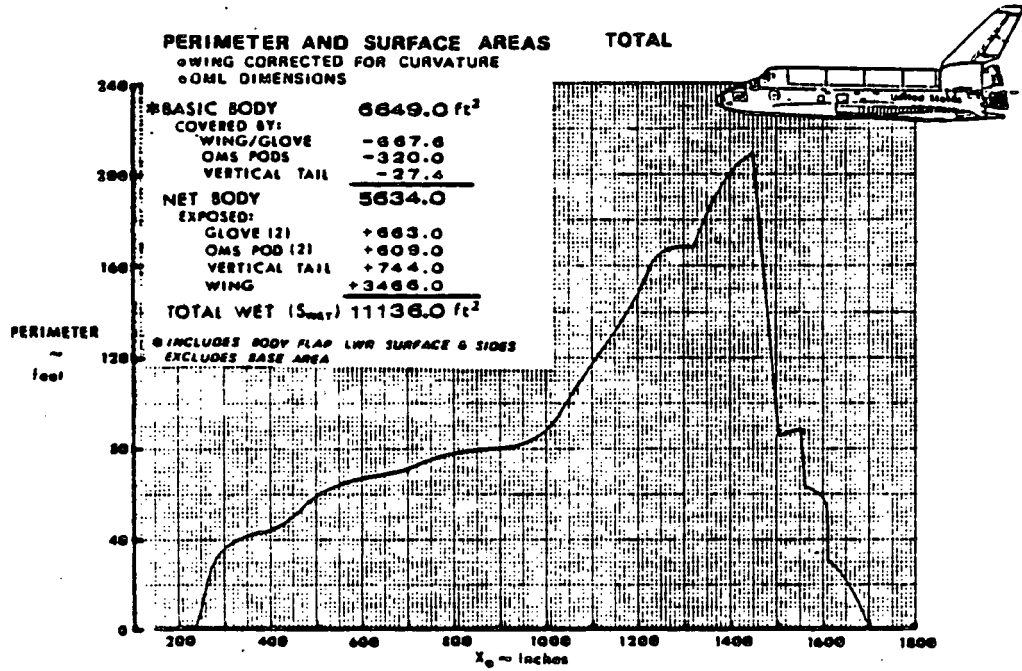


Figure 3.1.5.4-4
PERIMETER DISTRIBUTION

ORIGINAL PAGE IS
OF POOR QUALITY

3.2 SURFACE DESIGN REQUIREMENTS

3.2 SURFACE DESIGN REQUIREMENTS. The aerodynamic integrity of the Space Shuttle Vehicle is dependent on the efficiency of all surfaces exposed to the airflow such that surface design requirements are critical to the definition of the vehicle aerodynamic characteristics. The allowable aerodynamic surface alignments, Outer Mold Line (OML) fairing and smoothness requirements, and the sealing requirements which establish deviations affecting both aerodynamic and aerothermodynamic characteristics of the vehicle are discussed in this subsection [3.2].

3.2.1 SOLID ROCKET BOOSTERS. The pre-flight OML surface finish on the SRB is basically that of the surface coating or materials applied to the exterior structure and protuberances. A spray-on ablative material (MSA-1) with a weather sealer top coat is applied to areas such as the forward skirt and protuberances, including the cable systems tunnel. Cork is used extensively on the aft skirt, forward nose cap, and separation motor fairings. External thermal protection is not required for the steel motor case segments but paint is applied to provide corrosion resistance.

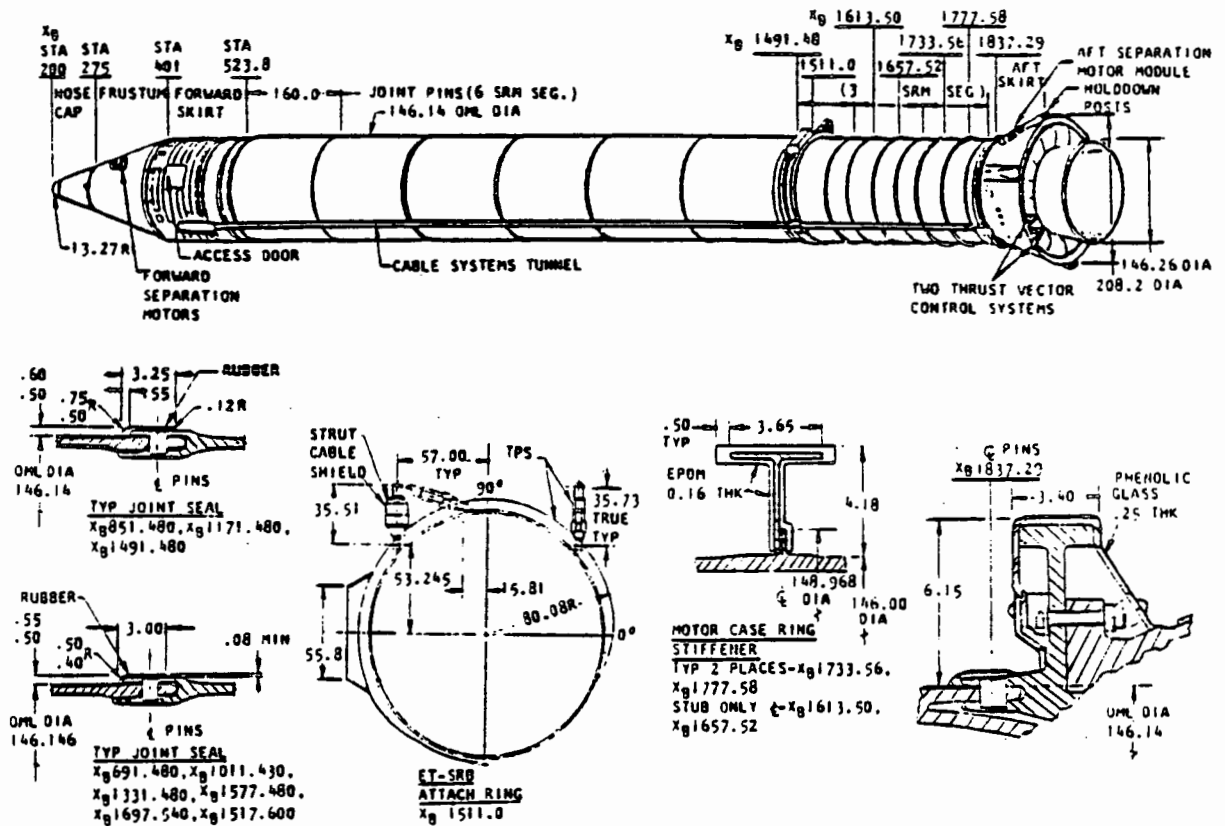


Figure 3.2.1-1
TYPICAL SRB PROTUBERANCES

ORIGINAL PAGE IS
OF POOR QUALITY

Significant protuberances are defined in Reference 3-8 as those larger than a threshold size which could cause a change in drag or thermal environment. The maximum height and width of such protuberances are not to exceed a specified distance beyond a nominal OML defined for static ambient conditions. The threshold size for significant protuberances is defined in the reference for three radial regions at the stations where the protuberances are located (see under 3.2.2, SIGNIFICANT PROTUBERANCES). Typical examples of protuberances which may deviate from the threshold size requirements include the cable systems tunnel, motor case segment joint flanges, aft case stiffener rings, and the SRB/ET attach ring and struts. Figure 3.2.1-1 illustrates some typical examples of these protuberances.

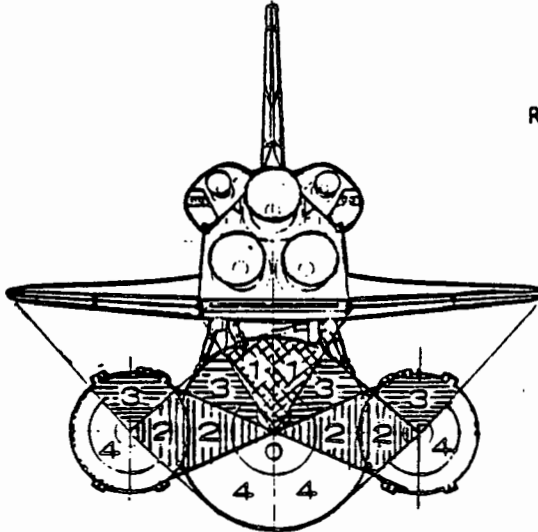
- 3.2.2 EXTERNAL TANK. Two versions of the External Tank exist - the heavy weight and the lightweight tank. Both versions are currently planned for use operationally. Dimensionally detailed descriptions of the external surfaces, OML definition, and protuberances are contained in Reference 3-8. The External Tank mold lines and aerodynamic fairings are not to exceed a nominal mold line defined for static ambient conditions as specified in the reference for both the heavy and light weight tanks.

The pre-flight OML surface finish on the ET consists of the nose cone surface insulating/ablative material, ogive area insulation, and a spray-on foam insulation applied over most of the ET exterior (including higher temperature ablative insulators). The nose cone insulating/ablative material (SLA561) is machined to 0.63 ± 0.03 inches and is normally controlled to within 20 percent of the specified thickness. The ogive insulation is 2-inches thick, reducing to 1-inch at ET station 851 (intertank juncture). The initial smoothness of the spray-on foam insulation (SOFI) is that required to obtain the specified thickness and OML tolerances, although, that sprayed on the intertank area ribs can vary considerably (1.00, + 0.75, -0.50 inch on the rib tops with a minimum of 0.30 inch required on the rib sides).

Significant ET protuberances are defined for four radial regions of the tank at the ET stations where the protuberances are located. The maximum allowable height and width of significant protuberances are calculated in the following manner:

SIGNIFICANT PROTUBERANCES

THERMAL ENVIRONMENT



| | | | | |
|---|--------|---|--|----------------------------|
| } | REGION | 1 | | $\Delta = 0.15 + .0003(X)$ |
| | | 2 | | $\Delta = 0.15 + .0004(X)$ |
| | | 3 | | $\Delta = 0.15 + .001(X)$ |
| | | 4 | | $\Delta = 0.15 + .002(X)$ |

WIDTH-NOT TO EXCEED Δ

Δ is the maximum allowable height above OML.
X is the distance in inches from the nose of the element (ET or SRB) to the station where the protuberance is located.

$$X_{ET} = (X_{PROT} - 322.5)$$

$$X_{SRB} = (X_{PROT} - 200.0)$$

NOTE:

- (1) No criteria for SRB aft of SSME exit plane.
- (2) This criteria does not apply when protuberances of different elements are facing each other. Each of these cases should be treated individually.
- (3) Not applicable to uniformly distributed TPS surface roughness or to tolerances on TPS OML. Protuberance heights are measured from OML of TPS.
- (4) All protuberances > 1.0 will be reported regardless of criteria.

AERODYNAMICS

All protuberances > 1 inch from the vehicle moldline (projected above TPS or hard structure) and greater than 2 feet in width on the Shuttle Integrated Vehicle will require Level II approval.

All protuberances will be reported regardless of criteria.

Typical examples of protuberances which may deviate from the threshold size requirements include the forward and aft Orbiter attach structure; the LO_2 feed, pressure, and anti-geyser lines; LH_2 feed, pressure, and recirculation lines; and the electrical conduit.

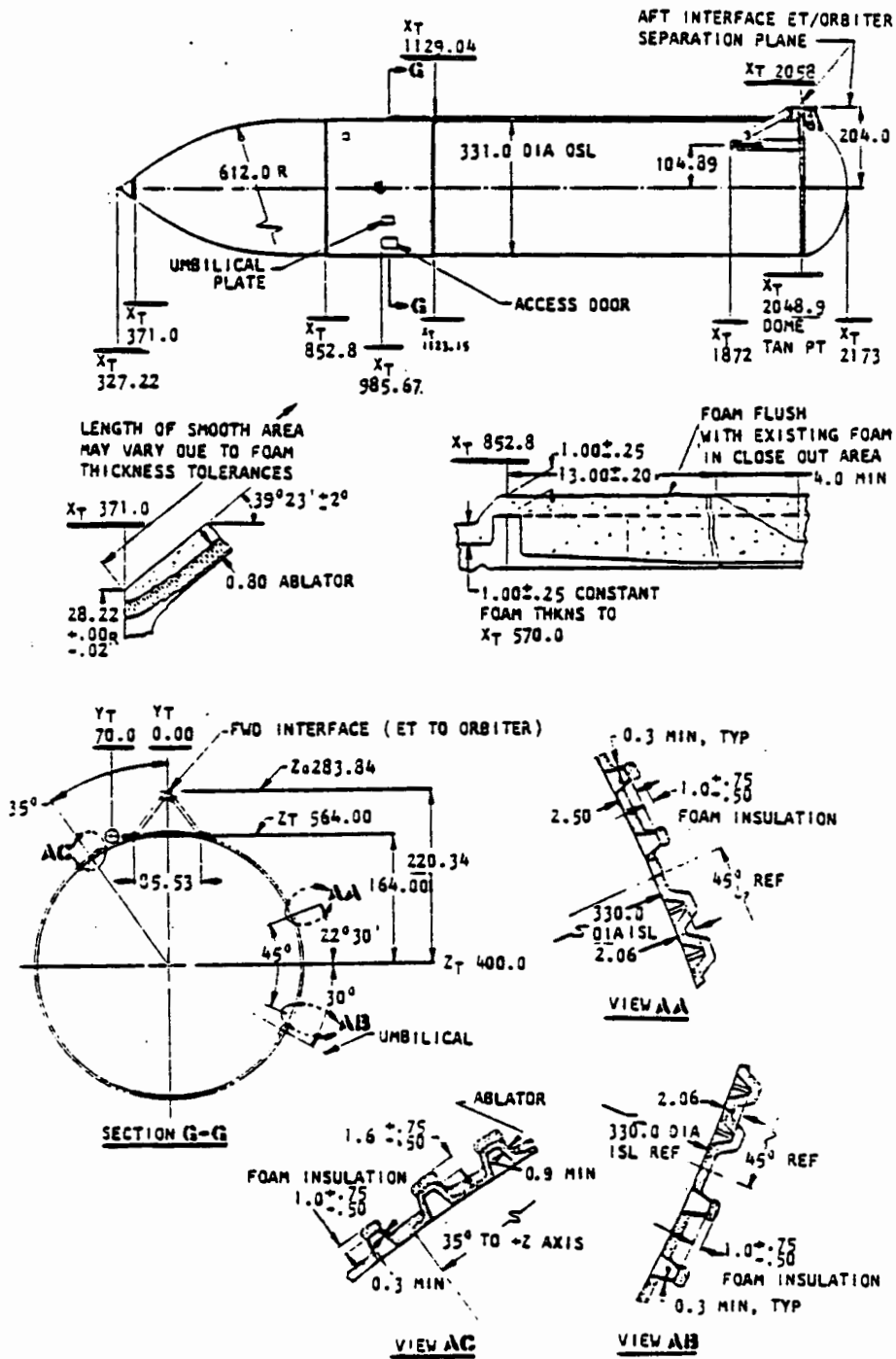


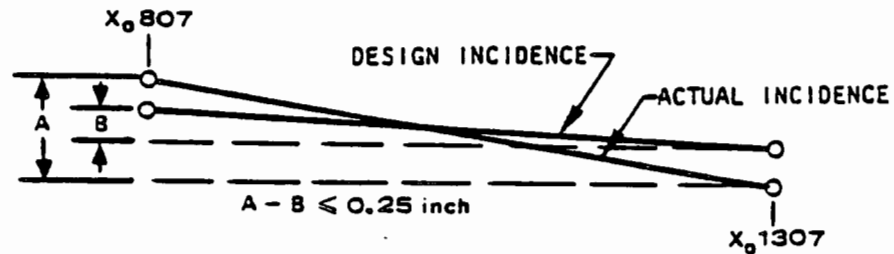
Figure 3.2.2-1
TYPICAL ET PROTUBERANCES

ORIGINAL PAGE IS
OF POOR QUALITY

3.2.3 ORBITER VEHICLE. The Orbiter Vehicle surface design requirements, allowable surface alignments, OML fairing and smoothness, and the sealing requirements which established deviations affecting both aerodynamic and aerothermodynamic characteristics are outlined below.

WING INCIDENCE TOLERANCE

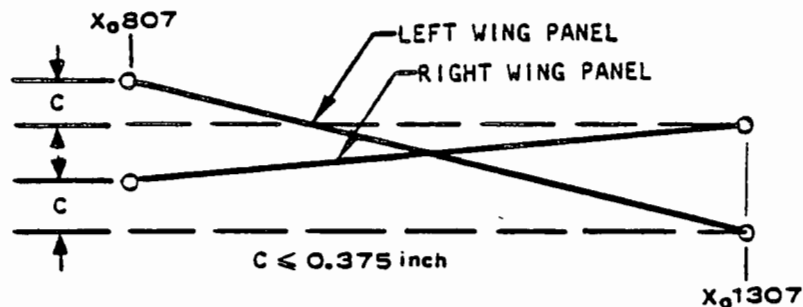
X-Z PLANE AT WING-FUSELAGE JUNCTURE Y₀105



- | | <u>CRITERIA</u> | <u>RATIONALE</u> |
|---|--------------------|---|
| <ul style="list-style-type: none"> • MAXIMUM ALLOWABLE WING INCIDENCE TOLERANCE AT WING-FUSELAGE JUNCTURE FOR THE LEADING EDGE ELEMENT RELATIVE TO THE TRAILING EDGE ELEMENT (FUSELAGE AND WING SUPPORTED IN MATING TOOLING) | <p>≤ 0.25 INCH</p> | <p>MAINTAIN ACCEPTABLE IMPACT ON ELEVON REQUIREMENTS DUE TO STRUCT. MISALIGNMENTS</p> |

WING DIFFERENTIAL INCIDENCE TOLERANCE

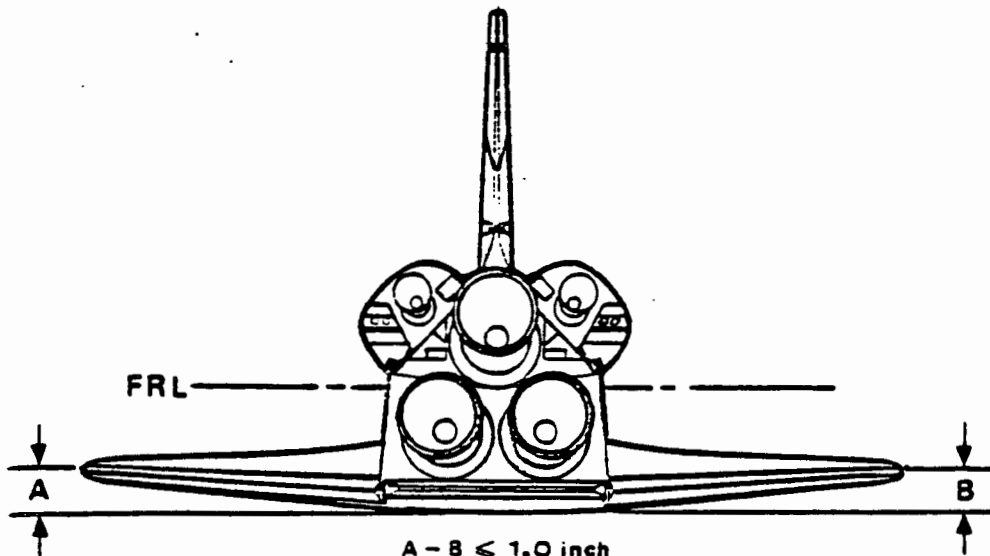
X-Z PLANE AT WING-FUSELAGE JUNCTURE Y₀105



- | | <u>CRITERIA</u> | <u>RATIONALE</u> |
|--|---------------------|---|
| <ul style="list-style-type: none"> • MAX ALLOWABLE DIFFERENTIAL INCIDENCE BETWEEN THE LEFT AND RIGHT WING PANELS AT THE WING-FUSELAGE JUNCTURE (VEHICLE SUPPORTED IN TOOLING JIG) | <p>≤ 0.375 INCH</p> | <p>MINIMIZE DEGRADATION OF AILERON EFFECTIVENESS DUE TO STRUCTURAL MISALIGNMENT</p> |

WING'S DIFFERENTIAL INCIDENCE TOLERANCE EQUALS LEFT WING'S INCIDENCE TOLERANCE MINUS RIGHT WING'S INCIDENCE TOLERANCE
OR, $C = (A - B)_{\text{LEFT WING}} - (A - B)_{\text{RIGHT WING}}$

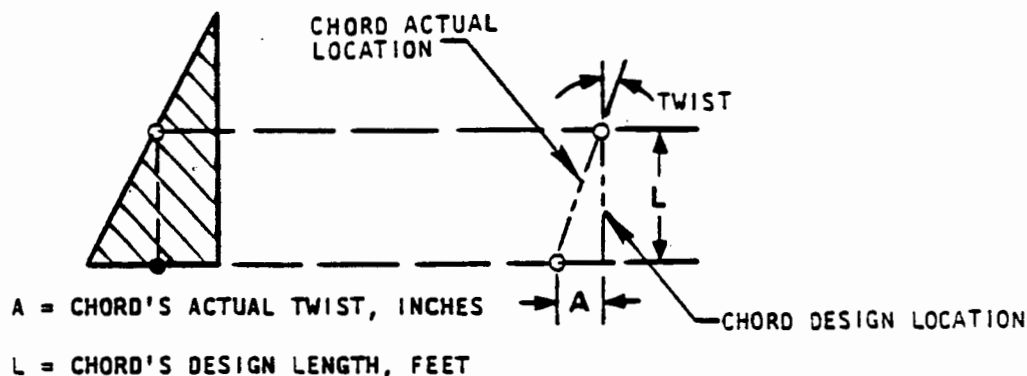
DIFFERENTIAL DEFLECTION OF WING TIPS



- MAXIMUM DIFFERENTIAL DEFLECTION OF WING TIPS (FUSELAGE AND WING SUPPORTED IN MATING TOOLING)

RATIONALE: MINIMIZE ASYMMETRIC LIFT AND ROLL

MAXIMUM ALLOWABLE TWIST TOLERANCE

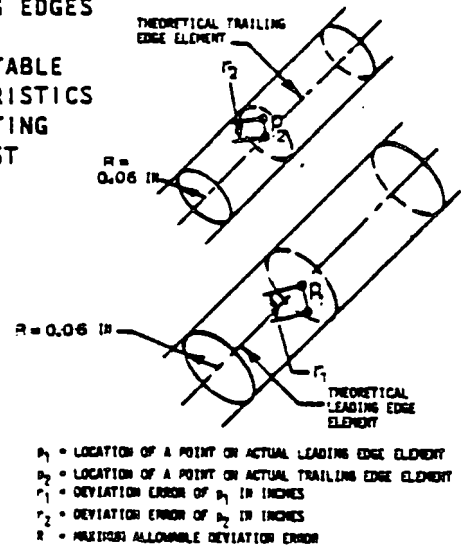


$$\text{LIFTING SURFACE TWIST TOLERANCE} = \frac{A}{L}, \frac{\text{INCHES}}{\text{FOOT}}$$

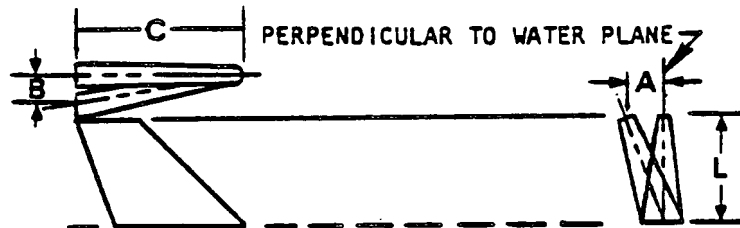
- | | <u>CRITERIA</u> | <u>RATIONALE</u> |
|---|-----------------------|--|
| • MAXIMUM ALLOWABLE TWIST TOLERANCE FOR ANY LIFTING SURFACE (WING OR TAIL (VEHICLE IN TOOLING JIG)) | ≤ 0.005 INCH PER FOOT | MAINTAIN SURFACE AERO EFFICIENCY AND REDUCE CONTROL REQUIREMENTS |
| • THE MAXIMUM ALLOWABLE DIFFERENTIAL TWIST TOLERANCE PER 12 INCH SPANWISE DISTANCE (VEHICLE IN TOOLING JIG) | ≤ 0.005 INCH PER FOOT | |

ERROR IN LOCATION OF LEADING AND TRAILING EDGES

- | <u>CRITERIA</u> | <u>RATIONALE</u> |
|---|--|
| <ul style="list-style-type: none"> • ACTUAL L.E. ELEMENT SHOULD LIE WITHIN AN 0.06 INCH-RADIUS CYLINDER FROM THE DESIGN LEADING EDGE ELEMENT • ACTUAL T.E. SHOULD LIE WITHIN 0.06 INCH-RADIUS CYLINDER FROM THE THEORETICAL TRAILING EDGE • REQUIREMENTS CHECKED AFTER LEADING AND TRAILING EDGE ASSEMBLIES HAVE BEEN FULLY FASTENED TO CENTER SECTION OF THE SURFACE. | <p>PROVIDE ACCEPTABLE AERO CHARACTERISTICS WITHOUT IMPACTING WEIGHT AND COST</p> |



VERTICAL TAIL CANT AND INCIDENCE TOLERANCE



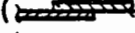
$$\text{CANT TOLERANCE} = \frac{A \text{ INCHES}}{L \text{ FOOT}}$$

$$\text{INCIDENCE TOLERANCE} = \frac{B \text{ INCHES}}{C \text{ FOOT}}$$

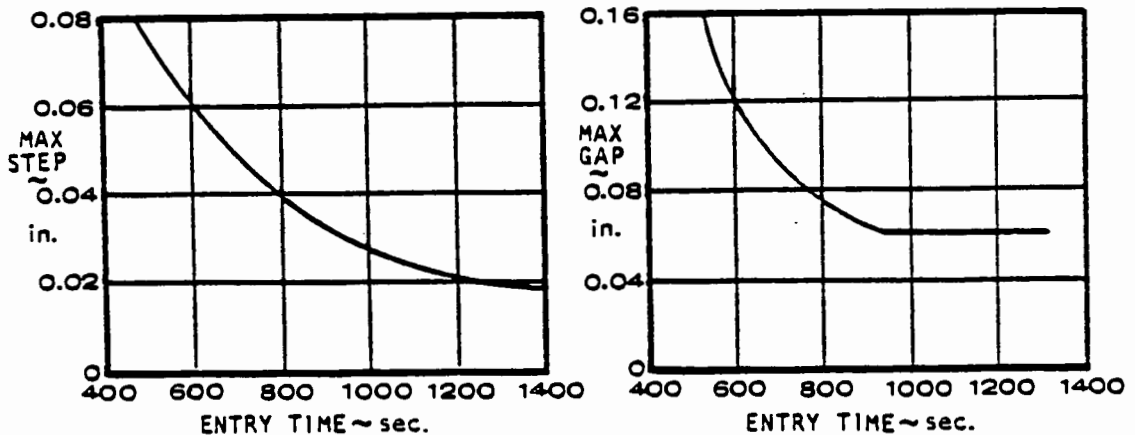
- | <u>CRITERIA</u> | <u>RATIONALE</u> |
|--|---|
| <ul style="list-style-type: none"> • MAXIMUM ALLOWABLE VERTICAL TAIL CANT (VEHICLE IN TOOLING JIG) • MAXIMUM ALLOWABLE INCIDENCE TOLERANCE OF THE VERTICAL TAIL (VEHICLE IN TOOLING JIG) | <p> ≤ 0.025 INCH PER FOOT ≤ 0.0125 INCH MAINTAIN VERTICAL TAIL AERO EFFICIENCY AND REDUCE CONTROL REQUIREMENTS </p> |


The aerodynamic criteria pertaining to surface discontinuities and waviness are based on aerodynamic efficiency requirements of lifting surfaces and the prevention of premature transition from laminar to turbulent boundary layers during the high heating portion of entry. The prevention of premature separation of the boundary layer on all fixed and movable lifting surfaces is also important. Aerodynamic efficiency is affected to a much greater extent by surface conditions over forward regions of components rather than aft regions.

Tolerance criteria are, therefore, generally more severe for forward sections of the vehicle surfaces and are somewhat relaxed for aft portions.

Surface discontinuities consist of steps and gaps. A step is an abrupt deviation from the faired contour; e.g., a lap joint (). The tolerance for a forward facing step is generally the same as for a rearward facing step unless specifically noted otherwise. The step requirements (cf. Figure 3.2.3-2) apply to all surface irregularities which have a dimension normal to the OML except RCC areas. RCC step and gap criteria are shown below based on trajectory 2689.

**RCC/RCC STEP AND GAP CRITERIA
BASED ON TRAJECTORY 2689**



A gap is defined as an abrupt negative deviation from a faired contour followed by an abrupt positive deviation such as is caused by a poorly matched butt joint () or spaces between TPS tiles. TPS gap criteria are outlined below and apply to all surface gaps with the exception of RCC areas (given above) and control surface gaps. Gaps shall not allow any increase in air leakage.

TPS GAP CRITERIA (PRE-FLIGHT)

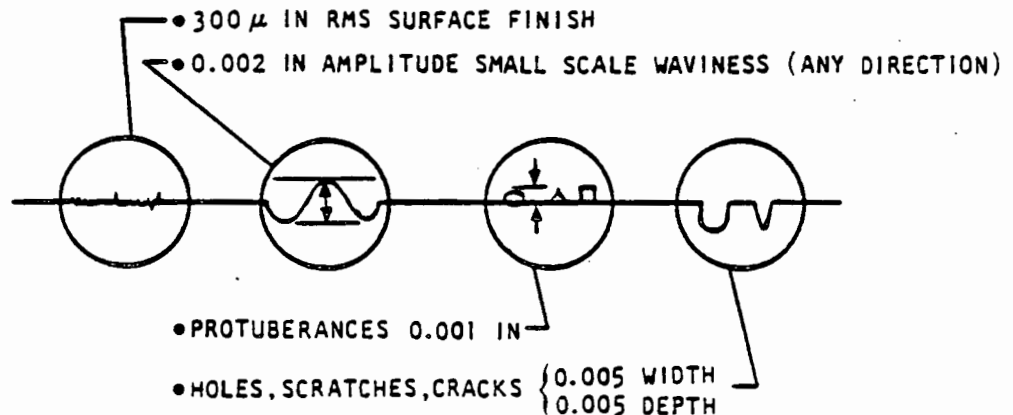
- BASIC REQUIREMENT: MINIMIZE GAP WIDTH AT THE AERODYNAMIC SURFACE
 - LOWER SURFACE: 0.045±0.020 inch
(BELOW A LINE: X₀238, Z₀336 TO X₀582, Z₀320
AND X₀>582, Z₀320; LOWER SURFACE OF WING;
GLOVE L.E. TO LRS1; UPPER AND LOWER BODY
FLAP; BASE HEAT SHIELD)
 - UPPER SURFACE: 0.055±0.020 inch
(ALL SURFACES NOT DEFINED ABOVE)
- TILE PATTERNED SO THAT NO GAPS ARE ALIGNED WITH LOCAL SURFACE STREAMLINES DURING ENTRY.
- TPS GAP EDGE RADIUS: 0.06 inch (MAXIMUM)

A wave is defined as a smooth variation from a faired contour. The wave height (H) is the distance measured normal to the surface between a low point on the surface and an adjacent high point. The wavelength (λ) is twice the distance from a low point on the surface to an adjacent high point. (See Figure 3.2.3-1 for surface waviness criteria and Figure 3.2.3-2 for maximum allowable gaps). The waviness requirement applies to all external surfaces.

The master lines OML fairing requirements permit no reflex fairing on lower surfaces. Reflex fairing is permitted on upper surfaces. Continuous second derivatives of equations defining the surface of the lower forward fuselage are required. The maximum manufacturing fairing deviation from the theoretical fairing is ± 0.06 inch consistent with the OML smoothness requirements, TPS thickness requirements, and aerodynamic surface alignment requirements. Maximum surface irregularities, including RMS surface finish, are defined below.

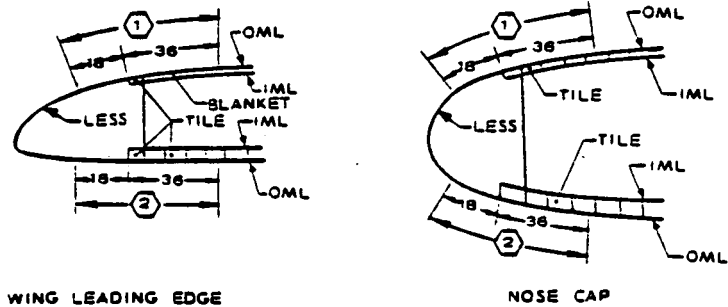
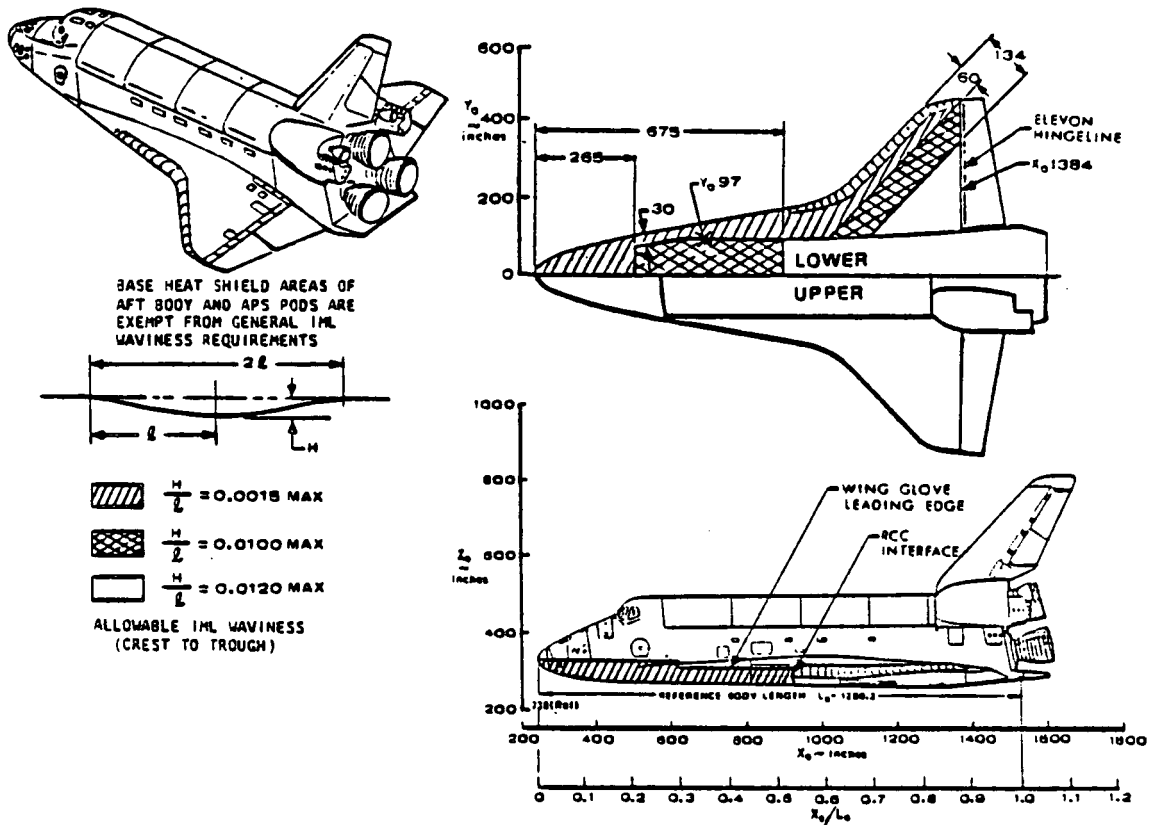
MICRO SURFACE FINISH CRITERIA

- APPLIES TO ALL EXTERNAL SURFACES (HRSI, LRSI, FRSI, RCC AND METALLIC TPS)
- DEFINITION OF MAXIMUM ALLOWABLE SMALL SCALE IRREGULARITIES



PENETRATION CRITERIA

- NOSE LANDING GEAR DOOR OML
 - STEPS ± 0.017 inch MAXIMUM ANY DIRECTION
 - LONGITUDINAL GAPS 0.034 inch WIDE x 0.034 inch DEEP OR EQUIVALENT AREA, ONE GAP PER DOOR INTERFACE.
 - TRANSVERSE GAPS 0.045 \pm 0.020 inch (FILLED WITH HIGH PRESSURE GRADIENT THERMAL BARRIER).
- FORWARD EXTERNAL TANK ATTACHMENT OML
 - STEPS ± 0.017 inch MAXIMUM
 - GAPS 0.030 inch MAXIMUM (BASED ON 3.0 inches MAXIMUM CIRCLE DIAMETER).



① $\frac{H}{L} = 0.0150$

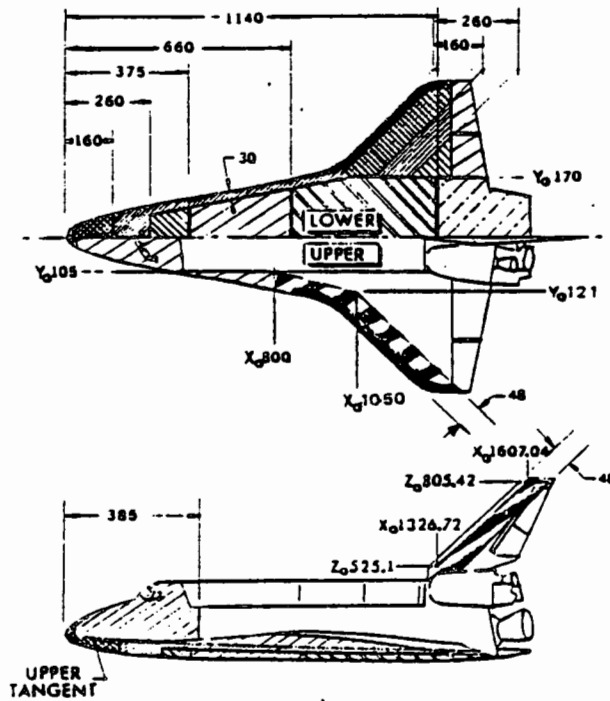
② $\frac{H}{L} = 0.0015$

LESS/WING UP'R SURFACE
NOSE CAP/BODY UP'R SURF. ABOVE MMB

LESS/WING UP'R SURFACE
NOSE CAP/BODY UP'R SURF. BELOW MMB

OUTER MOLD LINE WAVINESS CRITERIA

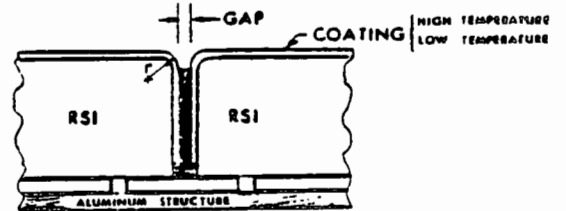
Figure 3.2.3-1
ORBITER VEHICLE SURFACE WAVINESS CRITERIA



MAXIMUM ALLOWABLE STEPS

| | | | |
|--|--------------------------------------|--|------------------------------------|
| | ± 0.017 in. | | ± 0.025 in. |
| | ± 0.020 in. | | ± 0.035 in. |
| | ± 0.030 in. | | ± 0.040 in. |
| | FORWARD FACING (UPSTREAM) +0.060 in. | | AFT FACING (DOWNSTREAM) -0.060 in. |

AFRSI ± 0.12 EXCEPT WING & VT LE



MAXIMUM ALLOWABLE GAP

Lower Surface: 0.045 ± 0.020 inches
 Upper Surface: 0.055 ± 0.020 inches
 TPS Gap Edge Radius: 0.060 inches (Maximum)

STEPS +0.05, -0.12
 NOTE: NO FWD FACING STEPS ALLOWED AT TILE/BLANKET BUTT JOINTS

Figure 3.2.3-2
 ORBITER OML STEP AND GAP CRITERIA

Surface irregularities due to protuberances such as air data probes, umbilical attachment, vents, and nozzle ports must be assessed on an individual basis. Such items are shown on Figure 3.2.3-3.

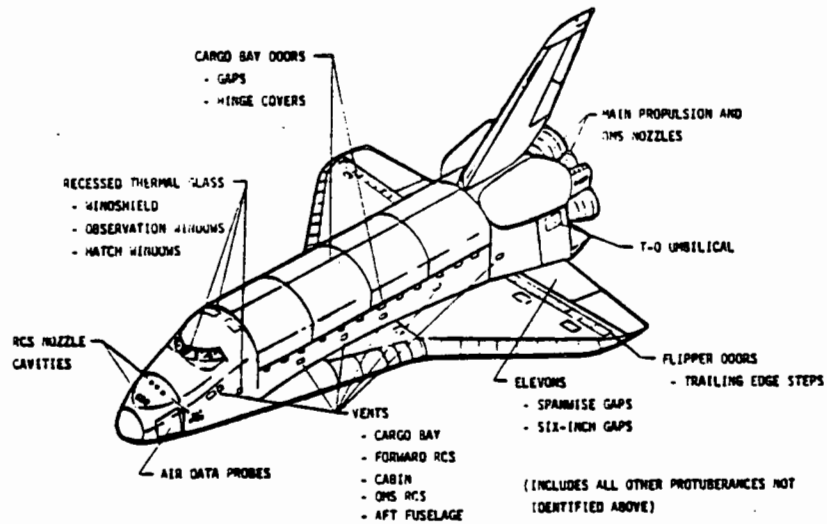


Figure 3.2.3-3
 PROTUBERANCE ITEMS REQUIRING SPECIAL TREATMENT

The prevention of unprogrammed air leakage from inside the Orbiter or through lifting surfaces is important in maintaining lift effectiveness and minimum total drag. An unsealed surface has more profile drag and drag-due-to-lift than a sealed surface.

OUTER MOLD LINE SEALING REQUIREMENTS DURING ENTRY

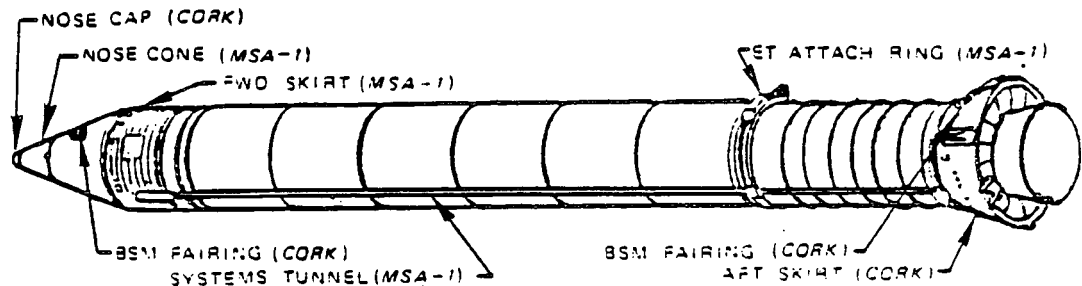
(Beyond the scope of this book, refer to Reference 3-11)

3.3 THERMAL PROTECTION SYSTEM

3.3 THERMAL PROTECTION SYSTEM. The Thermal Protective System (TPS) is designed to protect the primary airframe structure from the effects of aerodynamic heating during ascent and entry. The basic TPS for the SRB's is a spray-on ablative material with a weather sealer. Ablative composites are used on the ET in areas of high aerodynamic heating and in those areas subjected to plume heating. In general, the Orbiter TPS consists of reusable surface insulation tiles.

3.3.1 SOLID ROCKET BOOSTERS. The requirement for thermal protection of the SRB's is less extensive than for either the ET or Orbiter Vehicle. Thermal protection is required in those areas subjected to maximum aerodynamic and plume heating where aluminum skin is employed such as the nose cone, forward skirt, aft skirt, and BSM fairings. Several protuberances (rings and attach structure) also require special protective materials for instrumentation and electrical cables.

The two primary materials used for insulation on the SRB's are Marshall Sprayable Ablator (MSA-1) and cork. The MSA-1 is used on the forward skirt and cone areas, systems tunnel, and around the ET attach ring of the SRB. This material is sprayed on and built up to a thickness of 0.125 to 0.25 inch. Cork is bonded to the aft skirt, BSM fairings, and nose cap with a urethane adhesive with a thickness ranging from 0.25 to 0.50 inch. Both materials (MSA-1 and cork) are readily removed for SRB refurbishment.



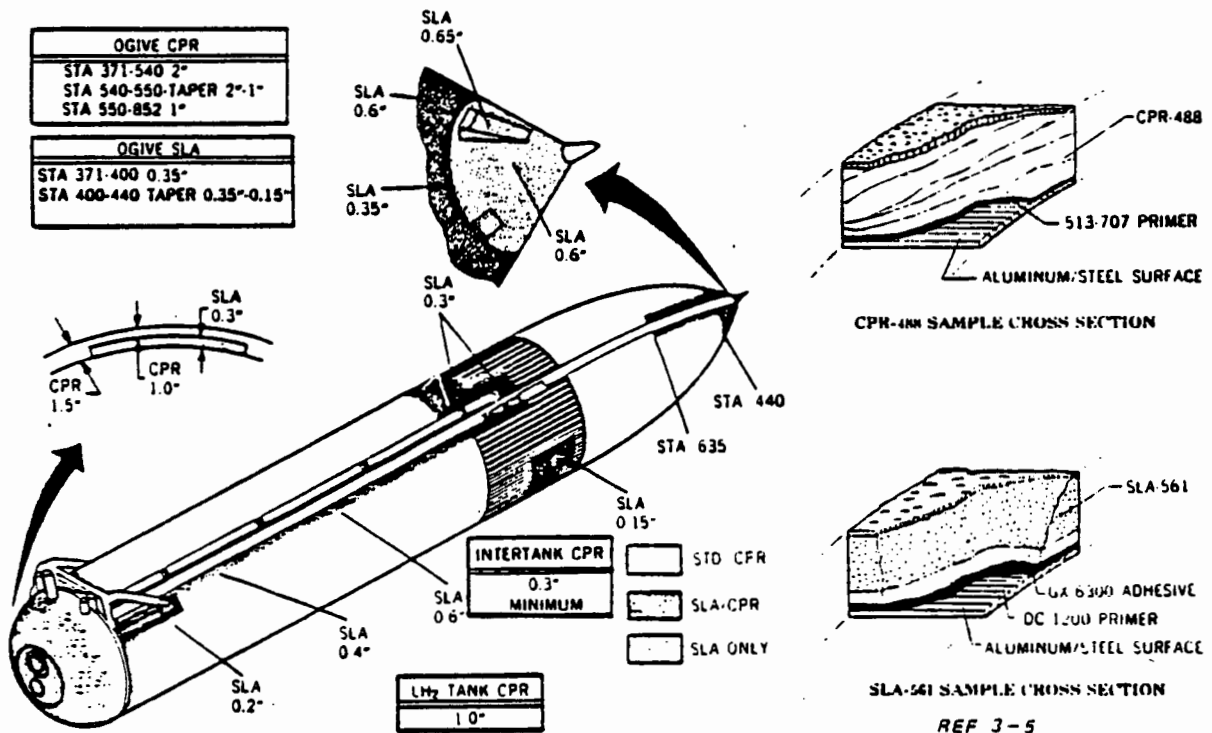
SRB THERMAL PROTECTION

Detailed SRB thermal protection system descriptions are given in Reference 3-10.

3.3.2 EXTERNAL TANK. The major portion of the ET thermal protection is provided by Spray-On Foam Insulation (SOFI) which is applied over most of the ET exterior, including higher temperature ablative insulators. The SOFI (CPR-488) is a light weight (2.4 lb/ft³), low conductivity (0.014 BTU/ft²-hr^oF at 75^oF) material which provides for heating rates up to 10 BTU/ft²-sec and temperatures above 300^oF. Application of the SOFI is carefully controlled to provide the required strength, adhesion, thickness, and surface finish without machining. SOFI thickness is defined by pre-launch requirements for stable, high-quality propellants and a minimum of air condensation and ice formation.

Ablative materials are used on ET surface areas where ascent flight heating rates exceed the SOFI temperature limits. These ablative materials maintain design temperature limits for the structure, system components, and propellant boil-off rates as aerodynamic and plume heating char the SOFI. The ablator thickness and required heating rates are derived from the worst case mission environment which, for the most part, is an Abort-Once-Around (AOA).

The primary ablative material used is SLA-561 (for heating rates up to 25 BTU/ft²-sec) which is a highly filled composite of silicone rubber base with a nominal density of 18 lb/ft³ and a thermal conductivity of 0.45 BTU/ft-hr.^oF at 75^oF. A similar material of higher density (30 lb/ft³), MA-225, is used for heating rates up to 75 BTU/ft²-sec. An over-coat is applied to the ablator material to prevent moisture accumulation in the porous filler material. Certain areas of the ET use SLA type ablative material under a CPR foam insulator as indicated in the sketch.



ET THERMAL PROTECTION

Two light weight urethane foams (BX-250) are also applied in smaller areas with lower thermal requirements (less than 200^oF substrate) such as the LO₂ tank forward bulkhead and aft dome and on the LH₂ forward dome. Detailed ET thermal protection system descriptions can be obtained from Reference 3-5. The ET Thermal Protection is summarized in Table 3.3.2-1.

Table 3.3.2-1
EXTERNAL TANK THERMAL PROTECTION

| ET COMPONENT | TPS MATERIAL | THICKNESS |
|--|-----------------|--------------------------------------|
| | | inches |
| Acreage | | |
| Nose Fairing | SLA-561 | 0.6 |
| LO ₂ Vent Louvers | SLA-561 | None |
| Conduit Fairing | SLA-561 | 0.65 |
| LO ₂ Tank Ogive | CPR-488/SLA-561 | Taper |
| LO ₂ Tank Barrel | CPR-488 | 1.0 |
| LO ₂ Tank Fwd Bulkhead | BX-250 | 0.5 |
| LO ₂ Tank Aft Dome | BX-250 | 0.5 |
| Intertank | CPR-488/SLA-561 | 0.5* |
| LH ₂ Tank Fwd Dome | BX-250 | 0.5 |
| LH ₂ Tank Aft Dome | CPR-488/SLA-561 | 1.0* |
| LH ₂ Tank Barrel | CPR-488/SLA-561 | 1.0* |
| Penetration | | |
| LO ₂ Feedline | CPR-488 | 1.0 |
| GO ₂ Pressurization Line | None Req. | --- |
| LH ₂ Feedline | SLA-561/CPR | 0.6/1.0 |
| LH ₂ Recirculation Line | SLA-561/CPR | 0.6/1.0 |
| GH ₂ Pressurization Line | None Req. | --- |
| Electrical Cable Tray | SLA-561/MA-255 | 0.3-0.65 |
| LH ₂ Vent Line | BX-250 | 0.5 |
| LO ₂ Feedline Fairing | SLA-561 | 0.2 |
| GH ₂ Press Line Fairing | SLA-561 | 0.23 |
| Intertank Fairing | SLA-561 | 0.4 |
| Structural Attachments | | |
| LO ₂ Feedline (5) | SLA-561/CPR-488 | 0.4/1.0 |
| GO ₂ Pressure Line, GH ₂ Pressure Line, Cable Tray on LH ₂ Tank (14) | SLA-561/CPR-488 | 0.4/1.0 |
| LO ₂ Press Line/Cable Tray-LO ₂ Tank (17) | SLA-561/CPR-488 | 0.4/1.0 |
| Interface Structure | | |
| Fwd ET/ORB Attachment Strut | MA-255 | 0.5 |
| Aft ET/ORB Thrust Strut | SLA-561/SOFI | 0.15/1.0 |
| Aft ET/ORB Vertical Strut | SLA-561/SOFI | 0.75/1.0 |
| Aft ET/ORB Diagonal Strut | SLA-561/SOFI | 0.75/1.0 |
| Aft ET/ORB Crossbeam | SLA-561 | 0.50 Fwd/Aft Face 0.25 Top/Bottom |
| Fwd ET/SRB Attachment | None Req. | --- |
| LO ₂ Line Aft Interface Attachment | SOFI | 1.0 |
| LH ₂ Line Aft Interface Attachment | SOFI | 1.0 |
| Isolator Requirements | | |
| ET/SRB Aft Attachment (4) | Glass Phenolic | 0.4 |
| ET/ORB Fwd Attachment (2) | Glass Phenolic | 0.5 |
| ET/ORB Aft Vertical Attachment (2) | Glass Phenolic | 0.4 |
| ET/ORB Aft Sway Attachment (1) | Glass Phenolic | 0.4 |
| LO ₂ Feedline Attachment (8) | Glass Phenolic | 0.4 |
| LO ₂ Pressurization Line/Cable Tray (14) | Glass Phenolic | 0.5 |
| LH ₂ Pressurization Line Attachment (15) | Glass Phenolic | 0.5 |
| Miscellaneous | | |
| Intertank Umbilical Carrier Plate | None Req. | --- |

3.3.3 ORBITER VEHICLE. The Orbiter Vehicle TPS is required to provide adequate capability for assuring safe Earth return and intact landing following Abort-Once-Around (AOA) and Return-To-Launch-Site (RTL) abort. In general, the TPS consists of Reusable Surface Insulation (RSI) tiles of four types having a 100-mission capability. The four types of insulation used are:

FRSI (flexible RSI) to 700°F (entry) and 750°F (ascent)

AFRSI (advanced flexible RSI) 700°F to 1200°F (nominal)

LRSI (low temperature RSI) 700°F to 1200°F (nominal)

HRSI (high temperature RSI) 1200°F to 2300°F (nominal)

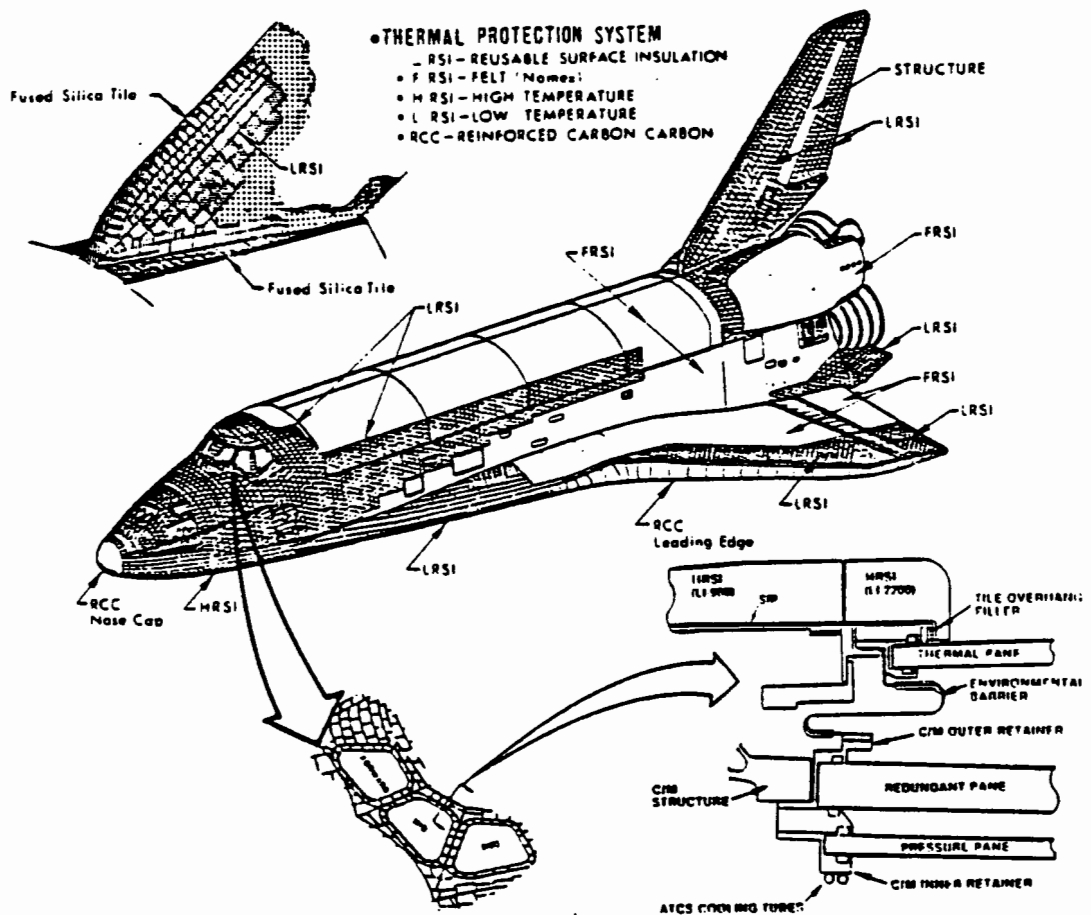


Figure 3.3.3-1

ORBITER THERMAL PROTECTION
(OV102 and OV099)

Orbiter Vehicle 102 was flown on the first five and on the ninth flights (STS-1 through STS-5 and STS-9). Orbiter Vehicle 099 was used on flights six through eight (STS-6, -7, and -8). The Thermal Protection System for OV102 during these flights is shown in Figure 3.3.3-1. OV099 TPS during flight STS-6 was similar to OV102 except that the OMS pods on OV099 were protected with AFRSI. The AFRSI on the highly curved forward edge of the OMS pods sustained severe damage during this flight. Consequently, AFRSI on the OMS pod leading edge and canopy was replaced with tile and/or FRSI for subsequent flights.

The Thermal Protection System for OV103 and OV104 is shown in Figure 3.3.3-2. Following flight STS-9, OV102 was returned to Palmdale, California for extensive modification from a flight test vehicle to a fully operational vehicle and the 102 MOD OMS pod TPS was made similar to that for OV103.

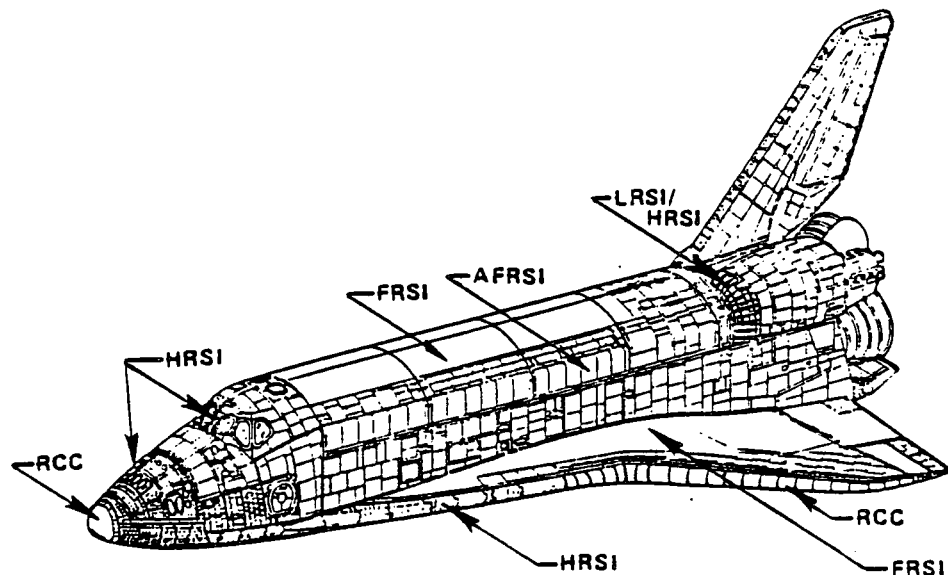


Figure 3.3.3-2

ORBITER THERMAL PROTECTION

(OV103 and OV104)

Tile gaps and steps influence the aerodynamic characteristics (particularly drag). Orbiter mold line criteria are given in Section 3.2.3. A more detailed description of the TPS is given in Reference 3-9.

3.4 AIR DATA SYSTEM

3.4 AIR DATA SYSTEMS. The air data systems are designed to provide air data relative to the vehicle at altitudes where winds, in conjunction with vehicle speeds, can produce relatively large errors in inertially derived air data. Orbiter Vehicle 102 will contain both the Ascent Air Data System (AADS) and the Orbiter Air Data System (ADS) for at least four flights. The remainder of the Operational Flights will contain only the ADS on the Orbiter.

ASCENT AIR DATA SYSTEM (AADS). The air data from the AADS are used in the Mach range 0.6 through 3.5. The AADS probe is located at the nose of the External Tank and is instrumented to measure total and static pressures as shown in Figure 3.4-1.

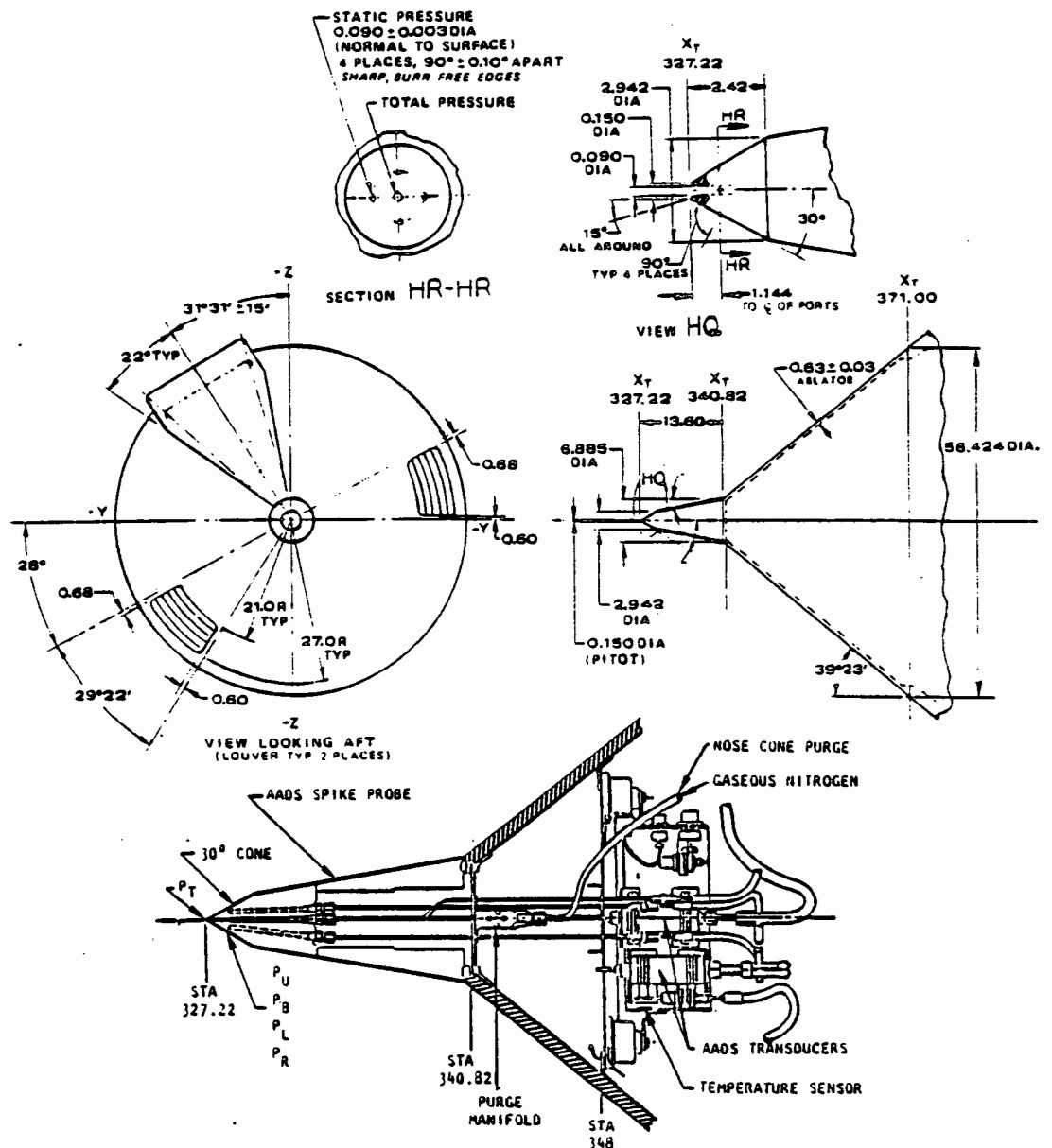


Figure 3.4-1
ASCENT AIR DATA SYSTEM

3.4-1

AIR DATA SYSTEM (ADS). At approximately 100,000 feet of altitude ($M \approx 3.5$) two air data probes are extended from the Orbiter forebody (FS 299, WP 324) to sense vehicle flight conditions. One probe is located on each side of the Orbiter forebody canted 10 degrees, nose down, relative to the FRL. The ADS probe is illustrated in Figure 3.4-2. The air data probe is instrumented to measure total temperature (T_T), local static pressure (P_S), and angle of attack from three pressure ports, (P_1 , P_2 and P_T).

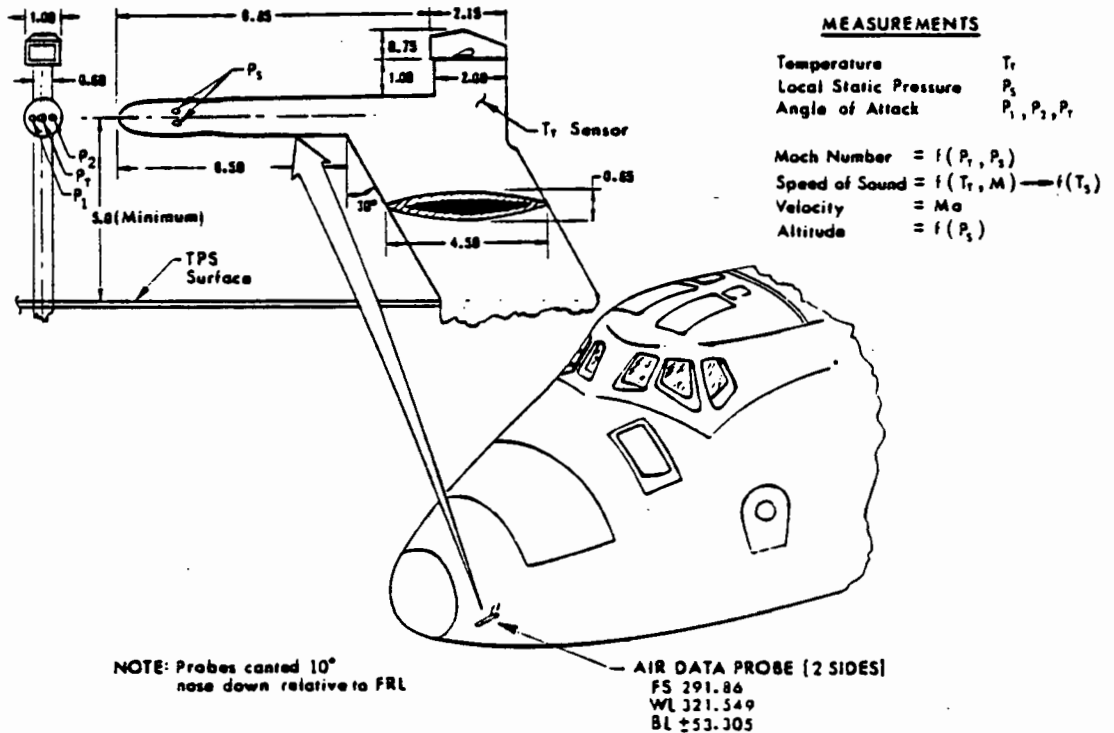


Figure 3.4-2
AIR DATA SYSTEM PROBE

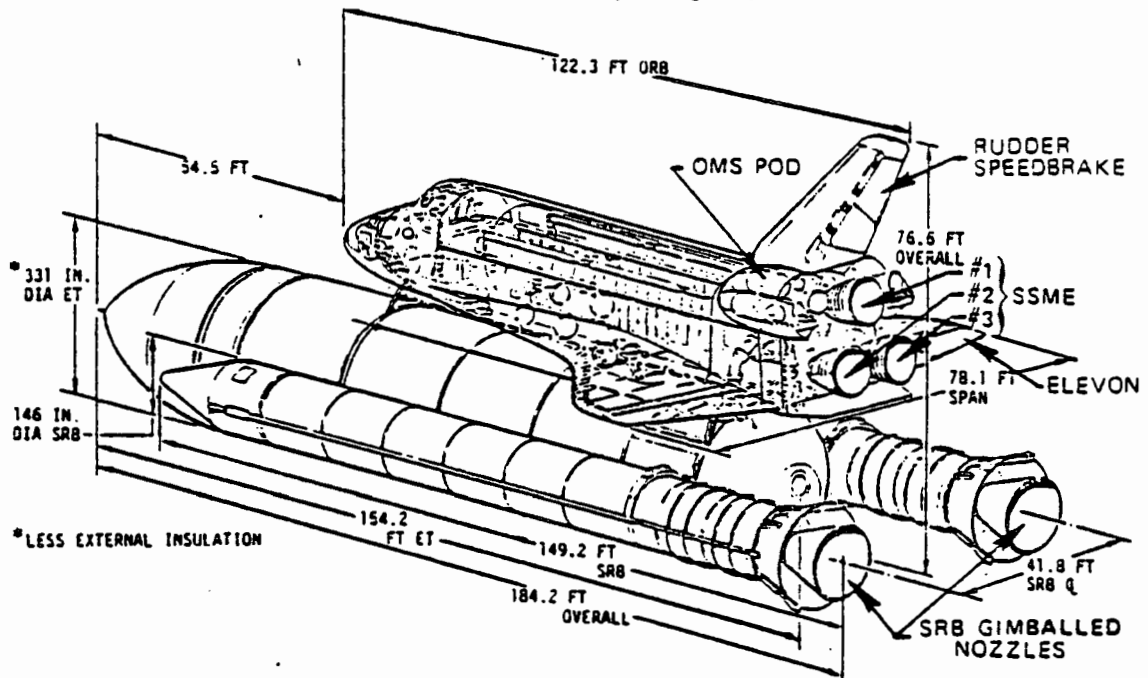
3.5 CONTROL SYSTEMS

3.5 CONTROL SYSTEMS. Space Shuttle control during the launch phase is achieved through a combination of aerodynamic surface controls, thrust vector gimbaling, and reaction controls. Orbiter Vehicle control during the entry phase is accomplished by blending RCS attitude control from the two aft OMS pods with aerodynamic surface controls. Surface deflections and gibal limits are presented, as well as the sign conventions applicable to developed forces and moments. Each form of control is discussed separately in the ensuing paragraphs of this section [3.5].

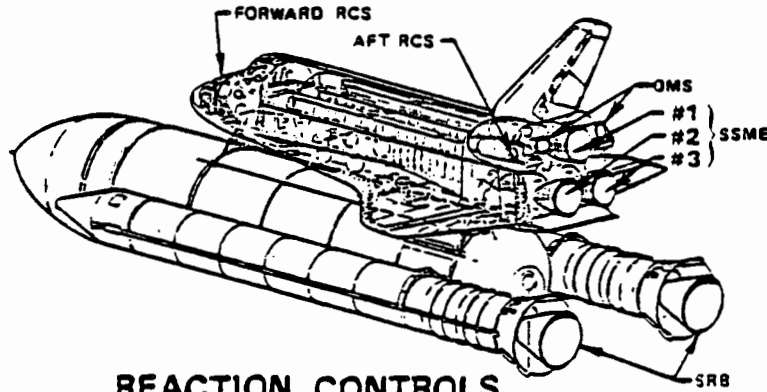
First stage boost relies primarily on SRB thrust gimbaling for control while the Space Shuttle Main Engine (SSME) gimbaling and elevon controls are used as load relief mechanisms. During SRB thrust tailoff, prior to SRB separation, primary control is switched to the SSME's where it remains throughout the entire second stage flight phase. During SRB staging, Booster Separation Motors (BSM's) are used to remove the SRB's from the proximity of the Orbiter and External Tank. No other form of control is available to alter the course of the SRB's during their descent to Earth. Throughout Orbiter/ET staging, and until such time as orbital insertion has been achieved, control of the Orbiter is attained by means of the Orbital Maneuvering System (OMS) engines. Once in orbit, Reaction Control System (RCS) jets are used to orient and change the course of the Orbiter vehicle.

The Return-To-Launch-Site (RTLS) abort separation of the Orbiter and ET utilizes a combination of elevon and RCS jet firing for control during mated coast (pre-separation), separation, and post-separation Orbiter recovery.

Rudder, speedbrake, or body flap controls are not used to any great extent during the launch phase or separation maneuver but are important to the Orbiter Vehicle entry flight phase.



3.5.1 REACTION CONTROLS. Reaction controls for the Space Shuttle Vehicle are comprised of the SRB thrust vector control, SSME thrust vector control, OMS thrust vector control, and the forward and aft RCS. Each system is discussed separately in the ensuing paragraphs.



REACTION CONTROLS

3.5.1.1 SRB THRUST VECTOR CONTROL. Solid Rocket Booster nozzle gimbaling, or Thrust Vector Control (TVC) is used for first stage control during boost. The SRB TVC subsystem consists of two hydraulic power units located adjacent to one another and two servoactuators, all of which are located in the aft skirt of each SRB as shown in Figure 3.5.1-1.

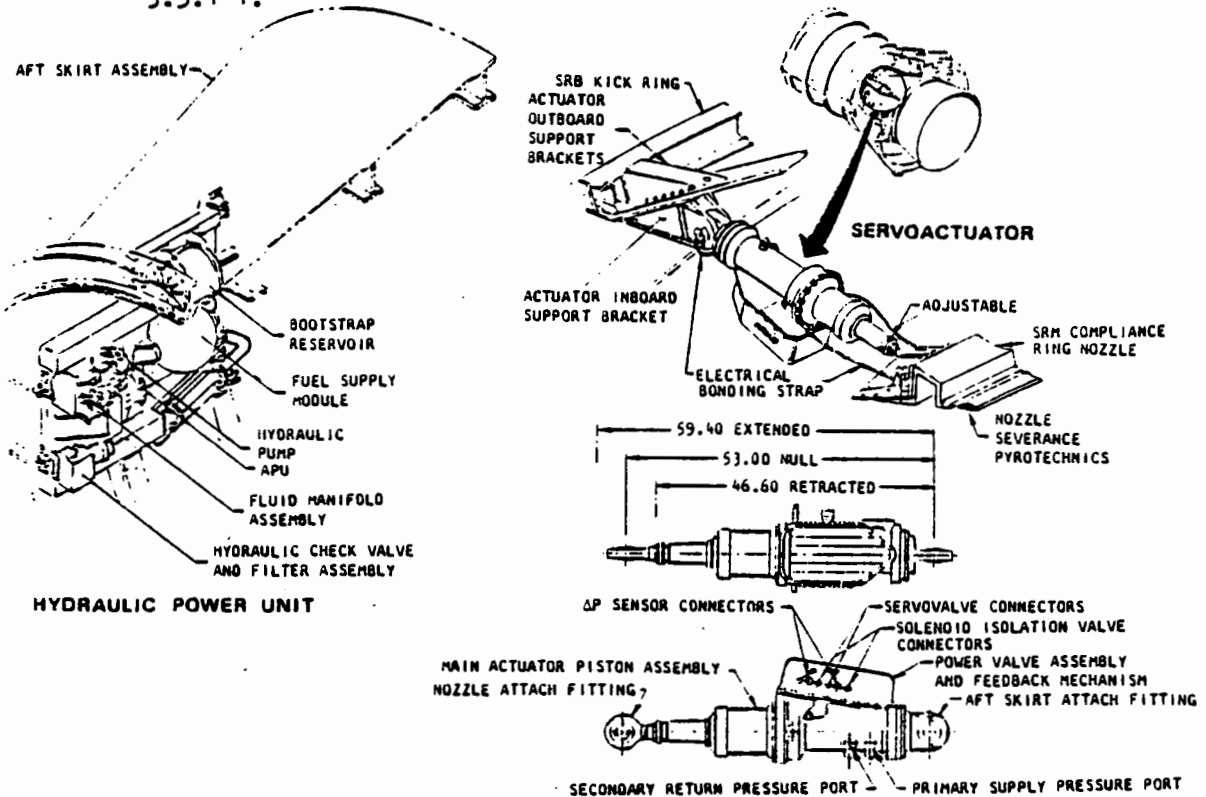


Figure 3.5.1-1
SRB THRUST VECTOR CONTROL

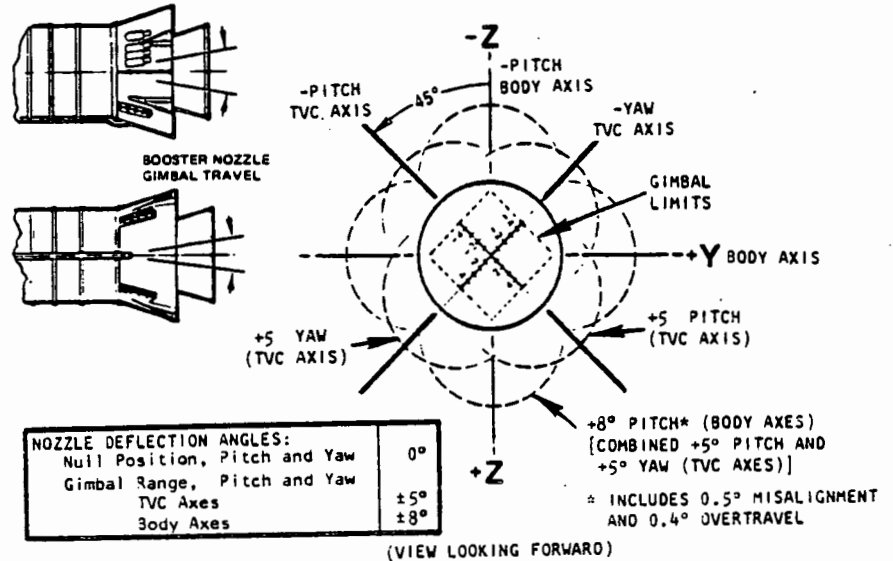
REF 3-4

The two hydraulic power units drive the two dual action servoactuators which provide attitude control for each of the SRB's in response to control commands

from the GN&C computers in the Orbiter Vehicle.

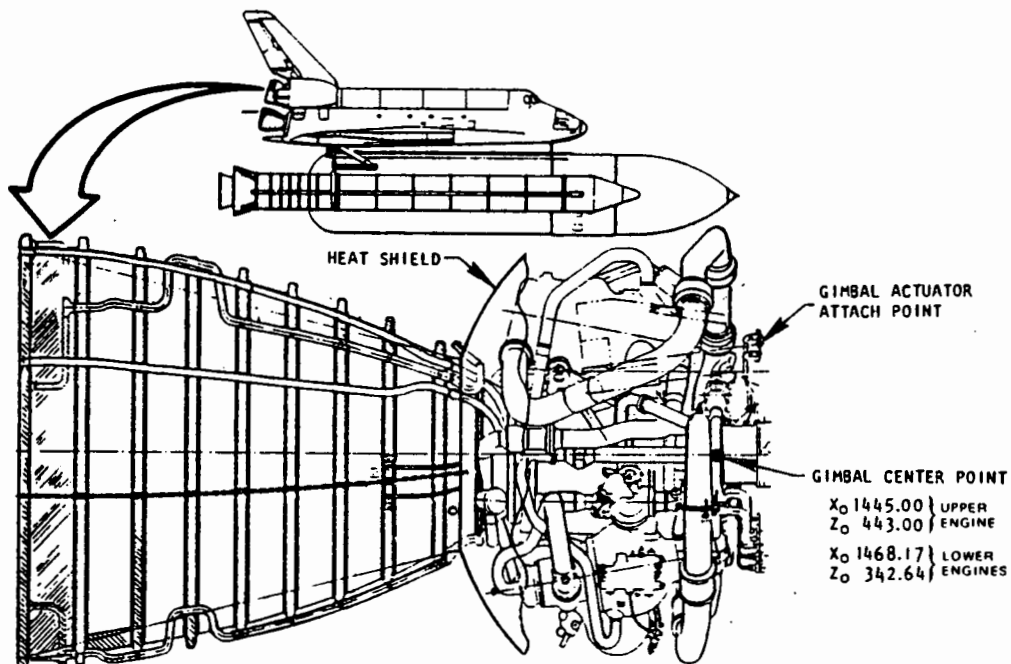
The servoactuators are located on the outboard sides of the SRB's, 45-degrees to the Y-axis, and are used to position the SRB nozzles in the pitch and yaw axes as commanded. SRB deflection angles are ± 5 degrees in the pitch and yaw TVC axes which correspond to ± 8 degrees in the body axis system.

At burnout, prior to separation, the TVC subsystem is designed to return each nozzle to the null position which is maintained from separation to splashdown.



SRB NOZZLE DEFLECTION ANGLES

3.5.1.2 SSME THRUST VECTOR CONTROL. The primary use of the Space Shuttle Main Engines is to provide thrust during first-stage boost. These engines are not used for control during the first stage, except to counter trajectory changes resulting from wind dispersions and immediately preceding first stage separation when the SRB's are nulled to zero (see Section 3.5.1.1) and shut down.



SPACE SHUTTLE MAIN ENGINE

SSME nozzle gimbaling is used for control during second stage flight. The nozzles can be deflected ± 11 -degrees in pitch and ± 9 -degrees in yaw from the null position as shown in Figure 3.5.1.2-1.

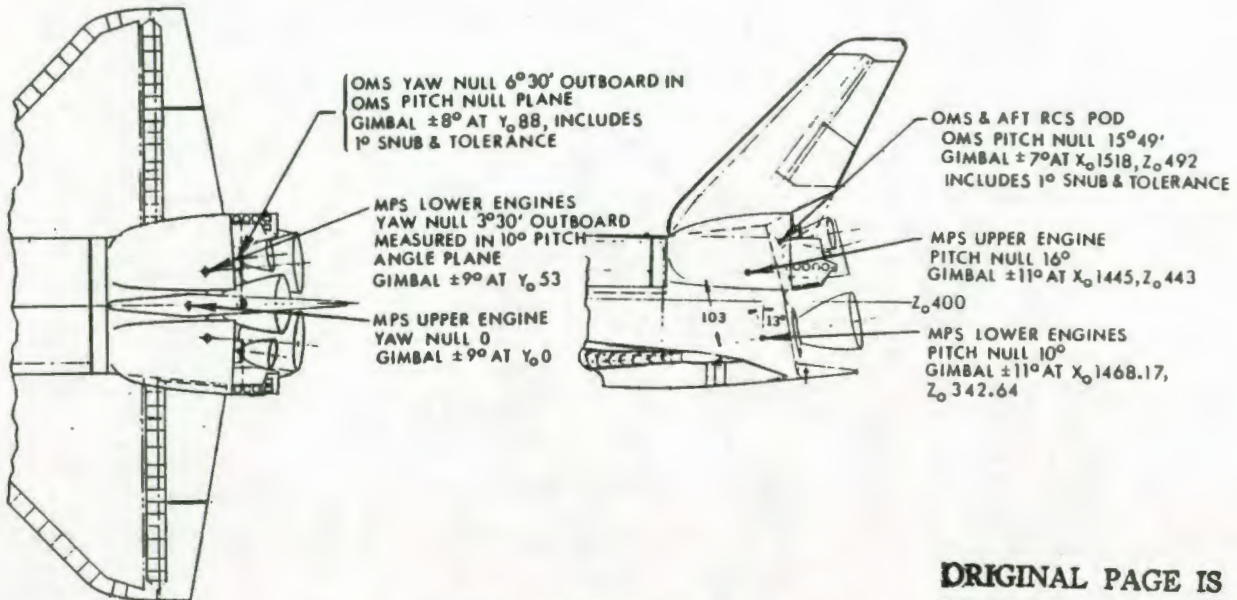
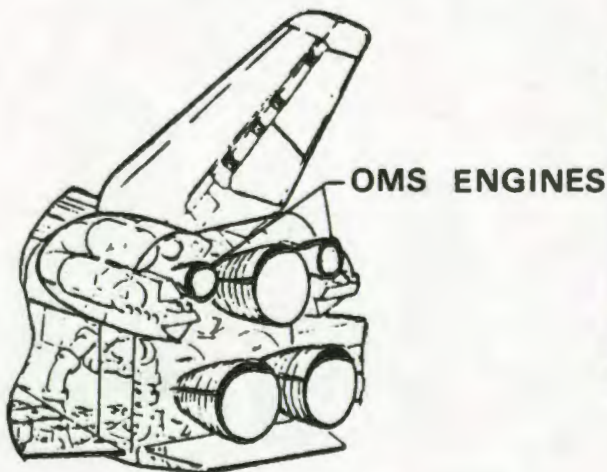


Figure 3.5.1.2-1
OMS AND SSME GIMBAL LIMITS

ORIGINAL PAGE IS
OF POOR QUALITY

3.5.1.3 OMS THRUST VECTOR CONTROL. At the end of second stage boost, prior to Orbiter-ET separation, vehicle control passes from the SSME's to the Orbital Maneuvering System (OMS) engines. The gimbal angle ranges for the OMS engines are shown in Figure 3.5.1.2-1 of the preceding section. The Orbital Maneuvering System engines are shown in the sketch and photograph below.



ORBITAL MANEUVERING SYSTEM

3.5.1.4 REACTION CONTROL SYSTEM. Attitude control and three-axis translation of the Orbiter Vehicle during orbit insertion and on-orbit operations is achieved by use of both forward and aft RCS thrusters. The aft RCS thrusters are also used to control the Orbiter and ET (mated coast) and the Orbiter alone during the RTLS abort separation maneuver. Details of the RCS and thruster identification are given in Figure 3.5.1.4-1.

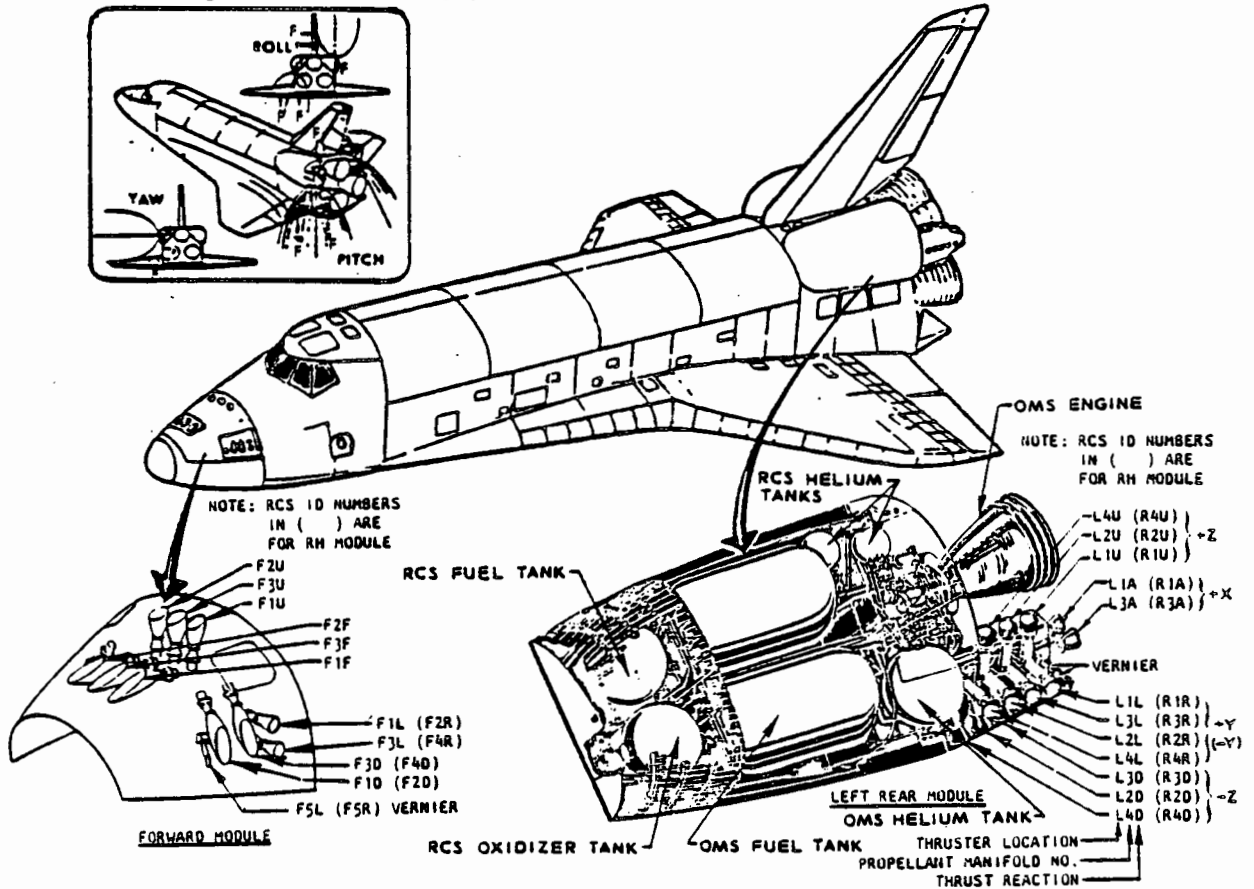


Figure 3.5.1.4-1
RCS THRUSTER IDENTIFICATION

Attitude control of the Orbiter Vehicle during entry is provided by the aft RCS in roll and pitch up to dynamic pressure levels of 10 and 20 psf, respectively. The RCS thrusters are located in the OMS pods as shown in the figure. For dynamic pressure levels exceeding 20 psf, sufficient elevon (elevator-aileron) control authority is available and the roll and pitch thrusters are deactivated. The blanketing effect of the wing at high angles of attack necessitates the use of yaw thrusters to augment the rudder control until the angle of attack is reduced to approximately ten degrees. Aft RCS jet/aerodynamic interaction, illustrated in the inset, can result in net effects which oppose the thrust moments alone, thus making it critical to flight safety and performance to be aware of induced RCS flow field interactions.



RCS jet-to-freestream momentum ratio was the primary correlating parameter for the side firing jet interactions. The analytical model developed indicates the total reaction control moments to be the sum of thrust, impingement, and interaction terms; i.e., the equation is of the form:

$$M_{RCS} = M_{THRUST} + M_{IMPINGEMENT} + M_{INTERACTION}$$

The force and moment terms due to RCS jet thrust as obtained from Reference 3-10 are presented in Table 3.5.1.4-1. These values have been included for reference only and are not intended for design purposes. The values are based on a nominal vacuum thrust of 870 pounds/jet and average moment arms for each jet group. All moments are referenced to 65 percent of body length and WL375. The effect of jet angle cant is also included in the values presented in the table.

Table 3.5.1.4-1
REFERENCE JET FORCES AND MOMENTS

| JET GROUP | LONGITUDINAL ONE SIDE FIRING | | | LATERAL-DIRECTIONAL LH SIDE FIRING ONLY (RH SIDE - USE OPPOSITE SIGN) | | |
|-------------|---------------------------------|-----------|-----------|---|-----------|-----------|
| | N_{JET} | A_{JET} | M_{JET} | Y_{JET} | X_{JET} | Z_{JET} |
| | LB/JET | LB/JET | FT-LB/JET | LB/JET | FT-LB/JET | FT-LB/JET |
| DOWN FIRING | + 802 | - 170 | - 31,140 | + 292 | - 9,422 | + 8,996 |
| UP FIRING | - 870 | 0 | + 32,791 | 0 | 0 | - 9,570 |
| SIDE FIRING | + 22 | 0 | - 856 | + 871 | - 33,282 | + 6,373 |

Impingement forces were determined by use of a computer program based on modified Newtonian impact theory and a modified vacuum plume flow field. These impingement forces (or moments) account for the RCS plume impinging on the Orbiter Vehicle surface(s) and are provided as a function of freestream static pressure, P_{∞} .

The interaction terms were determined by wind tunnel test data. The RCS jets were simulated by high pressure air discharged through non-metric ports in the wind tunnel model of the Orbiter Vehicle. The aerodynamic increment due to jet firing was computed and forces (or moments) due to the interaction of the jet plume were computed from:

$$M_{INTERACTION} = (C_{m_{RCS}}^{ON} - C_{m_{RCS}}^{OFF}) \bar{q} S \bar{c} - M_{IMPINGEMENT}$$

The procedure for determining RCS jet effectiveness during the thrust build-up and shut-down transient firing periods (as shown in Figure 3.5.1.4-2) is as follows:

STEP 1 - Evaluate RCS interaction and impingement effects for the full power condition (i.e., $P_{\text{CHAMBER}} = 152 \text{ psia} \approx 870 \text{ lb thrust level}$)

STEP 2 - Reduce the results of STEP 1 to the actual momentary pressure level using the ratio $P_{\text{CACTUAL}} / P_{\text{CFULL POWER}}$

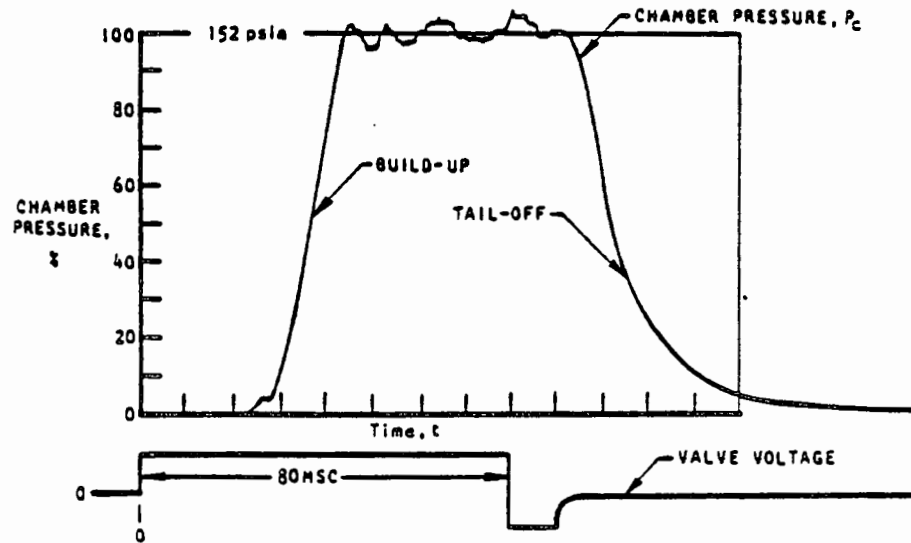
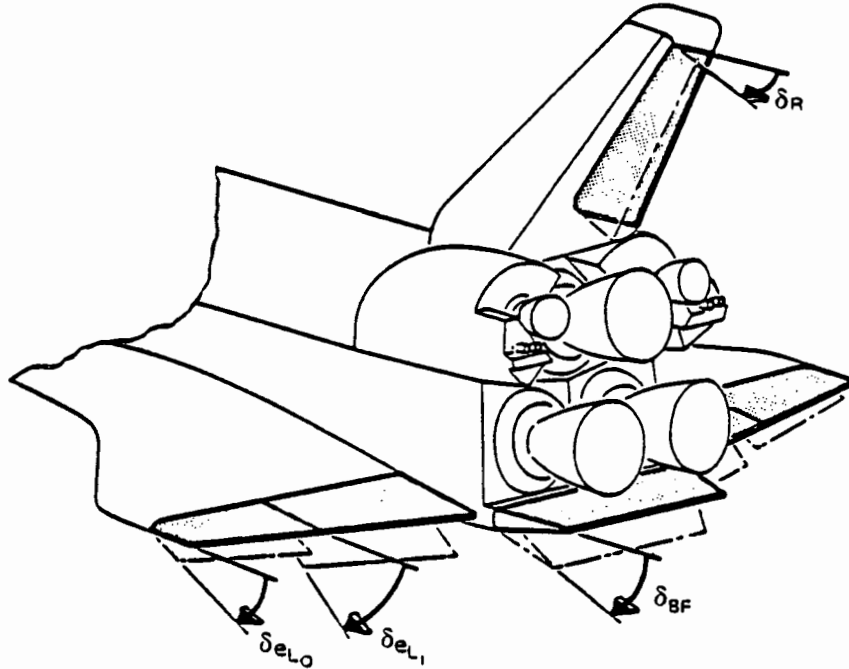


Figure 3.5.1.4-2
RCS PRIMARY THRUSTER CHAMBER PRESSURE
-TYPICAL 80-MILLISECOND PULSE-

3.5.2 AERODYNAMIC CONTROLS. Orbiter Vehicle aerodynamic control surface deflections, forces, and hinge moments are summarized in the sketch and table below. In general, control surface deflection angles are measured in a plane perpendicular to the control surface hinge axis. An exception is the rudder/speedbrake control surface(s) deflection which is measured in a plane parallel to the Fuselage Reference Plane (FRP). Each aerodynamic control surface is discussed separately in the ensuing paragraphs of this section.



| CONTROL SURFACE | POSITIVE DEFLECTION | MAXIMUM DISPLACEMENT | RATE | ANGLE | AERODYNAMIC FORCES and MOMENTS | HINGE MOMENT | |
|-----------------|--|---|---------|-------------------------------|--------------------------------|-------------------------|--|
| | | degrees | deg/sec | | | | |
| ELEVONS | | | | | | | |
| ELEVATOR | $\delta_e = \frac{1}{2}(\delta_{eL} - \delta_{eR})$ | $\left. \begin{array}{l} -35 \text{ TE UP} \\ -20 \text{ TE DOWN} \end{array} \right\}$ | 20.0 | $-\alpha, -\theta$ $+\phi$ | $-C_m$ $+C_L$ | $-C_{he}$ $-C_{hel}$ | |
| LEFT | $\delta_{eL} = \frac{1}{2}(\delta_{eL} + \delta_{eL})$ | | 20.0 | $-\phi$ $+\phi$ | $-C_L$ $+C_L$ | $-C_{heR}$ | |
| RIGHT | $\delta_{eR} = \frac{1}{2}(\delta_{eR} + \delta_{eR})$ | | | | | | |
| AILERON | $\delta_a = \frac{1}{2}(\delta_{eL} - \delta_{eR})$ | | | | | | |
| RUDDER | δ_R | $\pm 22.8^*$ | 10.0 | $+\beta, -\psi$ | $+C_{V_s}, -C_n$ | $-C_{hR}$ | |
| SPEEDBRAKE | δ_{SB} | 0 TO 87.2 | 5.0 | $+\alpha, +\theta$ | $+C_m$ | | |
| BODY FLAP | δ_{BF} | $\left\{ \begin{array}{l} -11.70 \text{ TE UP} \\ +22.53 \text{ TE DOWN} \end{array} \right.$ | 1.3 | $-\alpha, -\theta$ | $-C_m$ | $-C_{hBF}$ | |

*Refer to Figure 3.5.2.2-2 for rudder limits.
Figure 3.5.2-1 presents the speedbrake and body flap control schedules.

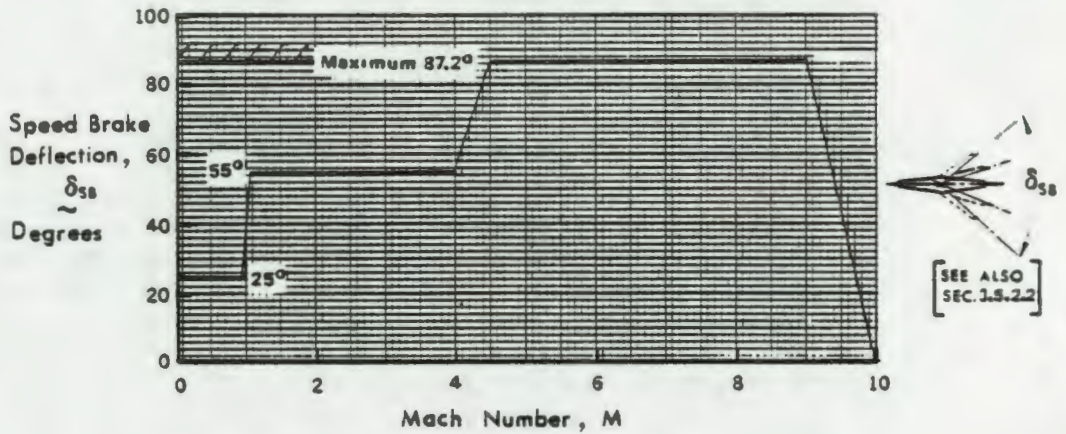
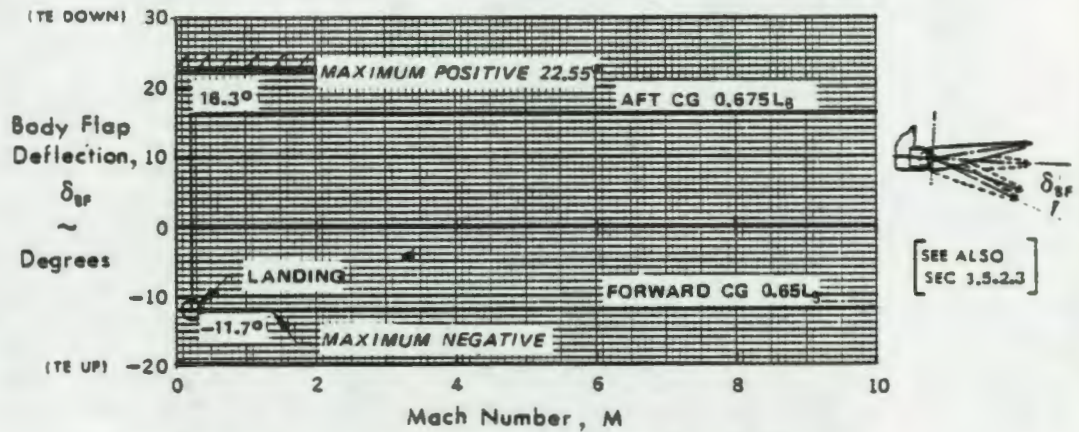
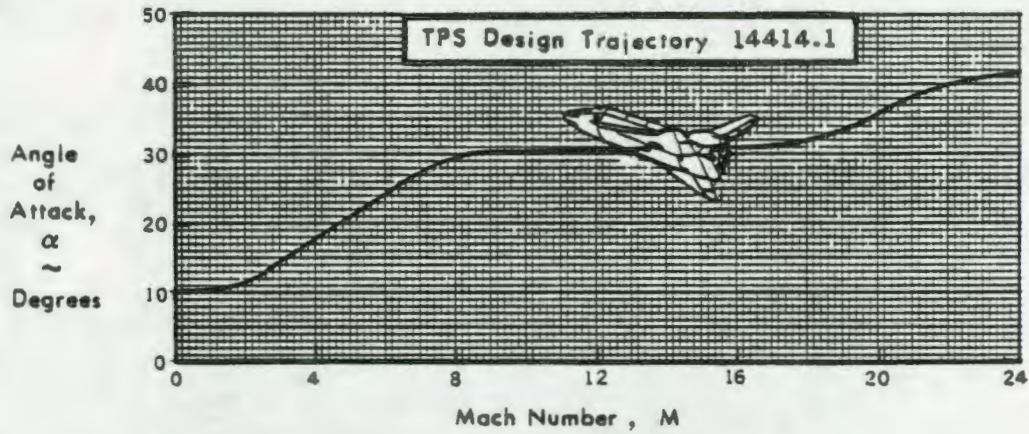


Figure 3.5.2-1
CONTROL SCHEDULES

3.5.2.1 ELEVONS. The elevons are divided into four segments, right- and left-inboard and right- and left-outboard. Gaps between the fuselage and elevon and between the inboard and outboard segments, to which the data herein are applicable, are those baselined in MCR 0315. A typical elevon control installation is shown in Figure 3.5.2.1-1.

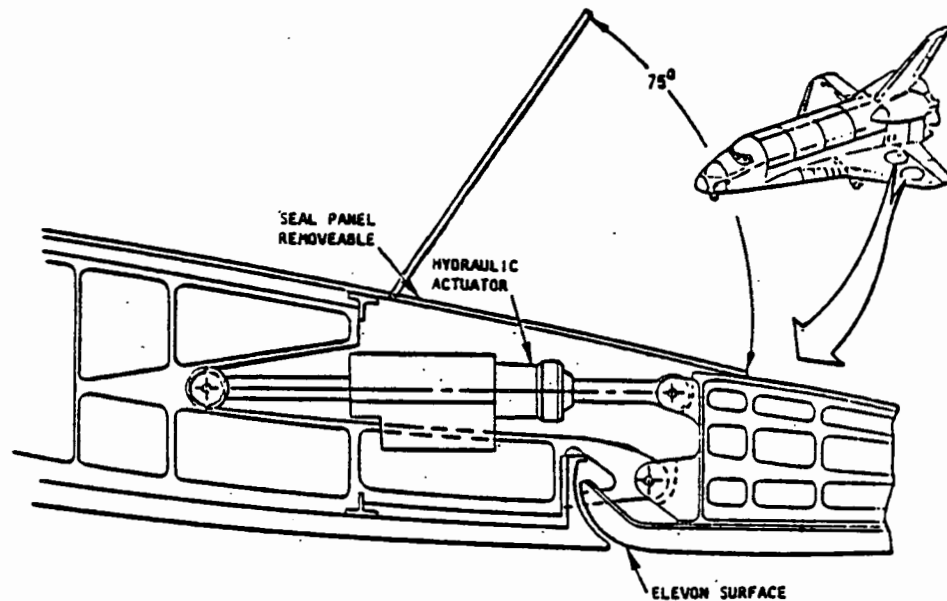
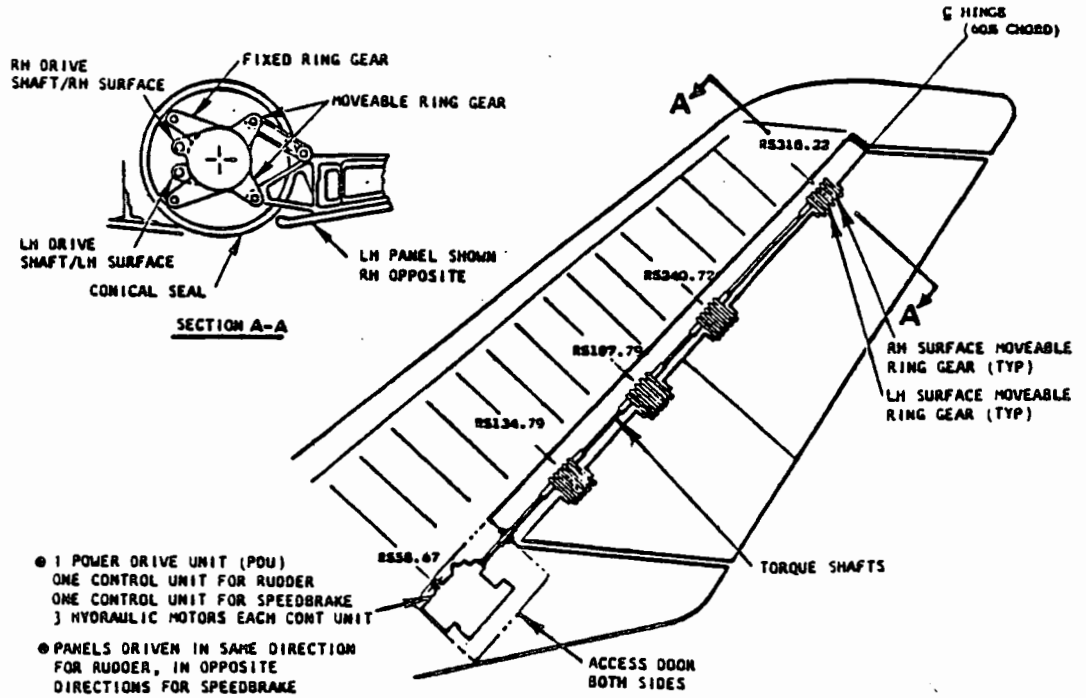


Figure 3.5.2.1-1
ELEVON CONTROL

The surfaces are hydraulic-actuated with four actuators to control each of the four segments. These surfaces are employed for pitch and roll control and pitch and roll trim. Maximum control surface deflections and rates are given in the table under Section 3.5.2. The elevon deflection range is -35 degrees (trailing edge up) to +20 degrees (trailing edge down) except during entry where it is limited to +10 degrees to prevent excessive heating. The aileron function deflections are also shown in the table.

3.5.2.2 RUDDER/SPEEDBRAKE. Directional control of the Orbiter is achieved aerodynamically by means of the rudder. During entry, at high angles of attack, the rudder is augmented by RCS (see Section 3.5.1, paragraph 3.5.1.4). The rudder is split into four panels, two per side (upper and lower), which are deflected together for yaw control and deployed symmetrically, in opposition, for drag modulation (speedbrake function). Each pair (upper and lower) of panels is actuated by power hinges driven by a common torque shaft as illustrated in Figure 3.5.2.2-1.



- 1 POWER DRIVE UNIT (POU)
- ONE CONTROL UNIT FOR RUDDER
- ONE CONTROL UNIT FOR SPEEDBRAKE
- 3 HYDRAULIC MOTORS EACH CONT UNIT
- PANELS DRIVEN IN SAME DIRECTION FOR RUDDER, IN OPPOSITE DIRECTIONS FOR SPEEDBRAKE

Figure 3.5.2.2-1
RUDDER/SPEED BRAKE CONTROL

Rudder/speed brake deflections are given in Figure 3.5.2.2-2 and in the table of Section 3.5.2.

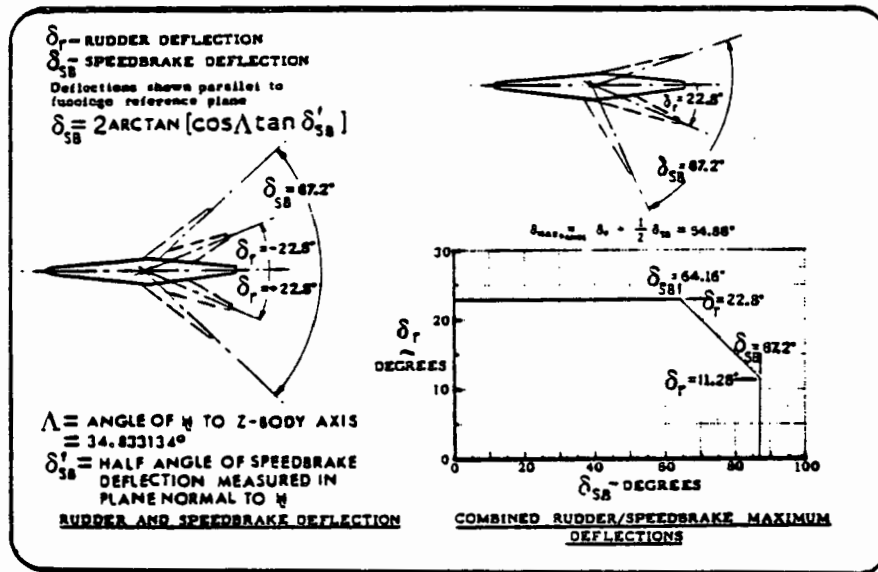


Figure 3.5.2.2-2
ORBITER RUDDER/SPEED BRAKE DEFLECTIONS

3.5.2.3 BODY FLAP. Trim capability to relieve elevon loads is obtained by body flap deflection actuated by power hinges as shown in Figure 3.5.2.3-1.

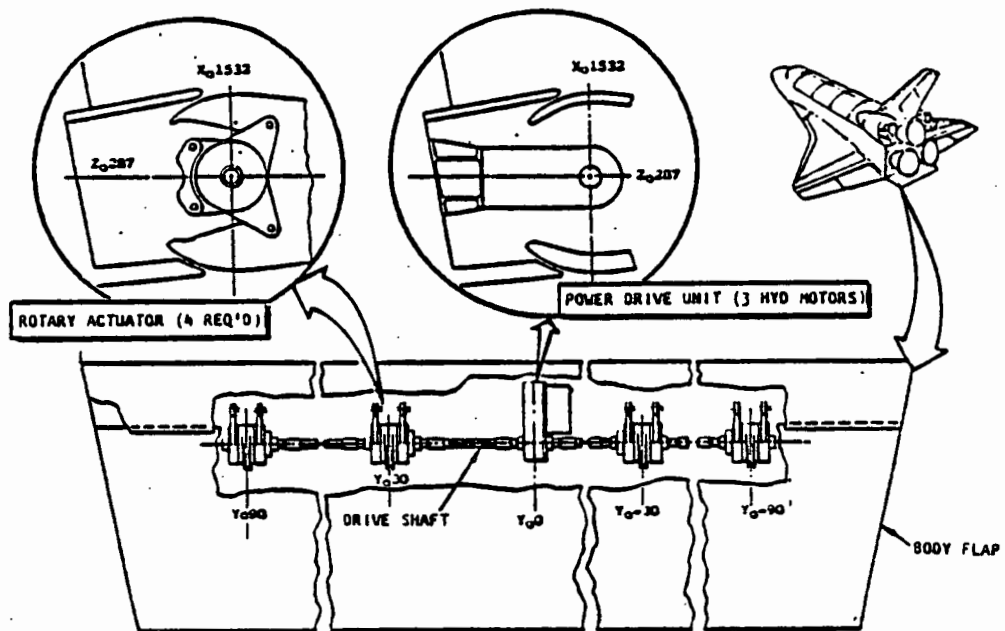


Figure 3.5.2.3-1
BODY FLAP CONTROL

Body flap deflection is from -11.7 degrees (trailing edge up) for entry with a forward center of gravity to +16.3 degrees (trailing edge down) for entry with an aft center of gravity. Maximum positive body flap deflection is +22.5 degrees as shown in Figure 3.5.2.3-2.

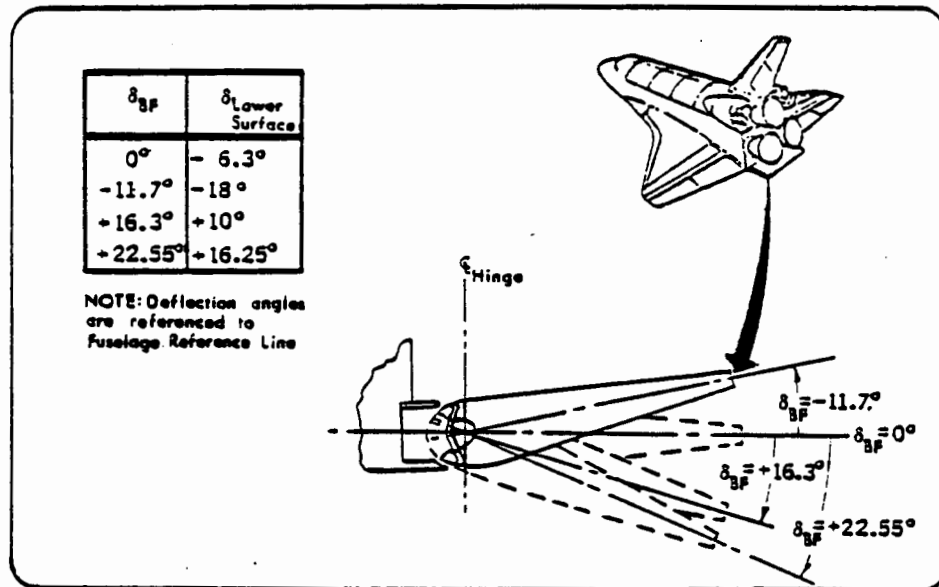


Figure 3.5.2.3-2
BODY FLAP DEFLECTION

3.6 LANDING GEAR

ORIGINAL PAGE IS
OF POOR QUALITY

3.6 LANDING GEAR. The Orbiter Vehicle landing gear consists of a double-wheel steerable nose gear and two, double-wheel, wing-mounted, main gear. Figure 3.6-1 presents the nose gear installation. Steering capability is ± 10 degrees and the crosswind constraint is 20 knots maximum.

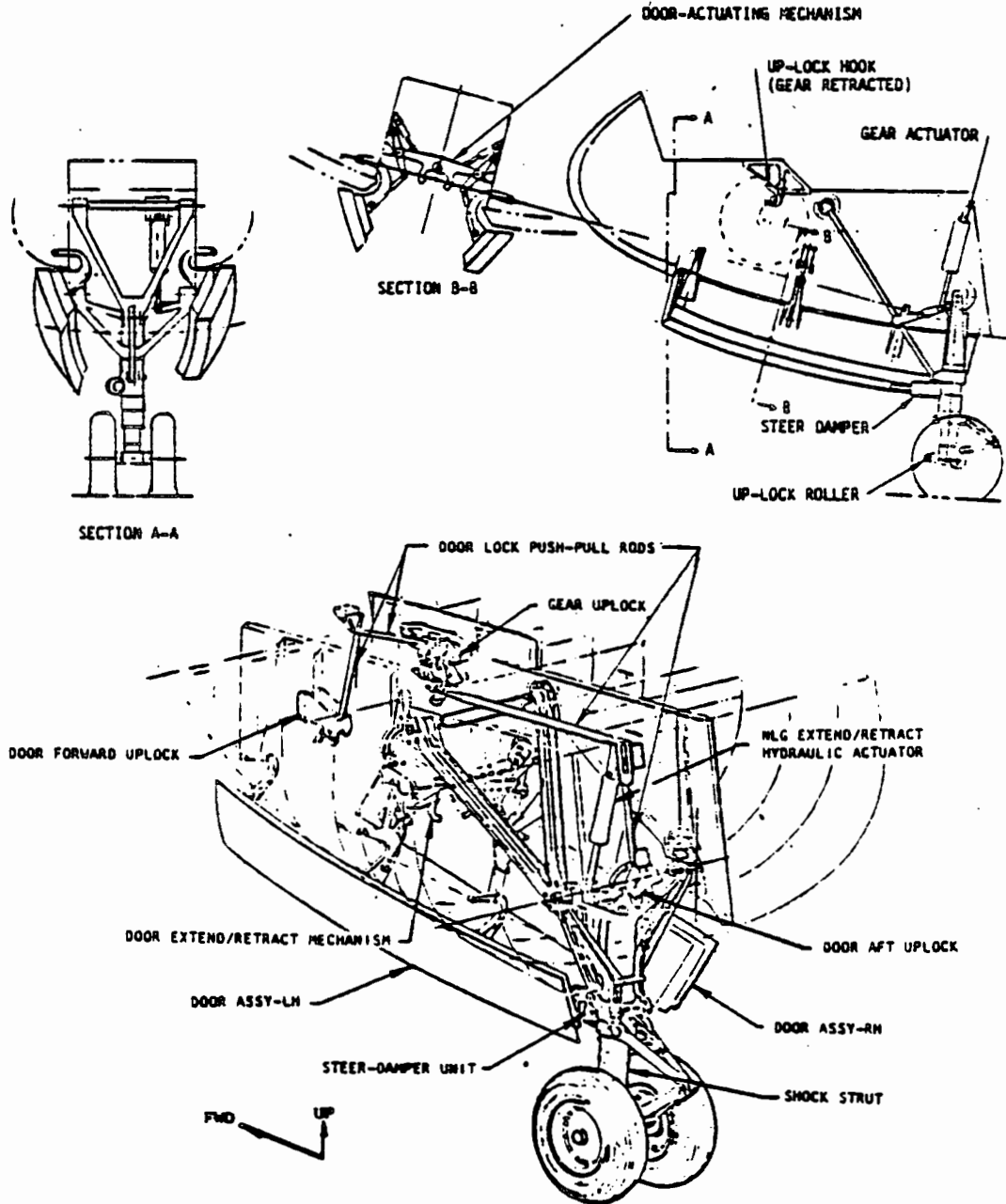


Figure 3.6-1
NOSE GEAR INSTALLATION

Figure 3.6-2 presents the main gear installation. The gear is designed for a maximum landing velocity of 221 knots. Maximum allowable sink rate for the Orbiter Vehicle with a 65,000 pound payload is 6.0 fps. Gear deployment is 300 knots maximum.

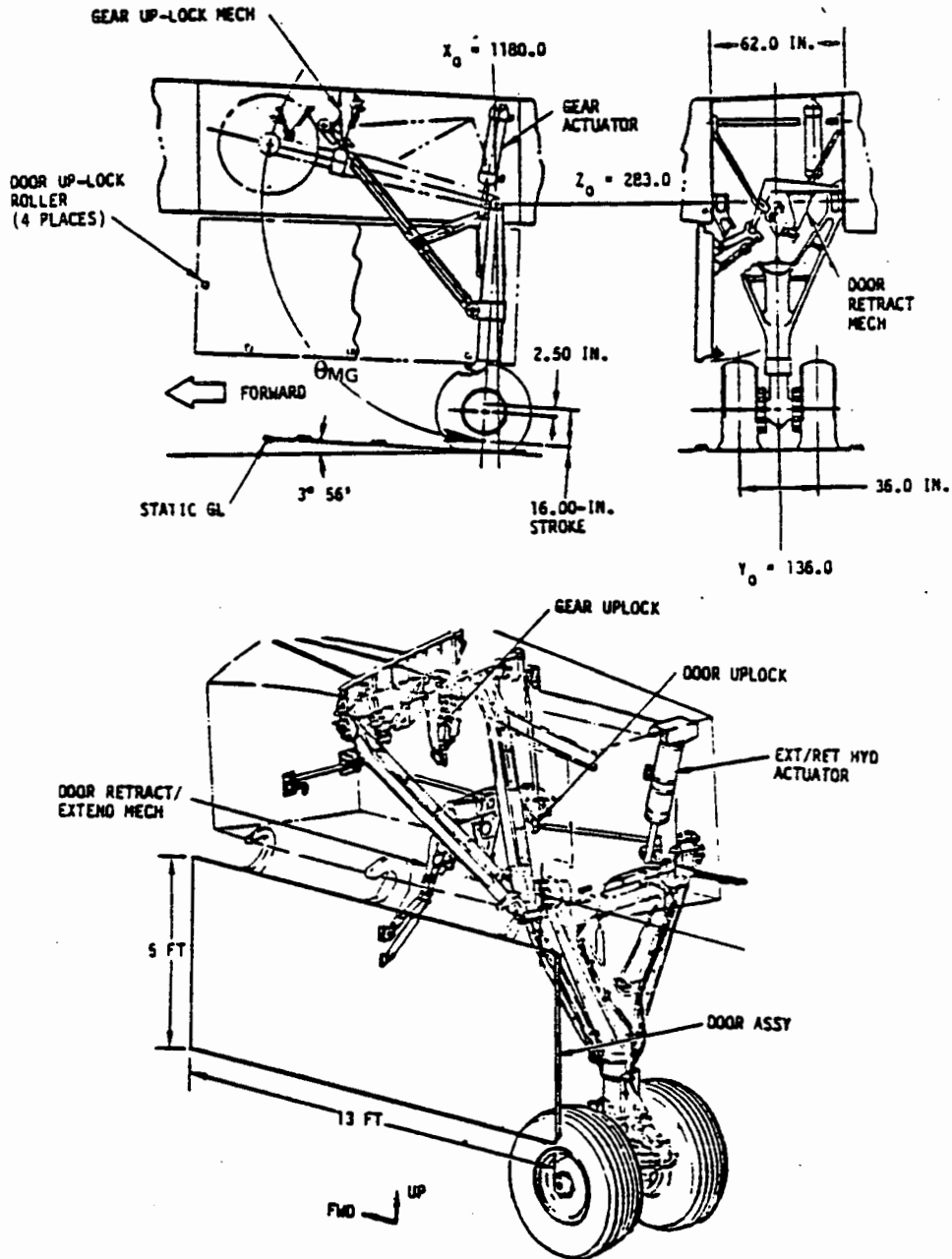
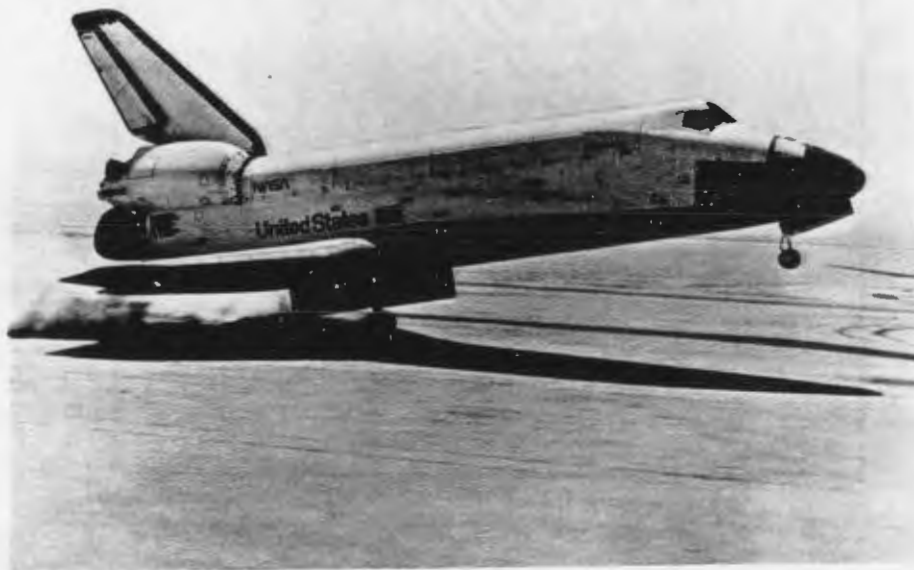


Figure 3.6-2
MAIN GEAR INSTALLATION

Ground effect, as shown in the data sections of this report, is given as a function of the ratio of height-above-ground to wing span (h/b_w). The height-above-ground is measured to a point on the vehicle just aft of the trailing edge of the inboard section of the elevon (FS1506.84, WL282.71). Height-above-ground as a function of angle of attack is given in Figure 3.6-3 for various values of the ratio (h/b_w).

The touchdown attitude is restricted by the ground scrape angle (α_s) as illustrated on Figure 3.6-3. Scrape angle(s) is given for three landing gear strut conditions: fully extended; static; and fully compressed, tires flat when the body flap is in the landing position (-11.7 degrees). The effect of elevon deflection (trailing edge down) is to further restrict the touchdown attitude as shown on the figure.



ORBITER LANDING

ORIGINAL PAGE IS
OF POOR QUALITY

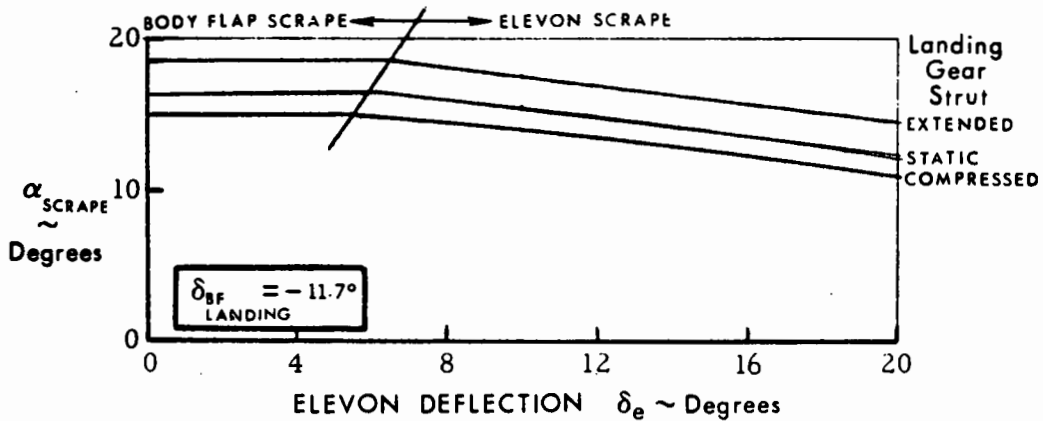
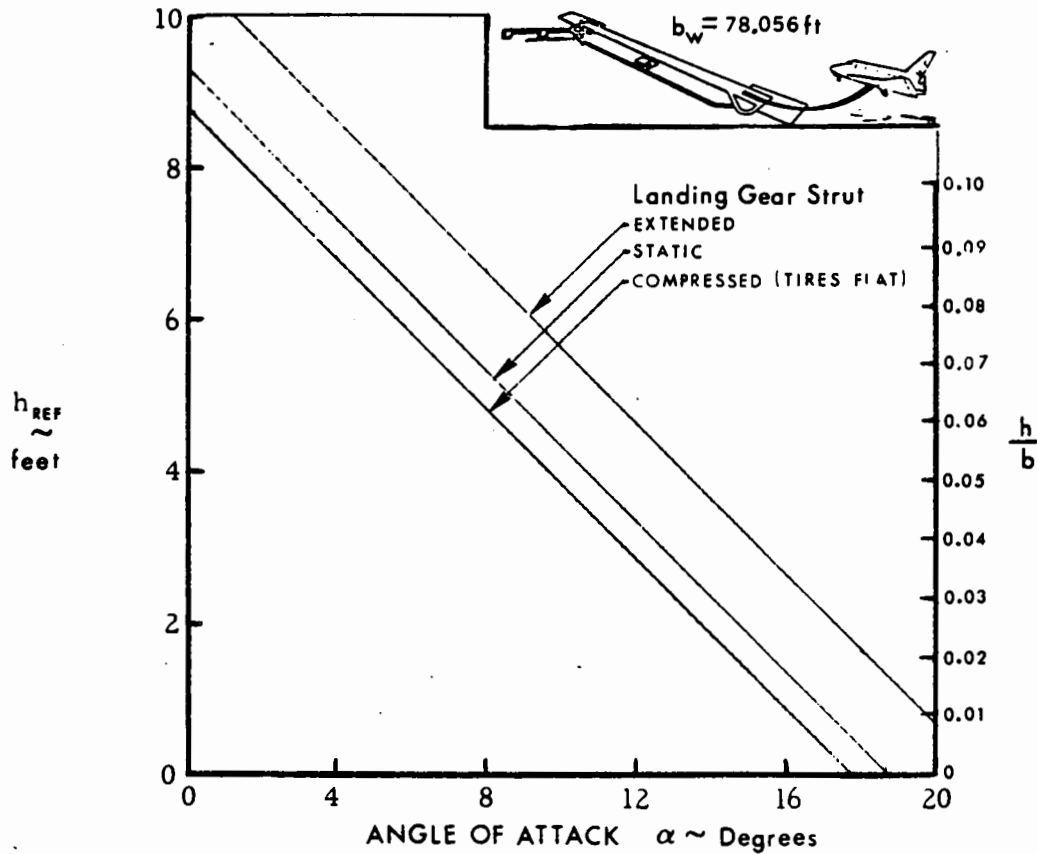
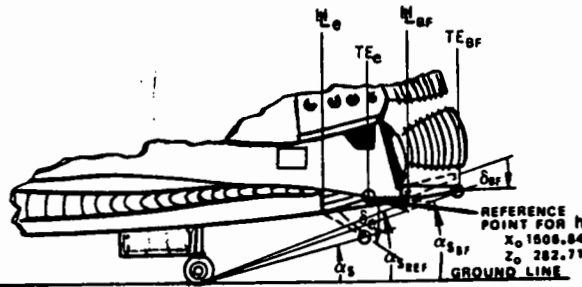


Figure 3.6-3
GROUND CLEARANCE

ORIGINAL PAGE IS
OF POOR QUALITY

3.7 SHUTTLE INFRARED LEESIDE TEMPERATURE SENSING

3.7 SHUTTLE INFRARED LEESIDE TEMPERATURE SENSING. The objectives of the Shuttle Infrared Leeside Temperature Sensing (SILTS) experiment are to:

- o Obtain benchmark leeside aeroheating data on a full-scale vehicle in a true entry environment.
- o Establish a ground to flight extrapolation for leeside aerodynamic heating data.
- o Assess the capability of various ground facilities to simulate the full scale flight environment on the leeside of an aerodynamic vehicle.
- o Establish a leeside flow model for development of analytical prediction techniques.
- o Explore Reynolds number and scale effects on leeside vortex and boundary layer development.
- o Determine real gas effects on leeside flow.
- o Establish the validity of existing flow-fields models.

This experiment will support the NASA/OAST goals of developing technology for advanced aerospace transportation systems. The knowledge derived from the SILTS experiments may also allow modification of the Orbiter upper surface Thermal Protection System and, thereby, reduce both weight and refurbishment costs. SILTS will be implemented on OV-102 for a minimum of three flights. Leeside heating effects will be measured for approximately 30 minutes beginning five minutes prior to entry (400,000 feet altitude).

The SILTS Experiment is to be mounted in a pod-like structure which will replace the tip of the vertical tail as shown in Figure 3.7-1. Data will be recorded on an OEX tape recorder located remotely from the experiment. The experiment system consists of an IR Camera/Dome Assembly, Data & Control Module, and a Pressure System Module. The dome assembly contains window covers, a Window Cooling System, and the IR camera mount and indexing mechanism which provides alternate views through two windows.

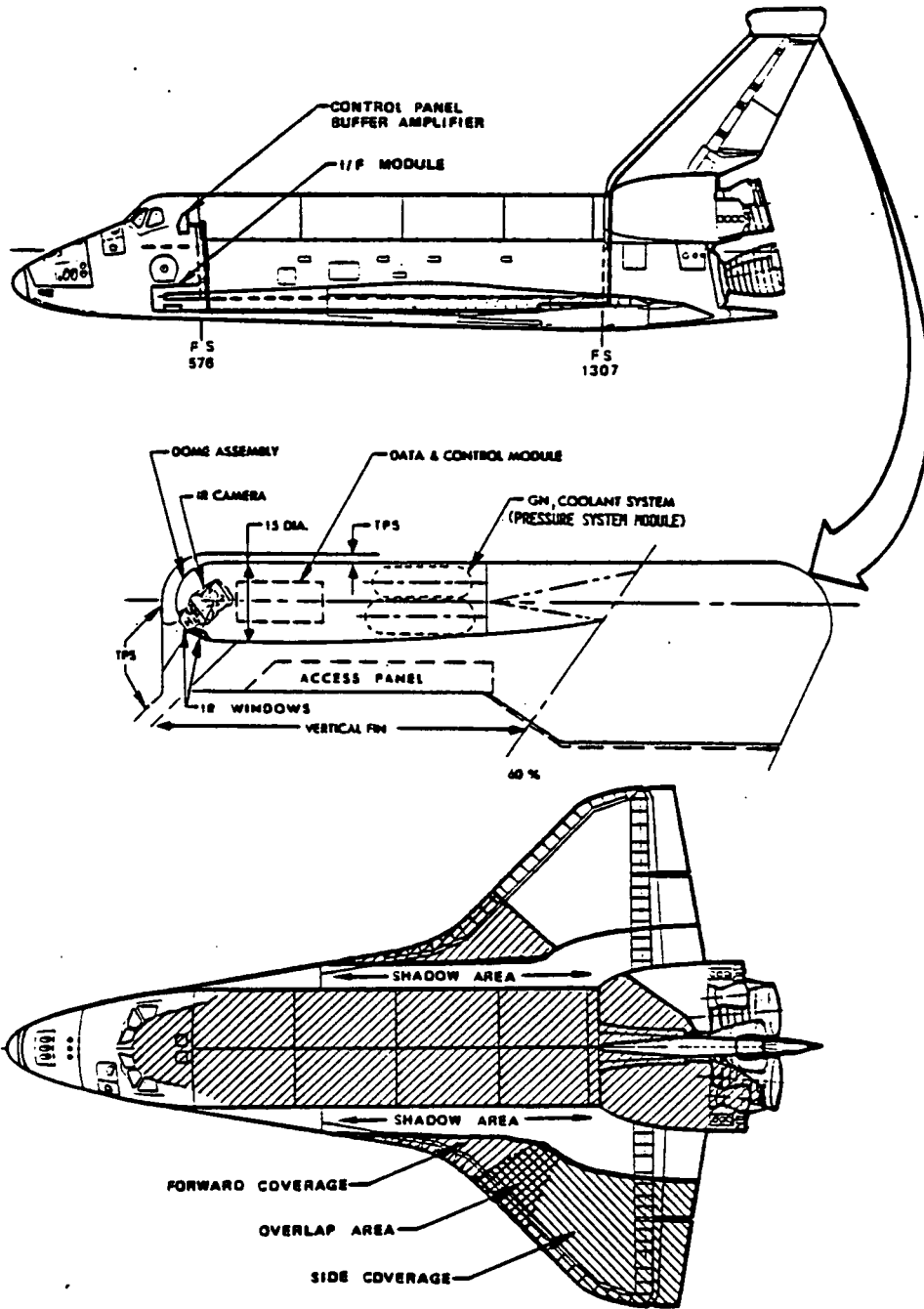


Figure 3.7-1
SILTS EXPERIMENT

4.0 AERODYNAMIC DATA USAGE

4.0 AERODYNAMIC DATA USAGE

The Space Shuttle Vehicle moves along trajectories that are dependent upon the vehicle's inertia characteristics, Earth's gravitational field, propulsive and reaction forces, and the aerodynamic forces and moments acting on it. The aerodynamic forces and moments acting on the vehicle are functions of the velocity, density of the medium through which it flies, vehicle geometry, and the angle that the relative wind makes with the vehicle.

The trajectories along which the Space Shuttle Vehicle can fly are limited only by the propulsive characteristics, the aerodynamic characteristics, and the vehicle's structural and thermal integrity. These limitations dictate the maximum performance and maneuverability of the spacecraft. If the spacecraft is to fly steadily along any arbitrary flight path (trajectory), the forces acting on it must be in static equilibrium (if the path is straight) or in dynamic equilibrium (if the path is curved or accelerated). It is, therefore, convenient to represent the spacecraft by a set of mutually perpendicular axes with their origin at some specified reference center. Aerodynamic reference systems for the launch vehicle are discussed in Section 3.1.1 and, for the Orbiter vehicle, in Section 3.1.5.

4.0

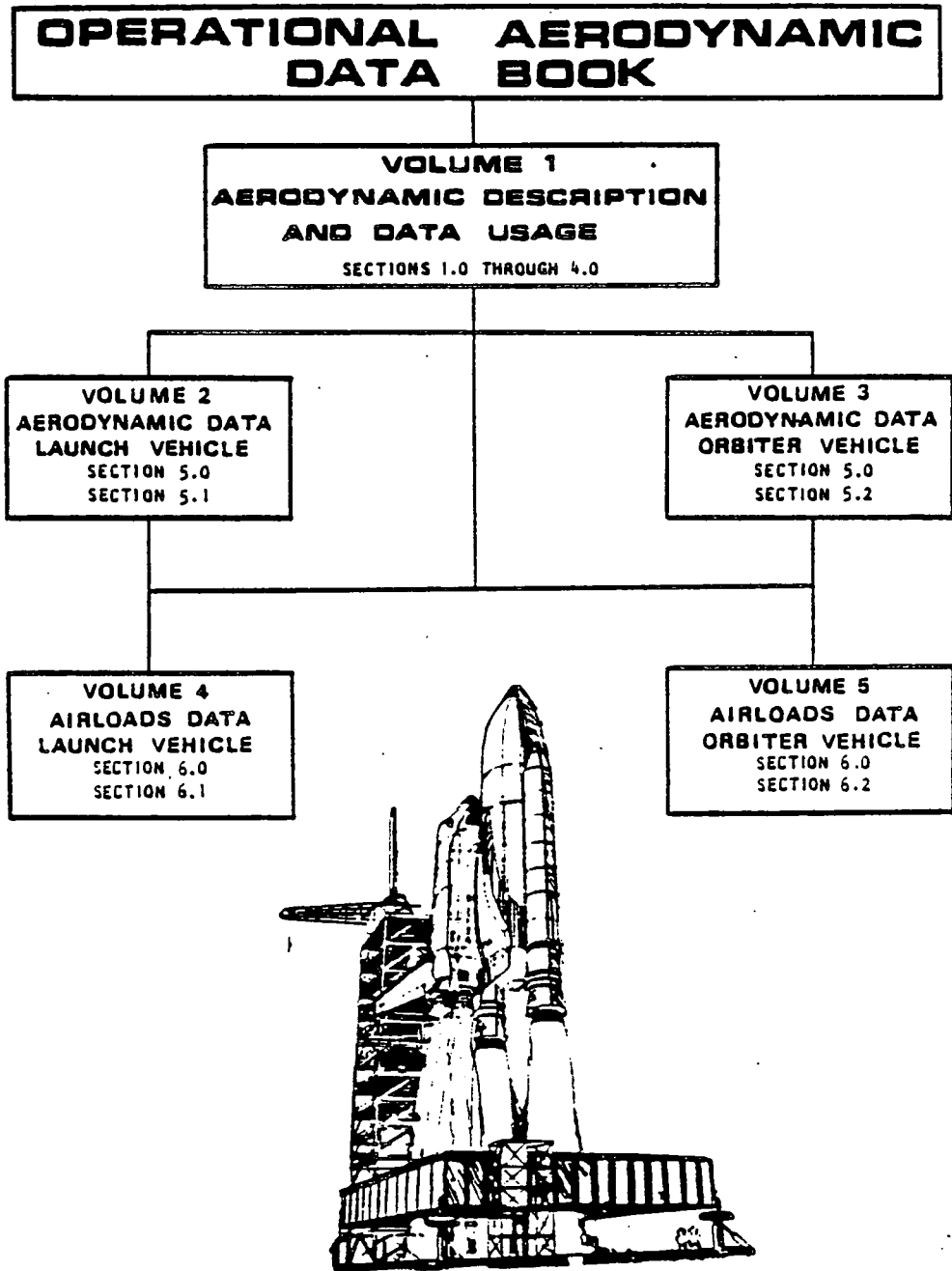
REFERENCES

- 4-1 NASA SP-3070, "Summary of Transformation Equations and Equations of Motion Used in Free-Flight and Wind Tunnel Data Reduction and Analysis," Gainer, T.G., and S. Hoffman, Langley Research Center, Hampton, Virginia (1972).
- 4-2 Hoerner, S. F., FLUID DYNAMIC DRAG, published by author (1978)
- 4-3 NASA/MSFC Memorandum ED 32-76-62, "External Tank (ET) Static Stability Aerodynamics for Return-to-Launch-Site (RTLS) Disposal Trajectories," (July 23, 1976)
- 4-4 NASA/MSFC Memorandum ED 32-77-25, "Addendum to MSFC Memo ED 32-76-62, Entitled External Tank (ET) Static Stability Aerodynamics for Return-to-Launch-Site (RTLS) Disposal Trajectories," (April 12, 1977)
- 4-5 NASA/MSFC Memorandum ED 32-75-11, "Transmittal of 6DOF Aero Characteristics for ET Entry," (March 10, 1975)
- 4-6 U. S. Committee on Extension to the Standard Atmosphere, "U. S. Standard Atmosphere, 1962", Government Printing Office, Washington, D. C., 1962.
- 4-7 STS 83-0540, "Eastern Test Range Ignition Overpressure Operational Design Data Book," Rockwell International, Space Division, Downey, California (October 1983)
- 4-8 STS 84-0264, "Western Test Range Ignition Overpressure Design Data Book," Rockwell International, Space Division, Downey, California (July 1984)
- 4-9 SD 72-SH-0060-1M, "Aerodynamic Design Data Book, Volume 1, Orbiter Vehicle STS-1," Rockwell International, Space Division, Downey, California (November 1980)
- 4-10 WADC TN 57-28, "Methods of Estimating Base Pressures on Aircraft Configurations," WADC Technical Report, Wright-Patterson AFB, Dayton, Ohio (July 1957).
- 4-11 DAC Rept ES29074, "Charts for Determining Skin Friction Coefficients on Smooth and Rough Flat Plates at Mach Numbers up to 50 With and Without Heat Transfer," Douglas Aircraft, El Segundo, California (April 1959).
- 4-12 MD59-453, "External Drag Manual," North American Aviation, Inc., Missile Division, Downey, California (February 1960).
- 4-13 Hald, A., STATISTICAL THEORY WITH ENGINEERING APPLICATIONS, John Wiley & Sons, Inc., New York, New York (November 1962).
- 4-14 SD74-SH-0206-1H, "Aerodynamic Design Substantiation Report (Volume 1) Orbiter Vehicle," Rockwell International, Space Division, Downey, California (January 1975).

ORIGINAL PAGE IS
OF POOR QUALITY

4.1 LAUNCH VEHICLE AERODYNAMIC EQUATIONS

4.1 LAUNCH VEHICLE AERODYNAMIC EQUATIONS. Equations for use in ascent trajectory analyses, subsystems analyses, flight control analyses, and manned simulation studies are given for the body-axis system (cf. Section 3.1). These equations relate directly to the aerodynamic data presented in Volume 2; i.e., equations for the first-stage longitudinal aerodynamics (Volume 1, Section 4.1.1.1) make use of the data given under first-stage longitudinal aerodynamics (Volume 2, Section 5.1.1.1), etc.

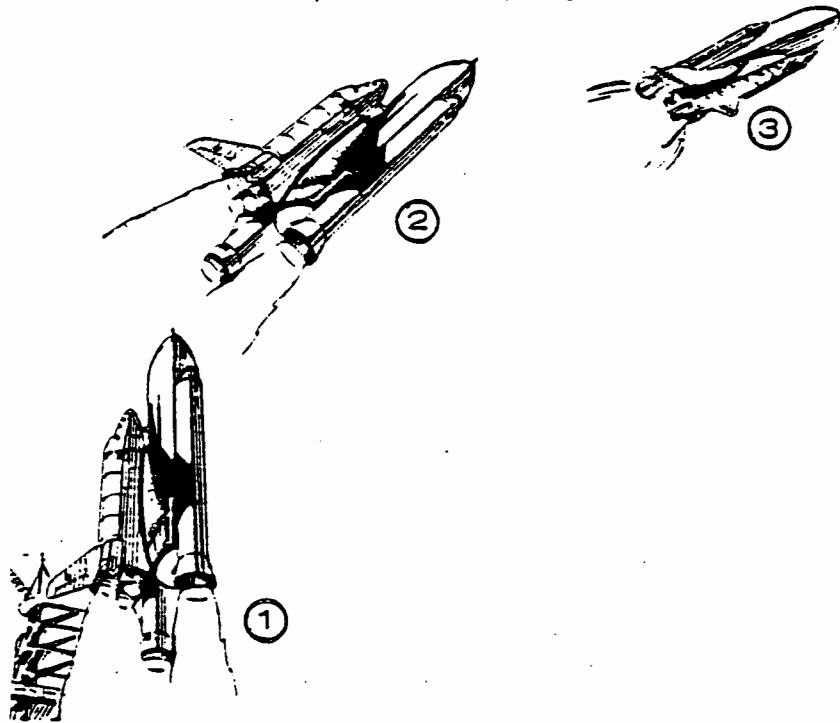


4.1.1 FIRST STAGE (INCLUDING ABORT)

4.1.1 **FIRST STAGE.** Aerodynamic characteristics pertaining to the first-stage ascent vehicle (including abort conditions) are defined for full-scale, rigid and elastic, forces and moments by the equations of the following sub-sections. The first-stage is comprised of the Orbiter Vehicle (OV), External Tank (ET), and two Solid Rocket Boosters (SRB). Two types of abort can occur during first-stage ascent; Intact Abort or Contingency Abort. The former consists of safe separation of the OV from the other Shuttle elements and occurs when a complete or partial loss of thrust from any one Space Shuttle Main Engine (SSME) is experienced. Loss of thrust from two or three SSME's constitute the latter or Contingency Abort condition. The contingency abort is usually considered where trajectory and remaining Shuttle capability permit crew survival. A Contingency Abort is accomplished by utilization of special guidance procedures and flight profiles similar to Glide-RTLS (cf. Section 4.1.5).

4.1.1.1 **LONGITUDINAL AERODYNAMICS.** The basic first-stage, operational, longitudinal forces and moment are defined for three phases or categories:

- 1) ground wind forces and moment
(function of wind direction).
- 2) transition from high to low attitudes
over the Mach range zero to 0.60
(function of pitch and yaw).
- 3) low attitude forces and moment
over the Mach range 0.60 to 4.50
(function of Mach number, angle of
attack, and sideslip angle).



The total longitudinal forces and moment for the first-stage are defined as:

$$\text{Normal Force, } N_{\text{TOTAL}} = \bar{q} S C_{N_{\text{TOTAL AERO}}} \text{ (lb)}$$

$$\text{Axial Force, } A_{\text{TOTAL}} = \bar{q} S C_{A_{\text{TOTAL AERO}}} \text{ (lb)}$$

$$\text{Pitching Moment, } M_{\text{TOTAL}} = \bar{q} S L_B C_{m_{\text{TOTAL AERO}}} \text{ (ft-lb)}$$

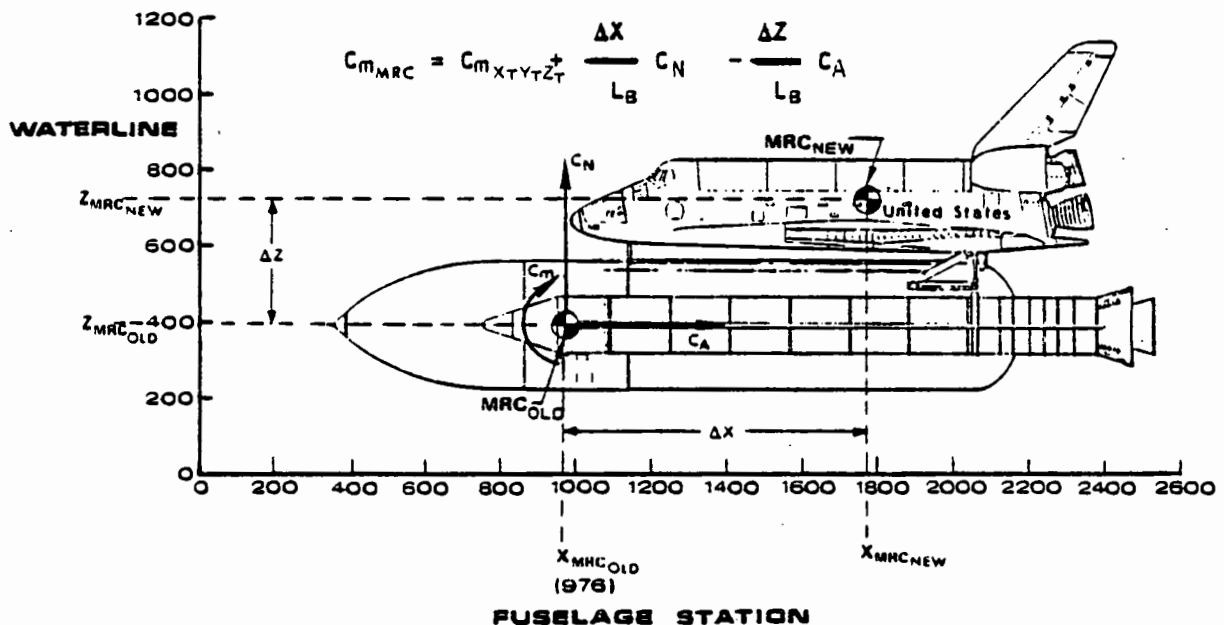
where, \bar{q} = dynamic pressure (lb/ft²)

S = Reference Wing Area (2690 ft²)

L_B = Reference Body Length (1290.3 in)
(see Figure 3.1.5-2b)

NOTE: 1. The first-stage Moment Reference Center is located at $X_T 976, Y_T 0, Z_T 400$.

2. To obtain pitching moment data about any other reference center:



where, $\Delta X = X_{\text{MRC NEW}} - 976$ inches
 $\Delta Z = Z_{\text{MRC NEW}} - 400$ inches

The total non-dimensional forces and moment coefficients are defined as:

GROUND WINDS ($M_\infty = 0$)

$$C_{(1)GW_{\text{TOTAL AERO}}} = (1 + k_{1,2} K_{1,KSC}^{\text{OR VAFB}}) C_{(1)W/O TOWER} + C_{(1)BASE}$$

TRANSITION ($0 \leq M_{\infty} \leq 4.5$)

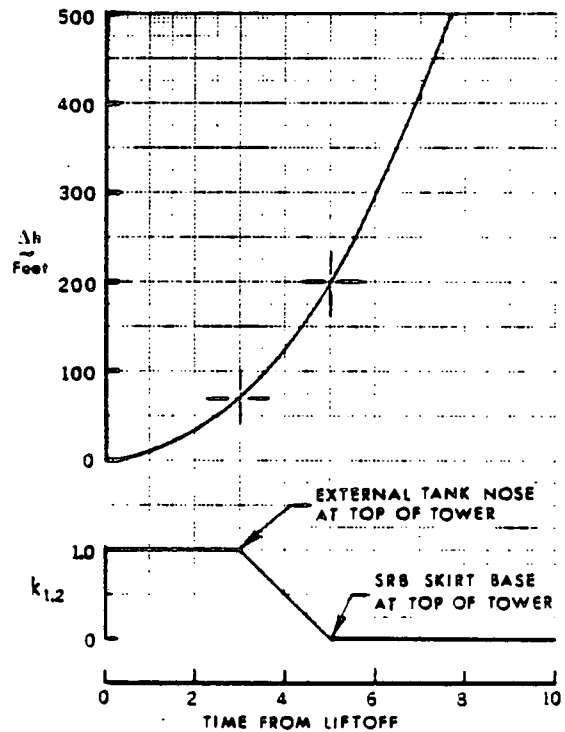
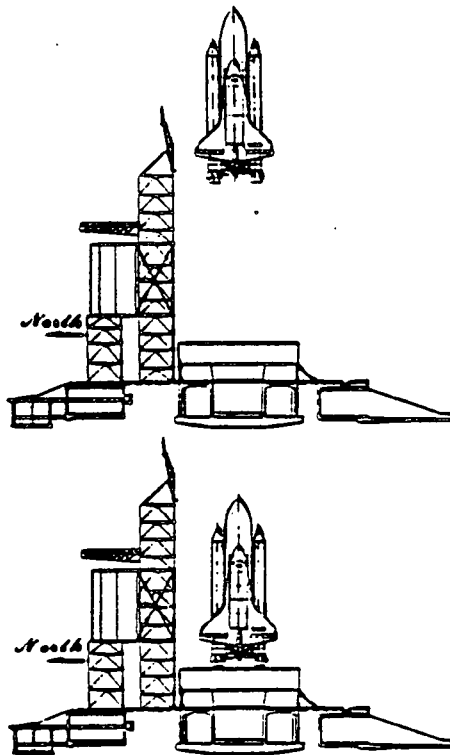
$$C_{() \text{ TRANS}}^{\text{TOTAL AERO}} = C_{() \text{ f TRANS}} + C_{() \text{ BASE}}$$

LOW ATTITUDE ($0.6 \leq M \leq 4.5$)

$$C_{() \text{ LOW ATT}}^{\text{TOTAL AERO}} = C_{() \text{ f LOW ATT}} + C_{() \text{ BASE}} + \Delta C_{() \text{ ELEVON}} + C_{() \frac{\dot{\alpha} L_B}{2V}} + C_{() \frac{q L_B}{2V}} + C_{() \text{ FLEX}}$$

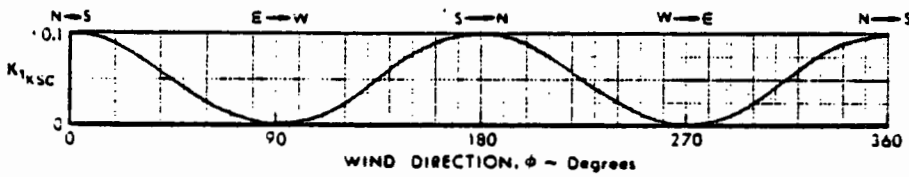
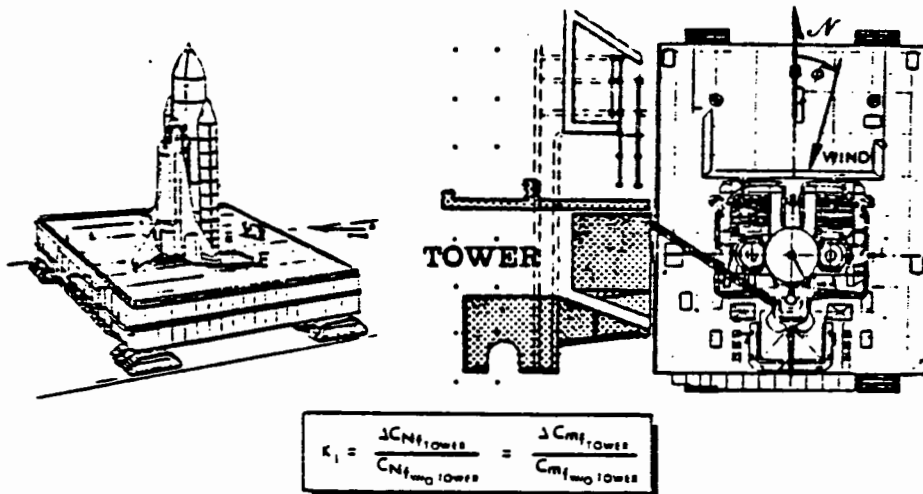
Where, the subscript () is used to denote either normal force (N), axial force (A), or pitching moment (m).

$k_{1,2}$ = post-lift off parameter

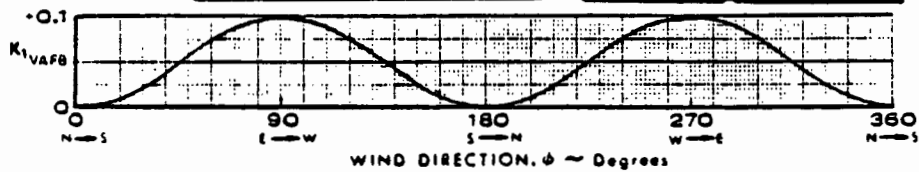
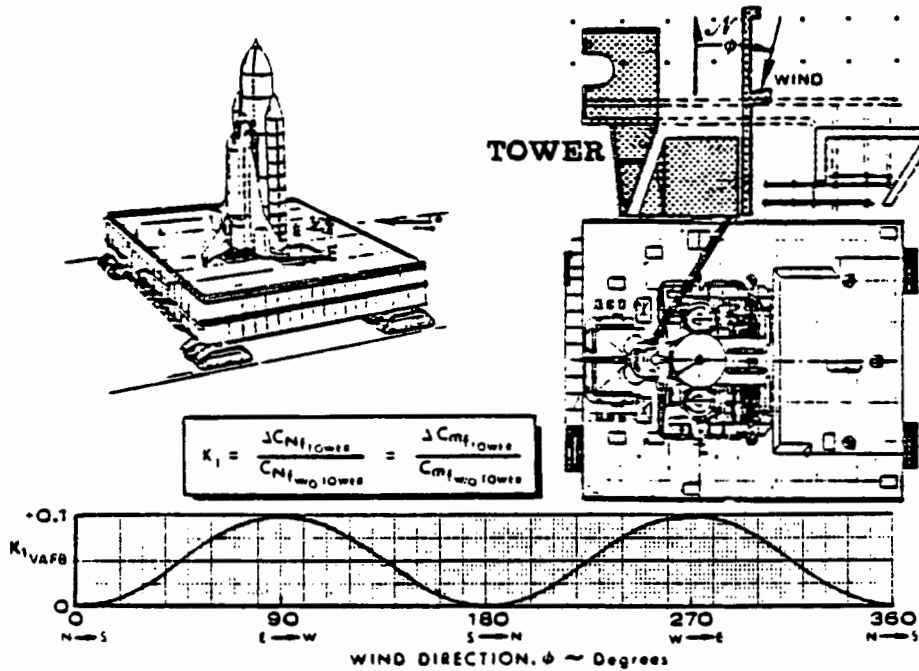


LIFTOFF TRAJECTORY AND POST-LIFTOFF INTERFERENCE PARAMETER

$K_{1 \text{ KSC}}$ = longitudinal tower interference factor
or
VAFB



(a) KENNEDY SPACE CENTER



(b) VANDENBURG AIR FORCE BASE

TOWER INTERFERENCE EFFECTS ON LAUNCH VEHICLE

$C_{()_{W/O TOWER}}$ = Basic force or moment coefficient
on crawler without tower

subscript: (N) (Figure 5.1.1.1.1-1, -2)
(A) (Figure 5.1.1.1.2-1, -2)
(m) (Figure 5.1.1.1.3-1, -2)

$C_{()_{TRANS}}$ = Basic forebody force or moment
coefficient during transition

subscript(N) $\left\{ \begin{array}{l} \cos\beta[-3.55(\sin|a|)^{1.17} + 0.046(1 - \sin|a|)] \\ \text{for } (-90^\circ \leq a \leq 0^\circ) \\ \cos\beta[3.25(\sin a)^{1.04} + 0.046(1 - \sin a)] \\ \text{for } (0^\circ < a \leq +90^\circ) \\ \text{(use in conjunction with Tables 5.1.1.1.1-1, -2} \\ \text{for } a, \beta > \pm 12^\circ) \end{array} \right.$

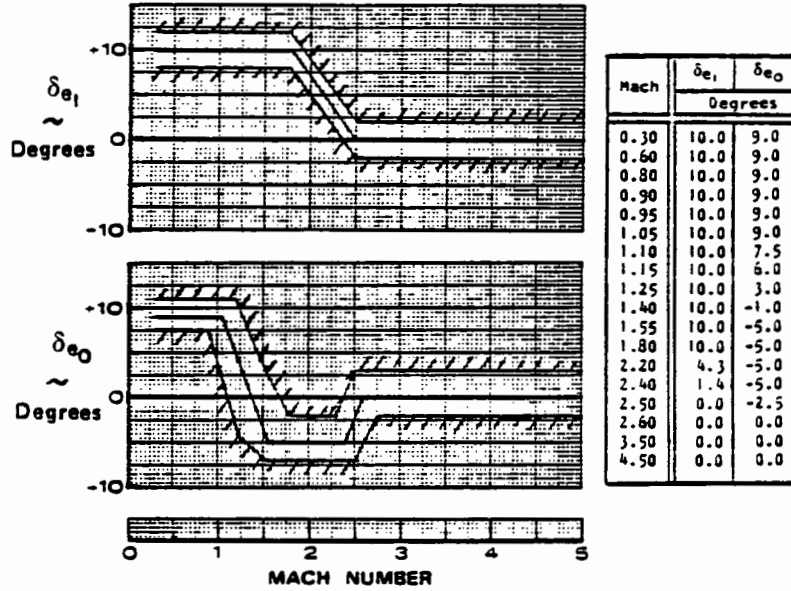
subscript(A) $\left\{ \begin{array}{l} 0.134 - 0.134[\sin(\sqrt{a^2 + \beta^2})] \\ \text{for } (-90^\circ \leq a \leq +90^\circ) \\ \text{if } (|a| + |\beta|) \geq 140^\circ, \text{ assume } C_A = 0 \\ \text{(use in conjunction with Tables 5.1.1.1.2-1, -2} \\ \text{for } a, \beta > \pm 12^\circ) \end{array} \right.$

subscript(m) $\left\{ \begin{array}{l} \{1.726(\sin|a|)^{1.67} - 0.059[1 - (\sin|a|)^{0.55}]\} \cos\beta \\ \text{for } (-90^\circ \leq a \leq 0^\circ) \\ \{-1.509(\sin a)^{1.14} - 0.059(1 - \sin a)\} \cos\beta \\ \text{for } (0^\circ < a \leq +90^\circ) \\ \text{(use in conjunction with Tables 5.1.1.1.3-1, -2} \\ \text{for } a, \beta > \pm 12^\circ) \end{array} \right.$

$C_{()_{FLOW ATT}}$ = Full-scale, rigid-body, proximity
forebody force or moment coefficient
(including forebody plume effects)

subscript: (N) (Figure 5.1.1.1.1-3)
(Tables 5.1.1.1.1-3 through -5)
(A) (Figure 5.1.1.1.2-3)
(Tables 5.1.1.1.2-3 through -5)
(m) (Figure 5.1.1.1.3-3)
(Tables 5.1.1.1.3-3 through -5)

NOTE: All control surfaces neutral except elevons
which follow Mach-deflection schedule

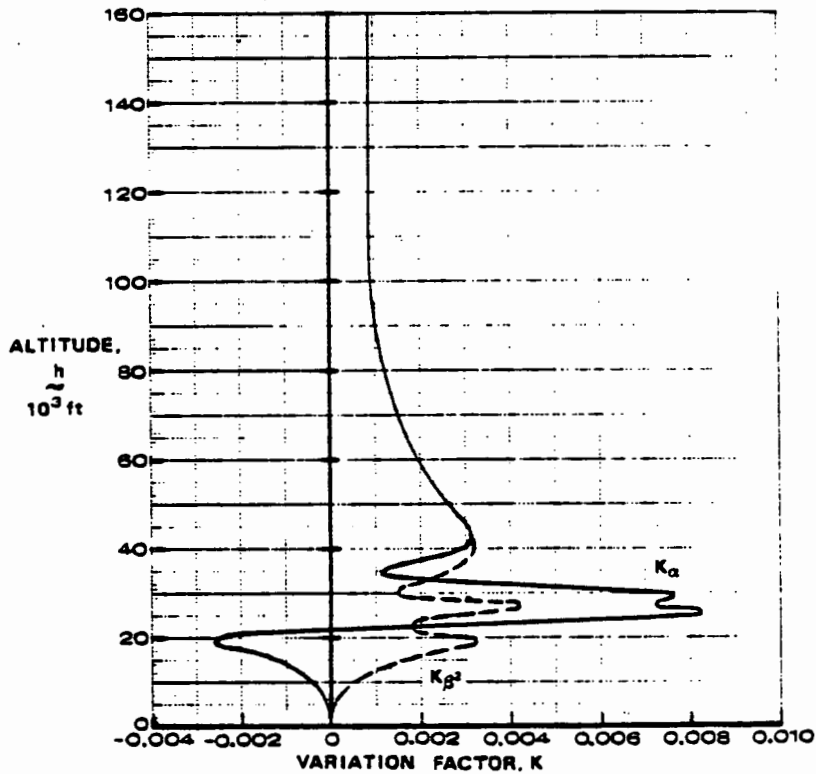


$C_{()_{BASE}}$ = Power-on base force or moment coefficient
(including effects of SSME and SRM plumes)

$$= \frac{F_{()_{BASE}}}{\bar{q}S} \Bigg|_{\substack{\alpha=0 \\ \beta=0}} \times [1 + K_{\alpha}\alpha + K_{\beta^2}\beta^2]$$

OR

$$= \frac{M_{BASE}}{\bar{q}SL_B} \Bigg|_{\substack{\alpha=0 \\ \beta=0}} \times [1 + K_{\alpha}\alpha + K_{\beta^2}\beta^2]$$



4.1.1-6

STS95-0118-1



The base terms for normal first-stage launch are:

$F_{N_{BASE}}$ (Figure 5.1.1.1.1-4)

$F_{N_{BASE}}^{THROTTLE}$ (Figure 5.1.1.1.1-5)

$F_{A_{BASE}}$ (Figure 5.1.1.1.2-4)

$F_{A_{BASE}}^{THROTTLE}$ (Figure 5.1.1.1.2-5)

M_{BASE} (Figure 5.1.1.1.3-4)

$M_{BASE}^{THROTTLE}$ (Figure 5.1.1.1.3-5)

The difference between normal launch aerodynamics and INTACT ABORT aerodynamics lies in the base term only, where a one SSME-out failure condition prevails. The base force and moment terms for one SSME-out condition are defined as:

$F_{N_{BASE}}^{#1 \text{ SSME OFF FIRST STAGE}}$ (Figure 5.1.1.1.1-6)

$F_{N_{BASE}}^{#2 \text{ (OR 3) SSME OFF FIRST STAGE}}$ (Figure 5.1.1.1.1-7)

$F_{A_{BASE}}^{#1 \text{ SSME OFF FIRST STAGE}}$ (Figure 5.1.1.1.2-6)

$F_{A_{BASE}}^{#2 \text{ (OR 3) SSME OFF FIRST STAGE}}$ (Figure 5.1.1.1.2-7)

$M_{BASE}^{#1 \text{ SSME OFF FIRST STAGE}}$ (Figure 5.1.1.1.3-6)

$M_{BASE}^{#2 \text{ (OR 3) SSME OFF FIRST STAGE}}$ (Figure 5.1.1.1.3-7)

A CONTINGENCY ABORT is characterized by two or more SSME-out conditions. The terms affected by contingency abort requirements are the forebody and base terms which are defined as follows:

C_{if} subscript (N), (A), or (m) $\left\{ \begin{array}{l} \text{Rockwell: (TSO datasets)} \\ \quad M = 0.6: \$TT443.CONT.STRUC.M060.DATA \\ \quad M = 0.9: \$TT443.CONT.STRUC.M090.DATA \\ \text{NASA:} \\ \quad \text{Rockwell tape A02578} \end{array} \right.$

F_{NBASE} #1 AND #2 SSME OFF (OR #1 AND #3) (Figure 5.1.1.1.1-8)

F_{NBASE} #2 AND #3 SSME OFF (Figure 5.1.1.1.1-9)

F_{NBASE} ALL SSME OFF (Figure 5.1.1.1.1-10)

F_{ABASE} #1 AND #2 SSME OFF (OR #1 AND #3) (Figure 5.1.1.1.2-8)

F_{ABASE} #2 AND #3 SSME OFF (Figure 5.1.1.1.2-9)

F_{ABASE} ALL SSME OFF (Figure 5.1.1.1.2-10)

M_{BASE} #1 AND #2 SSME OFF (OR #1 AND #3) (Figure 5.1.1.1.3-8)

M_{BASE} #2 AND #3 SSME OFF (Figure 5.1.1.1.3-9)

M_{BASE} ALL SSME OFF (Figure 5.1.1.1.3-10)

$\Delta C_{()_{ELEVON}}$ = Change in force or moment coefficient due to elevon deflection.

$$= Bx + Cx^2 + Dy + Exy + Fy^2$$

$$x = (\delta e_1 \quad - \delta e_1 \quad)$$

$$y = (\delta e_0 \quad - \delta e_0 \quad)$$

δe_1 = inboard deflection

δe_0 = outboard deflection

Coefficients B, C, D, E, and F

subscript: (N) $\beta = -6^\circ$ (Table 5.1.1.1.1-3)
 $\beta = 0^\circ$ (Table 5.1.1.1.1-4)
 $\beta = +6^\circ$ (Table 5.1.1.1.1-5)

(A) $\beta = -6^\circ$ (Table 5.1.1.1.2-3)
 $\beta = 0^\circ$ (Table 5.1.1.1.2-4)
 $\beta = +6^\circ$ (Table 5.1.1.1.2-5)

(m) $\beta = -6^\circ$ (Table 5.1.1.1.3-3)
 $\beta = 0^\circ$ (Table 5.1.1.1.3-4)
 $\beta = +6^\circ$ (Table 5.1.1.1.3-5)

$C_{()_{\dot{\alpha}}}$ = Change in force or moment coefficient due to rate of change of angle of attack, $\dot{\alpha}$ (per radian)*

subscript: (N) (assume zero)
(A) (assume zero)
(m) (see note ff $C_{()_q}$)

$C_{()_q}$ = Change in force or moment coefficient due to pitch rate, q (per radian)*

subscript: (N) (assume zero)
(A) (assume zero)
(m) (Figure 5.1.1.1.3-12)

NOTE: As presented here, $C_{m\dot{\alpha}} \equiv C_{m\dot{q}} + C_{m\dot{\alpha}}$ and should be treated as $C_{m\dot{q}}$.

$\Delta C_{()_{FLEX}}$ = Change in force or moment coefficient due to aeroelastic deformation

$$= \Delta C_{()_{\bar{q}}} = 650_{psf} \left(\frac{\bar{q}}{650} \right)$$

NOTE: See under Hinge Moments for alternate method.

*See reference 4-1 for rotary derivative transfer

subscript: (N) (Figure 5.1.1.1.1-11)
 (A) (Figure 5.1.1.1.2-11)
 (m) (Figure 5.1.1.1.3-11)

4.1.1.2 LATERAL-DIRECTIONAL AERODYNAMICS. The basic first-stage operational lateral-directional force and moments are defined under the same three categories listed in Section 4.1.1.1.

The total lateral-directional force and moments for the first stage are:

$$\text{Side Force, } Y_{\text{TOTAL}} = \bar{q} S C_{Y_{\text{TOTAL AERO}}}$$

$$\text{Yawing Moment, } N_{\text{TOTAL}} = \bar{q} S L_B C_{N_{\text{TOTAL AERO}}}$$

$$\text{Rolling Moment, } L_{\text{TOTAL}} = \bar{q} S L_B C_{l_{\text{TOTAL AERO}}}$$

NOTE: The first-stage moment reference center is located at $X_T 976$, $Y_T 0$, $Z_T 400$.
 To obtain yawing moment about any other MRC;

$$C_{n_{\text{MRC}}} = C_{n_{X_T Y_T Z_T}} - \frac{\Delta Y}{L_B} C_A + \frac{\Delta X}{L_B} C_Y$$

where, $\Delta X = X_{\text{MRC}_{\text{NEW}}} - 976$ inches

$$\Delta Y = Y_{\text{MRC}_{\text{NEW}}} - 0 \text{ inch}$$

$$C_{l_{\text{MRC}}} = C_{l_{X_T Y_T Z_T}} + \frac{\Delta Y}{L_B} C_N - \frac{\Delta Z}{L_B} C_Y$$

$$\Delta Z = Z_{\text{MRC}_{\text{NEW}}} - 400 \text{ inches}$$

The total non-dimensional force and moment coefficients are defined as:

GROUND WIND ($M = 0$)

$$C_{()_{\text{TOTAL AERO}}}^{\text{GW}} = (1 + k_1, 2k_2) C_{()_{\text{W/O TOWER}}}$$

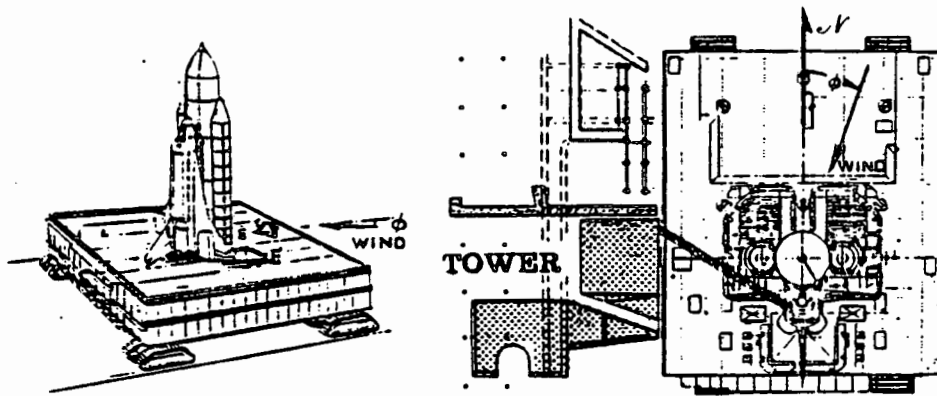
TRANSITION ($0 \leq M \leq 0.6$)

$$C_{()_{\text{TOTAL AERO}}}^{\text{TRANS}} = C_{()_{\text{TRANS}}}$$

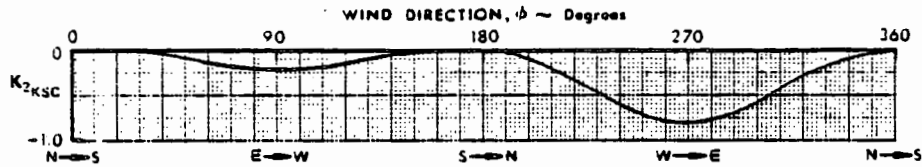
LOW ATTITUDE ($0.6 \leq M \leq 4.5$)

$$C_{()_{\text{TOTAL AERO}}}^{\text{LOW ATT}} = C_{()_{\text{FOREBODY}}} + \Delta C_{()_{\text{ELEVON}}} + C_{()_p} \frac{\rho L_B}{2V} + C_{()_r} \frac{r L_B}{2V} + C_{()_\beta} \frac{\beta L_B}{2V} + \Delta C_{()_{\text{FLEX}}}$$

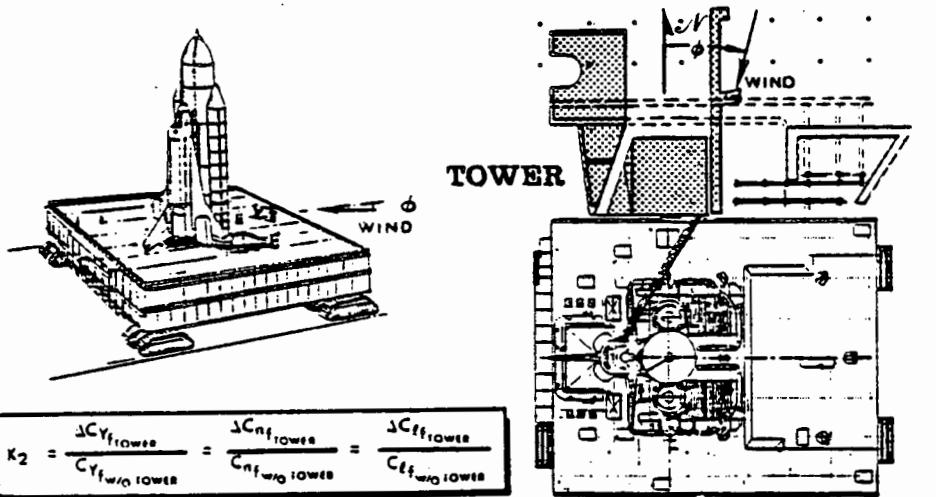
where, the subscript () is used to denote either side force (Y), yawing moment (n), or rolling moment (l).



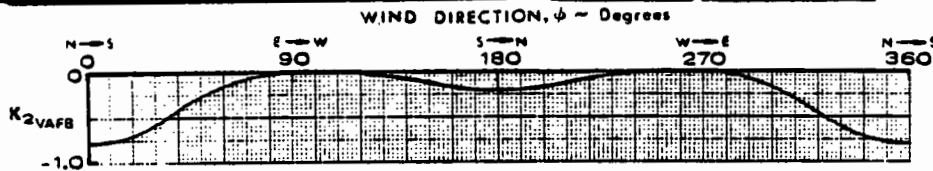
$$K_2 = \frac{\Delta C_{Y_{TOWER}}}{C_{Y_{W/D TOWER}}} = \frac{\Delta C_{n_{TOWER}}}{C_{n_{W/D TOWER}}} = \frac{\Delta C_{l_{TOWER}}}{C_{l_{W/D TOWER}}}$$



(a) KENNEDY SPACE CENTER



$$K_2 = \frac{\Delta C_{Y_{TOWER}}}{C_{Y_{W/D TOWER}}} = \frac{\Delta C_{n_{TOWER}}}{C_{n_{W/D TOWER}}} = \frac{\Delta C_{l_{TOWER}}}{C_{l_{W/D TOWER}}}$$



(b) VANDENBURG AIR FORCE BASE

TOWER INTERFERENCE EFFECTS ON LAUNCH VEHICLE

$C_{()W/O TOWER}$ = Basic force or moment coefficient
on crawler without tower

subscript: (Y) (Figure 5.1.1.2.1-1, -2)
(n) (Figure 5.1.1.2.2-1, -2)
(l) (Figure 5.1.1.2.3-1, -2)

$C_{()TRANS}$ = Basic forebody force or moment
coefficient during transition phase $(-90^\circ \leq \alpha \leq +90^\circ)$
 $(-90^\circ \leq \beta \leq +90^\circ)$

subscript (Y), $[2.03(\sin|\beta|)^{0.94} - 0.0123 - 2.02(\sin|\beta|)^2]\cos\alpha + 2.02(\sin|\beta|)^{2.73}$
 $\pm \beta + \mp C_Y$
for $\alpha, \beta > 12^\circ$, use in conjunction with Tables 5.1.1.2.1-1, -2

(n), $[\cos 2\alpha - 0.02][0.9638(\sin|\beta|) + 0.0022 - 0.966(\sin|\beta|)^2]$
 $+ 0.966(\sin|\beta|)^{2.12}$
 $\pm \beta + \pm C_n$
for $\alpha, \beta > 12^\circ$, use in conjunction with Tables 5.1.1.2.2-1, -2

(l), $[0.332(\sin|\beta|)^{0.97} + 0.0008 - 0.333(\sin|\beta|)^{1.9}]\cos\alpha + 0.333(\sin|\beta|)^{2.12}$
 $\pm \beta + \mp C_l$
for $\alpha, \beta > 12^\circ$, use in conjunction with Tables 5.1.1.2.3-1, -2

$C_{()FOREBODY}$ = Full-scale, rigid-body, proximity,
forebody force or moment coefficient
(including forebody plume effects)
NOTE: All control surfaces neutral except
elevons which follow the Mach -
deflection schedule given in
Section 4.1.1.1.

subscript: (Y) (Figures 5.1.1.2.1-3,-4)
(Tables 5.1.1.2.1-3 through 6)
(n) (Figures 5.1.1.1.1-3,-4)
(Tables 5.1.1.2.2-3 through 6)
(l) (Figures 5.1.1.1.3-3,-4)
(Tables 5.1.1.2.3-3 through 6)

$\Delta C_{()ELEVON}$ = Change in force or moment coefficient due to elevon
deflection

$$= Bx + Cx^2 + Dy + Exy + Fy^2$$

$$x = (\delta e_{I OFF NOM} - \delta e_{I NOM})$$

$$y = (\delta e_{O OFF NOM} - \delta e_{O NOM})$$

Coefficients B, C, D, E, and F

subscript: (Y) $\alpha = -8^\circ$ (Table 5.1.1.2.1-3)
 $\alpha = -4^\circ$ (Table 5.1.1.2.1-4)
 $\alpha = 0^\circ$ (Table 5.1.1.2.1-5)
 $\alpha = +4^\circ$ (Table 5.1.1.2.1-6)

C-3

(n) $\alpha = -8^\circ$ (Table 5.1.1.2.2-3)
 $\alpha = -4^\circ$ (Table 5.1.1.2.2-4)
 $\alpha = 0^\circ$ (Table 5.1.1.2.2-5)
 $\alpha = +4^\circ$ (Table 5.1.1.2.2-6)

(l) $\alpha = -8^\circ$ (Table 5.1.1.2.3-3)
 $\alpha = -4^\circ$ (Table 5.1.1.2.3-4)
 $\alpha = 0^\circ$ (Table 5.1.1.2.3-5)
 $\alpha = +4^\circ$ (Table 5.1.1.2.3-6)

$C_{()p}$ = Change in force or moment coefficient due to roll rate, p (per radian)*

subscript: (Y) (assume zero)
 (n) (Figure 5.1.1.2.2-5)
 (l) (Figure 5.1.1.2.3-5)

$C_{()r}$ = Change in force or moment coefficient due to yaw rate, r (per radian)*

subscript: (Y) (assume zero)
 (n) (Figure 5.1.1.2.2-6)
 (l) (Figure 5.1.1.2.3-6)

$C_{()\dot{\beta}}$ = Change in force or moment coefficient due to lateral acceleration, $\dot{\beta}$ (per radian)*

subscript: (Y) (assume zero)
 (n) (assume zero)
 (l) (assume zero)

$\Delta C_{()FLEX}$ = Incremental change in basic force or moment coefficient due to aeroelastic deformation

$$= \left(\frac{\Delta C_{()\beta_{FLEX}}}{\bar{q}} \right) \bar{q} \beta$$

subscript: (Y) (Figure 5.1.1.2.1-5)
 (n) (Figure 5.1.1.2.2-7)
 (l) (Figure 5.1.1.2.3-7)

*See reference 4-1 for rotary derivative transfer.

The difference between normal launch aerodynamics and INTACT ABORT aerodynamics lies in the base term only, where a one SSME-out failure condition prevails. No lateral-directional terms are affected by Intact Abort requirements.

A CONTINGENCY ABORT is characterized by two or more SSME-out conditions. The only changes to the nominal data are in the forebody aerodynamic coefficients for Mach 0.6 and 0.9 and represent an expansion of the α/β matrix to cover the following flight conditions:

| Mach | α -Range (deg.) | β -Range (deg.) |
|------|------------------------|-----------------------|
| 0.6 | -14 to +8 | -10 to +8 |
| 0.9 | -12 to +4 | - 6 to +6 |

These data set expansions are limited to the nominal trajectory elevation setting, $\delta e_1/\delta e_0 = 10/9$ degrees. The only terms affected by Contingency Abort requirements are as follows:

$C_{Y_{FOREBODY}}$ { Rockwell: (TSO datasets)
 M = 0.6: \$TT443.CONT.STRUC.MO60.DATA
 M = 0.9: \$TT443.CONT.STRUC.MO90.DATA
 NASA:
 M > 0.9, refer to normal launch data.

$C_{N_{FOREBODY}}$ { Rockwell: (TSO datasets)
 M = 0.6: \$TT443.CONT.STRUC.MO60.DATA
 M = 0.9: \$TT443.CONT.STRUC.MO90.DATA
 $C_{L_{FOREBODY}}$ { NASA:
 Rockwell Tape A02578

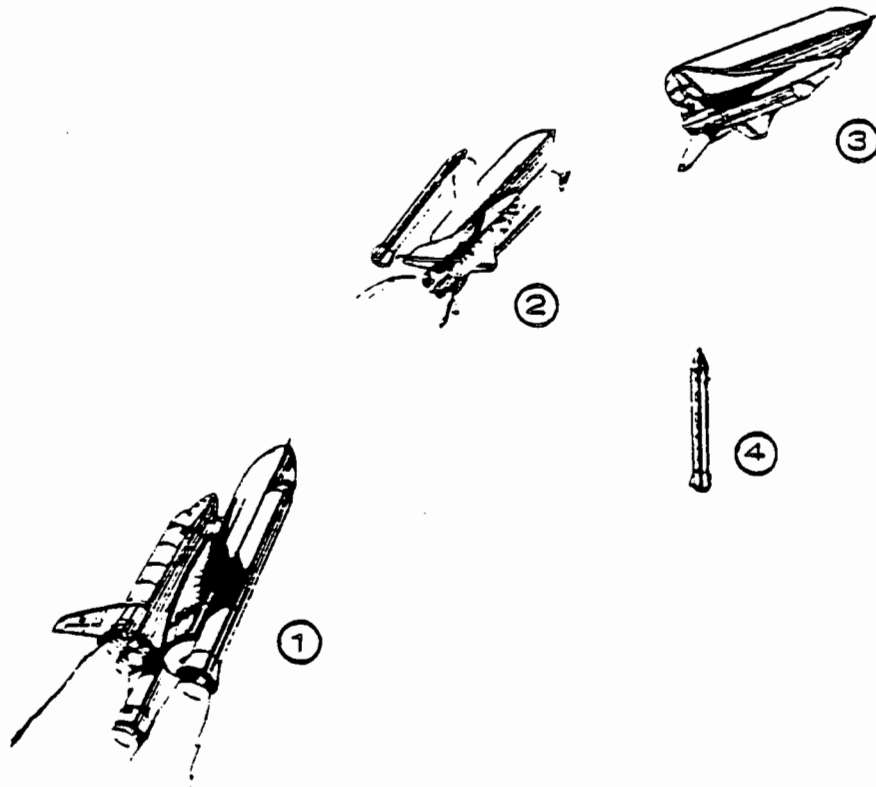
For M > 0.9 refer to normal launch data. There are no lateral-directional base force terms.

4.1.2 SOLID ROCKET BOOSTER SEPARATION

ORIGINAL PAGE IS
OF POOR QUALITY

4.1.2 SOLID ROCKET BOOSTER SEPARATION. The Solid Rocket Boosters (SRB's) are separated (at burn-out) from the Orbiter-plus External Tank (OT) by means of aerodynamic forces and moments and by the application of thrust from the Booster Separation Motors (BSM's). Longitudinal separation (ΔX) is achieved by means of the higher axial acceleration of the OT whereas, lateral (ΔY) and normal (ΔZ) separation are achieved by a combination of the BSM thrust and the aerodynamic forces and moments on the SRB's. The effects of SSME plumes on SRB separation trajectories are also taken into account. This section considers:

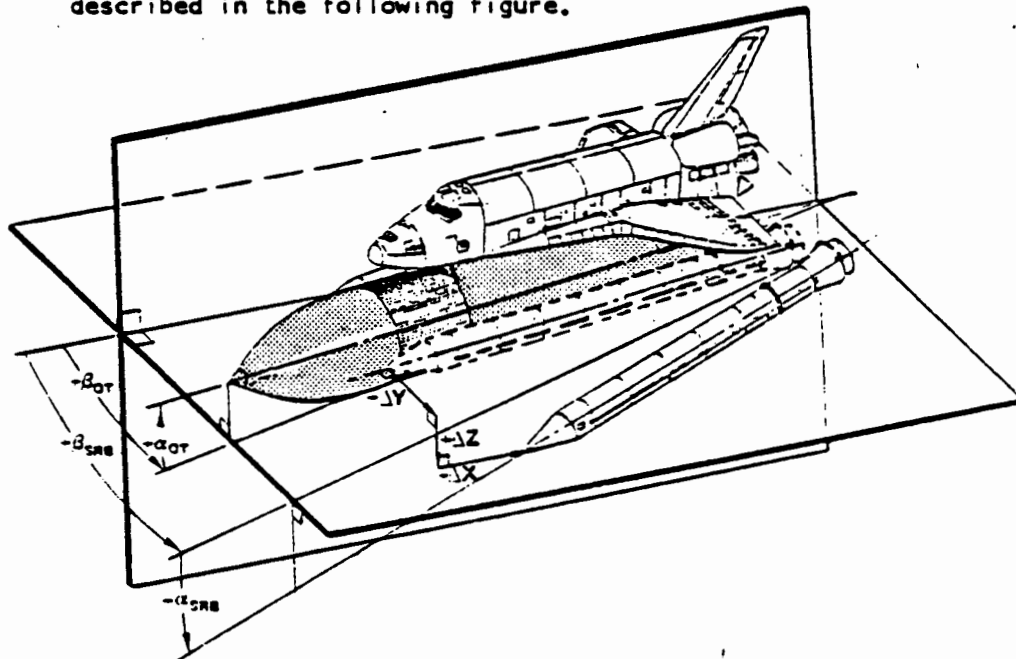
- (1) Pre-Separation Launch Vehicle Aerodynamics
- (2) Separation Proximity Aerodynamics
- (3) Separation Isolated Orbiter-plus-External Tank
- (4) Separation Isolated Solid Rocket Booster



Separation motion is initiated by firing the eight, solid propellant, Booster Separation Motors on each SRB (see Section 3.1.2). These motors produce 21,700 lb thrust each over a very short burn time (0.68 sec) which was selected to minimize impingement of the exhaust plume on the OT. Three basic aerodynamic phenomena must be taken into account in order to describe the separation motion. These are:

- 1) The BSM plume effect on the flow field surrounding the vehicle(s).
- 2) BSM plume impingement on the OT.
- 3) Proximity effect of the separating vehicles on one another.

Each of these items is a function of the orientation of the OT with respect to the freestream flow and the relative displacement and orientation between the separating vehicles. A set of eight independent variables are, therefore, required to define the separation motion (α_{OT} , β_{OT} , $\Delta\alpha$, $\Delta\beta$, ΔX , ΔY , ΔZ and the Separation Motor jet-to-freestream Momentum Ratio). The orientation variables are described in the following figure.



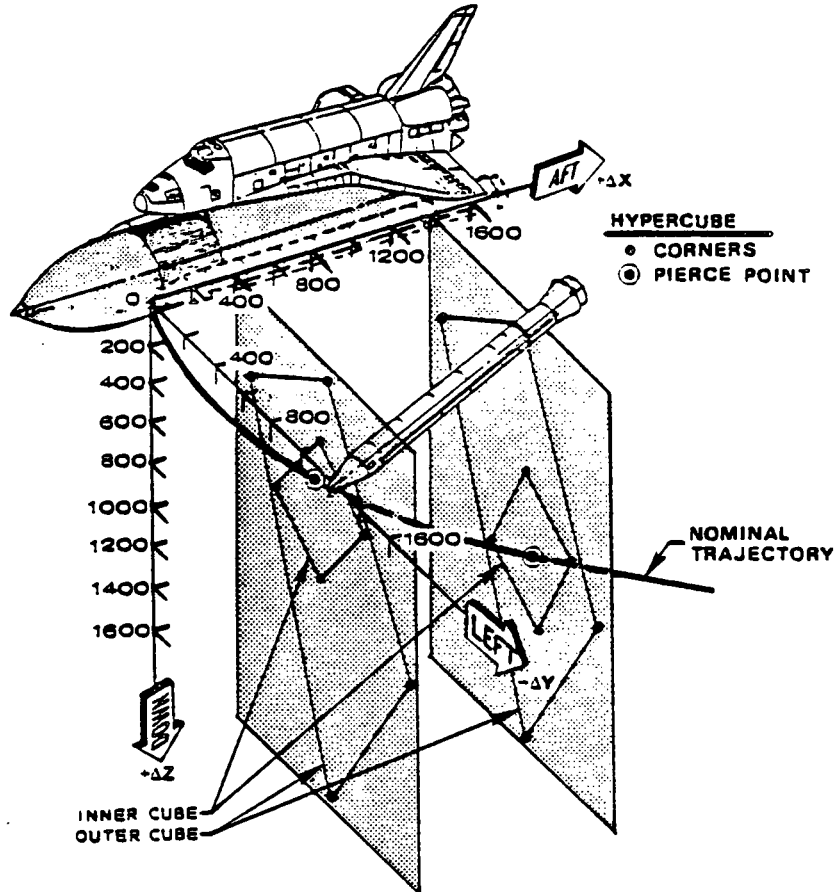
- NOTE: 1. ΔX , ΔY , ΔZ are orthogonal displacements of SRB nose from its mated position.
2. Angular orientation of SRB is about SRB nose.
3. ΔX - Positive aft
 ΔY - Positive outboard right
 ΔZ - Positive down

4. $\Delta\alpha \equiv (\alpha_{SRB} - \alpha_{OT})$
 $\Delta\beta \equiv (\beta_{SRB} - \beta_{OT})$
5. Separation Motor jet-to-freestream Momentum Ratio (MR) is also an independent variable.

Aerodynamic forces and moments are defined as a function of these parameters in the Orbiter-plus-External Tank (OT) and Solid Rocket Booster body-axis systems (see also Section 3.1).

*
* Particular attention should be given to the location
* of the MOMENT REFERENCE CENTERS Used in the separation
* data. These Moment Reference Centers differ for each
* configuration and also differ from the MRC used for
* nominal data.
*

The use of eight independent variables (hyperspace) in any data base is extremely cumbersome if the standard square data grid is used and, most of the data required to fill the grid, would exceed any reasonable expectation of use where SRB separation is concerned. A unique data organization concept was, therefore, developed by the NASA (JSC) which would handle the five independent proximity variables (ΔX , ΔY , ΔZ , $\Delta \alpha$, and $\Delta \beta$) by placing two, four-dimensional, arrays of data (ΔY , ΔZ , $\Delta \alpha$, and $\Delta \beta$) at various points along a fifth dimension (ΔX). This concept has been designated as a "hypercube" format consisting of "inner" and "outer" data sets which are not constrained to have parallel opposite sides and may, therefore, be shaped to match any physical constraints. An example of the hypercube boundaries surrounding the nominal SRB trajectory is shown in the following sketch.



4.1.2-3

The inner data set encompasses the flight parameters for a nominal separation trajectory with 3-sigma dispersions and the outer data set encompasses all potential separation conditions, including engine-out conditions. Data are provided at the vertices of the hypercubes and at an interior point within each hypercube to increase the data density in a particular region of interest and provide non-linear variation between hypercube corners. The longitudinal displacements (ΔX) at which the hypercubes are placed are selected in a manner which maintains constant intervals of time (rather than constant length intervals) to provide increased data density early in the separation motion when trends are being established. A low order polynomial surface was fit to the vertices and interior points for the purpose of interpolation on ΔY , ΔZ , $\Delta \alpha$, and $\Delta \beta$. Interpolation of the remaining independent variables (ΔX , α_{OT} , β_{OT} , and the plume scaling parameter) is handled in a linear fashion.

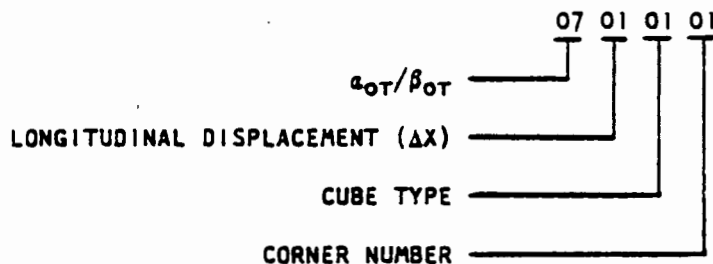
Each hypercube has a total of 34 data points comprised of 16 inner cube corners, 16 outer cube corners, plus the additional interior points located near the centers of each hypercube. Although the hypercube geometry remains the same for all values of α_{OT} and β_{OT} , the dependent variables (proximity coefficient, $\Delta C_{()} \equiv C_{()PROX} - C_{()ISOL}$, data) stored within are unique. These proximity coefficients are stored on ROCKWELL COMPUTER DISK PACK TU0110 in three separate data bases for the RH SRB (LH SRB data are obtained by appropriate transformation) under the following data set names:

MR = 0: TAERO1.JULY82.PWROFF.HYPC.PC0.DATA
 MR = 133.4: TAERO1.JULY82.PWRON.HYPC.PC900.DATA
 MR = 222.3: TAERO1.JULY82.PWRON.HYPC.PC1500.DATA

The nine proximity coefficients;

| | | |
|----------------------|----------------------|----------------------|
| $\Delta C_{N_{OT}}$ | $\Delta C_{m_{OT}}$ | $\Delta C_{Y_{OT}}$ |
| $\Delta C_{n_{OT}}$ | $\Delta C_{l_{OT}}$ | $\Delta C_{N_{SRB}}$ |
| $\Delta C_{m_{SRB}}$ | $\Delta C_{Y_{SRB}}$ | $\Delta C_{n_{SRB}}$ |

are followed by a coded index (consisting of four, two-digit numbers) which identifies the hypercube and corner number. This code is defined in the following manner:



| FIRST INTEGER | | SECOND INTEGER | | | | THIRD INTEGER | | FOURTH INTEGER | | | |
|---------------|--------------------------|----------------|------------|-----------|------------|---------------|-----------|----------------|---------------|----|----|
| CODE | α_{OT}/β_{OT} | PLUME-ON | | PLUME-OFF | | CODE | CUBE TYPE | CODE | CORNER NUMBER | | |
| | | CODE | ΔX | CODE | ΔX | | | | | | |
| 01 | -10/-10 | 00 | 0 | 00 | 0 | 00 | MATED | 01 | 1 | | |
| 02 | 0/-10 | 01 | 100 | 01 | 100 | 01 | INNER | 02 | 2 | | |
| 03 | 10/-10 | 02 | 200 | 02 | 300 | 02 | OUTER | 03 | 3 | | |
| 04 | -4/-5 | | | 03 | 600 | | | 04 | 4 | | |
| 05 | 4/-5 | | | 04 | 1100 | | | 05 | 1700 | 05 | 5 |
| 06 | -10/0 | | | 06 | | | | | | 06 | 6 |
| 07 | 0/0 | | | | | | | | | 07 | 7 |
| 08 | 10/0 | | | | | | | | | 08 | 8 |
| 09 | -4/5 | | | | | | | | | 09 | 9 |
| 10 | 4/5 | | | | | | | | | 10 | 10 |
| 11 | -10/10 | | | | | | | | | | |
| 12 | 0/10 | | | | | | | | | | |
| 13 | 10/10 | | | | | | | | | | |
| | | | | | | | | 17 | 17 | | |

The purpose of the coded index is to facilitate data interpolation by providing each set of aerodynamic coefficients for a specific set of independent variables with an unique identifying number. An illustration of the relationship between the coded index associated with the aerodynamic coefficient data stored on DISK PACK TU0110 and the corresponding independent variables is provided in the following example:

PLUME-ON (MR = 133.4) INNER HYPERCUBE

| INDEX CODE | α_{OT}/β_{OT} | ΔX | ΔY | ΔZ | $\Delta \alpha$ | $\Delta \beta$ | CORNER No. |
|---------------|--------------------------|------------|------------|------------|-----------------|----------------|------------|
| | Deg/Deg | in | in | in | Deg. | Deg. | |
| 07-01-01-01 | 0/0 | 100 | 60 | 110 | -4 | -1.5 | 1 |
| -02 | ↓ | ↓ | ↓ | ↓ | ↓ | 0 | 2 |
| -03 | ↓ | ↓ | ↓ | ↓ | ↓ | -1.5 | 3 |
| -04 | ↓ | ↓ | ↓ | ↓ | ↓ | 0 | 4 |
| -05 | ↓ | ↓ | ↓ | 70 | -4 | -1.5 | 5 |
| -06 | ↓ | ↓ | ↓ | ↓ | ↓ | 0 | 6 |
| -07 | ↓ | ↓ | ↓ | ↓ | ↓ | -1.5 | 7 |
| -08 | ↓ | ↓ | ↓ | ↓ | ↓ | 0 | 8 |
| -09 | ↓ | ↓ | 30 | 110 | -4 | -1.5 | 9 |
| -10 | ↓ | ↓ | ↓ | ↓ | ↓ | 0 | 10 |
| -11 | ↓ | ↓ | ↓ | ↓ | ↓ | -1.5 | 11 |
| -12 | ↓ | ↓ | ↓ | ↓ | ↓ | 0 | 12 |
| -13 | ↓ | ↓ | ↓ | 70 | -4 | -1.5 | 13 |
| -14 | ↓ | ↓ | ↓ | ↓ | ↓ | 0 | 14 |
| -15 | ↓ | ↓ | ↓ | ↓ | ↓ | -1.5 | 15 |
| -16 | ↓ | ↓ | ↓ | ↓ | ↓ | 0 | 16 |
| * 07-01-01-17 | ↓ | ↓ | 40 | 90 | -4 | -1.0 | 17 |

* INTERIOR HYPERCUBE POINT

A sample of the output for these conditions is provided in the following table:

PLUME-ON (MR = 133.4) INNER HYPERCUBE

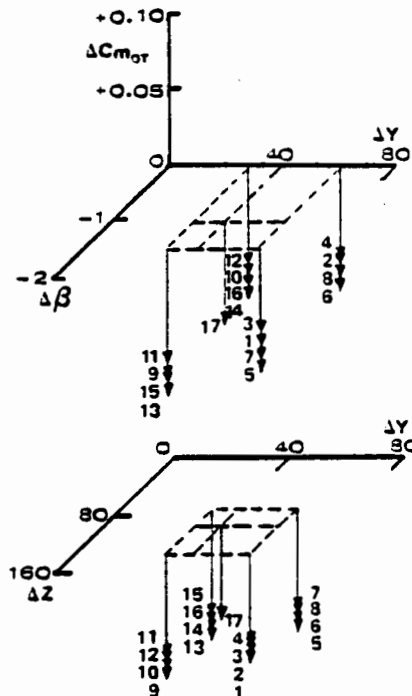
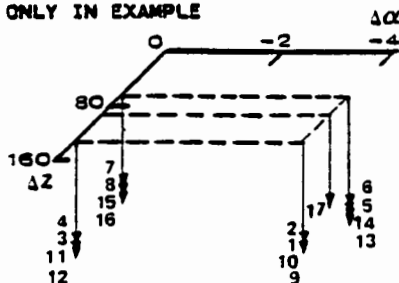
| C _{NOT} | C _{MOT} | C _{YOT} | C _{ROT} | C _{ZOT} | C _{NSRB} | C _{MSRB} | C _{YSRB} | C _{NSRB} | α_{OT}/β_{OT} | ΔX | TYPE | CORNER No. |
|------------------|------------------|------------------|------------------|------------------|-------------------|-------------------|-------------------|-------------------|--------------------------|------------|------|------------|
| -0.0136 | -0.0740 | 0.0037 | 0.0015 | 0.0012 | 0.0012 | 0.0068 | -0.0049 | -0.0028 | 07 | 01 | 01 | 01 |
| -0.0079 | -0.0737 | -0.0027 | 0.0038 | 0.0005 | -0.0007 | 0.0078 | 0.0015 | -0.0023 | 07 | 01 | 01 | 02 |
| -0.0101 | -0.0714 | 0.0032 | 0.0004 | 0.0007 | -0.0088 | 0.0081 | -0.0038 | -0.0057 | 07 | 01 | 01 | 03 |
| -0.0130 | -0.0710 | -0.0011 | 0.0018 | 0.0004 | -0.0071 | 0.0088 | 0.0018 | -0.0085 | 07 | 01 | 01 | 04 |
| -0.0812 | -0.0888 | 0.0181 | 0.0053 | 0.0010 | -0.0004 | 0.0049 | -0.0049 | -0.0017 | 07 | 01 | 01 | 05 |
| -0.0729 | -0.0875 | 0.0147 | 0.0054 | 0.0008 | -0.0028 | 0.0050 | 0.0005 | -0.0018 | 07 | 01 | 01 | 06 |
| -0.0381 | -0.0791 | 0.0222 | 0.0059 | 0.0008 | -0.0083 | 0.0038 | -0.0063 | -0.0058 | 07 | 01 | 01 | 07 |
| -0.0485 | -0.0803 | 0.0092 | 0.0014 | 0.0009 | -0.0071 | 0.0048 | 0.0009 | -0.0080 | 07 | 01 | 01 | 08 |
| -0.0382 | -0.0807 | -0.0673 | 0.0060 | 0.0013 | 0.0017 | 0.0088 | 0.0193 | -0.0031 | 07 | 01 | 01 | 09 |
| -0.0388 | -0.0805 | -0.0579 | -0.0078 | -0.0010 | 0.0 | 0.0077 | 0.0015 | -0.0010 | 07 | 01 | 01 | 10 |
| -0.0231 | -0.0732 | -0.0418 | -0.0102 | -0.0001 | -0.0076 | 0.0049 | -0.0033 | -0.0033 | 07 | 01 | 01 | 11 |
| -0.0238 | -0.0747 | -0.0437 | -0.0093 | -0.0003 | -0.0082 | 0.0054 | 0.0022 | -0.0048 | 07 | 01 | 01 | 12 |
| -0.0483 | -0.0937 | -0.0203 | -0.0030 | 0.0001 | 0.0017 | 0.0085 | -0.0027 | -0.0017 | 07 | 01 | 01 | 13 |
| -0.0532 | -0.0908 | -0.0202 | -0.0031 | 0.0001 | -0.0017 | 0.0070 | 0.0002 | -0.0010 | 07 | 01 | 01 | 14 |
| -0.0518 | -0.0838 | -0.0187 | -0.0073 | 0.0014 | -0.0090 | 0.0040 | -0.0030 | -0.0040 | 07 | 01 | 01 | 15 |
| -0.0552 | -0.0858 | -0.0192 | -0.0040 | 0.0003 | -0.0100 | 0.0038 | 0.0023 | -0.0048 | 07 | 01 | 01 | 16 |
| -0.0271 | -0.0835 | -0.0145 | -0.0011 | -0.0002 | 0.0014 | 0.0074 | -0.0028 | -0.0022 | 07 | 01 | 01 | 17 |

The OT proximity pitching moment coefficient from the table above is plotted in the figure below to illustrate the hypercube variable concept. The coefficient values are represented by arrows and identified by the appropriate hypercube corner numbers. Similar plots for the other eight proximity coefficients are presented in the appropriate data sections (Volume 2 of this report).

PLUME-ON (MR = 133.4) INNER HYPERCUBE
 $\Delta X = 100$ inches
 $\alpha_{OT}/\beta_{OT} = 0/0$

| CORNER No. | ΔY | ΔZ | $\Delta \alpha$ | $\Delta \beta$ | $\Delta C_{m_{OT}}$ |
|------------|------------|------------|-----------------|----------------|---------------------|
| | in | in | Deg. | Deg. | |
| 1 | 80 | 110 | -4 | -1.5 | -0.0740 |
| 2 | 80 | 110 | 0 | 0 | -0.0737 |
| 3 | 80 | 110 | 0 | -1.5 | -0.0714 |
| 4 | 80 | 110 | 0 | 0 | -0.0710 |
| 5 | 80 | 70 | -4 | -1.5 | -0.0888 |
| 6 | 80 | 70 | 0 | 0 | -0.0875 |
| 7 | 80 | 70 | 0 | -1.5 | -0.0791 |
| 8 | 80 | 70 | 0 | 0 | -0.0803 |
| 9 | 30 | 110 | -4 | -1.5 | -0.0807 |
| 10 | 30 | 110 | 0 | 0 | -0.0805 |
| 11 | 30 | 110 | 0 | -1.5 | -0.0732 |
| 12 | 30 | 110 | 0 | 0 | -0.0747 |
| 13 | 30 | 70 | -4 | -1.5 | -0.0937 |
| 14 | 30 | 70 | 0 | 0 | -0.0908 |
| 15 | 30 | 70 | 0 | -1.5 | -0.0838 |
| 16 | 30 | 70 | 0 | 0 | -0.0858 |
| *17 | 40 | 90 | -4 | -1.0 | -0.0835 |

*SHOWN ONLY IN EXAMPLE





The values associated with the hypercube corners for the entire PLUME-OFF and PLUME-ON data base are summarized in Table 4.1.2-1. The specific combinations of these values are presented in Section and follow the format used in the example for the PLUME-ON (MR = 133.4) INNER HYPERCUBE case.

**Table 4.1.2-1
PLUME-OFF AND PLUME-ON HYPERCUBE DATA BASE SUMMARY**

| PLUME-OFF | | | | | |
|------------|--------------------------|---------------------------|--|--------------------------------------|---------------------------|
| ΔX | ΔY | ΔZ | $\Delta \alpha$ | $\Delta \beta$ | LOCATION |
| Inches | Inches | Inches | Degrees | Degrees | |
| 0 | 0 | 0 | 0 | 0 | ORIGIN |
| 100 | 30, 80 40 | 70, 110 90 | - 4, 0 - 4 | - 1.5, 0 - 1.0 | INNER CUBE INTERIOR PT |
| | 10, 50, 90, 110 80 | 40, 80, 150, 250 170 | - 7, - 4, 0 - 4 | -5.5, -4.5, -2.5, -0.5, 1.0 - 2.0 | OUTER CUBE INTERIOR PT |
| 300 | 90, 170 130 | 180, 280 230 | - 9, - 5 - 7 | - 4, 0 - 2 | INNER CUBE INTERIOR PT |
| | 30, 130, 180, 280 170 | 40, 150, 400, 550 400 | -17, -14, -9, -7, -6.5, -2, 0 -10 | -15, - 9, - 7, - 1, 2 - 5 | OUTER CUBE INTERIOR PT |
| 600 | 140, 290 220 | 300, 480 380 | -15, - 5 -10 | - 8, - 1 -5 | INNER CUBE INTERIOR PT |
| | 90, 220, 250, 510 350 | 140, 280, 660, 800 800 | -30, -28, -15, -11, -9, -7, -2, 0 -15 | -20, -12, -11, - 7, 3 -8 | OUTER CUBE INTERIOR PT |
| 1100 | 250, 450 350 | 380, 630 500 | -21, -10 -16 | -15, - 3 - 9 | INNER CUBE INTERIOR PT |
| | 100, 370, 700 500 | 180, 400, 900 750 | -33, -22, -17, -13, -4, 0 -22 | -20, -18, -16, 3 -11 | OUTER CUBE INTERIOR PT |
| 1700 | 350, 650 500 | 500, 800 650 | -30, -15 -23 | -15, - 5 -10 | INNER CUBE INTERIOR PT |
| | 200, 800 500 | 300, 1000 900 | -34, -27, -15, - 5 -25 | -20, -16, 0, 8 -18 | OUTER CUBE INTERIOR PT |
| PLUME-ON | | | | | |
| 0 | 0 | 0 | 0 | 0 | ORIGIN |
| 100 | 30, 80 40 | 70, 110 90 | - 4, 0 - 4 | - 1.5, 0 - 1.0 | INNER CUBE INTERIOR PT |
| | 10, 50, 90, 110 80 | 40, 80, 150, 250 170 | - 7, - 4, 0 - 4 | -5.5, -4.5, -2.5, -0.5, 1.0 -2.0 | OUTER CUBE INTERIOR PT |
| 200 | 60, 110 90 | 130, 200 160 | - 7, - 4 - 4 | -2.5, -0.5 - 1.5 | INNER CUBE INTERIOR PT |
| | 20, 80, 150 ----- | 60, 90, 180, 280 ----- | - 7, 0 ----- | -6.5, -3.5, -1.0, 0.5 ----- | OUTER CUBE INTERIOR PT |

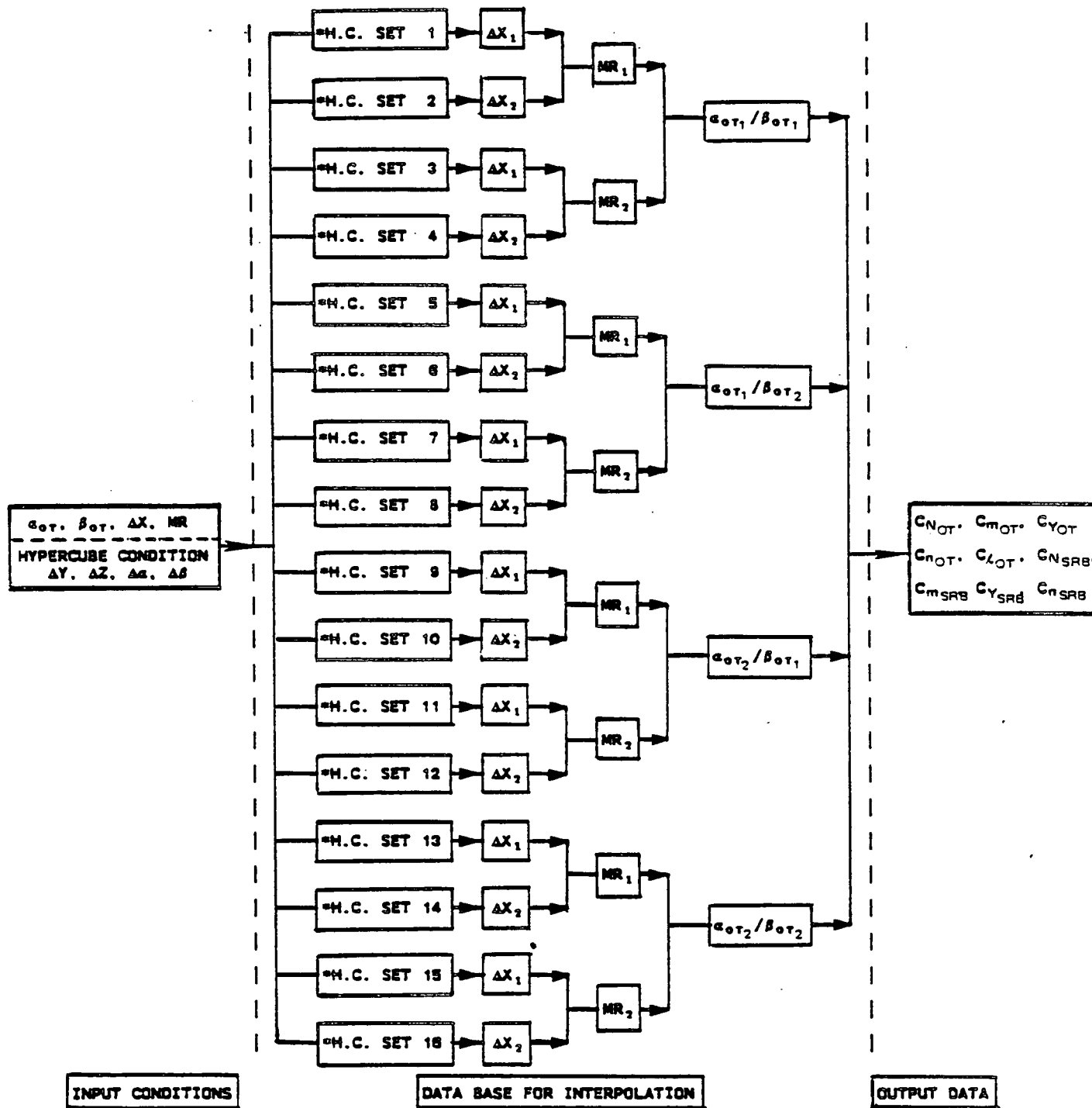
4.1.2-8

5T585-0119-1

Space Transportation
Systems Division



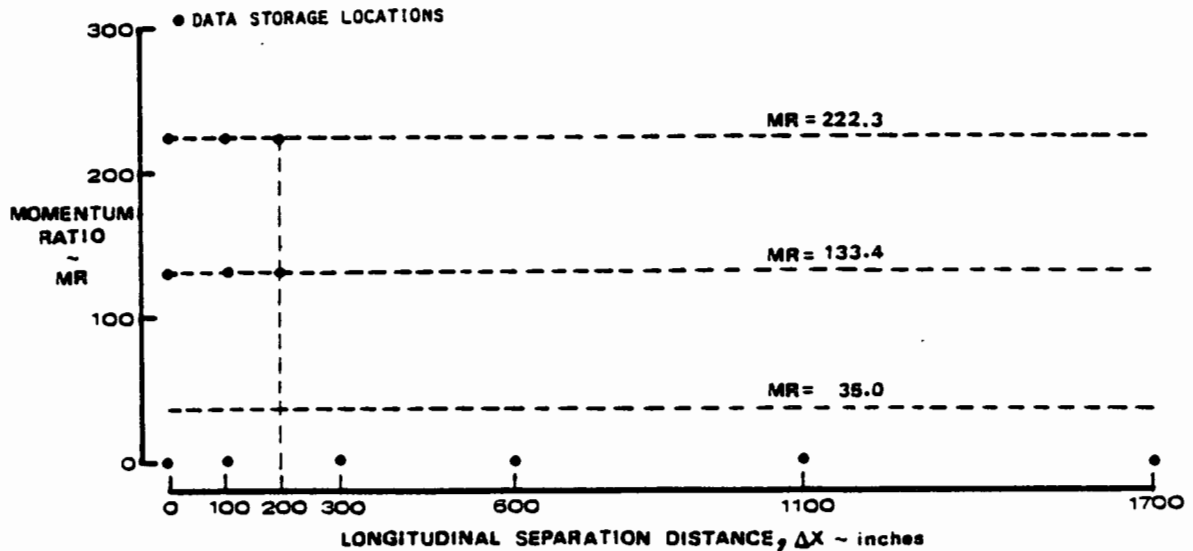
The hypercube data sets (sixteen) required to perform an interpolation for a given set (α_{OT} , β_{OT} , MR, ΔX , ΔY , ΔZ , Δa , and $\Delta \beta$) of input conditions are defined below. The order of interpolation is:



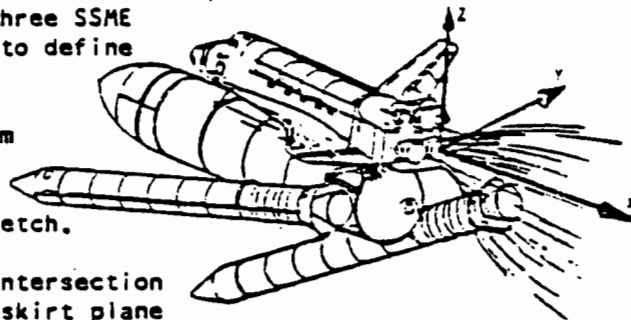
H.C. SET__ = HYPERCUBE POINTS 1 -17 (INNER OR OUTER)

Special rules, based on the SRB longitudinal separation position (ΔX), are to be observed in the interpolation on momentum ratio (MR) as indicated below:

- ① IF MR > 222.3, SET MR = 222.3
- ② IF MR < 35.0, SET MR = 0
- ③ IF MR \geq 133.4 AND $\Delta X \geq$ 200, SET $\Delta X = 200$
- ④ IF MR < 133.4 AND $\Delta X \geq$ 200, SET MR = 0



Space Shuttle Main Engine (SSME) plume impingement force and moment effects on SRB separation trajectories have been included to supplement the basic aerodynamic contribution. A plume oriented coordinate system, based on the number three SSME (lower right engine) is used to define impingement effects on the right hand SRB. The origin of the plume coordinate system is the intersection of the nozzle axis with the nozzle exit plane as shown in the sketch.



An SRB reference point, the intersection of the SRB axis with the aft skirt plane ($X_B 1930.64$), is used in the definition of SRB to OT relative position parameters. The plume property distributions in all radial planes containing the plume axis (i.e., any orientation, ϕ , of the SRB in Figure 4.1.2-1) are considered similar based on the assumption that the interaction of one SSME plume on another is neglected and discounting nozzle cant with respect to the freestream flow. This simplifies impingement calculations and data storage since the analysis of SRB movement can be limited to the X - Z plane of the plume coordinate system.

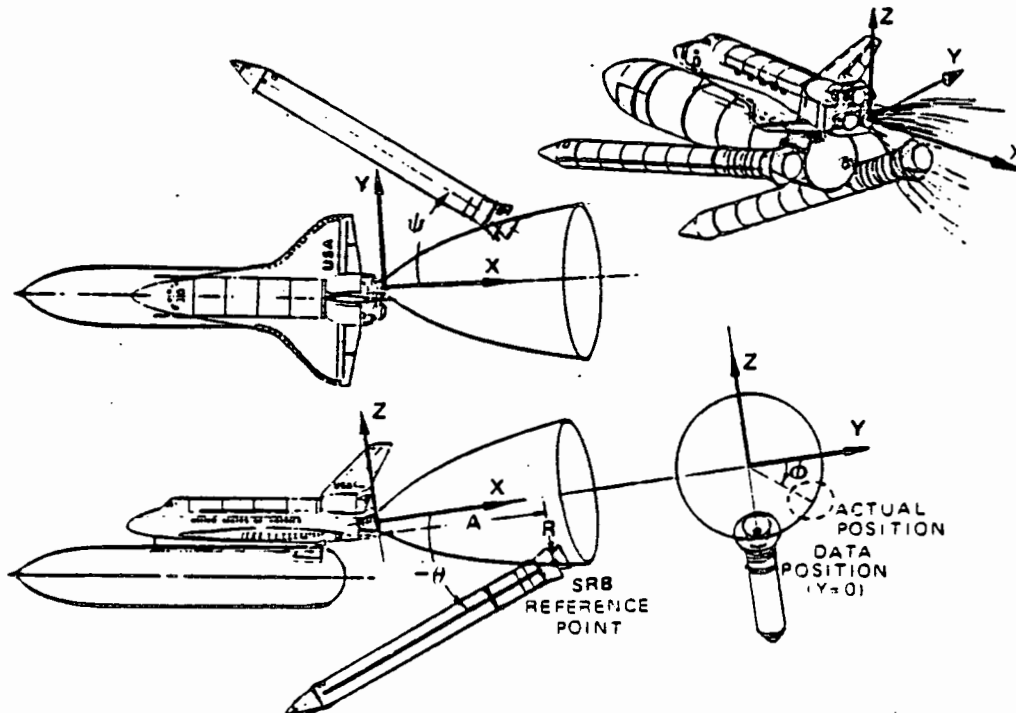


Figure 4.1.2-1
SSME PLUME IMPINGEMENT COORDINATE SYSTEM

The relative position parameters for the actual SRB are converted (Euler Transformations) into four independent variables in the plume coordinate system defined as follows:

- A Axial location of SRB reference point in plume measured in the X - Z plane.
- R Radial location of SRB reference point in plume.
- θ SRB pitch angle relative to the plume ζ measured in the X - Z plane.
- ψ SRB yaw angle relative to the plume ζ measured in the Z - Y plane.

Forces and moments due to impingement are then determined as a function of these variables through a table look-up and the results transformed to the proper SRB ϕ angle orientation by means of Euler relationships. The Euler transformation order from plume coordinate system to SRB coordinate system is pitch rotation followed by yaw rotation.

All of the tabulated plume impingement data are presented for the RH SRB entering the number three (lower right) SSME plume. Comparable impingement data for the LH SRB entering the number two (lower left) SSME plume are generated from the right SRB data by considering appropriate sign changes in the directional aerodynamic properties (side force, yawing moment, and the yaw angle, ψ). Roll induced plume impingement effects are considered negligible and are, therefore, not presented.

4.1.2.1 LONGITUDINAL AERODYNAMICS. Longitudinal aerodynamic force and moment equations pertaining to SRB separation are presented in two parts:

| | |
|----------------|------------------|
| PRE-SEPARATION | (LAUNCH VEHICLE) |
| | (PROXIMITY) |
| SEPARATION | (ISOLATED OT) |
| | (ISOLATED SRB) |

The separation configuration was shown on page 4.1.2-2. Definitions of the appropriate flight parameters are also given on page 4.1.2-2.

PRE-SEPARATION

LAUNCH VEHICLE. Launch Vehicle longitudinal aerodynamic forces and moment for the pre-separation phase are defined as:

$$C_{\text{AERO}}^{(\)\text{TOTAL}} = C_{\text{FOREBODY}}^{(\)} + C_{\text{BASE}}^{(\)} + \Delta C_{\text{ELEVON}}^{(\)} + C_{\dot{\alpha}}^{(\)} \frac{\dot{\alpha} L_B}{2V} + C_q^{(\)} \frac{q L_B}{2V} + \Delta C_{\text{FLEX}}^{(\)}$$

where the subscript () is used to denote normal force (N), axial force (A), or pitching moment (m).

$C_{\text{FOREBODY}}^{(\)}$ = Full-scale, rigid, mated forebody force or moment coefficient (including forebody plume effects) with all control surfaces neutral.

| | |
|----------------|-------------------|
| subscript: (N) | Table 5.1.2.1.1-1 |
| (A) | Table 5.1.2.1.2-1 |
| (m) | Table 5.1.2.1.3-1 |

$C_{\text{BASE}}^{(\)}$ = Power-on base force or moment coefficient (including effects of SSME and SRM plumes).

| | |
|----------------|---------------------|
| subscript: (N) | cf. Section 4.1.1.1 |
| (A) | cf. Section 4.1.1.1 |
| (m) | cf. Section 4.1.1.1 |

$\Delta C_{\text{ELEVON}}^{(\)}$ = Change in force or moment coefficient due to elevon deflection.

| | |
|----------------|---------------------|
| subscript: (N) | cf. Section 4.1.1.1 |
| (A) | cf. Section 4.1.1.1 |
| (m) | cf. Section 4.1.1.1 |

$C_{\dot{\alpha}}^{(\)}$ = Change in force or moment coefficient due to rate of change of angle of attack, $\dot{\alpha}$, (per radian).

| | |
|----------------|---------------------|
| subscript: (N) | cf. Section 4.1.1.1 |
| (A) | cf. Section 4.1.1.1 |
| (m) | cf. Section 4.1.1.1 |

$C_{()q}$ = Change in force or moment coefficient due to pitch rate, q (per radian).

subscript: (N) cf. Section 4.1.1.1
(A) cf. Section 4.1.1.1
(m) cf. Section 4.1.1.1

$\Delta C_{()FLEX}$ = Change in force or moment coefficient due to aeroelastic deformation.

subscript: (N) cf. Section 4.1.1.1
(A) cf. Section 4.1.1.1
(m) cf. Section 4.1.1.1

SEPARATION

The total separation force and moment coefficients have been subdivided into three components:

1. ISOLATED VEHICLE (LSRB, RSRB, OT)
2. PROXIMITY EFFECT (LSRB, RSRB, OT)
3. SSME PLUME EFFECT (LSRB, RSRB)

Total separation force, (N) or (A), coefficients are defined as:

$$C_{()_{AERO} | RSRB}^{TOTAL} = C_{()_{ISOLATED} | RSRB} + \Delta C_{()_{PROXIMITY} | RSRB} + \frac{1}{qS} \Delta F_{()_{SSME PLUME} | RSRB}$$

$$C_{()_{AERO} | LSRB}^{TOTAL} = C_{()_{ISOLATED} | LSRB} + \Delta C_{()_{PROXIMITY} | LSRB} + \frac{1}{qS} \Delta F_{()_{SSME PLUME} | LSRB}$$

$$C_{()_{AERO} | OT}^{TOTAL} = C_{()_{ISOLATED} | OT} + \frac{1}{K} \left[\Delta C_{()_{PROXIMITY} | OT}^{RSRB} + \Delta C_{()_{PROXIMITY} | OT}^{LSRB} \right]$$

The total separation pitching moment (m) coefficient is defined as:

$$C_{(m)_{AERO} | RSRB}^{TOTAL} = C_{(m)_{ISOLATED} | RSRB} + \Delta C_{(m)_{PROXIMITY} | RSRB} + \frac{1}{qS L_B} \Delta M_{SSME PLUME | RSRB}$$

$$C_{(m)_{AERO} | LSRB}^{TOTAL} = C_{(m)_{ISOLATED} | LSRB} + \Delta C_{(m)_{PROXIMITY} | LSRB} + \frac{1}{qS L_B} \Delta M_{SSME PLUME | LSRB}$$

$$C_{(m)_{AERO} | OT}^{TOTAL} = C_{(m)_{ISOLATED} | OT} + \frac{1}{K} \left[\Delta C_{(m)_{PROXIMITY} | OT}^{RSRB} + \Delta C_{(m)_{PROXIMITY} | OT}^{LSRB} \right]$$

ISOLATED VEHICLE. The isolated vehicle force or moment coefficients are defined as:

$$C_{()ISOLATEDOT} = C_{()FOREBODYOT} + C_{()BASEOT} + \left[C_{()a} \frac{\dot{a}L}{2V} + C_{()q} \frac{qL}{2V} \right]$$

= Plume-off, free-air, force or moment coefficient for the isolated OT.

where, $C_{()FOREBODYOT}$ = Full-scale, rigid, forebody force or moment coefficient (including forebody plume effects) with all control surfaces neutral.

| | | |
|------------|-----|-------------------|
| subscript: | (N) | Table 5.1.2.1.1-2 |
| | (A) | Table 5.1.2.1.2-2 |
| | (m) | Table 5.1.2.1.3-2 |

$C_{()BASEOT}$ = OT base force or moment coefficient.

| | | |
|------------|-----|---------------------|
| subscript: | (N) | cf. Section 4.1.1.1 |
| | (A) | cf. Section 4.1.1.1 |
| | (m) | cf. Section 4.1.1.1 |

[] = OT rotary derivatives.

| | | |
|------------|-----|---------------|
| subscript: | (N) | Assume zero. |
| | (A) | Non-existent. |
| | (m) | Assume zero. |

$C_{()ISOLATEDSRB}$ = Full-scale, free-air, force or moment coefficient for the isolated SRB.

| | | |
|------------|-----|-------------------|
| subscript: | (N) | Table 5.1.2.1.1-3 |
| | (A) | Table 5.1.2.1.2-3 |
| | (m) | Table 5.1.2.1.3-3 |

PROXIMITY. Booster Separation Motor (BSM) plume-on and plume-off separation aerodynamics are presented as proximity increments for the Orbiter-plus-External Tank (OT) and for the RIGHT-HAND Solid Rocket Booster (RSRB). LEFT-HAND Solid Rocket Booster (LSRB) data are obtained by interpolating in the RSRB DATA BASE.

 * NOTE: The sign of the interpolated RSRB *
 * longitudinal coefficients should *
 * NOT be changed for application to *
 * the LSRB. *
 * However, the sign of β , $\Delta\beta$, and ΔY *
 * must be reversed prior to using the *
 * RSRB data base. *

| | ORB/ET | RSRB |
|-----------|--------------|--------------|
| MOMENT | X_T 1097.0 | X_B 1258.5 |
| REFERENCE | Y_T 0.0 | Y_B 0.0 |
| CENTER | Z_T 450.0 | Z_B 0.0 |

The proximity data should be obtained from Disk Pack TU0110 and used with the HYPERCUBE interpolator subroutine of the Rockwell SVDS Separation Trajectory Program (Reference 4-). The proximity increments include both impingement and flow interference effects of the BSM plumes.

$\Delta C_{RSRB}^{()PROX} |_{OT}$ = Orbiter-plus-External Tank force or moment proximity increment due to the presence of the RSRB.

$\Delta C_{LSRB}^{()PROX} |_{OT}$ = Orbiter-plus-External Tank force or moment proximity coefficient increment due to the presence of the LSRB.

$\Delta C_{OT}^{()PROX} |_{RSRB}$ = RSRB force or moment proximity coefficient increment due to the presence of the OT.

$\Delta C_{OT}^{()PROX} |_{LSRB}$ = LSRB force or moment proximity coefficient increment due to the presence of the OT.

| |
|---|
| $\Delta C^{()PROX} = C^{()PROXIMITY} - C^{()ISOLATED}$ <p style="text-align: center;">PLUME-ON PLUME-OFF</p> |
|---|

K = Plume indicator factor.
 1 BSM plume-on
 2 BSM plume-off

SSME PLUME EFFECTS. The incremental force, (N) or (A), and moment (m) due to impingement of the SSME plume on the SRB was discussed on pages 4.1.2-10 and -11. The effect of the SSME plumes on the left- and right-hand SRB's is described as a dimensional force (pounds) or moment (foot-pounds).

$\Delta F_{RSRB}^{()SSME} |_{PLUME}$ = Incremental force due to impingement of SSME plume-on RSRB.
 subscript: (N) Table 5.1.2.1.1-4
 (A) Table 5.1.2.1.2-4

$\Delta F_{LSRB}^{()SSME} |_{PLUME}$ = Incremental force due to impingement of SSME plume-on LSRB. (Use same tables as for impingement on RSRB with appropriate conversion of yaw angle, ψ).

$\Delta M_{RSRB}^{SSME} |_{PLUME}$ = Incremental pitching moment due to impingement of SSME plume on RSRB.
 Table 5.1.2.1.3-4

$\Delta M_{LSRB}^{SSME} |_{PLUME}$ = Incremental pitching moment due to impingement of SSME plume on LSRB. (Use same tables as for impingement on RSRB with appropriate conversion of yaw angle, ψ).

4.1.2.2. LATERAL-DIRECTIONAL AERODYNAMICS. Lateral directional aerodynamic force and moment equations pertaining to SRB separation are presented in two parts:

| | |
|----------------|--|
| PRE-SEPARATION | (LAUNCH VEHICLE) |
| SEPARATION | (PROXIMITY) (ISOLATED OT) (ISOLATED SRB) |

The separation configuration was shown on page 4.1.2-2. Definitions of the appropriate flight parameters are also given on page 4.1.2-2.

PRE-SEPARATION

LAUNCH VEHICLE. Launch Vehicle lateral directional aerodynamic force and moments for the pre-separation phase are defined as:

$$C_{()TOTAL} = C_{()FOREBODY} + \Delta C_{()ELEVON} + C_{()p} \frac{pL}{2V} + C_{()r} \frac{rL}{2V} + C_{()\dot{\beta}} \frac{\dot{\beta}L}{2V} + \Delta C_{()FLEX}$$

where the subscript () is used to denote side force (Y), yawing moment (n), or rolling moment (l).

$C_{()FOREBODY}$ = Full-scale, rigid, mated forebody force or moment coefficient (including forebody plume effects) with all control surfaces neutral.

| | |
|----------------|-------------------|
| subscript: (Y) | Table 5.1.2.2.1-1 |
| (n) | Table 5.1.2.2.2-1 |
| (l) | Table 5.1.2.2.3-1 |

$\Delta C_{()ELEVON}$ = Change in force or moment coefficient due to elevon deflection.

| | |
|----------------|---------------------|
| subscript: (Y) | cf. Section 4.1.1.2 |
| (n) | cf. Section 4.1.1.2 |
| (l) | cf. Section 4.1.1.2 |

$C_{()p}$ = Change in force or moment coefficient due to roll rate, p (per radian).

| | |
|----------------|--------------------|
| subscript: (Y) | Assume zero |
| (n) | Figure 5.1.1.2.2-5 |
| (l) | Figure 5.1.1.2.3-5 |

$C_{()r}$ = Change in force or moment coefficient due to yaw rate, r (per radian).

| | |
|----------------|--------------------|
| subscript: (Y) | Assume zero |
| (n) | Figure 5.1.1.2.2-6 |
| (l) | Figure 5.1.1.2.3-6 |

$C_{()\dot{\beta}}$ = Change in force or moment coefficient due to lateral acceleration, $\dot{\beta}$ (per radian).

subscript: (Y) Assume zero
(n) Assume zero
(l) Assume zero

$\Delta C_{()FLEX}$ = Change in force or moment coefficient due to aeroelastic deformation.

subscript: (Y) Figure 5.1.1.2.1-5
(n) Figure 5.1.1.2.2-7
(l) Figure 5.1.1.2.3-7

SEPARATION

The total separation force and moment coefficients have been subdivided into three components:

1. ISOLATED VEHICLE (LSRB, RSRB, OT)
2. PROXIMITY EFFECT (LSRB, RSRB, OT)
3. SSME PLUME EFFECT (LSRB, RSRB)

Total separation force (Y) coefficient is defined as:

$$C_{(Y)TOTAL}^{AERO} \Big|_{RSRB} = C_{(Y)ISOLATED} \Big|_{RSRB} + \Delta C_{(Y)PROXIMITY} \Big|_{RSRB} + \frac{1}{qS} \Delta F_{(Y)SSME}^{PLUME} \Big|_{RSRB}$$

$$C_{(Y)TOTAL}^{AERO} \Big|_{LSRB} = C_{(Y)ISOLATED} \Big|_{LSRB} + \Delta C_{(Y)PROXIMITY} \Big|_{LSRB} + \frac{1}{qS} \Delta F_{(Y)SSME}^{PLUME} \Big|_{LSRB}$$

$$C_{(Y)TOTAL}^{AERO} \Big|_{OT} = C_{(Y)ISOLATED} \Big|_{OT} + \frac{1}{K} \left[\Delta C_{(Y)PROXIMITY} \Big|_{OT} + \Delta C_{(Y)PROXIMITY} \Big|_{OT} \right]$$

The total separation yawing moment () coefficient is defined as:

$$C_{(n)TOTAL}^{AERO} \Big|_{RSRB} = C_{(n)ISOLATED} \Big|_{RSRB} + \Delta C_{(n)PROXIMITY} \Big|_{RSRB} + \frac{1}{qSL_B} \Delta \tau_{(n)SSME}^{PLUME} \Big|_{RSRB}$$

$$C_{(n)TOTAL}^{AERO} \Big|_{LSRB} = C_{(n)ISOLATED} \Big|_{LSRB} + \Delta C_{(n)PROXIMITY} \Big|_{LSRB} + \frac{1}{qSL_B} \Delta \tau_{(n)SSME}^{PLUME} \Big|_{LSRB}$$

$$C_{(n)TOTAL}^{AERO} \Big|_{OT} = C_{(n)ISOLATED} \Big|_{OT} + \frac{1}{K} \left[\Delta C_{(n)PROXIMITY} \Big|_{OT} + \Delta C_{(n)PROXIMITY} \Big|_{OT} \right]$$

ISOLATED VEHICLE. The isolated vehicle force or moment coefficients are defined as:

$$C_{() ISOLATED OT} = C_{() FOREBODY OT} + \left[C_{() p} \frac{pL}{2V} + C_{() r} \frac{rL}{2V} + C_{() \dot{\beta}} \frac{\dot{\beta}L}{2V} \right]$$

= Plume-off, free-air, force or moment coefficient for the isolated OT.

where, $C_{() FOREBODY OT}$ = Full-scale, rigid, forebody force or moment coefficient (including forebody plume effects) with all control surfaces neutral.

subscript: (Y) Table 5.1.2.2.1-2
(n) Table 5.1.2.2.2-2
(L) Table 5.1.2.2.3-2

[] = OT rotary derivatives.

subscript: (Y) Assume zero.
(n) Assume zero.
(L) Assume zero.

$C_{() ISOLATED SRB}$ = Full-scale, free-air, force or moment coefficient for the isolated SRB.

subscript: (Y) Table 5.1.2.2.1-3
(n) Table 5.1.2.2.2-3
(L) Table 5.1.2.2.3-3

PROXIMITY. Booster Separation Motor (BSM) plume-on and plume-off separation aerodynamics are presented as proximity increments for the Orbiter-plus-External Tank (OT) and for the RIGHT-HAND Solid Rocket Booster (RSRB). LEFT-HAND Solid Rocket Booster (LSRB) data are obtained by interpolating in the RSRB DATA BASE.

* NOTE: Reverse the sign of the interpolated *
* RSRB lateral-directional coefficients *
* for application to the LSRB. *
* The sign of β , $\Delta\beta$, and ΔY must be *
* reversed prior to using the RSRB *
* data base. *

| | | |
|-----------|----------------|----------------|
| | ORB/ET | RSRB |
| MOMENT | { X_T 1097.0 | { X_B 1258.5 |
| REFERENCE | { Y_T 0.0 | { Y_B 0.0 |
| CENTER | { Z_T 450.0 | { Z_B 0.0 |

The proximity data should be obtained from Disk Pack TU0110 and used with the HYPERCUBE interpolator subroutine of the Rockwell SVDS Separation Trajectory Program (Reference 4-6). The proximity increments include both impingement and flow interference effects of the BSM plumes.

$\Delta C_{() \text{PROX}} \left| \begin{matrix} \text{RSRB} \\ \text{OT} \end{matrix} \right.$ = Orbiter-plus-External Tank force or moment proximity increment due to the presence of the RSRB.

$\Delta C_{() \text{PROX}} \left| \begin{matrix} \text{LSRB} \\ \text{OT} \end{matrix} \right.$ = Orbiter-plus-External Tank force or moment proximity coefficient increment due to the presence of the LSRB. Signs of ΔY , β , and $\Delta\beta$ for the LSRB must be reversed before using the RSRB data base. Sign of resulting coefficient should be changed.

$\Delta C_{() \text{PROX}} \left| \begin{matrix} \text{OT} \\ \text{RSRB} \end{matrix} \right.$ = RSRB force or moment proximity coefficient increment due to the presence of the OT.

$\Delta C_{() \text{PROX}} \left| \begin{matrix} \text{OT} \\ \text{LSRB} \end{matrix} \right.$ = LSRB force or moment proximity coefficient increment due to the presence of the OT. Signs of ΔY , β , and $\Delta\beta$ for the LSRB must be reversed before using the RSRB data base. Sign of resulting coefficient should be changed.

| |
|--|
| $\Delta C_{() \text{PROX}} = C_{() \text{PROXIMITY PLUME-ON}} - C_{() \text{ISOLATED PLUME-OFF}}$ |
|--|

K = Plume indicator factor.
 1 BSM plume-on
 2 BSM plume-off

SSME PLUME EFFECTS. The incremental force (Y) and yawing moment (M) due to impingement of the SSME plume on the SRB was discussed on pages 4.1.2-10 and -11. The effect of the SSME plumes on the left- and right-hand SRB's is described as a dimensional force (pounds) or moment (foot-pounds).

$\Delta F_{() \text{SSME PLUME}} \left| \begin{matrix} \text{RSRB} \\ \text{RSRB} \end{matrix} \right.$ = Incremental force due to impingement of SSME plume-on RSRB.
 subscript: (Y) Table 5.1.2.2.1-4

$\Delta F_{() \text{SSME PLUME}} \left| \begin{matrix} \text{LSRB} \\ \text{LSRB} \end{matrix} \right.$ = Incremental force due to impingement of SSME plume-on LSRB. (Use same tables as for impingement on RSRB with appropriate conversion of yaw angle, ψ .)

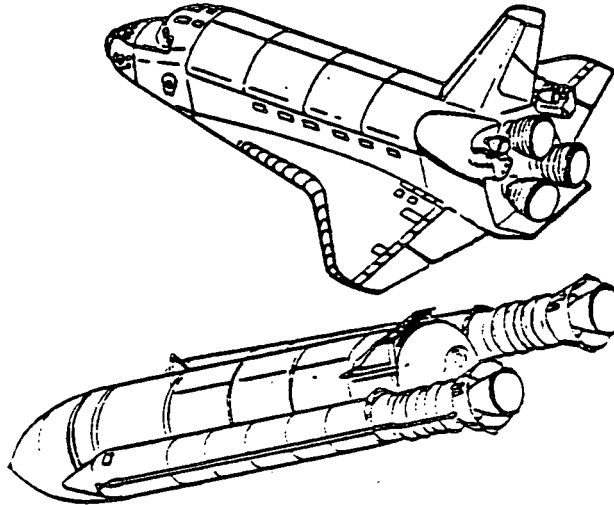
$\Delta M_{() \text{SSME PLUME}} \left| \begin{matrix} \text{RSRB} \\ \text{RSRB} \end{matrix} \right.$ = Incremental yawing moment due to impingement of SSME plume on LSRB.
 Table 5.1.2.2.2-4

$\Delta M_{() \text{SSME PLUME}} \left| \begin{matrix} \text{LSRB} \\ \text{LSRB} \end{matrix} \right.$ = Incremental yawing moment due to impingement of SSME plume on LSRB. (Use same tables as for impingement on RSRB with appropriate conversion of yaw angle, ψ .)

4.1.3 CONTINGENCY SEPARATION

ORIGINAL PAGE IS
OF POOR QUALITY

4.1.3 **CONTINGENCY SEPARATION.** Contingency Abort separation is defined as the separation of the Orbiter Vehicle from the ET + SRB's (SRB's thrusting). The separation configuration is shown in the sketch.



4.1.3.1 **LONGITUDINAL AERODYNAMICS.** Aerodynamic force and moment coefficients pertaining to Contingency Abort longitudinal separation aerodynamics are defined for initial separation conditions only.

$C_{() \text{TOTAL AERO}}$ = Full scale, rigid-body, total force or moment coefficient.
(NO SSME plumes; all control surfaces neutral)

| | |
|----------------|---|
| subscript: (N) | Orbiter (Table 5.1.3.1.1-1) ET + SRB's (Table 5.1.3.1.1-2) |
| (A) | Orbiter (Table 5.1.3.1.2-1) ET + SRB's (Table 5.1.3.1.2-2) |
| (m) | Orbiter (Table 5.1.3.1.3-1) ET + SRB's (Table 5.1.3.1.3-2) |



NOTES: 1. The Moment Reference Centers for the two separating vehicles are;

| | ORBITER | ET + SRB's |
|----------------|---------|------------|
| X _T | 976.0 | 322.5 |
| Y _T | 0.0 | 0.0 |
| Z _T | 736.5 | 400.0 |

2. For a MRC other than given;

$$C_{m_{MRC}} = C_{m_{X_T Y_T Z_T}} + \frac{\Delta X}{L_B} C_N - \frac{\Delta Z}{L_B} C_A$$

$$\text{and, } \left. \begin{aligned} \Delta X &= X_{MRC} - 976.0 \\ \Delta Z &= Z_{MRC} - 736.5 \end{aligned} \right\} \text{ORBITER}$$

$$\left. \begin{aligned} \Delta X &= X_{MRC} - 322.5 \\ \Delta Z &= Z_{MRC} - 400.0 \end{aligned} \right\} \text{ET plus SRB's}$$

4.1.3.2 LATERAL-DIRECTIONAL AERODYNAMICS. Aerodynamic force and moment coefficients pertaining to Contingency Abort lateral-directional separation aerodynamics are defined for zero sideslip initial separation conditions only.

$C_{()_{TOTAL AERO}}$ = Full-scale, rigid-body, total force or moment coefficient.
(NO SSME plumes; all control surfaces neutral).

| | | |
|----------------|------------|---------------|
| subscript: (Y) | Orbiter | (assume zero) |
| | ET + SRB's | (assume zero) |
| (n) | Orbiter | (assume zero) |
| | ET + SRB's | (assume zero) |
| (l) | Orbiter | (assume zero) |
| | ET + SRB's | (assume zero) |

ORIGINAL PAGE IS
OF POOR QUALITY

4.1.4 SECOND-STAGE (INCLUDING ABORT)

4.1.4 SECOND-STAGE
(INCLUDING ABORT)

4.1.4 SECOND-STAGE. Aerodynamic characteristics pertaining to the second-stage ascent vehicle are defined for full-scale, rigid-body, forces and moments by the equations given in the following sub-sections. The second-stage is comprised of the Orbiter Vehicle (OV) and the External Tank (ET). Where applicable, the figure numbers which relate the data of Volume 2 to the particular element of the equations are given.

4.1.4.1 LONGITUDINAL AERODYNAMICS. The basic second-stage operational longitudinal forces and moment are defined for two categories of flight:

1. low attitude forces and moment as functions of Mach number, angle of attack, and sideslip angle over the Mach range 0.6 to 10.0.
2. hypersonic, viscous interaction effects from continuum to the free molecular flow regime.

The total longitudinal forces and moment for the second-stage are (identical to first-stage) defined in Section 4.1.1.1. The total non-dimensional forces and moment coefficients are obtained from:

$$C_{\text{TOTAL AERO}}^{(\)} = C_{\text{FOREBODY}}^{(\)} + C_{\text{BASE}}^{(\)} + C_{\text{q}}^{(\)} \frac{\dot{\alpha} L_B}{2V} + C_{\text{q}}^{(\)} \frac{q L_B}{2V}$$

where, the subscript () is used to denote either normal force (N), axial force (A), or pitching moment (m).

$C_{\text{FOREBODY}}^{(\)}$ = Full-scale, rigid-body, proximity forebody force or moment coefficient

NOTE: All control surfaces neutral.

| | | |
|------------|-------------|---------------------|
| | $C_{(\)f}$ | (0.6 ≤ M ≤ 10.0) |
| subscript: | (N) | (Table 5.1.4.1.1-1) |
| | (A) | (Table 5.1.4.1.2-1) |
| | (m) | (Table 5.1.4.1.3-1) |

| | | |
|------------|------------------|---------------------|
| | $C_{(\)f_{CF}}$ | (Kn ≤ 0.01) |
| subscript: | (N) | (Table 5.1.4.1.1-2) |
| | (A) | (Table 5.1.4.1.2-2) |
| | (m) | (Table 5.1.4.1.3-2) |

| | | |
|--|------------------|--------------------|
| | $C_{(\)f_{TF}}$ | (0.01 ≤ Kn ≤ 10.0) |
|--|------------------|--------------------|

Empirical transitional flow relationship.

$$= [C_{(\)f_{FMF}} - C_{(\)f_{CF}}] \sin[9.009(Kn - 0.01)] + C_{(\)f_{CF}}$$



| | |
|-----------------|---------------------|
| $C_{()_{FMF}}$ | (Kn \geq 10.0) |
| subscript: (N) | (Table 5.1.4.1.1-2) |
| (A) | (Table 5.1.4.1.2-2) |
| (m) | (Table 5.1.4.1.3-2) |

where, TF = transitional flow
FMF = free molecular flow
CF = continuum flow

The following assumptions are applicable to second-stage data:

- (1) Specific heat ratio, γ , is constant for all altitudes
- (2) Universal gas constant, \bar{R} , is constant for all altitudes
- (3) The speed of sound at any altitude is;

$$a = (\gamma g_c R_{\infty} T_{\infty})^{1/2}$$

where,

$$\gamma = 1.405 \qquad g_c = 32.174 \frac{\text{lb-ft}}{\text{lb-sec}^2}$$

$$R_{\infty} = \frac{\bar{R}}{M} \frac{\text{ft-lb}}{\text{lb-}^{\circ}\text{R}} \qquad T_{\infty} = \text{Temperature, } ^{\circ}\text{R}$$

$$\bar{R} = 1544 \frac{\text{ft-lb}}{\text{Mol-}^{\circ}\text{R}} \qquad M = \text{Molecular Weight, } \frac{\text{lb}}{\text{Mol}}$$

$$(4) \text{ Knudsen number, } Kn = 0.1407 \frac{\lambda_{\infty} \left(\frac{P_{\infty}}{\rho_{\infty}} \right)^{1/2}}{V_{\infty}}$$

where,

$$\lambda_{\infty} = \text{mean free path} \qquad V_{\infty} = \text{freestream velocity}$$

$$P_{\infty} = \text{freestream pressure} \qquad \rho_{\infty} = \text{freestream density}$$

(See Table 4.1.4-1)

Table 4.1.4-1
 VARIATION OF ATMOSPHERIC PARAMETERS WITH ALTITUDE
 (U.S. STANDARD ATMOSPHERE, 1962)

| ALTITUDE | FREESTREAM PRESSURE P_{∞} | FREESTREAM DENSITY ρ_{∞} | MOLECULAR MEAN FREE PATH, λ_{∞} | GAS CONSTANT R_{∞} | FREESTREAM TEMPERATURE T_{∞} |
|-----------|--|--|--|---------------------------------|---|
| feet | lb/ft ² | lb/ft ³ | feet | ft/°R | °R |
| 0 | 2.1160 ⁺³ | 7.647 ⁻² | 2.18 ⁻⁷ | 53.31 | 518.67 |
| 100,000 | 2.3272 ⁺¹ | 1.068 ⁻³ | 1.06 ⁻⁵ | 53.31 | 408.57 |
| 125,000 | 7.7688 | 3.301 ⁻⁴ | 5.00 ⁻⁵ | 53.31 | 441.17 |
| 150,000 | 2.8419 | 1.112 ⁻⁴ | 1.53 ⁻⁴ | 53.31 | 479.07 |
| 175,000 | 1.1000 | 4.260 ⁻⁵ | 4.05 ⁻⁴ | 53.31 | 483.94 |
| 200,000 | 4.1344 ⁻¹ | 1.696 ⁻⁵ | 1.00 ⁻³ | 53.31 | 457.00 |
| 225,000 | 1.4272 ⁻¹ | 6.598 ⁻⁶ | 2.50 ⁻³ | 53.31 | 405.46 |
| 250,000 | 4.2480 ⁻² | 2.263 ⁻⁶ | 7.30 ⁻³ | 53.31 | 351.83 |
| 275,000 | 1.0706 ⁻² | 6.171 ⁻⁷ | 2.70 ⁻² | 53.31 | 325.17 |
| 300,000 | 2.6429 ⁻³ | 1.488 ⁻⁷ | 1.16 ⁻¹ | 53.31 | 332.90 |
| 325,000 | 7.2888 ⁻⁴ | 3.652 ⁻⁸ | 4.80 ⁻¹ | 53.43 | 373.20 |
| 350,000 | 2.3723 ⁻⁴ | 1.012 ⁻⁸ | 1.62 | 53.82 | 435.14 |
| 375,000 | 9.2814 ⁻⁴ | 3.183 ⁻⁹ | 5.30 | 54.42 | 535.14 |
| 400,000 | 4.4590 ⁻⁵ | 1.164 ⁻⁹ | 1.42 ⁺¹ | 55.20 | 693.61 |
| 425,000 | 2.4787 ⁻⁵ | 4.952 ⁻¹⁰ | 3.20 ⁺¹ | 55.95 | 945.78 |
| 450,000 | 1.7570 ⁻⁵ | 2.600 ⁻¹⁰ | 6.15 ⁺¹ | 56.58 | 1193.77 |
| 475,000 | 1.2756 ⁻⁵ | 1.552 ⁻¹⁰ | 1.00 ⁺² | 57.07 | 1439.66 |
| 500,000 | 9.7590 ⁻⁶ | 1.020 ⁻¹⁰ | 1.50 ⁺² | 57.48 | 1663.48 |
| 550,000 | 6.2168 ⁻⁶ | 5.453 ⁻¹¹ | 2.76 ⁺² | 58.37 | 1951.36 |
| 600,000 | 4.1852 ⁻⁶ | 3.350 ⁻¹¹ | 4.49 ⁺² | 59.25 | 2106.85 |
| 650,000 | 2.9089 ⁻⁶ | 2.177 ⁻¹¹ | 6.70 ⁺² | 60.29 | 2214.53 |
| 700,000 | 2.0667 ⁻⁶ | 1.467 ⁻¹¹ | 9.92 ⁺² | 61.34 | 2295.37 |
| 750,000 | 1.4962 ⁻⁶ | 1.009 ⁻¹¹ | 1.41 ⁺³ | 62.43 | 2372.21 |
| 800,000 | 1.1004 ⁻⁶ | 7.135 ⁻¹¹ | 1.95 ⁺³ | 63.56 | 2424.00 |
| 850,000 | 8.1973 ⁻⁷ | 5.121 ⁻¹² | 2.68 ⁺³ | 64.74 | 2470.23 |
| 900,000 | 6.1797 ⁻⁷ | 3.724 ⁻¹² | 3.65 ⁺³ | 65.98 | 2513.06 |
| 950,000 | 4.7105 ⁻⁷ | 2.742 ⁻¹² | 4.80 ⁺³ | 67.25 | 2552.57 |
| 1,000,000 | 3.6286 ⁻⁷ | 2.046 ⁻¹² | 6.30 ⁺³ | 68.56 | 2584.22 |

(Ref. 4-6)

$C_{()BASE}$ = Power-on base force or moment coefficient
(including effects of SSME plumes)

subscript: (N), $\frac{F_{NBASE}}{\bar{q}S}$ F_{NBASE} (Figure 5.1.4.1.1-1)

(A), $\frac{F_{ABASE}}{\bar{q}S}$ F_{ABASE} (Figure 5.1.4.1.2-1)

(m), $\frac{M_{BASE}}{\bar{q}SL_b}$ M_{BASE} (Figure 5.1.4.1.3-1)

The base term for second-stage INTACT ABORT is defined for any one SSME-out condition by:

$$\frac{F_{()BASE}}{\bar{q}S} \quad \text{OR} \quad \frac{M_{BASE}}{\bar{q}SL_b}$$

where, F_{NBASE} (Figure 5.1.4.1.1-2)
1 SSME OFF
SECOND STAGE

F_{ABASE} (Figure 5.1.4.1.2-2)
1 SSME OFF
SECOND STAGE

M_{BASE} (Figure 5.1.4.1.3-2)
1 SSME OFF
SECOND STAGE

The base term for second-stage CONTINGENCY ABORT is defined for two or more SSME-out conditions by:

$F_{N_{BASE}}$
2 SSME OFF
SECOND STAGE (Figure 5.1.4.1.1-3)

$F_{N_{BASE}}$
ALL SSME OFF
SECOND STAGE (Figure 5.1.4.1.1-4)

$F_{A_{BASE}}$
2 SSME OFF
SECOND STAGE (Figure 5.1.4.1.2-3)

$F_{A_{BASE}}$
ALL SSME OFF
SECOND STAGE (Figure 5.1.4.1.2-4)

M_{BASE}
2 SSME OFF
SECOND STAGE (Figure 5.1.4.1.3-3)

M_{BASE}
ALL SSME OFF
SECOND STAGE (Figure 5.1.4.1.3-4)

$C_{l\dot{\alpha}}$ = Change in force or moment coefficient due to rate of change of angle of attack, $\dot{\alpha}$ (per radian)*

subscript (N) (Assume zero)
(A) (Assume zero)
(m) (See note C_{mq})

$C_{l\dot{q}}$ = Change in force or moment coefficient due to pitch rate, \dot{q} (per radian)*

subscript (N) (Assume zero)
(A) (Assume zero)
(m) (Figure 5.1.4.1.3-5)

NOTE: $C_{mq} = C_{mq} + C_{m\dot{q}}$
(treat as C_{mq})

4.1.4.2 LATERAL-DIRECTIONAL AERODYNAMICS. The second-stage basic operational lateral-directional force and moments are defined for low attitudes as functions of Mach number, angle of attack, and sideslip angle over the Mach range 0.6 to 10.0. The total force and moments are as defined in Section 4.1.2.1. The total non-dimensional force and moment coefficients are obtained from:

* See Reference 4-1 for rotary derivative transfer.



$$C_{() \text{ TOTAL AERO}} = C_{() \text{ FOREBODY}} + C_{()p} \frac{\rho L_B}{2V} + C_{()r} \frac{r L_B}{2V} + C_{() \dot{\beta}} \frac{\dot{\beta} L_B}{2V}$$

where,

$C_{() \text{ FOREBODY}}$ = Full-scale, rigid-body, proximity force or moment coefficient
NOTE: All control surfaces neutral.

subscript: (Y) (Table 5.1.4.2.1-1)
(n) (Table 5.1.4.2.2-1)
(l) (Table 5.1.4.2.3-1)

$C_{()p}$ = Change in forebody force or moment coefficient due to roll rate, p (per radian)*

subscript: (Y), = $C_{Yp_{\alpha=0^\circ}} + \frac{\partial C_{Yp}}{\partial \alpha} \alpha$ (Undefined)
(n), = $C_{np_{\alpha=0^\circ}} + \frac{\partial C_{np}}{\partial \alpha} \alpha$ (Figure 5.1.4.2.2-1)
(l), = $C_{lp_{\alpha=0^\circ}} + \frac{\partial C_{lp}}{\partial \alpha} \alpha$ (Figure 5.1.4.2.3-1)

$C_{()r}$ = Change in forebody force or moment coefficient due to yaw rate, r (per radian)*

subscript: (Y), = $C_{Yr_{\alpha=0^\circ}} + \frac{\partial C_{Yr}}{\partial \alpha} \alpha$ (Undefined)
(n), = $C_{nr_{\alpha=0^\circ}} + \frac{\partial C_{nr}}{\partial \alpha} \alpha$ (Figure 5.1.4.2.2-2)
(l), = $C_{lr_{\alpha=0^\circ}} + \frac{\partial C_{lr}}{\partial \alpha} \alpha$ (Figure 5.1.4.2.3-2)

$C_{() \dot{\beta}}$ = Change in forebody force or moment coefficient due to lateral acceleration, $\dot{\beta}$ (per radian)*

subscript: (Y), = $C_{Y \dot{\beta}}$ (Undefined)
(n), = $C_{n \dot{\beta}}$ (Undefined)
(l), = $C_{l \dot{\beta}}$ (Undefined)

No second stage lateral-directional terms are affected by INTACT ABORT requirements.

No second-stage lateral-directional terms are affected by CONTINGENCY ABORT requirements.

*op. cit.

4.1.5 EXTERNAL TANK SEPARATION

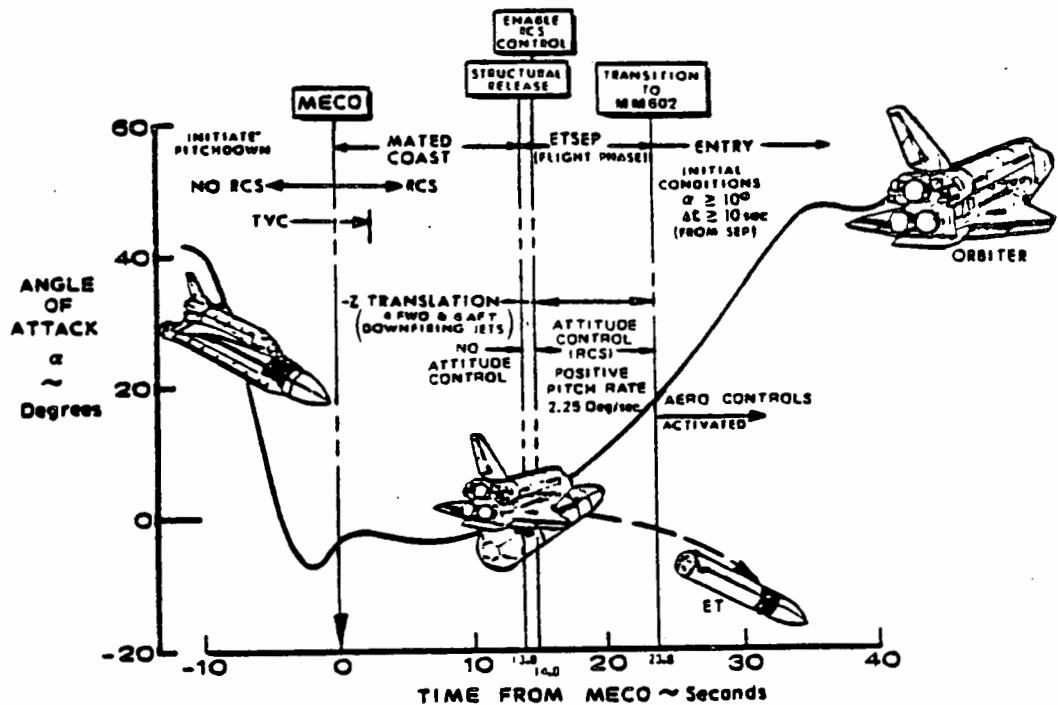
ORIGINAL PAGE IS
OF POOR QUALITY

4.1.5

EXTERNAL TANK SEPARATION. Separation of the Orbiter Vehicle from the External Tank is accomplished during one of the following flight modes:

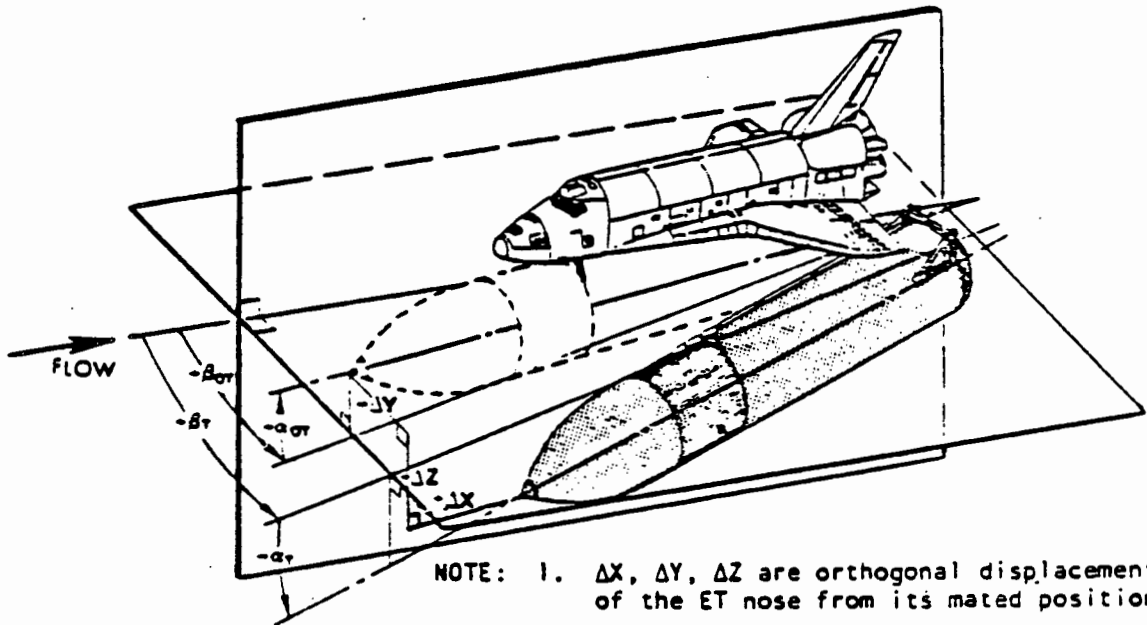
- 1) Nominal Mission just prior to Orbit Insertion
- 2) Return-to-Launch-Site (RTLS) Abort
- 3) Abort-Once Around (AOA)
- 4) Abort-To-Orbit (ATO)
- 5) Trans-Atlantic Abort Landing (TAL)

Separation during modes (1), (3), and (4) occurs at altitudes where the aerodynamics of the vehicle(s) are of little or no concern and will, therefore, not be discussed. External Tank separation aerodynamic data are limited to modes (2) and (5). Data for RTLS separation have been limited to Mach 6.0 over a flight dynamic pressure range of 5 to 10 psf. Nominal conditions at separation have been defined as a dynamic pressure of 8 psf and an angle of attack of -4 degrees. The Launch Vehicle data (Volume 2) include the effects of jet impingement and plume/flow field interaction resulting from the Reaction Control System (RCS) jet firings. Separation during TAL abort utilizes freestream aerodynamics for both Orbiter and ET in conjunction with RCS impingement effects from the forward down-firing jets on the ET as a function of ET separation position and attitude and aft jet impingement effects on the Orbiter wing. The flight conditions for TAL abort are Mach 25.0 and dynamic pressures less than 1 psf. No jet/freestream interaction effects are present in Mode (5).



4.1.5-1

Flight parameters used in describing the proximity aerodynamics are shown in the following sketch.



- NOTE: 1. ΔX , ΔY , ΔZ are orthogonal displacements of the ET nose from its mated position.
2. ΔX - positive aft
 ΔY - positive outboard right
 ΔZ - positive down
3. $\Delta\alpha \equiv (\alpha_T - \alpha_{OT})$
 $\Delta\beta \equiv (\beta_T - \beta_{OT})$

Aerodynamic forces and moments are defined as a function of these parameters in the Orbiter-plus-External Tank (OT) body-axis system.

 *
 * Particular attention should be given to the location *
 * of the MOMENT REFERENCE CENTERS used in the separation *
 * data. These Moment Reference Centers differ for each *
 * configuration and also differ from the MRC used for *
 * nominal data. *
 *

At MECO plus 10 seconds and continuing for approximately thirty seconds, LH_2 pressure build-up is vented through the LH_2 dump line. The proximity of the dump line exit to the wing results in gaseous plume impingement forces which affect the Orbiter aerodynamics during ET separation (see Volume 2, Section 5.1.5).

4.1.5.1 RTLS ABORT. Aerodynamic forces and moments pertaining to Orbiter and External Tank separation during the RTLS abort mode are defined for three phases of the separation maneuver:

| | | |
|-----------------|---|------------------------|
| PRE-SEPARATION | } | TURN-AROUND MANEUVER |
| | | MATED COAST |
| SEPARATION | | PROXIMITY |
| POST-SEPARATION | } | ISOLATED ORBITER |
| | | ISOLATED EXTERNAL TANK |

Nominal conditions at RTLS separation are considered to be a dynamic pressure of 8.0 psf with the vehicle at -4 degrees angle of attack. The data of Volume 2 (Section 5.1.5) are, however, presented for freestream dynamic pressures of 5.0, 7.5, 8.0, and 10.0 psf. A value of jet-to-freestream momentum ratio (ϕ_j/ϕ_∞) is associated with each dynamic pressure (\bar{q}) and is denoted as the plume scaling parameter with the following relationship:

$$\bar{q}_{FLGHT} = \frac{\dot{m} v_j / 2S}{\phi_j / \phi_\infty} = \frac{0.1543}{\phi_j / \phi_\infty} \quad (\text{Based on single RCS jet})$$

4.1.5.1.1 LONGITUDINAL AERODYNAMICS

PRE-SEPARATION (TURN-AROUND MANEUVER). The total aerodynamic forces and moment coefficients are defined as:

$$C_{N \text{ TOTAL AERO}} = C_{Nf} + C_{N \text{ BASE}}$$

$$C_{A \text{ TOTAL AERO}} = C_{Af} + C_{A \text{ BASE}} + K C_{A_{3-D} \text{ BASE}} \cos \alpha$$

$$C_{m \text{ TOTAL AERO}} = C_{mf} + C_{m \text{ BASE}}$$

where, $C_{()f}$ = Second-stage, forebody force
or moment coefficient
-180° ≤ α ≤ +180°

subscript: (N)
(A)
(m)

(Table 5.1.5.1.1.1-1)
(Table 5.1.5.1.1.2-1)
(Table 5.1.5.1.1.3-1)

$C_{()BASE}$ = Power-on, base force or moment coefficient (including effects of SSME plumes)

subscript: (N) $= \frac{1}{\bar{q}_{REF} S} F_{NBASE}$ (see Figure 5.1.4.1.1-2)

(A) $= \frac{1}{\bar{q}_{REF} S} F_{ABASE}$ (see Figure 5.1.4.1.2-2)

(m) $= \frac{1}{\bar{q}_{REF} S L_B} M_{BASE}$ (see Figures 5.1.4.1.3-2)

K = Factor relating to presence of C_{A3-D}_{BASE} term

$$K = \begin{cases} 0 & -90^\circ \leq \alpha \leq +90^\circ \\ 1.0 & \begin{cases} +90^\circ < \alpha \leq +180^\circ \\ -90^\circ > \alpha \geq -180^\circ \end{cases} \end{cases}$$

C_{A3-D}_{BASE} = Empirical three-dimensional base axial force coefficient (Reference 4-2)

THREE-DIMENSIONAL BASE
AXIAL FORCE COEFFICIENT

| MACH | 1.0 | 2.0 | 3.0 | 4.0 | 5.0 | 6.0 | 7.0 | 8.0 | 9.0 | 10.0 |
|------------------------|--------|--------|--------|--------|--------|--------|--------|--------|--------|--------|
| $C_{A3-D}_{BASE}^{**}$ | 0.0722 | 0.0602 | 0.0344 | 0.0224 | 0.0155 | 0.0103 | 0.0086 | 0.0069 | 0.0062 | 0.0052 |

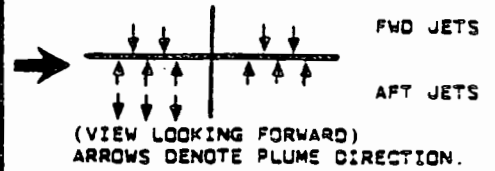
*Reference Area is 2690 ft.

PRE-SEPARATION (MATED COAST). The available RCS roll/pitch commands for the mated coast phase of the RTL maneuver are presented in Table 4.1.5.1.1-1 with a description of the associated jets being fired. Jet control commands (denoted by the circles on the Table) are used in conjunction with one of the following three conditions of YAW COMMAND (UZCMD):

| UZCMD | CONDITION |
|-------|---|
| +1 | 2 forward left side-firing plus 1 aft right side-firing jets. |
| 0 | No side-firing jets. |
| -1 | 2 forward right side-firing plus 1 aft left side-firing jets. |

Table 4.1.5.1.1-1
ROLL/PITCH COMMAND GENERATION FOR RTLS MATED COAST

| JYCMD | UXCMD | NZLA | PZLA | NZRA | PZRA | NZLF | NZRF |
|-------|---------------------------|------------------|-----------------------|-----------------------|-----------------------|-----------------------|-----------------------|
| ⊕5 | ⊕2 ⊕0 ⊖2 | 3 2 0 0 | 3 3 3 3 | 0 0 2 3 | 3 3 3 3 | 2 2 2 2 | 2 2 2 2 |
| +4 | +2 +1 0 -1 -2 | 3 2 0 0 | 3 3 3 3 | 0 0 2 3 | 3 3 3 3 | 2 2 1 2 2 | 2 2 1 2 2 |
| +3 | +2 +1 0 -1 -2 | 3 2 0 0 | 3 3 3 3 | 0 0 2 3 | 3 3 3 3 | 1 1 0 1 1 | 1 1 0 1 1 |
| +2 | +2 +1 0 -1 -2 | 3 2 0 0 | 3 3 2 3 3 | 0 0 0 2 3 | 3 3 2 3 3 | 0 0 0 0 0 | 0 0 0 0 0 |
| +1 | +2 +1 0 -1 -2 | 3 2 0 0 | 2 2 1 2 2 | 0 0 0 2 3 | 2 2 1 2 2 | 0 0 0 0 0 | 0 0 0 0 0 |
| ⊖0 | ⊕2 ⊕0 ⊖2 | 3 2 0 0 | 1 1 0 1 1 | 0 0 0 2 3 | 1 1 0 1 1 | 0 0 0 0 0 | 0 0 0 0 0 |
| -1 | +2 +1 0 -1 -2 | 3 3 1 1 | 0 0 0 0 | 1 1 1 2 3 | 0 0 0 0 0 | 0 0 0 0 0 | 0 0 0 0 0 |
| -2 | +2 +1 0 -1 -2 | 3 3 2 2 | 0 0 0 0 | 2 2 2 3 3 | 0 0 0 0 0 | 0 0 0 0 0 | 0 0 0 0 0 |
| ⊖3 | ⊕2 ⊕0 ⊖2 | 3 3 3 3 | 0 0 0 0 | 3 3 3 3 | 0 0 0 0 | 0 0 0 0 | 0 0 0 0 |



DEFINITIONS:

UYCMD = Pitch Command
 UXCMD = Roll Command
 NZLA = Negative 'Z' Left Aft Thrusters
 PZLA = Positive 'Z' Left Aft Thrusters

NZRA = Negative 'Z' Right Aft Thrusters
 PZRA = Positive 'Z' Right Aft Thrusters
 NZLF = Negative 'Z' Left Forward Thrusters
 NZRF = Negative 'Z' Right Forward Thrusters

NOTE: Numbers refer to number of jets firing.

REFERENCE: SD78-SH-0003A (FLIGHT CONTROL PSSR Volume 2 Ascent; Sections 4.5 - 4.5.1.2)

Orbiter-plus-External Tank mated coast aerodynamic forces and moment coefficients are defined as:

$$C_{(1)} \begin{matrix} \text{TOTAL} \\ \text{AERO} \end{matrix} = C_{(1)} \begin{matrix} \beta \\ \text{RCS ON} \end{matrix}$$

where,
 $\beta > 0^\circ$

$$C_{(1)} \begin{matrix} \beta \\ \text{RCS ON} \end{matrix} = C_{(1)} \begin{matrix} \beta=0^\circ \\ \text{RCS OFF} \end{matrix} + \Delta C_{(1)} \begin{matrix} \beta=0^\circ \\ \end{matrix} + \Delta C_{(1)} \begin{matrix} \beta \\ \beta > 0^\circ \end{matrix} + \frac{\beta}{4} (C_{(1)} \begin{matrix} \beta=+4^\circ \\ \text{RCS ON} \end{matrix} - C_{(1)} \begin{matrix} \beta=0^\circ \\ \text{RCS OFF} \end{matrix})$$

$\beta < 0^\circ$

$$C_{(1)} \begin{matrix} \beta \\ \text{RCS ON} \end{matrix} = C_{(1)} \begin{matrix} \beta=0^\circ \\ \text{RCS OFF} \end{matrix} + \Delta C_{(1)} \begin{matrix} \beta=0^\circ \\ \end{matrix} + \Delta C_{(1)} \begin{matrix} \beta \\ \beta < 0^\circ \end{matrix} - \frac{\beta}{4} (C_{(1)} \begin{matrix} \beta=-4^\circ \\ \text{RCS ON} \end{matrix} - C_{(1)} \begin{matrix} \beta=0^\circ \\ \text{RCS OFF} \end{matrix})$$

$C_{(1)} \begin{matrix} \beta \\ \text{RCS OFF} \end{matrix}$ = RCS-off, full-scale, rigid body second-stage force or moment coefficient with SSME power-off for $\beta = -4^\circ, 0^\circ, +4^\circ$

subscript: (N)
(A)
(m)

(Table 5.1.5.1.1.1-2)
(Table 5.1.5.1.1.2-2)
(Table 5.1.5.1.1.3-2)

$$\Delta C_{(1)} \begin{matrix} \beta=0^\circ \\ \end{matrix} = \left[C_{(1)} \begin{matrix} \beta=0^\circ \\ \text{RCS ON} \end{matrix} - C_{(1)} \begin{matrix} \beta=0^\circ \\ \text{RCS OFF} \end{matrix} \right]$$

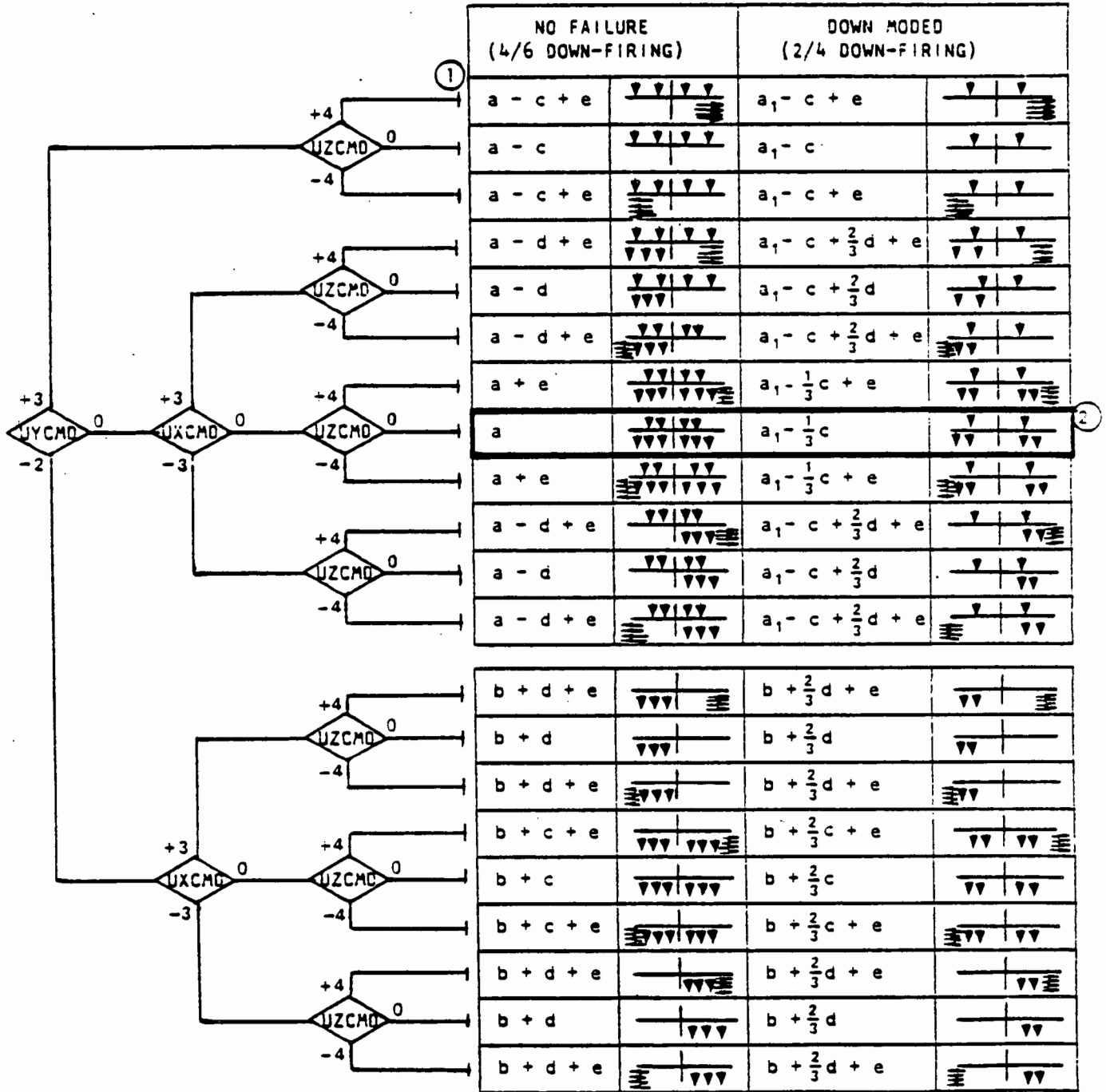
$$\Delta C_{(1)} \begin{matrix} \beta \\ \beta > 0^\circ \end{matrix} = \frac{1}{4} \left[\left(C_{(1)} \begin{matrix} \beta=+4^\circ \\ \text{RCS ON} \end{matrix} - C_{(1)} \begin{matrix} \beta=+4^\circ \\ \text{RCS OFF} \end{matrix} \right) - \Delta C_{(1)} \begin{matrix} \beta=0^\circ \\ \end{matrix} \right]$$

$$\Delta C_{(1)} \begin{matrix} \beta \\ \beta < 0^\circ \end{matrix} = - \frac{1}{4} \left[\left(C_{(1)} \begin{matrix} \beta=-4^\circ \\ \text{RCS ON} \end{matrix} - C_{(1)} \begin{matrix} \beta=-4^\circ \\ \text{RCS OFF} \end{matrix} \right) - \Delta C_{(1)} \begin{matrix} \beta=0^\circ \\ \end{matrix} \right]$$

| \bar{q} psf | ϕ_j/ϕ_m | Subscript | $\beta < 0^\circ$ | $\beta = 0^\circ$ | $\beta > 0^\circ$ |
|--------------------|----------------------------|-------------|---|--|--|
| | | | Table No. for RCS-ON | | |
| 5.0 7.5 10.0 | 0.0303 0.0202 0.0151 | N N N | 5.1.5.1.1.1-3 5.1.5.1.1.1-6 5.1.5.1.1.1-9 | 5.1.5.1.1.1-4 5.1.5.1.1.1-7 5.1.5.1.1.1-10 | 5.1.5.1.1.1-5 5.1.5.1.1.1-8 5.1.5.1.1.1-11 |
| 5.0 7.5 10.0 | 0.0303 0.0202 0.0151 | A A A | 5.1.5.1.1.2-3 5.1.5.1.1.2-6 5.1.5.1.1.2-9 | 5.1.5.1.1.2-4 5.1.5.1.1.2-7 5.1.5.1.1.2-10 | 5.1.5.1.1.2-5 5.1.5.1.1.2-8 5.1.5.1.1.2-11 |
| 5.0 7.5 10.0 | 0.0303 0.0202 0.0151 | m m m | 5.1.5.1.1.3-3 5.1.5.1.1.3-6 5.1.5.1.1.3-9 | 5.1.5.1.1.3-4 5.1.5.1.1.3-7 5.1.5.1.1.3-10 | 5.1.5.1.1.3-5 5.1.5.1.1.3-8 5.1.5.1.1.3-11 |

SEPARATION (PROXIMITY). The RTLS separation aerodynamics (including RCS jet plume effects) are defined for Mach 6.0. The nominal (no failure) separation sequence, from structural release to transition to Major Mode 602 (Figure 4.1.5-1), consists of a -Z translation (4 forward and 6 aft down-firing RCS jets) without attitude control for approximately 1-second duration after structural release, followed by RCS attitude control maneuvers where pitch rate is not to exceed +2.25 degrees per second. Down-moding occurs in the case of a jet failure resulting in a 2 forward and 4 aft down-firing translation jet configuration. Once initiated, down-moding continues throughout the attitude control phase of separation. The -Z translation burn is denoted by UXCMD = UYCMD = UZCMD = 0 in Table 4.1.5.1.1-2 (heavy outline). All other values of UXCMD, UYCMD, and UZCMD shown in the table apply to the attitude control phase of separation. The terms a, a₁, b, c, d, and e appearing in the table are further defined in Tables 4.1.5.1.1-3, -4, and -5. Synthesis of RCS configurations is required in the evaluation of aerodynamic coefficient sideslip derivatives because of the unavailability of wind tunnel test results for the basic RCS configurations RC06 (term c), RC21 (term d), and RC07 (term e) used in Table 4.1.5.1.1-2.

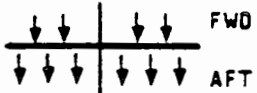

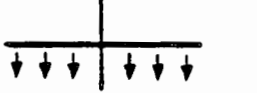
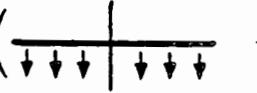
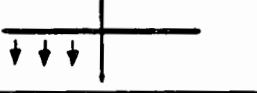
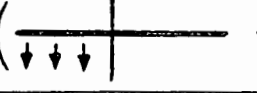
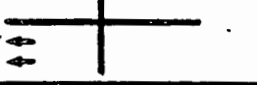
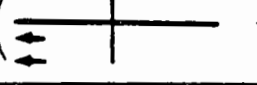
Table 4.1.5.1.1-2
RTLS SEPARATION TRANSLATION AND ATTITUDE CONTROL MANEUVERS



NOTE: 1. Terms a, a₁, b, c, d, and e are defined in Tables 4.1.5.1.1-3, -4, and -5.

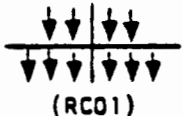
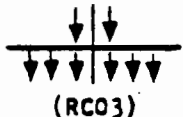
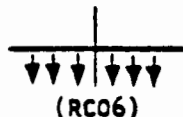
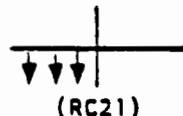
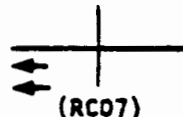
2. -Z Translation burn ~ Structural release to MM602 (cf. Figure 4.1.5-1).

Table 4.1.5.1.1-3
RCS + PROXIMITY EFFECT FOR ZERO DEGREES SIDESLIP

| TERM | CONFIGURATION | SYNTHESIS | DISK PACK |
|----------------|---|--|------------------------|
| a |  | RC01: DISK PACK (INCLUDES JET INTERACTION, PROXIMITY, AND COUPLING EFFECT). | TU0095 (APPENDIX A) |
| a ₁ |  | RC03: DISK PACK (INCLUDES JET INTERACTION, PROXIMITY, AND COUPLING EFFECT). | TU0095 (APPENDIX A) |
| b | (PROXIMITY w/o RCS) | (POWER OFF PROXIMITY AERC) | TU0110 (APPENDIX A) |
| c |  | RC06: ( - RCS OFF) | |
| d |  | RC21: ( - RCS OFF) | |
| e |  | RC07: ( - RCS OFF) | |

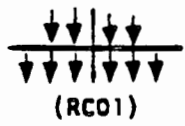
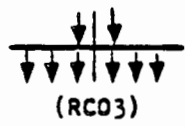
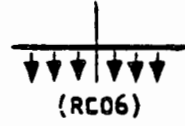
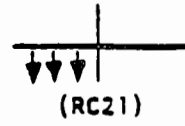
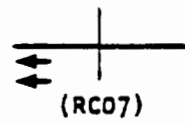
NOTE: Terms c, d, and e represent RCS effects only.

Table 4.1.5.1.1-4
SIDESLIP DERIVATIVE OF RCS + PROXIMITY EFFECT
FOR SIDESLIP LESS THAN ZERO DEGREES

| TERM | CONFIGURATION | SYNTHESIS | DISK PACK |
|----------------|---|---|------------------------|
| a |  | $-\left[\left(\begin{array}{c} \downarrow \downarrow \downarrow \downarrow \\ \downarrow \downarrow \downarrow \downarrow \end{array} \right)_{\beta=3^\circ} - \left(\begin{array}{c} \downarrow \downarrow \downarrow \downarrow \\ \downarrow \downarrow \downarrow \downarrow \end{array} \right)_{\beta=0^\circ} \right] / 3^\circ$ | TU0095 (APPENDIX A) |
| a ₁ |  | $-\left[\left(\begin{array}{c} \downarrow \downarrow \\ \downarrow \downarrow \downarrow \downarrow \end{array} \right)_{\beta=3^\circ} - \left(\begin{array}{c} \downarrow \downarrow \\ \downarrow \downarrow \downarrow \downarrow \end{array} \right)_{\beta=0^\circ} \right] / 3^\circ$ | TU0095 (APPENDIX A) |
| b | (PROXIMITY w/o RCS) | $-\left[(\text{PROXIMITY})_{\beta=3^\circ} - (\text{PROXIMITY})_{\beta=0^\circ} \right] / 3^\circ$ | TU0110 (APPENDIX A) |
| c |  | $\left(\begin{array}{c} \downarrow \downarrow \\ \downarrow \downarrow \downarrow \downarrow \end{array} \right)_{-\beta} - \left[\left(\begin{array}{c} \downarrow \downarrow \\ \uparrow \uparrow \uparrow \uparrow \end{array} \right)_{\beta} \left(\begin{array}{c} \downarrow \downarrow \\ \uparrow \uparrow \uparrow \uparrow \end{array} \right)_{\beta} \right]$ <p>(RC03; ΔZ = 1000) (RC59) (RC11)</p> | |
| d |  | $\left(\begin{array}{c} \downarrow \downarrow \downarrow \downarrow \\ \uparrow \uparrow \uparrow \uparrow \end{array} \right)_{-\beta} - \left(\begin{array}{c} \downarrow \downarrow \downarrow \downarrow \\ \uparrow \uparrow \uparrow \uparrow \end{array} \right)_{\beta}$ <p>(RC38) (RC62)</p> | |
| e |  | $-\left(\begin{array}{c} \downarrow \downarrow \downarrow \downarrow \\ \downarrow \downarrow \downarrow \downarrow \end{array} \right)_{-\beta} + \left(\begin{array}{c} \downarrow \downarrow \downarrow \downarrow \\ \downarrow \downarrow \downarrow \downarrow \end{array} \right)_{\beta}$ <p>(RC113) (RC01; ΔZ = 1000)</p> | |

NOTE: Terms c, d, and e represent RCS effects only.

Table 4.1.5.1.1-5
SIDESLIP DERIVATIVE OF RCS + PROXIMITY EFFECT
FOR SIDESLIP GREATER THAN ZERO DEGREES

| TERM | CONFIGURATION | SYNTHESIS | DISK PACK |
|----------------|---|---|------------------------|
| a |  | $\left[\left(\begin{array}{c} \downarrow \downarrow \downarrow \downarrow \\ \downarrow \downarrow \downarrow \downarrow \end{array} \right)_{\beta=3^\circ} - \left(\begin{array}{c} \downarrow \downarrow \downarrow \downarrow \\ \downarrow \downarrow \downarrow \downarrow \end{array} \right)_{\beta=0^\circ} \right] / 3^\circ$ | TU0095 (APPENDIX A) |
| a ₁ |  | $\left[\left(\begin{array}{c} \downarrow \downarrow \\ \downarrow \downarrow \downarrow \downarrow \end{array} \right)_{\beta=3^\circ} - \left(\begin{array}{c} \downarrow \downarrow \\ \downarrow \downarrow \downarrow \downarrow \end{array} \right)_{\beta=0^\circ} \right] / 3^\circ$ | TU0095 (APPENDIX A) |
| b | (PROXIMITY w/o RCS) | $\left[(\text{PROXIMITY})_{\beta=3^\circ} - (\text{PROXIMITY})_{\beta=0^\circ} \right] / 3^\circ$ | TU0110 (APPENDIX A) |
| c |  | $\left(\begin{array}{c} \downarrow \downarrow \downarrow \downarrow \\ \downarrow \downarrow \downarrow \downarrow \end{array} \right)_{-\beta} - \left[\left(\begin{array}{c} \downarrow \downarrow \\ \uparrow \uparrow \uparrow \uparrow \end{array} \right)_{-\beta} - \left(\begin{array}{c} \uparrow \uparrow \uparrow \uparrow \\ \uparrow \uparrow \uparrow \uparrow \end{array} \right)_{-\beta} \right]$ <p>(RC03; ΔZ = 1000) (RC59) (RC11)</p> | |
| d |  | $\left(\begin{array}{c} \downarrow \downarrow \downarrow \downarrow \\ \uparrow \uparrow \uparrow \uparrow \end{array} \right)_{-\beta} - \left(\begin{array}{c} \downarrow \downarrow \downarrow \downarrow \\ \uparrow \uparrow \uparrow \uparrow \end{array} \right)_{-\beta}$ <p>(RC38) (RC62)</p> | |
| e |  | $\left(\begin{array}{c} \downarrow \downarrow \downarrow \downarrow \\ \downarrow \downarrow \downarrow \downarrow \end{array} \right)_{-\beta} + \left(\begin{array}{c} \downarrow \downarrow \downarrow \downarrow \\ \downarrow \downarrow \downarrow \downarrow \end{array} \right)_{-\beta}$ <p>(RC113) (RC01; ΔZ = 1000)</p> | |

NOTE: Terms c, d, and e represent RCS effects only.

The total force and moment coefficients for the Orbiter and ET over the applicable dynamic pressure range are obtained in the following manner:

$$C_{\text{AERO}}^{(\text{TOTAL})} \Big|_{\text{ORB}} \Big|_{5 \leq \bar{q} \leq 10 \text{ psf}} = C_{\text{RCS OFF}}^{(\text{ISOLATED})} + \left(\Delta C_{\bar{q}=8 \text{ psf}} + \Delta C_{\bar{q} \text{ effect}} \right) \Big|_{\text{ORB}} \Big|_{\text{ET}}$$

$$C_{\text{AERO}}^{(\text{TOTAL})} \Big|_{\text{ET}} \Big|_{5 \leq \bar{q} \leq 10 \text{ psf}} = C_{\text{RCS OFF}}^{(\text{ISOLATED})} + \left(\Delta C_{\bar{q}=8 \text{ psf}} + \Delta C_{\bar{q} \text{ effect}} \right) \Big|_{\text{ET}} \Big|_{\text{ORB}}$$

$$\Delta C_{\bar{q}=8 \text{ psf}} = \left[C_{\text{RCS PLUME} + \text{PROXIMITY}}^{(\text{RCS PLUME})} - C_{\text{RCS OFF}}^{(\text{ISOLATED})} \right]_{\bar{q}=8 \text{ psf}}$$

$$\Delta C_{\bar{q} \text{ effect}} = \left[C_{\text{RCS PLUME} + \text{PROXIMITY}}^{(\text{RCS PLUME})} - C_{\text{RCS OFF}}^{(\text{ISOLATED})} \right]_{\bar{q}=8 \text{ psf}} - \Delta C_{\bar{q}=8 \text{ psf}}$$

where,

$C_{\text{RCS PLUME} + \text{PROXIMITY}}^{(\text{RCS PLUME})}$ = Aerodynamic force or moment coefficient for the Orbiter in the presence of the ET (or the ET in the presence of the Orbiter) including the effect of RCS plumes (c.f. $\Delta C_{\bar{q}}$ definition)

| | |
|---------------|-------------|
| subscript (N) | (not given) |
| (A) | (not given) |
| (m) | (not given) |

$C_{\text{RCS OFF}}^{(\text{ISOLATED})}$ = Freestream aerodynamic force or moment coefficient with RCS-OFF

| | | |
|----------------|-----------------------|------------------------|
| subscript: (N) | Orbiter Vehicle (ORB) | (Volume 3) |
| | External Tank (ET) | (Table 5.1.5.1.1-12) |
| (A) | Orbiter Vehicle (ORB) | (Volume 3) |
| | External Tank (ET) | (Table 5.1.5.1.1.2-12) |
| (m) | Orbiter Vehicle (ORB) | (Volume 3) |
| | External Tank (ET) | (Table 5.1.5.1.1.3-12) |

NOTE: Orbiter pitching moment coefficients from Volume 3 of this report must be converted as follows:

$$C_m \begin{Bmatrix} x_0 1089.6 \\ y_0 0.0 \\ z_0 375.0 \end{Bmatrix} = C_m \begin{Bmatrix} x_0 1076.7 \\ y_0 0.0 \\ z_0 375.0 \end{Bmatrix} \left(\frac{\bar{c}_w}{L_B} \right) + \left(\frac{\Delta X}{L_B} \right) C_N - \left(\frac{\Delta Z}{L_B} \right) C_A$$

where; $\Delta X = 1089.6 - 1076.7 = 12.9$ in.
 $\Delta Z = 375.0 - 375.0 = 0.0$ in.
 $\bar{c}_w = 474.72$ in.
 $L_B = 1290.30$ in.

$\Delta C_{()ORB|ET}$ = Effect of ET on Orbiter due to proximity for all β at other \bar{q} effect than nominal dynamic pressure.

$\Delta C_{()ET|ORB}$ = Effect of Orbiter on ET due to proximity for all β at other \bar{q} effect than nominal dynamic pressure.

| \bar{q} psf | ϕ_j/ϕ_∞ | Subscript | Table |
|------------------|----------------------|-----------|----------------|
| 5.0 | 0.0303 | N | 5.1.5.1.1.1-13 |
| 7.5 | 0.0202 | N | 5.1.5.1.1.1-14 |
| 10.0 | 0.0151 | N | 5.1.5.1.1.1-15 |
| 5.0 | 0.0303 | A | 5.1.5.1.1.2-13 |
| 7.5 | 0.0202 | A | 5.1.5.1.1.2-14 |
| 10.0 | 0.0151 | A | 5.1.5.1.1.2-15 |
| 5.0 | 0.0303 | m | 5.1.5.1.1.3-13 |
| 7.5 | 0.0202 | m | 5.1.5.1.1.3-14 |
| 10.0 | 0.0151 | m | 5.1.5.1.1.3-15 |

* C A U T I O N *

$\Delta C_{()ORB|ET}$ = $\left\{ \begin{array}{l} \text{STRUCTURAL RELEASE TO MM602 - Fully coupled} \\ \text{RCS + Proximity effect (Disk Pack TU0095).} \\ \text{BEYOND MM602 - Plume-off proximity effect} \\ \text{(Disk Pack TU0095) combined with isolated} \\ \text{Orbiter (no proximity) RCS effect.} \end{array} \right.$

* $\bar{q} = 8 \text{psf}$ *

$\Delta C_{l1}{}_{ORB|ET}$ = Effect of ET on Orbiter due to
proximity at nominal dynamic
 $\bar{q} = 8 \text{ psf}$ pressure for applicable RCS
command.


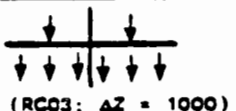
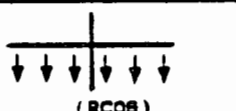
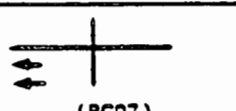

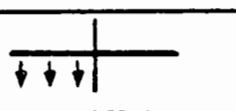

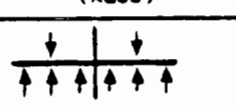
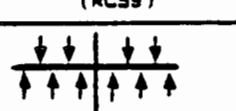
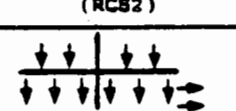
$$= \left[\Delta C_{l1}{}_{\beta=0 \text{ deg}} + \Delta C_{l1}{}_{\beta} \times \beta \right]_{ORB|ET}$$

subscript: (N) $\bar{q} = 8 \text{ psf}$ (Table 4.1.5.1.1-2)
(A) (Table 4.1.5.1.1-2)
(m) (Table 4.1.5.1.1-2)

$\Delta C_{l1}{}_{\beta=0 \text{ deg}}{}_{ORB|ET}$ = RCS + Proximity effect for Orbiter (See Table 4.1.5.1.1-3
at $\beta = 0^\circ$ and nominal dynamic and -6).
 $\bar{q} = 8 \text{ psf}$ pressure.

$\Delta C_{l1}{}_{\beta}{}_{ORB|ET}$ = Sideslip derivative of Orbiter $\beta < 0$: (Table 4.1.5.1.1-4
RCS + Proximity effect at and -6)
 $\bar{q} = 8 \text{ psf}$ nominal dynamic pressure. $\beta > 0$: (Tables 4.1.5.1.1-5
and -6)

Table 4.1.5.1.1-6
COEFFICIENT DATA LOCATION

| RCS CONFIGURATION | SUBSCRIPT | Table | | |
|---|-----------|-------------------|-------------------|-------------------|
| | | $\beta < 0^\circ$ | $\beta = 0^\circ$ | $\beta > 0^\circ$ |
|  (RCO1: $\Delta Z = 1000$) | N | S.1.5.1.1.1-17 | | S.1.5.1.1.1-17 |
| | A | S.1.5.1.1.2-17 | | S.1.5.1.1.2-17 |
| | m | S.1.5.1.1.3-17 | | S.1.5.1.1.3-17 |
|  (RCO3: $\Delta Z = 1000$) | N | S.1.5.1.1.1-17 | | S.1.5.1.1.1-17 |
| | A | S.1.5.1.1.2-17 | | S.1.5.1.1.2-17 |
| | m | S.1.5.1.1.3-17 | | S.1.5.1.1.3-17 |
|  (RCO8) | N | | S.1.5.1.1.1-16 | |
| | A | | S.1.5.1.1.2-16 | |
| | m | | S.1.5.1.1.3-16 | |
|  (RCO7) | N | | S.1.5.1.1.1-16 | |
| | A | | S.1.5.1.1.2-16 | |
| | m | | S.1.5.1.1.3-16 | |
|  (RC11) | N | S.1.5.1.1.1-17 | | S.1.5.1.1.1-17 |
| | A | S.1.5.1.1.2-17 | | S.1.5.1.1.2-17 |
| | m | S.1.5.1.1.3-17 | | S.1.5.1.1.3-17 |
|  (RC21) | N | | S.1.5.1.1.1-16 | |
| | A | | S.1.5.1.1.2-16 | |
| | m | | S.1.5.1.1.3-16 | |
|  (RC38) | N | S.1.5.1.1.1-17 | | S.1.5.1.1.1-17 |
| | A | S.1.5.1.1.2-17 | | S.1.5.1.1.2-17 |
| | m | S.1.5.1.1.3-17 | | S.1.5.1.1.3-17 |
|  (RC59) | N | S.1.5.1.1.1-17 | | S.1.5.1.1.1-17 |
| | A | S.1.5.1.1.2-17 | | S.1.5.1.1.2-17 |
| | m | S.1.5.1.1.3-17 | | S.1.5.1.1.3-17 |
|  (RC52) | N | S.1.5.1.1.1-17 | | S.1.5.1.1.1-17 |
| | A | S.1.5.1.1.2-17 | | S.1.5.1.1.2-17 |
| | m | S.1.5.1.1.3-17 | | S.1.5.1.1.3-17 |
|  (RC113) | N | S.1.5.1.1.1-17 | | S.1.5.1.1.1-17 |
| | A | S.1.5.1.1.2-17 | | S.1.5.1.1.2-17 |
| | m | S.1.5.1.1.3-17 | | S.1.5.1.1.3-17 |

$\Delta C_{(1)ET|ORB}$ = Effect of Orbiter on ET due to
RCS + proximity at nominal
 $\bar{q} = 8 \text{ psf}$ dynamic pressure.

$$= [\Delta C_{(1)\beta=0^\circ} + \Delta C_{(1)\beta} \times \beta]_{ET|ORB}^{\bar{q}=8\text{psf}}$$

$\Delta C_{(1)\beta=0^\circ ET|ORB}$ = RCS + Proximity effect for ET
at $\beta = 0^\circ$ and nominal dynamic
 $\bar{q} = 8 \text{ psf}$ pressure.

Nominal Separation (RC01)
Down-Mode Separation (RC03)

subscript: (N) (Disk Pack TU0095 ; Appendix A)
(A) (Disk Pack TU0095 ; Appendix A)
(m) (Disk Pack TU0095 ; Appendix A)

$\Delta C_{(1)\beta ET|ORB}$ = Sideslip derivative of ET
RCS + Proximity effect at
 $\bar{q} = 8 \text{ psf}$ nominal dynamic pressure.

$$= \frac{1}{3} [\Delta C_{(1)\beta=3^\circ} - \Delta C_{(1)\beta=0^\circ}]_{ET|ORB}$$

$\Delta C_{(1)\beta=3^\circ ET|ORB}$ = RCS + Proximity effect for ET
at $\beta = 3^\circ$ and nominal dynamic
 $\bar{q} = 8 \text{ psf}$ pressure.

Nominal Separation (RC01)
Down-Mode Separation (RC03)

subscript: (N) (Disk Pack TU0095 ; Appendix A)
(A) (Disk Pack TU0095 ; Appendix A)
(m) (Disk Pack TU0095 ; Appendix A)

POST-SEPARATION (ISOLATED ORBITER). The Orbiter free-air aerodynamic force and moment coefficients during the post-separation recovery phase are provided in Volume 3 of this report. Orbiter pitching moment coefficients from Volume 3 must be converted as follows:

$$C_m \begin{pmatrix} x_0 1089.6 \\ y_0 0.0 \\ z_0 375.0 \end{pmatrix} = C_m \begin{pmatrix} x_0 1076.7 \\ y_0 0.0 \\ z_0 375.0 \end{pmatrix} \left(\frac{\bar{c}_w}{L_B} \right) + \left(\frac{\Delta X}{L_B} \right) C_N - \left(\frac{\Delta Z}{L_B} \right) C_A$$

where; $\Delta X = 1089.6 - 1076.7 = 12.9 \text{ in.}$
 $\Delta Z = 375.0 - 375.0 = 0.0 \text{ in.}$
 $\bar{c}_w = 474.72 \text{ in.}$
 $L_B = 1290.30 \text{ in.}$

POST-SEPARATION (ISOLATED EXTERNAL TANK). Isolated External Tank aerodynamics for the post-separation disposal trajectory studies (of no significance to the RTLS separation maneuver) are defined in the NASA/MSFC memoranda (References 4-3, 4-4 and 4-5).

These documents present both longitudinal and lateral-directional data in the missile axis system; however, equations are provided to transform the coefficients to the body axis system.

Isolated data applicable to the RTLS separation maneuver (compatible with the references) are presented in Volume 2, as indicated under

C) ISOLATED above.
RCS OFF

References 4-3 and 4-4 contain the ET static aerodynamic coefficients for Mach numbers between zero and ten. All data are provided with associated accuracy envelopes which account for experimental tolerances or accuracies on the limited experimental data base, tolerances on analytical predictions, and an additional envelope to account for large Reynolds number effects at subsonic and hypersonic Mach numbers. The data presented in these references provide a full matrix of information over a Mach range from 0.6 to 8.0 and angles of attack between zero and 180 degrees with roll angles between zero and 360 degrees.

Reference 4-5 provides the static stability aerodynamics for Mach numbers between 10 and 30. Static, inviscid, aerodynamic coefficients are presented in both tabulated and graphical form in the missile axis system with appropriate equations for transformation to the body axis system. Tolerances are provided for the inviscid coefficients. Incremental coefficients for viscous and free molecular flow effects are also given. These increments are to be combined with the inviscid flow coefficients to obtain total coefficients for any given Mach number and altitude. This reference [4-5] also includes tabulations of the primary moment damping derivations for Mach 20 at an altitude of 215,000 feet.

4.1.5.1.2 LATERAL-DIRECTIONAL AERODYNAMICS

PRE-SEPARATION (TURN-AROUND MANEUVER). The total aerodynamic force and moment coefficients are defined as:

$$*C_{(1)TOTAL} = C_{(1)f} \equiv C_{(1)|\beta=0^{\circ}}_{RCS OFF}$$

AERO

where, $C_{(1)f}$ = Second-stage, forebody force or moment coefficient

| | |
|----------------|-----------------------|
| subscript: (Y) | (Table 5.1.5.1.2.1-1) |
| (n) | (Table 5.1.5.1.2.2-1) |
| (L) | (Table 5.1.5.1.2.3-1) |

PRE-SEPARATION (MATED COAST). The available RCS roll/pitch commands for the mated coast phase of the RTLS maneuver are presented in Table 4.1.5.1.1-1 with a description of the associated jets being fired. Jet control commands (denoted by circles on the table) are used in conjunction with one of the following three conditions of yaw command (UZCMD):

| UZCMD | CONDITION |
|-------|--|
| +1 | 2 forward left side-firing plus 1 aft right side-firing jets. |
| 0 | No side-firing jets. |
| -1 | 2 forward right side-firing plus 1 aft left side-firing jets. |

Orbiter-plus-External Tank mated coast aerodynamic force and moment coefficients are defined as:

$$C_{(1)TOTAL} = C_{(1)|\beta}_{RCS ON}$$

AERO

where,

$$\beta > 0^{\circ}$$

$$C_{(1)|\beta}_{RCS ON} = C_{(1)|\beta=0^{\circ}}_{RCS OFF} + \Delta C_{(1)|\beta=0^{\circ}} + \Delta C_{(1)|\beta}_{\beta > 0^{\circ}} \times \beta + \frac{\beta}{4} (C_{(1)|\beta=-4^{\circ}} - C_{(1)|\beta=0^{\circ}})_{RCS OFF}$$

$$\beta < 0^{\circ}$$

$$C_{(1)|\beta}_{RCS ON} = C_{(1)|\beta=0^{\circ}}_{RCS OFF} + \Delta C_{(1)|\beta=0^{\circ}} + \Delta C_{(1)|\beta}_{\beta < 0^{\circ}} \times \beta - \frac{\beta}{4} (C_{(1)|\beta=-4^{\circ}} - C_{(1)|\beta=0^{\circ}})_{RCS OFF}$$

*NOTE: (1) Rotary derivatives have been assumed negligible.
(2) Control surface deflections have not been considered.

$C_{(1)}|_{\beta} =$ RCS-off, full, scale, rigid body second stage force or moment coefficient with SSME power-off for $\beta = -4^\circ, 0^\circ, +4^\circ$. $\equiv C_{(1)f}$

subscript: (Y) (Table 5.1.5.1.2.1-1)
(n) (Table 5.1.5.1.2.2-1)
(l) (Table 5.1.5.1.2.3-1)

$$\Delta C_{(1)}|_{\beta=0^\circ} = \left[C_{(1)}|_{\beta=0^\circ}^{\text{RCS ON}} - C_{(1)}|_{\beta=0^\circ}^{\text{RCS OFF}} \right]$$

$$\Delta C_{(1)}|_{\beta > 0^\circ} = \frac{1}{4} \left[\left(C_{(1)}|_{\beta=+4^\circ}^{\text{RCS ON}} - C_{(1)}|_{\beta=+4^\circ}^{\text{RCS OFF}} \right) - \Delta C_{(1)}|_{\beta=0^\circ} \right]$$

$$\Delta C_{(1)}|_{\beta < 0^\circ} = -\frac{1}{4} \left[\left(C_{(1)}|_{\beta=-4^\circ}^{\text{RCS ON}} - C_{(1)}|_{\beta=-4^\circ}^{\text{RCS OFF}} \right) - \Delta C_{(1)}|_{\beta=0^\circ} \right]$$

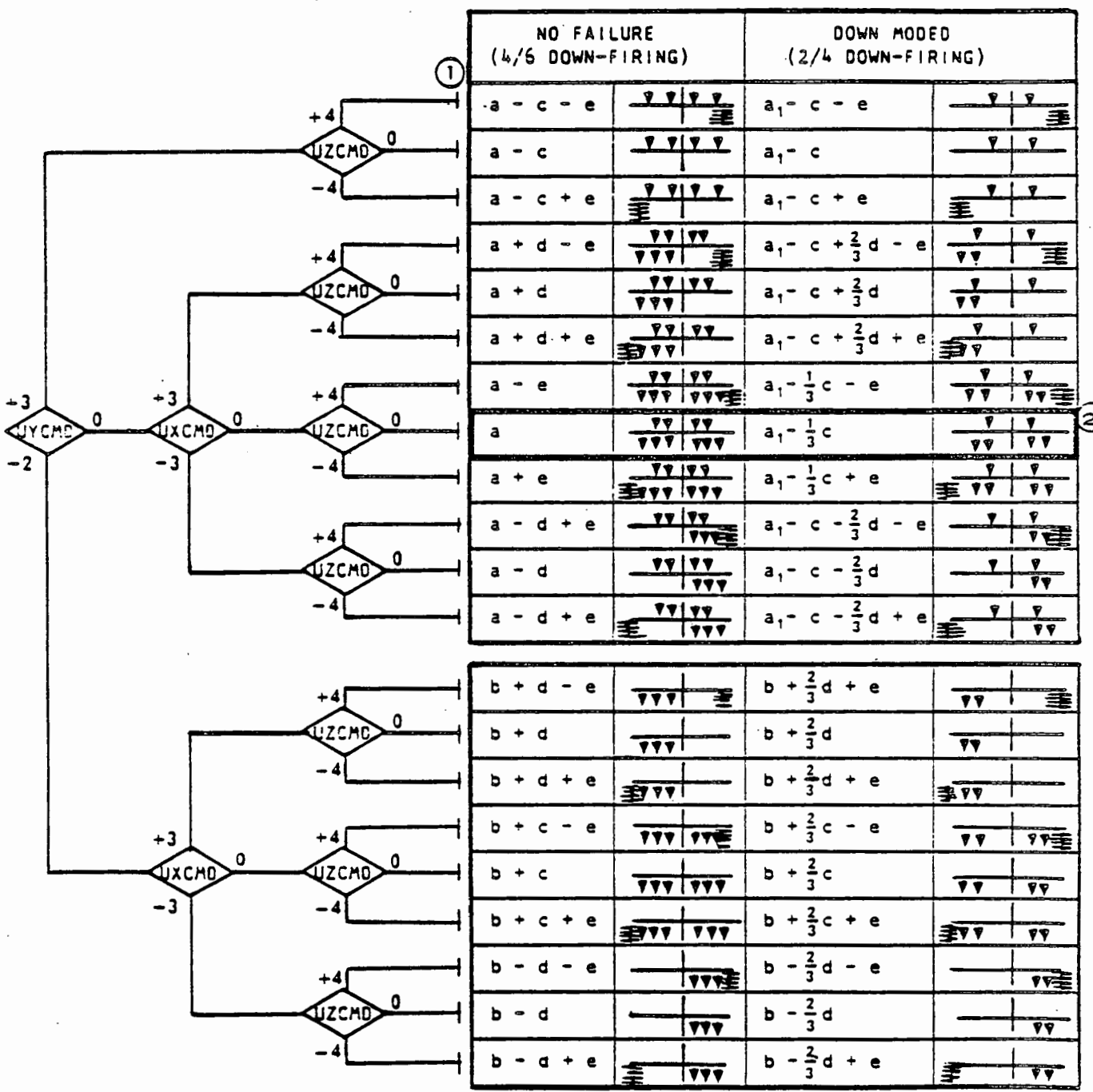
| \bar{q} psf | ϕ_j/ϕ_m | Subscript | $\beta < 0^\circ$ | $\beta = 0^\circ$ | $\beta > 0^\circ$ |
|------------------|-----------------|-----------|----------------------|-------------------|-------------------|
| | | | Table No. for RCS-ON | | |
| 5.0 | 0.0303 | Y | 5.1.5.1.2.1-2 | 5.1.5.1.2.1-3 | 5.1.5.1.2.1-4 |
| 7.5 | 0.0202 | Y | 5.1.5.1.2.1-5 | 5.1.5.1.2.1-6 | 5.1.5.1.2.1-7 |
| 10.0 | 0.0151 | Y | 5.1.5.1.2.1-8 | 5.1.5.1.2.1-9 | 5.1.5.1.2.1-10 |
| 5.0 | 0.0303 | n | 5.1.5.1.2.2-2 | 5.1.5.1.2.2-3 | 5.1.5.1.2.2-4 |
| 7.5 | 0.0202 | n | 5.1.5.1.2.2-5 | 5.1.5.1.2.2-6 | 5.1.5.1.2.2-7 |
| 10.0 | 0.0151 | n | 5.1.5.1.2.2-8 | 5.1.5.1.2.2-9 | 5.1.5.1.2.2-10 |
| 5.0 | 0.0303 | l | 5.1.5.1.2.3-2 | 5.1.5.1.2.3-3 | 5.1.5.1.2.3-4 |
| 7.5 | 0.0202 | l | 5.1.5.1.2.3-5 | 5.1.5.1.2.3-6 | 5.1.5.1.2.3-7 |
| 10.0 | 0.0151 | l | 5.1.5.1.2.3-8 | 5.1.5.1.2.3-9 | 5.1.5.1.2.3-10 |

SEPARATION (PROXIMITY). The RTLS separation aerodynamics (including RCS jet plume effects) are defined for Mach 6.0. The nominal (no failure) separation sequence, from structural release to transition to Major Mode 602 (Figure 4.1.5-1), consists of a -Z translation (4 forward and 6 aft down-firing RCS jets) without attitude control for approximately 1-second duration after structural release, followed by RCS attitude control maneuvers where pitch rate is not to exceed +2.25 degrees per second. Down-moding occurs in the case of a jet failure resulting in a 2 forward and 4 aft down-firing translation jet configuration. Once initiated, down-moding continues throughout the attitude control phase of separation. The -Z translation burn is denoted by UXCMD = UYCMD = UZCMD = 0 in Table 4.1.5.1.2-1 (heavy outline). All other values of UXCMD, UYCMD, and UZCMD shown in the



table apply to the attitude control phase of separation. The terms a, a₁, b, c, d, and e appearing in the table are further defined in Tables 4.1.5.1.1-3, -4, and -5. Synthesis of RCS configurations is required in the evaluation of aerodynamic coefficient sideslip derivatives because of the unavailability of wind tunnel test results for the basic RCS configurations RC06 (term c), RC21 (term d), and RC07 (term e) used in Table 4.1.5.1.2-1.

Table 4.1.5.1.2-1
RTLS SEPARATION TRANSLATION AND ATTITUDE CONTROL MANEUVERS



NOTE: 1. Terms a, a₁, b, c, d, and e are defined in Tables 4.1.5.1.1-3, -4, and -5.
2. -Z Translation burn ~ Structural release to MM602 (cf. Figure 4.1.5-1).

The total force and moment coefficients for the Orbiter and ET over the applicable dynamic pressure range are obtained in the following manner:

$$C_{(1) \text{ TOTAL AERO}}^{5 \leq \bar{q} \leq 10 \text{ psf}} = C_{(1) \text{ ISOLATED RCS OFF}} + \left(\Delta C_{(1) \bar{q}=8 \text{ psf}} + \Delta C_{(1) \bar{q} \text{ effect}} \right)_{\text{ORB|ET}}$$

$$C_{(1) \text{ TOTAL AERO}}^{5 \leq \bar{q} \leq 10 \text{ psf}} = C_{(1) \text{ ISOLATED RCS OFF}} + \left(\Delta C_{(1) \bar{q}=8 \text{ psf}} + \Delta C_{(1) \bar{q} \text{ effect}} \right)_{\text{ET|ORB}}$$

$$\Delta C_{(1) \bar{q}=8 \text{ psf}} = \left(C_{(1) \text{ RCS PLUME + PROXIMITY}} - C_{(1) \text{ ISOLATED RCS OFF}} \right)_{\bar{q}=8 \text{ psf}}$$

$$\Delta C_{(1) \bar{q} \text{ effect}} = \left(C_{(1) \text{ RCS PLUME + PROXIMITY}} - C_{(1) \text{ ISOLATED RCS OFF}} \right)_{\bar{q} \neq 8 \text{ psf}} - \Delta C_{(1) \bar{q}=8 \text{ psf}}$$

where,

$C_{(1) \text{ RCS PLUME + PROXIMITY}}$ = Aerodynamic force or moment coefficient for the Orbiter in the presence of the ET (or the ET in the presence of the Orbiter) including the effect of RCS plumes (c.f. $\Delta C_{(1)}$ definition)

subscript: (Y) (not given)
(n) (not given)
(l) (not given)

$C_{(1) \text{ ISOLATED RCS OFF}}$ = Freestream aerodynamic force or moment coefficient with RCS-OFF

| | | |
|----------------|-----------------------|------------------------|
| subscript: (Y) | Orbiter Vehicle (ORB) | (Volume 3) |
| | External Tank (ET) | (Table 5.1.5.1.2.1-11) |
| (n) | Orbiter Vehicle (ORB) | (Volume 3) |
| | External Tank (ET) | (Table 5.1.5.1.2.2-11) |
| (l) | Orbiter Vehicle (ORB) | (Volume 3) |
| | External Tank (ET) | (Table 5.1.5.1.2.3-11) |

NOTE: (1) Orbiter yawing moment coefficients from Volume 3 of this report must be converted as follows:

$$C_n \begin{bmatrix} x_0 1039.6 \\ y_0 0.0 \\ z_0 375.0 \end{bmatrix} = C_n \begin{bmatrix} x_0 1076.7 \\ y_0 0.0 \\ z_0 375.0 \end{bmatrix} \left(\frac{b_w}{L_B} \right) - \left(\frac{\Delta Y}{L_B} \right) C_A + \left(\frac{\Delta X}{L_B} \right) C_Y$$

where; $\Delta Y = 0.0$ in.
 $\Delta X = 1089.6 - 1076.7 = 12.9$ in.
 $b_w = 936.68$ in.
 $L_B = 1290.30$ in.

NOTE: (2) Orbiter rolling moment coefficients from Volume 3 of this report must be converted as follows:

$$C_l \begin{Bmatrix} x_0 & 1089.6 \\ y_0 & 0.0 \\ z_0 & 375.0 \end{Bmatrix} = C_l \begin{Bmatrix} x_0 & 1076.7 \\ y_0 & 0.0 \\ z_0 & 375.0 \end{Bmatrix} \left(\frac{b_w}{L_B} \right) + \left(\frac{\Delta Y}{L_B} \right) C_N - \left(\frac{\Delta Z}{L_B} \right) C_Y$$

where; $\Delta Y = 0.0$ in.
 $\Delta Z = 0.0$ in.
 $b_w = 936.68$ in.
 $L_B = 1290.30$ in.

$\Delta C_{l(ORB)|ET}$
 \bar{q}_{effect} = Effect of ET on Orbiter due to proximity for all β at other than nominal dynamic pressure.

$\Delta C_{l(ET)|ORB}$
 \bar{q}_{effect} = Effect of Orbiter on ET due to proximity for all β at other than nominal dynamic pressure.

| \bar{q} psf | ϕ_j/ϕ_m | Subscript | Table |
|------------------|-----------------|-----------|----------------|
| 5.0 | 0.0303 | Y | 5.1.5.1.2.1-12 |
| 7.5 | 0.0202 | Y | 5.1.5.1.2.1-12 |
| 10.0 | 0.0151 | Y | 5.1.5.1.2.1-12 |
| 5.0 | 0.0303 | n | 5.1.5.1.2.2-12 |
| 7.5 | 0.0202 | n | 5.1.5.1.2.2-12 |
| 10.0 | 0.0151 | n | 5.1.5.1.2.2-12 |
| 5.0 | 0.0303 | l | 5.1.5.1.2.3-12 |
| 7.5 | 0.0202 | l | 5.1.5.1.2.3-12 |
| 10.0 | 0.0151 | l | 5.1.5.1.2.3-12 |

 * CAUTION *

$\Delta C_{l(ORB)|ET}$
 $\bar{q} = 8 \text{ psf}$ =

{ STRUCTURAL RELEASE TO MM602 - Fully coupled
 RCS + Proximity effect (Disk Pack TU0095).
 BEYOND MM602 - Plume-off proximity effect
 (Disk Pack TU0095) combined with isolated
 Orbiter (no proximity) RCS effect.

$\Delta C_{(1)ORB|ET}$
 $\bar{q}=8psf$ = Effect of ET on Orbiter due to proximity at nominal dynamic pressure for applicable RCS command.

$$= \left[\Delta C_{(1)\beta=0} + \Delta C_{(1)\beta} \times \beta \right]_{ORB|ET}$$

subscript: (Y)
(n)
(l)

$\bar{q}=8psf$

(Table 4.1.5.1.2-1)
(Table 4.1.5.1.2-1)
(Table 4.1.5.1.2-1)

$\Delta C_{(1)\beta=0}$
 $\bar{q}=8psf$ = RCS + Proximity effect for Orbiter at $\beta = 0^\circ$ and nominal dynamic pressure.

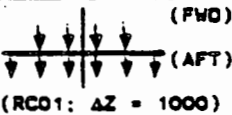
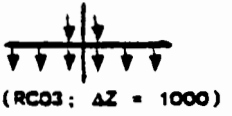
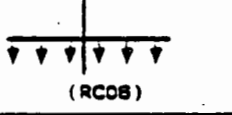
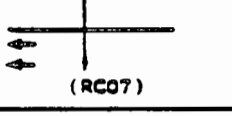
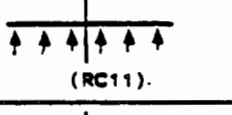
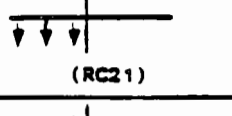
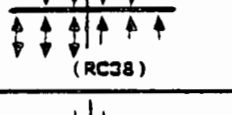
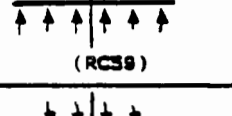

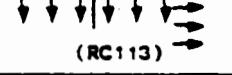
(Tables 4.1.5.1.1-3
and 4.1.5.1.2-2)

$\Delta C_{(1)\beta}$
 $\bar{q}=8psf$ = Sideslip derivative of Orbiter RCS + Proximity effect at nominal dynamic pressure.

$\beta < 0$: (Tables 4.1.5.1.1-4
and 4.1.5.1.2-2)

$\beta > 0$: (Tables 4.1.5.1.1-5
and 4.1.5.1.2-2)

Table 4.1.5.1.2-2
COEFFICIENT DATA LOCATION

| RCS CONFIGURATION | SUBSCRIPT | Table | | |
|---|-----------|-------------------|-------------------|-------------------|
| | | $\beta < 0^\circ$ | $\beta = 0^\circ$ | $\beta > 0^\circ$ |
|  | Y | S.1.5.2.1-14 | | S.1.5.2.1-14 |
| | n | S.1.5.2.2-14 | | S.1.5.2.2-14 |
| | l | S.1.5.2.3-14 | | S.1.5.2.3-14 |
|  | Y | S.1.5.2.1-14 | | S.1.5.2.1-14 |
| | n | S.1.5.2.2-14 | | S.1.5.2.2-14 |
| | l | S.1.5.2.3-14 | | S.1.5.2.3-14 |
|  | Y | | S.1.5.2.1-13 | |
| | n | | S.1.5.2.2-13 | |
| | l | | S.1.5.2.3-13 | |
|  | Y | | S.1.5.2.1-13 | |
| | n | | S.1.5.2.2-13 | |
| | l | | S.1.5.2.3-13 | |
|  | Y | S.1.5.2.1-14 | | S.1.5.2.1-14 |
| | n | S.1.5.2.2-14 | | S.1.5.2.2-14 |
| | l | S.1.5.2.3-14 | | S.1.5.2.3-14 |
|  | Y | | S.1.5.2.1-13 | |
| | n | | S.1.5.2.2-13 | |
| | l | | S.1.5.2.3-13 | |
|  | Y | S.1.5.2.1-14 | | S.1.5.2.1-14 |
| | n | S.1.5.2.2-14 | | S.1.5.2.2-14 |
| | l | S.1.5.2.3-14 | | S.1.5.2.3-14 |
|  | Y | S.1.5.2.1-14 | | S.1.5.2.1-14 |
| | n | S.1.5.2.2-14 | | S.1.5.2.2-14 |
| | l | S.1.5.2.3-14 | | S.1.5.2.3-14 |
|  | Y | S.1.5.2.1-14 | | S.1.5.2.1-14 |
| | n | S.1.5.2.2-14 | | S.1.5.2.2-14 |
| | l | S.1.5.2.3-14 | | S.1.5.2.3-14 |
|  | Y | S.1.5.2.1-14 | | S.1.5.2.1-14 |
| | n | S.1.5.2.2-14 | | S.1.5.2.2-14 |
| | l | S.1.5.2.3-14 | | S.1.5.2.3-14 |

$\Delta C_{(1)ET|ORB}$
 $\bar{q} = 8 \text{ psf}$ = Effect of Orbiter on ET due to
RCS + proximity at nominal
dynamic pressure.

$$= \left[\Delta C_{(1)\beta=0^\circ} + \Delta C_{(1)\beta} \times \beta \right]_{ET|ORB}^{\bar{q}=8 \text{ psf}}$$

$\Delta C_{(1)\beta=0^\circ}$
 $\bar{q} = 8 \text{ psf}$ = RCS + Proximity effect for ET
at $\beta = 0^\circ$ and nominal dynamic
pressure.

Nominal Separation (RC01)
Down-Mode Separation (RC03)

subscript: (Y) (Disk Pack TU0095 ; Appendix A)
(n) (Disk Pack TU0095 ; Appendix A)
(l) (Disk Pack TU0095 ; Appendix A)

$\Delta C_{(1)\beta} ET|ORB$
 $\bar{q} = 8 \text{ psf}$ = Sideslip derivative of ET
RCS + Proximity effect at
nominal dynamic pressure.

$$= \frac{1}{3} \left[\Delta C_{(1)\beta=3^\circ} + \Delta C_{(1)\beta=0^\circ} \right]_{ET|ORB}^{\bar{q}=8 \text{ psf}}$$

$\Delta C_{(1)\beta=3^\circ}$
 $\bar{q} = 8 \text{ psf}$ = RCS + Proximity effect for ET
at $\beta = 3^\circ$ and nominal dynamic
pressure.

Nominal Separation (RC01)
Down-Mode Separation (RC03)

subscript: (Y) (Disk Pack TU0095 ; Appendix A)
(n) (Disk Pack TU0095 ; Appendix A)
(l) (Disk Pack TU0095 ; Appendix A)

POST-SEPARATION (ISOLATED ORBITER). The Orbiter free-air aerodynamic force and moment coefficients during the post-separation recovery phase are provided in Volume 3 of this report.

NOTE: (1) Orbiter yawing moment coefficients from Volume 3 of this report must be converted as follows:

$$C_n \begin{Bmatrix} x_c 1089.6 \\ y_o 0.0 \\ z_o 375.0 \end{Bmatrix} = C_n \begin{Bmatrix} x_c 1076.7 \\ y_o 0.0 \\ z_o 375.0 \end{Bmatrix} \left(\frac{b_w}{L_B} \right) - \left(\frac{\Delta Y}{L_B} \right) C_A + \left(\frac{\Delta X}{L_B} \right) C_Y$$

where; $\Delta Y = 0.0 \text{ in.}$
 $\Delta X = 1089.6 - 1076.7 = 12.9 \text{ in.}$

NOTE: (2) Orbiter rolling moment coefficients from Volume 3 of this report must be converted as follows:

$$C_{\ell} \begin{Bmatrix} x_0 1089.6 \\ y_0 0.0 \\ z_0 375.0 \end{Bmatrix} = C_{\ell} \begin{Bmatrix} x_0 1076.7 \\ y_0 0.0 \\ z_0 375.0 \end{Bmatrix} \left(\frac{b_w}{L_B} \right) + \left(\frac{\Delta Y}{L_B} \right) C_N - \left(\frac{\Delta Z}{L_B} \right) C_Y$$

where; $\Delta Y = 0.0$ in.
 $\Delta Z = 0.0$ in.

POST-SEPARATION (ISOLATED EXTERNAL TANK). Isolated External Tank aerodynamics for the post-separation disposal trajectory studies (of no significance to the RTLS separation maneuver) are defined in the NASA/MSFC memoranda (References 4-3, 4-4 and 4-5).

These documents present both longitudinal and lateral-directional data in the missile axis system; however, equations are provided to transform the coefficients to the body axis system.

Isolated data applicable to the RTLS separation maneuver (compatible with the references) are presented in Volume 2, as indicated under

() ISOLATED above.
RCS OFF

References 4-3 and 4-4 contain the ET static aerodynamic coefficients for Mach numbers between zero and ten. All data are provided with associated accuracy envelopes which account for experimental tolerances or accuracies on the limited experimental data base, tolerances on analytical predictions, and an additional envelope to account for large Reynolds number effects at subsonic and hypersonic Mach numbers. The data presented in these references provide a full matrix of information over a Mach range from 0.6 to 8.0 and angles of attack between zero and 180 degrees with roll angles between zero and 360 degrees.

Reference 4-5 provides the static stability aerodynamics for Mach numbers between 10 and 30. Static, inviscid, aerodynamic coefficients are presented in both tabulated and graphical form in the missile axis system with appropriate equations for transformation to the body axis system. Tolerances are provided for the inviscid coefficients. Incremental coefficients for viscous and free molecular flow effects are also given. These increments are to be combined with the inviscid flow coefficients to obtain total coefficients for any given Mach number and altitude. This reference [4-5] also includes tabulations of the primary moment damping derivations for Mach 20 at an altitude of 215,000 feet.

4.1.5.2 TRANSATLANTIC ABORT LANDING (TAL). Aerodynamic forces and moments pertaining to Orbiter and External Tank separation during the intact TAL abort mode (Mach = 25.0 and dynamic pressure less than 1.0 psf) are defined for two phases of the separation maneuver:

| | |
|----------------|-------------|
| PRE-SEPARATION | MATED COAST |
| SEPARATION | PROXIMITY |

Post-separation isolated Orbiter and External Tank aerodynamics were defined in Section 4.1.5.1. RCS plume effects are limited to plume impingement (no jet/flowfield interaction) due to the extreme altitude (dynamic pressure less than 1 psf) at which TAL abort occurs. Plume impingement on the Orbiter is limited to the aft down-firing RCS jets and confined to the upper wing and fuselage. Forward down-firing jet impingement affects only the ET. The plume impingement effects were numerically determined by means of a Method-Of-Characteristics solution to the nozzle-plume flowfield followed by impingement calculations based on Newtonian impact theory. Scarfed nozzle effects for the forward down-firing jets were not accounted for in the impingement calculations.

Impingement data for the forward down-firing jets are based on two left-hand jets. Right-hand jet data are obtained from the left-hand data set by applying appropriate sign changes to ΔY , $\Delta \beta$, and the lateral-directional force and moment coefficients. Single down-firing jet impingement values are obtained by halving the two jet effect.

Relative displacements and attitudes of the ET with respect to its mated position (ΔX , ΔY , ΔZ , $\Delta \alpha$, and $\Delta \beta$) were defined in Section 4.1.5. Data are provided for the following combinations of parameters:

$\Delta X = 0$ inches
 $\Delta Y = +100, 0, -100, -200, -300, -400$ inches
 $\Delta Z = 0, 100, 300, 400, 700, 1000$ inches
 $\Delta \alpha = 0, -2.5$ degrees
 $\Delta \beta = -5, 0, +5$ degrees

The longitudinal displacement (ΔX) of the ET during separation is negligible; therefore, the data base for $\Delta X = 0$ may be used for all values of ΔX experienced during separation.

4.1.5.2.1 LONGITUDINAL AERODYNAMICS

PRE-SEPARATION (MATED COAST). The total aerodynamic forces and moment are defined below where forces are in pounds and the moment is in foot-pounds. Forces and moments are used in this section rather than coefficients due to the manner of generating impingement effects.

$$\begin{aligned}
 F_{N \text{ TOTAL AERO}} &= \bar{q} S C_{Nf|_{OET}} + F_{N \text{ BASE}} + F_{N \text{ IMP (FWD JETS)}} + F_{N \text{ IMP (AFT JETS)}} \\
 F_{A \text{ TOTAL AERO}} &= \bar{q} S C_{Af|_{OET}} + F_{A \text{ BASE}} + F_{A \text{ IMP (FWD JETS)}} + F_{A \text{ IMP (AFT JETS)}} \\
 M_{\text{TOTAL AERO}} &= \bar{q} S L_B C_{mf|_{OET}} + M_{\text{BASE}} + M_{\text{IMP (FWD JETS)}} + M_{\text{IMP (AFT JETS)}}
 \end{aligned}$$

where,

$C_{i|_{OET}}$ = Second -stage, forebody force or moment coefficient ($-180^\circ \leq \alpha \leq +180^\circ$).

subscript: (N) (Table 5.1.5.1.1.1-1)
(A) (Table 5.1.5.1.1.2-1)
(m) (Table 5.1.5.1.1.3-1)

NOTE: Pitching moment coefficient must be converted to the Mated Coast Moment Reference Center (MRC) as follows:

$$C_{mf} \begin{Bmatrix} x_T 1734.0 \\ y_T 0.0 \\ z_T 634.3 \end{Bmatrix} = C_{mf} \begin{Bmatrix} x_T 976.0 \\ y_T 0.0 \\ z_T 400.0 \end{Bmatrix} + \left(\frac{\Delta X}{L_B} \right) C_{Nf} - \left(\frac{\Delta Z}{L_B} \right) C_{Af}$$

where, $\Delta X = 1734.0 - 976.0 = 758.0$ in.
 $\Delta Z = 634.3 - 400.0 = 243.3$ in.
 $L_B = 1290.3$ in.

Power-on base force or moment (including effects of SSME plumes). $\left\{ \begin{array}{l} F_{N \text{ BASE}} \quad (\text{Figure 5.1.4.1.1-2}) \\ F_{A \text{ BASE}} \quad (\text{Figure 5.1.4.1.2-2}) \\ M_{\text{BASE}} \quad (\text{Figure 5.1.4.1.3-2}) \end{array} \right.$

NOTE: Pitching moment must be converted to the Mated Coast MRC as follows:

$$M_{\text{BASE}} \begin{Bmatrix} x_T 1734.0 \\ y_T 0.0 \\ z_T 634.3 \end{Bmatrix} = M_{\text{BASE}} \begin{Bmatrix} x_T 976.0 \\ y_T 0.0 \\ z_T 400.0 \end{Bmatrix} + \left(\frac{\Delta X}{12} \right) F_{N \text{ BASE}} - \left(\frac{\Delta Z}{12} \right) F_{A \text{ BASE}}$$

where, ΔX and ΔZ are as above.

Plume impingement forces or moment on ET due to forward downfiring RCS jets. (NOTE: No impingement on Orbiter) $\left\{ \begin{array}{l} F_{N \text{ IMP (FWD JETS)}} \quad (\text{Table 5.1.5.2.1.1-1}) \\ F_{A \text{ IMP (FWD JETS)}} \quad (\text{Table 5.1.5.2.1.2-1}) \\ M_{\text{IMP (FWD JETS)}} \quad (\text{Table 5.1.5.2.1.3-1}) \end{array} \right.$

NOTE: Pitching moment must be converted to the Mated Coast MRC as follows:

$$M_{\text{IMP (FWD JETS)}} = M_{\text{IMP (FWD JETS)}} + \left(\frac{\Delta X}{12}\right) F_{N \text{ IMP (FWD JETS)}} - \left(\frac{\Delta Z}{12}\right) F_{A \text{ IMP (FWD JETS)}}$$

$$\begin{Bmatrix} X_T \\ Y_T \\ Z_T \end{Bmatrix} = \begin{Bmatrix} X_T \\ Y_T \\ Z_T \end{Bmatrix}$$

$$\begin{Bmatrix} 1734.0 \\ 0.0 \\ 634.3 \end{Bmatrix} = \begin{Bmatrix} 1328.7 \\ 0.0 \\ 416.4 \end{Bmatrix}$$

where, $\Delta X = 1734.0 - 1328.7 = 405.3$ in.
 $\Delta Z = 634.3 - 416.4 = 217.9$ in.

Plume impingement forces or moment on Orbiter due to aft downfiring RCS jets. (NOTE: No impingement on ET)

$$\left\{ \begin{array}{l} F_{N \text{ IMP (AFT JETS)}} \\ F_{A \text{ IMP (AFT JETS)}} \\ M_{\text{IMP (AFT JETS)}} \end{array} \right. \quad \begin{array}{l} \text{(See Volume 3)} \\ \text{(See Volume 3)} \\ \text{(See Volume 3)} \end{array}$$

NOTE: Pitching moment must be converted to the Mated Coast MRC as follows:

$$M_{\text{IMP (AFT JETS)}} = M_{\text{IMP (AFT JETS)}} + \left(\frac{\Delta X}{12}\right) F_{N \text{ IMP (AFT JETS)}} - \left(\frac{\Delta Z}{12}\right) F_{A \text{ IMP (AFT JETS)}}$$

$$\begin{Bmatrix} X_T \\ Y_T \\ Z_T \end{Bmatrix} = \begin{Bmatrix} X_T \\ Y_T \\ Z_T \end{Bmatrix}$$

$$\begin{Bmatrix} 1734.0 \\ 0.0 \\ 634.3 \end{Bmatrix} = \begin{Bmatrix} 1076.7 \\ 0.0 \\ 375.0 \end{Bmatrix}$$

where, $\Delta X = 1734.0 - (1076.7 + 741.0) = -83.7$ in.
 $\Delta Z = 634.3 - (375.0 + 336.5) = -77.2$ in.

SEPARATION (PROXIMITY). The total aerodynamic forces and moment for the Orbiter and ET during separation are defined below where forces are in pounds and moments are in foot-pounds. Forces and moments are used in this section rather than coefficients due to the manner of generating impingement effects.

$$F_{N \text{ TOTAL AERO}} \Big|_{\text{ORB}} = \bar{q} S C_N \Big|_{\text{ORB}} + F_{N \text{ IMP (AFT JETS)}} \Big|_{\text{ORB}}$$

$$F_{N \text{ TOTAL AERO}} \Big|_{\text{ET}} = \bar{q} S C_N \Big|_{\text{ET}} + F_{N \text{ IMP (FWD JETS)}} \Big|_{\text{ET}}$$

$$F_{A \text{ TOTAL AERO}} \Big|_{\text{ORB}} = \bar{q} S C_A \Big|_{\text{ORB}} + F_{A \text{ IMP (AFT JETS)}} \Big|_{\text{ORB}}$$

$$F_{A \text{ TOTAL AERO}} \Big|_{\text{ET}} = \bar{q} S C_A \Big|_{\text{ET}} + F_{A \text{ IMP (FWD JETS)}} \Big|_{\text{ET}}$$

$$M_{\text{TOTAL AERO}} \Big|_{\text{ORB}} = \bar{q} S L_B C_m \Big|_{\text{ORB}} + M_{\text{IMP (AFT JETS)}} \Big|_{\text{ORB}}$$

$$M_{\text{TOTAL AERO}} \Big|_{\text{ET}} = \bar{q} S L_B C_m \Big|_{\text{ET}} + M_{\text{IMP (FWD JETS)}} \Big|_{\text{ET}}$$

where,

$C_{()}|_{ORB}$ = Isolated Orbiter (no SSME plumes)
force or moment coefficient.

subscript: (N) (See Volume 3)
(A) (See Volume 3)
(m) (See Volume 3)

NOTE: Pitching moment coefficient must be converted
to Orbiter proximity MRC as follows:

$$C_{m}|_{ORB} = \left(\frac{\bar{c}_w}{L_B}\right) C_{m}|_{ORB} + \left(\frac{\Delta X}{L_B}\right) C_{N}|_{ORB} - \left(\frac{\Delta Z}{L_B}\right) C_{A}|_{ORB}$$

$$\left\{ \begin{matrix} X_0 & 1089.6 \\ Y_0 & 0.0 \\ Z_0 & 375.0 \end{matrix} \right\} \quad \left\{ \begin{matrix} X_0 & 1076.7 \\ Y_0 & 0.0 \\ Z_0 & 375.0 \end{matrix} \right\}$$

where, $\Delta X = 1089.6 - 1076.7 = 12.9$ in.
 $\Delta Z = 0.0$
 $L_B = 1290.3$ in.
 $\bar{c}_w = 474.82$ in.

$C_{()}|_{ET}$ = Isolated ET force or moment coefficient.

subscript: (N) (Table 5.1.5.1.1.1-12)
(A) (Table 5.1.5.1.1.2-12)
(m) (Table 5.1.5.1.1.3-12)

NOTE: ET pitching moment data are at correct MRC.

$F_{N IMP}$ (AFT JETS) | ORB (See Volume 3)
 $F_{A IMP}$ (AFT JETS) | ORB (See Volume 3)
 M_{IMP} (AFT JETS) | ORB (See Volume 3)

NOTE: Pitching moment must be converted to Orbiter
separation MRC as follows:

$$M_{IMP}|_{ORB} = M_{IMP}|_{ORB} + \left(\frac{\Delta X}{12}\right) F_{N IMP}|_{ORB} - \left(\frac{\Delta Z}{12}\right) F_{A IMP}|_{ORB}$$

$$\left\{ \begin{matrix} X_0 & 1089.6 \\ Y_0 & 0.0 \\ Z_0 & 375.0 \end{matrix} \right\} \quad \left\{ \begin{matrix} X_0 & 1076.7 \\ Y_0 & 0.0 \\ Z_0 & 375.0 \end{matrix} \right\}$$

where, $\Delta X = 1089.6 - 1076.7 = 12.9$ in.
 $\Delta Z = 0.0$

$F_{N IMP}$ (FWD JETS) | ET (Table 5.1.5.2.1.1-1)
 $F_{A IMP}$ (FWD JETS) | ET (Table 5.1.5.2.1.2-1)
 M_{IMP} (FWD JETS) | ET (Table 5.1.5.2.1.3-1)

NOTE: ET pitching moment data are at the correct MRC.

POST-SEPARATION (ISOLATED ORBITER). The Orbiter free-air aerodynamic force and moment coefficients during the post-separation recovery phase are provided in Volume 3 of this report as defined in Section 4.1.5.1.1.

POST-SEPARATION (ISOLATED EXTERNAL TANK). Isolated External Tank aerodynamics for the post-separation disposal trajectory studies (of no significance to the RTLS separation maneuver) are defined in Section 4.1.5.1.1.

4.1.5.2.2 LATERAL/DIRECTIONAL AERODYNAMICS.

PRE-SEPARATION (MATED COAST). The total aerodynamic force and moments are defined below where forces are in pounds and moments are in foot-pounds. Forces and moments are used in this section rather than coefficients due to the manner of generating impingement effects. There are no lateral/directional base force or moment effects to be concerned with.

$$F_{Y \text{ TOTAL AERO}} = \bar{q} S C_{Y|OET} + F_{Y \text{ IMP (FWD JETS)}} + F_{Y \text{ IMP (AFT JETS)}}$$

$$K_{TOTAL AERO} = \bar{q} S L_B C_{n|OET} + K_{IMP (FWD JETS)} + K_{IMP (AFT JETS)}$$

$$L_{TOTAL AERO} = \bar{q} S L_B C_{L|OET} + L_{IMP (FWD JETS)} + L_{IMP (AFT JETS)}$$

where,

$C_{()|OET}$ = Second-stage force or moment coefficient
 Subscript: (Y) (Table 5.1.5.1.2.1-1)
 (n) (Table 5.1.5.1.2.2-1)
 (L) (Table 5.1.5.1.2.3-1)

NOTE: Yawing and rolling moment coefficients are at the correct Mated Coast MRC.

| | | |
|--|---|------------------------|
| Plume impingement force or moments on ET due to forward downfiring RCS jets (NOTE: No impingement on Orbiter) | $\left\{ \begin{array}{l} F_{Y \text{ IMP (FWD JETS)}} \\ K_{IMP (FWD JETS)} \\ L_{IMP (FWD JETS)} \end{array} \right.$ | (Figure 5.1.5.2.2.1-1) |
| | | (Figure 5.1.5.2.2.2-1) |
| | | (Figure 5.1.5.2.2.3-1) |

NOTE: Yawing and rolling moments must be converted to the Mated Coast MRC as follows:

$$F_{IMP}^{(FWD\ JETS)} = F_{IMP}^{(FWD\ JETS)} + \left(\frac{\Delta X}{12}\right) F_{Y_{IMP}}^{(FWD\ JETS)} - \left(\frac{\Delta Y}{12}\right) F_{A_{IMP}}^{(FWD\ JETS)}$$

$$\begin{Bmatrix} X_T & 1734.0 \\ Y_T & 0.0 \\ Z_T & 634.3 \end{Bmatrix} \quad \begin{Bmatrix} X_T & 1328.7 \\ Y_T & 0.0 \\ Z_T & 416.4 \end{Bmatrix}$$

$$L_{IMP}^{(FWD\ JETS)} = L_{IMP}^{(FWD\ JETS)} + \left(\frac{\Delta Y}{12}\right) F_{N_{IMP}}^{(FWD\ JETS)} - \left(\frac{\Delta Z}{12}\right) F_{Y_{IMP}}^{(FWD\ JETS)}$$

$$\begin{Bmatrix} X_T & 1734.0 \\ Y_T & 0.0 \\ Z_T & 634.3 \end{Bmatrix} \quad \begin{Bmatrix} X_T & 1328.7 \\ Y_T & 0.0 \\ Z_T & 416.4 \end{Bmatrix}$$

where, $\Delta X = 1734.0 - 1328.7 = 405.3$ in.
 $\Delta Y = 0.0$
 $\Delta Z = 634.3 - 416.4 = 217.9$ in.

Plume impingement force or moments on Orbiter due to aft downfiring RCS jets. (NOTE: No impingement on ET.)

$$\left. \begin{array}{l} F_{Y_{IMP}}^{(AFT\ JETS)} \\ F_{N_{IMP}}^{(AFT\ JETS)} \\ L_{IMP}^{(AFT\ JETS)} \end{array} \right\} \begin{array}{l} \text{(See Volume 3)} \\ \text{(See Volume 3)} \\ \text{(See Volume 3)} \end{array}$$

NOTE: Yawing and rolling moments must be converted to the Mated Coast MRC as follows:

$$F_{IMP}^{(AFT\ JETS)} = F_{IMP}^{(AFT\ JETS)} + \left(\frac{\Delta X}{12}\right) F_{Y_{IMP}}^{(AFT\ JETS)} - \left(\frac{\Delta Y}{12}\right) F_{A_{IMP}}^{(AFT\ JETS)}$$

$$\begin{Bmatrix} X_T & 1734.0 \\ Y_T & 0.0 \\ Z_T & 634.3 \end{Bmatrix} \quad \begin{Bmatrix} X_O & 1076.7 \\ Y_O & 0.0 \\ Z_O & 375.0 \end{Bmatrix}$$

$$L_{IMP}^{(AFT\ JETS)} = L_{IMP}^{(AFT\ JETS)} + \left(\frac{\Delta Y}{12}\right) F_{N_{IMP}}^{(AFT\ JETS)} - \left(\frac{\Delta Z}{12}\right) F_{Y_{IMP}}^{(AFT\ JETS)}$$

$$\begin{Bmatrix} X_T & 1734.0 \\ Y_T & 0.0 \\ Z_T & 634.3 \end{Bmatrix} \quad \begin{Bmatrix} X_O & 1076.7 \\ Y_O & 0.0 \\ Z_O & 375.0 \end{Bmatrix}$$

where, $\Delta X = 1734.0 - (1076.7 + 741) = -83.7$
 $\Delta Y = 0.0$
 $\Delta Z = 634.3 - (375.0 + 336.5) = -77.2$

SEPARATION (PROXIMITY). The total aerodynamic force and moments for the Orbiter and ET during separation are defined below where forces are in pounds and moments are in foot-pounds. Forces and moments are used in this section rather than coefficients due to the manner of generating impingement effects.

$$F_{Y \text{ TOTAL AERO}}|_{\text{ORB}} = \bar{q} S C_{Y}|_{\text{ORB}} + F_{Y \text{ IMP (AFT JETS)}}|_{\text{ORB}}$$

$$F_{Y \text{ TOTAL AERO}}|_{\text{ET}} = \bar{q} S C_{Y}|_{\text{ET}} + F_{Y \text{ IMP (FWD JETS)}}|_{\text{ET}}$$

$$M_{\text{ TOTAL AERO}}|_{\text{ORB}} = \bar{q} S L_B C_{n}|_{\text{ORB}} + M_{\text{ IMP (AFT JETS)}}|_{\text{ORB}}$$

$$M_{\text{ TOTAL AERO}}|_{\text{ET}} = \bar{q} S L_B C_{n}|_{\text{ET}} + M_{\text{ IMP (FWD JETS)}}|_{\text{ET}}$$

$$L_{\text{ TOTAL AERO}}|_{\text{ORB}} = \bar{q} S L_B C_{\ell}|_{\text{ORB}} + L_{\text{ IMP (AFT JETS)}}|_{\text{ORB}}$$

$$L_{\text{ TOTAL AERO}}|_{\text{ET}} = \bar{q} S L_B C_{\ell}|_{\text{ET}} + L_{\text{ IMP (FWD JETS)}}|_{\text{ET}}$$

where,

$C_{()}|_{\text{ORB}}$ = Isolated Orbiter (no SSME plumes) force or moment coefficient.

subscript: (Y) (See Volume 3)
(n) (See Volume 3)
(L) (See Volume 3)

NOTE: Yawing and rolling moment coefficients must be converted to Orbiter proximity MRC as follows:

$$C_{n}|_{\text{ORB}} = \left(\frac{\bar{C}_W}{L_B} \right) C_{n}|_{\text{ORB}} + \left(\frac{\Delta X}{L_B} \right) C_{Y}|_{\text{ORB}} - \left(\frac{\Delta Y}{L_B} \right) C_{A}|_{\text{ORB}}$$

$$\begin{Bmatrix} X_O 1089.6 \\ Y_O 0.0 \\ Z_O 375.9 \end{Bmatrix} \quad \begin{Bmatrix} X_O 1076.7 \\ Y_O 0.0 \\ Z_O 375.0 \end{Bmatrix}$$

$$C_{\ell}|_{\text{ORB}} = \left(\frac{\bar{C}_W}{L_B} \right) C_{\ell}|_{\text{ORB}} + \left(\frac{\Delta Y}{L_B} \right) C_{n}|_{\text{ORB}} - \left(\frac{\Delta Z}{L_B} \right) C_{Y}|_{\text{ORB}}$$

$$\begin{Bmatrix} X_O 1089.6 \\ Y_O 0.0 \\ Z_O 375.0 \end{Bmatrix} \quad \begin{Bmatrix} X_O 1076.7 \\ Y_O 0.0 \\ Z_O 375.0 \end{Bmatrix}$$

where, $\Delta X = 1089.6 - 1076.7 = 12.9$ in.

$\Delta Y = 0.0$

$\Delta Z = 0.0$

$C_{()|ET}$ = Isolated ET force or moment coefficient

subscript: (Y) (Table 5.1.5.1.2.1-11)
(n) (Table 5.1.5.1.2.2-11)
(L) (Table 5.1.5.1.2.3-11)

NOTE: ET yawing and rolling moment coefficient data are at the correct MRC.

$F_{Y IMP (AFT JETS)|ORB}$ (See Volume 3)

$F_{(AFT JETS)|ORB}$ (See Volume 3)

$\mathcal{L}_{IMP (AFT JETS)|ORB}$ (See Volume 3)

NOTE: Yawing and rolling moments must be converted to Orbiter separation MRC as follows:

$$F_{IMP|ORB} = F_{IMP|ORB} + \left(\frac{\Delta X}{12}\right) F_{Y IMP|ORB} - \left(\frac{\Delta Y}{12}\right) F_{A IMP|ORB}$$

$$\left\{ \begin{array}{l} X_O 1089.6 \\ Y_O 0.0 \\ Z_O 375.0 \end{array} \right\} \left\{ \begin{array}{l} X_O 1076.7 \\ Y_O 0.0 \\ Z_O 375.0 \end{array} \right\}$$

$$\mathcal{L}_{IMP|ORB} = \mathcal{L}_{IMP|ORB} + \left(\frac{\Delta Y}{12}\right) F_{N IMP|ORB} - \left(\frac{\Delta Z}{12}\right) F_{Y IMP|ORB}$$

$$\left\{ \begin{array}{l} X_O 1089.6 \\ Y_O 0.0 \\ Z_O 375.0 \end{array} \right\} \left\{ \begin{array}{l} X_O 1076.7 \\ Y_O 0.0 \\ Z_O 375.0 \end{array} \right\}$$

where, $\Delta X = 1089.6 - 1076.7 = 12.9$ in
 $\Delta Y = 0.0$
 $\Delta Z = 0.0$

$F_{Y IMP (FWD JETS)|ET}$ (Table 5.1.5.2.2.1-1)

$F_{(FWD JETS)|ET}$ (Table 5.1.5.2.2.2-1)

$\mathcal{L}_{IMP (FWD JETS)|ET}$ (Table 5.1.5.2.2.3-1)

NOTE: ET yawing and rolling moment data are at the correct MRC

POST-SEPARATION (ISOLATED ORBITER). The Orbiter free-air aerodynamic force and moment coefficients during the post-separation recovery phase are provided in Volume 3 of this report.

POST-SEPARATION (ISOLATED EXTERNAL TANK). Isolated External Tank aerodynamics for the post-separation disposal trajectory (of no significance to TAL abort separation) are defined in Section 4.1.5.1.2

4.1.6 HINGE MOMENTS

ORIGINAL PAGE IS
OF POOR QUALITY

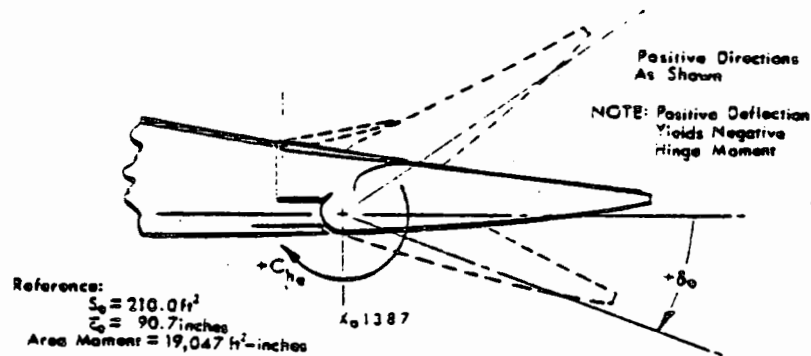
4.1.6 HINGE MOMENTS. Inboard and outboard elevon hinge moment coefficients are presented in both graphical and tabular form for the Mach range 0 to 4.5. Angle of sideslip range is -8° to $+8^\circ$ for angles of attack of -8° , -4° , 0° , and $+4^\circ$. All data are presented for the right-hand panel only (to obtain left-hand panel data, use values tabulated for corresponding negative sideslip angles).

The elevon control hinge moment coefficients are based on theoretical reference dimensions. The reference area is 210 ft² and the reference length (mean aerodynamic chord) is 90.7 inches. These reference values were used for each panel so that the total hinge moment is the sum of the individual panel moments:

where,

$$HM_{eTOTAL} = HM_{eINBOARD} + HM_{eOUTBOARD}$$

$$HM_e = C_{he} (\bar{q} S_e \bar{c}_e)$$



OR

$$HM_{eTOTAL} = \bar{q} S_e \bar{c}_e (C_{heINBOARD} + C_{heOUTBOARD})$$

| ELEVON DEFLECTION | | HINGE MOMENT |
|-------------------|-----------------|--------------|
| Elevon | $+ \delta_e$ | $-C_{he}$ |
| Right | $+ \delta_{eR}$ | $-C_{heR}$ |
| Left | $+ \delta_{eL}$ | $-C_{heL}$ |

The hinge moment coefficients are then described by:

$$C_{he_{TOTAL1}} = C_{he_{INBOARD}} + \Delta C_{he_{ELEVON1}} + \Delta C_{he_{IFLEX}}$$

$$C_{he_{TOTAL0}} = C_{he_{OUTBOARD}} + \Delta C_{he_{ELEVON0}} + \Delta C_{he_{OFLEX}}$$

where;

$$C_{he_{INBOARD}} = \text{rigid-body, inboard elevon hinge moment coefficient} \quad (\text{Figure 5.1.6-1})$$

$$C_{he_{OUTBOARD}} = \text{rigid-body, outboard elevon hinge moment coefficient} \quad (\text{Figure 5.1.6-2})$$

$$\Delta C_{he_{ELEVON1(0)}} = \text{change in elevon hinge moment coefficient due to deflection of inboard panel, } \delta_{e1}, \text{ or outboard panel, } \delta_{e0}$$

$$= Bx + Cx^2 + Dy + Exy + Fy^2$$

$$\text{with } x = (\delta_{e1_{OFF\ NOM}} - \delta_{e1_{NOM}})$$

$$y = (\delta_{e0_{OFF\ NOM}} - \delta_{e0_{NOM}})$$

and coefficients B, C, D, E, & F

Inboard (Tables 5.1.6-1 through -4)

Outboard (Tables 5.1.6-5 through -8)

$$\Delta C_{he_{IFLEX}} = \text{Change in inboard elevon hinge moment coefficient due to aeroelastic deformation.}$$

$$= C_{he_{TOTAL1}} - (C_{he_{INBOARD}} + \Delta C_{he_{ELEVON1}})$$

nominal δ_{e1}/δ_{e0} (Figure 5.1.6-3)

off-nominal δ_{e1}/δ_{e0} (See Section 5.1.8)

$\Delta C_{he\delta_{FLEX}}$ = Change in outboard elevon hinge moment coefficient due to aeroelastic deformation.

$$= C_{he_{TOTAL_0}} - (C_{he_{OUTBOARD}} + \Delta C_{he_{ELEVON_0}})$$

nominal $\delta_{e_1} / \delta_{e_0}$ (Figure 5.1.6-4)

off-nominal $\delta_{e_1} / \delta_{e_0}$ (See Section 5.1.8)

An alternate method of determining the change in the longitudinal coefficients due to aeroelastic deformation at or near the zero sideslip condition (due to rotation of the elevon about its hinge line) is proportional to the hinge moment on the elevon. The change in the longitudinal coefficients may be obtained by determining the rigid coefficient values from the appropriate tables (Sections 5.1.1.1.1-1, 5.1.1.1.1-2, or 5.1.1.1.1-3, and Section 5.1.8) at both the rigid and flexible elevon deflection angles and subtracting the "rigid" from the "flexible" value. The flexible elevon deflection is obtained by:

$$\delta_{e_1}^F = \delta_{e_1} + \Delta \delta_{e_{FLEX_1}}$$

where,

$$\Delta \delta_{e_{FLEX_1}} = K_1 \bar{q} S_e \bar{c}_e C_{he_{TOTAL_{FLEX_1}}}$$

K_1 = Inboard elevon spring constant $(1.547 \times 10^{-6} \text{ deg/in.-lb})$

K_0 = Outboard elevon spring constant $(3.323 \times 10^{-6} \text{ deg/in.-lb})$

$C_{he_{TOTAL_{FLEX_1}}}$ = Total inboard flexible hinge moment coefficient

$$= \frac{-(C_{he_{OUTBOARD}} + \Delta C_{he_{ELEVON_0}})(C_{he_{\delta_{e_1} K_0} \bar{q} S_e \bar{c}_e}) - (C_{he_{INBOARD}} + \Delta C_{he_{ELEVON_1}})(1 - C_{he_{\delta_{e_0} K_0} \bar{q} S_e \bar{c}_e})}{C_{he_{\delta_{e_0} K_0} \bar{q} S_e \bar{c}_e}(C_{he_{\delta_{e_1} K_1} \bar{q} S_e \bar{c}_e}) - (1 - C_{he_{\delta_{e_1} K_1} \bar{q} S_e \bar{c}_e})(1 - C_{he_{\delta_{e_0} K_0} \bar{q} S_e \bar{c}_e})}$$

$C_{he_{TOTAL_{FLEX_0}}}$ = Total outboard flexible hinge moment coefficient

$$= \frac{-(C_{he_{INBOARD}} + \Delta C_{he_{ELEVON_1}})(C_{he_{\delta_{e_1} K_1} \bar{q} S_e \bar{c}_e}) - (C_{he_{OUTBOARD}} + \Delta C_{he_{ELEVON_0}})(1 - C_{he_{\delta_{e_1} K_1} \bar{q} S_e \bar{c}_e})}{C_{he_{\delta_{e_0} K_0} \bar{q} S_e \bar{c}_e}(C_{he_{\delta_{e_1} K_1} \bar{q} S_e \bar{c}_e}) - (1 - C_{he_{\delta_{e_1} K_1} \bar{q} S_e \bar{c}_e})(1 - C_{he_{\delta_{e_0} K_0} \bar{q} S_e \bar{c}_e})}$$

$$C_{he_{\delta_{e_0}}} = D + E_x + 2F_y$$

$$C_{he_{\delta_{e_1}}} = B + 2C_x + E_y$$



Coefficients B, C, D, E, & F

(Tables 5.1.6-1 through -4)

$$C_{heo\delta_{e0}} = D + Ex + 2Fy$$

$$C_{heo\delta_{e1}} = B + 2Cx + Ey$$

Coefficients B, C, D, E, & F

(Tables 5.1.6-5 through -8)

ORIGINAL PAGE IS
OF POOR QUALITY

4.1.7 UNCERTAINTIES

4.1.7 UNCERTAINTIES

4.1.7 **AERODYNAMIC DATA UNCERTAINTIES.** This section defines the aerodynamic data uncertainties and associated terms for the mated vehicle, its elements (Orbiter, External Tank, and Solid Rocket Boosters), and components (wing, elevons, and vertical tail). Uncertainties for SRB and RTLS abort separations are also defined.

Laboratory (wind tunnel), experimental, and flight test data are always accompanied by measurement precision error. It, therefore, becomes important to assign some parameter, such as a limit of error, to represent the precision of data measurements. The error in a measurement is the observed value minus the true value, where the true value is unknown. Errors can be classified as either accidental or systematic. Accidental errors are those which, in a large number of measurements, will be negative as often as positive and will, therefore, affect a mean value only slightly. Systematic errors, arising from the same cause, will affect the mean value in the same sense (either positive OR negative) and, rather than balance one another, will result in a definite bias to a mean. Examples of systematic errors would be model support effects, wind tunnel wall effects, blockage, engine gimbal biases, thrust biases, flight mass summaries, and the like. When all systematic errors have been eliminated (insofar as possible), the sample of individual repeated measurements of a quantity can be considered with the objective of securing the best estimate of the true value and assessing the degree of reproducibility which has been obtained. The best estimate of the unknown true value has been obtained from Space Shuttle test flights utilizing flight data measurements coupled with extensive analysis of flight to predicted comparisons. The best estimate of the unknown true value is the mean value of all these comparisons.

4.1.7.1 **LAUNCH VEHICLE, ELEMENTS, AND COMPONENTS.** The true values (wind tunnel data adjusted to flight levels and trends) of the aerodynamic characteristics of the total launch vehicle, the elements, and the components are given in the data section [5.1]. Uncertainties, described in this section, represent deviations from those true values and describe the scattering of observations about the mean. These deviations about the mean should be treated as three-sigma errors normally distributed for statistical error analyses where uncertainties need to be combined. Sigma is defined as the standard deviation, or limit in the probability sense, of the square-root of the average value of the squared deviation of individual values from the mean as the number of values is increased indefinitely.

The element, component, and total vehicle uncertainties may be used for a variety of analyses and combined, therefore, in a variety of ways. Uncertainties are defined for:

| | | |
|---------------------------------|---|---------------|
| Orbiter Vehicle | } | ELEMENTS |
| External Tank | | |
| Left-Hand Solid Rocket Booster | | |
| Right-Hand Solid Rocket Booster | | |
| Wing | } | COMPONENTS |
| Inboard/Outboard Elevons | | |
| Vertical Tail | | |
| First-Stage | } | TOTAL VEHICLE |
| Second-Stage | | |

Guidelines intended for usage of the uncertainties are included. The following items are applicable (unless otherwise specified):

- (1) Transfer of all moment uncertainty terms and moment coefficients may be performed separately, prior to summation.
- (2) For Mach numbers exceeding 6.0, the uncertainties applicable at Mach 6.0 are to be retained.

4.1.7.1.1 TRAJECTORY ANALYSIS/GUIDANCE, NAVIGATION, AND CONTROL. The uncertainties defined in this sub-section are intended for use in ascent trajectory analyses, subsystem analyses, flight control analyses, day of launch commit-to-flight analyses, and manned simulation studies. These definitions apply to the first and second stage configurations only.

Equations specifying the use of the uncertainties as related to the total vehicle are included. Each of the six aerodynamic forebody coefficients are to be treated separately and the base coefficients are to be combined separately. A total incremental result is specified by appropriate equations. The total forebody aerodynamic coefficient uncertainties are obtained for four flight regimes as outlined below.

```

*****
*
*   Note that all moments are about a Moment Reference Center
*   (MRC) of XT976, YT0, ZT400 EXCEPT for the ground wind
*   phase where the MRC is at XT2468.
*
*****

```

It has been assumed that users will be comparing analyses performed WITH uncertainties to analyses conducted WITHOUT uncertainties.

GROUND WINDS (M = 0).

$$\Delta C_{() \text{ TOTAL AERO}} = |(1 + k_{1,2} K_{1 \text{ OR } 2}) C_{() \text{ W/O TOWER}}|$$

where, () = the symbol applicable to coefficient being analyzed:
 N = Normal Force
 A = Axial Force
 m = Pitching Moment
 Y = Side Force
 n = Yawing Moment
 l = Rolling Moment

$k_{1,2}$ = post lift-off parameter

K_1 = LONGITUDINAL tower interference factor

K_2 = LATERAL-DIRECTIONAL tower interference factor

TRANSITION (0 ≤ M ≤ 0.6)

$$\Delta C_{() \text{ TOTAL AERO}} = \left| \Delta C_{() \text{ FIRST STAGE M=0.60}} \left[1 - \left(\frac{|\alpha \text{ or } \beta| - 12}{78} \right) \right] + \left| C_{() \text{ TRAN @ 90°}} \left(\frac{|\alpha \text{ or } \beta| - 12}{78} \right) \right| \right|$$

Longitudinal $12^\circ \leq \alpha \leq 90^\circ$
 Lateral-Directional $12^\circ \leq \beta \leq 90^\circ$

where, () = (as above)

$\Delta C_{() \text{ FIRST STAGE M=0.60}}$ = First-stage uncertainty at M = 0.6.

$C_{() \text{ TRAN @ 90°}}$ = Transition coefficient at $\alpha = 90^\circ$

LOW ATTITUDE (M ≥ 0.6).

$$\Delta C_{() \text{ TOTAL AERO}} = \Delta C_{() f}$$

where, () = (as above)

Table 4.1.7.1.1-1 presents a summary of the total vehicle uncertainties, the figures where they may be found, and the manner in which they are to be correlated when analyzing the effect on a specific parameter due to the application of any uncertainty. In order to perform an uncertainty analysis on any of the six aerodynamic coefficients or the base terms, the following procedure is to be followed:

1. Determine uncertainty to be analyzed and locate in Table under 'INCREMENTAL COEFFICIENT MULTIPLIER'.
2. Look at column under uncertainty and note the row(s) where a plus or minus one is located. In the column at the left of the table under 'ΔC' find the terms which correspond to the row(s) noted above.
3. Above terms are to be correlated using the multipliers (± 1) in the table. Careful attention must be given to the order of the signs on the multipliers (i.e., ± 1 as opposed to $\neq 1$).

Example: ΔC_{Af} to be analyzed
 ΔC_{Af} correlated with $\Delta C'_m |_{\Delta C_A}$ as follows:

$$+\Delta C_{Af} + \Delta C'_m |_{\Delta C_A}$$

$$-\Delta C_{Af} - \Delta C'_m |_{\Delta C_A}$$

(note signs on terms)

4. When more than one column appears under the uncertainty to be analyzed, each column with every combination shown should be analyzed separately with respect to the other columns, as in step 3.

HYPERSONIC VISCOUS.

NOTE: Provided for longitudinal aerodynamics only.

$$\Delta C_{() \text{TOTAL AERO}} = \left| \Delta C_{() \text{SECOND STAGE}} \right| F_1 + \left| C_{() \text{FMF}} \right| F_2$$

where, () = (as above)

subscripts: $\frac{\text{SECOND}}{\text{STAGE}}$ = Second-stage uncertainty

FMF = Free-molecular coefficient

$$F_1 = \begin{cases} 1 & , \text{Kn} \leq 0.01 \\ \sin 90 - \left(\frac{10}{\text{Kn}} \right) * 90 & , 0.01 \leq \text{Kn} \leq 10.0 \\ 0 & , \text{Kn} > 10.0 \end{cases}$$

$$F_2 = \begin{cases} 0 & , \text{Kn} \leq 0.01 \\ \sin \left(\frac{10}{\text{Kn}} \right) * 90 & , 0.01 \leq \text{Kn} \leq 10.0 \\ 1 & , \text{Kn} > 10.0 \end{cases}$$

Kn = Knudsen number.

Table 4.1.7.1.1-1
TOTAL VEHICLE UNCERTAINTIES SUMMARY

| ΔC | CODE | TABLE NUMBER | | INCREMENTAL COEFFICIENT MULTIPLIER (REQUIRED TO FORM CORRELATED UNCERTAINTY ASSESSMENTS DUE TO) | | | | | | | | | | | | | |
|--------------------------------------|--------|--------------|--------------|--|------------------|----|------------------|------------------|----|----|----|------------------|------------------|-------|---|----|---|
| | | FIRST-STAGE | SECOND-STAGE | ΔC _{Ai} | ΔC _{Ni} | | ΔC _{mi} | ΔC _{Yi} | | | | ΔC _{ni} | ΔC _{Li} | ΔBASE | | | |
| | | UNCERTAINTY | UNCERTAINTY | | | | | | | | | | | | | | |
| ΔC _{Ai} | DCA | 5.1.7.1.1-1 | 5.1.7.1.1-2 | ±1 | 0 | 0 | 0 | 0 | 0 | 0 | 0 | 0 | 0 | 0 | 0 | | |
| ΔC _{Ni} | DCN | ↑ | ↑ | 0 | ±1 | ±1 | ↓ | ↓ | ↓ | ↓ | ↓ | ↓ | ↓ | ↓ | ↓ | | |
| ΔC _{mi} | DPM | | | 0 | 0 | ±1 | ↓ | ↓ | ↓ | ↓ | ↓ | ↓ | ↓ | ↓ | ↓ | ↓ | |
| ΔC _{Yi} | DCY | | | 0 | 0 | 0 | ±1 | ±1 | ±1 | ±1 | ↓ | ↓ | ↓ | ↓ | ↓ | ↓ | |
| ΔC _{ni} | DYM | | | 0 | 0 | 0 | 0 | 0 | 0 | 0 | ±1 | ↓ | ↓ | ↓ | ↓ | ↓ | |
| ΔC _{Li} | DRM | | | 0 | 0 | ↓ | ↓ | ↓ | ↓ | ↓ | 0 | ±1 | ↓ | ↓ | ↓ | ↓ | |
| ΔC _{mi} ΔC _{Ai} | DCMTA | | | ±1 | ±1 | ±1 | ↓ | ↓ | ↓ | ↓ | ↓ | ↓ | ↓ | ↓ | ↓ | ↓ | ↓ |
| ΔC _{mi} ΔC _{Ni} | DCMTN | | | 0 | 0 | 0 | ±1 | ±1 | ↓ | ↓ | ↓ | ↓ | ↓ | ↓ | ↓ | ↓ | ↓ |
| Δ(ΔC _{mi})ΔC _{Ni} | DDCMTN | | | 0 | 0 | 0 | ±1 | ±1 | ↓ | ↓ | ↓ | ↓ | ↓ | ↓ | ↓ | ↓ | ↓ |
| ΔC _{ni} ΔC _{Yi} | DCYMT | | | 0 | 0 | 0 | 0 | 0 | ±1 | ±1 | ±1 | ±1 | ↓ | ↓ | ↓ | ↓ | ↓ |
| Δ(ΔC _{ni})ΔC _{Yi} | DDCYMT | | | 0 | 0 | 0 | 0 | 0 | ±1 | ±1 | ±1 | ±1 | ↓ | ↓ | ↓ | ↓ | ↓ |
| ΔC _{Li} ΔC _{Yi} | DCLT | | | 0 | 0 | 0 | 0 | 0 | ±1 | ±1 | ±1 | ±1 | ↓ | ↓ | ↓ | ↓ | ↓ |
| Δ(ΔC _{Li})ΔC _{Yi} | DDCLT | | | 0 | 0 | 0 | 0 | 0 | ±1 | ±1 | ±1 | ±1 | ↓ | ↓ | ↓ | ↓ | ↓ |
| ΔF _{BASE} | DFAB | | | 5.1.7.1.1-3 | 5.1.7.1.1-3 | 0 | 0 | 0 | 0 | 0 | 0 | 0 | 0 | 0 | 0 | ±1 | ↓ |
| ΔF _{NBASE} | DFNB | | | 0 | 0 | 0 | 0 | 0 | 0 | 0 | 0 | 0 | 0 | 0 | 0 | ±1 | ↓ |
| ΔM _{BASE} ΔF _A | DMAB | | | 0 | 0 | 0 | 0 | 0 | 0 | 0 | 0 | 0 | 0 | 0 | 0 | ±1 | ↓ |
| ΔM _{BASE} ΔF _N | DMNB | 0 | 0 | 0 | 0 | 0 | 0 | 0 | 0 | 0 | 0 | 0 | 0 | ±1 | ↓ | | |

4.1.7-6

STS85-0118-1

4.1.7.1.2 STRUCTURES. The uncertainties defined in this sub-section pertain to the first-stage mated elements, wing, elevon, and vertical tail only. It has been assumed that users will be performing Monte Carlo/day-of-launch margin assessment analyses only. The following instructions are, therefore, directed toward this end.

4.1.7.1.2.1 MATED ELEMENTS. Equations defining the use of the uncertainties as related to the mated elements (Orbiter, External Tank, Left- and Right-Hand Solid Rocket Boosters) are provided and the uncertainty values to be used are given in Section 5.1.7.1.2.1.

The forebody force and moment uncertainty levels are obtained in the following manner:

$$\Delta C_{()LV} = \sum_{i=1}^4 [(\Delta C_{()i} / 3.0)(K_{()i})]$$

where, () = applicable symbol denoting particular coefficient being analyzed:

- N = Normal Force
- A = Axial Force
- m = Pitching Moment
- Y = Side Force
- n = Yawing Moment
- l = Rolling Moment

i = applicable number denoting particular element being analysed:

- 1 = Orbiter Vehicle
- 2 = External Tank
- 3 = Left-hand SRB
- 4 = Right-hand SRB

$K_{()i}$ = Sigma level randomly selected by Monte Carlo scheme (TO BE PROVIDED BY THE USER).

The forebody first-order transfer terms are obtained in the following manner:

$$\Delta C'_{m|\Delta C_A} = [0.2608(\Delta C_{A1}/3.0)(K_{A1})]$$

$$\Delta C'_{m|\Delta C_N} = \sum_{i=1}^4 [X_{P_i} (\Delta C_{N_i}/3.0)(K_{N_i})]$$

$$\Delta C'_{n|\Delta C_Y} = \sum_{i=1}^4 [X_{Y_i} (\Delta C_{Y_i}/3.0)(K_{Y_i})]$$

$$\Delta C'_{l|\Delta C_Y} = [Z_{R1} (\Delta C_{Y1}/3.0)(K_{Y1})]$$

$$\Delta C'_{n|\Delta C_A} = 0.0$$

$$\Delta C'_{l|\Delta C_N} = 0.0$$

The forebody second-order transfer terms are obtained in the following manner:

$$\Delta(\Delta C_{m}')_{\Delta C_N} = \sum_{i=1}^4 \{ (\Delta X_{P_i} / 3.0) (K_{P_i}) [C_{N_i} + (\Delta C_{N_i} / 3.0) (K_{N_i})] \}$$

$$\Delta(\Delta C_{n}')_{\Delta C_V} = \sum_{i=1}^4 \{ (\Delta X_{V_i} / 3.0) (K_{N_i}) [C_{V_i} + (\Delta C_{V_i} / 3.0) (K_{V_i})] \}$$

$$\Delta(\Delta C_{l}')_{\Delta C_V} = \{ (\Delta Z_{R_1} / 3.0) (K_{Z_1}) [C_{V_1} + (\Delta C_{V_1} / 3.0) (K_{V_1})] \}$$

The base terms are obtained in the following manner:

$$\Delta F_{A_{BASE}} = \sum_{i=1}^4 [(\Delta F_{A_{b_i}} / 3.0) (K_{A_{b_i}})]$$

$$\Delta F_{N_{BASE}} = [(\Delta F_{N_{b_1}} / 3.0) (K_{N_{b_1}})]$$

$$\Delta M_{BASE} |_{\Delta F_A} = [(\Delta F_{A_{b_1}} / 3.0) (K_{A_{b_1}}) (X_{P_b})]$$

$$\Delta M_{BASE} |_{\Delta F_N} = [(\Delta F_{N_{b_1}} / 3.0) (K_{N_{b_1}}) (Z_{P_b})]$$

Reference Table 5.1.7.1.2.1-1

FOREBODY NORMAL FORCE COEFFICIENT

C_{Nf} (CNO, CNE, CNS)
subscript: O - Orbiter
ET - External Tank
LSRB - Left-hand SRB
RSRB - Right-hand SRB

UNCERTAINTY

ΔC_{Nf} (DCNO, DCNE, DCNS)
subscript: O - Orbiter
ET - External Tank
LSRB - Left-hand SRB
RSRB - Right-hand SRB

FOREBODY AXIAL FORCE COEFFICIENT UNCERTAINTY

ΔC_{Af} (DCAO, DCAE, DCAS)
subscript: O - Orbiter
ET - External Tank
LSRB - Left-hand SRB
RSRB - Right-hand SRB

FOREBODY PITCHING MOMENT COEFFICIENT UNCERTAINTY

ΔC_{mf} (DCMO, DCME, DCMS)
subscript: O - Orbiter
ET - External Tank
LSRB - Left-hand SRB
RSRB - Right-hand SRB



Reference Table 5.1.7.1.2.1-2

FOREBODY SIDE FORCE COEFFICIENT

C_{Y_f} , (CYO, CYE, CYS)

subscript: 0 - Orbiter
ET - External Tank
LSRB - Left-hand SRB
RSRB - Right-hand SRB

UNCERTAINTY

ΔC_{Y_f} , (DCYO, DCYE, DCYS)

subscript: 0 - Orbiter
ET - External Tank
LSRB - Left-hand SRB
RSRB - Right-hand SRB

FOREBODY YAWING MOMENT COEFFICIENT UNCERTAINTY

ΔC_{n_f} , (DCYMO, DCYME, DCYMS)

subscript: 0 - Orbiter
ET - External Tank
LSRB - Left-hand SRB
RSRB - Right-hand SRB

FOREBODY ROLLING MOMENT COEFFICIENT UNCERTAINTY

ΔC_{l_f} , (DCLO, DCLE, DCLS)

subscript: 0 - Orbiter
ET - External Tank
LSRB - Left-hand SRB
RSRB - Right-hand SRB

Reference Table 5.1.7.1.2.1-3

LONGITUDINAL AERODYNAMIC CENTER-PITCH

X_p , (XPO, XPE, XPS)
subscript: 0 - Orbiter
ET - External Tank
LSRB - Left-hand SRB
RSRB - Right-hand SRB

UNCERTAINTY

ΔX_p , (DXPO, DXPE, DXPS)
subscript: 0 - Orbiter
ET - External Tank
LSRB - Left-hand SRB
RSRB - Right-hand SRB

LATERAL-DIRECTIONAL AERODYNAMIC CENTER

YAW
 X_y , (XYO, XYE, XYS)
subscript: 0 - Orbiter
ET - External Tank
LSRB - Left-hand SRB
RSRB - Right-hand SRB

UNCERTAINTY

ΔX_y , (DXYO, DXYE, DXYS)
subscript: 0 - Orbiter
ET - External Tank
LSRB - Left-hand SRB
RSRB - Right-hand SRB

ROLL

Z_R , (ZRO)
subscript: 0 - Orbiter
ET - External Tank
LSRB - Left-hand SRB
RSRB - Right-hand SRB

UNCERTAINTY

ΔZ_R , (DZRO)
subscript: 0 - Orbiter
ET - External Tank
LSRB - Left-hand SRB
RSRB - Right-hand SRB

Reference Table 5.1.7.1.1-3

POWER-ON BASE

NORMAL FORCE COEFFICIENT UNCERTAINTY

$$\Delta C_{N_b} = \Delta F_{N_b} / \bar{q}S$$

ΔF_{N_b} , (DFNB)

subscript: O - Orbiter
ET - External Tank
LSRB - Left-hand SRB
RSRB - Right-hand SRB

AXIAL FORCE COEFFICIENT UNCERTAINTY

$$\Delta C_{A_b} = \Delta F_{A_b} / \bar{q}S$$

ΔF_{A_b} , (DFABO, DFABE, DFABS)

subscript: O - Orbiter
ET - External Tank
LSRB - Left-hand SRB
RSRB - Right-hand SRB

\bar{q} = freestream dynamic pressure

S = reference area 2690.0 ft²

X_{p_b} = 1296.3 inches

Z_{p_b} = 336.5 inches

4.1.7.1.2.2 WING UNCERTAINTIES. The basic wing shear, bending, and torsion uncertainties are presented herein. The data are to be used primarily for structural margin assessment analyses.

The wing panel load coefficient uncertainties are based on a reference area of 2690 ft² and a reference length of 936.68 inches in bending and 474.8 inches in torsion. The moment reference center is located at (X₀1308, Y₀105, Z₀288). The following information is presented in Table 5.1.7.1.2.2-1.

SHEAR COEFFICIENT UNCERTAINTY

$$\Delta C_{S\text{WING}}, \text{ (DCSW)}$$

BENDING COEFFICIENT UNCERTAINTY

$$\Delta C_{B\text{WING}}, \text{ (DCBW)}$$

TORSION COEFFICIENT UNCERTAINTY

$$\Delta C_{T\text{WING}}, \text{ (DCTW)}$$

LATERAL-DIRECTIONAL AERODYNAMIC CENTER-BENDING

$$a.c._B, \text{ (ACB)}$$

UNCERTAINTY

$$\Delta a.c._B, \text{ (DACB)}$$

LONGITUDINAL AERODYNAMIC CENTER- TORSION

$$a.c._T, \text{ (ACT)}$$

UNCERTAINTY

$$\Delta a.c._T, \text{ (DACT)}$$

NOTE: For Mach numbers greater than 6.0 use the uncertainties given at 6.0.

4.1.7.1.2.3 **ELEVON UNCERTAINTIES.** The basic elevon hinge moment uncertainties are given for the inboard and outboard elevons. The data are to be used for trajectory shaping studies and structural margin assessment analyses.

The elevon control hinge moment coefficient uncertainties are based on theoretical reference dimensions. The reference area is 210 ft² and the reference length (mean aerodynamic chord) is 90.7 inches. The following information is presented in Table 5.1.7.1.2.2-1.

ΔC_{he_i} (DCHEI)
= Rigid-body, inboard elevon
hinge moment coefficient
uncertainty about the elevon
hinge line

ΔC_{he_o} (DCHEO)
= Rigid-body, outboard elevon
hinge moment coefficient
uncertainty about the elevon
hinge line

NOTE: For Mach numbers greater than 6.0 use the uncertainties given at 6.0.

4.1.7.1.2.4 VERTICAL UNCERTAINTIES. The basic vertical six component force and moment uncertainties are presented herein. The data are to be used primarily for structural margin assessment analyses.

The vertical tail panel load uncertainties are presented in coefficient form for normal force, axial force, pitching moment, root shear, bending, and torsion. The data are based on a reference area of 413.25 ft² and a reference length of 199.80 inches. The Moment Reference Center is located at (X_0 1414.3, Y_0 0, Z_0 503). The following information is presented in Table 5.1.7.1.2.4-1.

AXIAL FORCE COEFFICIENT UNCERTAINTY

$\Delta C_{\text{VERT AXIAL}}$, (DCAV)

SHEAR COEFFICIENT

$C_{\text{VERT SHEAR}}$, (CSV)

SHEAR COEFFICIENT UNCERTAINTY

$\Delta C_{\text{VERT SHEAR}}$, (DCSV)

NORMAL FORCE COEFFICIENT UNCERTAINTY

$\Delta C_{\text{VERT NORMAL}}$, (DCNV)

BENDING COEFFICIENT UNCERTAINTY

$\Delta C_{\text{VERT BENDING}}$, (DCBV)

PITCHING COEFFICIENT UNCERTAINTY

$\Delta C_{\text{VERT PITCHING}}$, (DCMV)

TORSION COEFFICIENT UNCERTAINTY

$\Delta C_{\text{VERT TORSION}}$, (DCTV)

LATERAL-DIRECTIONAL AERODYNAMIC CENTER

BENDING

a.c.g., (ACBV)

UNCERTAINTY

Δ a.c.g., (DACBV)



LONGITUDINAL AERODYNAMIC CENTER

TORSION

a.c.T, (ACTV)

UNCERTAINTY

Δ a.c.T, (DACTV)

NOTE: For Mach numbers greater than 6.0 use the uncertainties given at 6.0.

- 4.1.7.2 SEPARATION: Statistical principles have also been applied in defining separation tolerances about a mean. However, variations (as a result of the complexity of the model(s) used for separation testing) are not statistically distributed about a mean but either exist or do not exist when applied to the uncertainty evaluation.

For separation, tolerances represent the uncertainty associated with the ability of the test apparatus to achieve the exact programmed conditions (model position - attitude, jet plume pressure, etc.) as well as the inability to achieve an exact steady state measurement of the forces and moments on the test model. Variations, on the other hand, represent the uncertainty associated with differences between model and flight configurations and flow field simulation parameters. The assessment of separation uncertainties is considerably more complex than that for the launch configuration. The total uncertainty (i.e., combined tolerance and variation) is to be used in conducting flight simulation studies.

Wind tunnel data were used to define separation uncertainties because of the inaccuracies associated with flight measurements at the low flight dynamic pressure and the presence of booster separation motor (BSM) and SRB plume effects experienced during separation. Flight measurements data are not available for the external tank during RTLS abort separation.

Separation uncertainties are defined for:

- 4.1.7.2.1 SOLID ROCKET BOOSTERS (SRB)
- 4.1.7.2.2 RETURN-TO-LAUNCH-SITE (RTLS) INTACT ABORT
- 4.1.7.2.3 TRANS-ATLANTIC ABORT LANDING (TAL) INTACT ABORT

4.1.7.2.1 SOLID ROCKET BOOSTER (SRB). Uncertainties to be used with the SRB separation aerodynamic data base presented in Section 4.1.2 are defined herein. These uncertainties are based on: (1) a data interpolation error; (2) an SRB configuration asymmetry error; and (3) a BSM plume simulation error. The values furnished represent total uncertainties (i.e., combined tolerance-variation effect) and are applicable to the SRB separation total aerodynamic coefficients. Uncertainties are provided for both the SRB's and the Orbiter-plus-External Tank (OET) configurations for two conditions: 1) Booster Separation Motor (BSM) plume-on; and 2) BSM plume-off. The same plume-on uncertainties are to be used for all plume momentum ratios. The proposed uncertainties for each aerodynamic coefficients are applicable to any combination of separation attitude and vehicle-to-vehicle relative attitude and position (i.e., α , β , $\Delta\alpha$, $\Delta\beta$, Δx , Δy , and Δz). The uncertainty for a particular force or moment during SRB separation is calculated from the coefficient uncertainty, $\Delta C_{()_{TOTAL AERO}}$, as follows:

$$\Delta()_{TOTAL AERO} = \bar{q} S \Delta C_{()_{TOTAL AERO}}$$

(N) = Normal Force
(Y) = Side Force

$$\Delta()_{TOTAL AERO} = \bar{q} S L_B \Delta C_{()_{TOTAL AERO}}$$

(M) = Pitching Moment
(Y) = Yawing Moment
(R) = Rolling Moment

Axial force is not utilized in SRB separation dynamic studies. Uncertainties are presented for the pre-separation phase (first-stage vehicles) and the separation phase (OET and SRB's in proximity).

PRE-SEPARATION

First stage (SSME power-on) uncertainties, defined in section 4.1.7.1, will be used for the SSME power-off SRB pre-separation maneuver with the exception of base force and moment terms which will be neglected. The pre-separation flight conditions are identical with those at the end of first stage boost. These uncertainties are presented as a function of Mach number and angle-of-attack (longitudinal) or sideslip angle (lateral-directional). The last uncertainty value shown should be used for angle-of-attack or sideslip values exceeding ± 8 degrees.

SEPARATION (PROXIMITY)

Uncertainties for the proximity phase of SRB separation are defined for the total aerodynamic coefficients as follows:

$\Delta C_{()}^{TOTAL AERO}$ = Total uncertainty on force or moment coefficient for OET in the presence of both SRB's for BSM plume-on and - off operation.
| OET

Subscript: (N)
(M)
(Y)
(L)
(R) } (Table 5.1.7.2.1-1)

$\Delta C_{()}^{TOTAL AERO}$ = Total uncertainty on force or moment coefficient for left or right SRB in presence of OET and other SRB for BSM plume-on and plume-off.
| SRB

Subscript: (N)
(M)
(Y)
(L)
(R) } (Table 5.1.7.2.1-2)



Axial force is not defined for either vehicle during the SRB separation maneuver; and rolling moment for the SRB is zero as a result of configuration symmetry.

POST-SEPARATION (ISOLATED VEHICLE)

The uncertainties for the Orbiter-plus-Tank (OET) and SRB's in free air following completion of SRB separation are defined in Section 4.1.7.1.

4.1.7.2.2 RETURN-TO-LAUNCH-SITE (RTLS) INTACT ABORT. Uncertainties to be used with the RTLS abort separation aerodynamics presented in Section 4.1.5.1 are provided herein for use in conducting RTLS abort separation trajectory studies. The uncertainties are comprised of tolerances and variations which are combined in RSS fashion to give a total aerodynamic uncertainty for application to the data base. Tolerances consist of wind tunnel and plume scaling measurement errors; whereas, variations deal with experimental-to-flight scaling errors. These uncertainties were derived for normal separation at Mach 6.0 and a dynamic pressure of ≈ 8.0 psf. They are, however, equally applicable to off-nominal separation conditions over the range of 5 to 10 psf. The uncertainties are applicable to any combination of separation attitude and position (i.e., α , β , $\Delta\alpha$, $\Delta\beta$, Δx , ΔY , ΔZ). The uncertainty for a particular force or moment during RTLS separation is calculated from the coefficient uncertainty, ΔC (), as follows:

()
TOTAL
AERO

$$\Delta ()_{\text{TOTAL AERO}} = \bar{q} S \Delta C ()_{\text{TOTAL AERO}}$$

(N) = Normal Force
(A) = Axial Force
(Y) = Side Force

$$\Delta ()_{\text{TOTAL AERO}} = \bar{q} S L_B \Delta C ()_{\text{TOTAL AERO}}$$

(M) = Pitching Moment
(N) = Yawing Moment
(R) = Rolling Moment

PRE-SEPARATION (TURN-AROUND MANEUVER)

Uncertainties for the pre-separation turn-around maneuver prior to RTLS abort separation are the same as second stage launch vehicle uncertainties defined in Section 4.1.7.1. These uncertainties are presented as a function of Mach number and angle-of-attack (longitudinal) or sideslip angle (lateral-directional). The last uncertainty value shown should be used for angle-of-attack or sideslip values exceeding ± 8 degrees.

PRE-SEPARATION (MATED COAST)

Uncertainties for the mated coast maneuver prior to RTLS abort separation are defined for the total aerodynamic coefficient as follows:

$$\Delta C_{() \text{ TOTAL AERO}} \Big|_{\text{OET}} = \text{Total uncertainty force or moment coefficient for the Orbiter-plus-tank (OET) for RCS-on and off operation}$$

Subscript: (N)
(A)
(~~W~~)
(Y)
(V)
(L) } (Table 5.1.7.2.2-1)

The values provided in Table 5.1.7.2.2-1 are to be used for all combinations of angle-of-attack and sideslip and dynamic pressure between 5 and 10 psf.

SEPARATION (PROXIMITY)

Uncertainties for the proximity phase of RTLS abort separation are defined for the total aerodynamic coefficient as follows:

$\Delta C_{()}^{TOTAL AERO} |_{ORB}$ = Total uncertainty on force or moment coefficient for the Orbiter during separation.

Subscript: (N)
(A)
(W)
(Y)
(H)
(S) } (Table 5.1.7.2.2-2)

$\Delta C_{()}^{TOTAL AERO} |_{ET}$ = Total uncertainty on force or moment coefficient for the ET during separation.

Subscript: (N)
(A)
(W)
(Y)
(H)
(S) } (Table 5.1.7.2.2-3)

POST-SEPARATION (ISOLATED VEHICLE)

Uncertainties for the Post-separation isolated Orbiter are presented in Volume 3. Post-separation isolated ET uncertainties are found in Section 4.1.7.1.

4.1.7.2.3 TRANSATLANTIC ABORT LANDING (TAL) INTACT ABORT. Uncertainties to be used with the TAL abort separation aerodynamics data base presented in Section 4.1.5.2. are defined herein. These uncertainties are based on: (1) tolerances consisting of wind tunnel measurement errors; and (2) empirical error factors related to plume modeling accuracy which are presented as percentages of the plume impingement force or moment. These uncertainties were derived for nominal separation at Mach 25 and dynamic pressure less than 1.0 psf. The uncertainties are applicable to any combination of separation attitude and position (i.e., α , β , $\Delta\alpha$, $\Delta\beta$, Δx , Δy , Δz).

PRE-SEPARATION (MATED COAST)

Uncertainties for the mated vehicle maneuver prior to TAL abort separation are defined for the total aerodynamic force or moment as follows:

$$\Delta F_{N_{\text{TOTAL AERO}}} \Big|_{\text{OET}} = \left(\left\{ \Delta C_{N_{\text{OET}}} \bar{q} S \right\}^2 + \left\{ K_N \left[F_{N_{\text{IMP}}} + F_{N_{\text{IMP}}} \right] \right\}^2 \right)^{\frac{1}{2}}$$

(FWD JETS) (AFT JETS)

$$\Delta F_{A_{\text{TOTAL AERO}}} \Big|_{\text{OET}} = \left(\left\{ \Delta C_{A_{\text{OET}}} \bar{q} S \right\}^2 + \left\{ K_A \left[F_{A_{\text{IMP}}} + F_{A_{\text{IMP}}} \right] \right\}^2 \right)^{\frac{1}{2}}$$

(FWD JETS) (AFT JETS)

$$\Delta M_{\text{TOTAL AERO}} \Big|_{\text{OET}} = \left(\left\{ \Delta C_{M_{\text{OET}}} \bar{q} S L_B \right\}^2 + \left\{ K_M \left[M_{\text{IMP}} + M_{\text{IMP}} \right] \right\}^2 \right)^{\frac{1}{2}}$$

(FWD JETS) (AFT JETS)

$$\Delta F_{Y_{\text{TOTAL AERO}}} \Big|_{\text{OET}} = \left(\left\{ \Delta C_{Y_{\text{OET}}} \bar{q} S \right\}^2 + \left\{ K_Y \left[F_{Y_{\text{IMP}}} + F_{Y_{\text{IMP}}} \right] \right\}^2 \right)^{\frac{1}{2}}$$

(FWD JETS) (AFT JETS)

$$\Delta K_{\text{TOTAL AERO}} \Big|_{\text{OET}} = \left(\left\{ \Delta C_{K_{\text{OET}}} \bar{q} S L_B \right\}^2 + \left\{ K_N \left[K_{\text{IMP}} + K_{\text{IMP}} \right] \right\}^2 \right)^{\frac{1}{2}}$$

(FWD JETS) (AFT JETS)

$$\Delta \mathcal{L}_{\text{TOTAL AERO}} \Big|_{\text{OET}} = \left(\left\{ \Delta C_{\mathcal{L}_{\text{OET}}} \bar{q} S L_B \right\}^2 + \left\{ K_{\mathcal{L}} \left[\mathcal{L}_{\text{IMP}} + \mathcal{L}_{\text{IMP}} \right] \right\}^2 \right)^{\frac{1}{2}}$$

(FWD JETS) (AFT JETS)

where:

$\Delta C_{()_{OET}}$ = OET force or moment coefficient tolerance based on RSS of isolated Orbiter and ET tolerances.

Subscript: (N)
(A)
(M)
(Y)
(Z)
(S) } (Table 5.1.7.2.3-1)

$K_{()}$ = Impingement uncertainty based on fraction of impingement force or moment.

Subscript: (N)
(A)
(M)
(Y)
(Z)
(S) } (Table 5.1.7.2.3-2)

Plume impingement force or moment on ET due to forward downfiring RCS jets (Note: No impingement on Orbiter.) $F_{N_{IMP}}$ (Table 5.1.5.2.1.1-1)
(FWD JETS)

$F_{A_{IMP}}$ (Table 5.1.5.2.1.2-1)
(FWD JETS)

M_{IMP} (Table 5.1.5.2.1.3-1)
(FWD JETS)

$F_{Y_{IMP}}$ (Table 5.1.5.2.2.1-1)
(FWD JETS)

M'_{IMP} (Table 5.1.5.2.2.2-1)
(FWD JETS)

L_{IMP} (Table 5.1.5.2.2.3-1)
(FWD JETS)

Plume impingement force
or moment on Orbiter due
to aft downfiring RCS jets
(Note: No impingement
on ET).

$F_{N_{IMP(AFT JET)}}$ (See Volume 3)

$F_{A_{IMP(AFT JET)}}$ (See Volume 3)

$M_{IMP(AFT JET)}$ (See Volume 3)

$F_{Y_{IMP(AFT JET)}}$ (See Volume 3)

$F_{X_{IMP(AFT JET)}}$ (See Volume 3)

$L_{IMP(AFT JET)}$ (See Volume 3)

SEPARATION (PROXIMITY)

Uncertainties for the proximity phase of TAL abort separation are defined for the total aerodynamic force or moment as follows:

$$\Delta F_{N \text{ TOTAL AERO}} \Big|_{\text{ORB}} = \left(\left\{ \Delta C_N \Big|_{\text{ORB}} \bar{q} S \right\}^2 + \left\{ K_N F_{N \text{ IMP (AFT JETS)}} \right\}^2 \right)^{\frac{1}{2}}$$

$$\Delta F_{N \text{ TOTAL AERO}} \Big|_{\text{ET}} = \left(\left\{ \Delta C_N \Big|_{\text{ET}} \bar{q} S \right\}^2 + \left\{ K_N F_{N \text{ IMP (FWD JETS)}} \right\}^2 \right)^{\frac{1}{2}}$$

$$\Delta F_{A \text{ TOTAL AERO}} \Big|_{\text{ORB}} = \left(\left\{ \Delta C_A \Big|_{\text{ORB}} \bar{q} S \right\}^2 + \left\{ K_A F_{A \text{ IMP (AFT JETS)}} \right\}^2 \right)^{\frac{1}{2}}$$

$$\Delta F_{A \text{ TOTAL AERO}} \Big|_{\text{ET}} = \left(\left\{ \Delta C_A \Big|_{\text{ET}} \bar{q} S \right\}^2 + \left\{ K_A F_{A \text{ IMP (FWD JETS)}} \right\}^2 \right)^{\frac{1}{2}}$$

$$\Delta M_{\text{ TOTAL AERO}} \Big|_{\text{ORB}} = \left(\left\{ \Delta C_m \Big|_{\text{ORB}} \bar{q} S L_B \right\}^2 + \left\{ K_m M_{\text{ IMP (AFT JETS)}} \right\}^2 \right)^{\frac{1}{2}}$$

$$\Delta M_{\text{ TOTAL AERO}} \Big|_{\text{ET}} = \left(\left\{ \Delta C_m \Big|_{\text{ET}} \bar{q} S L_B \right\}^2 + \left\{ K_m M_{\text{ IMP (FWD JETS)}} \right\}^2 \right)^{\frac{1}{2}}$$

$$\Delta F_{Y \text{ TOTAL AERO}} \Big|_{\text{ORB}} = \left(\left\{ \Delta C_Y \Big|_{\text{ORB}} \bar{q} S \right\}^2 + \left\{ K_Y F_{Y \text{ IMP (AFT JETS)}} \right\}^2 \right)^{\frac{1}{2}}$$

$$\Delta F_{Y \text{ TOTAL AERO}} \Big|_{\text{ET}} = \left(\left\{ \Delta C_Y \Big|_{\text{ET}} \bar{q} S \right\}^2 + \left\{ K_Y F_{Y \text{ IMP (FWD JETS)}} \right\}^2 \right)^{\frac{1}{2}}$$

$$\Delta C_{\text{TOTAL AERO}} \Big|_{\text{ORB}} = \left(\left\{ \Delta C_n \Big|_{\text{ORB}} \bar{q} S L_B \right\}^2 + \left\{ K_n \mathcal{L}_{\text{IMP}} \Big|_{\text{AFT JETS}} \right\}^2 \right)^{\frac{1}{2}}$$

$$\Delta C_{\text{TOTAL AERO}} \Big|_{\text{ET}} = \left(\left\{ \Delta C_n \Big|_{\text{ET}} \bar{q} S L_B \right\}^2 + \left\{ K_n \mathcal{L}_{\text{IMP}} \Big|_{\text{FWD JETS}} \right\}^2 \right)^{\frac{1}{2}}$$

$$\Delta \mathcal{L}_{\text{TOTAL AERO}} \Big|_{\text{ORB}} = \left(\left\{ \Delta C_l \Big|_{\text{ORB}} \bar{q} S L_B \right\}^2 + \left\{ K_l \mathcal{L}_{\text{IMP}} \Big|_{\text{AFT JETS}} \right\}^2 \right)^{\frac{1}{2}}$$

$$\Delta \mathcal{L}_{\text{TOTAL AERO}} \Big|_{\text{ET}} = \left(\left\{ \Delta C_l \Big|_{\text{ET}} \bar{q} S L_B \right\}^2 + \left\{ K_l \mathcal{L}_{\text{IMP}} \Big|_{\text{FWD JETS}} \right\}^2 \right)^{\frac{1}{2}}$$

where,

$\Delta C_{(\)_{\text{ORB}}}$

= Orbiter force or moment coefficient tolerance base on RSS of isolated Orbiter tolerances.

Subscript: (N)
(A)
~~(W)~~
(Y)
~~(S)~~
(Q)

} (Table 5.1.7.2.3-3)

$\Delta C_{(\)_{\text{ET}}}$

= ET force or moment coefficient tolerance based on RSS of isolated ET tolerances.

Subscript: (N)
(A)
~~(W)~~
(Y)
~~(S)~~
(Q)

} (Table 5.1.7.2.3-4)

K () = Impingement uncertainties based on fraction of impingement force or moment.

Subscript: (N)
(A)
~~(X)~~
(Y)
~~(Z)~~
~~(W)~~ } (Table 5.1.7.2.3-2)

Plume impingement force or moment on Orbiter due to aft downfiring RCS jets (Note: No impingement on ET).

$F_{N\text{IMP(AFT JET)}}$ (See Volume 3)

$F_{A\text{IMP(AFT JET)}}$ (See Volume 3)

$M_{\text{IMP(AFT JET)}}$ (See Volume 3)

$F_{Y\text{IMP(AFT JET)}}$ (See Volume 3)

$M_{\text{IMP(AFT JET)}}$ (See Volume 3)

$L_{\text{IMP(AFT JET)}}$ (See Volume 3)

Plume impingement force or moment on ET due to forward downfiring RCS jets (Note: No impingement on Orbiter.) $F_{N,IMP}$ (Table 5.1.5.2.1.1-1)
(FWD JETS)

$F_{A,IMP}$ (Table 5.1.5.2.1.2-1)
(FWD JETS)

M_{IMP} (Table 5.1.5.2.1.3-1)
(FWD JETS)

$F_{Y,IMP}$ (Table 5.1.5.2.2.1-1)
(FWD JETS)

$\dot{\phi}_{IMP}$ (Table 5.1.5.2.2.2-1)
(FWD JETS)

\mathcal{L}_{IMP} (Table 5.1.5.2.2.3-1)
(FWD JETS)

POST-SEPARATION (ISOLATED VEHICLE)

Uncertainties for the post-separation isolated Orbiter are presented in Volume 3 Post-Separation isolated ET uncertainties are found in Section 4.1.7.1.

ORIGINAL PAGE IS
OF POOR QUALITY.

4.1.8 STRUCTURAL ANALYSIS DATA



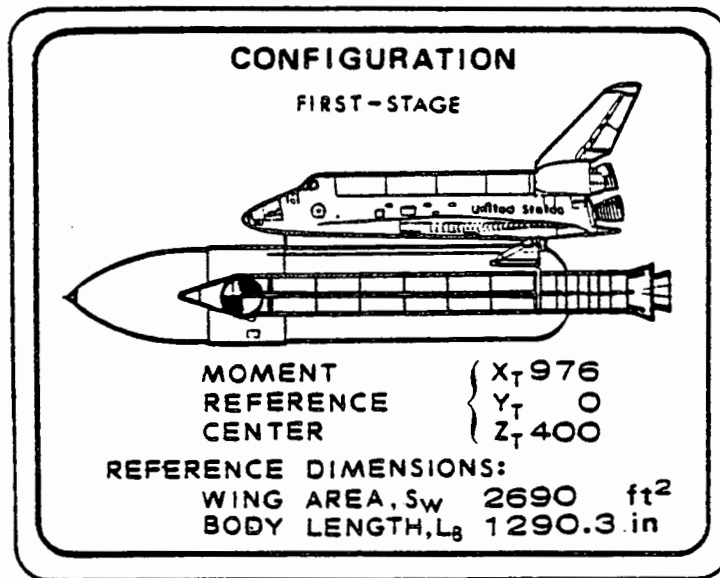
4.1.8 STRUCTURAL ANALYSIS DATA. Equations for use with the structural analysis data are given for the various elements and components. These equations relate directly to the aerodynamic data presented in Volume 2; e.g., equations for the longitudinal aerodynamics (Volume 1, Section 4.1.8.1) make use of the data given under longitudinal aerodynamics (Volume 2, Section 5.1.8.1), etc.

These equations apply to the first-stage only and are intended to provide Structural Engineering with element and component aerodynamic force and moment coefficients for the launch configuration. Attach structure increments are distributed to the elements in the following manner:

| | |
|------------|--|
| Orbiter/ET | All on ET, except forward bipod X-load; one-half on the Orbiter; one-half on the ET. |
| RH SRB/ET | One-half on the RHSRB; One-half on the ET. |
| LH SRB/ET | One-half on the LHSRB; One-half on the ET. |

See Section 3.0 for element and attach structure geometry.

4.1.8.1 LONGITUDINAL AERODYNAMICS. The first-stage mated vehicle aerodynamic forces and moment for the longitudinal degrees-of-freedom are presented for various Mach numbers from 0.60 to 2.50, inboard/outboard elevon deflections, and various angles of attack and sideslip for the total vehicle and its elements. The element data (Orbiter, External Tank, Solid Rocket Boosters) are "in the presence of" one another. Data are based on the Launch Vehicle baseline configuration (cf. Figure 3.1.1-6). Aerodynamic forces and moment are given in the body-axis system about a Moment Reference Center located as shown in the sketch for the TOTAL LAUNCH VEHICLE and for the ELEMENTS (Orbiter, RHSRB, LHSRB, and ET).



Data are provided for nine elevon settings and are presented in order of increasing Mach number.

| MACH No. | RANGE Degrees | | $\delta_{e_i}/\delta_{e_0}$ | | | | | | | | |
|----------|---------------|----------|-----------------------------|-------|--------|--------|--------|---------|--------|--------|---------|
| | α | β | Degrees | | | | | | | | |
| 0.60 | -8 to +8 | -8 to +8 | +8/+5 | +8/+9 | +2/+11 | +10/+5 | +10/+9 | +10/+11 | +12/+5 | +12/+9 | +12/+11 |
| 0.80 | -8 to +8 | -8 to +8 | +8/+5 | +8/+9 | +8/+11 | +10/+5 | +10/+9 | +10/+11 | +12/+5 | +12/+9 | +12/+11 |
| 0.90 | -8 to +4 | -8 to +6 | +8/+5 | +8/+9 | +8/+11 | +10/+5 | +10/+9 | +10/+11 | +12/+5 | +12/+9 | +12/+11 |
| 1.05 | -8 to +4 | -8 to +6 | +8/+5 | +8/+9 | +8/+11 | +10/+5 | +10/+9 | +10/+11 | +12/+5 | +12/+9 | +12/+11 |
| 1.10 | -8 to +4 | -8 to +6 | +8/+5 | +6/+9 | +8/+11 | +10/+5 | +10/+9 | +10/+11 | +12/+5 | +12/+9 | +12/+11 |
| 1.15 | -8 to +4 | -8 to +6 | +8/-2 | +8/+5 | +8/+9 | +10/-2 | +10/+5 | +10/+9 | +12/-2 | +12/+5 | +12/+9 |
| 1.25 | -8 to +4 | -8 to +6 | +8/-2 | +8/+5 | +8/+9 | +10/-2 | +10/+5 | +10/+9 | +12/-2 | +12/+5 | +12/+9 |
| 1.40 | -8 to +4 | -8 to +6 | +8/-7 | +8/-2 | +8/+5 | +10/-7 | +10/-2 | +10/+5 | +12/-7 | +12/-2 | +12/+5 |
| 1.55 | -8 to +4 | -8 to +6 | +8/-7 | +8/-2 | +8/+5 | +10/-7 | +10/-2 | +10/+5 | +12/-7 | +12/-2 | +12/+5 |
| 1.80 | -6 to +6 | -6 to +6 | +4/-7 | +4/-5 | +4/-2 | +10/-7 | +10/-5 | +10/-2 | +12/-7 | +12/-5 | +12/-2 |
| 2.20 | -6 to +6 | -6 to +6 | 0/-7 | 0/-5 | 0/-2 | +4/-7 | +4/-5 | +4/-2 | +10/-7 | +10/-5 | +10/-2 |
| 2.50 | -6 to +6 | -6 to +6 | 0/-7 | 0/-2 | 0/+2 | +4/-7 | +4/-2 | +4/+2 | +10/-7 | +10/-2 | +10/+2 |



The first-stage basic aerodynamic coefficient data are described in the following manner:

$$C_{()\text{FOREBODY}} = C'_{()\text{FOREBODY}} + \Delta C_{()\text{PLUME}} + \Delta C_{()\text{ATTACH}} + \Delta C^*_{()\text{FLEX}}$$

where;

$C_{()\text{FOREBODY}}$ = Full-scale, rigid body, proximity forebody force or moment coefficient (including plume effects and attach structure effects) for each element at the noted elevon settings (9 per Mach number).

| subscript: (N) | MACH | TABLE |
|----------------|------|----------------------------|
| | 0.60 | 5.1.8.1.1- 1 through - 9 |
| | 0.80 | 5.1.8.1.1- 10 through - 18 |
| | 0.90 | 5.1.8.1.1- 19 through - 27 |
| | 1.05 | 5.1.8.1.1- 28 through - 36 |
| | 1.10 | 5.1.8.1.1- 37 through - 45 |
| | 1.15 | 5.1.8.1.1- 46 through - 54 |
| | 1.25 | 5.1.8.1.1- 55 through - 63 |
| | 1.40 | 5.1.8.1.1- 64 through - 72 |
| | 1.55 | 5.1.8.1.1- 73 through - 81 |
| | 1.80 | 5.1.8.1.1- 82 through - 90 |
| | 2.20 | 5.1.8.1.1- 91 through- 99 |
| | 2.50 | 5.1.8.1.1-100 through -108 |

| subscript: (A) | MACH | TABLE |
|----------------|------|----------------------------|
| | 0.60 | 5.1.8.1.2- 1 through - 9 |
| | 0.80 | 5.1.8.1.2- 10 through - 18 |
| | 0.90 | 5.1.8.1.2- 19 through - 27 |
| | 1.05 | 5.1.8.1.2- 28 through - 36 |
| | 1.10 | 5.1.8.1.2- 37 through - 45 |
| | 1.15 | 5.1.8.1.2- 46 through - 54 |
| | 1.25 | 5.1.8.1.2- 55 through - 63 |
| | 1.40 | 5.1.8.1.2- 64 through - 72 |
| | 1.55 | 5.1.8.1.2- 73 through - 81 |
| | 1.80 | 5.1.8.1.2- 82 through - 90 |
| | 2.20 | 5.1.8.1.2- 91 through- 99 |
| | 2.50 | 5.1.8.1.2-100 through -108 |

| subscript: (m) | MACH | TABLE |
|----------------|------|----------------------------|
| | 0.60 | 5.1.8.1.3- 1 through - 9 |
| | 0.80 | 5.1.8.1.3- 10 through - 18 |
| | 0.90 | 5.1.8.1.3- 19 through - 27 |
| | 1.05 | 5.1.8.1.3- 28 through - 36 |
| | 1.10 | 5.1.8.1.3- 37 through - 45 |
| | 1.15 | 5.1.8.1.3- 46 through - 54 |
| | 1.25 | 5.1.8.1.3- 55 through - 63 |
| | 1.40 | 5.1.8.1.3- 64 through - 72 |
| | 1.55 | 5.1.8.1.3- 73 through - 81 |
| | 1.80 | 5.1.8.1.3- 82 through - 90 |
| | 2.20 | 5.1.8.1.3- 91 through- 99 |
| | 2.50 | 5.1.8.1.3-100 through -108 |

* Not included in tabulated totals.

$C'_{()FOREBODY}$ = Full-scale, rigid body, proximity forebody force or moment coefficient exclusive of plume and attach structure increments.

| | MACH | TABLE |
|----------------|------|-------------|
| subscript: (N) | (| NOT GIVEN) |
| (A) | (| NOT GIVEN) |
| (m) | (| NOT GIVEN) |

$\Delta C'_{()PLUME}$ = Incremental forebody force or moment coefficient due to the effect of jet plumes.

| | MACH | TABLE |
|----------------|------|-------------|
| subscript: (N) | (| NOT GIVEN) |
| (A) | (| NOT GIVEN) |
| (m) | (| NOT GIVEN) |

$\Delta C'_{()ATTACH}$ = Incremental forebody force or moment coefficient due to the effect of ET and SRB attach structure.

| | MACH | TABLE |
|----------------|------|---------------|
| subscript: (N) | 0.60 | 5.1.8.1.1-109 |
| | 0.80 | 5.1.8.1.1-110 |
| | 0.90 | 5.1.8.1.1-111 |
| | 1.05 | 5.1.8.1.1-112 |
| | 1.10 | 5.1.8.1.1-113 |
| | 1.15 | 5.1.8.1.1-114 |
| | 1.25 | 5.1.8.1.1-115 |
| | 1.40 | 5.1.8.1.1-116 |
| | 1.55 | 5.1.8.1.1-117 |
| | 1.80 | 5.1.8.1.1-118 |
| | 2.20 | 5.1.8.1.1-119 |
| | 2.50 | 5.1.8.1.1-120 |

| | MACH | TABLE |
|----------------|------|---------------|
| subscript: (A) | 0.60 | 5.1.8.1.2-109 |
| | 0.80 | 5.1.8.1.2-110 |
| | 0.90 | 5.1.8.1.2-111 |
| | 1.05 | 5.1.8.1.2-112 |
| | 1.10 | 5.1.8.1.2-113 |
| | 1.15 | 5.1.8.1.2-114 |
| | 1.25 | 5.1.8.1.2-115 |
| | 1.40 | 5.1.8.1.2-116 |
| | 1.55 | 5.1.8.1.2-117 |
| | 1.80 | 5.1.8.1.2-118 |
| | 2.20 | 5.1.8.1.2-119 |
| | 2.50 | 5.1.8.1.2-120 |

| subscript: (m) | MACH | TABLE |
|----------------|------|---------------|
| | 0.60 | 5.1.8.1.3-109 |
| | 0.80 | 5.1.8.1.3-110 |
| | 0.90 | 5.1.8.1.3-111 |
| | 1.05 | 5.1.8.1.3-112 |
| | 1.10 | 5.1.8.1.3-113 |
| | 1.15 | 5.1.8.1.3-114 |
| | 1.25 | 5.1.8.1.3-115 |
| | 1.40 | 5.1.8.1.3-116 |
| | 1.55 | 5.1.8.1.3-117 |
| | 1.80 | 5.1.8.1.3-118 |
| | 2.20 | 5.1.8.1.3-119 |
| | 2.50 | 5.1.8.1.3-120 |

$\Delta C_{() FLEX}$ = Change in force or moment coefficient due to
aeroelastic deformation.

subscript: (N) (Figure 5.1.8.1.1-1)
 (A) (Figure 5.1.8.1.2-1)
 (m) (Figure 5.1.8.1.3-1)

NOTE: Not available for ET or SRB.

The total aerodynamic force or moment coefficient for the first-stage is:

$$C_{() TOTAL} = C_{() FOREBODY} + \Delta C_{() BASE}$$

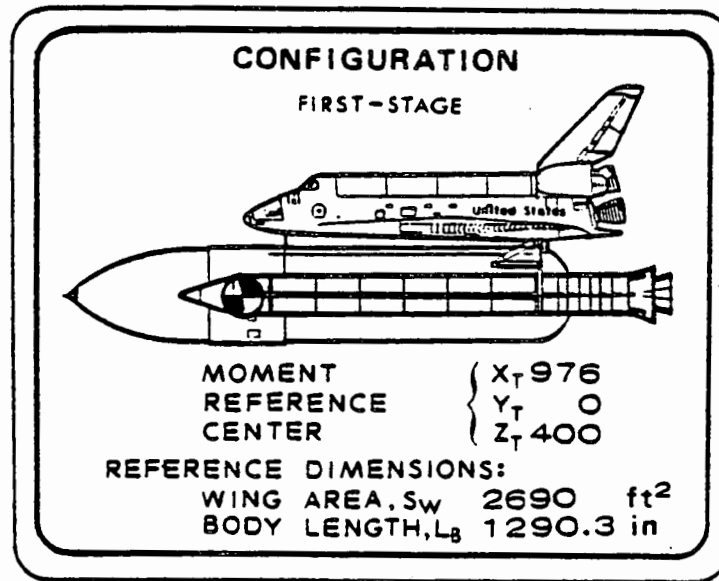
where;

$C_{() FOREBODY}$ = Defined above.

$C_{() BASE}$ = Power-on base force or moment (See Section 4.1.1.1)
coefficient (including effects
of SSME and SRM plumes).

subscript: (N) TO BE APPLIED TO ORBITER ELEMENT ONLY.
 subscript: (A) TO BE APPLIED TO ORBITER, ET AND SRB ELEMENTS.
 subscript: (m) TO BE APPLIED TO ORBITER ELEMENT ONLY.

4.1.8.2 LATERAL-DIRECTIONAL AERODYNAMICS. The first-stage mated vehicle aerodynamic forces and moment for the longitudinal degrees-of-freedom are presented for various Mach numbers from 0.60 to 2.50, inboard/outboard elevon deflections, and various angles of attack and sideslip for the total vehicle and its elements. The element data (Orbiter, External Tank, Solid Rocket Boosters) are "in the presence of" one another. Data are based on the Launch Vehicle baseline configuration (cf. Figure 3.1.1-6). Aerodynamic forces and moment are given in the body-axis system about a Moment Reference Center located as shown in the sketch for the TOTAL LAUNCH VEHICLE and for the ELEMENTS (Orbiter, RHSRB, LHSRB, and ET).



Data are provided for nine elevon settings and are presented in order of increasing Mach number.

| MACH No. | RANGE Degrees | | $\delta e_i / \delta e_0$ Degrees | | | | | | | | |
|----------|---------------|----------|-----------------------------------|-------|--------|--------|--------|---------|--------|--------|---------|
| | α | β | | | | | | | | | |
| 0.60 | -8 to +8 | -8 to +8 | +8/+5 | +8/+9 | +8/+11 | +10/+5 | +10/+9 | +10/+11 | +12/+5 | +12/+9 | +12/+11 |
| 0.80 | -8 to +8 | -6 to +6 | +8/+5 | +8/+9 | +8/+11 | +10/+5 | +10/+9 | +10/+11 | +12/+5 | +12/+9 | +12/+11 |
| 0.90 | -8 to +4 | -6 to +6 | +6/+5 | +8/+9 | +8/+11 | +10/+5 | +10/+9 | +10/+11 | +12/+5 | +12/+9 | +12/+11 |
| 1.05 | -8 to +4 | -6 to +6 | +8/+5 | +8/+9 | +8/+11 | +10/+5 | +10/+9 | +10/+11 | +12/+5 | +12/+9 | +12/+11 |
| 1.10 | -8 to +4 | -6 to +6 | +8/+5 | +8/+9 | +8/+11 | +10/+5 | +10/+9 | +10/+11 | +12/+5 | +12/+9 | +12/+11 |
| 1.15 | -8 to +4 | -6 to +6 | +8/-2 | +8/+5 | +8/+9 | +10/-2 | +10/+5 | +10/+9 | +12/-2 | +12/+5 | +12/+9 |
| 1.25 | -8 to +4 | -6 to +6 | +8/-2 | +8/+5 | +8/+9 | +10/-2 | +10/+5 | +10/+9 | +12/-2 | +12/+5 | +12/+9 |
| 1.40 | -8 to +4 | -6 to +6 | +8/-7 | +8/-2 | +8/+5 | +10/-7 | +10/-2 | +10/+5 | +12/-7 | +12/-2 | +12/+5 |
| 1.55 | -8 to +4 | -6 to +6 | +8/-7 | +8/-2 | +8/+5 | +10/-7 | +10/-2 | +10/+5 | +12/-7 | +12/-2 | +12/+5 |
| 1.80 | -6 to +6 | -6 to +6 | +4/-7 | +4/-5 | +4/-2 | +10/-7 | +10/-5 | +10/-2 | +12/-7 | +12/-5 | +12/-2 |
| 2.20 | -6 to +6 | -6 to +6 | 0/-7 | 0/-5 | 0/-2 | +4/-7 | +4/-5 | +4/-2 | +10/-7 | +10/-5 | +10/-2 |
| 2.50 | -6 to +6 | -6 to +6 | 0/-7 | 0/-2 | 0/+2 | +4/-7 | +4/-2 | +4/+2 | +10/-7 | +10/-2 | +10/+2 |

The first-stage basic aerodynamic coefficient data are described in the following manner:

$$C_{(Y)}^{\text{FOREBODY}} = C_{(Y)}^{\text{FOREBODY}} + \Delta C_{(Y)}^{\text{PLUME}} + \Delta C_{(Y)}^{\text{ATTACH}} + \Delta C_{(Y)}^{\text{FLEX}}$$

where;

$C_{(Y)}^{\text{FOREBODY}}$ = Full-scale, rigid body, proximity forebody force or moment coefficient (including plume effects and attach structure effects) for each element at the noted elevon settings (9 per Mach number).

| subscript: (Y) | MACH | TABLE |
|----------------|------|----------------------------|
| | 0.60 | 5.1.8.2.1- 1 through - 9 |
| | 0.80 | 5.1.8.2.1- 10 through - 18 |
| | 0.90 | 5.1.8.2.1- 19 through - 27 |
| | 1.05 | 5.1.8.2.1- 28 through - 36 |
| | 1.10 | 5.1.8.2.1- 37 through - 45 |
| | 1.15 | 5.1.8.2.1- 46 through - 54 |
| | 1.25 | 5.1.8.2.1- 55 through - 63 |
| | 1.40 | 5.1.8.2.1- 64 through - 72 |
| | 1.55 | 5.1.8.2.1- 73 through - 81 |
| | 1.80 | 5.1.8.2.1- 82 through - 90 |
| | 2.20 | 5.1.8.2.1- 91 through- 99 |
| | 2.50 | 5.1.8.2.1-100 through -108 |

| subscript: (n) | MACH | TABLE |
|----------------|------|----------------------------|
| | 0.60 | 5.1.8.2.2- 1 through - 9 |
| | 0.80 | 5.1.8.2.2- 10 through - 18 |
| | 0.90 | 5.1.8.2.2- 19 through - 27 |
| | 1.05 | 5.1.8.2.2- 28 through - 36 |
| | 1.10 | 5.1.8.2.2- 37 through - 45 |
| | 1.15 | 5.1.8.2.2- 46 through - 54 |
| | 1.25 | 5.1.8.2.2- 55 through - 63 |
| | 1.40 | 5.1.8.2.2- 64 through - 72 |
| | 1.55 | 5.1.8.2.2- 73 through - 81 |
| | 1.80 | 5.1.8.2.2- 82 through - 90 |
| | 2.20 | 5.1.8.2.2- 91 through- 99 |
| | 2.50 | 5.1.8.2.2-100 through -108 |

| subscript: (L) | MACH | TABLE |
|----------------|------|----------------------------|
| | 0.60 | 5.1.8.2.3- 1 through - 9 |
| | 0.80 | 5.1.8.2.3- 10 through - 18 |
| | 0.90 | 5.1.8.2.3- 19 through - 27 |
| | 1.05 | 5.1.8.2.3- 28 through - 36 |
| | 1.10 | 5.1.8.2.3- 37 through - 45 |
| | 1.15 | 5.1.8.2.3- 46 through - 54 |
| | 1.25 | 5.1.8.2.3- 55 through - 63 |
| | 1.40 | 5.1.8.2.3- 64 through - 72 |
| | 1.55 | 5.1.8.2.3- 73 through - 81 |
| | 1.80 | 5.1.8.2.3- 82 through - 90 |
| | 2.20 | 5.1.8.2.3- 91 through- 99 |
| | 2.50 | 5.1.8.2.3-100 through -108 |

* Not included in tabulated totals.



$C_{i, \text{FOREBODY}}$ = Full-scale, rigid body, proximity forebody force or moment coefficient exclusive of plume and attach structure increments.

| | MACH | TABLE |
|----------------|------|-------------|
| subscript: (Y) | (| NOT GIVEN) |
| (n) | (| NOT GIVEN) |
| (A) | (| NOT GIVEN) |

$\Delta C_{i, \text{PLUME}}$ = Incremental forebody force or moment coefficient due to the effect of jet plumes.

| | MACH | TABLE |
|----------------|------|-------------|
| subscript: (Y) | (| NOT GIVEN) |
| (n) | (| NOT GIVEN) |
| (A) | (| NOT GIVEN) |

$\Delta C_{i, \text{ATTACH}}$ = Incremental forebody force or moment coefficient due to the effect of ET and SRB attach structure.

| | MACH | TABLE |
|----------------|------|---------------|
| subscript: (Y) | 0.60 | 5.1.8.2.1-109 |
| | 0.80 | 5.1.8.2.1-110 |
| | 0.90 | 5.1.8.2.1-111 |
| | 1.05 | 5.1.8.2.1-112 |
| | 1.10 | 5.1.8.2.1-113 |
| | 1.15 | 5.1.8.2.1-114 |
| | 1.25 | 5.1.8.2.1-115 |
| | 1.40 | 5.1.8.2.1-116 |
| | 1.55 | 5.1.8.2.1-117 |
| | 1.80 | 5.1.8.2.1-118 |
| | 2.20 | 5.1.8.2.1-119 |
| | 2.50 | 5.1.8.2.1-120 |

| | MACH | TABLE |
|----------------|------|---------------|
| subscript: (n) | 0.60 | 5.1.8.2.2-109 |
| | 0.80 | 5.1.8.2.2-110 |
| | 0.90 | 5.1.8.2.2-111 |
| | 1.05 | 5.1.8.2.2-112 |
| | 1.10 | 5.1.8.2.2-113 |
| | 1.15 | 5.1.8.2.2-114 |
| | 1.25 | 5.1.8.2.2-115 |
| | 1.40 | 5.1.8.2.2-116 |
| | 1.55 | 5.1.8.2.2-117 |
| | 1.80 | 5.1.8.2.2-118 |
| | 2.20 | 5.1.8.2.2-119 |
| | 2.50 | 5.1.8.2.2-120 |

| subscript: (λ) | MACH | TABLE |
|--------------------------|------|---------------|
| | 0.60 | 5.1.8.2.3-109 |
| | 0.80 | 5.1.8.2.3-110 |
| | 0.90 | 5.1.8.2.3-111 |
| | 1.05 | 5.1.8.2.3-112 |
| | 1.10 | 5.1.8.2.3-113 |
| | 1.15 | 5.1.8.2.3-114 |
| | 1.25 | 5.1.8.2.3-115 |
| | 1.40 | 5.1.8.2.3-116 |
| | 1.55 | 5.1.8.2.3-117 |
| | 1.80 | 5.1.8.2.3-118 |
| | 2.20 | 5.1.8.2.3-119 |
| | 2.50 | 5.1.8.2.3-120 |

$\Delta C_{() FLEX}$ = Change in force or moment coefficient due to aeroelastic deformation.

$$= \left(\frac{\Delta C_{() \beta FLEX}}{\bar{q}} \right) \bar{q} \beta$$

subscript: (Y) (Figure 5.1.8.2.1-1)
 (n) (Figure 5.1.8.2.2-1)
 (λ) (Figure 5.1.8.2.3-1)

NOTE: Not available for ET or SRB.

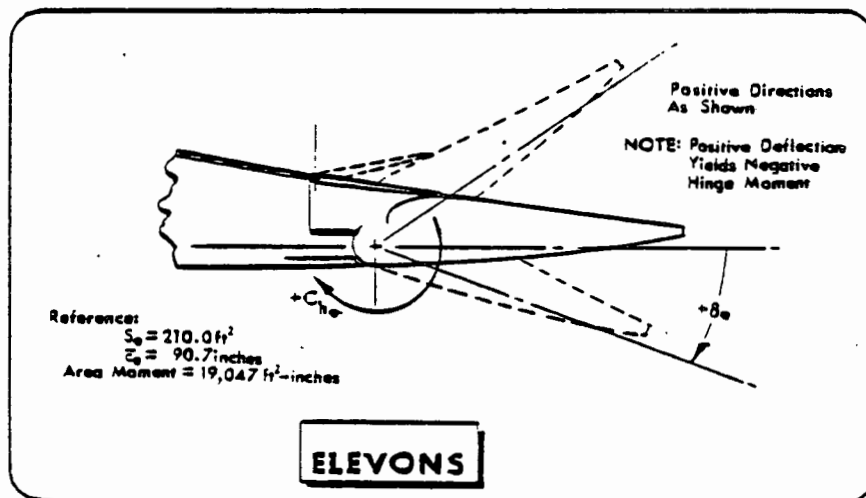
4.1.8.3 ELEVON AND WING PANEL LOADS. The elevon and wing panel loads are presented in coefficient for the inboard and outboard elevon hinge moments and wing root shear, bending and torsion. Data are presented for the right-hand wing panel and include the glove. To obtain left-hand panel data, use values tabulated for corresponding negative sideslip angles.

ELEVON CONTROL HINGE MOMENT. The elevon control hinge moment coefficients are base on theoretical reference dimensions. The reference area is 210.0 ft and the reference length (mean aerodynamic chord) is 90.7 inches. These reference values were used for each panel so that the total hinge moment is the sum of the individual panel moments:

$$HM_{eTOTAL} = HM_{eINBOARD} + HM_{eOUTBOARD}$$

where;

$$HM_e = C_{h_e} (\bar{q} S_e \bar{c}_e)$$



or,

$$HM_{eTOTAL} = \bar{q} S_e \bar{c}_e (C_{h_{eINBOARD}} + C_{h_{eOUTBOARD}})$$

and the hinge moment coefficients are described by:

$$C_{h_{eTOTALI}} = C_{h_{eINBOARD}} + \Delta C_{h_{ePLUMEI}} + \Delta C_{h_{eFLEXI}}^*$$

$$C_{h_{eTOTALO}} = C_{h_{eOUTBOARD}} + \Delta C_{h_{ePLUME0}} + \Delta C_{h_{eFLEX0}}^*$$

*Not included in tabulated totals.

where;

- $C_{heTOTALI}$ = Rigid-body, inboard elevon hinge moment coefficient. (Table 5.1.8.3-1 through -108)
- $C_{heTOTALO}$ = Rigid-body, outboard elevon hinge moment coefficient. (Table 5.1.8.3-1 through -108)
- $\Delta C_{hePLUMEI}$ = Change in elevon hinge moment coefficient due to plume effect on inboard elevon. (Not Given)
- $\Delta C_{hePLUME O}$ = Change in elevon hinge moment coefficient due to plume effect on outboard elevon. (Not Given)
- $\Delta C_{heFLEXI}$ = Change in inboard elevon hinge moment coefficient due to aeroelastic deformation. (Table 5.1.8.3-109 through -112)
- $\Delta C_{heFLEXO}$ = Change in outboard elevon hinge moment coefficient due to aeroelastic deformation. (Table 5.1.8.3-113 through -116)

WING PANEL LOADS. The wing panel loads consist of wing root shear, bending, and torsion coefficients based on a reference area of 2690 ft² and a reference length of 936.68 inches in bending and 474.80 inches in torsion. The Moment Reference Center is located at (X₀1307, Y₀105, Z₀288).

$$\begin{aligned}
 C_{WING\ SHEAR\ TOTAL} &= C_{WING\ SHEAR\ PLUME-OFF} + \Delta C_{SPLUME} + \Delta C_{SFLEX}^* \\
 C_{WING\ BENDING\ TOTAL} &= C_{WING\ BENDING\ PLUME-OFF} + \Delta C_{BPLUME} + \Delta C_{BFLEX}^* \\
 C_{WING\ TORSION\ TOTAL} &= C_{WING\ TORSION\ PLUME-OFF} + \Delta C_{TPLUME} + \Delta C_{TFLEX}^*
 \end{aligned}$$

*Not included in tabulated totals.

where;

| | | |
|---------------------------------|---|-----------------------------------|
| $C_{\text{WING SHEAR TOTAL}}$ | = Wing root shear coefficient. | (Tables 5.1.8.3-1 through -108) |
| $\Delta C_{\text{S PLUME}}$ | = Change in Shear coefficient due to plume effects. | (Not Given) |
| $\Delta C_{\text{S FLEX}}$ | = Change in shear coefficient due to aeroelastic deformation. | (Tables 5.1.8.3-117 through -12) |
| $C_{\text{WING BENDING TOTAL}}$ | = Wing root bending coefficient. | (Tables 5.1.8.3-1 through -108) |
| $\Delta C_{\text{B PLUME}}$ | = Change in bending coefficient due to plume effects. | (Not Given) |
| $\Delta C_{\text{B FLEX}}$ | = Change in bending coefficient due to aeroelastic deformation. | (Tables 5.1.8.3-117 through -120) |
| $C_{\text{WING TORSION TOTAL}}$ | = Wing root torsion coefficient. | (Tables 5.1.8.3-1 through -108) |
| $\Delta C_{\text{T PLUME}}$ | = Change in torsion coefficient due to plume effects. | (Not Given) |
| $\Delta C_{\text{T FLEX}}$ | = Change in torsion coefficient due to aeroelastic deformation. | (Tables 5.1.8.3-117 through -120) |

4.1.8.4 VERTICAL TAIL LOADS. The vertical tail panel loads are presented in coefficient form for normal force, axial force, pitching moment, root shear, bending, and torsion. The data are based on a reference area of 413.25 ft and a reference length of 199.80 inches. The Moment Reference Center is located at (X₀1414.3, Y₀0.0, Z₀503.0).

$$C_{\text{VERT AXIAL TOTAL}} = C_{\text{VERT AXIAL}} + \Delta C_{\text{A FLEX}}^*$$

$$C_{\text{VERT SHEAR TOTAL}} = C_{\text{VERT SHEAR}} + \Delta C_{\text{S FLEX}}^* + \Delta C_{\text{S PLUME}}$$

$$C_{\text{VERT NORMAL TOTAL}} = C_{\text{VERT NORMAL}} + \Delta C_{\text{N FLEX}}^*$$

$$C_{\text{VERT BENDING TOTAL}} = C_{\text{VERT BENDING}} + \Delta C_{\text{B FLEX}}^* + \Delta C_{\text{B PLUME}}$$

$$C_{\text{VERT PITCHING TOTAL}} = C_{\text{VERT PITCHING}} + \Delta C_{\text{P FLEX}}^*$$

$$C_{\text{VERT TORSION TOTAL}} = C_{\text{VERT TORSION}} + \Delta C_{\text{T FLEX}}^* + \Delta C_{\text{T PLUME}}$$

where;

| | | |
|--------------------------------|--|--------------------------------|
| $C_{\text{VERT AXIAL TOTAL}}$ | = Vertical axial force coefficient. | (Tables 5.1.8.4-1 through -12) |
| $\Delta C_{\text{A FLEX}}^*$ | = Change in axial force coefficient due to aeroelastic deformation. | (Not Defined) |
| $C_{\text{VERT SHEAR TOTAL}}$ | = Vertical root shear coefficient. | (Tables 5.1.8.4-1 through -12) |
| $\Delta C_{\text{S FLEX}}^*$ | = Change in shear coefficient due to aeroelastic deformation. | (Figure 5.1.8.4-1) |
| $\Delta C_{\text{S PLUME}}$ | = Change in shear coefficient due to plume effects. | (Not Given) |
| $C_{\text{VERT NORMAL TOTAL}}$ | = Vertical normal force coefficient. | (Tables 5.1.8.4-1 through -12) |
| $\Delta C_{\text{N FLEX}}^*$ | = Change in normal force coefficient due to aeroelastic deformation. | (Not Defined) |

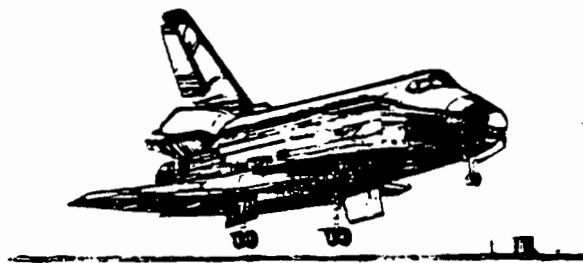
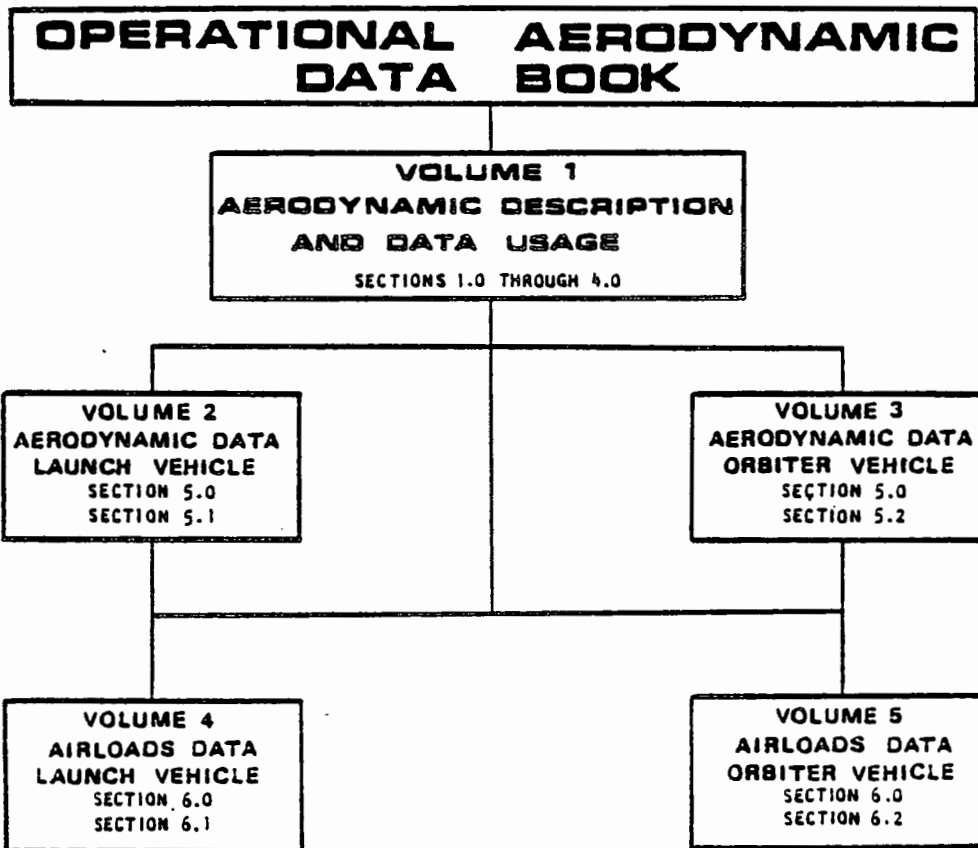
*Not included in tabulated totals.

| | | |
|----------------------------------|---|--------------------------------|
| $C_{\text{VERT BENDING TOTAL}}$ | = Vertical root bending coefficient. | (Tables 5.1.8.4-1 through -12) |
| $\Delta C_{\text{B FLEX}}$ | = Change in bending coefficient due to aeroelastic deformation. | (Figure 5.1.8.4-2) |
| $\Delta C_{\text{B PLUME}}$ | = Change in bending coefficient due to plume effects. | (Not Given) |
| $C_{\text{VERT PITCHING TOTAL}}$ | = Vertical pitching moment coefficient. | (Tables 5.1.8.4-1 through -12) |
| $\Delta C_{\text{P FLEX}}$ | = Change in pitching moment coefficient due to aeroelastic deformation. | (Not Defined) |
| $C_{\text{VERT TORSION TOTAL}}$ | = Vertical root torsion coefficient. | (Tables 5.1.8.4-1 through -12) |
| $\Delta C_{\text{T FLEX}}$ | = Change in torsion coefficient due to aeroelastic deformation. | (Figure 5.1.8.4-3) |
| $\Delta C_{\text{T PLUME}}$ | = Change in torsion coefficient due to plume effects. | (Not Given) |

4.2 ORBITER VEHICLE AERODYNAMIC EQUATIONS

ORIGINAL PAGE IS
OF POOR QUALITY

4.2 ORBITER VEHICLE AERODYNAMIC EQUATIONS. Equations for use in entry trajectory analyses, subsystems analyses, flight control analyses, and manned simulation studies are defined in this section. These equations relate directly to the aerodynamic data presented in Volume 3; i.e., equations for the Orbiter Vehicle longitudinal aerodynamics (Volume 1, Section 4.2.1.1) make use of the data given under longitudinal aerodynamics (Volume 3, Section 5.2.1.1), etc.



The forces and moments presented herein are defined for three phases or categories:

1.) ON-ORBIT (PAYLOAD BAY DOORS OPEN)

The payload bay doors open data are intended for use in simulators for on-orbit (600,000 feet or higher) station keeping. These data are presented as a function of angle of attack (0 to 360 degrees) and sideslip (0 to 180 degrees) only. The aerodynamic control surfaces (elevon, aileron, body flap, speedbrake, and rudder) are considered to be ineffective. Attitude control is obtained through the use of RCS. The RCS effects are to be used in this flight regime with the appropriate P_{∞} for impingement effects and ϕ_1/ϕ_{∞} for jet interaction.

2.) ON-ORBIT (PAYLOAD BAY DOORS CLOSED)

The payload bay doors closed data are intended for use in simulators for on-orbit and abort missions for altitudes in excess of 300,000 feet and large variations in attitude. These data are presented as functions of angle of attack (0 to 360 degrees), sideslip (0 to 180 degrees), and altitude. The aerodynamic control surfaces (elevon, aileron, body flap, speedbrake, and rudder) are considered to be ineffective due to the low dynamic pressure ($q < 2$ psf). Attitude control is obtained through the use of RCS. The RCS effects are to be applied in this flight regime with the appropriate P_{∞} for impingement effects and ϕ_1/ϕ_{∞} for jet interaction.

3.) ENTRY

The aerodynamic data presented are for use in entry simulations from 600,000 feet through landing. The angle of attack and sideslip data are restricted to cover only those conditions expected during a normal End-Of-Mission type entry. Aerodynamic control surface effectiveness (elevon, aileron, body flap, speedbrake, and rudder) is provided for use when the dynamic pressure becomes significant ($q > 2$ psf) and the RCS functions are terminated. The RCS data can be used from 600,000 feet to $q = 10$ psf ($\approx 260,000$ feet) for roll, $q = 40$ psf ($\approx 240,000$ feet) for pitch, and Mach 1.0 (50,000 feet) for yaw.

4.2.1 ORBITAL AND ENTRY AERODYNAMICS

ORIGINAL PAGE IS
OF POOR QUALITY

4.2.1 ORBITAL AND ENTRY AERODYNAMICS. Certain calculations and definitions are required prior to obtaining data from the Digital File and/or Data Tables of Volume 3. These definitions and calculations are given in this section [4.2] and will be referred to as "Pre-Lookup" definitions and calculations.

PRE-LOOKUP DEFINITIONS AND CALCULATIONS

δ_{SB} = Speedbrake deflection (defined in freestream direction - See Section 3.5.2.2).

δ_{BF} = Body Flap deflection.
NOTE: RIGID values indicated by lack of superscript.
FLEXIBLE values indicated by superscript "f".

$$\delta_{BF}^f = \delta_{BF} + \Delta\delta_{BF}$$

$$\Delta\delta_{BF} = K_{BF} \bar{q} S_{BF} \bar{c}_{BF} C_{h_{BF}}^f$$

$$K_{BF} = 1.817 \times 10^{-6} \text{ degrees/inch-pound}$$

$C_{h_{BF}}^f$ = Flexible Body Flap hinge moment coefficient.
(See Section 4.2.2.2.)

$\delta e_{() \text{ or } ()}$ = elevon deflection
first subscript indicates left-hand or right-hand panel.
second subscript indicates inboard or outboard panel.
NOTE: RIGID values indicated by lack of superscript.
FLEXIBLE values indicated by the superscript, "f".

$$= \frac{1}{2}(\delta e_L + \delta e_O) = \frac{1}{2}(\delta e_{L1} + \delta e_{R1})$$

$$\delta e_L = \frac{1}{2}(\delta e_{L1} + \delta e_{R1})$$

$$\delta e_O = \frac{1}{2}(\delta e_{L0} + \delta e_{R0})$$

$$\delta e_L = \frac{1}{2}(\delta e_{L_1} + \delta e_{L_0}) = \delta e + \delta a$$

$$\delta e_R = \frac{1}{2}(\delta e_{R_1} + \delta e_{R_0}) = \delta e - \delta a$$

$\delta a_{()}$ or $()$ = aileron deflection
 first subscript indicates left-hand
 or right-hand panel.
 second subscript indicates inboard
 or outboard panel.
 NOTE: RIGID values indicated by lack of
 superscript.
 FLEXIBLE values indicated by the
 superscript, "f".

$$\delta a = \frac{1}{2}(\delta e_L - \delta e_R) = \frac{1}{2}(\delta a_1 + \delta a_0)$$

$$\delta a_1 = \frac{1}{2}(\delta e_{L_1} - \delta e_{R_1})$$

$$\delta a_0 = \frac{1}{2}(\delta e_{L_0} - \delta e_{R_0})$$

Modify initial rigid elevon deflection with flexible increment

$$\delta e_{L_1}^f = \delta e_{L_1} + \Delta \delta e_{L_1}$$

$$\delta e_{L_0}^f = \delta e_{L_0} + \Delta \delta e_{L_0}$$

$$\delta e_{R_1}^f = \delta e_{R_1} + \Delta \delta e_{R_1}$$

$$\delta e_{R_0}^f = \delta e_{R_0} + \Delta \delta e_{R_0}$$

$$\text{where, } \Delta \delta e_{L_1} = K_1 \bar{q} S_e \bar{c}_e C_{he_{L_1}}^f, \quad \Delta \delta e_{R_1} = K_1 \bar{q} S_e \bar{c}_e C_{he_{R_1}}^f,$$

$$\Delta \delta e_{L_0} = K_0 \bar{q} S_e \bar{c}_e C_{he_{L_0}}^f, \quad \Delta \delta e_{R_0} = K_0 \bar{q} S_e \bar{c}_e C_{he_{R_0}}^f$$

$$K_1 = 1.547 \times 10^{-6} \text{ degrees/inch-pound}$$

$$K_0 = 3.323 \times 10^{-6} \text{ degrees/inch-pound}$$

$$\left. \begin{array}{l} C_{HeL_i}^f \\ C_{HeL_o}^f \\ C_{HeR_i}^f \\ C_{HeR_o}^f \end{array} \right\} \quad (\text{See Section 4.2.2.1})$$

$$\delta e_{TOTAL}^f = \frac{1}{4} [\delta e_{L_i}^f + \delta e_{L_o}^f + \delta e_{R_i}^f + \delta e_{R_o}^f]$$

The basic equations are followed by written explanations of the meanings of the various elements contained in the equations. These are, in turn, followed with term by term definitions of each element and where these elements are located; either on the digital tape and/or in Volume 3 of this Data Book.

MOMENT TRANSFER EQUATIONS

The aerodynamic data contained in Volume 3 of this report are given for a MOMENT REFERENCE CENTER located at $X_0 1076.7$, $Y_0 0.0$, $Z_0 375.0$. To obtain moments about any other Reference Center:

$$C_{m_{MRC}} = C_{m_{0.65L_B}} + \frac{\Delta X}{c_w} C_N - \frac{\Delta Z}{c_w} C_A$$

$$C_{n_{MRC}} = C_{n_{0.65L_B}} + \frac{\Delta X}{b_w} C_Y - \frac{\Delta Y}{b_w} C_A$$

$$C_{l_{MRC}} = C_{l_{0.65L_B}} + \frac{\Delta Y}{b_w} C_N - \frac{\Delta Z}{b_w} C_Y$$

or

$$M_{MRC} = M_{0.65L_B} + \Delta X(N) - \Delta Z(A)$$

$$N_{MRC} = N_{0.65L_B} + \Delta X(Y) - \Delta Y(A)$$

$$L_{MRC} = L_{0.65L_B} + \Delta Y(N) - \Delta Z(Y)$$

where, $\Delta X = X_{MRC} - 1076.7$ inches
 $\Delta Y = Y_{MRC} - 0$ inch
 $\Delta Z = Z_{MRC} - 375$ inches

Additional moment transfer equations (including dynamic derivatives) may be obtained from Reference 4-1.

REACTION CONTROL SYSTEM (See also Section 3.5.1.4)

NOTE: For RCS, Thrust value, $T_i = 870$ lb-force.

DEFINITION:

n_{LHD} = number of operating left-hand down-firing jets
 $= L4D + L2D + L3D$

n_{LHS} = number of operating left-hand side firing jets
 $= L4L + L2L + L3L + L1L$

n_{LHU} = number of operating left-hand up-firing jets
 $= L4U + L2U + L1U$

n_{RHD} = number of operating right-hand down-firing jets
 $= R4D + R2D + R3D$

n_{RHS} = number of operating right-hand side firing jets
 $= R4R + R2R + R3R + R1R$

n_{RHU} = number of operating right-hand up-firing jets
 $= R4U + R2U + R1U$

MOMENTUM RATIO:

$$\frac{\phi_J}{\phi_{\infty}} = \left(\frac{\dot{m}_J V_J}{\bar{q}_{\infty} A_{REF}} \right) \left(\frac{A_{REF}}{2S_{REF}} \right) n = 0.1543 \left(\frac{n}{\bar{q}_{\infty}} \right)$$

$$\frac{\phi_J}{\phi_{\infty}} \Big|_{LHD} = 0.1543 \left(\frac{n_{LHD}}{\bar{q}_{\infty}} \right)$$

$$\frac{\phi_J}{\phi_{\infty}} \Big|_{RHD} = 0.1543 \left(\frac{n_{RHD}}{\bar{q}_{\infty}} \right)$$

$$\frac{\phi_J}{\phi_{\infty}} \Big|_{LHU} = 0.1543 \left(\frac{n_{LHU}}{\bar{q}_{\infty}} \right)$$

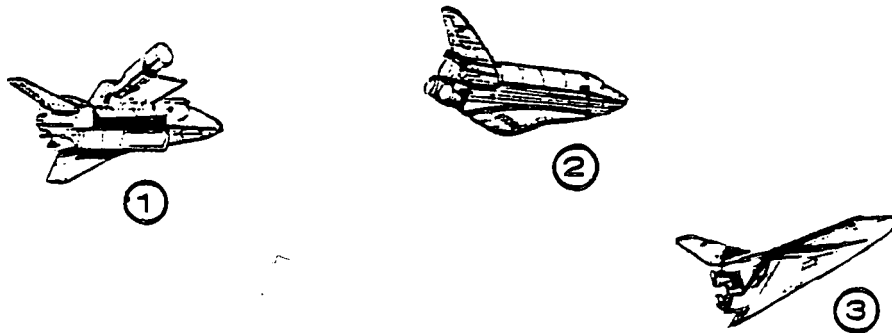
$$\frac{\phi_J}{\phi_{\infty}} \Big|_{RHU} = 0.1543 \left(\frac{n_{RHU}}{\bar{q}_{\infty}} \right)$$

$$\frac{\phi_J}{\phi_{\infty}} \Big|_{LHS} = 0.1543 \left(\frac{n_{LHS}}{\bar{q}_{\infty}} \right)$$

$$\frac{\phi_J}{\phi_{\infty}} \Big|_{RHS} = 0.1543 \left(\frac{n_{RHS}}{\bar{q}_{\infty}} \right)$$

4.2.1.1 LONGITUDINAL AERODYNAMICS. The basic aerodynamic characteristics for the longitudinal degrees-of-freedom are presented as full-scale, rigid and elastic, forces and moment in both the stability and body axis systems (cf. Section 3.1.5). These forces and moments are defined for three phases or categories:

- 1.) ON-ORBIT (PAYLOAD BAY DOORS OPEN)
- 2.) ON-ORBIT (PAYLOAD BAY DOORS CLOSED)
- 3.) ENTRY



The total longitudinal forces and moment for the Orbiter Vehicle are defined as:

$$\begin{aligned} \text{LIFT FORCE, } L_{\text{TOTAL}} &= \bar{q} S_w C_{L_{\text{TOTAL}}} + L_{\text{RCS}} \quad (\text{lb}) \\ \text{NORMAL FORCE, } N_{\text{TOTAL}} &= \bar{q} S_w C_{N_{\text{TOTAL}}} + N_{\text{RCS}} \quad (\text{lb}) \\ \text{DRAG FORCE, } D_{\text{TOTAL}} &= \bar{q} S_w C_{D_{\text{TOTAL}}} + D_{\text{RCS}} \quad (\text{lb}) \\ \text{AXIAL FORCE, } A_{\text{TOTAL}} &= \bar{q} S_w C_{A_{\text{TOTAL}}} + A_{\text{RCS}} \quad (\text{lb}) \\ \text{PITCHING MOMENT, } M_{\text{TOTAL}} &= \bar{q} S_w \bar{c}_w C_{m_{\text{TOTAL}}} + M_{\text{RCS}} \quad (\text{ft-lb}) \end{aligned}$$

where, \bar{q} = dynamic pressure (lb/ft²)

S_w = Wing Reference Area (2690.00 ft²)

\bar{c}_w = Wing Mean Aerodynamic Chord (39.56 feet)
(see Figure 3.1.5-2b)

RCS flow field interactions are defined as contributions to the total forces or moment rather than coefficients since the terms due to jet thrust and impingement are independent of dynamic pressure and cannot, therefore, be normalized in the conventional manner.

The total non-dimensional force and moment coefficients are defined as:

ON-ORBIT (PAYLOAD BAY DOORS OPEN)

$$C_{TOTAL} = C_{PLB DRS OPEN}$$

ON-ORBIT (PAYLOAD BAY DOORS CLOSED)

$$C_{TOTAL} = C_{h=300K ft} + K_{TRAN} [C_{h=600K ft} - C_{h=300K ft}]$$

ENTRY

$$C_{TOTAL} = C_{BASIC} + \Delta C_{HIGH ALT} + \Delta C_{REAL GAS} + \Delta C_{VISCOUS INTERACTION} + \Delta C_{BF} + \Delta C_{ELEVATOR/AILERON} + \Delta C_{PLUNGING} + \Delta C_{PITCH RATE} + \Delta C_{LG} + \Delta C_{GE} + \Delta C_{SILTS POD} + \Delta C_{VEHICLE}$$

where, the subscript () denotes lift force (L), normal force (N), drag force (D), axial force (A), or pitching moment (M) and;

$C_{PLB DRS OPEN}$ = Basic, full-scale, freestream, rigid body force or moment coefficient when vehicle is in orbit with payload bay doors open (altitude = 600,000 feet).

$C_{h=600K ft}$ = Basic, full-scale, freestream, rigid body force or moment coefficient when vehicle is in orbit with payload bay doors closed (altitude = 600,000 feet).

$C_{h=300K ft}$ = Basic, full-scale, rigid body force or moment coefficient when vehicle, with payload bay doors closed, is at an altitude of 300,000 feet.

K_{TRAN} = Transition factor for use between 600,000 feet and 300,000 feet of altitude.

C_{BASIC} = Basic, full-scale, freestream, rigid body force or moment coefficient.

$\Delta C_{HIGH ALT}$ = Change in force or moment coefficient due to high altitude effects ($h > 285,000$ ft).

$\Delta C_{REAL GAS}$ = Change in force or moment coefficient due to real gas effects.

$\Delta C_{VISCOUS INTERACTION}$ = Change in force or moment coefficient due to viscous interaction, \bar{V}'_{∞} , effects.

ΔC_{BF} = Change in force or moment coefficient due to body flap deflection, δ_{BF} .



$\Delta C_{() \text{ELEVATOR/AILERON}}$ = Change in force or moment coefficient due to elevator deflection (δe) and aileron deflection (δa).

$\Delta C_{() \text{PLUNGING}}$ = Change in force or moment coefficient due to rate of change of angle of attack, $\dot{\alpha}$, (per radian).

$\Delta C_{() \text{PITCH RATE}}$ = Change in force or moment coefficient due to pitch rate, q , (per radian).

$\Delta C_{() \text{LG}}$ = Change in force or moment coefficient due to fully extended landing gear.
NOTE: θ_{MG} = angle between main gear fully retracted and fully extended positions.

$$\theta_{MG} = \begin{cases} 0.0^\circ, & \text{Fully Retracted} \\ 98.0^\circ, & \text{Fully Extended} \end{cases}$$

$\Delta C_{() \text{GE}}$ = Change in force or moment coefficient due to proximity of ground.

h/b = ratio of height above ground to wing span at reference point $\begin{cases} X_0 1506.84 \\ Z_0 282.71 \end{cases}$
(See also Section 3.6)

$\Delta C_{() \text{SILTS POD}}$ = Change in force or moment coefficient due to addition of SILTS POD.

$\Delta C_{() \text{VEHICLE}}$ = Change in force or moment coefficient due to geometry differences between vehicles (e.g., OV099, OV102, OV103, or OV104).



| | DIGITAL FILE No. | TABLE (or FIGURE) No. |
|---|------------------------|-----------------------------|
| $C_{()_{\text{PLB DRS OPEN}}} = C_{()_{\text{PLBDO}}} f(a, \beta)$ | | |
| subscript: (L) | A 1 | 5.2.1.1.1- 1 |
| (N) | A 2 | 5.2.1.1.1- 18 |
| (D) | A 3 | 5.2.1.1.2- 1 |
| (A) | A 4 | 5.2.1.1.2- 18 |
| (m) | A 5 | 5.2.1.1.3- 1 |
| $C_{()_{h=600K ft}} = C_{()_{\text{PLBDC}}} f(a, \beta, h = 600K ft.)$ | | |
| subscript: (L) | A 6 | 5.2.1.1.1- 2 |
| (N) | A 7 | 5.2.1.1.1- 19 |
| (D) | A 8 | 5.2.1.1.2- 2 |
| (A) | A 9 | 5.2.1.1.2- 19 |
| (m) | A 10 | 5.2.1.1.3- 2 |
| $C_{()_{h=300K ft}} = C_{()_{\text{PLBDC}}} f(a, \beta, h = 300K ft.)$ | | |
| subscript: (L) | A 6 | 5.2.1.1.1- 2 |
| (N) | A 7 | 5.2.1.1.1- 19 |
| (D) | A 8 | 5.2.1.1.2- 2 |
| (A) | A 9 | 5.2.1.1.2- 19 |
| (m) | A 10 | 5.2.1.1.3- 2 |
| $K_{\text{TRAN}} = K_{\text{TRAN}} f(h)$ | A130 | 5.2.1.1.1- 17 |
| $C_{()_{\text{BASIC}}} = C_{()_{\text{B}}} f(\delta_{\text{SB}}, a, M)$ | | |
| subscript: (L) | A 11 | 5.2.1.1.1- 3 |
| (N) | A 12 | 5.2.1.1.1- 20 |
| (D) | A 13 | 5.2.1.1.2- 3 |
| (A) | A 14 | 5.2.1.1.2- 20 |
| (m) | A 15 | 5.2.1.1.3- 3 |
| $\Delta C_{()_{\text{HIGH ALT}}} = \Delta C_{()_{\text{HA}}} f(a, h)$ | | |
| subscript: (L) | A 16 | 5.2.1.1.1- 4 |
| (N) | A 17 | 5.2.1.1.1- 21 |
| (D) | A 18 | 5.2.1.1.2- 4 |
| (A) | A 19 | 5.2.1.1.2- 21 |
| (m) | A 20 | 5.2.1.1.3- 4 |



| DIGITAL FILE No. | TABLE (or FIGURE) No. |
|------------------------|-----------------------------|
|------------------------|-----------------------------|

$$\Delta C_{() \text{REAL GAS}} = \Delta C_{() \text{RG}} f(\alpha, M)$$

| | | |
|----------------|------|---------------|
| subscript: (L) | A 21 | 5.2.1.1.1- 5 |
| (N) | A 22 | 5.2.1.1.1- 22 |
| (D) | A 23 | 5.2.1.1.2- 5 |
| (A) | A 24 | 5.2.1.1.2- 22 |
| (m) | A 25 | 5.2.1.1.3- 5 |

$$\Delta C_{() \text{VISCIOUS INTERACTION}} = \Delta C_{() \text{VI}} f(\alpha, \bar{V}_w')$$

| | | |
|----------------|------|---------------|
| subscript: (L) | A 26 | 5.2.1.1.1- 6 |
| (N) | A 27 | 5.2.1.1.1- 23 |
| (D) | A 28 | 5.2.1.1.2- 6 |
| (A) | A 29 | 5.2.1.1.2- 23 |
| (m) | A 30 | 5.2.1.1.3- 6 |

$$\Delta C_{() \text{BF}} = \Delta C_{() \text{BF}} f(\delta_{\text{BF}}^f, \alpha, M)$$

| | | |
|----------------|------|---------------|
| subscript: (L) | A 31 | 5.2.1.1.1- 7 |
| (N) | A 32 | 5.2.1.1.1- 24 |
| (D) | A 33 | 5.2.1.1.2- 7 |
| (A) | A 34 | 5.2.1.1.2- 24 |
| (m) | A 35 | 5.2.1.1.3- 7 |



$$\Delta C_{() \text{ELEVATOR/AILERON}} = \frac{1}{2} \left[K_{() \delta_{eL}} \Delta C_{() e_{L1}} + (1 - K_{() \delta_{eL}}) \Delta C_{() e_{L0}} + K_{() \delta_{eR}} \Delta C_{() e_{R1}} + (1 - K_{() \delta_{eR}}) \Delta C_{() e_{R0}} \right]$$

$K_{() \delta_{eL \text{ or } R}}$ = Elevon partial span factor to be used for elevon-body flap interconnect flight system where δ_e is limited to $\pm 5^\circ$ and inboard and outboard angles are not equal.
NOTE: subscript L = left-hand panels
R = right-hand panels

$\Delta C_{() e_{L1, L0} \text{ or } R1, R0}$ = Change in force or moment coefficient due to individual elevon deflection, δ_{eL1} , δ_{eL0} , δ_{eR1} , or δ_{eR0} .

| | DIGITAL FILE No. | TABLE (or FIGURE) No. |
|---|------------------------|-----------------------------|
| $K_{() \delta_{eL}} = K_{() \text{SPLIT ELEVON}} f(\delta_{eL}, M)$ | | |
| subscript: (L) | A 36 | 5.2.1.1.1- 8 |
| (N) | A 37 | 5.2.1.1.1- 25 |
| (D) | A 38 | (0.50) |
| (A) | A 39 | (0.50) |
| (m) | A 40 | 5.2.1.1.3- 8 |
| $\Delta C_{() e_{L1}} = \Delta C_{() e} f(\delta_{eL1}, \alpha, M)$ | | |
| subscript: (L) | A 41 | 5.2.1.1.1- 9 |
| (N) | A 42 | 5.2.1.1.1- 26 |
| (D) | A 43 | 5.2.1.1.2- 9 |
| (A) | A 44 | 5.2.1.1.2- 26 |
| (m) | A 45 | 5.2.1.1.3- 9 |
| $\Delta C_{() e_{L0}} = \Delta C_{() e} f(\delta_{eL0}, \alpha, M)$ | | |
| subscript: (L) | A 41 | 5.2.1.1.1- 9 |
| (N) | A 42 | 5.2.1.1.1- 26 |
| (D) | A 43 | 5.2.1.1.2- 9 |
| (A) | A 44 | 5.2.1.1.2- 26 |
| (m) | A 45 | 5.2.1.1.3- 9 |
| $K_{() \delta_{eR}} = K_{() \text{SPLIT ELEVON}} f(\delta_{eR}, M)$ | | |
| subscript: (L) | A 36 | 5.2.1.1.1- 8 |
| (N) | A 37 | 5.2.1.1.1- 25 |
| (D) | A 38 | (0.50) |
| (A) | A 39 | (0.50) |
| (m) | A 40 | 5.2.1.1.3- 8 |



| | |
|------------------------|-----------------------------|
| DIGITAL FILE No. | TABLE (or FIGURE) No. |
|------------------------|-----------------------------|

$$\Delta C_{(l)eR_1} = \Delta C_{(l)e} f(\delta e_{R_1}, \alpha, M)$$

| | | |
|----------------|------|---------------|
| subscript: (L) | A 41 | 5.2.1.1.1- 9 |
| (N) | A 42 | 5.2.1.1.1- 26 |
| (D) | A 43 | 5.2.1.1.2- 9 |
| (A) | A 44 | 5.2.1.1.2- 26 |
| (m) | A 45 | 5.2.1.1.3- 9 |

$$\Delta C_{(l)eR_0} = \Delta C_{(l)e} f(\delta e_{R_0}, \alpha, M)$$

| | | |
|----------------|------|---------------|
| subscript: (L) | A 41 | 5.2.1.1.1- 9 |
| (N) | A 42 | 5.2.1.1.1- 26 |
| (D) | A 43 | 5.2.1.1.2- 9 |
| (A) | A 44 | 5.2.1.1.2- 26 |
| (m) | A 45 | 5.2.1.1.3- 9 |

$$\Delta C_{(l)PLUNGING} = C_{(l)\dot{\alpha}} \frac{\dot{\alpha} \bar{c}}{2V}$$

NOTE: This coefficient has been included to preserve completeness of the overall equation.

$C_{(l)\dot{\alpha}}$ = Change in force or moment coefficient due to rate of change of angle of attack, $\dot{\alpha}$, (per radian).

| | |
|------------------------|-----------------------------|
| DIGITAL FILE No. | TABLE (or FIGURE) No. |
|------------------------|-----------------------------|

$$C_{(l)\dot{\alpha}} = C_{(l)\dot{\alpha}} f(\alpha, M)$$

| | | |
|----------------|------|-------------|
| subscript: (L) | none | zero valued |
| (N) | none | zero valued |
| (D) | none | zero valued |
| (A) | none | zero valued |
| (m) | none | zero valued |

$$\Delta C_{(l)PITCH RATE} = \eta_{(l)q} \left\{ C_{(l)q} + \left[K_{SB BF} \left(\frac{\delta_{SB} - 25}{75} \right) + (1 - K_{SB BF}) \left(\frac{\delta_{BF}}{13.75} \right) \right] \Delta C_{(l)q_{SB BF}} \right\} \frac{q \bar{c}}{2V}$$

$\eta_{(l)q}$ = Pitch rate flexible-to-rigid ratio

$C_{(l)q}$ = Change in force or moment coefficient due to pitch rate, q , (per radian).



$K_{\text{SB}}^{\text{BF}}$ = constant.
 $\Delta C_{(l)q}^{\text{SB}}^{\text{BF}}$ = Incremental effect of speedbrake/body flap on pitch damping.

| | DIGITAL FILE No. | TABLE (or FIGURE) No. |
|--|------------------------|-----------------------------|
| $\eta_{(l)q} = \eta_{(l)q} f(\bar{q}, M)$ | | |
| subscript: (L) | F 16 | (1.0) |
| (N) | F 17 | (1.0) |
| (D) | F 18 | (1.0) |
| (A) | F 19 | (1.0) |
| (m) | F 20 | 5.2.1.1.3- 18 |
| $C_{(l)q} = C_{(l)q} f(\alpha, M)$ | | |
| subscript: (L) | A 46 | 5.2.1.1.1- 10 |
| (N) | A 47 | 5.2.1.1.1- 27 |
| (D) | A 48 | zero valued |
| (A) | A 49 | 5.2.1.1.2- 27 |
| (m) | A 50 | 5.2.1.1.3- 10 |
| $K_{\text{SB}}^{\text{BF}} = 0.50$ | | none |
| $\Delta C_{(l)q}^{\text{SB}}^{\text{BF}} = \Delta C_{(l)q}^{\text{SB}}^{\text{BF}} f(\alpha, M)$ | | |
| subscript: (L) | A 51 | zero valued |
| (N) | A 52 | zero valued |
| (D) | A 53 | zero valued |
| (A) | A 54 | zero valued |
| (m) | A 55 | 5.2.1.1.3- 11 |
| $\Delta C_{(l)LG} = \Delta C_{(l)LG} f(\alpha, \theta_{MG})$ | | |
| subscript: (L) | A 56 | 5.2.1.1.1- 12 |
| (N) | A 57 | 5.2.1.1.1- 28 |
| (D) | A 58 | 5.2.1.1.2- 12 |
| (A) | A 59 | 5.2.1.1.2- 28 |
| (m) | A 60 | 5.2.1.1.3- 12 |

$$\Delta C_{()GE} = C_{()GE_{BASIC}} + \Delta C_{()GE_{BF}}$$

$\Delta C_{()GE_{BASIC}}$ = Change in basic force or moment coefficient due to ground effects ($\delta_{BF} = -11.7^\circ$).

$\Delta C_{()GE_{BF}}$ = Incremental change in body flap force or moment coefficient due to ground effects.

| | DIGITAL FILE No. | TABLE (or FIGURE) No. |
|---|------------------------|-----------------------------|
| $\Delta C_{()GE_{BASIC}} = \Delta C_{()GE_{BASIC}} f(h/b, \alpha, \delta_{BF}^i)$ | | |
| subscript: (L) | A 61 | 5.2.1.1.1- 13 |
| (N) | A 62 | 5.2.1.1.1- 29 |
| (D) | A 63 | 5.2.1.1.2- 13 |
| (A) | A 64 | 5.2.1.1.2- 29 |
| (m) | A 65 | 5.2.1.1.3- 13 |
| $\Delta C_{()GE_{BF}} = \Delta C_{()GE_{BF}} f(h/b, \alpha, \delta_{BF}^i)$ | | |
| subscript: (L) | A 66 | 5.2.1.1.1- 14 |
| (N) | A 67 | 5.2.1.1.1- 30 |
| (D) | A 68 | 5.2.1.1.2- 14 |
| (A) | A 69 | 5.2.1.1.2- 30 |
| (m) | A 70 | 5.2.1.1.3- 14 |
| $\Delta C_{()SILTS_{POD}} = \Delta C_{()SP} f(M, SP \text{ FLAG})$ 0 off 1 on | | |
| subscript: (L) | A 71 | 5.2.1.1.1- 15 |
| (N) | A 72 | 5.2.1.1.1- 31 |
| (D) | A 73 | 5.2.1.1.2- 15 |
| (A) | A 74 | 5.2.1.1.2- 31 |
| (m) | A 75 | 5.2.1.1.3- 15 |
| $\Delta C_{()VEHICLE} = \Delta C_{()VEH} f(M, \text{VEHICLE})$ | | |
| subscript: (L) | A 76 | 5.2.1.1.1- 16 |
| (N) | A 77 | 5.2.1.1.1- 32 |
| (D) | A 78 | 5.2.1.1.2- 16 |
| (A) | A 79 | 5.2.1.1.2- 32 |
| (m) | A 80 | 5.2.1.1.3- 16 |

(NOTE: The term VEHICLE is given as Vehicle Number; i.e., 99, 102, 103, 104)

RCS flow field interactions have been subdivided into three components:

1. RCS JET THRUST (subscript JT)
2. RCS JET PLUME IMPINGEMENT (subscript IMP)
3. RCS JET PLUME INTERACTION WITH FLOW FIELD (subscript JI)

The effect of the RCS may be described as a dimensional force (pounds) or moment (foot-pounds) in terms of the significant contributing elements by:

$$()_{RCS} = ()_{JT} + [()_{SURF} + \Delta()_e + \Delta()_{BF}]_{IMP} + \bar{q} S_w [\Delta C_{()} + \Delta C_{()_e} + \Delta C_{()_{BF}}]_{JI}$$

where, () indicates Normal Force (N) or Axial Force (A) and;

$$(M)_{RCS} = (M)_{JT} + [(M)_{SURF} + \Delta(M)_e + \Delta(M)_{BF}]_{IMP} + \bar{q} S_w \bar{c}_w [\Delta C_{(m)} + \Delta C_{(m)_e} + \Delta C_{(m)_{BF}}]_{JI}$$

where, (M) indicates Pitching Moment.

$$()_{JT} = \text{Thrust Force or Moment resulting from number (n) of jets being fired (Reference Data only).}$$

$$= K_A \{ K_{MJL} [()_{JT_U} + ()_{JT_S} + ()_{JT_D}]_L + K_{MJR} [()_{JT_U} + ()_{JT_S} + ()_{JT_D}]_R \}$$

$$K_{MJL} = 1.018423 - 0.009423(n_{LHU} + n_{LHS} + n_{LHD})$$

$$K_{MJR} = 1.018423 - 0.009423(n_{RHU} + n_{RHS} + n_{RHD})$$

$$(N)_{JT_{UL}} = - (L4U + L2U + L1U)T$$

$$(N)_{JT_{SL}} = 0.0257(L4L + L2L + L3L + L1L)T$$

$$(N)_{JT_{DL}} = 0.9215(L4D + L2D + L3D)T$$

$$(N)_{JT_{UR}} = - (R4U + R2U + R1U)T$$

$$(N)_{JT_{SR}} = 0.0257(R4R + R2R + R3R + R1R)T$$

$$(N)_{JT_{DR}} = 0.9215(R4D + R2D + R3D)T$$

$$(A)_{JT_{UL}} = (A)_{JT_{SL}} = (A)_{JT_{UR}} = (A)_{JT_{SR}} = 0$$

$$(A)_{JT_{DL}} = - 0.1959(L4D + L2D + L3D)T$$

$$(A)_{JT_{DR}} = - 0.1959(R4D + R2D + R3D)T$$

$$(M)_{JT_{UL}} = [36.6083(L4U) + 37.6917(L2U) + 38.7750(L1U)]T$$



$$(M)_{JTSL} = -[0.9408(L4L) + 0.9687(L2L) + 0.9965(L3L) + 1.0244(L1L)]T$$

$$(M)_{JTDL} = -[34.7532(L4D) + 35.7940(L2D) + 36.8347(L3D)]T$$

$$(M)_{JTUR} = +[36.6083(R4U) + 37.6917(R2U) + 38.7750(R1U)]T$$

$$(M)_{JTSR} = -[0.9408(R4R) + 0.9687(R2R) + 0.9965(R3R) + 1.0244(R1R)]T$$

$$(M)_{JTD R} = -[34.7532(R4D) + 35.7940(R2D) + 36.8347(R3D)]T$$

K_A = Altitude-Thrust correction factor.

$K_{MJL \text{ or } R}$ = Multiple jet firing thrust correction factor for left (right) hand jets

$()_{SURF IMP}$ = Force or Moment resulting from jet impingement on Orbiter Vehicle surface(s).

$$= ()_{SURF IMP S} (n_{LH} + n_{RH})_S + ()_{SURF IMP D} (n_{LH} + n_{RH})_D$$

$\Delta()_{eIMP}$ = Change in impingement Force or Moment due to elevon deflection.

$$= \Delta()_{eIMP_{LD}} n_{LHD} + \Delta()_{eIMP_{RD}} n_{RHD}$$

$\Delta()_{BFIMP}$ = Change in impingement Force or Moment due to body flap deflection.

$$= \Delta()_{BFIMP_D} (n_{LH} + n_{RH})_D$$

$\Delta C()_{JI}$ = Change in Force or Moment coefficient due to jet interaction.

$$= \Delta C()_{JILU} + \Delta C()_{JIRU} + \Delta C()_{JILS} + \Delta C()_{JIRS} + \Delta C()_{JILD} + \Delta C()_{JIRD}$$

$\Delta C()_{eJI}$ = Change in jet interaction Force or Moment coefficient due to elevon deflection.

$$= \Delta C()_{eJILS} + \Delta C()_{eJIRS} + \Delta C()_{eJILD} + \Delta C()_{eJIRD}$$

$\Delta C()_{BFJI}$ = Change in jet interaction Force or Moment coefficient due to body flap deflection.

$$= \Delta C()_{BFJILD} + \Delta C()_{BFJIRD}$$

| | DIGITAL FILE No. | TABLE (or FIGURE) No. |
|---|------------------------|-----------------------------|
| $K_A = f(h)$ | J 31 | 5.2.1.1.1- 44 |
| $()_{SURF} = ()_{IMP_S} f(P_{\infty})$ IMP S | | |
| component: (N) | J 1 | 5.2.1.1.1- 35 |
| (A) | J 2 | 5.2.1.1.2- 35 |
| (m) | J 3 | 5.2.1.1.3- 19 |
| $()_{SURF} = ()_{IMP_D} f(P_{\infty})$ IMP D | | |
| component: (N) | J 4 | 5.2.1.1.1- 36 |
| (A) | J 5 | 5.2.1.1.2- 36 |
| (m) | J 6 | 5.2.1.1.3- 20 |
| $\Delta()_{e_{IMP_{LD}}} = \Delta()_{e_{IMP_D}} f(P_{\infty}, \delta e_L^f)$ | | |
| component: (N) | J 7 | 5.2.1.1.1- 37 |
| (A) | J 8 | 5.2.1.1.2- 37 |
| (m) | J 9 | 5.2.1.1.3- 21 |
| $\Delta()_{e_{IMP_{RD}}} = \Delta()_{e_{IMP_D}} f(P_{\infty}, \delta e_R^f)$ | | |
| component: (N) | J 7 | 5.2.1.1.1- 37 |
| (A) | J 8 | 5.2.1.1.2- 37 |
| (m) | J 9 | 5.2.1.1.3- 21 |
| $\Delta()_{BF_{IMP_D}} = \Delta()_{BF_{IMP_D}} f(P_{\infty}, \delta_{BF}^f)$ | | |
| component: (N) | J 10 | 5.2.1.1.1- 38 |
| (A) | J 11 | 5.2.1.1.2- 38 |
| (m) | J 12 | 5.2.1.1.3- 22 |
| $\Delta C_{()_{JLU}} = \Delta C_{()_{JU}} f\left(\frac{\phi_J}{\phi_{\infty}} \Big _{LHU}, \alpha\right)$ | | |
| subscript: (N) | J 13 | 5.2.1.1.1- 39 |
| (A) | J 14 | 5.2.1.1.2- 39 |
| (m) | J 15 | 5.2.1.1.3- 23 |
| $\Delta C_{()_{JRU}} = \Delta C_{()_{JU}} f\left(\frac{\phi_J}{\phi_{\infty}} \Big _{RHU}, \alpha\right)$ | | |
| subscript: (N) | J 13 | 5.2.1.1.1- 39 |
| (A) | J 14 | 5.2.1.1.2- 39 |
| (m) | J 15 | 5.2.1.1.3- 23 |

| | DIGITAL FILE No. | TABLE (or FIGURE) No. |
|---|------------------------|---|
| $\Delta C_{()J1L5} = \Delta C_{()J1S} f \left(\frac{\phi_J}{\phi_\infty} \Big _{LH5}, a \right)$ | | |
| subscript: (N) (A) (m) | J 16 J 17 J 18 | 5.2.1.1.1- 40 5.2.1.1.2- 40 5.2.1.1.3- 24 |
| $\Delta C_{()J1R5} = \Delta C_{()J1S} f \left(\frac{\phi_J}{\phi_\infty} \Big _{RH5}, a \right)$ | | |
| subscript: (N) (A) (m) | J 16 J 17 J 18 | 5.2.1.1.1- 40 5.2.1.1.2- 40 5.2.1.1.3- 24 |
| $\Delta C_{()J1L0} = \Delta C_{()J1D} f \left(\frac{\phi_J}{\phi_\infty} \Big _{LH0}, a \right)$ | | |
| subscript: (N) (A) (m) | J 19 J 20 J 21 | 5.2.1.1.1- 41 5.2.1.1.2- 41 5.2.1.1.3- 25 |
| $\Delta C_{()J1R0} = \Delta C_{()J1D} f \left(\frac{\phi_J}{\phi_\infty} \Big _{RH0}, a \right)$ | | |
| subscript: (N) (A) (m) | J 19 J 20 J 21 | 5.2.1.1.1- 41 5.2.1.1.2- 41 5.2.1.1.3- 25 |
| $\Delta C_{()eJ1L5} = \Delta C_{()eJ1S} f \left(\frac{\phi_J}{\phi_\infty} \Big _{LH5}, a, \delta e_L^f \right)$ | | |
| subscript: (N) (A) (m) | J 22 J 23 J 24 | (zero valued) (zero valued) (zero valued) |
| $\Delta C_{()eJ1R5} = \Delta C_{()eJ1S} f \left(\frac{\phi_J}{\phi_\infty} \Big _{RH5}, a, \delta e_R^f \right)$ | | |
| subscript: (N) (A) (m) | J 22 J 23 J 24 | (zero valued) (zero valued) (zero valued) |

| | DIGITAL FILE No. | TABLE (or FIGURE) No. |
|---|------------------------|---|
| $\Delta C_{(l)e_{JL}L_D} = \Delta C_{(l)e_{JD}} f\left(\frac{\phi_J}{\phi_\infty} \Big _{LHD}, a, \delta e_L^f\right)$ | | |
| subscript: (N) (A) (m) | J 25 J 26 J 27 | 5.2.1.1.1- 42 5.2.1.1.2- 42 5.2.1.1.3- 26 |
| $\Delta C_{(l)e_{JR}D} = \Delta C_{(l)e_{JD}} f\left(\frac{\phi_J}{\phi_\infty} \Big _{RHD}, a, \delta e_R^f\right)$ | | |
| subscript: (N) (A) (m) | J 25 J 26 J 27 | 5.2.1.1.1- 42 5.2.1.1.2- 42 5.2.1.1.3- 26 |
| $\Delta C_{(l)BF_{JL}L_D} = \Delta C_{(l)BF_{JD}} f\left(\frac{\phi_J}{\phi_\infty} \Big _{LHD}, a, \delta e_{BF}^f\right)$ | | |
| subscript: (N) (A) (m) | J 28 J 29 J 30 | 5.2.1.1.1- 43 (zero valued) 5.2.1.1.3- 27 |
| $\Delta C_{(l)BF_{JR}D} = \Delta C_{(l)BF_{JD}} f\left(\frac{\phi_J}{\phi_\infty} \Big _{RHD}, a, \delta e_{BF}^f\right)$ | | |
| subscript: (N) (A) (m) | J 28 J 29 J 30 | 5.2.1.1.1- 43 (zero valued) 5.2.1.1.3- 27 |

NOTE: The effects of the RCS on LIFT and DRAG may be computed from;

$$(L)_{RCS} = (N)_{RCS} \cos \alpha - (A)_{RCS} \sin \alpha$$

$$(D)_{RCS} = (N)_{RCS} \sin \alpha + (A)_{RCS} \cos \alpha$$

4.2.1.2 LATERAL-DIRECTIONAL AERODYNAMICS. The basic aerodynamic characteristics for the lateral-directional degrees-of-freedom are presented as full-scale, rigid and elastic, force and moments in the body-axis system (cf. Section 3.1.5). The lateral-directional characteristics are defined under the same three categories listed in Section 4.2.1.1,

The total lateral-directional force and moments for the Orbiter Vehicle are defined as:

$$\text{SIDE FORCE, } Y_{\text{TOTAL}} = \bar{q} S_w C_{Y_{\text{TOTAL}}} + Y_{\text{RCS}} \quad (\text{lb})$$

$$\text{YAWING MOMENT, } N_{\text{TOTAL}} = \bar{q} S_w b_w C_{n_{\text{TOTAL}}} + N_{\text{RCS}} \quad (\text{ft-lb})$$

$$\text{ROLLING MOMENT, } L_{\text{TOTAL}} = \bar{q} S_w b_w C_{l_{\text{TOTAL}}} + L_{\text{RCS}} \quad (\text{ft-lb})$$

where, \bar{q} = dynamic pressure (lb/ft²)

S_w = Wing Reference Area (2690.00 ft²)

b_w = Wing Span (78.057 ft)
(see Figure 3.1.5-2b)

RCS flow field interactions are defined as contributions to the total force or moments rather than coefficients since the terms due to jet thrust and impingement are independent of dynamic pressure and cannot, therefore, be normalized in the conventional manner.

The total non-dimensional force and moment coefficients are defined as:

ON-ORBIT (PAYLOAD BAY DOORS OPEN)

$$C_{()TOTAL} = C_{()PLB DRS OPEN}$$

ON-ORBIT (PAYLOAD BAY DOORS CLOSED)

$$C_{()TOTAL} = C_{()h=300K ft} + K_{TRAN} [C_{()h=600K ft} - C_{()h=300K ft}]$$

ENTRY

$$C_{()TOTAL} = C_{()SIDESLIP} + \Delta C_{()AILERON} + \Delta C_{()RUDDER} + \Delta C_{()ROLL RATE} + \Delta C_{()YAW RATE} \\ + \Delta C_{()SILTS POD} + \Delta C_{()VEHICLE}$$

where, the subscript () denotes side force (Y), yawing moment (n), or rolling moment (l) and;

$C_{()PLB DRS OPEN}$ = Basic, full-scale, freestream, rigid body force or moment coefficient when vehicle is in orbit with payload bay doors open (altitude = 600,000 feet).

$C_{()h=600K ft}$ = Basic, full-scale, freestream, rigid body force or moment coefficient when vehicle is in orbit with payload bay doors closed (altitude = 600,000 feet).

$C_{()h=300K ft}$ = Basic, full-scale, rigid body force or moment coefficient when vehicle, with payload bay doors closed, is at an altitude of 300,000 feet.

K_{TRAN} = Transition factor for use between 600,000 feet and 300,000 feet of altitude.

$C_{()SIDESLIP}$ = Basic, full-scale, freestream, force or moment coefficient due to sideslip angle, β .

$\Delta C_{()AILERON}$ = Change in force or moment coefficient due to aileron deflection, δ_a .

$\Delta C_{()RUDDER}$ = Change in force or moment coefficient due to rudder deflection, δ_R .



- $\Delta C_{(1)}$ _{ROLL RATE} = Change in force or moment coefficient due to roll rate, p , (per radian).
- $\Delta C_{(1)}$ _{YAW RATE} = Change in force or moment coefficient due to yaw rate, r , (per radian).
- $\Delta C_{(1)}$ _{SILTS POD} = Change in force or moment coefficient due to addition of SILTS POD.
- $\Delta C_{(1)}$ _{VEHICLE} = Change in force or moment coefficient due to geometry differences between vehicles (e.g., OV099, OV102, OV103 or OV104).

| | DIGITAL FILE No. | TABLE (or FIGURE) No. |
|--|------------------------|-----------------------------|
| $C_{(1)}$ _{PLB DRS OPEN} = $C_{(1)}$ _{PLBDO} $f(a, \beta)$ | | |
| subscript: (Y) | A 81 | 5.2.1.2.1- 1 |
| (n) | A 82 | 5.2.1.2.2- 1 |
| (l) | A 83 | 5.2.1.2.3- 1 |
| $C_{(1)}$ _{h=600K ft} = $C_{(1)}$ _{PLBDC} $f(a, \beta, h = 600K \text{ ft})$ | | |
| subscript: (Y) | A 84 | 5.2.1.2.1- 2 |
| (n) | A 85 | 5.2.1.2.2- 2 |
| (l) | A 86 | 5.2.1.2.3- 2 |
| $C_{(1)}$ _{h=300K ft} = $C_{(1)}$ _{PLBDC} $f(a, \beta, h = 300K \text{ ft})$ | | |
| subscript: (Y) | A 84 | 5.2.1.2.1- 2 |
| (n) | A 85 | 5.2.1.2.2- 2 |
| (l) | A 86 | 5.2.1.2.3- 2 |
| K_{TRAN} = K_{TRAN} $f(h)$ | A130 | 5.2.1.2.1- 17 |

$$C_{(1)SIDESLIP} = [1 - \eta_{(1)VT}] C_{(1)\delta_{SB}=25^\circ} - [1 - \eta_{(1)VT}] \Delta C_{(1)\beta_{VT}} \beta + \eta_{(1)VT} C_{(1)\delta_{SB}=\delta_{SB}} \\ + \Delta C_{(1)\beta_{HIGH}} \beta + \Delta C_{(1)\beta_e} \beta + \Delta C_{(1)\beta_{LG}} \beta + \Delta C_{(1)\beta_{GE}} \beta$$

$\eta_{(1)VT}$ = Vertical tail flexible-to-rigid ratio .

$C_{(1)\delta_{SB}=25^\circ}$ = Basic force or moment coefficient with speedbrake set at 25°.

$\Delta C_{(1)\beta_{VT}}$ = Change in basic force or moment coefficient of vertical tail due to sideslip.

$C_{(1)\delta_{SB}=\delta_{SB}}$ = Basic force or moment coefficient with speedbrake deflection, δ_{SB} .

$\Delta C_{(1)\beta_{HIGH}} \beta$ = Change in force or moment coefficient due to high altitude effects ($h > 285,000$ ft).

$\Delta C_{(1)\beta_e}$ = Change in force or moment coefficient due to elevon deflection, δ_e .

$\Delta C_{(1)\beta_{LG}}$ = Change in force or moment coefficient due to fully extended landing gear.

NOTE: θ_{MG} = angle between main gear fully retracted and fully extended positions

$$\theta_{MG} = \begin{cases} 0.0^\circ, & \text{Fully Retracted} \\ 98.0^\circ, & \text{Fully Extended} \end{cases}$$

$\Delta C_{(1)\beta_{GE}}$ = Change in force or moment coefficient due to ground effect.



| | DIGITAL FILE No. | TABLE (or FIGURE) No. |
|--|------------------------|-----------------------------|
| $\eta_{(1)VT} = \eta_{(1)VT} f(\bar{a}, M)$ | | |
| subscript: (Y) | F 4 | 5.2.1.2.1- 19 |
| (n) | F 5 | 5.2.1.2.2- 19 |
| (l) | F 6 | 5.2.1.2.3- 19 |
| $C_{(1)\delta_{SB}=25} = C_{(1)B} f(\beta , a, M, \delta_{SB} = 25^\circ) \text{SIGN}(\beta)$ | | |
| subscript: (Y) | A 87 | 5.2.1.2.1- 3 |
| (n) | A 88 | 5.2.1.2.2- 3 |
| (l) | A 89 | 5.2.1.2.3- 3 |
| $\Delta C_{(1)\beta_{VT}} = \Delta C_{(1)\beta_{VT}} f(a, M)$ | | |
| subscript: (Y) | F 1 | 5.2.1.2.1- 18 |
| (n) | F 2 | 5.2.1.2.2- 18 |
| (l) | F 3 | 5.2.1.2.3- 18 |
| $C_{(1)\delta_{SB}=\delta_{SB}} = C_{(1)B} f(\beta , a, M, \delta_{SB}) \text{SIGN}(\beta)$ | | |
| subscript: (Y) | A 87 | 5.2.1.2.1- 3 |
| (n) | A 88 | 5.2.1.2.2- 3 |
| (l) | A 89 | 5.2.1.2.3- 3 |
| $\Delta C_{(1)\beta_{HIGH}} = \Delta C_{(1)\beta_{HA}} f(a, h)$ | | |
| subscript: (Y) | A 90 | 5.2.1.2.1- 4 |
| (n) | A 91 | 5.2.1.2.2- 4 |
| (l) | A 92 | 5.2.1.2.3- 4 |
| $\Delta C_{(1)\beta_e} = \Delta C_{(1)\beta_e} f(\delta_e, a, M)$ | | |
| subscript: (Y) | A 93 | 5.2.1.2.1- 5 |
| (n) | A 94 | 5.2.1.2.2- 5 |
| (l) | A 95 | 5.2.1.2.3- 5 |
| $\Delta C_{(1)\beta_{LG}} = \Delta C_{(1)\beta_{LG}} f(a, \theta_{MG})$ | | |
| subscript: (Y) | A 96 | 5.2.1.2.1- 6 |
| (n) | A 97 | 5.2.1.2.2- 6 |
| (l) | A 98 | 5.2.1.2.3- 6 |
| $\Delta C_{(1)\beta_{GE}} = \Delta C_{(1)\beta_{GE}} f(h/b)$ | | |
| subscript: (Y) | A 99 | (zero valued) |
| (n) | A100 | (zero valued) |
| (l) | A101 | 5.2.1.2.3- 7 |

$$\Delta C_{() \text{AILERON}} = [K_{() \delta_a}^f \delta a_i^f + (1 - K_{() \delta_a}^f) \delta a_o^f] C_{() \delta_a} + \Delta C_{() \delta_{aGE}}^f \delta a^f$$

δa = Aileron deflection (See Section 4.2.1).

$K_{() \delta_a}$ = Elevon partial span factor to be used for elevon-body flap interconnect flight system where δe is limited to $\pm 5^\circ$ and inboard and outboard angles are not equal.

$C_{() \delta_a}$ = Change in force or moment coefficient with change in aileron deflection, δa , when inboard and outboard angles are equal.

$\Delta C_{() \delta_{aGE}}$ = Change in force or moment coefficient with change in aileron deflection, δa , when inboard and outboard angles are equal and vehicle is in proximity of ground.

| | DIGITAL FILE No. | TABLE (or FIGURE) No. |
|--|------------------------|-----------------------------|
| $K_{() \delta_a} = K_{() \text{SPLIT ELEVON}}^f f(\delta e, M)$ | | |
| subscript: (Y) | A102 | (0.60) |
| (n) | A103 | 5.2.1.2.2- 8 |
| (l) | A104 | 5.2.1.2.3- 8 |
| $C_{() \delta_a} = C_{() \delta_a}^f f(\delta e, a, M)$ | | |
| subscript: (Y) | A105 | 5.2.1.2.1- 9 |
| (n) | A106 | 5.2.1.2.2- 9 |
| (l) | A107 | 5.2.1.2.3- 9 |
| $\Delta C_{() \delta_{aGE}} = \Delta C_{() \delta_{aGE}}^f f(h/b, \phi)$ | | |
| subscript: (Y) | A108 | (zero valued) |
| (n) | A109 | (zero valued) |
| (l) | A110 | 5.2.1.2.3- 10 |

$$\Delta C_{()RUDDER} = \eta_{()\delta_R} C_{()\delta_R} \delta_R$$

$\eta_{()\delta_R}$ = Rudder flexible-to-rigid ratio.

$C_{()\delta_R}$ = Change in force or moment coefficient with change in rudder deflection.

δ_R = Rudder deflection.

| | DIGITAL FILE No. | TABLE (or FIGURE) No. |
|---|------------------------|-----------------------------|
| $\eta_{()\delta_R} = \eta_{()\delta_R} f(\bar{q}, M)$ | | |
| subscript: (Y) | F 7 | 5.2.1.2.1- 20 |
| (n) | F 8 | 5.2.1.2.2- 20 |
| (L) | F 9 | 5.2.1.2.3- 20 |
| $C_{()\delta_R} = C_{()\delta_R} f(\delta_{SB}, \alpha, M)$ | | |
| subscript: (Y) | A111 | 5.2.1.2.1- 11 |
| (n) | A112 | 5.2.1.2.2- 11 |
| (L) | A113 | 5.2.1.2.3- 11 |

$$\Delta C_{()ROLL RATE} = \eta_{()p} C_{()p} \left(\frac{pb}{2V} \right)$$

$\eta_{()p}$ = Roll rate flexible-to-rigid ratio.

$C_{()p}$ = Change in force or moment coefficient due to roll rate, p.

| | DIGITAL FILE No. | TABLE (or FIGURE) No. |
|---|------------------------|-----------------------------|
| $\eta_{()p} = \eta_{()p} f(\bar{q}, M)$ | | |
| subscript: (Y) | F 10 | (1.0) |
| (n) | F 11 | 5.2.1.2.2- 21 |
| (L) | F 12 | 5.2.1.2.3- 21 |
| $C_{()p} = C_{()p} f(\alpha, M)$ | | |
| subscript: (Y) | A114 | (zero valued) |
| (n) | A115 | 5.2.1.2.2- 12 |
| (L) | A116 | 5.2.1.2.3- 12 |

$$\Delta C_{() \text{ YAW RATE}} = \eta_{() r} \bar{C}_{() r} \left(\frac{rb}{2V} \right)$$

$\eta_{() r}$ = Yaw rate flexible-to-rigid ratio

$C_{() r}$ = Change in force or moment coefficient due to yaw rate, r.

| DIGITAL FILE No. | TABLE (or FIGURE) No. |
|------------------------|-----------------------------|
|------------------------|-----------------------------|

$$\eta_{() r} = \eta_{() r} f(\bar{q}, M)$$

| | | |
|----------------|------|---------------|
| subscript: (Y) | F 13 | (1.0) |
| (n) | F 14 | 5.2.1.2.2- 22 |
| (l) | F 15 | 5.2.1.2.3- 22 |

$$C_{() r} = C_{() r} f(a, M)$$

| | | |
|----------------|------|---------------|
| subscript: (Y) | A117 | (zero valued) |
| (n) | A118 | 5.2.1.2.2- 13 |
| (l) | A119 | 5.2.1.2.3- 13 |

$$\Delta C_{() \text{ SILTS POD}} = \Delta C_{() \beta_{SP}} \beta + \Delta C_{() \delta_{RSP}} \delta_R$$

$\Delta C_{() \beta_{SP}}$ = Change in force or moment coefficient with sideslip angle due to addition of SILTS pod.

$\Delta C_{() \delta_{RSP}}$ = Change in force or moment coefficient with rudder deflection due to addition of SILTS pod.

| | DIGITAL FILE No. | TABLE (or FIGURE) No. |
|---|------------------------|-----------------------------|
| $\Delta C_{(i)}\beta_{SP} = \Delta C_{(i)}\beta_{SP} f(M, SP \text{ FLAG})$ | | |
| | 0 off | |
| | 1 on | |
| subscript: (Y) | A120 | 5.2.1.2.1- 14 |
| (n) | A121 | 5.2.1.2.2- 14 |
| (l) | A122 | 5.2.1.2.3- 14 |
| $\Delta C_{(i)}\delta_{RSP} = \Delta C_{(i)}\delta_{RSP} f(M, SP \text{ FLAG})$ | | |
| | 0 off | |
| | 1 on | |
| subscript: (Y) | A123 | 5.2.1.2.1- 15 |
| (n) | A124 | 5.2.1.2.2- 15 |
| (l) | A125 | 5.2.1.2.3- 15 |
| $\Delta C_{(i)}\text{VEHICLE} = \Delta C_{(i)}\text{VEH} f(M, \text{VEHICLE})$ | | |
| subscript: (Y) | A126 | 5.2.1.2.1- 16 |
| (n) | A127 | 5.2.1.2.2- 16 |
| (l) | A128 | 5.2.1.2.3- 16 |

NOTE: The term VEHICLE is given as Vehicle number; i.e.,
99, 102, 103, 104)

RCS flow field interactions have been subdivided into three components:

1. RCS JET THRUST (subscript JT)
2. RCS JET PLUME IMPINGEMENT (subscript IMP)
3. RCS JET PLUME INTERACTION WITH FLOW FIELD (subscript JI)

The effect of the RCS may be described as a dimensional force (pounds) or moment (foot-pounds) in terms of the significant contributing elements by:

$$(Y)_{RCS} = (Y)_{JT} + [(Y)_{SURF} + \Delta(Y)_e + \Delta(Y)_{BF}]_{IMP} + \bar{q} S_{WB} [\Delta C_{(Y)} + \Delta C_{(Y)_e} + \Delta C_{(Y)_{BF}}]_{JI}$$

where, (Y) indicates Side Force and;

$$()_{RCS} = ()_{JT} + [()_{SURF} + \Delta()_e + \Delta()_{BF}]_{IMP} + \bar{q} S_{WB} [\Delta C_{()} + \Delta C_{()_e} + \Delta C_{()_{BF}}]_{JI}$$

where, () indicates Yawing Moment (n), or Rolling Moment (l).

$$()_{JT} = \text{Thrust Force or Moment resulting from number (n) of jets being fired (Reference Data only).}$$

$$= K_A \left\{ K_{MJL} [()_{JTU} + ()_{JTS} + ()_{JTD}]_L + K_{MJR} [()_{JTU} + ()_{JTS} + ()_{JTD}]_R \right\}$$

$$K_{MJL} = 1.018423 - 0.009423(n_{LHU} + n_{LHS} + n_{LHD})$$

$$K_{MJR} = 1.018423 - 0.009423(n_{RHU} + n_{RHS} + n_{RHD})$$

$$(Y)_{JTUL} = (Y)_{JTUR} = 0$$

$$(Y)_{JTS_L} = 1.0006(L4L + L2L + L3L + L1L)T$$

$$(Y)_{JTD_L} = 0.3354(L4D + L2D + L3D)T$$

$$(Y)_{JTS_R} = -1.0006(R4R + R2R + R3R + R1R)T$$

$$(Y)_{JTD_R} = -0.3354(R4D + R2D + R3D)T$$

$$(n)_{JTUL} = (n)_{JTUR} = 0$$

$$(n)_{JTS_L} = -[36.6303(L4L) + 37.7143(L2L) + 38.7983(L3L) + 39.8822(L1L)]T$$

$$(n)_{JTD_L} = -[10.4508(L4D) + 10.8927(L2D) + 11.2084(L3D)]T$$

$$(n)_{JTS_R} = [36.6303(R4R) + 37.7143(R2R) + 38.7983(R3R) + 39.8822(R1R)]T$$

$$(n)_{JTD_R} = [10.4508(R4D) + 10.8927(R2D) + 11.2084(R3D)]T$$

$$(\ell)_{JT_{UL}} = -11(L4U + L2U + L1U)T$$

$$(\ell)_{JT_{SL}} = 7.3252(L4L + L2L + L3L + L1L)T$$

$$(\ell)_{JT_{DL}} = [10.3409(L4D) + 10.3406(L2D) + 10.3411(L3D)]T$$

$$(\ell)_{JT_{UR}} = 11(R4U + R2U + R1U)T$$

$$(\ell)_{JT_{SR}} = -7.3252(R4R + R2R + R3R + R1R)T$$

$$(\ell)_{JT_{DR}} = -[10.3409(R4D) + 10.3406(R2D) + 10.3411(R3D)]T$$

$$K_A = \text{Altitude-Thrust correction factor}$$

$$K_{MJ_{L \text{ or } R}} = \text{Multiple jet firing thrust correction factor for left (right) hand jets}$$

$$(\)_{SURF IMP} = \text{Force or Moment resulting from jet impingement on Orbiter Vehicle surface(s).}$$

$$= (\)_{SURF IMP U} (n_{LH} - n_{RH})_U + (\)_{SURF IMP S} (n_{LH} - n_{RH})_S + (\)_{SURF IMP D} (n_{LH} - n_{RH})_D$$

$$\Delta(\)_{e_{IMP}} = \text{Change in impingement Force or Moment due to elevon deflection.}$$

$$= \Delta(\)_{e_{IMP L D}} n_{LHD} - \Delta(\)_{e_{IMP R D}} n_{RHD}$$

$$\Delta(\)_{BF_{IMP}} = \text{Change in impingement Force or Moment due to body flap deflection.}$$

$$= \Delta(\)_{BF_{IMP}} (n_{LH} - n_{RH})_D$$

$$\Delta C(\)_{JI} = \text{Change in Force or Moment coefficient due to jet interaction.}$$

$$= \Delta C(\)_{JILU} - \Delta C(\)_{JIRU} + \Delta C(\)_{JILS} - \Delta C(\)_{JIRS} + \Delta C(\)_{JILD} - \Delta C(\)_{JIRD}$$

$$\Delta C(\)_{e_{JI}} = \text{Change in jet interaction Force or Moment coefficient due to elevon deflection.}$$

$$= \Delta C(\)_{e_{JILS}} - \Delta C(\)_{e_{JIRS}} + \Delta C(\)_{e_{JILD}} - \Delta C(\)_{e_{JIRD}}$$

$$\Delta C(\)_{BF_{JI}} = \text{Change in jet interaction Force or Moment coefficient due to body flap deflection.}$$

$$= \Delta C(\)_{BF_{JILD}} - \Delta C(\)_{BF_{JIRD}}$$

| | DIGITAL FILE No. | TABLE (or FIGURE) No. |
|--|------------------------|---|
| $K_A = f(h)$ | J 31 | 5.2.1.2.1- 32 |
| $()_{SURF} = ()_{IMP_U} f(P_{\infty})$ component: (Y) (n) (l) | J 41 J 42 J 43 | 5.2.1.2.1- 23 5.2.1.2.2- 23 5.2.1.2.3- 23 |
| $()_{SURF} = ()_{IMP_S} f(P_{\infty})$ component: (Y) (n) (l) | J 44 J 45 J 46 | 5.2.1.2.1- 24 5.2.1.2.2- 24 5.2.1.2.3- 24 |
| $()_{SURF} = ()_{IMP_D} f(P_{\infty})$ component: (Y) (n) (l) | J 47 J 48 J 49 | 5.2.1.2.1- 25 5.2.1.2.2- 25 5.2.1.2.3- 25 |
| $\Delta()_{e_{IMP_{L_D}}} = \Delta()_{e_{IMP_D}} f(P_{\infty}, \delta e_L^f)$ component: (Y) (n) (l) | J 50 J 51 J 52 | 5.2.1.2.1- 26 5.2.1.2.2- 26 5.2.1.2.3- 26 |
| $\Delta()_{e_{IMP_{R_D}}} = \Delta()_{e_{IMP_D}} f(P_{\infty}, \delta e_R^f)$ component: (Y) (n) (l) | J 50 J 51 J 52 | 5.2.1.2.1- 26 5.2.1.2.2- 26 5.2.1.2.3- 26 |
| $\Delta()_{BF_{IMP_D}} = \Delta()_{BF_{IMP_D}} f(P_{\infty}, \delta_{BF}^f)$ component: (Y) (n) (l) | J 53 J 54 J 55 | (zero valued) 5.2.1.2.2- 27 5.2.1.2.3- 27 |
| $\Delta C()_{J_{L_U}} = \Delta C()_{J_{L_U}} f\left(\frac{\phi_J}{\phi_{\infty}} \Big _{L_{H_U}}, \alpha\right)$ subscript: (Y) (n) (l) | J 56 J 57 J 58 | 5.2.1.2.1- 28 5.2.1.2.2- 28 5.2.1.2.3- 28 |

| | DIGITAL FILE No. | TABLE (or FIGURE) No. |
|---|------------------------|-----------------------------|
| $\Delta C_{()JIRU} = \Delta C_{()JIU} f\left(\frac{\phi_J}{\phi_\infty} \Big _{RHU}, \alpha\right)$ | | |
| subscript: (Y) | J 56 | 5.2.1.2.1- 28 |
| (n) | J 57 | 5.2.1.2.2- 28 |
| (l) | J 58 | 5.2.1.2.3- 28 |
| $\Delta C_{()JILS} = \Delta C_{()JIS} f\left(\frac{\phi_J}{\phi_\infty} \Big _{LHS}, \alpha\right)$ | | |
| subscript: (Y) | J 59 | 5.2.1.2.1- 29 |
| (n) | J 60 | 5.2.1.2.2- 29 |
| (l) | J 61 | 5.2.1.2.3- 29 |
| $\Delta C_{()JIRS} = \Delta C_{()JIS} f\left(\frac{\phi_J}{\phi_\infty} \Big _{RHS}, \alpha\right)$ | | |
| subscript: (Y) | J 59 | 5.2.1.2.1- 29 |
| (n) | J 60 | 5.2.1.2.2- 29 |
| (l) | J 61 | 5.2.1.2.3- 29 |
| $\Delta C_{()JILD} = \Delta C_{()JID} f\left(\frac{\phi_J}{\phi_\infty} \Big _{LHD}, \alpha\right)$ | | |
| subscript: (Y) | J 62 | 5.2.1.2.1- 30 |
| (n) | J 63 | 5.2.1.2.2- 30 |
| (l) | J 64 | 5.2.1.2.3- 30 |
| $\Delta C_{()JIRD} = \Delta C_{()JID} f\left(\frac{\phi_J}{\phi_\infty} \Big _{RHD}, \alpha\right)$ | | |
| subscript: (Y) | J 62 | 5.2.1.2.1- 30 |
| (n) | J 63 | 5.2.1.2.2- 30 |
| (l) | J 64 | 5.2.1.2.3- 30 |
| $\Delta C_{()eJILS} = \Delta C_{()eJIS} f\left(\frac{\phi_J}{\phi_\infty} \Big _{LHS}, \alpha, \delta e_L\right)$ | | |
| subscript: (Y) | J 65 | (zero valued) |
| (n) | J 66 | (zero valued) |
| (l) | J 67 | (zero valued) |

| | DIGITAL FILE No. | TABLE (or FIGURE) No. |
|---|------------------------|-----------------------------|
| $\Delta C_{(l)e_{JIRS}} = \Delta C_{(l)e_{JIS}} f\left(\frac{\phi_J}{\phi_{\infty}} \Big _{RHS}, a, \delta e_R^f\right)$ | | |
| subscript: (Y) | J 65 | (zero valued) |
| (n) | J 66 | (zero valued) |
| (l) | J 67 | (zero valued) |
| $\Delta C_{(l)e_{JILD}} = \Delta C_{(l)e_{JID}} f\left(\frac{\phi_J}{\phi_{\infty}} \Big _{LHD}, a, \delta e_L^f\right)$ | | |
| subscript: (Y) | J 68 | (zero valued) |
| (n) | J 69 | (zero valued) |
| (l) | J 70 | 5.2.1.2.3- 31 |
| $\Delta C_{(l)e_{JIRD}} = \Delta C_{(l)e_{JID}} f\left(\frac{\phi_J}{\phi_{\infty}} \Big _{RHD}, a, \delta e_R^f\right)$ | | |
| subscript: (Y) | J 68 | (zero valued) |
| (n) | J 69 | (zero valued) |
| (l) | J 70 | 5.2.1.2.3- 31 |
| $\Delta C_{(l)BF_{JILD}} = \Delta C_{(l)BF_{JID}} f\left(\frac{\phi_J}{\phi_{\infty}} \Big _{LHD}, a, \delta BF^f\right)$ | | |
| subscript: (Y) | J 71 | (zero valued) |
| (n) | J 72 | (zero valued) |
| (l) | J 73 | (zero valued) |
| $\Delta C_{(l)BF_{JIRD}} = \Delta C_{(l)BF_{JID}} f\left(\frac{\phi_J}{\phi_{\infty}} \Big _{RHD}, a, \delta BF^f\right)$ | | |
| subscript: (Y) | J 71 | (zero valued) |
| (n) | J 72 | (zero valued) |
| (l) | J 73 | (zero valued) |

ORIGINAL PAGE IS
OF POOR QUALITY

4.2.2 HINGE MOMENTS

4.2.2 HINGE MOMENTS

4.2.2 HINGE MOMENTS. The Orbiter Vehicle control surface hinge moment coefficients are defined for both rigid and elastic (flexible) values for the elevon, body flap, and rudder/speedbrake.

4.2.2.1 ELEVON CONTROL. The elevon control hinge moment coefficients are based on theoretical (NOT TRUE) reference dimensions. These reference values were used for each panel so that the total hinge moment is the sum of the individual panel hinge moments:

$$HM_{eTOTAL} = HM_{eINBOARD} + HM_{eOUTBOARD}$$

$$\text{where, } HM_e = C_{he}(\bar{q} S_e \bar{c}_e)$$

$$\text{Reference Area, } S_e = 210.0 \text{ ft}^2$$

$$\text{Mean Aerodynamic Chord, } \bar{c}_e = 90.7 \text{ inches}$$

$$\text{Area Moment, } S_e \bar{c}_e = 19,047.0 \text{ ft}^2\text{-inches}$$

Elevon hinge moments are defined positive in the same sense as for positive deflection; i.e., trailing edge down. However, a positive deflection results in a negative hinge moment.

$$C_{he()TOTAL} = C_{he()I} + C_{he()O} \quad (\text{Applicable to either flex or rigid.})$$

$$C_{he()I}^f = \frac{C_{he()I}}{1 - C_{he()I\delta_e} K_I \bar{q} S_e \bar{c}_e}$$

$$C_{he()O}^f = \frac{C_{he()O}}{1 - C_{he()O\delta_e} K_O \bar{q} S_e \bar{c}_e}$$

$$C_{he()I\delta_e} = \frac{1}{2\delta_e} [C_{he()IPOS} - C_{he()INEG}]$$

$$C_{he()O\delta_e} = \frac{1}{2\delta_e} [C_{he()OPOS} - C_{he()ONEG}]$$

$C_{he()I}$ = Rigid or Flexible (superscript "f")
elevon hinge moment coefficient for
inboard panel.
subscript:(L) = left-hand panel
(R) = right-hand panel

$C_{he()O}$ = Rigid or Flexible (superscript "f")
elevon hinge moment coefficient for
outboard panel.
subscript:(L) = left-hand panel
(R) = right-hand panel

$C_{he(i)} \delta_e$ = Change in elevon hinge moment coefficient with change in elevon deflection for inboard panel.
subscript: (L) = left-hand panel
(R) = right-hand panel

$C_{he(i)} \delta_{e, POS}$
(NEG) = Inboard elevon hinge moment coefficient for a positive (negative) elevon deflection from nominal.

$C_{he(o)} \delta_e$ = Change in elevon hinge moment coefficient with change in elevon deflection for outboard panel.
subscript: (L) = left-hand panel
(R) = right-hand panel

$C_{he(o)} \delta_{e, POS}$
(NEG) = Outboard elevon hinge moment coefficient for a positive (negative) elevon deflection from nominal.

$\delta e'$ = 1 degree (recommended).

K_i = 1.547×10^{-6} degrees/inch-pound

K_o = 3.323×10^{-6} degrees/inch-pound

| | | DIGITAL FILE No. | TABLE (or FIGURE) No. |
|-----------------------------|---|------------------------|-----------------------------|
| $C_{he(i)}$ | = $C_{he_i} f(\delta e_{(i)}, \alpha, M)$ | A131 | 5.2.2.1-1 |
| $C_{he(i)} \delta_{e, POS}$ | = $C_{he_i} f(\delta e_{(i)} + \delta e', \alpha, M)$ | A131 | 5.2.2.1-1 |
| $C_{he(i)} \delta_{e, NEG}$ | = $C_{he_i} f(\delta e_{(i)} - \delta e', \alpha, M)$ | A131 | 5.2.2.1-1 |
| $C_{he(o)}$ | = $C_{he_o} f(\delta e_{(o)}, \alpha, M)$ | A132 | 5.2.2.1-2 |
| $C_{he(o)} \delta_{e, POS}$ | = $C_{he_o} f(\delta e_{(o)} + \delta e', \alpha, M)$ | A132 | 5.2.2.1-2 |
| $C_{he(o)} \delta_{e, NEG}$ | = $C_{he_o} f(\delta e_{(o)} - \delta e', \alpha, M)$ | A132 | 5.2.2.1-2 |

4.2.2.2 BODY FLAP CONTROL. The body flap control hinge moment coefficients are based on theoretical (NOT TRUE) reference dimensions.

$$HM_{BF} = C_{hBF} (\bar{q} S_{BF} \bar{c}_{BF})$$

$$\text{where, Reference Area, } S_{BF} = 135.0 \text{ ft}^2$$

$$\text{Mean Aerodynamic Chord, } \bar{c}_{BF} = 81.0 \text{ inches}$$

$$\text{Area Moment, } S_{BF} \bar{c}_{BF} = 10,935.0 \text{ ft}^2\text{-inches}$$

Body Flap hinge moments are defined positive in the same sense as for positive deflection; i.e., trailing edge down. However, a positive deflection results in a negative hinge moment.

$$C_{hBF}^f = \frac{C_{hBF}}{1 - C_{hBF\delta_{BF}} K_{BF} \bar{q} S_{BF} \bar{c}_{BF}}$$

$$C_{hBF} = C_{hBF\delta_{SB}=25^\circ} + \Delta C_{hBF\delta_{SB}=\delta_{SB}}$$

$$C_{hBF\delta_{BF}} = \frac{1}{2\delta_{BF}'} [C_{hBF_{POS}} - C_{hBF_{NEG}}]$$

$C_{hBF\delta_{SB}=25^\circ}$ = Basic body flap hinge moment coefficient with speedbrake set at 25° .

$\Delta C_{hBF\delta_{SB}=\delta_{SB}}$ = Change in body flap hinge moment coefficient due to speedbrake deflection, δ_{SB} .

$C_{hBF\delta_{BF}}$ = Change in body flap hinge moment coefficient with change in body flap deflection.

$C_{hBF_{POS}}$
(NEG) = Body flap hinge moment coefficient for a positive (negative) body flap deflection from nominal.

δ_{BF}' = 1 degree (recommended).

K_{BF} = 1.817×10^{-6} degrees/inch-pound



| | DIGITAL FILE No. | TABLE (or FIGURE) No. |
|--|------------------------|-----------------------------|
| $Ch_{BF\delta_{SB}=25^\circ} = Ch_{BF\text{BASIC}} f(\delta_{BF}, a, M)$ | A133 | 5.2.2.2-1 |
| $Ch_{BF\text{POS}} = Ch_{BF\text{BASIC}} f(\delta_{BF} + \delta'_{BF}, a, M)$ | A133 | 5.2.2.2-1 |
| $Ch_{BF\text{NEG}} = Ch_{BF\text{BASIC}} f(\delta_{BF} - \delta'_{BF}, a, M)$ | A133 | 5.2.2.2-1 |
| $\Delta Ch_{BF\delta_{SB}=\delta_{SB}} = \Delta Ch_{BF\delta_{SB}=\delta_{SB}} f(\delta_{SB}, a, M)$ | A134 | 5.2.2.2-2 |

4.2.2.3 RUDDER/SPEEDBRAKE CONTROL. The rudder/speedbrake control hinge moment coefficients are based on theoretical (NOT TRUE) reference dimensions

$$\text{RUDDER: } HM_R = HM_{\text{RIGHT}} - HM_{\text{LEFT}}$$

$$\text{SPEEDBRAKE: } HM_{\text{SB}} = HM_{\text{RIGHT}} + HM_{\text{LEFT}}$$

$$\text{where, } HM_{\text{SB}} = C_{h_{\text{SB}}} (\bar{q} S_{\text{SB}} \bar{c}_{\text{R}})$$

$$\text{Reference Area, } S_{\text{SB}} = 100.15 \text{ ft}^2$$

$$\text{Mean Aerodynamic Chord, } \bar{c}_{\text{R}} = 73.20 \text{ inches}$$

$$\text{Area Moment, } S_{\text{SB}} \bar{c}_{\text{R}} = 7331.00 \text{ ft}^2\text{-inc}$$

Rudder hinge moments are defined positive in the same sense as for positive deflection; i.e., trailing edge left. Speedbrake panel hinge moments are positive in a direction which tends to collapse the panel.

$$HM_{\text{RIGHT}} = (C_{h_{\text{PANEL}}} + C_{h_{\text{SIDESLIP}}} + C_{h_{\text{RUDDER}}}) (\bar{q} S_{\text{SB}} \bar{c}_{\text{R}})$$

$$HM_{\text{LEFT}} = (C_{h_{\text{PANEL}}} - C_{h_{\text{SIDESLIP}}} - C_{h_{\text{RUDDER}}}) (\bar{q} S_{\text{SB}} \bar{c}_{\text{R}})$$

$C_{h_{\text{PANEL}}}$ = Right or Left panel hinge moment coefficient for $\beta = \delta_R = 0^\circ$.

$C_{h_{\text{SIDESLIP}}}$ = Right panel hinge moment coefficient due to sideslip angle, β .

$C_{h_{\text{RUDDER}}}$ = Right panel hinge moment coefficient due to rudder deflection, δ_R .

$$C_{h_{\text{PANEL}}} = C_{h_{\text{PANEL}}}^{\delta_{\text{BF}}=0^\circ} + \Delta C_{h_{\text{PANEL}}}^{\delta_{\text{BF}}=\delta_{\text{BF}}}$$

$C_{h_{\text{PANEL}}}^{\delta_{\text{BF}}=0^\circ}$ = Basic panel hinge moment coefficient with body flap deflection set at zero degrees.

$\Delta C_{h_{\text{PANEL}}}^{\delta_{\text{BF}}=\delta_{\text{BF}}}$ = Change in panel hinge moment coefficient due to body flap deflection, δ_{BF} .

| | DIGITAL FILE No. | TABLE (or FIGURE) No. |
|--|------------------------|-----------------------------|
| $C_{H_{PANEL}} = C_{H_{SB}} \text{ BASIC } f(\delta_{SB}, \alpha, M)$ $\delta_{BF} = 0$ | A135 | 5.2.2.3-1 |
| $\Delta C_{H_{PANEL}} = \Delta C_{H_{SB_{BF}}} f(\delta_{BF}, \alpha, M)$ $\delta_{BF} = \delta_{BF}$ | A136 | 5.2.2.3-2 |

$$C_{H_{SIDESLIP}} = \eta_{HM\beta} C_{H\beta} \beta$$

$\eta_{HM\beta}$ = Rudder/Speedbrake hinge moment sideslip
Flexible-to-Rigid ratio.

$C_{H\beta}$ = Change in right panel hinge moment coefficient
with change in sideslip angle.

| | DIGITAL FILE No. | TABLE (or FIGURE) No. |
|---|------------------------|-----------------------------|
| $\eta_{HM\beta} = \eta_{HM\beta} f(\bar{q}, M)$ | F 21 | 5.2.2.3- 5 |
| $C_{H\beta} = C_{H\beta} f(\delta_{SB}, \alpha, M)$ | A137 | 5.2.2.3- 3 |

$$C_{H_{RUDDER}} = \eta_{HM\delta_R} C_{H\delta_R} \delta_R$$

$\eta_{HM\delta_R}$ = Rudder/Speedbrake hinge moment rudder
Flexible-to-Rigid ratio.

$C_{H\delta_R}$ = Change in right panel hinge moment coefficient
with change in rudder deflection

| | DIGITAL FILE No. | TABLE (or FIGURE) No. |
|---|------------------------|-----------------------------|
| $\eta_{HM\delta_R} = \eta_{HM\delta_R} f(\bar{q}, M)$ | F 22 | 5.2.2.3- 6 |
| $C_{H\delta_R} = C_{H\delta_R} f(\delta_{SB}, \alpha, M)$ | A138 | 5.2.2.3- 4 |

4.2.3 AERODYNAMIC UNCERTAINTIES

4.2.3 AERODYNAMIC UNCERTAINTIES

This section presents the aerodynamic data uncertainties associated with the operational aerodynamic data of the foregoing sections. Certain calculations and definitions are required prior to obtaining data from the Digital File and/or Data Tables of Volume 3. These definitions and calculations are given in this section and will be referred to as "Pre-Lookup" definitions and calculations.

PRE-LOOKUP DEFINITIONS AND CALCULATIONS:

$$\begin{aligned}\Delta\alpha &= \text{Incremental change in angle of attack} \\ &\quad (\text{from reference angle of attack}). \\ &= \alpha_{\text{NOM}} - \alpha_{\text{REF}}\end{aligned}$$

$$\begin{aligned}\Delta\delta_e &= \text{Incremental change in elevon deflection} \\ &\quad (\text{from reference elevon deflection}). \\ &= \delta_{e\text{NOM}} - \delta_{e\text{REF}}\end{aligned}$$

$$\begin{aligned}\Delta\delta_{\text{BF}} &= \text{Incremental change in body flap deflection} \\ &\quad (\text{from reference body flap deflection}). \\ &= \delta_{\text{BFNOM}} - \delta_{\text{BFREF}}\end{aligned}$$

$$\begin{aligned}\Delta\delta_{\text{SB}} &= \text{Incremental change in speedbrake deflection} \\ &\quad (\text{from reference speedbrake deflection}). \\ &= \delta_{\text{SBNOM}} - \delta_{\text{SBREF}}\end{aligned}$$

where, α_{NOM} = Nominal angle of attack.

α_{REF} = Reference angle of attack.

$\delta_{e\text{NOM}}$ = Nominal elevon deflection

$\delta_{e\text{REF}}$ = Reference elevon deflection

δ_{BFNOM} = Nominal body flap deflection

δ_{BFREF} = Reference body flap deflection

δ_{SBNOM} = Nominal speedbrake deflection

δ_{SBREF} = Reference speedbrake deflection

| | | DIGITAL FILE No. | TABLE (or FIGURE) No. |
|-----------------------|------------------------------|------------------------|-----------------------------|
| a_{REF} | $= a_{REF} f(M)$ | U 1 | 5.2.3-1 |
| δe_{REF} | $= \delta e_{REF} f(M)$ | U 2 | 5.2.3-2 |
| $\delta \theta_{REF}$ | $= \delta \theta_{REF} f(M)$ | U 3 | 5.2.3-3 |
| δs_{REF} | $= \delta s_{REF} f(M)$ | U 4 | 5.2.3-4 |

$$\frac{\phi_J}{\phi_\bullet} \Big|_{DIFF_U} = \text{Differential Momentum Ratio between left- and right-hand up firing jets.}$$

$$= \text{ABS} \left(\frac{\phi_J}{\phi_\bullet} \Big|_{LHU} - \frac{\phi_J}{\phi_\bullet} \Big|_{RHU} \right)$$

$$\frac{\phi_J}{\phi_\bullet} \Big|_{DIFF_S} = \text{Differential Momentum Ratio between left- and right-hand side firing jets.}$$

$$= \text{ABS} \left(\frac{\phi_J}{\phi_\bullet} \Big|_{LHS} - \frac{\phi_J}{\phi_\bullet} \Big|_{RHS} \right)$$

$$\frac{\phi_J}{\phi_\bullet} \Big|_{DIFF_D} = \text{Differential Momentum Ratio between left- and right-hand down firing jets.}$$

$$= \text{ABS} \left(\frac{\phi_J}{\phi_\bullet} \Big|_{LHD} - \frac{\phi_J}{\phi_\bullet} \Big|_{RHD} \right)$$

4.2.3.1 LONGITUDINAL AERODYNAMIC DATA UNCERTAINTIES. The total longitudinal aerodynamic data with uncertainties should be computed in the following manner:

$$L_{TOTAL} = \bar{q}S (C_{L_{TOTAL}} \pm \Delta C_{L_{UNC}}) + L_{RCS} \pm \Delta L_{RCS_{UNC}}$$

$$N_{TOTAL} = \bar{q}S (C_{N_{TOTAL}} \pm \Delta C_{N_{UNC}}) + N_{RCS} \pm \Delta N_{RCS_{UNC}}$$

$$D_{TOTAL} = \bar{q}S (C_{D_{TOTAL}} \pm \Delta C_{D_{UNC}}) + D_{RCS} \pm \Delta D_{RCS_{UNC}}$$

$$A_{TOTAL} = \bar{q}S (C_{A_{TOTAL}} \pm \Delta C_{A_{UNC}}) + A_{RCS} \pm \Delta A_{RCS_{UNC}}$$

$$M_{TOTAL} = \bar{q}S \bar{c} (C_{M_{TOTAL}} \pm \Delta C_{M_{UNC}}) + M_{RCS} \pm \Delta M_{RCS_{UNC}}$$

The non-dimensional force and moment coefficient uncertainties are defined as:

$$\Delta C_{()_{UNC}} = \left[\Delta C_{()_{U_{FREE AIR}}^2} + \Delta C_{()_{U_{GE}}^2} \right]^{1/2}$$

where, the subscript () denotes lift force (L), normal force (N), drag force (D), axial force (A), or pitching moment (M) and;

$$\begin{aligned} \Delta C_{()_{U_{FREE AIR}}} &= \text{Free-air force or moment coefficient uncertainty.} \\ &= \Delta C_{()_{U_{BASIC}}} + \Delta(\Delta C_{()})_{U_{ALT}} \end{aligned}$$

$$\Delta C_{()_{U_{BASIC}}} = \text{Basic, force or moment coefficient uncertainty.}$$

$$\Delta(\Delta C_{()})_{U_{ALT}} = \text{Change in force or moment coefficient uncertainty due to high altitude.}$$

$$\Delta C_{()_{U_{GE}}} = \text{Change in force or moment coefficient uncertainty due to proximity of the ground.}$$

| | DIGITAL FILE No. | TABLE (or FIGURE) No. |
|--|------------------------|-----------------------------|
| $\Delta C_{()U \text{ BASIC}} = \Delta C_{()U} f(M, \Delta \delta e, \Delta \alpha)$ | | |
| subscript: (L) | U 6 | 5.2.3.1.1-1 |
| (N) | U 7 | 5.2.3.1.1-7 |
| (D) | U 8 | 5.2.3.1.2-1 |
| (A) | U 9 | 5.2.3.1.2-7 |
| (m) | U 10 | 5.2.3.1.3-1 |
| $\Delta(\Delta C_{()})_{U \text{ ALT}} = \Delta(\Delta C_{()})_{U \text{ HA}} f(h)$ | | |
| subscript: (L) | U 11 | 5.2.3.1.1-2 |
| (N) | U 12 | 5.2.3.1.1-8 |
| (D) | U 13 | 5.2.3.1.2-2 |
| (A) | U 14 | 5.2.3.1.2-8 |
| (m) | U 15 | 5.2.3.1.3-2 |
| $\Delta C_{()U \text{ GE}} = \Delta C_{()U \text{ GE}} f(h/b, \Delta \alpha)$ | | |
| subscript: (L) | U 16 | 5.2.3.1.1-3 |
| (N) | U 17 | 5.2.3.1.1-9 |
| (D) | U 18 | 5.2.3.1.2-3 |
| (A) | U 19 | 5.2.3.1.2-9 |
| (m) | U 20 | 5.2.3.1.3-3 |

The following uncertainties are for use in linearized stability analyses and other sensitivity studies.

$$*\Delta C_{()_{UNC}} = \Delta C_{()_{\alpha_{UNC}}} \Delta \alpha + \Delta C_{()_{\delta_{e_{UNC}}}} \Delta \delta_e$$

$$*\Delta C_{()_{\alpha_{UNC}}} = \Delta C_{()_{\alpha_U}}$$

$$*\Delta C_{()_{\delta_{e_{UNC}}}} = \left[\Delta C_{()_{\delta_{e_U_{BASIC}}}}^2 + \Delta C_{()_{\delta_{e_U_{GE}}}}^2 \right]^{1/2}$$

where, $\Delta C_{()_{\alpha_U}}$ = Basic angle of attack derivative uncertainty.
 $\Delta C_{()_{\delta_{e_U_{BASIC}}}}$ = Basic elevon deflection derivative uncertainty.
 $\Delta C_{()_{\delta_{e_U_{GE}}}}$ = Change in elevon deflection derivative uncertainty due to proximity of the ground.

| | DIGITAL FILE No. | TABLE (or FIGURE) No. |
|---|------------------------|-----------------------------|
| $\Delta C_{()_{\alpha_U}} = \Delta C_{()_{\alpha_U}} f(M)$ | | |
| subscript: (L) | U 21 | 5.2.3.1.1- 4 |
| (N) | U 22 | 5.2.3.1.1-10 |
| (D) | U 23 | 5.2.3.1.2- 4 |
| (A) | U 24 | 5.2.3.1.2-10 |
| (m) | U 25 | 5.2.3.1.3- 4 |
| $\Delta C_{()_{\delta_{e_U_{BASIC}}}} = \Delta C_{()_{\delta_{e_U_{BASIC}}}} f(M, \Delta \alpha)$ | | |
| subscript: (L) | U 26 | 5.2.3.1.1- 5 |
| (N) | U 27 | 5.2.3.1.1-11 |
| (D) | U 28 | 5.2.3.1.2- 5 |
| (A) | U 29 | 5.2.3.1.2-11 |
| (m) | U 30 | 5.2.3.1.3- 5 |
| $\Delta C_{()_{\delta_{e_U_{GE}}}} = \Delta C_{()_{\delta_{e_U_{GE}}}} f(h/b)$ | | |
| subscript: (L) | U 31 | 5.2.3.1.1- 6 |
| (N) | U 32 | 5.2.3.1.1-12 |
| (D) | U 33 | 5.2.3.1.2- 6 |
| (A) | U 34 | 5.2.3.1.2-12 |
| (m) | U 35 | 5.2.3.1.3- 6 |

NOTE: Terms marked by asterisk (*) are to be used in linearized analyses only and are NOT to be combined with total values.

The RCS forces and moment uncertainties are defined as:

$$\Delta(\)_{RCSUNC} = \left\{ \left[\Delta(\)_{IMPUNC} \right]^2 + \left[\Delta C_{()JIUNC} \bar{q} S \right]^2 \right\}^{1/2}$$

where; () indicates Normal Force (N) or Axial Force (A) and,

$$\Delta(L)_{RCSUNC} = \Delta(N)_{RCSUNC}$$

$$\Delta(D)_{RCSUNC} = \Delta(A)_{RCSUNC}$$

$$\Delta(M)_{RCSUNC} = \left\{ \left[\Delta(M)_{IMPUNC} \right]^2 + \left[\Delta C_{(M)JIUNC} \bar{q} S \bar{c} \right]^2 \right\}^{1/2}$$

where; (L) indicates Lift Force, (D) indicates Drag Force,
and (M) indicates Pitching Moment.

$\Delta(\)_{IMPUNC}$ = Force or Moment Uncertainty resulting from
jet impingement on Orbiter Vehicle surface(s).

$$= \left\{ \left[\Delta(\)_{IMPUNC_U} \right]^2 + \left[\Delta(\)_{IMPUNC_S} \right]^2 + \left[\Delta(\)_{IMPUNC_D} \right]^2 \right\}^{1/2}$$

$$\text{where; } \Delta(\)_{IMPUNC_U} = \Delta(\)_{IMP_{U_U}} (n_{LH_U} + n_{RH_U})$$

$$\Delta(\)_{IMPUNC_S} = \Delta(\)_{IMP_{U_S}} (n_{LH_S} + n_{RH_S})$$

$$\Delta(\)_{IMPUNC_D} = \Delta(\)_{IMP_{U_D}} (n_{LH_D} + n_{RH_D})$$

$\Delta C_{()JIUNC}$ = Force or Moment Coefficient Uncertainty
due to jet interaction.

$$= \left\{ \left[\Delta C_{()JIUNC_U} \right]^2 + \left[\Delta C_{()JIUNC_S} \right]^2 + \left[\Delta C_{()JIUNC_D} \right]^2 \right\}^{1/2}$$

$$\text{where; } \Delta C_{()JIUNC_U} = \left\{ \left[\Delta C_{()JIUNC_{LU}} \right]^2 + \left[\Delta C_{()JIUNC_{RU}} \right]^2 \right\}^{1/2}$$

$$\Delta C_{()JIUNC_S} = \left\{ \left[\Delta C_{()JIUNC_{LS}} \right]^2 + \left[\Delta C_{()JIUNC_{RS}} \right]^2 \right\}^{1/2}$$

$$\Delta C_{()JIUNC_D} = \left\{ \left[\Delta C_{()JIUNC_{LD}} \right]^2 + \left[\Delta C_{()JIUNC_{RD}} \right]^2 \right\}^{1/2}$$

where; (N) indicates Normal Force, (A) indicates Axial Force,
and (M) indicates Pitching Moment.

| | DIGITAL FILE No. | TABLE (or FIGURE) No. |
|--|------------------------|-----------------------------|
| $\Delta()_{IMP_{UU}} = \Delta()_{IMP_{UU}} f(P_{\infty})$ | | |
| component: (N) | U101 | (zero valued) |
| (A) | U102 | (zero valued) |
| (m) | U103 | (zero valued) |
| $\Delta()_{IMP_{US}} = \Delta()_{IMP_{US}} f(P_{\infty})$ | | |
| component: (N) | U104 | (zero valued) |
| (A) | U105 | (zero valued) |
| (m) | U106 | (zero valued) |
| $\Delta()_{IMP_{UD}} = \Delta()_{IMP_{UD}} f(P_{\infty})$ | | |
| component: (N) | U107 | 5.2.3.1.1-15 |
| (A) | U108 | 5.2.3.1.2-15 |
| (m) | U109 | 5.2.3.1.3-15 |
| $\Delta C()_{J1U_{LU}} = \Delta C()_{J1U_{LU}} f\left(\frac{\phi_J}{\phi_{\infty}} \Big _{LH_U}, \Delta \alpha\right)$ | | |
| subscript: (N) | U110 | 5.2.3.1.1-16 |
| (A) | U111 | 5.2.3.1.2-16 |
| (m) | U112 | 5.2.3.1.3-16 |
| $\Delta C()_{J1U_{RU}} = \Delta C()_{J1U_{RU}} f\left(\frac{\phi_J}{\phi_{\infty}} \Big _{RH_U}, \Delta \alpha\right)$ | | |
| subscript: (N) | U110 | 5.2.3.1.1-16 |
| (A) | U111 | 5.2.3.1.2-16 |
| (m) | U112 | 5.2.3.1.3-16 |
| $\Delta C()_{J1U_{LS}} = \Delta C()_{J1U_{LS}} f\left(\frac{\phi_J}{\phi_{\infty}} \Big _{LH_S}, \Delta \alpha\right)$ | | |
| subscript: (N) | U113 | 5.2.3.1.1-17 |
| (A) | U114 | 5.2.3.1.2-17 |
| (m) | U115 | 5.2.3.1.3-17 |
| $\Delta C()_{J1U_{RS}} = \Delta C()_{J1U_{RS}} f\left(\frac{\phi_J}{\phi_{\infty}} \Big _{RH_S}, \Delta \alpha\right)$ | | |
| subscript: (N) | U113 | 5.2.3.1.1-17 |
| (A) | U114 | 5.2.3.1.2-17 |
| (m) | U115 | 5.2.3.1.3-17 |



| | DIGITAL FILE No. | TABLE (or FIGURE) No. |
|--|------------------------|-----------------------------|
| $\Delta C_{()JIU_{LD}} = \Delta C_{()JIU_D} f \left(\frac{\phi_J}{\phi_{\infty}} \Big _{LHD}, \Delta a \right)$ | | |
| subscript: (N) | U116 | 5.2.3.1.1-18 |
| (A) | U117 | 5.2.3.1.2-18 |
| (m) | U118 | 5.2.3.1.3-18 |
| $\Delta C_{()JIU_{RD}} = \Delta C_{()JIU_D} f \left(\frac{\phi_J}{\phi_{\infty}} \Big _{RHD}, \Delta a \right)$ | | |
| subscript: (N) | U116 | 5.2.3.1.1-18 |
| (A) | U117 | 5.2.3.1.2-18 |
| (m) | U118 | 5.2.3.1.3-18 |

LIFT-TO-DRAG RATIO

$$\pm \Delta(L/D)_{UNC} = \left[\Delta(L/D)_{U_{FREE AIR}}^2 + \Delta(L/D)_{U_{GE}}^2 \right]^{1/2}$$

where, $\Delta(L/D)_{U_{FREE AIR}}$ = Total free-air lift-to-drag uncertainty.
 $= \Delta(L/D)_{U_{BASIC}} + \Delta(L/D)_{U_{ALT}}$

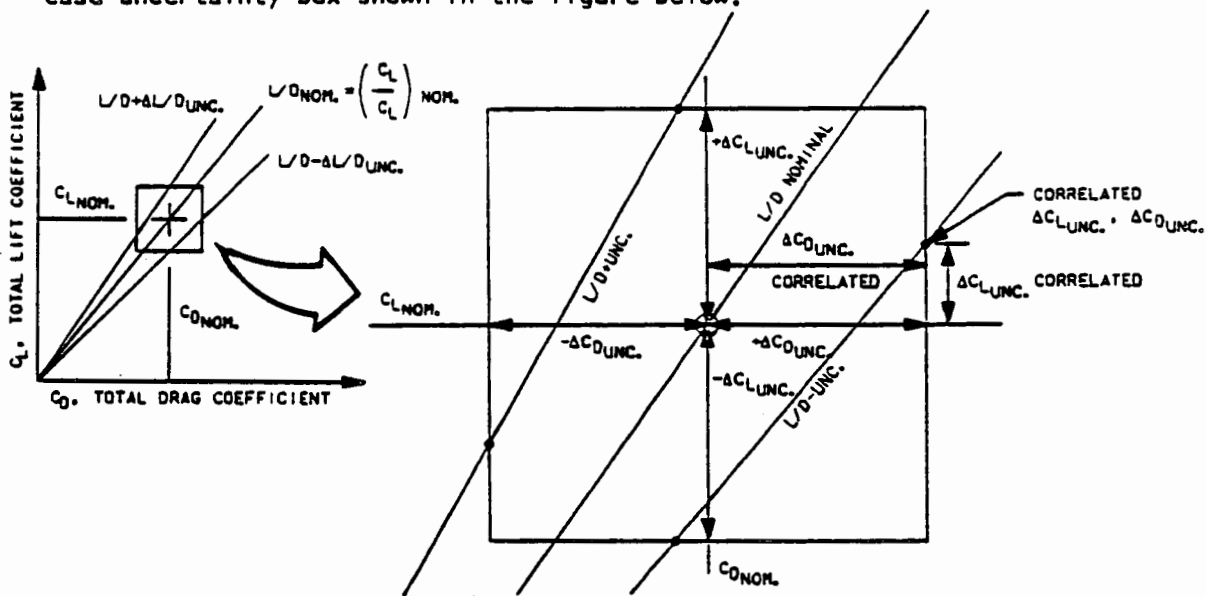
$\Delta(L/D)_{U_{BASIC}}$ = Basic lift-to-drag uncertainty.

$\Delta(L/D)_{U_{ALT}}$ = Change in lift-to-drag uncertainty due to high altitude.

$\Delta(L/D)_{U_{GE}}$ = Change in lift-to-drag uncertainty due to proximity of the ground.

| | DIGITAL FILE No. | TABLE (or FIGURE) No. |
|---|------------------|-----------------------|
| $\Delta(L/D)_{U_{BASIC}} = \Delta(L/D)_{U_{f(M, \Delta \alpha)}}$ | U 36 | 5.2.3.1.4-1 |
| $\Delta(L/D)_{U_{ALT}} = \Delta(L/D)_{U_{f(h)}}$ | U 37 | 5.2.3.1.4-2 |
| $\Delta(L/D)_{U_{GE}} = \Delta(L/D)_{U_{f(h/b)}}$ | U 38 | 5.2.3.1.4-3 |

Correlation of C_L and C_D Uncertainties With L/D Uncertainties. The basic lift and drag uncertainties presented above are to be used to form the worst case uncertainty box shown in the figure below.



4.2.3.1-7

Since the lift and drag uncertainties are highly correlated, certain areas of the box are outside the three-sigma probability limit. To determine the three-sigma limits on lift and drag, it is necessary to develop the nominal L/D line and apply the $\pm\Delta(L/D)$ uncertainty to it as follows:

$$(L/D)_{\text{MAX}}^{\text{MIN}} = \left(\frac{C_L}{C_D} \right)_{\text{NOM}} \pm \Delta \left(\frac{L}{D} \right)_{\text{UNC}}$$

The intersection of the L/D \pm UNCERTAINTY line with the worst case box yields the correlated ΔC_L and ΔC_D uncertainty points. These cases can be computed using the following equations.

To find C_D at max or min C_L and L/D use:

$$C_{L \text{ MAX}}^{\text{MIN}} = C_{L \text{ NOM}} \pm \Delta C_{L \text{ UNC}}$$

$$(L/D)_{\text{MAX}}^{\text{MIN}} = \frac{C_{L \text{ NOM}}}{C_{D \text{ NOM}}} \pm \Delta \left(\frac{L}{D} \right)_{\text{UNC}}$$

$$C_{D @ C_L \text{ MAX}}^{\text{MIN}} = \frac{C_{L \text{ MAX}}}{(L/D)_{\text{MAX}}}$$

$$C_{D @ C_L \text{ MIN}}^{\text{MIN}} = \frac{C_{L \text{ MIN}}}{(L/D)_{\text{MIN}}}$$

To find C_L at max or min C_D and L/D use:

$$C_{D \text{ MAX}}^{\text{MIN}} = C_{D \text{ NOM}} \pm \Delta C_{D \text{ UNC}}$$

$$C_{L @ C_D \text{ MAX}}^{\text{MIN}} = (L/D)_{\text{MIN}} C_{D \text{ MAX}}$$

$$C_{L @ C_D \text{ MIN}}^{\text{MIN}} = (L/D)_{\text{MAX}} C_{D \text{ MIN}}$$

4.2.3.2 LATERAL-DIRECTIONAL AERODYNAMIC DATA UNCERTAINTIES. The total lateral-directional aerodynamic data with uncertainties should be computed in the following manner:

$$Y_{TOTAL} = \bar{q}S \left(C_{Y_{TOTAL}} \pm \Delta C_{Y_{UNC}} \right) + Y_{RCS} \pm \Delta Y_{RCS_{UNC}}$$

$$N_{TOTAL} = \bar{q}Sb \left(C_{n_{TOTAL}} \pm \Delta C_{n_{UNC}} \right) + N_{RCS} \pm \Delta N_{RCS_{UNC}}$$

$$L_{TOTAL} = \bar{q}Sb \left(C_{L_{TOTAL}} \pm \Delta C_{L_{UNC}} \right) + L_{RCS} \pm \Delta L_{RCS_{UNC}}$$

The non-dimensional force and moment coefficient uncertainties are defined as:

$$\Delta C_{()_{UNC}} = \left[(\Delta C_{()_{\beta_{UNC}}} \beta)^2 + (\Delta C_{()_{\delta a_{UNC}}} \delta a)^2 + (\Delta C_{()_{\delta r_{UNC}}} \delta r)^2 \right]^{1/2} + C_{()_{O_{UNC}}}$$

where, the subscript () denotes side force (Y), yawing moment (n), or rolling moment (L) and;

$\Delta C_{()_{\beta_{UNC}}}$ = Total sideslip derivative uncertainty due to sideslip angle.

$$= \left[\Delta C_{()_{\beta_{U_{FREE_{AIR}}}}}^2 + \Delta C_{()_{\beta_{U_{GE}}}}^2 \right]^{1/2}$$

$\Delta C_{()_{\beta_{U_{FREE_{AIR}}}}}$ = Free-air sideslip derivative uncertainty due to sideslip angle.

$$= \Delta C_{()_{\beta_{U_{BASIC}}}} + \Delta(\Delta C_{()_{\beta}})_{U_{ALT}}$$

$\Delta C_{()_{\beta_{U_{BASIC}}}}$ = Basic sideslip derivative uncertainty due to sideslip angle.

$\Delta(\Delta C_{()_{\beta}})_{U_{ALT}}$ = Change in sideslip derivative uncertainty due to high altitude.

$\Delta C_{()_{\beta_{U_{GE}}}}$ = Change in sideslip derivative uncertainty due to proximity of ground.

$\Delta C_{l\delta_a}_{UNC}$ = Total aileron derivative uncertainty due to aileron deflection.

$$= \left[\Delta C_{l\delta_a}_{FREE\ AIR}^2 + \Delta C_{l\delta_a}_{GE}^2 \right]^{1/2}$$

$\Delta C_{l\delta_a}_{FREE\ AIR}$ = Free-air aileron derivative uncertainty due to aileron deflection.

$\Delta C_{l\delta_a}_{GE}$ = Change in aileron derivative uncertainty due to proximity of the ground.

$\Delta C_{l\delta_r}_{UNC}$ = Basic rudder derivative uncertainty due to rudder deflection.

$\Delta C_{l\delta_o}_{UNC}$ = Bent airframe uncertainty.

 * CAUTION *
 * APPLICATION OF RUDDER DERIVATIVES MUST BE SUCH THAT CHANGES TO THE *
 * SIGN OF THE BASIC DERIVATIVE ARE AVOIDED; i.e., *
 * *
 * $C_{Y\delta_r} - \Delta C_{Y\delta_r}_{UNC} \geq 0$ *
 * $C_{n\delta_r} + \Delta C_{n\delta_r}_{UNC} \leq 0$ *
 * $C_{L\delta_r} - \Delta C_{L\delta_r}_{UNC} \geq 0$ *
 * *****

| | DIGITAL FILE No. | TABLE (or FIGURE) No. |
|--|------------------------|-----------------------------|
| $\Delta C_{(1)\beta_{U_{BASIC}}} = \Delta C_{(1)\beta_U} f(M, \Delta a)$ | | |
| subscript: (Y) | U 41 | 5.2.3.2.1-1 |
| (n) | U 42 | 5.2.3.2.2-1 |
| (L) | U 43 | 5.2.3.2.3-1 |
| $\Delta(\Delta C_{(1)\beta})_{U_{ALT}} = \Delta(\Delta C_{(1)\beta})_{U_{HA}} f(h)$ | | |
| subscript: (Y) | U 44 | 5.2.3.2.1-2 |
| (n) | U 45 | 5.2.3.2.2-2 |
| (L) | U 46 | 5.2.3.2.3-2 |
| $\Delta C_{(1)\beta_{U_{GE}}} = \Delta C_{(1)\beta_{U_{GE}}} f(h/b)$ | | |
| subscript: (Y) | U 47 | 5.2.3.2.1-3 |
| (n) | U 48 | 5.2.3.2.2-3 |
| (L) | U 49 | 5.2.3.2.3-3 |
| $\Delta C_{(1)\delta_{aU_{FREE AIR}}} = \Delta C_{(1)\delta_{aU}} f(M, \Delta \delta e, \Delta a)$ | | |
| subscript: (Y) | U 50 | 5.2.3.2.1-4 |
| (n) | U 51 | 5.2.3.2.2-4 |
| (L) | U 52 | 5.2.3.2.3-4 |
| $\Delta C_{(1)\delta_{aU_{GE}}} = \Delta C_{(1)\delta_{aU_{GE}}} f(h/b)$ | | |
| subscript: (Y) | U 53 | 5.2.3.2.1-5 |
| (n) | U 54 | 5.2.3.2.2-5 |
| (L) | U 55 | 5.2.3.2.3-5 |
| $\Delta C_{(1)\delta_{rU_{UNC}}} = \Delta C_{(1)\delta_{rU}} f(M, \Delta a)$ | | |
| subscript: (Y) | U 56 | 5.2.3.2.1-6 |
| (n) | U 57 | 5.2.3.2.2-6 |
| (L) | U 58 | 5.2.3.2.3-6 |
| $C_{(1)O_{UNC}} = C_{(1)O_U} f(M, A)$ | | |
| subscript: (Y) | U 59 | 5.2.3.2.1-7 |
| (n) | U 60 | 5.2.3.2.2-7 |
| (L) | U 61 | 5.2.3.2.3-7 |

NOTE: (1) A = Asymmetry type =

1.0 Combined normally with other uncertainties.

2.0 Combined with nominal $C_{n\beta}$ and $C_{L\beta}$
 $\Delta C_{n\beta_{UNC}}$ and $\Delta C_{L\beta_{UNC}}$ are set equal to zero.

(2) Values of $C_{nO_{UNC}}$ and $C_{LO_{UNC}}$ are ALWAYS of OPPOSITE sign.

The RCS force and moment uncertainties are defined as:

$$\Delta(Y)_{RCSUNC} = \left\{ [\Delta(Y)_{IMPUNC}]^2 + [\Delta C(Y)_{JIUNC} \bar{q}S]^2 \right\}^{1/2}$$

where; (Y) indicates Side Force and,

$$\Delta(\)_{RCSUNC} = \left\{ [\Delta(\)_{IMPUNC}]^2 + [\Delta C(\)_{JIUNC} \bar{q}S b]^2 \right\}^{1/2}$$

where; () indicates Yawing Moment (n), or Rolling Moment (L).

$\Delta(\)_{IMPUNC}$ = Force or Moment Uncertainty resulting from jet impingement on Orbiter Vehicle surface(s).

$$= \left\{ [\Delta(\)_{IMPUNC_U}]^2 + [\Delta(\)_{IMPUNC_S}]^2 + [\Delta(\)_{IMPUNC_D}]^2 \right\}^{1/2}$$

$$\Delta(\)_{IMPUNC_U} = \Delta(\)_{IMP_{UJ}} (n_{LHU} - n_{RHU})$$

$$\Delta(\)_{IMPUNC_S} = \Delta(\)_{IMP_{US}} (n_{LHS} - n_{RHS})$$

$$\Delta(\)_{IMPUNC_D} = \Delta(\)_{IMP_{UD}} (n_{LHD} - n_{RHD})$$

$\Delta C(\)_{JIUNC}$ = Force or Moment Coefficient Uncertainty due to jet interaction.

$$= \left\{ [\Delta C(\)_{JIUNC_U}]^2 + [\Delta C(\)_{JIUNC_S}]^2 + [\Delta C(\)_{JIUNC_D}]^2 \right\}^{1/2}$$

| | DIGITAL FILE No. | TABLE (or FIGURE) No. |
|---|------------------------|-----------------------------|
| $\Delta(\)_{IMP_{UU}} = \Delta(\)_{IMP_{UU}} f(P_{\infty})$ | | |
| component: (Y) | U119 | 5.2.3.2.1-8 |
| (n) | U120 | 5.2.3.2.2-8 |
| (L) | U121 | 5.2.3.2.3-8 |
| $\Delta(\)_{IMP_{US}} = \Delta(\)_{IMP_{US}} f(P_{\infty})$ | | |
| component: (Y) | U122 | (zero valued) |
| (n) | U123 | (zero valued) |
| (L) | U124 | (zero valued) |
| $\Delta(\)_{IMP_{UD}} = \Delta(\)_{IMP_{UD}} f(P_{\infty})$ | | |
| component: (Y) | U125 | 5.2.3.2.1-10 |
| (n) | U126 | 5.2.3.2.2-10 |
| (L) | U127 | 5.2.3.2.3-10 |
| $\Delta C_{()J1UNC_U} = \Delta C_{()J1U_U} f\left(\frac{\phi_J}{\phi_{\infty}} \middle \text{DIFF}_U, \Delta a\right)$ | | |
| subscript: (Y) | U128 | 5.2.3.2.1-11 |
| (n) | U129 | 5.2.3.2.2-11 |
| (L) | U130 | 5.2.3.2.3-11 |
| $\Delta C_{()J1UNC_S} = \Delta C_{()J1U_S} f\left(\frac{\phi_J}{\phi_{\infty}} \middle \text{DIFF}_S, \Delta a\right)$ | | |
| subscript: (Y) | U131 | 5.2.3.2.1-12 |
| (n) | U132 | 5.2.3.2.2-12 |
| (L) | U133 | 5.2.3.2.3-12 |
| $\Delta C_{()J1UNC_D} = \Delta C_{()J1U_D} f\left(\frac{\phi_J}{\phi_{\infty}} \middle \text{DIFF}_D, \Delta a\right)$ | | |
| subscript: (Y) | U134 | 5.2.3.2.1-13 |
| (n) | U135 | 5.2.3.2.2-13 |
| (L) | U136 | 5.2.3.2.3-13 |

4.2.3.3 AERODYNAMIC HINGE MOMENT UNCERTAINTIES. The total aerodynamic hinge moments with uncertainties are defined for the elevon, body flap, and rudder/ speedbrake.

4.2.3.3.1 ELEVON CONTROL. The total aerodynamic elevon hinge moments with uncertainties should be computed in the following manner:

$$HM_{e1_TOTAL} = \bar{q} S_e \bar{c}_e (C_{he1} \pm \Delta C_{he1_UNC})$$

$$HM_{e0_TOTAL} = \bar{q} S_e \bar{c}_e (C_{he0} \pm \Delta C_{he0_UNC})$$

The non-dimensional elevon hinge moment coefficient uncertainties are defined as:

$$\Delta C_{he1_UNC} = \Delta C_{he1U}$$

$$\Delta C_{he0_UNC} = \Delta C_{he0U}$$

where, ΔC_{he1_UNC} = Inboard elevon hinge moment coefficient uncertainty.

ΔC_{he0_UNC} = Outboard elevon hinge moment coefficient uncertainty.

| | | DIGITAL FILE No. | TABLE (or FIGURE) No. |
|-------------------|--|------------------------|-----------------------------|
| ΔC_{he1U} | $= \Delta C_{he1U} f(M, \Delta\delta e, \Delta\alpha)$ | U 71 | 5.2.3.3.1-1 |
| ΔC_{he0U} | $= \Delta C_{he0U} f(M, \Delta\delta e, \Delta\alpha)$ | U 72 | 5.2.3.3.1-2 |

NOTE: To obtain total elevon hinge moment coefficient uncertainties, RSS inboard and outboard values.

$$\Delta C_{heUNC} = \left[\Delta C_{he1_UNC}^2 + \Delta C_{he0_UNC}^2 \right]^{1/2}$$

4.2.3.3.2 BODY FLAP CONTROL. The total aerodynamic body flap hinge moment with uncertainties should be computed in the following manner:

$$HM_{BF_TOTAL} = \bar{q}S_{BF}\bar{c}_{BF}(C_{h_{BF}} \pm \Delta C_{h_{BF_UNC}})$$

The non-dimensional body flap hinge moment coefficient uncertainty is defined as:

$$\Delta C_{h_{BF_UNC}} = \Delta C_{h_{BFU}}$$

where, $\Delta C_{h_{BF_UNC}}$ = Body flap hinge moment coefficient uncertainty.

$$\Delta C_{h_{BFU}} = \Delta C_{h_{BFU}} f(M, \Delta \alpha)$$

DIGITAL
FILE
No.

TABLE
(or FIGURE)
No.

U 73

5.2.3.3.2-1

4.2.3.3.3 RUDDER/SPEEDBRAKE CONTROL. The total rudder/speedbrake hinge moments with uncertainties should be computed in the following manner:

TOTAL RUDDER/SPEEDBRAKE (RIGHT OR LEFT HAND) PANEL:

$$HM_{R/SB_{RH}} = \bar{q}S_{R/SB}\bar{c}_{R/SB}(C_{h_{PANEL}} + C_{h_{SIDESLIP}} + C_{h_{RUDDER}} \pm \Delta C_{h_{R/SB_{UNC}}})$$

$$HM_{R/SB_{LH}} = \bar{q}S_{R/SB}\bar{c}_{R/SB}(C_{h_{PANEL}} - C_{h_{SIDESLIP}} - C_{h_{RUDDER}} \pm \Delta C_{h_{R/SB_{UNC}}})$$

TOTAL SPEEDBRAKE:

$$HM_{SB} = \bar{q}S_{R/SB}\bar{c}_{R/SB}(2C_{h_{PANEL}} \pm \Delta C_{h_{SB_{UNC}}})$$

TOTAL RUDDER:

$$HM_R = \bar{q}S_{R/SB}\bar{c}_{R/SB}(2C_{h_{SIDESLIP}} + 2C_{h_{RUDDER}} \pm \Delta C_{h_{R_{UNC}}})$$

The non-dimensional rudder/speedbrake (left- or right-hand panel) hinge moment coefficient uncertainties are defined as:

$$\Delta C_{hR/SBUNC} = \left[\Delta C_{hSB_U}^2 + (\Delta C_{h\beta_U} \beta)^2 + (\Delta C_{h\delta_{rU}} \delta_r)^2 \right]^{1/2}$$

where, ΔC_{hSB_U} = Left or right hand speedbrake panel hinge moment coefficient uncertainty.

$\Delta C_{h\beta_U}$ = Rudder panel hinge moment coefficient uncertainty due to sideslip.

$\Delta C_{h\delta_{rU}}$ = Rudder panel hinge moment coefficient uncertainty due to rudder deflection.

| | | | DIGITAL FILE No. | TABLE (or FIGURE) No. |
|---------------------------|-----------------------------|-----------------------|------------------------|-----------------------------|
| ΔC_{hSB_U} | = ΔC_{hSB_U} | $f(M, \Delta \alpha)$ | U 74 | 5.2.3.3.3-1 |
| $\Delta C_{h\beta_U}$ | = $\Delta C_{h\beta_U}$ | $f(M)$ | U 75 | 5.2.3.3.3-2 |
| $\Delta C_{h\delta_{rU}}$ | = $\Delta C_{h\delta_{rU}}$ | $f(M)$ | U 76 | 5.2.3.3.3-3 |

NOTE: To obtain total speedbrake hinge moment uncertainty:

$$\Delta C_{hSBUNC} = \left[2(1 + \rho_{C_{hR/SB_{RH}} C_{hR/SB_{LH}}}) \Delta C_{hR/SBUNC}^2 \right]^{1/2}$$

and to obtain total rudder hinge moment uncertainty:

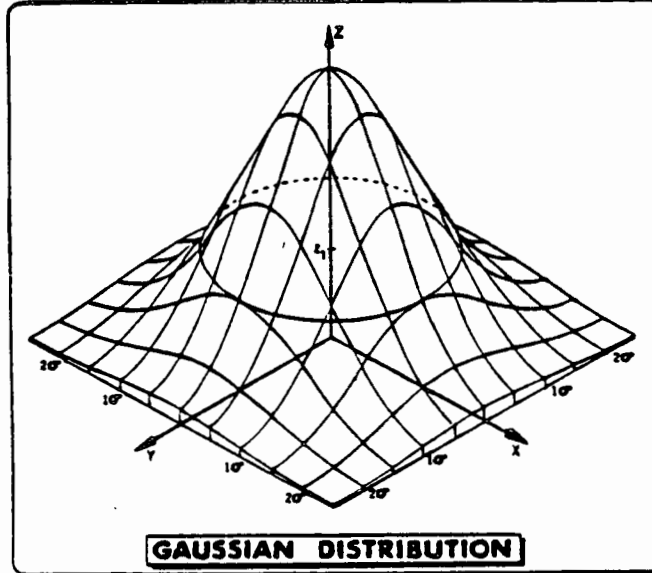
$$\Delta C_{hRUNC} = \left[2(1 - \rho_{C_{hR/SB_{RH}} C_{hR/SB_{LH}}}) \Delta C_{hR/SBUNC}^2 \right]^{1/2}$$

where, $\rho_{C_{hR/SB_{RH}} C_{hR/SB_{LH}}}$ = Correlation coefficient relating right and left hand rudder/speedbrake hinge moment coefficient.

| | | | DIGITAL FILE No. | TABLE (or FIGURE) No. |
|--|------------------------------|--------|------------------------|-----------------------------|
| $\rho_{C_{hR/SB_{RH}} C_{hR/SB_{LH}}}$ | = $\rho_{C_{hR/SB_{RH,LH}}}$ | $f(M)$ | U 91 | 5.2.3.4-8 |

4.2.3.4 AERODYNAMIC DATA UNCERTAINTY CORRELATION COEFFICIENTS.

Aerodynamic data uncertainty correlation coefficients are presented in this section. Correlation coefficients describe the degree of linear relationship between two aerodynamic coefficients. For statistical error



analysis where uncertainties need to be combined, the uncertainties can be treated as three-sigma (3σ) errors normally distributed about the mean.

Uncertainty envelopes can be statistically defined. A two-dimensional Gaussian probability density distribution is represented by a bell-shaped surface in the x, y, z space shown in the sketch (Reference 4-13). The curve formed by the intersection of the distribution surface and a vertical plane parallel to one of the coordinate planes is a curve of the

same shape as the normal distribution curve; i.e., a sigma "cut" where the height (or z) represents the proportionate number of errors of the value x (or y) and the greater the value of z , the more closely the errors are clustered about the maximum ordinate (x or $y = 0$). Therefore, z can be considered as a precision index or a measure of the concentration of measurements about their mean and may be seen from the sketch to be inversely related to sigma. Sigma (σ) is defined as the standard deviation, or limit in the probability sense, of the square root of the average value of the squared deviation of individual values from the mean as the number of values is increased indefinitely.

If a plane normal to the vertical axis, Z , is drawn at z_1 , then the intersection of this plane with the surface will describe a curve formed by the locus of points with probability density z . The curve will be a circle, provided that the standard deviations are equal for both x and y values. When this condition is not satisfied or x and y are linearly correlated ($-1 < \rho_{XY} < +1$), the circle deforms into a contour ellipse of the form:

$$\frac{1}{1 - \rho_{XY}^2} \left\{ \left(\frac{x - \bar{x}}{\sigma_X} \right)^2 - 2\rho_{XY} \left(\frac{x - \bar{x}}{\sigma_X} \right) \left(\frac{y - \bar{y}}{\sigma_Y} \right) + \left(\frac{y - \bar{y}}{\sigma_Y} \right)^2 \right\} = \chi_{f=2}^2 (P)$$

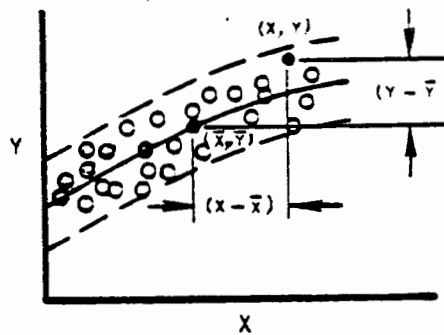
where \bar{x} and \bar{y} are the normal or mean values, σ_X and σ_Y are the standard deviations, ρ_{XY} is the correlation coefficient between x and y , and $\chi_{f=2}^2 (P)$ represents the value of the χ^2 distribution for two degrees of freedom corresponding to a given probability level (P). In order that all ellipses

generated will be tangent to a three-sigma rectangle ($\chi^2_{f=2} = 9.00$) which corresponds to a probability level of $P = 0.98889$ and the equation of the contour probability ellipse becomes:

$$\frac{1}{1 - \rho_{XY}^2} \left\{ \left(\frac{x - \bar{x}}{\sigma_X} \right)^2 - 2\rho_{XY} \left(\frac{x - \bar{x}}{\sigma_X} \right) \left(\frac{y - \bar{y}}{\sigma_Y} \right) + \left(\frac{y - \bar{y}}{\sigma_Y} \right)^2 \right\} = 9.00$$

or

$$\frac{1}{1 - \rho_{XY}^2} \left\{ \left(\frac{x - \bar{x}}{3\sigma_X} \right)^2 - 2\rho_{XY} \left(\frac{x - \bar{x}}{3\sigma_X} \right) \left(\frac{y - \bar{y}}{3\sigma_Y} \right) + \left(\frac{y - \bar{y}}{3\sigma_Y} \right)^2 \right\} = 1.00$$



An n-dimensional Gaussian probability density distribution is represented by a "surface" in n-dimensional (X_1, X_2, \dots, X_n) space. The locus of points with a given probability density will form a contour "surface" given by the following matrix expression:

$$(x_n - \bar{x}_n) M_n^{-1} (x_n - \bar{x}_n) = \chi^2_{f=n}$$

where x_n is a random vector, \bar{x}_n is a mean vector, and M_n is the covariance matrix.

If the n-parameters consist of m-pairs of variables and each pair is assumed uncorrelated and independent of all other pairs, then the resulting equation for the contour "surface" is:

$$\sum_{i=1}^m \frac{1}{1 - \rho_{X_i Y_i}^2} \left\{ \left(\frac{x_i - \bar{x}_i}{\sigma_{X_i}} \right)^2 - 2\rho_{X_i Y_i} \left(\frac{x_i - \bar{x}_i}{\sigma_{X_i}} \right) \left(\frac{y_i - \bar{y}_i}{\sigma_{Y_i}} \right) + \left(\frac{y_i - \bar{y}_i}{\sigma_{Y_i}} \right)^2 \right\} = \chi^2_{f=2m}$$

$$\sum_{i=1}^m F_i = \sum_{i=1}^m \chi_i^2 = \chi^2_{f=2m}$$

Where F_i is the contour ellipse equation for each individual pair of variables and χ_i^2 is that portion of the $\chi^2_{f=2m}$ value associated with the F_i ellipse. The total $\chi^2_{f=2m}$ value can be apportioned among the

individual pairs in any manner consistent with the restriction $0 \leq \chi^2 \leq 9.0$.

Use of the above equations is contingent on the following assumptions:

1. Aerodynamic coefficients are normally distributed, and
2. Aerodynamic uncertainties are three-sigma levels.

These correlation coefficients are to be used in the above equations or in the equation forms given in Table 4.2.3.4-1 which describe the statistical determination for combining uncertainties of functions of the aerodynamic coefficients.


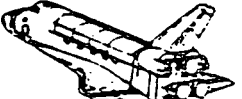


TABLE 4.2.3.4-1

COMBINING UNCERTAINTIES OF FUNCTIONS OF AERODYNAMIC COEFFICIENTS



| No | FUNCTION | MEAN VALUE | UNCERTAINTY | REMARKS |
|----|--|---|---|---|
| 1 | $y = \sum_{i=1}^n K_i x_i$ | $\bar{y} = \sum_{i=1}^n K_i \bar{x}_i$ | $\Delta y = \sqrt{\sum_{i=1}^n K_i^2 (\Delta x_i)^2 + 2 \sum_{i < j} K_i K_j \rho_{ij} \Delta x_i \Delta x_j}$ | $K_i =$ constant $\rho_{ij} =$ correlation coefficient |
| 2 | $y = x_1 x_2$ | $\bar{y} = \bar{x}_1 \bar{x}_2 + \rho_{12} \Delta x_1 \Delta x_2$ | $\Delta y = \sqrt{(1 + \rho_{12}^2) [\Delta x_1 \Delta x_2]^2 + (\Delta x_1)^2 \bar{x}_2^2 + \bar{x}_1^2 (\Delta x_2)^2 + 2 \rho_{12} \bar{x}_1 \bar{x}_2 \Delta x_1 \Delta x_2}$ | Exact expression for a bivariate normal distribution |
| 3 | $y = x_1 x_2 \pm x_3 x_4$ | $\bar{y} = \bar{x}_1 \bar{x}_2 + \rho_{12} \Delta x_1 \Delta x_2 \pm \bar{x}_3 \bar{x}_4 + \rho_{34} \Delta x_3 \Delta x_4$ | $\Delta y = \sqrt{(1 + \rho_{12}^2) [\Delta x_1 \Delta x_2]^2 + (\Delta x_1)^2 \bar{x}_2^2 + \bar{x}_1^2 (\Delta x_2)^2 + 2 \rho_{12} \bar{x}_1 \bar{x}_2 \Delta x_1 \Delta x_2 + (1 + \rho_{34}^2) (\Delta x_3 \Delta x_4)^2 + (\Delta x_3)^2 \bar{x}_4^2 + \bar{x}_3^2 (\Delta x_4)^2 + 2 \rho_{34} \bar{x}_3 \bar{x}_4 \Delta x_3 \Delta x_4 \pm 2 [(\rho_{13} \Delta x_1 \Delta x_3) + (\rho_{14} \Delta x_1 \Delta x_4) + (\rho_{23} \Delta x_2 \Delta x_3) + (\rho_{24} \Delta x_2 \Delta x_4) + (\rho_{31} \Delta x_3 \Delta x_1) + (\rho_{32} \Delta x_3 \Delta x_2) + (\rho_{41} \Delta x_4 \Delta x_1) + (\rho_{42} \Delta x_4 \Delta x_2)] \bar{x}_1 \bar{x}_2}$ | Exact expression for a multivariate normal distribution |
| 4 | $z_1 = \sum_{i=1}^n K_i x_i$ $z_2 = \sum_{j=1}^n M_j y_j$ | $\bar{z}_1 = \sum_{i=1}^n K_i \bar{x}_i$ $\bar{z}_2 = \sum_{j=1}^n M_j \bar{y}_j$ | Δz_1 & Δz_2 from function 1 above $\rho_{z_1, z_2} = \left(\sum_{i=1}^n \sum_{j=1}^n K_i M_j \rho_{x_i y_j} \Delta x_i \Delta y_j \right) / \Delta z_1 \Delta z_2$ | $K_i, M_j =$ constant $\rho_{x_i y_j} =$ correlation coefficient |
| 5 | $y = G(x_1, x_2, \dots, x_n)$ | $\bar{y} = G(\bar{x}_1, \bar{x}_2, \dots, \bar{x}_n)$ | $\Delta y = \sqrt{\sum_{i=1}^n \left(\left[\frac{\partial G}{\partial x_i} \right] \Delta x_i \right)^2 + 2 \sum_{i < j} \left[\frac{\partial G}{\partial x_i} \right] \left[\frac{\partial G}{\partial x_j} \right] \rho_{ij} \Delta x_i \Delta x_j}$ | Linearized theory |
| 6 | $y = \frac{x_1}{x_2}$ | $\bar{y} = \frac{\bar{x}_1}{\bar{x}_2}$ | $\Delta y = \sqrt{\frac{(\Delta x_1)^2}{\bar{x}_2^2} + \frac{\bar{x}_1^2 (\Delta x_2)^2}{\bar{x}_2^4} - \frac{2 \rho (\Delta x_1) (\Delta x_2) \bar{x}_1}{\bar{x}_2^3}}$ | Derived from Equation No. 5 |

LONGITUDINAL CORRELATION COEFFICIENTS. The correlation coefficients to be used with the longitudinal aerodynamic uncertainties are:

$\rho_{C_L C_D}$ = Correlation coefficient relating lift and drag.

$\rho_{C_L C_m}$ = Correlation coefficient relating lift and pitching moment.

$\rho_{C_D C_m}$ = Correlation coefficient relating drag and pitching moment.

| | DIGITAL FILE No. | TABLE (or FIGURE) No. |
|--|------------------------|-----------------------------|
| $\rho_{C_L C_D} = \rho_{C_L C_D} f(M)$ | U 81 | 5.2.3.4-1 |
| $\rho_{C_L C_m} = \rho_{C_L C_m} f(M)$ | U 82 | 5.2.3.4-2 |
| $\rho_{C_D C_m} = \rho_{C_D C_m} f(M)$ | U 83 | 5.2.3.4-3 |

individual pairs in any manner consistent with the restriction $0 \leq \chi_i^2 \leq 9.0$.

Use of the above equations is contingent on the following assumptions:

1. Aerodynamic coefficients are normally distributed, and
2. Aerodynamic uncertainties are three-sigma levels.

These correlation coefficients are to be used in the above equations or in the equation forms given in Table 4.2.3.4-1 which describe the statistical determination for combining uncertainties of functions of the aerodynamic coefficients.


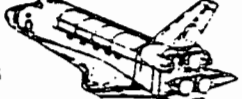


TABLE 4.2.3.4-1

COMBINING UNCERTAINTIES OF FUNCTIONS OF AERODYNAMIC COEFFICIENTS



| No | FUNCTION | MEAN VALUE | UNCERTAINTY | REMARKS |
|----|--|---|---|---|
| 1 | $y = \sum_{i=1}^n K_i X_i$ | $\bar{y} = \sum_{i=1}^n K_i \bar{X}_i$ | $\Delta y = \sqrt{\sum_{i=1}^n K_i^2 [\Delta X_i]^2 + 2 \sum_{i < j} K_i K_j \rho_{ij} \Delta X_i \Delta X_j}$ | $K_i = \text{constant}$ $\rho_{ij} = \text{correlation coefficient}$ |
| 2 | $y = X_1 X_2$ | $\bar{y} = \bar{X}_1 \bar{X}_2 + \rho_{12} \Delta X_1 \Delta X_2$ | $\Delta y = \sqrt{(1 + \rho_{12}^2) [\Delta X_1 \Delta X_2]^2 + (\Delta X_1)^2 \bar{X}_2^2 + \bar{X}_1^2 (\Delta X_2)^2 + 2 \rho_{12} \bar{X}_1 \bar{X}_2 \Delta X_1 \Delta X_2}$ | Exact expression for a bivariate normal distribution |
| 3 | $y = X_1 X_2 \pm X_3 X_4$ | $\bar{y} = \bar{X}_1 \bar{X}_2 + \rho_{12} \Delta X_1 \Delta X_2 + \bar{X}_3 \bar{X}_4 + \rho_{34} \Delta X_3 \Delta X_4$ | $\Delta y = \sqrt{(1 + \rho_{12}^2) [\Delta X_1 \Delta X_2]^2 + (\Delta X_1)^2 \bar{X}_2^2 + \bar{X}_1^2 (\Delta X_2)^2 + 2 \rho_{12} \bar{X}_1 \bar{X}_2 \Delta X_1 \Delta X_2 + (1 + \rho_{34}^2) (\Delta X_3 \Delta X_4)^2 + (\Delta X_3)^2 \bar{X}_4^2 + \bar{X}_3^2 (\Delta X_4)^2 + 2 \rho_{34} \bar{X}_3 \bar{X}_4 \Delta X_3 \Delta X_4 \pm 2 [(\rho_{12} \Delta X_1 \Delta X_2) \cdot (\rho_{34} \Delta X_3 \Delta X_4) + (\rho_{12} \Delta X_1 \Delta X_2) \cdot (\rho_{34} \Delta X_3 \Delta X_4) + (\rho_{12} \Delta X_1 \Delta X_2) \bar{X}_3 \bar{X}_4 + (\rho_{34} \Delta X_3 \Delta X_4) \bar{X}_1 \bar{X}_2 + (\rho_{12} \Delta X_1 \Delta X_2) \bar{X}_3 \bar{X}_4 + (\rho_{34} \Delta X_3 \Delta X_4) \bar{X}_1 \bar{X}_2]}$ | Exact expression for a multivariate normal distribution |
| 4 | $z_1 = \sum_{i=1}^n K_i X_i$ $z_2 = \sum_{j=1}^n M_j Y_j$ | $\bar{z}_1 = \sum_{i=1}^n K_i \bar{X}_i$ $\bar{z}_2 = \sum_{j=1}^n M_j \bar{Y}_j$ | Δz_1 & Δz_2 from function 1 above $\rho_{z_1 z_2} = \left(\sum_{i=1}^n \sum_{j=1}^n K_i M_j \rho_{X_i Y_j} \Delta X_i \Delta Y_j \right) / \Delta z_1 \Delta z_2$ | $K_i, M_j = \text{constant}$ $\rho_{X_i Y_j} = \text{correlation coefficient}$ |
| 5 | $y = G(X_1, X_2, \dots, X_n)$ | $\bar{y} = G(\bar{X}_1, \bar{X}_2, \dots, \bar{X}_n)$ | $\Delta y = \sqrt{\sum_{i=1}^n \left(\left[\frac{\partial G}{\partial X_i} \right] \Delta X_i \right)^2 + 2 \sum_{i < j} \left[\frac{\partial G}{\partial X_i} \right] \left[\frac{\partial G}{\partial X_j} \right] \rho_{ij} \Delta X_i \Delta X_j}$ | Linearized theory |
| 6 | $y = \frac{X_1}{X_2}$ | $\bar{y} = \frac{\bar{X}_1}{\bar{X}_2}$ | $\Delta y = \sqrt{\frac{(\Delta X_1)^2}{\bar{X}_2^2} + \frac{\bar{X}_1^2 (\Delta X_2)^2}{\bar{X}_2^4} - \frac{2 \rho (\Delta X_1) (\Delta X_2) \bar{X}_1}{\bar{X}_2^3}}$ | Derived from Equation No. 5 |

CONTROL SURFACE HINGE MOMENT CORRELATION COEFFICIENTS. Correlation coefficients to be used with the rudder/speedbrake panel hinge moment uncertainties are:

$\rho_{C_{hR/SBRH} C_{hR/SBLH}}$ = Correlation coefficient relating right- and left-hand rudder/speedbrake hinge moment coefficient.

$\rho_{C_{n\delta_r} C_{n\delta_r}}$ = Correlation coefficient relating yawing moment and hinge moment due to rudder deflection.

$\rho_{C_{l\delta_r} C_{n\delta_r}}$ = Correlation coefficient relating rolling moment and hinge moment due to rudder deflection.

| | DIGITAL FILE No. | TABLE (or FIGURE) No. |
|--|------------------------|-----------------------------|
| $\rho_{C_{hR/SBRH} C_{hR/SBLH}} = \rho_{C_{hR/SBRH.LH}}$ f(M) | U 91 | 5.2.3.4- 8 |
| $\rho_{C_{n\delta_r} C_{n\delta_r}} = \rho_{C_{n\delta_r} C_{n\delta_r}}$ f(M) | U 92 | 5.2.3.4- 9 |
| $\rho_{C_{l\delta_r} C_{n\delta_r}} = \rho_{C_{l\delta_r} C_{n\delta_r}}$ f(M) | U 93 | 5.2.3.4-10 |

4.3 LAUNCH VEHICLE AIRLOADS EQUATIONS

ORIGINAL PAGE IS
OF POOR QUALITY

4.3 LAUNCH VEHICLE AIRLOADS EQUATIONS

This section presents the airloads data base equations and methodology for obtaining the external pressure distribution and aerodynamic loads distribution for the Space Shuttle Vehicle during the first stage of launch and consists of the following subsections:

- 4.3.1 External Pressure Distribution and Airloads Analysis
- 4.3.2 Plume Effects
- 4.3.3 Skin Friction
- 4.3.4 Engine Nozzle Airloads
- 4.3.5 Attach Structure Airloads
- 4.3.6 ET and SRB Protuberance Airloads
- 4.3.7 Distributed Airloads

The ignition overpressure airloads experienced at the time of the SRB and SSME ignition are not included in this document but are provided in References 4-7 and 4-8. The referenced documents describe the procedures used to determine the pressure environment induced by the SRB and SSME ignition overpressure for the Eastern and Western test ranges respectively.

4.3.1 EXTERNAL PRESSURE DISTRIBUTION AND AIRLOADS ANALYSIS. This section presents the external surface pressure distribution data base and methodology for obtaining the loading distributions for the geometric elements of the first stage of the Space Shuttle Vehicle (SSV). The pressure data for the SSV are grouped for two regions; the forebody and the base of the vehicle. The pressure distribution for the base of the SSV is included in Section 4.3.2 (Plume Effects).

Detailed forebody pressure distributions are available for each exposed surface of the Launch Vehicle; i.e., the upper wing, lower wing, fuselage, vertical fin, External Tank, and Solid Rocket Booster. The pressure distribution is provided as a function of the principal bi-variant coordinates of the surface and is in tabular form for the non-dimensional pressure coefficient; i.e.,

$$C_p = \frac{[P - P_\infty]}{\bar{q}_\infty}$$

where; C_p = Local pressure coefficient

P = Local surface pressure

P_∞ = Free stream static pressure

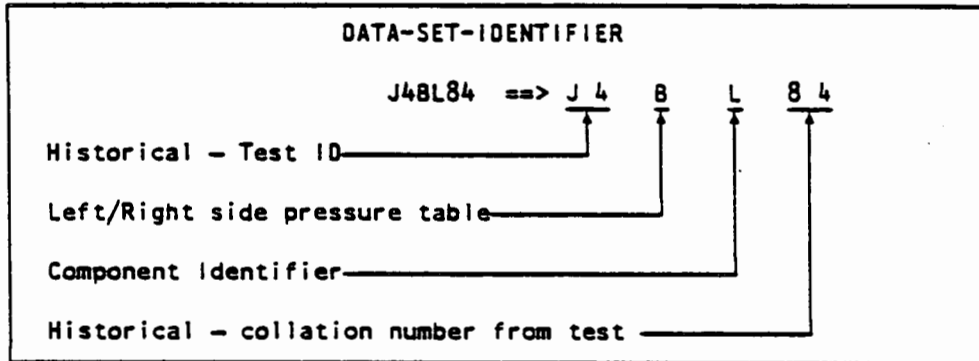
\bar{q}_∞ = Free stream dynamic pressure

The pressure data tables are grouped by configuration, by Mach number, and by control surface setting. Each configuration consists of a set of geometric surfaces and each surface contains a set of pressure tables for vehicle attitude; i.e., angle of attack and sideslip.

Due to the large volume of pressure points used to define the data base (approximately 50 million), the data are stored on mass storage devices. An identifier system has been devised for the total data base to access the required data quickly. This identifier system consists of a unique six character data-set-identifier, DS10, and two indices.

The six characters in a typical dataset identifier, such as J4BL84, have the following meaning:

DATA-SET-IDENTIFIER DESCRIPTION



The first two (J4) and last two (84) characters are historical and define the test and collation sequence of the test data for the original data base. These were maintained to provide uniqueness to the DSID. The third and fourth characters of the DSID define the characteristics of the data table. The third character is used to define the left or right side of the vehicle table with the letter, "R", being used for the right side and any other character for the left. The fourth character defines the geometric surface of the vehicle. These are defined in the table below. The DSID's and index definition of the data are defined in Tables 6.1.3-2 and 6.1.3-3.

COMPONENT IDENTIFIERS USED

| COMPONENT IDENTIFIER | COMPONENT NAME | DIMENSION VARIABLES | |
|----------------------|------------------------|---------------------|-------|
| | | X | Y |
| B | ORBITER FUSELAGE | X/LB | PHI |
| L | LOWER WING | X/CW | 2Y/BW |
| U | UPPER WING | X/CW | 2Y/BW |
| V | LEFT VERTICAL | X/CV | Z/BV |
| S | SRM BOOSTER | X/LS | PHI |
| T | EXTERNAL TANK | X/LT | PHI |
| I | ORBITER ATTACH REGIONS | X/LB | 2Y/BW |

The pressures were originally generated for a symmetrical loading distribution about the lateral plane and were defined for the left side of the vehicle only. The right side was defined as the left side pressure for the opposite sideslip angle. For the asymmetric loading conditions, the same procedure was used. The pressures for the right side of the vehicle are the appropriately defined tables but with opposite sideslip angles.

The use of tabulated pressure data in numerical integration techniques usually requires that the tables be a filled matrix for each

coordinate provided. The forces generated by the pressures are obtainable by integration over the exposed areas. The incremental vector force $[dF_{(i)}]$ on any exposed incremental area $[dS_{(i)}]$ with a reference pressure $[P_{\infty}]$ on the reverse side is:

$$dF_{(i)} = [P - P_{\infty}] dS_{(i)}$$

or in coefficient form:

$$dC_{(i)} = \frac{1}{S_{REF}} C_p dS_{(i)}$$

where; $dC_{(i)}$ = the incremental force coefficient

$dS_{(i)}$ = the vector areas of integration

(i) = the vector directions of the forces and areas

C_p = the local pressure coefficient

S_{REF} = the reference area

A bi-variant coordinate system is used to define the pressure distribution for each surface. The wing and vertical fin coordinates are a rectangular system of the local non-dimensional chord and span locations. The rectangular coordinate axis system of the wing and vertical fin is defined as zero at the leading edge of the panel and unity at the trailing edge in the streamwise (longitudinal) direction. The cross-flow direction is defined as unity at the wing and vertical fin tip, zero at the Orbiter centerline on the wing, and zero for the vertical fin at Orbiter Water Plane 500.

Representative displays of the pressure coefficient table for the upper wing, lower wing, and vertical fin are given in Tables 6.1.1-1, 6.1.1-2, and 6.1.1-3 and corresponding Figures 6.1.1-1, 6.1.1-2, and 6.1.1-3, respectively. The integration scheme employs superimposition of the pressure data on a finite element geometric model of the external structure. The models used for the upper wing, lower wing, and vertical fin are shown on Figures 6.1.1-4, 6.1.1-5, and 6.1.1-6, respectively.

The Orbiter fuselage, External Tank, and Solid Rocket Boosters reference axes are cylindrical coordinates. The streamwise (longitudinal) axis of the cylindrical coordinate system of the fuselage, External Tank, and Solid Rocket Booster is defined as zero at the nose of each element and unity at the base with the scaling length of each element being used as the reference length of the element. The radial coordinate is defined as positive around the left side of the element, starting with zero at the lower centerline. The only exception to this definition is the right hand Solid Rocket Booster where the positive direction is on the right side of the element.

Representative displays of the pressure coefficient table for the fuselage, External Tank, and Solid Rocket Booster are given in Tables 6.1.1-4, 6.1.1-5 and 6.1.1-6 and corresponding Figures 6.1.1-7, 6.1.1-8 and 6.1.1-9, respectively. The radial coordinates of these data are unwrapped on a flat surface for clarity. The finite element models used for the fuselage, External Tank, and Solid Rocket Booster are shown on Figures 6.1.1-10, 6.1.1-11, and 6.1.1-12.

Pressure data are provided for the first stage mated vehicle for various Mach numbers, inboard/outboard elevon deflections, and angles of attack and sideslip. The element pressure tables are provided for the following conditions:

| MACH NO. | ELEVON DEFLECTIONS DEGREES | | | | | | | | |
|-------------|-------------------------------|------|------|-------|-------|-------|-------|-------|-------|
| | 0.60 | 8/ 5 | 8/ 9 | 8/11 | 10/ 5 | 10/ 9 | 10/11 | 12/ 5 | 12/ 9 |
| 0.80 | 8/ 5 | 8/ 9 | 8/11 | 10/ 5 | 10/ 9 | 10/11 | 12/ 5 | 12/ 9 | 12/11 |
| 0.90 | 8/ 5 | 8/ 9 | 8/11 | 10/ 5 | 10/ 9 | 10/11 | 12/ 5 | 12/ 9 | 12/11 |
| 1.05 | 8/ 5 | 8/ 9 | 8/11 | 10/ 5 | 10/ 9 | 10/11 | 12/ 5 | 12/ 9 | 12/11 |
| 1.10 | 8/ 5 | 8/ 9 | 8/11 | 10/ 5 | 10/ 9 | 10/11 | 12/ 5 | 12/ 9 | 12/11 |
| 1.25 | 8/-2 | 8/ 5 | 8/ 9 | 10/-2 | 10/ 5 | 10/ 9 | 12/-2 | 12/ 5 | 12/ 9 |
| 1.40 | 8/-7 | 8/-2 | 8/ 5 | 10/-7 | 10/-2 | 10/ 5 | 12/-7 | 12/-2 | 12/ 5 |
| 1.55 | 8/-7 | 8/-2 | 8/ 5 | 10/-7 | 10/-2 | 10/ 5 | 12/-7 | 12/-2 | 12/ 5 |
| 1.80 | -- | 4/-5 | 4/-2 | -- | 10/-5 | 10/-2 | 12/-7 | 12/-5 | 12/-2 |
| 2.20 | -- | 0/-5 | 0/-2 | -- | 4/-5 | 4/-2 | 10/-5 | 10/-2 | -- |
| 2.50 | 0/-7 | 0/-2 | 0/ 2 | 4/-7 | 4/-2 | -- | -- | -- | -- |

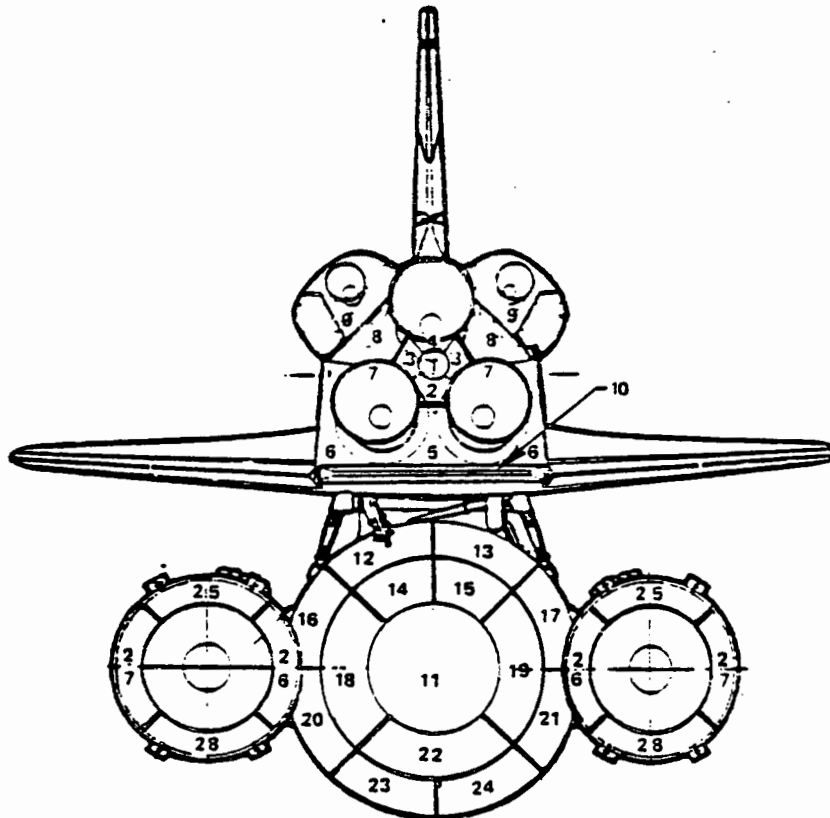
Data are presented for the elevon settings listed and the following angle of attack and sideslip ranges:

| MACH NO. | RANGE ~ DEGREES | |
|-------------|-----------------|----------|
| | α | β |
| 0.60 | -8 to +8 | -8 to +8 |
| 0.80 | -8 to +6 | -6 to +6 |
| 0.90 | -8 to +4 | -6 to +6 |
| 0.95 | -8 to +4 | -6 to +6 |
| 1.05 | -8 to +4 | -6 to +6 |
| 1.10 | -8 to +4 | -6 to +6 |
| 1.25 | -8 to +8 | -8 to +8 |
| 1.40 | -8 to +6 | -6 to +6 |
| 1.55 | -8 to +4 | -6 to +6 |
| 1.80 | -8 to +4 | -6 to +6 |
| 2.20 | -8 to +4 | -6 to +6 |
| 2.50 | -8 to +4 | -6 to +6 |

4.3.2 PLUME EFFECTS. This section presents the effects of the plume interaction with the surrounding flow. The principal effect of the gaseous mixing of the plume with the local flow is to create a recirculated flow region which repressurizes the base regions of the SSV and changes the local forebody pressures in the aft regions of the various SSV components. The use of the data for these phenomena is described in the following subsections and the data are presented in Volume 4 of this report.

BASE PRESSURE. This sub-section presents the base pressure distribution on the Orbiter, External Tank, and Solid Rocket Boosters during the launch phase. The power-on load distributions on the base region of the SSV are based on high-q boost conditions. The base regions considered are the bases of the fuselage, wings, and vertical fin of the Orbiter and the bases of the External Tank and the Solid Rocket Boosters.

The pressure distributions on the fuselage, ET, and SRB base regions vary due to geometric contours and protuberances which alter the recirculated flow directions and magnitudes. Based on flight and wind tunnel test results, the pressure is defined as approximately constant over each zone of the bases. These zones (10 for the Orbiter, 14 for the External Tank, and 4 for each of the Solid Rocket Boosters) and the areas encompassed are illustrated below and presented in Figures 6.1.2-1 through 6.1.2-4.



4.3.2-1

The base pressure on the upper surface of the body flap is a function of the plume mixing with the surrounding stream and is presented as part of the Orbiter base with the pressure distribution for the lower surface of the body flap being provided as part of the Orbiter fore-body fuselage pressure tables in Section 4.3.1.

The base pressures are presented for baseline conditions of zero angles of attack (α) and sideslip (β) and pressures for flight values other than $(\alpha, \beta) = (0, 0)$ are obtained by use of the following equation.

$$C_p(\alpha, \beta) = C_p(0, 0) * [1 + K_1\alpha + K_2\beta^2]$$

where; $C_p(\alpha, \beta)$ = Base pressure coefficient
(function of angle of attack
and sideslip)

$C_p(0, 0)$ = Base pressure coefficient
when angle of attack and
sideslip are zero degrees

α = Angle of attack, degrees

β = Angle of sideslip, degrees

K_1, K_2 = Constants given in the following
table

| MACH NO. | RANGE OF APPLICATION | | CONSTANTS | |
|-------------|----------------------|---------|-----------|---------|
| | α | β | K_1 | K_2 |
| 0.60 | -8 → +8 | -8 → +8 | -0.00047 | 0.00083 |
| 0.80 | -8 → +6 | -6 → +6 | -0.00146 | 0.00191 |
| 0.90 | -8 → +4 | -6 → +6 | -0.00247 | 0.00308 |
| 1.05 | -8 → +4 | -6 → +6 | 0.00731 | 0.00238 |
| 1.10 | -8 → +4 | -6 → +6 | 0.00772 | 0.00392 |
| 1.25 | -8 → +4 | -6 → +6 | 0.00284 | 0.00199 |
| 1.40 | -8 → +4 | -6 → +6 | 0.00196 | 0.00297 |
| 1.55 | -8 → +4 | -6 → +6 | 0.00305 | 0.00313 |
| 1.80 | -6 → +6 | -6 → +6 | 0.00271 | 0.00271 |
| 2.20 | -6 → +6 | -6 → +6 | 0.00208 | 0.00208 |
| 2.50 | -6 → +6 | -6 → +6 | 0.00158 | 0.00158 |

The pressures acting on the base regions of the wing, and vertical fin were obtained by using two-dimensional wake pressures (Reference 4-10). Tables listing the base pressure coefficients for the various Mach numbers are included on Figures 6.1.2-5 through 6.1.2-9.

FOREBODY EFFECTS. The interaction of the SSME and SRB plumes with the surrounding local air flow affects the pressure on the forebody of the SSV. The magnitude of pressure changes and regions of influence of these changes were measured during wind tunnel test. These are illustrated on the figures listed below.

FOREBODY PLUME EFFECTS

| ELEMENT | MACH NUMBER | | | | | |
|-----------------------|-----------------|------|------|------|------|------|
| | 0.60 | 0.90 | 1.05 | 1.10 | 1.25 | 1.40 |
| | Figure 6.1.2-() | | | | | |
| WING | 10 | 11 | 12 | 13 | 14 | 15 |
| FUSELAGE/VERTICAL FIN | 16 | 16 | 17 | 17 | 18 | 18 |
| EXTERNAL TANK | 19 | 20 | 21 | 22 | 23 | 24 |
| SOLID ROCKET BOOSTERS | 25 | 26 | 27 | 28 | 29 | 30 |

4.3.3 SKIN FRICTION AND SURFACE ROUGHNESS. This section presents the skin friction on the SSV and surface roughness drag of the TPS tiles and protuberances of the Orbiter.

SKIN FRICTION. The full scale skin friction was computed for design flight conditions using the fully turbulent flat plate skin friction for a wall-to-freestream temperature ratio (T_w/T_∞) of 1.0 and an equivalent sand roughness height (k) of 0.002 inches for all surfaces (Reference 4-11). The resultant local skin friction coefficients, presented as functions of the distance from the leading edge or nose, are given in Figures 6.1.3-1 and 6.1.3-6 for Mach numbers through the high dynamic pressure flight regime.

A modification constant has been applied to account for disturbances caused by shock/boundary layer interaction, proturbances, and pressure gradients. To obtain the skin friction in the vicinity of these disturbances, a multiplying factor (MF) is provided on Figures 6.1.3-7 through 6.1.3-17. The resultant local shear stress due to skin friction in the axial direction is

$$\tau = C_F * (MF) * \bar{q}_\infty$$

and the net axial force due to skin friction (independent of the angle of attack and the angle of sideslip) is:

$$C\tau = \frac{1}{S_{REF}} \int [C_F(x, y) (MF)] dS$$

- where; τ = Local shear stress (skin friction)
- C_F = Local skin friction coefficient
- MF = Multiplying factor to the skin friction
- from shock/boundary layer interaction.
- \bar{q}_∞ = Free stream dynamic pressure
- $C\tau$ = Skin friction force coefficient due
to shear stress
- dS = Wetted surface unit area
- S_{REF} = Reference area

Integration of the local skin friction over the wetted areas provides the global skin friction force coefficient of each segment. This resultant force vector for each element is in the direction of the aerodynamic stream. The vehicle axial, side, and normal components of the skin friction are obtained by the usual rotation equations; i.e.,

$$C_{()} = C_r * [\text{rotation vector}]$$

where; $C_{()}$ = Vehicle component force coefficient

() = A-, Y-, N- direction of force

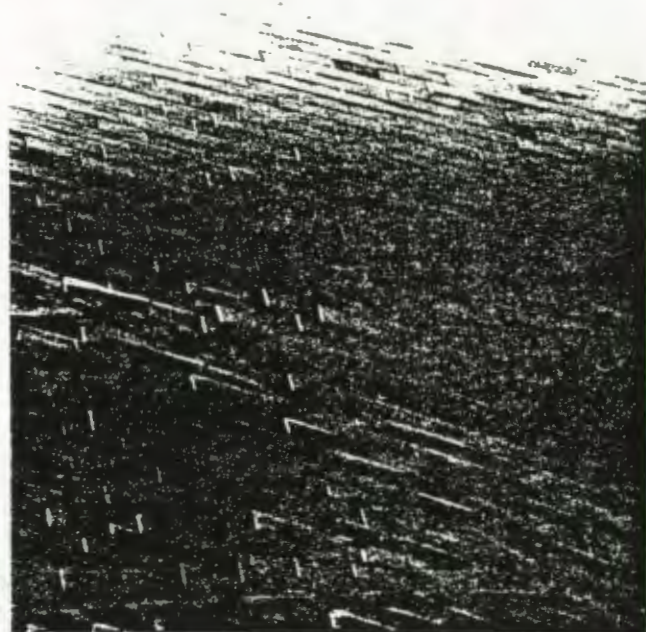
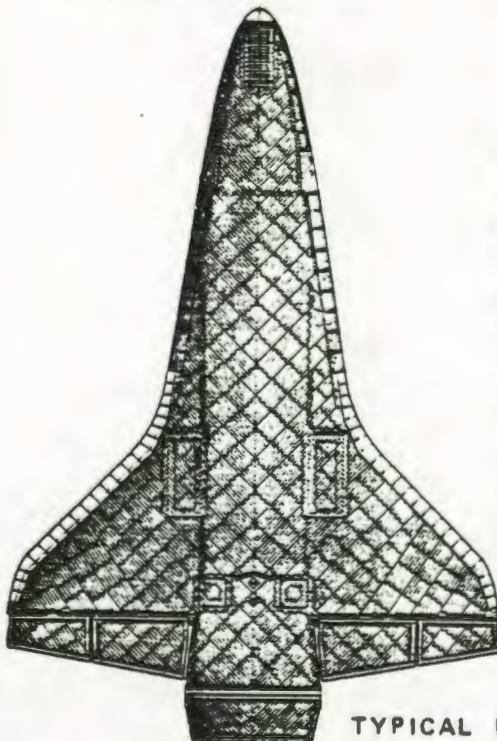
SKIN FRICTION ROTATION VECTORS

| ELEMENT | A | Y | N |
|-----------------------|------|--------------|---------------|
| FUSELAGE | 1.0* | $\sin \beta$ | $\sin \alpha$ |
| WING | 1.0 | $\sin \beta$ | 0 |
| VERTICAL FIN | 1.0 | 0 | $\sin \alpha$ |
| EXTERNAL TANK | 1.0 | $\sin \beta$ | $\sin \alpha$ |
| SOLID ROCKET BOOSTERS | 1.0 | $\sin \beta$ | $\sin \alpha$ |

$$* \cos \beta \approx \cos \alpha \approx 1.0$$

The total skin friction force vector for each element is provided on Figures 6.1.3-19 through 6.1.3-23 for the wing, fuselage, vertical tail, External Tank, and Solid Rocket Boosters.

TPS ROUGHNESS AND ORBITER PROTUBERANCES. Axial forces acting on the Orbiter fuselage as a result of the the TPS tiles and various local protuberances have been included in Volume 4 of this report. These forces were extracted from Section 6.2 of this report. The magnitudes of these corrections and their points of application are shown on Figure 6.1.3-24



TYPICAL LOWER SURFACE

4.3.3-2

4.3.4 ENGINE NOZZLE LOADS. This section presents the incremental loads on the Orbiter due to asymmetric loading on the SSME and OMS nozzles at vehicle angles of sideslip. The values presented in Figure 6.1.4-1 were determined by use of cross-flow theory and exposed nozzle areas. The incremental Orbiter side load is determined by:

$$\Delta C_Y = c\beta$$

where; ΔC_Y = Side force coefficient increment
(function of angle of sideslip)

β = Angle of sideslip, degrees

c = Proportionality constant

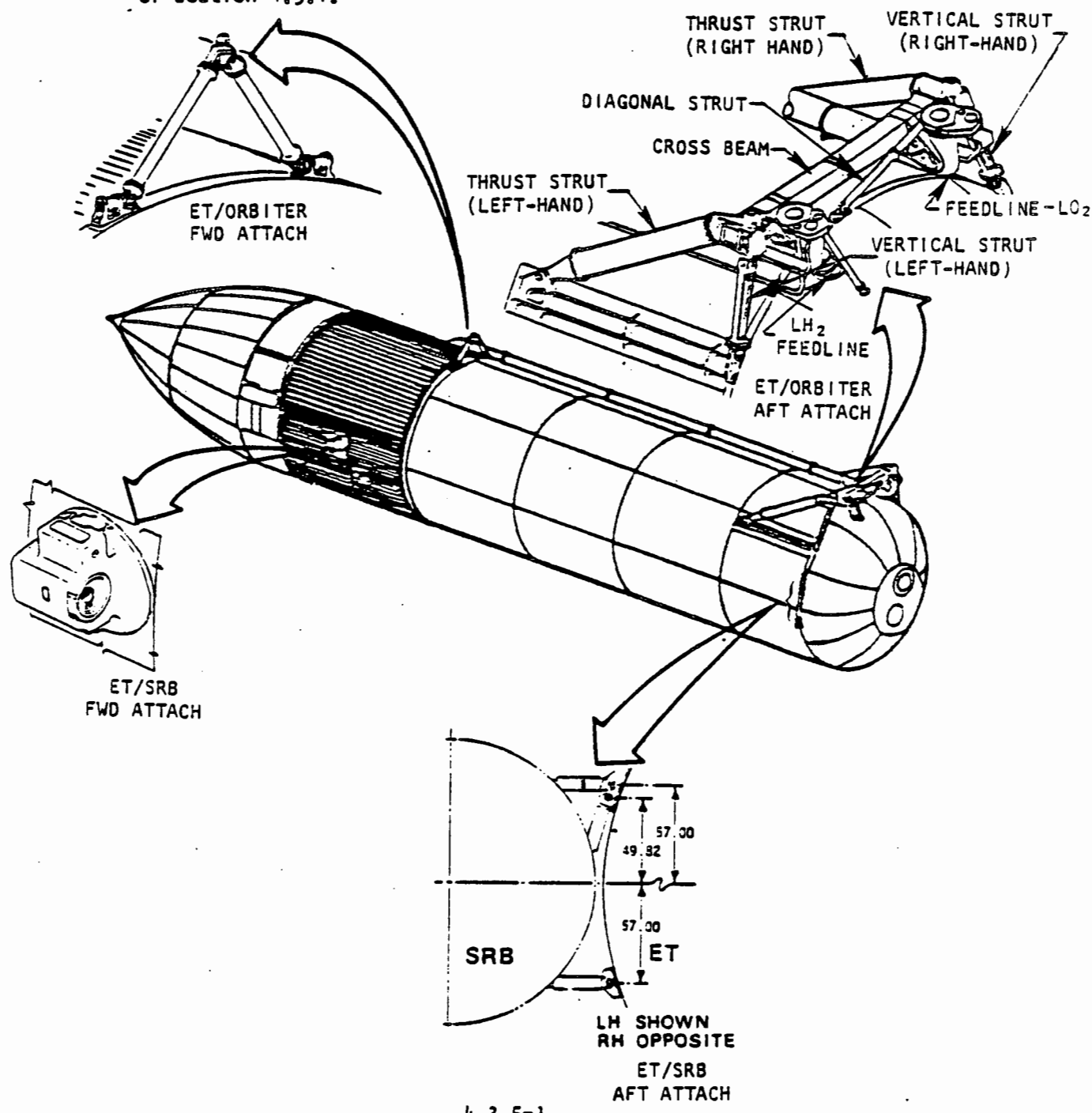
The proportionality constant, c , is defined as follows:

The upper SSME and OMS nozzles Figure 6.1.4-1

The lower SSME nozzles Figure 6.1.4-2

The yawing and rolling moment increments for the Orbiter are determined by use of the above force increments and the appropriate moment arms from the load point of application indicated on the figures.

4.3.5 ATTACH STRUCTURE LOADS. This section presents the loads on the attach structure which connect the Orbiter with the ET and the ET with the SRB's (cf. Section 3.1.4). The presence of the attach structure has two effects; it alters the vehicle pressure distributions in the vicinity of the attach structure and produces aerodynamic loads on itself. The interference influences on the Orbiter and ET pressure distributions are included as part of the integrated pressure loads of Section 4.3.1.



4.3.5-1

The total loads on the attach structure, determined from an evaluation of force data, have been apportioned among the various elements of the attach structure based on their respective projected areas. The loads on the attach structure are presented as a build-up of the various elements. The data were curve-fit as functions of angles of attack [α] and sideslip [β]; i.e.,

$$C_{()} = a + b\alpha + c\beta$$

- where; $C_{()}$ = Aerodynamic force coefficient
 () = A, Y, N components of force
 α = Angle of attack, degrees
 β = Angle of sideslip, degrees
 a
 b = Proportionality constants
 c

These proportionality constants for each of the element loads are plotted and tabulated in Section 6.1.3 for Mach numbers through the high dynamic pressure range of the launch trajectory. The constants and the load point are provided in the figures listed below:

ATTACH STRUCTURE FORCES

| ELEMENT | A | Y | N |
|---------------------------------|------------------|-----|-----|
| | Figure 6.1.5-() | | |
| Forward ET/Orbiter bipod | 1 | 2 | 3 |
| Right Thrust Strut | 4 | 5 | 6 |
| Left Thrust Strut | 7 | 8 | 9 |
| Right Vertical Strut | 10 | 11 | 12 |
| Left Vertical Strut | 13 | 14 | 15 |
| LH2 Vertical Feedline | 16 | 17 | 18 |
| L02 Vertical Feedline | 19 | 20 | 21 |
| Cross Beam | 22 | = 0 | = 0 |
| ET diagonal Strut | 23 | = 0 | 24 |
| ET/SRB Forward Attach Structure | 25 | = 0 | 26 |
| ET/SRB Aft Attach Structure | 27 | = 0 | 28 |

4.3.6 ET and SRB PROTUBERANCE LOADS. This section presents the loads on the External Tank and Solid Rocket Booster protuberances defined in Sections 3.1.2, 3.1.3, and 3.1.4. The locations of these protuberances are shown in Figures 3.1.3-2 (a through e) and 3.1.2-2 (a through d). The aerodynamic loads of the protuberances are presented as airloads on the protuberances and the resultant forces and moments on the SSV.

4.3.6.1 GLOBAL PROTUBERANCE AERODYNAMIC LOADS. The protuberance aerodynamic forces and moments on the SSV were determined by grouping protuberances in an assembly and calculating an equivalent force and point of application. The groupings established were the feedline assemblies on the ogive and cylinder sections of the External Tank and the aft-attach ring and skirt flange and burst ring assemblies on the Solid Rocket Booster. The coefficients of force for these four assemblies are presented as a function of the angles of attack and sideslip as:

$$F_{()} = C_{()} * \bar{q}_{\infty} * S_{()}_{REF}$$

where; () = represents the protuberance x-, y-, or z-axis direction

$C_{()}$ = force coefficient

\bar{q}_{∞} = free stream dynamic pressure

$S_{()}_{REF}$ = reference area (= 2690 sq. ft.)

The coefficients of force are presented as a function of the angle of attack and the angle of sideslip as:

$$C_{()} = a + b\alpha + c\beta + d\alpha^2 + e\beta^2 + f\alpha\beta$$

where; α = Angle of attack, degrees

β = Angle of sideslip, degrees

$\left. \begin{array}{l} a, b, \\ c, d, \\ e, f \end{array} \right\}$ = Proportionality constants

The proportionality constants for the global protuberance loads are plotted and tabulated in Section 6.1.6.1. These constants and the load points are provided in the curves listed below:

PROTUBERANCE AERODYNAMIC LOADS

| ELEMENT | A | Y | N |
|------------------------------|--------------------|----|----|
| | Figures 6.1.6.1-() | | |
| External Tank: | | | |
| Ogive Feedline Assembly | 1 | 5 | 7 |
| Cylinder Feedline Assembly | 2 | 6 | 8 |
| Solid Rocket Booster: | | | |
| Aft-Attach Structural Ring | 3 | -- | -- |
| Skirt Flange and Burst Rings | 4 | -- | -- |

4.3.6.2 **PROTUBERANCE AIRLOADS.** Detailed aerodynamic loads for each protuberance are presented to provide information on the magnitude of the load imposed on each protuberance during the launch. Unless otherwise specified, the protuberance airloads provided are external environment loads only and do not consider internal pressures or back-face pressures. For example, the upper surfaces of the attach fittings are exposed to a general pressure environment which does not act on the bottom surface because they are mounted on the main structure. However, a pressure differential results in an actual load on the fitting and must be considered in determining the total load on the fitting. Other examples of local environment loads are on the SRB systems tunnel and range safety cable tray; the internal pressures are also required for the total load assessment. This type of additional loading information is obtained from the source creating the load. That is, internal pressures are obtained from venting analysis. For the most part, the incremental loads provided are due to the local pressure environment.

PROTUBERANCE LOAD AXIS SYSTEM. The loads presented in Section 6.1.6.2 are in a protuberance axis coordinate system and thus provide local loads on the protuberance. The axis system for each protuberance is described with the appropriate protuberance in Section 6.1.6.2. In general, the protuberance body-axis is aligned with the axial direction, generally parallel to the local flow field, and the radial direction normal to the local surface and directed outward. The circumferential direction is perpendicular to the axial and radial directions and tangent to the surface of the ET or SRB. The loads are assumed to act at the protuberance area centroid, unless otherwise specified.

DATA FORMAT AND USAGE. The protuberance loads are obtained by using the tables and plots of force coefficients presented in Section 6.1.6.2. The loads are obtained by use of the following equation:

$$F_{()} = C_{()} * \bar{q}_{\infty} * (\bar{q}_E / \bar{q}_{\infty}) * S_{()}_{REF}$$

where; () = represents the protuberance x-, y-, or z-axis direction
 $C_{()}$ = force coefficient
 \bar{q}_{∞} = free stream dynamic pressure
 \bar{q}_E = equivalent dynamic pressure
 $S_{()}_{REF}$ = reference area of the protuberance

The coefficients of force are presented as a function of the angle of attack and the angle of sideslip as:

$$C_{(1)} = a + b\alpha + c\beta + d\alpha^2 + e\beta^2 + f\alpha\beta$$

where; α = Angle of attack, degrees
 β = Angle of sideslip, degrees
 $\left. \begin{array}{l} a, b, \\ c, d, \\ e, f \end{array} \right\}$ = Proportionality constants

The equivalent dynamic pressure in the above equation is due to the local changes in the local flow field and flow directions. This term is used to realign the magnitude and direction of forces due to the change of SSV angles of attack and sideslip. The equivalent dynamic pressure term is used synonymously as the cross-flow dynamic pressure, local dynamic pressure and an effective dynamic pressure depending on the protuberance and force direction. Each protuberance and force calculation is defined independently and caution must be exercised in the use of the equations given in Section 6.1.6.2.

Due to the large number of equations required to define the aerodynamic load acting on each protuberance, the equations and required data are presented together in Section 6.1.6.2.

4.3.7 DISTRIBUTED AIRLOADS. This section presents the wing span loading distribution of shear, bending and torsion. These loads are obtainable from the tabulated pressure tables of Appendix B of this report. Using the net unit load across the wing as the pressure difference, $\Delta P = P_L - P$ or $\Delta P = \bar{q}_\infty \Delta C_p$, the distribution of loads are obtainable by integration in the chord and span directions.

The shear of any segment of the wing from the tip to an inboard station is defined as:

$$N = \bar{q}_\infty S_{REF} C_N$$

$$C_N = - \frac{b \bar{c}}{S_{REF}} \sum \Delta C_p dx dy$$

The bending of any segment of the wing from the tip to an inboard station is defined as:

$$B = \bar{q}_\infty S_{REF} b C_B$$

$$C_B = - \frac{b \bar{c}}{2 S_{REF}} \sum (Y - Y_R) \Delta C_p dx dy$$

The torsion of any segment of the wing from the tip to an inboard station is defined as:

$$T = \bar{q}_\infty S_{REF} b C_T$$

$$C_T = - \frac{b \bar{c}}{S_{REF}} \sum \frac{c}{\bar{c}} (X_R - X) \Delta C_p dx dy$$

The reference parameters used are:

$$S_{REF} = 2690.0 \text{ sq. ft. -- Wing reference area}$$

$$b = 468.34 \text{ in. -- Wing semi-span}$$

$$\bar{c} = 474.80 \text{ in -- Mean aerodynamic chord}$$

Distributions of wing span loading of shear, bending and torsion are presented in Section 6.1.7.

ORIGINAL PAGE IS
OF POOR QUALITY.

4.4 ORBITER VEHICLE AIRLOADS EQUATIONS

4.4 ORBITER VEHICLE AIRLOADS EQUATIONS

This section is to be provided at a later date.